Mathematical Problems in Engineering

Decision Making Methods and Applications in Civil Engineering

Guest Editors: Jurgita Antucheviciene, Zdeněk Kala, Mohamed Marzouk, and Egidijus Rytas Vaidogas

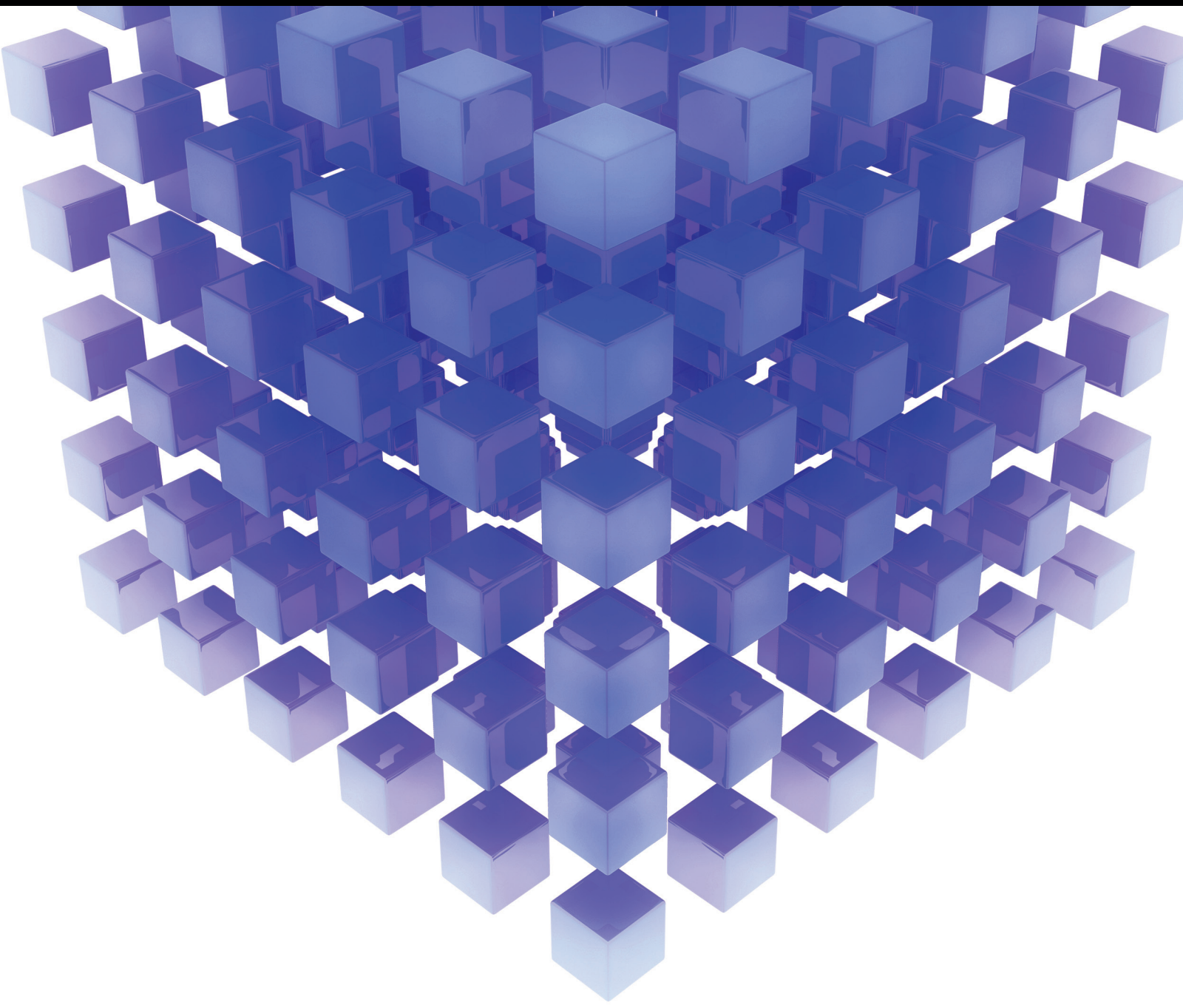

Decision Making Methods and Applications in Civil Engineering

Mathematical Problems in Engineering

Decision Making Methods and Applications in Civil Engineering

Guest Editors: Jurgita Antucheviciene, Zdenek Kala, Mohamed Marzouk, and Egidijus Rytas Vaidogas

Editorial Board

Contents

Hindawi Publishing Corporation
Mathematical Problems in Engineering
Volume 2015, Article ID 160569, 3 pages
http://dx.doi.org/10.1155/2015/160569

Editorial
Decision Making Methods and Applications in Civil Engineering

Jurgita Antucheviciene,[1] Zdeněk Kala,[2] Mohamed Marzouk,[3] and Egidijus Rytas Vaidogas[4]

[1]*Department of Construction Technology and Management, Faculty of Civil Engineering, Vilnius Gediminas Technical University, Saulėtekio Alėja 11, LT-10223 Vilnius, Lithuania*
[2]*Department of Structural Mechanics, Faculty of Civil Engineering, Brno University of Technology, Veveří Street 95, 602 00 Brno, Czech Republic*
[3]*Department of Structural Engineering, Faculty of Engineering, Cairo University, Giza 12613, Egypt*
[4]*Department of Labour Safety and Fire Protection, Faculty of Civil Engineering, Vilnius Gediminas Technical University, Saulėtekio Alėja 11, LT-10223 Vilnius, Lithuania*

Correspondence should be addressed to Jurgita Antucheviciene; jurgita.antucheviciene@vgtu.lt

Received 28 September 2015; Accepted 30 September 2015

This special issue aims at providing recent developments about the decision making (DM) in the field of civil engineering. This field is vast and plays an important role in the life of modern society. A very large number of decisions must be made in the life cycle of constructed objects. The decisions will be required in the time span starting from conceptualisation of these objects and covering design, construction, occupation, and decommissioning. Methods of DM can facilitate making these decisions in formal and not fully formal, partially intuitive way. The present special issue provides numerous examples on how can this be done.

Articles published in this special issue prove that useful information for making construction related decisions can be obtained by methods which do not belong to a formal DM, for instance, sensitivity analysis, stochastic analysis, mathematical optimization, occupational safety, and risk assessment. Classical disciplines of engineering are also useful tool for facilitating decisions in civil engineering. However, all of these methods can be seen as means of providing input information for a formal DM.

The formal DM methods, with application of which this special issue is concerned to a large measure, were intensively developed and applied to various engineering systems in recent decades. They are known as methods of multiple criteria decision making (MCDM). Articles included in this issue show how to apply such MCDM methods as AHP, ANP, and TOPSIS to making decisions related to construction industry and partially to transportation. Obviously, methods of MCDM were developed outside the field of civil engineering and their applications are very diverse. Several useful reviews of these methods are provided in the books [1, 2] as well as journal articles [3–8]. However, one can also find MCDM reviews devoted specifically to civil engineering as well as the related areas of infrastructure and asset management [9–11]. Systematically classified information on MCDM methods and applications can be found in the newly published review [12].

The problematics of DM cannot be resolved by means of MCDM alone. Sometimes intuition and sound engineering judgement will be as useful for making decisions as formal mathematical methods. A necessary base for such judgement is results of common engineering and sometimes managerial analysis. Several articles of this special issue demonstrate how to solve problems of DM in this not fully formal way.

In "Three-Dimensional Numerical Analysis of the Tunnel for Polyaxial State of Stress" by W. Qiu et al., the authors explore the mechanical behavior of rock masses around excavation under different value of intermediate principal stress. A new polyaxial strength criterion is used in numerical simulation to investigate the influence of intermediate principal stress. A mathematical relationship is established between

polyaxial failure criterion and Mohr-Coulomb failure criterion and they are applied in the numerical simulation, respectively. Results indicate that there are some differences of intermediate principal stress influence on the mechanical behavior of rock masses based on the both criteria.

In "Solving Civil Engineering Problems by Means of Fuzzy and Stochastic MCDM Methods: Current State and Future Research" by J. Antucheviciene et al., a review of DM methods, developed for dealing with uncertainties by means of fuzzy logic and probabilistic modelling and applied to solving problems of civil engineering, is provided. Several methodological difficulties emerging from uncertainty quantification in MCDM are identified. Prospects of using MCDM under uncertainty in developing areas of civil engineering are discussed.

The paper "A Novel Model of Set Pair Analysis Coupled with Extenics for Evaluation of Surrounding Rock Stability" by M. Wang et al. studies the problem of evaluation of surrounding rock stability as a complex and uncertain problem, involving numerous factors of fuzziness, uncertainty, and variability. A novel DM model, based on the set pair analysis (SPA) coupled with extenics, considering incompatibility, certainty, and uncertainty of evaluation indicators, is presented to analyze the surrounding rock stability.

Q. Hou and X. Zhou present the paper "Cross-Efficiency Evaluation Method with Compete-Cooperate Matrix" and investigate the question of cross-efficiency evaluation method as an effective data envelopment analysis (DEA) method with self-assessment and peer-assessment to evaluate and rank decision making units (DMUs). In this paper, a symmetric (nonsymmetric) compete-cooperate matrix is introduced and compete-cooperate cross-efficiency method is proposed to evaluate DMUs with diverse (relative) relationships. Numerical demonstration is provided to illustrate the reasonability and practicability of the proposed method.

In "Naïve Bayesian Classifier for Selecting Good/Bad Projects during the Early Stage of International Construction Bidding Decisions" by W. Jang et al., a method for increasing firms' profit rates and enhancing the efficiency of Korean contractors bidding decisions during early stages of a project cycle is suggested. Naïve Bayesian classifier is used as a screening tool that increases practical applicability using binomial variables with limited information obtained during early stages of construction projects.

In the paper "Service Station Evaluation Problem in Catering Service of High-Speed Railway: A Fuzzy QFD Approach Based on Evidence Theory," X. Wu et al. offer the MCDM approach for the service station evaluation problem in catering service of high-speed railway (SSEP-CSHR). The selection of potential service stations for CSHR is carried out using two-phase fuzzy quality function deployment (F-QFD) with regard to a series of practical criteria and basic requirements in context of CSHR.

J. Cho et al. propose quality function deployment (QFD) to select market products for building envelope solution in "QFD Based Benchmarking Logic Using TOPSIS and Suitability Index." Technique for Order of Preference by Similarity to Ideal Solution (TOPSIS) and Suitability Index (SI) are used to provide performance improvement criteria and allow analysis on suitability of the building envelope solution based on user's required performance criteria, respectively.

In "Planning Tunnel Construction Using Markov Chain Monte Carlo (MCMC)," J. P. Vargas et al. propose a simulation algorithm which can be regarded as a variant of the MCMC method. It provides the user with a reliable assessment of excavation times in case of utilizing the standard method of drilling and blasting.

In "Performance Requirements on Remodeling Apartment Housing and TOPSIS Evaluation" by J. Cho and J. Chun, the authors look into the problem of performance evaluation of remodeling apartment housing. They suggest applying the TOPSIS to measure performance improvement degree on remodeling design solutions before and after remodeling. The method presents the objective composite performance score with multiperformance properties and allows user to decide the weight for performance.

The paper "Use of a Combination of MRSS-ANP for Making an Innovative Landfill Siting Decision Model" by M. K. Younes et al. explores the use of a median ranked sample set (MRSS) and an analytic network process (ANP) when ranking the associated environmental, social, land use, and operational criteria and selecting a suitable landfill site. The proposed integrated model minimizes the uncertainty and the subjectivity of human judgments and may become a valuable tool for the decision makers.

Q. Wang et al. showed and applied a mechanical model of prestressed steel cantilever to study the optimal position of the transverse external tendon in the paper entitled "Structural Optimization of Steel Cantilever Used in Concrete Box Girder Bridge Widening," The reasonability and feasibility of the optimal design are verified by stress state analysis using finite element method. The structural optimization helps the designer to find the most suitable shape and layout of a steel cantilever from structural and architectural points of view.

The authors of "BIM Application to Select Appropriate Design Alternative with Consideration of LCA and LCCA" Y. Shin and K. Cho consider how to analyze the information needed to conduct life cycle assessment (LCA) and life cycle cost analysis (LCCA) using a building information modeling. Decision makers can use the results of the assessments at early phases of projects to evaluate different alternatives taking into account economic and environmental perspectives.

In "A Straight-Line Method for Analyzing Residual Drawdowns at an Observation Well" a new straight-line method to estimate the aquifer parameters by using the residual drawdowns at the observation is presented by M. Çimen. In hydraulic engineering, determination of the transmissivity and storage coefficients of a confined aquifer is important for effective groundwater resources.

The paper "Predicted Thermal Sensation Index for the Hot Environment in the Spinning Workshop" by R.-L. Yang et al. proposes a new heat index, named predicted thermal sensation (PTS) index, to effectively evaluate the general thermal sensation of the textile worker exposed to the hot environment in the spinning workshop. Compared to other indices, the PTS index can more effectively predict the mean thermal response of a large group of workers.

The paper "Sustainability-Related Decision Making in Industrial Buildings: An AHP Analysis" by J. Cuadrado et al. proposes an application of AHP method to serve as a sustainability related DM tool in industrial building projects during the design stage. Accompanied by an economic valuation of the actions to be undertaken, this tool means that the most cost-effective solution may be selected from among the various options.

I.-H. Han et al. consider the problem of DM related to occupational safety on the construction site. In the paper "Decision Making Method Based on Importance-Dangerousness Analysis for the Potential Risk Behavior of Construction Laborers," they propose an analytical technique allowing to quantitatively assess the risk to construction workers. This technique can serve as a practical tool for making decisions concerning the potentiality of workplace accidents.

In "Map Matching Based on Conditional Random Fields and Route Preference Mining for Uncertain Trajectories" by M. Xu et al., the problem of offline map matching accuracy of uncertain GPS trajectories is investigated. A map matching algorithm based on conditional random fields (CRF) and route preference mining is proposed. The experimental results show that the proposed algorithm is more accurate than existing methods, especially in the case of a low sampling rate.

The present special issue does not crystallize any special problem or methodological stream of DM in civil engineering. It rather demonstrates how diverse problems of DM in the field of construction and related fields can be. Articles included in this issue are, to a great extent, a result of a random choice. Out of 63 manuscripts submitted to the special issue, only 17 were finally accepted for publication. Unfortunately, 8 manuscripts were simply withdrawn and we, guest editors, are very sad about this. Several of them were of very high scientific quality.

Despite the certain randomness inherent in the final selection of manuscripts for publication, we think that the special issue could be interesting to all those who have to make decisions in the vast field of civil engineering.

Acknowledgments

A large number of people contributed in various ways to making this special issue possible. First of all, we thank professor Edmundas Kazimieras Zavadskas for having proposed the topic of this issue. Let us also thank the authors of articles published in the issue for their contribution. We are grateful to all the reviewers for their valuable work.

Jurgita Antucheviciene
Zdeněk Kala
Mohamed Marzouk
Egidijus Rytas Vaidogas

References

[1] J. R. Figueira, S. Greco, and M. Ehrgott, Eds., *Multiple Criteria Decision Analysis: State of the Art Surveys*, Springer, Berlin, Germany, 2005.

[2] M. Ehrgott, J. R. Figueira, and S. Greco, Eds., *Trends in Multiple Criteria Decision Analysis*, Springer, New York, NY, USA, 2010.

[3] M. M. Wiecek, Matthias Ehrgott, G. Fadel, and J. Rui Figueira, "Multiple criteria decision making for engineering," *Omega*, vol. 36, no. 3, pp. 337–339, 2008.

[4] E. K. Zavadskas and Z. Turskis, "Multiple criteria decision making (MCDM) methods in economics: an overview," *Technological and Economic Development of Economy*, vol. 17, no. 2, pp. 397–427, 2011.

[5] M. Behzadian, S. K. Otaghsara, M. Yazdani, and J. Ignatius, "A state-of the-art survey of TOPSIS applications," *Expert Systems with Applications*, vol. 39, no. 17, pp. 13051–13069, 2012.

[6] E. K. Zavadskas, Z. Turskis, and S. Kildiene, "State of art surveys of overviews on MCDM/MADM methods," *Technological and Economic Development of Economy*, vol. 20, no. 1, pp. 165–179, 2014.

[7] A. Mardani, A. Jusoh, and E. K. Zavadskas, "Fuzzy multiple criteria decision-making techniques and applications—two decades review from 1994 to 2014," *Expert Systems with Applications*, vol. 42, no. 8, pp. 4126–4148, 2015.

[8] C. Kahraman, S. C. Onar, and B. Oztaysi, "Fuzzy multicriteria decision-making: a literature review," *International Journal of Computational Intelligence Systems*, vol. 8, no. 4, pp. 637–666, 2015.

[9] D. Jato-Espino, E. Castillo-Lopez, J. Rodriguez-Hernandez, and J. C. Canteras-Jordana, "A review of application of multi-criteria decision making methods in construction," *Automation in Construction*, vol. 45, pp. 151–162, 2014.

[10] G. Kabir, R. Sadiq, and S. Tesfamariam, "A review of multi-criteria decision-making methods for infrastructure management," *Structure and Infrastructure Engineering: Maintenance, Management, Life-Cycle Design and Performance*, vol. 10, no. 9, pp. 1176–1210, 2014.

[11] L. F. Gay and S. K. Sinha, "Resilience of civil infrastructure systems: literature review for improved asset management," *International Journal of Critical Infrastructures*, vol. 9, no. 4, pp. 330–350, 2013.

[12] A. Mardani, A. Jusoh, K. MD Nor, Z. Khalifah, N. Zakwan, and A. Valipour, "Multiple criteria decision-making techniques and their applications—a review of the literature from 2000 to 2014," *Economic Research-Ekonomska Istraživanja*, vol. 28, no. 1, pp. 516–571, 2015.

Hindawi Publishing Corporation
Mathematical Problems in Engineering
Volume 2015, Article ID 281640, 14 pages
http://dx.doi.org/10.1155/2015/281640

Research Article

BIM Application to Select Appropriate Design Alternative with Consideration of LCA and LCCA

Young-su Shin and Kyuman Cho

Department of Architectural Engineering, Chosun University, 309 Pilmun-daero, Dong-gu, Gwangju 501-759, Republic of Korea

Correspondence should be addressed to Kyuman Cho; cho129@chosun.ac.kr

Received 27 March 2015; Accepted 10 June 2015

Academic Editor: Mohamed Marzouk

Advancements in building materials and technology have led to the rapid development of various design solutions. At the same time, life cycle assessment (LCA) and life cycle cost analysis (LCCA) of such solutions have become a great burden to engineers and project managers. To help conduct LCA and LCCA conveniently, this study (i) analyzed the information needed to conduct LCA and LCCA, (ii) evaluated a way to obtain such information in an easy and accurate manner using a building information modeling tool, and (iii) developed an Excel spreadsheet-based framework that allowed for the simultaneous implementation of LCA and LCCA. The framework developed for LCA and LCCA was applied to a real building case to evaluate three possible alternatives for an external skin system. The framework could easily and accurately determine which skin system had good properties in terms of the LCA and LCCA performance. Therefore, these results are expected to assist in decision making based on the perspectives of economic and environmental performances in the early phases of a project, where various alternatives can be created and evaluated.

1. Introduction

During the planning, design, and construction of a building, cost management has traditionally been recognized as one of the most important decision-making factors for project participants in the construction industry. Cost planning in the planning and design phase of a project and monitoring and controlling in the construction phase of a project are very important management activities that can determine the success of a construction project. Over the last 10 years, consideration of the life cycle cost (LCC) to analyze the economic feasibility has been one of the greatest changes in the field of project cost management [1]. LCC analysis (LCCA) is most effective when it is conducted in the initial phases (i.e., planning and design phases) of a construction project. For this reason, project managers or engineers have analyzed the economic feasibility of various alternatives with a focus on the diverse elements of building, construction methods, and items [2].

In addition to considering the LCC concept, attention has been given to greenhouse gas (GHG) emissions in all industries around the globe. In particular, buildings are believed to have a considerable impact on the environment because they account for more than 39% of the total primary energy consumed and approximately 39% of the GHG emissions that occur in the United States [3]. Consequently, many studies have been conducted to both evaluate and reduce the GHG emissions that occur in the building production cycle. In particular, the methodology of life cycle assessment (LCA) is widely used. LCA is used to evaluate the GHG emissions throughout the entire process, including the material production, transport, assembly, operation, and demolition of a building. Just as with LCCA, LCA is effective when applied to the planning and design phases of a construction project. LCA evaluates GHG emissions based on a comparison of various alternatives as it focuses on the construction production system, including the materials and construction methods required in the early phase to complete the construction of a building [4].

LCA and LCCA have three major points in common: (i) their effects can be maximized if they are conducted in the early phase of a project, (ii) they can be conducted for a production system that includes all the elements of the building and construction methods, and (iii) they provide

an analysis process that facilitates the selection of the optimal alternative by evaluating the economic and environmental performances of the alternatives [2, 4, 5]. On the other hand, it is difficult to apply the two techniques to buildings, compared to other "products," because of the following unique characteristics of construction projects: (i) buildings are large in size, with a wide variety of materials used in construction projects; (ii) there are a larger number of people involved in construction projects, and the demands of the project owner change frequently; and (iii) because each building is unique, the production system is less standardized compared to those for most other manufactured goods [6, 7].

Based on this background, this study was conducted to develop a method for improving the performance of LCA and LCCA utilizing the three-dimensional parametric building information modeling (BIM) approach.

This study was conducted using the following four steps. In step 1, a literature review was conducted to analyze the LCA and LCCA process and analysis methods, while simultaneously examining their limitations and problems. In step 2, the information and data required for LCA and the LCCA were analyzed based on the results from step 1. The analysis led to (i) the information required to conduct both the LCA and LCCA and (ii) additional information that was required to utilize each technique. In step 3, the BIM was adopted as an approach to provide information and data for the LCA and LCCA implementations, which were analyzed in step 2. In addition, a spreadsheet-based framework, which compiled the information outflow from the BIM, was developed to conduct the LCA and LCCA simultaneously. In step 4, a case study, in which the developed framework was applied to a real building project, focused on identifying the applicability of the research output. The case study facilitated an in-depth analysis of the usefulness of the framework that was suggested in the present study.

2. Step 1: State of the Art

2.1. LCA. The LCA concept is generally accepted within the environmental research field. When applied to buildings, LCA encompasses the analysis and assessment of the environmental effects of building materials, components, and assemblies throughout the entire life of the building, including its construction, use, and demolition [8]. Because of the increase in the number of methods for LCA and examples of its use, international organizations such as the International Standard Organization (ISO) have worked on the standardization of LCA, which has resulted in the ISO 14040 series. In particular, ISO 14041 covers the "definition and inventory analysis of LCA" and is recognized as the standard for the LCA technique in many cases. According to ISO 14041, LCA could be applied in the following four steps. (i) The LCA goal and scope are defined to secure the reliability of the analysis results by clarifying the scope of the target product. (ii) A life cycle input-output inventory analysis is conducted to establish the life cycle inventory database (LCI DB), which contains a large volume of process and production data, including the raw material inputs, energy use, main product to coproducts ratio, production rates, and equivalent environmental releases. The unit process datasets form the basis of every LCI DB and the foundation of all LCA applications. A unit process dataset is obtained by quantifying the inputs and outputs in relation to a quantitative reference flow from a specific process. These inputs and outputs are generated from mathematical relationships based on the raw data. Consequently, a "unit process" is defined as the "smallest element considered in the life cycle inventory analysis" in ISO 14040. (iii) An environment impact assessment is performed based on the results of the inventory analysis, and (iv) the evaluated data is interpreted. LCA can be used in a variety of ways to manage an environmental load, compare alternatives, and establish environmental policy [9].

In the construction field, many studies have been conducted to evaluate the environmental performance based on LCA analysis. Hong et al. [3] suggested an integrated model for assessing the cost and CO_2 emissions and calculated the CO_2 emissions based on the strength of ready-mixed concrete. In another study, Hong et al. [10] introduced a green roof system with energy saving measures focusing on elementary schools in Seoul, South Korea, to analyze the cost and CO_2 emissions. Khan et al. [11] developed decision-making methodology that integrated the LCA concept into risk analysis theory for identifying optimal plant design in the project early phase. Lee et al. [12] confirmed that the difference in CO_2 emissions depended on the strength of the concrete according to the period of use. Cole [8] confirmed the difference in CO_2 emissions using different major structural systems of buildings.

2.2. LCCA. LCCA is used to evaluate the economic feasibility based on the calculation of the equivalent values of all the important costs that occur within the life span, with particular focus on buildings or the major components of buildings [13]. An LCCA is conducted using the following four steps. (i) The analysis target is identified, which is the first step toward making a cost-effective decision by creating and evaluating the alternatives that can meet the minimum performance standards. (ii) The basic assumptions are established for the LCCA, including the analysis period and discount rate. In addition, the initial investment cost, operating cost, alteration/replacement cost, and other associated costs are confirmed, and the time of the occurrence of each cost is verified. Because these cost items occur at different points in time, it is important to convert each cost to the value at a single point in time. (iii) The LCC is calculated for each alternative by adding up the costs according to the type for each alternative. (iv) The related indices are calculated to evaluate the economic feasibility (the LCCA), including the net savings, savings-to-investment ratio, and payback period. In addition, a sensitivity analysis can be implemented to complement the LCCA methodology, which will provide reliability to the LCCA results.

Many previous studies have examined LCCA. Early studies on the LCC focused on minimizing the installation cost in the initial phases of building construction and maintenance, along with the replacement cost in the operation phase. Recently, attention has been given to studies on the energy cost in the operation phase, with the goal of evaluating

the environmental performance of various materials and construction methods. For example, Uygunoğlu and Keçebaş [14] analyzed the energy saving performance in relation to the form and thickness of a concrete block and examined the payback period accordingly. Wong et al. [15] conducted an LCCA when green roof systems were used, which aimed at proving economic effects. Zhang and Wang [16] examined the economic performance of thermal power plants using LCCA. Chang et al. [17] used LCCA to analyze the water-conservation and energy saving effects of green roof systems and examined the cost-reduction effects of those systems. Akadiri et al. [18] developed an assessment model based on the use of diverse sustainable materials and suggested cost-reduction effects that could be attributed to the use of sustainable materials. Fu et al. [19] suggested a new algorithm for calculating the carbon emission in order to optimize building plans in terms of sustainability through comparing the five LCA tools.

2.3. Integration of BIM into LCA and LCCA. While BIM definitions vary significantly according to the organization and researcher, the common concept is that the BIM is a program or process for extracting and reusing data by developing a model, which is presented in a multidimensional virtual space, using the data on the life cycle of a construction project [20, 21]. Currently, BIM is used widely in the construction industry because of the following advantages: (i) a graphic user interface, which provides a work environment where the operator can observe the work visually, (ii) convenient modification and addition because object-based modeling can be performed, which leads to excellent design changes and alternative comparisons, and (iii) the production of diverse information with high usability. In other words, one-time modeling allows for the production of various design documents and quick and accurate quantity estimation for various alternatives [22].

Several previous studies on BIM have been conducted, but very few studies have been conducted that describe the integration of BIM into LCA and LCCA. Basbagill et al. [23] developed a combined BIM-LCA method to figure out which materials and superstructure designs could be effective in terms of CO_2 emissions reduction according to BIM prescriptions for replacing materials in different types of structures. Consequently, it is possible to provide a method to help engineers select materials and superstructures appropriately during the early phases of a project. Han et al. [24] suggested an optimization method for building components that integrates genetic algorithms into the BIM approach, along with the LCCA result for each component. In this research, the BIM approach was utilized to calculate the energy consumption as a function of the installation of each component. Ristimäki et al. [25] developed a model for combining LCA and LCCA, in which a single energy system was adopted. This research demonstrated that the developed model was limited to a small part of a building, because of the difficulty in acquiring the data necessary to conduct the two analysis methods simultaneously. Iddon and Firth [26] analyzed CO_2 emissions of a small dwelling house during the planning phase, where they utilized the BIM approach to consider various alternatives to building components, including structure and envelope systems. In the previous research referenced above, BIM has been used mostly to conveniently generate various design alternatives for conducting LCA or LCCA analysis, but there have been few ideas or theories on how BIM could not only be integrated to conduct LCA and LCCA, but also how to conduct them simultaneously.

2.4. Problem Statements. Given the increased focus on the economic and environmental performances of construction projects, most of the elements comprising projects have been considered in evaluations of their performances using LCA and LCCA. Despite this, the previous studies that were conducted had the following limitations. (i) The analyses were limited to a small number of design alternatives, because a large volume of data was needed to implement the LCA and LCCA. (ii) Some recycling of previous data was needed for each implementation of the LCA and LCCA because of the unique characteristics of construction projects. (iii) There has been little research focused on the application of the BIM approach for conducting LCA and LCCA simultaneously, for the purposes of reducing and recycling the information required for the two methods.

Based on this background and the identified problems, this paper proposes a method for efficiently performing LCA and LCCA, while reducing and recycling the information required for the two methods. This paper (i) identifies the information needed to conduct the LCA and LCCA (in step 2), (ii) shows how the information required for the two methods can be obtained conveniently using a BIM approach (in step 3), and (iii) demonstrates how the LCA and LCCA can be computed simultaneously, based on the developed framework, which incorporates the information obtained using the BIM approach (in step 3).

3. Step 2: Identifying Data Required for Conducting LCA and LCCA

As the first stage for developing a method that facilitates the LCA and LCCA implementation, in step 2, the information required for conducting the two methods was identified, along with each phase of the LCA and LCCA (i.e., construction, operation, and disposal) and the target activities of that phase, as listed in Table 1.

3.1. Required Data for LCA and LCCA in Construction Phase. According to the LCA methodology by the ISO, the target activities of the LCA in the construction phase of a building consist of the production, transport, and assembly of materials. According to Hong et al. [3], an examination of previous studies related to LCA showed that the environmental impact factors generated in the construction phase can generally be calculated using (1). As shown in this equation, the quantity of environmental emissions in the construction phase for system A (EQ_A^{Con}) is the sum of the environmental impacts from the releases during production, transport, and assembly:

(1) Environmental emissions in the production process: if system A consists of i materials, the environmental

Table 1: Data required for conducting LCA and LCCA.

Life cycle phase	Target activities for conducting LCA and LCCA	Required information for LCA			Required information for LCC		
		Q	EF	Additions	Q	UC	Additions
Construction	Manufacturing factory	●	●	—	●	●	(i) Unit cost, including labor and equipment costs. It can be found using RS Means data
	Transporting	●	●	(i) Fuel type (ii) Fuel consumptions			
	Assembling site	●	●				
Operation	Maintenance and repair	●	●	(i) Operation period (ii) Repair cycle (iii) Repair rate	●	●	(i) Operation period (ii) Repair cycle (iii) Repair rate
	Replacement	●	●	(i) Replacement cycle	●	●	(i) Replacement cycle
	Operating		●	(i) Energy consumption		●	(i) Energy consumption
Disposal	Disposal	●	●	(i) Fuel type (ii) Fuel consumptions	●	●	(i) Unit cost for disposal

※Q = quantity of materials, EF = emission factor, and UC = unit cost.

impacts generated in the production process can be calculated by multiplying the quantity of each material (Q_a^M) and the emission factor of the environmental release when manufacturing that material (EF_a^M). In general, the emission factor of each material can be referred from the LCI DB of the countries.

(2) Environmental emissions in the transport process: if manufactured materials are transported to the construction site by j number of vehicles, the environmental impacts can be calculated by multiplying the quantity of each vehicle (Q_b^V) by the emission factor of the environmental release of that vehicle (EF_b^V).

(3) Environmental emissions in the assembly process on site: if k number of the equipment is used to assemble the materials at the construction site, the environmental impacts can be calculated by multiplying the quantity of equipment (Q_c^E) by the emission factor of the environmental release of the individual pieces of equipment (EF_b^E).

(4) To determine the emission factors of the transport vehicles and installation equipment, (i) the fuel type (i.e., gasoline, diesel, etc.) for each vehicle and piece of equipment for conducting the work should first be identified, and then (ii) the emission factors, along with the fuel type, can be found by referring to the LCI DB [27].

(5) With consideration of the above environmental impacts in each element, the amount of environmental emissions in the construction phase can be calculated using

$$EQ_A^{Con} = \sum_{a=1}^{i} \left(Q_a^M \times EF_a^M\right) + \sum_{b=1}^{j} \left(Q_b^V \times EF_b^V\right) + \sum_{c=1}^{k} \left(Q_c^E \times EF_c^E\right), \quad (1)$$

where EQ_A^{Con} = the quantity of environmental emissions in the construction phase for system A, Q_a^M = the quantity of material a comprising system A, EF_a^M = the emission factor of the environmental release while manufacturing material a, Q_b^V = the number of vehicles used to transport material b, EF_b^V = the emission factor of the vehicle used for material b, Q_c^E = the pieces of installation equipment, and EF_c^E = the emission factor of the equipment.

Generally, according to Dell'Isola and Kirk [13], the costs of items in the construction phase to conduct the LCCA can be calculated using (2). If system A would consist i of materials, the installation costs of system A (C_A^{Ins}) can be determined by multiplying the quantity of each material in the system by the installation cost of a unit area (i.e., unit cost). The unit cost generally refers to reported data such as from RS Means. Thus, such data includes the labor cost and equipment cost per unit area:

$$C_A^{Ins} = \sum_{a=1}^{i} \left(Q_a^M \times UC_a\right), \quad (2)$$

where C_A^{Ins} = the installation cost of system A, Q_a^M = the quantity of material a comprising system A, and UC_a = the unit cost for installing material a (i.e., \$/m^2).

As described above and listed in Table 1, to conduct the LCA and LCCA in the construction phase, it is necessary to obtain the following information: (i) the quantity of each material in the targeted system and the quantity of each set of equipment for transportation and installation, (ii) the emission factor of each material and piece of equipment, and (iii) additional information such as the fuel type and fuel consumption of equipment, as well as the unit installation cost.

3.2. Required Data for LCA and LCCA in Operation Phase. The target activities of the LCA in the building operation phase consist of maintenance and repair (M&R), replacement, and operation. According to previous studies, the quantity of environmental emissions generated during the operation phase can be calculated as follows [28]:

(1) Environmental impacts for M&R and replacement: these can be calculated in the same manner as

the environmental impacts during the construction phase. Along with the expected occurrence times for the replacement and M&R of the system, environmental impacts can be calculated considering the quantity and emission factors of the material, transport vehicle, and installation equipment.

(2) Environmental impacts during operation: these are calculated by multiplying (i) the annual quantity of energy consumption (Q_a^E) for each type (i.e., heating, air-conditioning, appliance, etc.) needed for the operation of buildings, (ii) the emission factors of environmental release depending on the energy type (EF_a^E), and (iii) the period in operation (n) (refer to (3)):

$$EQ_A^O = \left(Q_a^E \times EF_a^E\right) \times n, \tag{3}$$

where EQ_A^O = the quantity of environmental emissions during the operation phase for system A, Q_a^E = the annual energy consumption of the system, EF_a^E = the emission factor of environmental release depending on the energy type, and n = the period in operation.

The LCCA during the operation phase includes the M&R and energy costs, which can be calculated using (4) and (5), respectively:

(1) Maintenance, repair and replacement costs (C_A^{MR}): along with the expected occurrence times of the M&R and the replacement of the system, the costs are calculated by multiplying (i) the quantity of each item (Q_d^{MR}) in system A that requires maintenance, repair, and replacement by (ii) the unit cost (UC_d^{MR}) for such target activities. Moreover, because M&R and replacement costs will be incurred in the future, the equivalent present worth of the costs discounted at the interest rate (DR) for the M&R and replacement time (T_d) should be considered (please refer to [13] for the details):

$$C_A^{MR} = \sum_{d=1}^{l} \left(Q_d^{MR} \times UC_d^{MR} \times \frac{1}{(1+DR)^{T_d}} \right), \tag{4}$$

where C_A^{MR} = the present worth of total M&R and replacement costs of system A, Q_d^{MR} = the quantity of each item comprising the system that requires M&R and replacement, UC_d^{MR} = the unit cost for M&R and replacement, DR = the discount rate, and T_d = the M&R and replacement time of each item.

(2) The operation energy cost (C_A^E) is the product of the quantity of annual energy consumption (Q_a^E) and the unit cost of the energy source (UC^E). Moreover, because the cost is a future cost that occurs annually, the discount rate (DR) for the operation period (n) is considered to convert the cost to an equivalent present value in total (please refer to [13] for the details):

$$C_A^E = \left(Q_a^E \times UC^E\right) \times \frac{(1+DR)^n - 1}{DR\,(1+DR)^n}, \tag{5}$$

where C_A^E = the present worth of total energy cost of system A during n years, Q_a^E = the annual energy consumption of the system, UC^E = the unit cost of the energy source, and n = the period in operation.

As described above and listed in Table 1, to conduct the LCA and LCCA during the operation phase, it is essential to obtain (i) the quantity information, (ii) information on the emission factor, and (iii) additional information such as information on the M&R and replacement (i.e., operation period, repair cycle, repair rate, replacement rate, etc.) and information on the energy (i.e., energy consumption and energy cost).

3.3. Required Data for LCA and LCCA in Disposal Phase. During the disposal phase of the building, the LCA and LCCA can be conducted based on (6) and (7), respectively [28]. The quantity of environmental emissions during the disposal (EQ_A^D) can be calculated considering the quantity of the disposal equipment (Q_e^{ED}) and the emission factor according to the energy type of the individual pieces of equipment (EF_e^{ED}) (refer to (6)). Therefore,

$$EQ_A^D = \sum_{e=1}^{m} \left(Q_e^{ED} \times EF_e^{ED}\right). \tag{6}$$

The disposal cost (C_A^D) can be calculated by multiplying the disposal quantity (Q_A^D) by the unit cost (UC_A^D) for the disposal work. Similar to the M&R cost, the disposal cost needs to be converted to an equivalent present cost discounted at a certain interest rate (DR) for the time of the disposal (T_d), because the cost will be incurred in the future (refer to (7)). Therefore,

$$C_A^D = Q_A^D \times UC_A^D \times \frac{1}{(1+DR)^{T_d}}. \tag{7}$$

As described above and listed in Table 1, the following are needed to conduct the LCA and LCCA during the disposal phase: (i) the quantity information, (ii) information on the emission factor, and (iii) additional information such as the fuel type and consumption of the equipment and unit cost for disposal.

3.4. Required Data for LCA and LCCA. As analyzed in this step, a large amount of information is needed to conduct the LCA and LCCA, which makes project managers hesitant to apply these techniques. In addition, even if they are used, it is difficult to apply them to a range of alternatives. Therefore, this study developed a method to overcome the problems associated with conducting LCA and LCCA based on "easiness of data acquisition" and "data recycling." This

section identifies the data required for LCA and LCCA, along with the project phase, and then classifies the data into two categories: (i) the data commonly required and (ii) additional data, as listed in Table 1.

4. Step 3: Framework for Conducting LCA and LCCA

In step 3, a framework for the LCA and LCCA was developed using the following process: (i) mapping between the required LCA and LCCA data analyzed in step 2 and the acquirable data from BIM and (ii) embodying the calculation methods (Equations (1) to (7)) and all the data needed for LCA and LCCA into an Excel spreadsheet-based framework.

4.1. Mapping Required Data for LCA and LCCA with BIM Data. Despite some differences between the different types of BIM software, the application of BIM generally facilitates the acquisition of the following data: (i) visual model data expressed in a three-dimensional space, (ii) information on a quantity estimation, (iii) information on the necessary energy consumption to operate a building through an energy simulation, and (iv) information on construction interference among work activities [29].

As listed in Table 1, it is important to obtain diverse information to conduct the LCA and LCCA. Therefore, mapping can be performed as follows between the data that can be obtained from the BIM and the information that is required to conduct the LCA and LCCA:

(i) Quantity information about the material resources for each alternative: as listed in Table 1, the basic data to conduct the LCA and LCCA are information on the quantity of the input resource for each life cycle of the building. Among such diverse quantity information, information about the quantity of materials used to form the relevant building is fundamental to conducting the LCA and LCCA. This is because information about the quantity of materials has the greatest influence on making a decision based on the results of the LCA and LCCA in the construction and operation phases. Such information about the quantity of materials can be readily obtained from BIM. Furthermore, information about the quantities of materials for various alternatives can be obtained in a convenient and accurate way in the feasibility phase of a project, in which the level of change in the design plan can be significant.

(ii) Energy consumption: considering the recent trend of using many energy saving techniques, energy consumption is the most important factor among the factors that affect the results of the LCA and LCCA in the operation phase of a building. If the BIM is used in the operation phase, it is possible to obtain information on the energy consumption in a case where various energy saving techniques are applied. In addition to a building information model of a particular building, information on the following building conditions is required for analyzing the building's energy consumption: its location, azimuthal angle, climate condition, mechanical systems, and thermal conductivity performance. Once these conditions have been established, the BIM software can calculate the energy consumption of the building, expressed by parameters such as the monthly energy balance.

In the delivery process for an environmentally friendly building, the following aspects have recently become important great issues: (i) information about the quantity of materials and data on the energy consumption are the most fundamental for conducting the LCA and LCCA for various design alternatives, depending on the application of energy saving techniques; and (ii) the convenient acquisition of such core data from the BIM can be a great benefit when the LCA and LCCA are implemented in the delivery process for an environmentally friendly building.

In the meantime, the remaining data listed in Table 1 (i.e., the LCI DB, machinery data, operation period, etc.) can be obtained based on the existing methodologies for the LCA and LCCA.

4.2. Framework for Conducting LCA and LCCA Using BIM. Because the data obtained from BIM are readily compatible with an Excel spreadsheet, the framework was established using the spreadsheet program, in which the LCA and LCCA implementation methods are automatically connected to each other. As shown in Figures 1 through 4, the framework consists of four sheets in total, including three sheets for conducting the LCA and LCCA in the construction phase, operation phase, and disposal phase and one sheet for summarizing the results from these three sheets. Meanwhile, the data on each sheet can be entered manually after it has been extracted automatically using BIM.

4.2.1. Worksheet for Construction Phase. As shown in Figure 1, cell lines 1 to 6 on the sheet represent the quantity information that is commonly required to conduct the LCA and LCCA for the system, which was extracted automatically using the BIM. In other words, cell lines 1 and 2 show the material information for each system, whereas cell lines 3 to 6 present the quantity information for each material, including the weight (i.e., cell line 3) and the equivalent volume (i.e., cell line 4), area (i.e., cell line 5), and length values (i.e., cell line 6) corresponding to this weight.

Cell lines 7 to 25 are used for inputting the information that is needed to conduct the LCA for the equipment that is used in manufacturing (cell lines 10 to 17), transport, and construction (cell lines 22 to 25). In addition, (i) the fuel type of the input equipment and vehicles for material manufacture, transport, and construction (i.e., electricity, diesel, and gasoline) and (ii) the capacity of the equipment and vehicles (i.e., kg/EA, m^3/EA, m^2/EA, and m/EA) make it possible to calculate the required amount of fuel for the equipment and vehicles for the manufacture, transport, and construction (i.e., cell lines 18 and 26). Subsequently, the emission factors

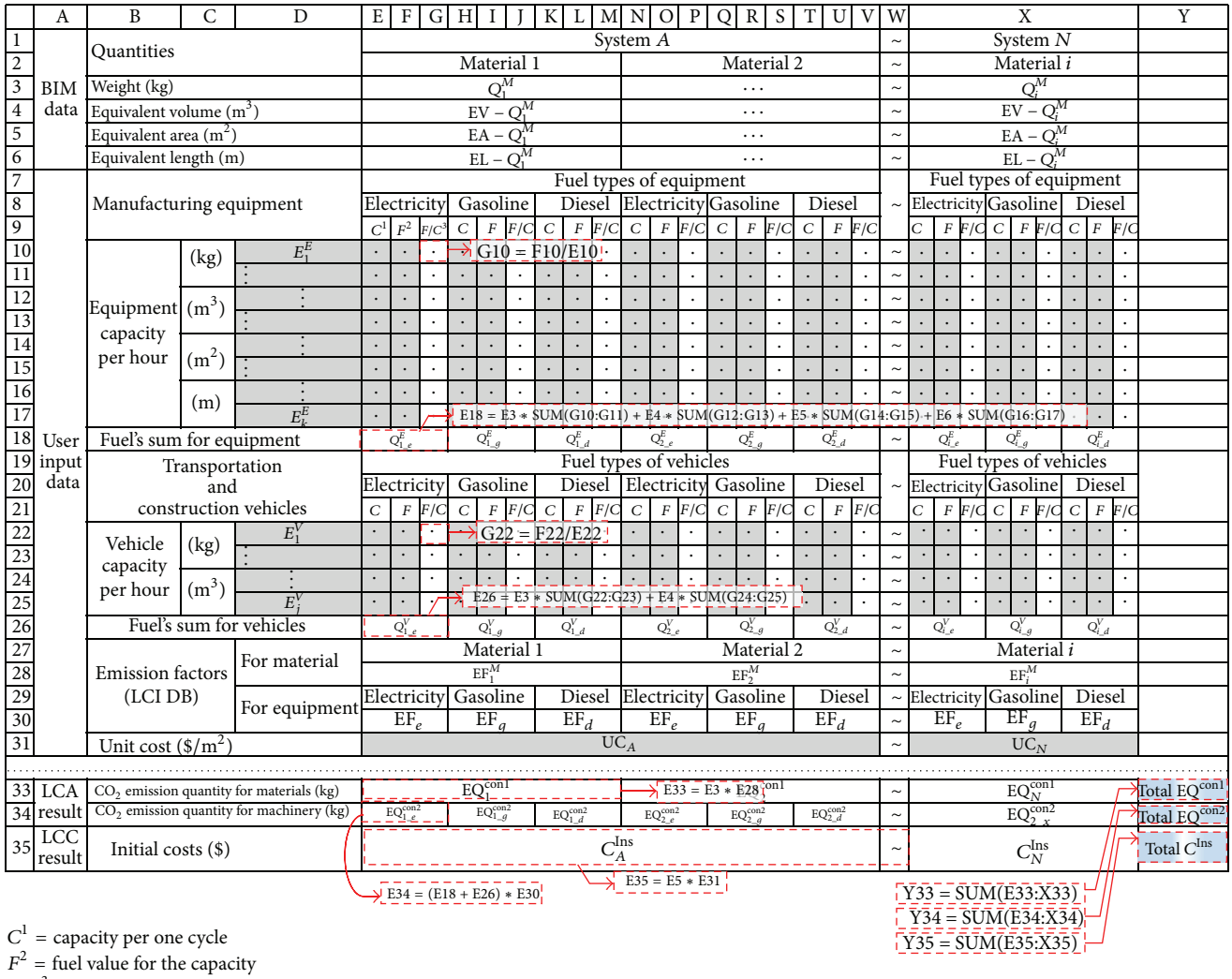

C^1 = capacity per one cycle
F^2 = fuel value for the capacity
F/C^3 = resource per unit capacity

Figure 1: Worksheet for LCA and LCC analysis in construction phase.

according to the type of material and equipment from the LCI DB (cell lines 27 to 30) are used to calculate the CO_2 emission quantity for materials and machinery (cell lines 33 and 34). To calculate the construction costs comprising the LCC, it is necessary to input the unit cost (cell line 31) of each system, which can be provided by RS Means, and so forth.

4.2.2. Worksheets for Operation and Disposal Phases. As shown in Figure 2 and (3) to (5), the material quantities and energy requirements per year, which can be extracted by the BIM program, are used to conduct the LCA and LCCA in the operation phase. Based on this information and program, if a user enters (i) the electricity price (i.e., cell (D7) in Figure 2), (ii) unit cost (i.e., adopted from the sheet "construction phases," cell (E31) in Figure 1), and (iii) operation information per system (i.e., cells (D9) to (D15) in Figure 2), they can automatically obtain the LCA and LCCA results in the operation phase.

The LCA and LCCA in the disposal phase are performed in a manner similar to that in the construction phase. They are also conducted based on the input values for the equipment used to demolish buildings (refer to Figure 3).

4.2.3. Worksheet for Summary. This sheet includes the results corresponding to "Total ~" on sheets 1 to 3 above (i.e., line 33, line 34, and line 35 of column Y on sheet 1; line 19, line 20, and line 21 of column L on sheet 2; and line 16 and line 17 of column Y on sheet 3) (refer to Figure 4).

5. Step 4: Case Application

A case application was conducted to verify the usability of the developed framework and the methodologies for conducting the LCA and LCCA. The following presents an overview of the building project selected for the application:

(i) Location: 868-4 Hak-dong, Dong-gu, Gwangju, Republic of Korea.

(ii) Structural system: steel-reinforced concrete structure.

	A	B	C	D	E	F	G	H	I	J	K	L
1	BIM data	Quantities		System A						~	System N	
2				Material 1			Material 2			~	Material i	
3		Equivalent area (m^2)		EA – Q_1^M			…			~	EA – Q_i^M	
4		Energy simulation	Source	Electricity								
5			Energy type	Heating	Hot-water supply	Air-conditioning	Ventilation fan	Appliance				
6			Energy requirement (MWh/yr)	ER_H	ER_{HW}	ER_{AC}	ER_V	ER_A				
7	User input data	Electricity price ($/MWh)		UC^E								
8		Unit cost[1] ($/$m^3$)		UC_A						~	UC_N	
9		Operate information	Replacement term (yr)	…						~	…	
10			Maintenance term (yr)	…						~	…	
11			Maintenance rate (%)	…						~	…	
12			Study period (yr)	…						~	…	
13			Number of replacement times	…						~	D16 = D3 * D8	
14			Number of maintenance times	…						~		
15			Discount rate (%)	…						~	D17 = (D3 * D8) * D11	
16		Replacement cost ($)		UC_A^{MR1}						~	UC_N^{MR1}	
17		Maintenance cost ($)		UC_A^{MR2}						~	UC_N^{MR2}	
19	LCA result	CO_2 emission quantity during operation phase (kg/yr)		EQ_H^E	EQ_{HW}^E	EQ_{AC}^E	EQ_V^E	EQ_A^E			L19 = SUM(D19:H19)	Total EQ^E
20	LCC result	Energy costs ($)		C^E							L20 = D20	Total C^E
21		R&M costs ($)		C_A^{MR}						~	L21 = SUM(D21:K21)	Total C^{MR}

Unit cost[1] = adopter from the sheet for "construction phase"

D21 = D16/(1 + D15)^(D9 * D13) + D17/(1 + D15)^(D10 * D14) + …

D20 = (SUM(D6:H6) * D7) * ((1 + D15)^D12 – 1)/(D15 * (1 + D15)^D12)

Figure 2: Worksheet for LCA and LCC analysis during operation phase.

	A	B	C	D	E	F	G	H	I	J	K	L	M	N	O	P	Q	R	S	T	U	V	W	X	Y
1	BIM data	Quantities			System A																		~	System N	
2					Material 1									Material 2									~	Material i	
3		Weight (kg)			Q_1^M									…									~	Q_i^M	
4		Equivalent volume (m^3)			EV – Q_1^M									…									~	EV – Q_i^M	
5	User input data	Disposal cost ($/kg)			UC_A^D																		~	UC_N^D	
6		Operate information	Study period (yr)		…																		~	…	
7			Discount rate (%)		…																		~	…	
8		Disposal equipment			Fuel types of equipment																			Fuel types of equipment	
9					Electricity			Gasoline			Diesel			Electricity			Gasoline			Diesel			~	Electricity	Gasoline	Diesel
10					C^1	F^2	F/C^3	C	F	F/C	C	F	F/C	C	F	F/C	C	F	F/C	C	F	F/C		C F F/C	C F F/C	C F F/C
11		Equipment capacity per hour	(m^3)	E_m^{ED}	·	·	·	G11 = F11/E11						·	·	·	·	·	·	·	·	·	~	· · ·	· · ·	· · ·
12		Fuel's sum for equipment			$Q_{1\_e}^{ED}$			$Q_{1\_g}^{ED}$			$Q_{1\_d}^{ED}$			$Q_{2\_e}^{ED}$			$Q_{2\_g}^{ED}$			$Q_{2\_d}^{ED}$			~	$Q_{i\_e}^{ED}$	$Q_{i\_g}^{ED}$	$Q_{i\_d}^{ED}$
13		Emission factors (LCI DB)	For equipment		Electricity			Gasoline			Diesel			Electricity			Gasoline			Diesel			~	Electricity	Gasoline	Diesel
14					EF_e			EF_g			EF_d			EF_e			EF_g			EF_d			~	EF_e	EF_g	EF_d
16	LCA result	CO_2 emission quantity for machinery (kg)			$EQ_{1\_e}^{ED}$			$EQ_{1\_g}^{ED}$			$EQ_{1\_d}^{ED}$			$EQ_{2\_e}^{ED}$			$EQ_{2\_g}^{ED}$			$EQ_{2\_d}^{ED}$			~	$EQ_{i\_x}^{ED}$		Total EQ^{ED}
17	LCC result	Disposal costs ($)			C_A^D																		~	C_N^D		Total C^D

E16 = E12 * E14

E17 = (E3 * E5)/(1 + E7)^E6

Y16 = SUM(E16:X16)

Y17 = SUM(E17:X17)

C^1 = capacity per one cycle
F^2 = fuel value for the capacity
F/C^3 = resource per unit capacity

Figure 3: Worksheet for LCA and LCC analysis in disposal phase.

	A	B	C
1	Assessment / Phase	$LCCO_2$	LCC
2	Construction	Total EQ^{con1} → B2 = "construction phase"!Y33	Total C^{Ins} → C2 = "construction phase"!Y35
3		Total EQ^{con2} → B3 = "construction phase"!Y34	
4	Operation	Total EQ^{E} → B4 = "operation phase"!L19	Total C^{MR} → C4 = "operation phase"!L20
5			Total C^{E} → C5 = "operation phase"!L21
6	Disposal	Total EQ^{ED} → B6 = "disposal phase"!Y16	Total C^{D} → C6 = "disposal phase"!Y17
7	SUM	Total emission quantity → B7 = SUM(B2:B6)	Total costs → C7 = SUM(C2:C6)

Figure 4: Summary worksheet for LCA and LCC analysis.

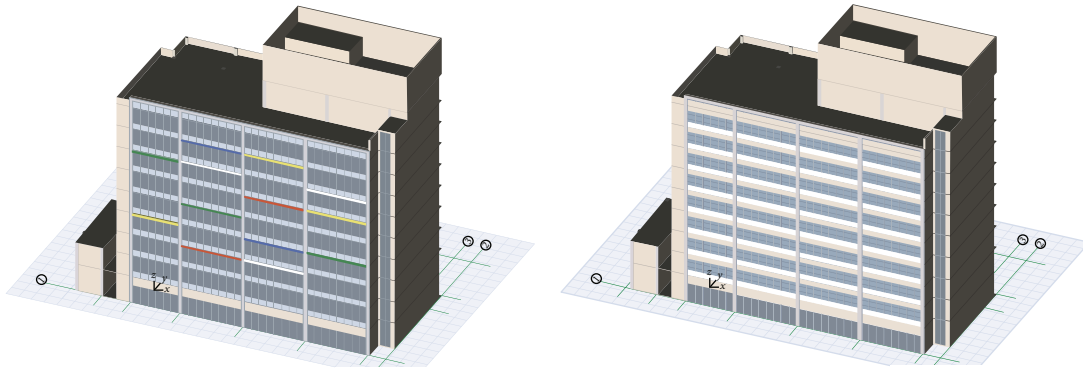

Original model and alternative model 2

(a)

Alternative model 1

(b)

Figure 5: Results of BIM for each alternative.

(iii) Type: office building.

(iv) Stories and floor area: 11 stories (one story below ground and 10 stories above ground), a building area of 881.68 m^2, and a gross floor area of 7,105.94 m^2.

Because it is important to obtain a large volume of data to conduct the LCA and LCCA for the entire building, the application of the developed framework was designed to focus only on the external skin of a building. In addition, the LCA and LCCA were conducted with particular focus on the construction and operation phases. Because the external skin of a building plays an important role in achieving energy efficiency, it has a remarkable effect on the results of the LCA and LCCA. Consequently, among the various alternatives for the skin of a building, it is possible to select the most valuable skin system based on the LCA and LCCA results, if the developed framework is used. In this study, the authors considered three alternatives for the external skin system, including the original external skin system. The following descriptions give an overview of each alternative:

(i) Original skin system: 22 mm double-glazed curtain wall (5 mm glass + 12 mm air layer + 5 mm glass) with a thermal transmittance of 2.79 W/m^3 K.

(ii) Alternative 1: cement brick wall with double-glazed windows (5 mm glass + 6-mm air layer + 5 mm glass) with a thermal transmittance of 3.25 W/m^3 K.

(iii) Alternative 2: 24 mm low-E glass curtain wall (6 mm glass + 12 mm argon layer + 6 mm low-E glass) with a thermal transmittance of 1.80 W/m^3 K.

5.1. Modeling and Data Acquisition. The modeling of the building was performed using the "ArchiCAD version 15" software in the following order: (i) creation of site, (ii) creation of structural columns, (iii) creation of bearing wall, and (iv) creation of the slab. After one story was completed, copy and paste commands, along with the grid system function, were used to complete the modeling of the floors (up to the 10th floor). Next, the modeling of the external skin system for each alternative was performed before entering the attribute information. The time required was approximately 12 h.

Figure 5 presents the completed 3D building information model. As mentioned, the modeling of the internal space was excluded from this case study because the purpose of the case application was to conduct the LCA and LCCA for each alternative external skin system. According to several previous studies, the skin system of a building critically affects its thermal conductivity performance. Consequently, the skin system could be regarded as one of the most important

Table 2: Quantity and energy data obtained by BIM.

Type of data from BIM			Properties of each alternative		
			Original skin	Alt. 1	Alt. 2
Quantity data	Aluminum frame	Volume (m^3)	20.96	18.53	20.96
		Weight (kg)	56,815	50,213	56,815
	Glass	Volume (m^3)	10.64	19.38	12.77
		Weight (kg)	25,321	46,123	30,385
	Cement brick	Volume (m^3)	—	68.16	—
		Weight (kg)	—	20,264	—
	Mortar	Volume (m^3)	—	6.41	—
		Weight (kg)	—	16,020	—
	Polystyrene	Volume (m^3)	—	14.2	—
		Weight (kg)	—	426	—
	Concrete	Volume (m^3)	—	31.24	—
		Weight (kg)	—	74,976	—
	Argon	Volume (m^3)	—	—	12.77
		Weight (kg)	—	—	17.62
Energy amount (MWh/yr)	Heating		311	323	308
	Hot-water supply		291	291	291
	Air-conditioning		2,653	2,737	2,487
	Ventilation fan		130	130	130
	Appliance		1,770	1,770	1,770
	Total consumption		5,155	5,251	4,986

factors affecting the energy consumption of a building. Therefore, this research was structured to conduct energy simulations based on numerous alternatives for building skin systems, while the other simulation conditions were fixed. As described in step 3, the additional information necessary for calculating the energy consumption during the operation phase was set as follows: (i) location (35°9′ in latitude and 125°54′ in longitude), (ii) bearing angle (340°), (iii) type of use (office building), (iv) climate data: KOR Kwangju_471560_IWEC [30], and (v) type of air-conditioning and heating system (central system).

Once the modeling was complete, (i) the element function of ArchiCAD was used to retrieve the quantity information for each alternative external skin, and (ii) EcoDesigner, which is an add-on function of ArchiCAD, was used to calculate the energy consumption for each alternative, all of which are listed in Table 2. According to the calculations, alternative 2, in which low-E glass was used, showed the lowest total energy consumption (4,986 MWh/yr).

5.2. Input Data for LCA and LCCA. To conduct the LCA and the LCCA for the three target alternatives, it was important to provide the information needed by the three worksheets (i.e., Figures 1, 2, and 3). For example, Figure 6 shows the input data and results for the worksheet in the construction phase when the original skin system (i.e., normal curtain wall) was used.

As shown in the figure, the information obtained from the BIM provided quantity information on aluminum and glass (i.e., cell (E3) to cell (E6) and cell (N3) to cell (N6) in Figure 6), which are the main materials comprising the original skin system. Second, because (i) three sets of equipment (i.e., aluminum cutter, notching clipper, and painter) were used for manufacturing the aluminum, (ii) they were operated by electricity, and (iii) they manufactured raw aluminum in "length" units; the equipment capacity and fuel requirement were entered into cells (E14) to (E16) and cells (F14) to (F16), respectively. Similarly, the capacity and fuel requirement of the equipment for glass manufacturing were entered, as shown in Figure 6 (i.e., cells (N10) to (N13) and cells (O10) to (O13)). In addition, the capacity and fuel requirement of the vehicles used for construction (i.e., a forklift, tower crane, and loader) were entered into lines 21 to 23, according to their fuel types. Finally, the unit cost of \$179.737/m^2 for the curtain wall installation work was entered based on the "Korean Price Information for Construction Work," which is similar to the cost data provided by RS Means in the USA [31].

To calculate the LCA and LCCA during the operation phase, (i) the analysis period used when simultaneously conducting the LCA and LCCA was determined to be 40 years, which was the life span of the reinforced concrete building as stipulated by legislation, and (ii) the discount rate for the LCCA was calculated based on the inflation rate and deposit interest rates over the past 10 years, which were provided by the Bank of Korea.

6. Results and Discussion

6.1. LCA and LCCA Results. Table 3 lists and Figure 7 shows the LCA results. As listed in Table 3, when a building is operated for 40 years, among the three alternatives, alternative 2 has the lowest CO_2 emission (low-E curtain wall system: 26,389,800 kg). The CO_2 emission of alternative 2 (i.e., 944,786 kg) is the highest among the three alternatives in

Table 3: LCA and LCCA results for each alternative.

Building skin system				Original skin	Alt. 1	Alt. 2
LCA results (kg)	CO_2 emission in construction phase	Manufacturing	Aluminum frame	839,987	750,011	839,987
			Glass	100,432	39,121	104,346
			Cement brick	—	21,391	—
			Mortar		16,873	
			Polystyrene		826	
			Concrete	—	13,231	—
			Argon	—	—	453
		Construction		940,419	841,453	944,786
	CO_2 emission in operation phase	Energy consumption	One year (kg/yr)	668,310	675,572	659,745
			40 years (kg)	26,732,400	27,022,880	26,389,800
	CO_2 emission in disposal phase	Disposal (kg)		21	104	22
	Total amount of CO_2 emission			**27,672,400 (kg)**	**27,864,438 (kg)**	**26,389,800 (kg)**
LCCA results (US $)	Construction phase	Initial investment costs		191,220	196,924	223,988
	Operation phase	Replacement and maintenance costs		136,765	132,938	160,201
		Energy costs		8,204,352	8,359,094	7,935,464
	Disposal phase	Disposal costs		9,565	14,507	10,154
	Total amount costs			**$8,541,902**	**$8,703,462**	**$8,329,808**

	A	B	C	D	E	F	G	H	I	J	K	L	M	N	O	P	Q	R	S	T	U	V	W
1	BIM data	Quantities			Normal curtail wall installation																		
2					Aluminum									Glass									
3		Weight (kg)			56,814.68									25,320.98									
4		Equivalent volume (m^3)			20.96									10.64									
5		Equivalent area (m^2)			(N/A)									1063.89									
6		Equivalent length (m)			2795.31									(N/A)									
7	User input data	Manufacturing equipment			Fuel types of equipment																		
8					Electricity			Gasoline			Diesel			Electricity			Gasoline			Diesel			
9					C^1	F^2	F/C^3	C	F	F/C	C	F	F/C	C	F	F/C	C	F	F/C	C	F	F/C	
10		Equipment capacity per hour	(kg)	Glass reinforcer										5000	90	0.018							
11				Glass multilayer										5000	94.5	0.0189							
12			(m^2)	Glass cutter										3	18	6							
13				Spattering equipment										0.4	60	150							
14			(m)	Aluminum cutter	2.5	16.5	6.6																
15				Nothing clipper	1.25	8	6.4																
16				Painter	0.4	0.3	0.75																
17		Fuel's sum for equipment			38,435.513			0			0			166,901.148			0			0			
18		Transportation and construction vehicles			Fuel types of vehicles																		
19					Electricity			Gasoline			Diesel			Electricity			Gasoline			Diesel			
20					C	F	F/C	C	F	F/C	C	F	F/C	C	F	F/C	C	F	F/C	C	F	F/C	
21		Vehicle capacity per hour	(kg)	Fork-lift							2000	4	0.002							2000	4	0.002	
22				Tower crane	12000	94.5	0.0079							12000	94.5	0.0079							
23			(m^3)	Loader							2.45	14.9	6.082							2.45	14.9	6.082	
24		Fuel's sum for vehicles			447.416			0			241.1			199.403			0			115.351			
25		Emission factors (LCI DB)		For material	Aluminum									Glass									
26					14.451									0.75083									
27				For equipment	Electricity			Gasoline			Diesel			Electricity			Gasoline			Diesel			
28					0.487218			0.06225			0.05644			0.487218			0.06225			0.05644			
29		Unit cost ($/$m^2$)			179.737																		
31	LCA result	CO_2 emission quantity for materials (kg)			821,028.941									19,011.751									840,041
32		CO_2 emission quantity for machinery (kg)			18,944.462			0			13.608			81,414.414			0			6.51			100,379
33	LCC result	Initial costs ($)			191,220.397																		191,220

C^1 = capacity per one cycle
F^2 = fuel value for the capacity
F/C^3 = resource per unit capacity

Figure 6: Example of application of worksheet for construction phase.

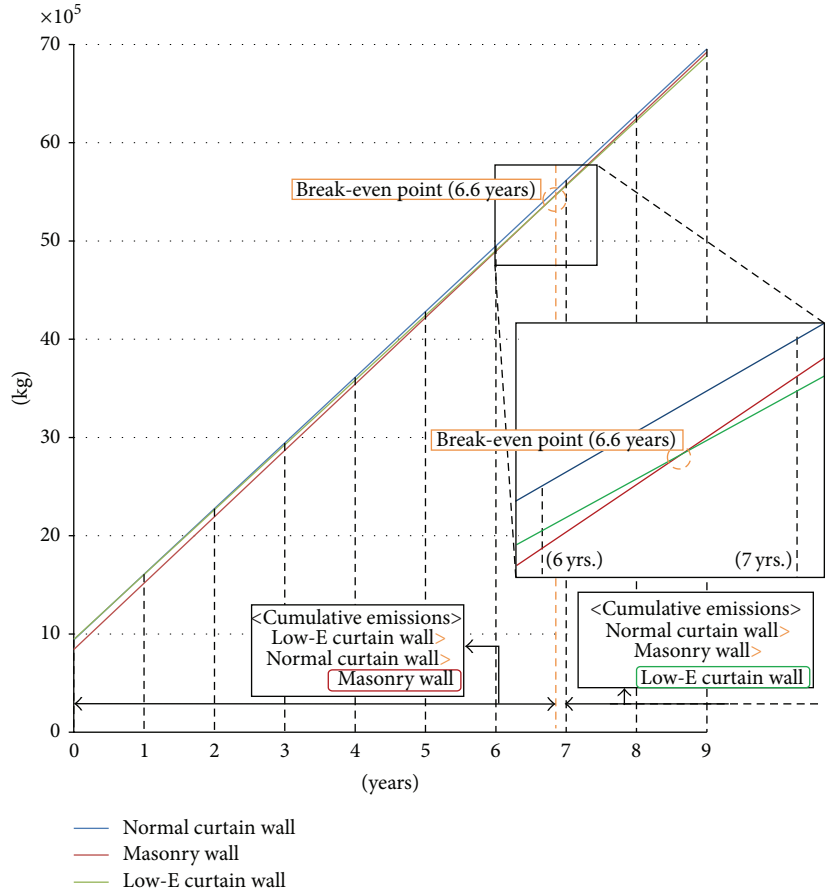

Figure 7: Results for accumulating LCA amount over years.

the construction phase but the lowest (659,745 kg/yr) in the operation phase. Therefore, alternative 2 was found to have the lowest total amount of CO_2 emissions. Figure 7 shows the cumulative CO_2 emissions over the operation time.

This alternative (low-E curtain wall system) can be considered to be the most environmentally friendly alternative after 8 years.

In addition, Table 3 lists and Figure 8 shows the LCCA results. As listed in Table 3, when the building is operated for 40 years, among the three alternatives, alternative 2 is the most economical (low-E curtain wall system: \$8,329,808). The initial investment cost of alternative 2 is the highest (\$223,988) among the three alternatives, whereas the energy cost of alternative 2 is the lowest (\$7,935,464). Therefore, alternative 2 was found to be the most economical in terms of the total amount cost. As shown in Figure 8, which depicts the cumulative LCC over the operation time, alternative 2 can be considered to be the most advantageous alternative in terms of the cost at the time point of 3.4 years because the energy cost is the lowest.

6.2. Advantages and Disadvantages of Applying BIM Technique to Conduct LCA and LCCA. Given the recent trends in the construction industry, which place emphasis on the economic and environmental performance, LCCA and LCA have been widely used. However, their implementation has been a great burden to engineers and project managers. The application of the results of this study will be useful in resolving such problems. In the case application results, it took approximately 12 hours to perform the BIM for the three alternatives for the external skin system, and the model provided information on the material quantities required and energy consumed, which are key items of information for conducting LCA and LCCA. The methodology suggested in this paper can be used to obtain LCA and LCCA results in an efficient manner.

The BIM made it possible to obtain the results of the quantity calculation immediately, and it is compatible with other software because commercial BIM programs can provide their results as Excel spreadsheet. Because various design documents are used to conduct the existing two-dimension-based quantity calculations, a large amount of time is required, and errors occasionally result. On the other hand, because the BIM can provide relevant information immediately, it is possible to save time in the early phase of the construction project and obtain more accurate quantity information. In addition, it is important to analyze the energy consumption that is required in the operation phase, wherein the LCA and the LCCA are conducted, which requires considerable time and effort. The energy evaluation function of

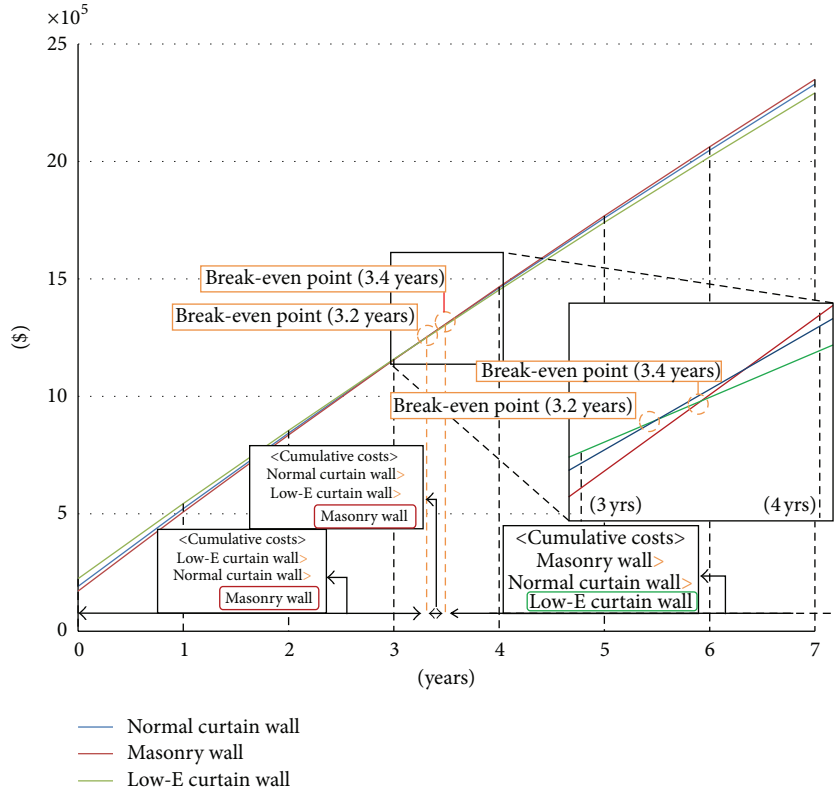

Figure 8: Results for accumulating LCC amount over years.

the BIM facilitates calculations of the energy consumption considering the environmental effects.

It is necessary to calculate the fuel consumption for a diverse range of machineries when the LCA is conducted. On the other hand, it is still a burden for engineers to analyze such requirements, because no information on the machinery can be gathered from the BIM results. The information related to machinery can be supported by COBIE spreadsheets [32]. In addition, for a quantity surveying task, it is common to use a margin to make the results of the task more adjustable, whereas there is no margin for the quantity calculation results provided by BIM. Therefore, it is important to add such a function to the BIM tool to make it possible to conduct the LCA and LCCA in a more accurate way. Finally, it is necessary to have macro or library functions as add-ons that allow for LCA and LCCA for the BIM in the future. In other words, if the macro or library functions, which can create the required data automatically, were added to the developed framework, it would be possible to conveniently gather the diverse data necessary for implementing the framework.

7. Conclusions

This study evaluated the usability of BIM to conduct LCA and LCCA in the early phase of a construction project. To accomplish this, (i) the methodology and information needed to conduct the LCA and LCCA were analyzed, (ii) mapping between the required information and the information that could be obtained using the BIM was conducted, and (iii) an Excel worksheet-based framework was developed. To identify the usability of the BIM to conduct the LCA and LCCA, a case application was conducted that analyzed three external skin systems for an actual building. Based on the possible diverse alternatives that were considered as a result of the characteristics of the early project phase, the BIM and developed framework could suggest alternatives with better performance in terms of the economic and environmental aspects. Therefore, if the framework developed in this study is applied, it is expected to be suitable for making important decisions in the early phases of a project.

BIM was applied to the framework developed in this study to obtain the quantity information and energy consumption of a project. Consequently, it was insufficient to verify the accuracy of the acquired information. Because the accuracy depended on the performance of the BIM software, this study did not conduct such verification. Rather, a test of the usability of the BIM and framework was performed. In the future, it will be necessary to develop a BIM library to help engineers and project managers gather the required information, including the LCI DB, to conduct the LCA and LCCA.

Conflict of Interests

The authors declare that there is no conflict of interests regarding the publication of this paper.

Acknowledgment

This study was supported by the Basic Science Research Program funded by the Ministry of Education, Science, and Technology (nos. 2014044260 and NRF-2014R1A1A1004766).

References

[1] E. P. Karan and J. Irizarry, "Extending BIM interoperability to preconstruction operations using geospatial analyses and semantic web services," *Automation in Construction*, vol. 53, pp. 1–12, 2015.

[2] W. Li, J. Zhu, and Z. Zhu, "The energy-saving benefit evaluation methods of the grid construction project based on life cycle cost theory," *Energy Procedia*, vol. 17, pp. 227–232, 2012.

[3] T. Hong, C. Ji, and H. Park, "Integrated model for assessing the cost and CO_2 emission (IMACC) for sustainable structural design in ready-mix concrete," *Journal of Environmental Management*, vol. 103, pp. 1–8, 2012.

[4] G. Zheng, Y. Jing, H. Huang, X. Zhang, and Y. Gao, "Application of life cycle assessment (LCA) and extenics theory for building energy conservation assessment," *Energy*, vol. 34, no. 11, pp. 1870–1879, 2009.

[5] Y. Huang, R. Bird, and O. Heidrich, "Development of a life cycle assessment tool for construction and maintenance of asphalt pavements," *Journal of Cleaner Production*, vol. 17, no. 2, pp. 283–296, 2009.

[6] C. Scheuer, G. A. Keoleian, and P. Reppe, "Life cycle energy and environmental performance of a new university building: modeling challenges and design implications," *Energy and Buildings*, vol. 35, no. 10, pp. 1049–1064, 2003.

[7] I. Z. Bribián, A. A. Usón, and S. Scarpellini, "Life cycle assessment in buildings: state-of-the-art and simplified LCA methodology as a complement for building certification," *Building and Environment*, vol. 44, no. 12, pp. 2510–2520, 2009.

[8] R. J. Cole, "Energy and greenhouse gas emissions associated with the construction of alternative structural systems," *Building and Environment*, vol. 34, no. 3, pp. 335–348, 1998.

[9] ISO, *ISO 14040, Life Cycle Assessment (LCA)—Principles and Guidelines*, Part 1.3, 97, International Organization for Standardization, 2008.

[10] T. Hong, J. Kim, and C. Koo, "LCC and $LCCO_2$ analysis of green roofs in elementary schools with energy saving measures," *Energy and Buildings*, vol. 45, pp. 229–239, 2012.

[11] F. I. Khan, R. Sadiq, and T. Husain, "GreenPro-I: a risk-based life cycle assessment and decision-making methodology for process plant design," *Environmental Modelling and Software*, vol. 17, no. 8, pp. 669–692, 2002.

[12] S. Lee, W. Park, and H. Lee, "Life cycle CO_2 assessment method for concrete using CO_2 balance and suggestion to decrease $LCCO_2$ of concrete in South-Korean apartment," *Energy and Buildings*, vol. 58, pp. 93–102, 2013.

[13] A. J. Dell'Isola and S. J. Kirk, *Life Cycle Costing for Facilities*, Construction Publishers & Consultants, Kingston, Mass, USA, 2003.

[14] T. Uygunoğlu and A. Keçebaş, "LCC analysis for energy-saving in residential buildings with different types of construction masonry blocks," *Energy and Buildings*, vol. 43, no. 9, pp. 2077–2085, 2011.

[15] N. H. Wong, S. F. Tay, R. Wong, C. L. Ong, and A. Sia, "Life cycle cost analysis of rooftop gardens in Singapore," *Building and Environment*, vol. 38, no. 3, pp. 499–509, 2003.

[16] G. Zhang and W. Wang, "The research of comprehensive evaluation model for thermal power equipment based on life cycle cost," *Systems Engineering Procedia*, vol. 4, pp. 68–78, 2012.

[17] N.-B. Chang, B. J. Rivera, and M. P. Wanielista, "Optimal design for water conservation and energy savings using green roofs in a green building under mixed uncertainties," *Journal of Cleaner Production*, vol. 19, no. 11, pp. 1180–1188, 2011.

[18] P. O. Akadiri, P. O. Olomolaiye, and E. A. Chinyio, "Multi-criteria evaluation model for the selection of sustainable materials for building projects," *Automation in Construction*, vol. 30, pp. 113–125, 2013.

[19] F. Fu, H. Luo, H. Zhong, and A. Hill, "Development of a carbon emission calculations system for optimizing building plan based on the LCA framework," *Mathematical Problems in Engineering*, vol. 2014, Article ID 653849, 13 pages, 2014.

[20] National Institute of Building Sciences, *Building SMART Alliance Strategic Goals*, National Institute of Building Sciences, 2007, http://www.nibs.org/?page=bsa.

[21] GSA, *GSA BIM Guide Overview*, US General Services Administration, Washington, DC, USA, 2007.

[22] B. Succar, "Building information modelling framework: a research and delivery foundation for industry stakeholders," *Automation in Construction*, vol. 18, no. 3, pp. 357–375, 2009.

[23] J. Basbagill, F. Flager, M. Lepech, and M. Fischer, "Application of life-cycle assessment to early stage building design for reduced embodied environmental impacts," *Building and Environment*, vol. 60, pp. 81–92, 2013.

[24] G. Han, J. Srebric, and E. Enache-Pommer, "Variability of optimal solutions for building components based on comprehensive life cycle cost analysis," *Energy and Buildings*, vol. 79, pp. 223–231, 2014.

[25] M. Ristimäki, A. Säynäjoki, J. Heinonen, and S. Junnila, "Combining life cycle costing and life cycle assessment for an analysis of a new residential district energy system design," *Energy*, vol. 63, pp. 168–179, 2013.

[26] C. R. Iddon and S. K. Firth, "Embodied and operational energy for new-build housing: a case study of construction methods in the UK," *Energy and Buildings*, vol. 67, pp. 479–488, 2013.

[27] Korea Life Cycle Inventory (LCI) Database, "LCI Database," 2015, http://www.edp.or.kr/lci/lci.asp.

[28] S. Tae, S. Shin, J. Woo, and S. Roh, "The development of apartment house life cycle CO_2 simple assessment system using standard apartment houses of South Korea," *Renewable and Sustainable Energy Reviews*, vol. 15, no. 3, pp. 1454–1467, 2011.

[29] BuildingSMART KOREA, *Overview of BIM—Definition of BIM*, BuildingSMART KOREA, 2015, http://www.buildingsmart.or.kr/overview/BIM.aspx.

[30] American Society of Heating and Refrigerating and Air-Conditioning Engineers, "Resources & Publications—International Weather for Energy Calculations," 2013, http://www.ashrae.org/resources–publications/bookstore/climate-data-center#iwec.

[31] Korea Price Information, 2013, http://www.kpi.or.kr.

[32] W. East, *COBIE (Construction-Operations Building Information Exchange)*, US Army Engineer Research and Development Center, US Army Corps of Engineers, Washington, DC, USA, 2007.

Hindawi Publishing Corporation
Mathematical Problems in Engineering
Volume 2015, Article ID 381926, 13 pages
http://dx.doi.org/10.1155/2015/381926

Research Article

Use of a Combination of MRSS-ANP for Making an Innovative Landfill Siting Decision Model

Mohammad K. Younes,[1] N. E. Ahmad Basri,[1] Z. M. Nopiah,[1] H. Basri,[1] and Mohammed F. M. Abushammala[2]

[1]*Department of Civil and Structural Engineering, Universiti Kebangsaan Malaysia, 43600 Bangi, Selangor, Malaysia*
[2]*Department of Civil Engineering, Middle East College, Knowledge Oasis Muscat, P.B. No. 79, 124 Al Rusayl, Oman*

Correspondence should be addressed to Mohammad K. Younes; mohyoumoh@hotmail.com

Received 4 April 2015; Revised 7 June 2015; Accepted 8 June 2015

Academic Editor: Jurgita Antucheviciene

Landfill siting is a complex, multicriteria decision-making problem that needs an extensive evaluation of environmental, social, land use, and operational criteria. Integration of a median ranked sample set (MRSS) and an analytic network process (ANP) has been implemented to rank the associated criteria and select a suitable landfill site. It minimizes the uncertainty and the subjectivity of human judgments. Four groups of experts with different backgrounds participated in this study, and each group contained four experts. The respondent preferences were ranked in a 4-by-4 matrix to obtain the judgment sets for the MRSS. These sets were subsequently analyzed using ANP to obtain the priorities in the landfill siting criteria. The results show that land topology and distance from surface water are the most influential factors, with priorities of 0.18 and 0.17, respectively. The proposed integrated model may become a promising tool for the environmental planners and decision makers.

1. Introduction

Facility site selection model is complex and needs extensive assessment and comparison efforts [1]. Proper landfill siting is essential to reduce the environmental and health impacts associated with its construction and operation [2]. In general, solid waste treatment and disposal facilities belong to a group of obnoxious or undesirable facilities, and, therefore, landfill siting faces two major challenges: (i) social objection represented by a phenomenon known as BANANA (build absolutely nothing anywhere near anyone) or NIMBY (not in my back yard) and (ii) the large number of technical, social, and environmental factors that must be considered in selecting the best location to minimize nuisances and maximize efficiency and social acceptance [3]. Solid waste landfill remains a convenient method for the disposal of an increasing amount of municipal solid waste, notably in developing countries [4]. Landfill site selection requires a different type of criteria processing to account for the unequal criteria importance [5–9]. Moreover, increasing the number of participating parties in the decision-making process widens its popularity and strengthens it [10], but analyzing and homogenizing the preferences of these stakeholders are complex issue, especially with conflict of interests among the participated interest groups.

Decision support systems like the analytic hierarchy process (AHP) and its generalization (ANP) have been widely implemented to handle the complex problems. Multicriteria decision-making (MCDM) using ANP is composed of the following steps: (i) identifying the factors and the components within the network together with their interactions and relations; (ii) conducting pairwise comparisons among the network elements and the main/subcriteria to build the unweighted supermatrix; (iii) obtaining the weighted supermatrix via weighting the blocks of the unweighted supermatrix by the corresponding priorities of the clusters (from which the resulting matrix is column stochastic); and (iv) developing the limit matrix by increasing the power of the weighted supermatrix until the weights converge [11].

The ANP is implemented to drive the relative priorities of the criteria using the judgment of individuals [12]. However, ANP implementation requires higher number of judgments

Table 1: Definition of the scale of importance [58].

Intensity of importance	Definition	Explanation
9	Extremely important	This activity is of the highest possible order of affirmation
7	Strongly important	This activity is strongly favored (dominant) over other activities
5	Moderately important	This activity is moderately favored over other activities
3	Slightly important	This activity is slightly favored over other activities
1	Equally important	This activity equally contributes to the objective
2, 4, 6, and 8		Intermediate importance between two adjacent responses

than AHP. Because of the ability of ANP to treat the interactions and feedback and thus justify the decision [13], ANP is widely used in many decision-making applications. However, ANP-based decisions are limited by the uncertainty in judgment during the pairwise comparison [14]. A previous study [1] combined ANP and data envelopment analysis to leverage both the available qualitative and quantitative data for the location of a landfill site. Additional studies [15, 16] implemented ANP to suggest the best location of a landfill site. Several researchers [17, 18] integrated a fuzzy set, AHP, and a weighted linear method to prioritize the site evaluation criteria and applied this process using Geographic Information System (GIS) software. Moreover, hybrid model of an ANP and a triangular fuzzy function were used by [14] to measure remedial countermeasures. A landfill site suitability analysis using an AHP and a compromised programming method was also reported [19]. An AHP was applied to find the weighted site evaluation criteria and was used in GIS to suggest the best landfill location [20].

The ranked sample set (RSS) was first proposed by Mc Intyre in 1952 to estimate the population mean, and since that time it was modified and developed many times [21, 22]. Applying of the RSS to estimate the population mean and median leads to notable gains in precision [23]. The MRSS is an adaptation of RSS, and, in this method, only the median observation is considered from each of randomly selected sets. The MRSS is advantageous (relative to RSS) because it minimizes the ranking errors and enhances the estimation efficiency [24]. The MRSS proposes promising applications in environmental researches because of its capability to represent a population without extensive observations [25]. For instance, the spray deposits on the leaves of apple trees were assessed using RSS [26]. An RSS method was also applied to collect samples from gasoline stations for analysis intended to verify the conformity of these stations with clean air regulations [27]. Prior sample knowledge was also integrated with RSS to minimize the cost of evaluating a stream habitat region for salmon [28].

This study presents a model to reduce the imprecision and vagueness of the human decision-making. It identifies the relative importance of landfill siting criteria as a case study. The presented model leverages the power of an expert system to extract knowledge that is subsequently applied to a hybrid MRSS-ANP system to obtain the criteria weights.

2. Methodology

Landfill siting is a multicriteria decision-making process. The proposed model decomposes this process into three levels: problem construction, criteria analysis, and selection [7]. Problem (case) construction determines the problem, aims, assessment criteria, the experts, and their groups. Criteria analysis extracts the expert knowledge and performs data analysis using MRSS. The selection step determines the importance of the landfill siting criteria using ANP and the rank of the final priorities.

2.1. Case Construction. The problem construction starts with a literature review used to determine the main and subcriteria of the landfill site selection. There are no general approaches to select a set of evaluation criteria but it can be selected through an examination of the relevant literature, analysis study, and expert opinions [29]. However, the criteria selection was based on the usage (the most commonly found in literature), expert opinions, and data availability. These criteria were subsequently arranged in a hierarchical structure, and the hierarchical tree defines the most general network. The landfill siting criteria were classified into four main groups: social [30, 31], operational [16, 18], environmental [32, 33], and land use [34–36]. Moreover, the subcriteria fall under each main group, as shown in Figure 1. After the initial classifying, the experts were determined and divided into four clusters (groups). A cluster analysis splits the data into meaningful groups that are usually associated or share characteristics [37]. The resulting groups involved the governmental sector, private sector, academia, and nongovernment organizations interested in solid waste and environmental issues.

A developed questionnaire asked the stakeholders to draw pairwise comparisons among the criteria and the subcriteria with respect to landfill site selection. The used questionnaire takes into account the interactions and feedbacks between the criteria. Table 1 shows the intensity of the importance of the criteria. The odd-numbered rankings were used to determine the criteria importance, whereas the entire range from 1 to 9 was used to develop the ANP multicriteria decision analysis.

2.2. Criteria Analysis. The stakeholders preferences were grouped into four random sets. Each set consists of the

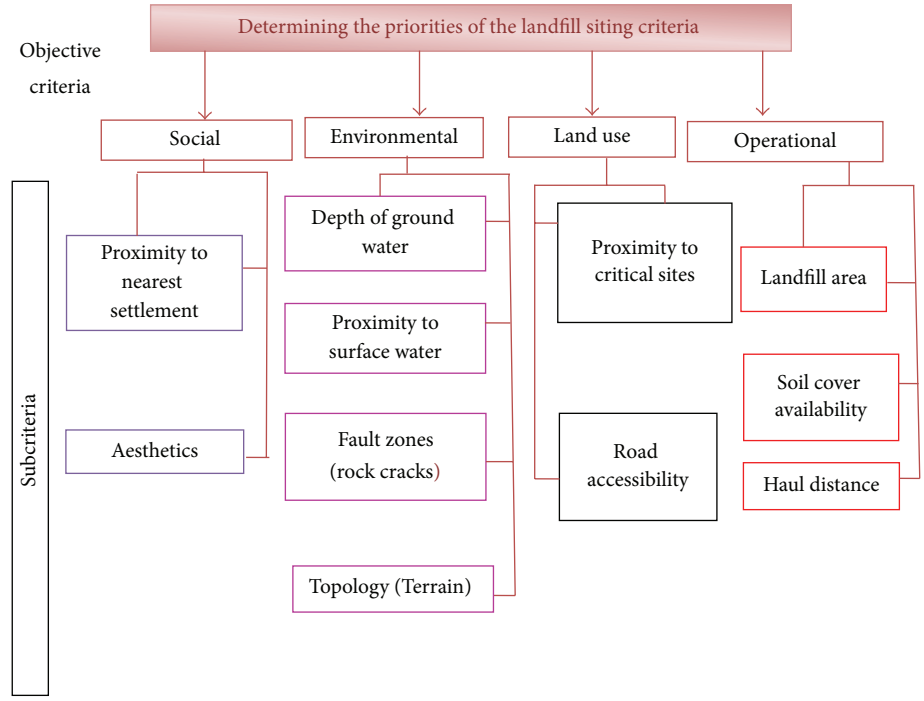

Figure 1: Hierarchical structure of the landfill siting criteria.

Table 2: Comparison of the importance of land use with the importance of operation methods.

Sector	Government	Private sector	NGO	Academia
Expert group number 1	7	0.33	0.20	1
Expert group number 2	1	3	1	0.14
Expert group number 3	7	5	3	7
Expert group number 4	3	3	3	0.20

responses of one government, private, academia, and NGO respondent. The respondents are experts in the field of solid waste management and landfill siting issues through their work experience. Table 2 shows an example of one of the comparisons by displaying the obtained preferences of the respondents and their sets. Next, these responses were ranked in increasing order for each individual set, as shown in Table 3. After that, the importance of the landfill siting criteria was obtained using the second scenario [21]:

(i) If the sample size, n, is odd, then the median is selected by $((n + 1)/2)$th. This observation can be denoted as $X_{(((n+1)/2):n)}$, and the general formula is

$$\left\{X_{(((n+1)/2):n)1}, X_{(((n+1)/2):n)2}, \ldots, X_{(((n+1)/2):n)n}\right\}. \quad (1)$$

(ii) If the sample size n is even,

then the median is selected by $(n/2)$th. This observation can be denoted as $X_{((n/2):n)}$, and the general formula is

$$\left\{X_{((n/2):n)1}, X_{((n/2):n)2}, \ldots, X_{((n/2):n)n}\right\}. \quad (2)$$

2.3. Final Priority Selection. The study aim is to determine the overall priority of each criterion and apply it in the case study considering the interactions and the feedbacks among the main and subcriteria. ANP systematically breaks down the problem to justify the decision [38, 39]. To capture the interactions and feedback, a hierarchical framework that contains all main and subcriteria must be constructed. Thus the comparisons can be performed and synthesized to determine the unweighted, weighted, and limit matrices that determine the priorities of importance of the landfill siting criteria. Figure 2 shows the interactions and feedback between the landfill siting components. An arrow and/or loop arrow specify the dependence and feedback for which the two-side (double) arrows indicate the influences between the elements on both groups. The inner-dependence or self-feedback is indicated by a loop arrow at the top of each group.

The resulting relative importance sets from the previous step contain the preferences of government, private, NGO, and academic stakeholders and are used in the ANP. This step is repeated for the sixty-three pairwise comparisons to build the comparison matrix (unweighted supermatrix). The inputs of the supermatrix depend on the presence and the type of dependence among the group elements that are shown in Figure 2. The matrix is subsequently input into the Super Decisions (version 2.2) software to develop the weighted and limit matrices [40]. The weights obtained in the limit matrix represent the final importance priorities. Finally, the integrated landfill siting procedures are summarized in Figure 3. This figure illustrates the guidelines for such decision-making problem.

2.4. Case Study. Selangor is the most populated and highly developed state in Malaysia; it has a diversified economy

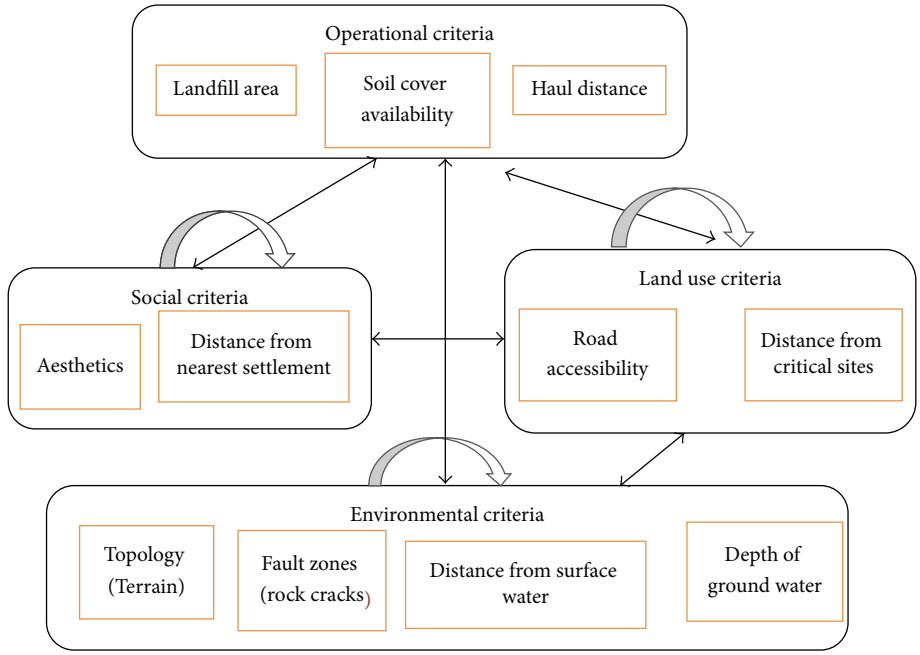

Figure 2: Interactions and feedback between criteria.

including industry, commerce, agriculture, and tourism. Moreover, Selangor completely surrounds two federal territories, which are Kuala Lumpur (KL), the national capital of Malaysia, and Putrajaya the federal capital. The areas of Selangor, Kuala Lumpur, and Putrajaya are 7,930, 243, and 92 km^2, respectively. There is a great demand to depend on scientific approach for determining a landfill site in Selangor due to increasing amounts of solid waste and land scarcity. Thus Boolean logic was implemented to exclude unsuitable areas that cannot be used as a disposal site [19]. The exclusion is done by overlaying technique and in dependence on constraint factors [6, 41]; these factors are based on Malaysian guidelines for development of solid waste sanitary landfill [42]. However, the Boolean logic is restrictive in nature [43]; thus, by its implementation, the study area is classified into two classes suitable area with value (1) and unsuitable area with value (0) as shown in Figure 4 and described in (3):

$$\text{Boolean Suitablity Index} = \prod_{j=1}^{n} b_j, \tag{3}$$

where Boolean Suitability Index has a value (0 or 1), b_j is the Suitability Index for each constraint criterion and has a value (0 or 1), and n the total number of constraint criteria [2]. Finally, the potential landfill sites were suggested based on assumed landfill area and ranked using the obtained MRSS-ANP weights and Suitability Index (SI), which is the sum of products of the standardized score of each criterion multiplied by the weight of each criterion:

$$\text{SI} = \sum W_i * C_i, \tag{4}$$

where W_i is weight of factor I and C_i is criteria grading of factor map i [34].

3. Results and Discussion

3.1. Case Construction. Figure 1 shows the developed hierarchical structure of the landfill site evaluation criteria. Each main criterion has an ultimate goal, that is, to maximize the preservation of nature (environmental), acceptance by the public (social), or appropriateness of the site (land use). Additionally, the target of operational criteria is minimizing the costs. The eleven subcriteria that share common characteristics were grouped together under the main criteria. Since the solid waste hauling distance, availability of soil cover for daily landfill operations, and landfill area are controlled during landfill construction or operation, they were classified under one group (operational) [43].

Moreover, land use involves the locations of critical sites highways and roads that are identified by the town planning department and these locations are highlighted for specific consideration in future plans. Examples of critical sites include airports, hospitals, railway, and other institutes [18]. Landfills serve large communities, but only subset of those communities commonly experiences the impacts of the landfill (typically the ones that are located near it) [44]. However, these effects can be minimized using special arrangements designed to reduce the nuisances caused during waste transportation and enhance the landscaping around the landfill to create a green buffer. The environmental criteria aim to conserve air, water, and soil and to minimize land altering activities [32] by applying the best available techniques and environmental practices to achieve these goals.

Figure 2 displays the dependence and feedback among the criteria. The environmental criteria do not relate to the aesthetics or distance from the nearest settlement; therefore, an interconnection or feedback between the environmental

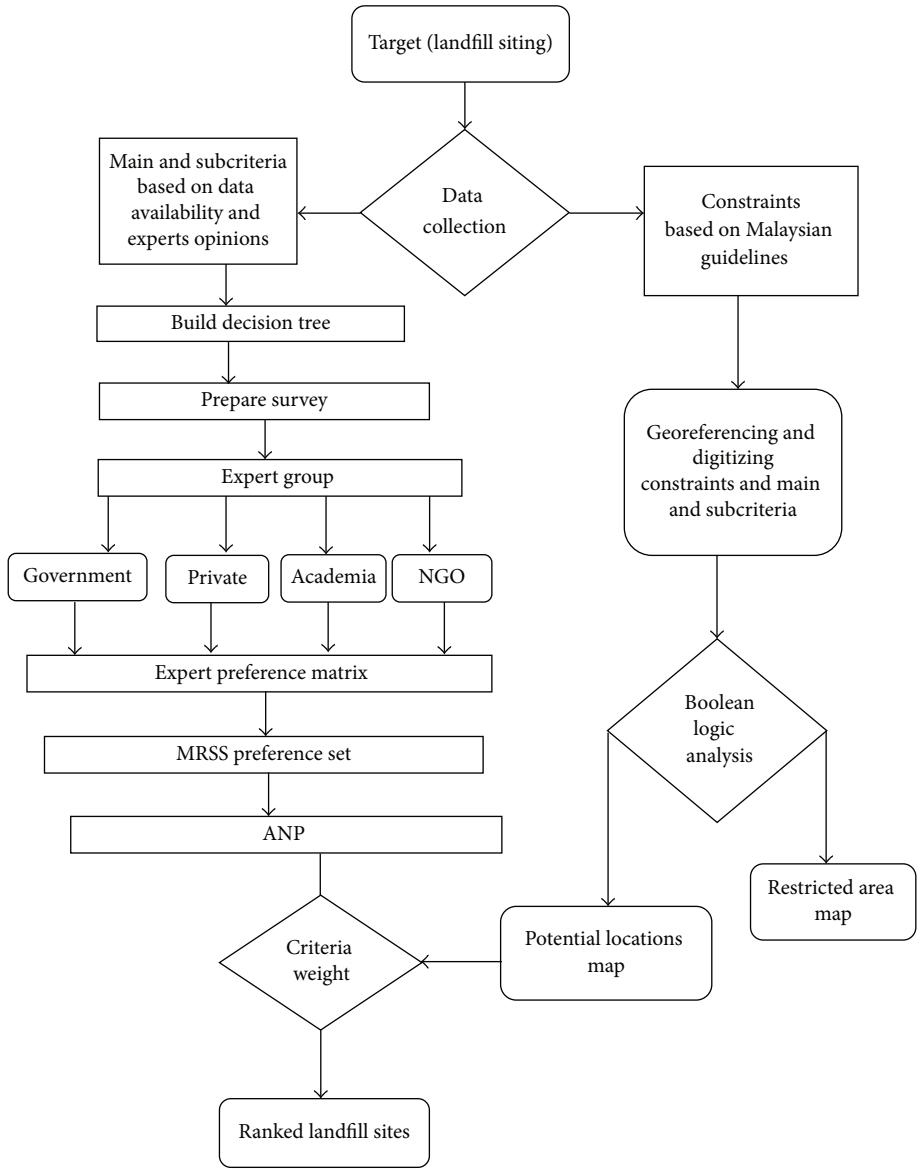

Figure 3: The landfill site selection algorithm.

and social main group is not shown. One or more of the remaining subcriteria relate to an additional criterion from outside of the group. For example, reciprocal effects were noted between the land topology and surface water. Surface water alters the land topology, whereas the topology affects the water runoff and maximizes or minimizes the movement of pollutants. Pairwise comparisons were used to compare the criteria and to allocate the criteria priorities using the Saaty method [39, 45]. The respondents were divided into four stakeholder sets to reduce vagueness and enhance quality.

3.2. Criteria Analysis. Based on the interactions and feedback among the criteria, sixty-three pairwise comparisons were required. The preferences of each respondent were recorded for each comparison. Every set of responses contained the opinion of one expert from each group, that is, government, private, academia, and NGO. Therefore, the response range within the same set is relatively large because of the conflicts of interest of the stakeholders. The expert responses within the same group were observed to converge, but outlier responses were noted due to human nature and the various backgrounds of the experts. For instance, one governmental expert might emphasize environmental concerns because of personal involvement in environmental regulations, whereas another governmental expert may emphasize planning and land development because of personal involvement in a planning department. Similarly, one NGO representative could emphasize conservation, whereas another NGO representative might emphasize service to society. Therefore, points of view can diverge within an identical group.

Sixty-three pairwise comparisons were performed to identify the relative importance of the landfill siting criteria. An example of one of these comparisons is shown in Table 2.

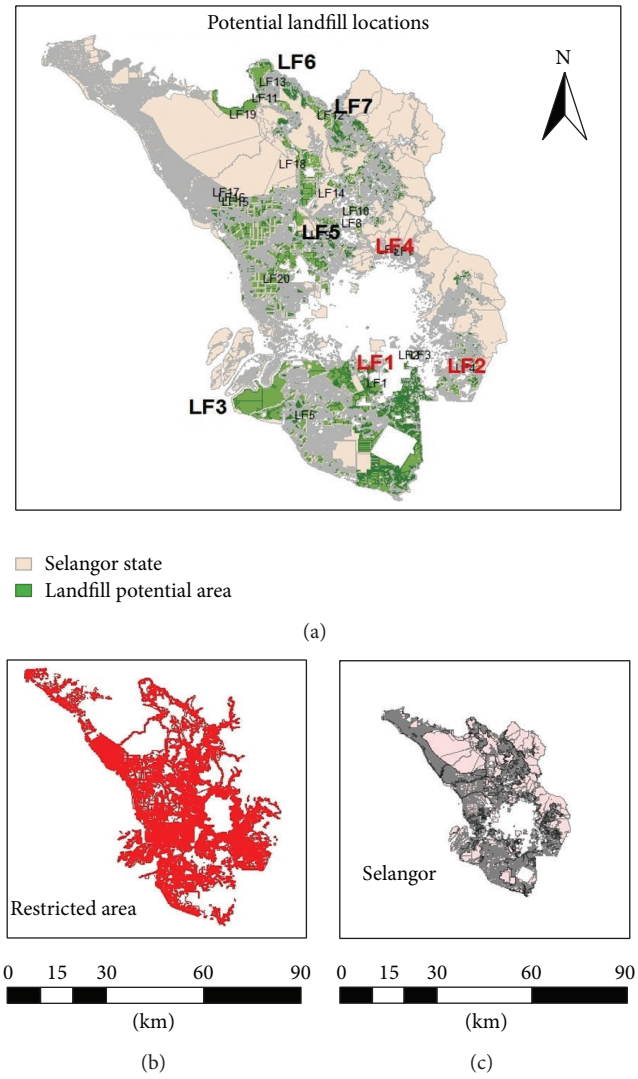

Figure 4: Selangor and potential landfill sites maps.

This table compares land use and operational methods to create a positive social impression with respect to the landfill site. For instance, the second expert in the first group indicates that operation method is slightly more important than the land use. In Table 3, the relative weights are ranked in increasing order. Because four preferences are contained in each set, the median weight set is determined using (2). Therefore, the second and the third quarters represent the MRSS and determine the relative importance set of the landfill siting criteria. The obtained relative importance set displayed in Table 3 is "1; 5; 7; 3." This technique guarantees representation of the best set regardless of the origin of the responses. This result is displayed in Table 3 in which an increasing response rank is required regardless of the sector.

3.3. Final Priority Selection. The ANP uses three matrices: unweighted supermatrix, weighted supermatrix, and limit matrix. The unweighted supermatrix is the relative importance of all main components and subcomponents.

Table 3: Ranked comparison of the importance of land use with operational methods.

Ranked experts preferences				
Expert group number 1	0.20	0.33	1	7
Expert group number 2	0.14	**1**	1	3
Expert group number 3	3	**5**	**7**	7
Expert group number 4	0.20	3	**3**	3

Table 4: Priorities group matrix of the main criteria.

Sector	Land use	Environmental	Operational	Social
Land use	0.183	0.143	0.116	0.540
Environmental	0.526	0.571	0.488	0.0
Operational	0.204	0.286	0.275	0.163
Social	0.087	0.0	0.121	0.297

Table 5: Final priorities of the main criteria.

Main criteria	Final priority
Land use	0.142
Environmental	0.546
Operational	0.262
Social	0.05

The weighted supermatrix clarifies the values of each group and its elements. The limit matrix represents the priorities results and is obtained by raising the weighted supermatrix to a high power to acquire constant values.

Table 4 shows the priorities group matrix. Zero values mean that there are no interconnections between the criteria in the matrix; this independence is shown in Figure 2 in which no interactions are displayed between the environmental and social groups. The priority value of each main criterion in Table 4 depends on the relationship between the criteria groups. For instance, operations have an importance of 0.286 with respect to minimizing the landfill effects on the environment. This importance decreases to 0.16 when considering the creation of a positive social opinion with respect to the landfill site.

The final priorities of the main criteria group are shown in Table 5, and the highest rank of 0.54 is shown for environmental criteria, followed by operational methods and techniques (priority rank of 0.26). A landfill should be located and designed to protect human health and to conserve the environment. Therefore, environmental criteria gained the highest rank and this is the present worldwide trend [29]. In addition, according to the obtained results we can conclude that the social and operational criteria are considered to be insignificant by stakeholders. However, such results were reported by many researchers. For instance, Ismail (2011) [46] reported ground water, surface water, and protected area as the most important factors followed by land slope. Afzali et al. (2011) ranked the surface water (19%) followed by ground water (13%) as the most important physical criteria. Nadi et al. (2010) [47] ranked the hydrology and water as the most important criteria (33.4%) and social and financial

Table 6: Weight priorities of the overall subcriteria.

Group	Criteria	Priority normalized by group	Final priority
Environmental	SW	0.317	0.173
	GW	0.157	0.085
	FZ	0.181	0.099
	TO	0.345	0.188
Land use	CS	0.409	0.058
	RA	0.591	0.083
Operational	HD	0.145	0.038
	LA	0.511	0.135
	SA	0.344	0.091
Social	AE	0.579	0.029
	NS	0.421	0.021

SW: proximity to surface water, GW: depth of ground water, FZ: proximity to fault zone, TO: topology, CS: proximity to critical site, RA: road accessibility, HD: haul distance, LA: landfill area, SA: soil availability, AE: aesthetic, and NS: nearest settlement.

Table 7: Summary of the rankings and SI for the potential landfill sites.

Site number	Environmental				Land use		Operational			Social		SI
	SW	GW	FZ	TO	CS	RA	HD	LA	SA	AE	NS	
LF1	0.173	0.085	0.040	0.113	0.058	0.017	0.038	0.135	0.091	0.029	0.004	0.782
LF2	0.173	0.068	0.040	0.113	0.058	0.083	0.038	0.135	0.091	0.029	0.004	0.832
LF3	0.035	0.017	0.020	0.188	0.058	0.083	0.038	0.135	0.091	0.029	0.008	0.702
LF4	0.138	0.068	0.099	0.113	0.058	0.083	0.038	0.135	0.091	0.023	0.013	0.859
LF5	0.104	0.085	0.020	0.075	0.058	0.066	0.038	0.135	0.091	0.017	0.021	0.711
LF6	0.138	0.051	0.040	0.150	0.058	0.064	0.038	0.135	0.091	0.017	0.004	0.787
LF7	0.035	0.017	0.099	0.113	0.058	0.083	0.038	0.135	0.091	0.029	0.008	0.706

criteria as the least important criteria with weight equal to 15.5% and 15.3, respectively. Demesouka et al. (2013) indicated the hydrology as the most important factor followed by the environmental criteria and ranked the social and economic factors as the least important or insignificant factors. In a study done by [48], the social and technoeconomic criteria gained the lowest importance of 9% and 6%, respectively. Moreover, such conclusion was also reported by Ismail (2011) for landfill siting in Malaysia because the social and operational (technical) criteria can be extended and modified. A study done by [49] reported that urban area and water resources are the most important criteria that should be considered for construction intermunicipality landfill. However, sometimes it is inappropriate to compare among studies from different countries because the obtained weights are dependent upon surveyed respondents, different studied factors, and different local and environmental conditions.

The final priorities of the factors related to landfill site selection are shown in Table 6. The overall highest rank is for land topology (18.8%) because of its direct effect on both surface water and groundwater as well as on soil erosion by control of water runoff [50]. Surface water is the second highest factor (17.3%). Surface water can easily become polluted and can therefore propagate pollutants. The third highest rank is for landfill area (13.5%); this ranking is due to the requirement to locate the landfill in a manner that reduces the price of the land because the land price represents the highest cost for a landfill. In addition, the landfill size must be optimized to minimize environmental effects and the costs associated with identifying a new landfill site.

However, applying (2) produced Table 8 that describes the preference sets of the performed sixty-three comparisons. Each element in the set represents the preferences of each expert group. Table 9 is a result of applying the preferences sets in ANP and represents the unweighted supermatrix. It is two-dimensional matrix of element by element, and it provides relative importance of all components (main criteria and subcriteria) [45]. The weighted and limit matrices are described by Tables 10 and 11, respectively. In the limit matrix, the constant values of each value are determined by taking the necessary limit of the weighted supermatrix [38]. Social criteria and haul distance got the lowest rank. The influence of these criteria on the design of a landfill can be minimized with suitable arrangements. For example, if appropriate transfer station is used, then the solid waste hauling cost is reduced. Additionally, planted buffer zones and special landscaping can reduce visual and odor pollution to minimize the nuisance to neighbors. Moreover, shifting traffic as far as possible

Table 8: MRSS preference sets.

Number	Comparison target	Comparison elements	MRSS preference sets
1	To create positive social opinion	Land use (operational)	0.33, 1, 7, and 3
2		Land use (social)	1, 1, 5, and 1
3		Operation (social)	0.2, 1, 0.2, and 1
4	To protect environmental elements	Environmental (land use)	1, 3, 5, and 5
5		Environmental (operational)	1, 1, 5, and 1
6		Land use (operational)	1, 1, 5, and 1
7	For sustainable and strategic land use planning	Environmental (land use)	1, 3, 3, and 3
8		Environmental (operational)	1, 1, 7, and 3
9		Environmental (social)	5, 1, 7, and 7
10		Land use (operational)	0.33, 0.2, 1, and 3
11		Land use (social)	1, 0.14, 3, and 3
12		Operation (social)	1, 1, 5, and 5
13	To minimize the operational cost and to operate the landfill with best available techniques and best environmental practices	Environmental (land use)	1, 7, 5, and 5
14		Environmental (operational)	1, 1, 3, and 3
15		Environmental (social)	1, 1, 5, and 3
16		Land use (operational)	0.33, 1, 1, and 1
17		Land use (social)	1, 0.2, 3, and 1
18		Operation (social)	5, 1, 5, and 3
19	To protect surface water	Proximity to critical sites (road accessibility)	0.2, 0.11, 0.33, and 1
20		Soil cove availability (landfill area)	0.33, 1, 5, and 1
21		Avoiding faulting zones (depth of ground water)	0.33, 0.14, 3, and 1
22		Avoiding faulting zones (topology)	1, 0.14, 3, and 1
23		Depth of ground water (topology)	3, 1, 1, and 1
24	To reduce the effects on fault zones	Landfill area (soil cover)	1, 0.2, 5, and 3
25		Proximity to surface water (depth of ground water)	1, 1, 3, and 1
26		Proximity to surface water (topology)	1, 1, 1, and 1
27		Depth of ground water (topology)	1, 1, 1, and 1
28	To protect the ground water from pollutants	Landfill area (soil cover)	1, 1, 5, and 1
29		Proximity to surface water (avoiding fault zones)	1, 1, 1, and 1
30		Proximity to surface water (topology)	1, 1, 0.2, and 0.3
31		Avoiding fault zones (topology)	1, 1, 5, and 3
32	To reduce altering the land topology	Landfill area (soil cover)	1, 0.14, 3, and 1
33		Proximity to surface water (avoiding fault zones)	1, 1, 3, and 3
34		Proximity to surface water (topology)	1, 1, 1, and 1
35		Avoiding fault zones (topology)	1, 0.2, 0.33, and 1
36	To protect the critical sites	Proximity to surface water (avoiding fault zones)	1, 1, 5, and 1
37		Proximity to surface water (depth of ground water)	1, 1, 5, and 7
38		Avoiding fault zones (depth of ground water)	1, 1, 3, and 3
39		Aesthetic (proximity to living settlement)	0.33, 1, 5, and 3
40		Road accessibility (proximity to critical sites)	0.33, 1, 1, and 3
41	To locate landfill in places easily accessed by roads	Proximity to surface water (topology)	0.33, 1, 0.2, and 0.2
42		Haul Distance (landfill Area)	5, 5, 5, and 5
43		Aesthetic (proximity to living settlement)	0.33, 1, 3, and 1
44	To minimize the solid waste haul distance	Proximity to surface water (topology)	1, 3, 5, and 1
45		Proximity to critical sites (road accessibility)	0.33, 0.2, 0.2, and 0.14
46		Landfill area (soil cover)	1, 1, 1, and 1
47		Aesthetic (proximity to living settlement)	0.33, 0.3, 1, and 1

Table 8: Continued.

Number	Comparison target	Comparison elements	MRSS preference sets
48	To determine the optimum landfill area	Proximity to surface water (avoiding fault zones)	1, 1, 3, and 3
49		Proximity to surface water(depth of ground water)	1, 1, 3, and 5
50		Proximity to surface water(topology)	3, 1, 7, and 7
51		Avoiding fault zones (depth of ground water)	1, 1, 3, and 3
52		Avoiding fault zones (topology)	3, 1, 7, and 3
53		Depth of ground water (topology)	0.33, 1, 3, and 3
54		Proximity to critical sites (road accessibility)	1, 1, 3, and 5
55		Solid waste haul distance (landfill area)	1, 1, 1, and 5
56		Solid waste haul distance (soil cover)	1, 1, 3, and 3
57		Landfill area (soil cover)	0.33, 1, 5, and 1
58		Aesthetic (proximity to living settlement)	0.33, 1, 1, and 1
59	To protect the soil cover from pollution	Proximity to surface water (topology)	0.33, 1, 0.2, and 0.33
60	To minimize the possibility of the landfill being seen	Proximity to critical sites (road accessibility)	0.33, 0.33, 1, and 1
61		Solid waste haul distance (landfill area)	1, 1, 3, and 1
62		Aesthetic (proximity to living settlement)	1, 0.33, 3, and 1
63	To locate the landfill as far as possible from settlements	Solid waste haul distance (landfill area)	1, 1, 7, and 7

Table 9: Unweighted supermatrix.

Group labels	Environmental			Land use			Operational			Social	
	SW	GW	FZ	TO	CS	RA	HD	LA	SA	AE	NS
Environmental											
SW	0.00	0.25	0.41	0.40	0.54	0.25	0.75	0.48	0.25	0.00	0.00
GW	0.55	0.00	0.26	0.00	0.16	0.00	0.00	0.15	0.00	0.00	0.00
FZ	0.21	0.46	0.00	0.20	0.30	0.00	0.00	0.29	0.00	0.00	0.00
TO	0.24	0.28	0.33	0.40	0.00	0.75	0.25	0.08	0.75	0.00	0.00
Land use											
CS	0.25	0.00	1.00	0.00	0.33	1.00	0.17	0.75	0.00	0.33	0.00
RA	0.75	0.00	0.00	1.00	0.67	0.00	0.83	0.25	0.00	0.67	1.00
Operational											
HD	0.00	0.00	0.00	0.00	0.00	0.83	0.00	0.49	0.00	0.67	0.83
LA	0.33	0.67	0.67	0.50	0.00	0.17	0.50	0.31	1.00	0.33	0.17
SA	0.67	0.33	0.33	0.50	0.00	0.00	0.50	0.20	0.00	0.00	0.00
Social											
AE	0.00	0.00	0.00	0.00	0.75	0.50	0.33	0.50	0.00	0.50	1.00
NS	0.00	0.00	0.00	0.00	0.25	0.50	0.67	0.50	0.00	0.55	0.00

from populated areas may minimize noise complaints. In general, these considerations are inexpensive and require minimal labor compared with the other criteria.

Finally, incorporating the participation of conflicting stakeholders minimizes the uncertainty and risk of reproducing homogenous decisions and enhances the quality of the decisions. Additionally, consistent and reliable results must be achieved [51, 52]. The landfill sitting factors and stakeholders are both predefined and grouped in sets. Stakeholder grouping and interviews are time-saving tools that effectively gather perceptions and values from the experts [53]. However, to ensure an efficient and unbiased representation of the expert judgments, an MRSS was used to rank and calculate the judgment sets [27, 54].

3.4. Case Study. As consequence of rapid urbanization and economic growth the solid waste generation is increased dramatically in Selangor state. Owing to this increase, the search for and the provision of an efficient solid waste management method has become an essential matter [55]. Landfill is the main solid waste disposal method in Malaysia [4]. Figure 4(c) shows the map of Selangor including Putrajaya and Kuala Lumpur cities. The restricted area that cannot be used to construct a landfill is shown in Figure 4(b).

Table 10: Weighted supermatrix.

Group labels	Environmental				Land use		Operational			Social	
	SW	GW	FZ	TO	CS	RA	HD	LA	SA	AE	NS
Environmental											
SW	0.00	0.17	0.24	0.23	0.36	0.13	0.37	0.23	0.16	0.00	0.00
GW	0.31	0.00	0.15	0.00	0.11	0.00	0.00	0.08	0.00	0.00	0.00
FZ	0.12	0.31	0.00	0.11	0.20	0.00	0.00	0.14	0.00	0.00	0.00
TO	0.14	0.19	0.19	0.23	0.00	0.39	0.12	0.04	0.48	0.00	0.00
Land use											
CS	0.04	0.00	0.14	0.00	0.08	0.18	0.02	0.09	0.00	0.18	0.00
RA	0.11	0.00	0.00	0.14	0.15	0.00	0.10	0.03	0.00	0.36	0.54
Operational											
HD	0.00	0.00	0.00	0.00	0.00	0.17	0.00	0.14	0.00	0.11	0.14
LA	0.09	0.22	0.19	0.14	0.00	0.03	0.14	0.09	0.36	0.05	0.03
SA	0.19	0.11	0.10	0.14	0.00	0.00	0.14	0.05	0.00	0.00	0.00
Social											
AE	0.00	0.00	0.00	0.00	0.08	0.04	0.04	0.06	0.00	0.15	0.30
NS	0.00	0.00	0.00	0.00	0.03	0.04	0.08	0.06	0.00	0.15	0.00

Table 11: Limit matrix.

Group labels	Environmental				Land use		Operational			Social	
	SW	GW	FZ	TO	CS	RA	HD	LA	SA	AE	NS
Environmental											
SW	0.173	0.173	0.173	0.173	0.173	0.173	0.173	0.173	0.173	0.173	0.173
GW	0.085	0.085	0.085	0.085	0.085	0.085	0.085	0.085	0.085	0.085	0.085
FZ	0.099	0.099	0.099	0.099	0.099	0.099	0.099	0.099	0.099	0.099	0.099
TO	0.188	0.188	0.188	0.188	0.188	0.188	0.188	0.188	0.188	0.188	0.188
Land use											
CS	0.058	0.058	0.058	0.058	0.058	0.058	0.058	0.058	0.058	0.058	0.058
RA	0.083	0.083	0.083	0.083	0.083	0.083	0.083	0.083	0.083	0.083	0.083
Operational											
HD	0.038	0.038	0.038	0.038	0.038	0.038	0.038	0.038	0.038	0.038	0.038
LA	0.135	0.135	0.135	0.135	0.135	0.135	0.135	0.135	0.135	0.135	0.135
SA	0.091	0.091	0.091	0.091	0.091	0.091	0.091	0.091	0.091	0.091	0.091
Social											
AE	0.029	0.029	0.029	0.029	0.029	0.029	0.029	0.029	0.029	0.029	0.029
NS	0.021	0.021	0.021	0.021	0.021	0.021	0.021	0.021	0.021	0.021	0.021

The restriction map was obtained by implementing the guidelines issued by Department of Environment. These guidelines determine the prohibited landfill construction areas that are urban, sensitive ecological areas, heritage and cultural sites, strategic agricultural area like paddy fields, flood plain zones, swamps and water bodies, and parks. Moreover, it suggests a buffer distance, like distance from human settlements (500 m), highways (300 m), floodplain areas (100 m), and proximity to surface water (100 m buffer). The restriction area represents 80% of the total Selangor area. The top map in Figure 4(a) shows the potential area in green color. After that, seven sites were determined as a potential landfill sites based on their area. The landfill area assumed to be around 100 hectare, and this assumption is based on Pariatamby and Tanaka (2014) recommendation [56] for minimum landfill size required for economically efficient gas collection system and the recommendation for potential impacts of landfill based on its size [57]. The ranks of the potential landfill sites are shown in Table 7. These ranks were obtained using the results of MRSS-ANP model for site evaluation criteria and Suitability Index (SI), which is the sum of products of the standardized score of each criterion multiplied by the weight of each criterion. The highest ranks are for sites numbers LF4 and LF2, with SI equal to 0.859 and 0.832, respectively, as shown in Figure 4.

4. Conclusions

The siting of undesirable facilities is a process characterized by uncertainty and complexity, as well as multiple and

conflicting criteria. Determining the site evaluation criteria and constructing the dependence and connections among these factors is the key preliminary step in the siting process. Therefore, an appropriate hierarchical structure must be constructed for the evaluation criteria, and the expert groups must be determined. However, participation of all potential stakeholders in decision-making process is essential to justify and increase the decision acceptance and quality. Moreover, it minimizes the risk and avoids production of identical decision. Stakeholders grouping and interviewing are efficient way to collect their perceptions. Moreover, MRSS is a statistical tool that guarantees gathering unbiased representation of the study society, and thus it was used in this study.

Environmental criteria were assigned the highest priority (54.6%). Environmental effects have the highest complexity and represent the core of the mitigation measures. The second highest criterion was operational methods and techniques. These processes are pivotal in reducing the effects of a landfill. Social criteria were the least important because the social issues related to landfill sites can be minimized by proper management. Overall, land topology and distance from surface water were the most important subcriteria and have weights equal to 18.8% and 17.3%, respectively, whereas aesthetics and proximity to the nearest settlement have the lowest priorities of 2.9% and 2.2%, respectively. These results can be justified as the proposed site is a sanitary landfill with gas and leachate collection system; therefore, the main pollution threats are from the outside, namely, from rainwater. The risk of odor pollution is low because of the applied mitigation measures, that is, leachate and gas collection and buffering zones around the site. Furthermore, the landfill area lacks vegetation; therefore, the topology of the land primarily controls the water runoff and permeability, thus directly affecting soil erosion and surface and ground water.

Finally, this paper incorporated an MRSS and ANP to obtain a methodological framework with which to evaluate the landfill siting criteria. Compared with a traditional ANP, several additional benefits can be achieved using an MRSS-ANP model. First, this process can enhance handling of the vagueness and imprecision associated with the pairwise comparison process. Second benefit is addressing the interactions, interdependencies, and feedback among the decision evaluation criteria. Third, the combined approach can assist the decision makers to more confidently justify their decisions with minimum funds and expertise. This approach serves as a guide for applying the complex MCDM process to real-life and environmental problems in which the adequate participation of stakeholders and influence factors must be considered. This study represents a first attempt to combine statistical analysis with an ANP to prioritize landfill siting criteria, and further sensitivity analyses are suggested for future work.

Appendix

For details see Tables 8, 9, 10, and 11.

Conflict of Interests

The authors declare that there is no conflict of interests regarding the publication of this paper.

Acknowledgments

The authors thank Universiti Kebangsaan Malaysia (UKM) and the Malaysian Ministry of Higher Education (MOHE) for funding through FRGS/1/2013/TK03/UKM/02/5.

References

[1] M. R. Khadivi and S. M. T. Fatemi Ghomi, "Solid waste facilities location using of analytical network process and data envelopment analysis approaches," *Waste Management*, vol. 32, no. 6, pp. 1258–1265, 2012.

[2] A. Afzali, J. M. V. Samani, and M. Rashid, "Municipal landfill site selection for isfahan city by use of fuzzy logic and analytic hierarchy process," *Iranian Journal of Environmental Health Science & Engineering*, vol. 8, no. 3, pp. 273–284, 2011.

[3] M. Colebrook and J. Sicilia, "Undesirable facility location problems on multicriteria networks," *Computers & Operations Research*, vol. 34, no. 5, pp. 1491–1514, 2007.

[4] S. T. Tan, H. Hashim, J. S. Lim, W. S. Ho, C. T. Lee, and J. Yan, "Energy and emissions benefits of renewable energy derived from municipal solid waste: analysis of a low carbon scenario in Malaysia," *Applied Energy*, vol. 136, pp. 797–804, 2014.

[5] K. Hadjibiros, D. Dermatas, and C. Laspidou, "Municipal solid waste management and landfill site selection in Greece: irrationality versus efficiency," *Global NEST Journal*, vol. 13, pp. 150–161, 2011.

[6] A. Al-Hanbali, B. Alsaaideh, and A. Kondoh, "Using GIS-based weighted linear combination analysis and remote sensing techniques to select optimum solid waste disposal sites within Mafraq City, Jordan," *Journal of Geographic Information System*, vol. 3, no. 4, pp. 267–278, 2011.

[7] D. Geneletti, "Combining stakeholder analysis and spatial multicriteria evaluation to select and rank inert landfill sites," *Waste Management*, vol. 30, no. 2, pp. 328–337, 2010.

[8] Y. Anifowose, K. Omole, and O. Akingbade, "Waste disposal site selection using remote sensing and GIS: a study of akure and its environs, Southwest-Nigeria," in *Proceedings of the COLERM*, vol. 2, pp. 526–533, 2012.

[9] M. I. Yesilnacar, M. L. Süzen, B. Ş. Kaya, and V. Doyuran, "Municipal solid waste landfill site selection for the city of Şanliurfa-Turkey: An example using MCDA integrated with GIS," *International Journal of Digital Earth*, vol. 5, no. 2, pp. 147–164, 2012.

[10] N. Holman, "Community participation: using social network analysis to improve developmental benefits," *Environment and Planning C: Government & Policy*, vol. 26, no. 3, pp. 525–543, 2008.

[11] T. L. Saaty, *Theory and Applications of the Analytic Network Process: Decision Making with Benefits, Opportunities, Costs, and Risks*, RWS Publications, 2005.

[12] T. L. Saaty, "Rank from comparisons and from ratings in the analytic hierarchy/network processes," *European Journal of Operational Research*, vol. 168, no. 2, pp. 557–570, 2006.

[13] C.-W. Tsui and U.-P. Wen, "A hybrid multiple criteria group decision-making approach for green supplier selection in the

TFT-LCD industry," *Mathematical Problems in Engineering*, vol. 2014, Article ID 709872, 13 pages, 2014.

[14] M. A. B. Promentilla, T. Furuichi, K. Ishii, and N. Tanikawa, "A fuzzy analytic network process for multi-criteria evaluation of contaminated site remedial countermeasures," *Journal of Environmental Management*, vol. 88, no. 3, pp. 479–495, 2008.

[15] G. Tuzkaya, S. Önüt, U. R. Tuzkaya, and B. Gülsün, "An analytic network process approach for locating undesirable facilities: an example from Istanbul, Turkey," *Journal of Environmental Management*, vol. 88, no. 4, pp. 970–983, 2008.

[16] S. Khan and M. N. Faisal, "An analytic network process model for municipal solid waste disposal options," *Waste Management*, vol. 28, no. 9, pp. 1500–1508, 2008.

[17] A. Aydi, M. Zairi, and H. B. Dhia, "Minimization of environmental risk of landfill site using fuzzy logic, analytical hierarchy process, and weighted linear combination methodology in a geographic information system environment," *Environmental Earth Sciences*, vol. 68, no. 5, pp. 1375–1389, 2013.

[18] P. V. Gorsevski, K. R. Donevska, C. D. Mitrovski, and J. P. Frizado, "Integrating multi-criteria evaluation techniques with geographic information systems for landfill site selection: a case study using ordered weighted average," *Waste Management*, vol. 32, no. 2, pp. 287–296, 2012.

[19] O. E. Demesouka, A. P. Vavatsikos, and K. P. Anagnostopoulos, "Suitability analysis for siting MSW landfills and its multicriteria spatial decision support system: method, implementation and case study," *Waste Management*, vol. 33, no. 5, pp. 1190–1206, 2013.

[20] M. Eskandari, M. Homaee, S. Mahmoodi, and E. Pazira, "Integrating GIS and AHP for municipal solid waste landfill site selection," *Journal of Basic and Applied Scientific Research*, vol. 3, no. 4, pp. 588–595, 2013.

[21] K. Ibrahim, M. Syam, and A. I. Al-Omari, "Estimating the population mean using stratified median ranked set sampling," *Applied Mathematical Sciences*, vol. 4, no. 45–48, pp. 2341–2354, 2010.

[22] K. Ibrahim, "On comparison of some variation of ranked set sampling," *Sains Malaysiana*, vol. 40, no. 4, pp. 397–401, 2011.

[23] C. E. Husby, E. A. Stasny, and D. A. Wolfe, "An application of ranked set sampling for mean and median estimation using USDA crop production data," *Journal of Agricultural, Biological, and Environmental Statistics*, vol. 10, no. 3, pp. 354–373, 2005.

[24] S. S. Hossain and H. A. Muttlak, "Hypothesis tests on the scale parameter using median ranked set sampling," *Statistica*, vol. 66, no. 4, pp. 415–433 (2007), 2006.

[25] J. V. Deshpande, J. Frey, and O. Ozturk, "Nonparametric ranked-set sampling confidence intervals for quantiles of a finite population," *Environmental and Ecological Statistics*, vol. 13, no. 1, pp. 25–40, 2006.

[26] R. Murray, M. Ridout, and J. Cross, "The use of ranked set sampling in spray deposit assessment," *Aspects of Applied Biology*, vol. 57, pp. 141–146, 2000.

[27] D. A. Wolfe, "Ranked set sampling: its relevance and impact on statistical inference," *ISRN Probability and Statistics*, vol. 2012, Article ID 568385, 32 pages, 2012.

[28] N. A. Mode, L. L. Conquest, and D. A. Marker, "Incorporating prior knowledge in environmental sampling: ranked set sampling and other double sampling procedures," *Environmetrics*, vol. 13, no. 5-6, pp. 513–521, 2002.

[29] M. N. A. Azman, M. S. S. Ahamad, T. A. Majid, A. S. Yahaya, and M. H. Hanafi, "Statistical evaluation of pre-selection criteria for industrialized building system (IBS)," *Journal of Civil Engineering and Management*, vol. 19, no. 1, pp. S131–S140, 2013.

[30] M. Mutlutürk and R. Karagüzel, "The Landfill Area Quality (LAQ) classification approach and its application in Isparta, Turkey," *Environmental & Engineering Geoscience*, vol. 13, no. 3, pp. 229–240, 2007.

[31] Z. Adeli and A. M. Khorshiddoust, "Application of geomorphology in urban planning: case study in landfill site selection," *Procedia—Social and Behavioral Sciences*, vol. 19, pp. 662–667, 2011.

[32] M. Zamorano, E. Molero, Á. Hurtado, A. Grindlay, and Á. Ramos, "Evaluation of a municipal landfill site in Southern Spain with GIS-aided methodology," *Journal of Hazardous Materials*, vol. 160, no. 2-3, pp. 473–481, 2008.

[33] A. A. Isalou, V. Zamani, B. Shahmoradi, and H. Alizadeh, "Landfill site selection using integrated fuzzy logic and analytic network process (F-ANP)," *Environmental Earth Sciences*, vol. 68, no. 6, pp. 1745–1755, 2013.

[34] Ş. Şener, E. Şener, B. Nas, and R. Karagüzel, "Combining AHP with GIS for landfill site selection: a case study in the Lake Beyşehir catchment area (Konya, Turkey)," *Waste Management*, vol. 30, no. 11, pp. 2037–2046, 2010.

[35] B. Nas, T. Cay, F. Iscan, and A. Berktay, "Selection of MSW landfill site for Konya, Turkey using GIS and multi-criteria evaluation," *Environmental Monitoring and Assessment*, vol. 160, no. 1–4, pp. 491–500, 2010.

[36] M. A. Alanbari, N. Al-Ansari, and H. K. Jasim, "GIS and multicriteria decision analysis for landfill site selection in Al-Hashimyah Qadaa," *Natural Science*, vol. 6, no. 5, pp. 282–304, 2014.

[37] S. P. S. Kushwah, K. Rawat, and P. Gupta, "Analysis and comparison of efficient techniques of clustering algorithms in data mining," *International Journal of Innovative Technology and Exploring Engineering*, vol. 1, no. 3, pp. 109–113, 2012.

[38] M. Sevkli, A. Oztekin, O. Uysal, G. Torlak, A. Turkyilmaz, and D. Delen, "Development of a fuzzy ANP based SWOT analysis for the airline industry in Turkey," *Expert Systems with Applications*, vol. 39, no. 1, pp. 14–24, 2012.

[39] T. L. Saaty and K. Peniwati, *Group Decision Making: Drawing Out and Reconciling Differences*, RWS Publications, 2013.

[40] R. Liu, J.-X. Yu, H.-C. Sun, and P. Tian, "Introduction to the ANP super decisions software and its application," *Systems Engineering-Theory & Practice*, vol. 8, article 024, 2003.

[41] H. Shahabi, S. Keihanfard, B. B. Ahmad, and M. J. T. Amiri, "Evaluating Boolean, AHP and WLC methods for the selection of waste landfill sites using GIS and satellite images," *Environmental Earth Sciences*, vol. 71, no. 9, pp. 4221–4233, 2014.

[42] Department of Environment, *EIA Guidelines for Development of Solid Waste Sanitary Landfill*, Department of Environment, Ministry of Natural Resources and Environment, Putrajaya, Malaysia, 2012.

[43] S. P. Gbanie, P. B. Tengbe, J. S. Momoh, J. Medo, and V. T. S. Kabba, "Modelling landfill location using Geographic Information Systems (GIS) and Multi-Criteria Decision Analysis (MCDA): case study Bo, Southern Sierra Leone," *Applied Geography*, vol. 36, pp. 3–12, 2013.

[44] C. Simsek, A. Elci, O. Gunduz, and N. Taskin, "An improved landfill site screening procedure under NIMBY syndrome constraints," *Landscape and Urban Planning*, vol. 132, pp. 1–15, 2014.

[45] T. L. Saaty, "Decision making with the analytic hierarchy process," *International Journal of Services Sciences*, vol. 1, no. 1, pp. 83–98, 2008.

[46] S. N. Ismail, *Assessing environmental impacts and siting consideration for landfill in Developing Countries: a case study of Malaysia [Ph.D. thesis]*, University of East Anglia, Norwich, UK, 2011.

[47] B. Nadi, A. Mahmud, N. Ahmad, B. Farjad, B. Arvinpil, and A. Amani, "Managing of urban solid waste by geoinformatics technology," *International Geoinformatics Research and Development Journal*, vol. 1, pp. 70–80, 2010.

[48] T. Z. Vasiljević, Z. Srdjević, R. Bajčetić, and M. V. Miloradov, "GIS and the analytic hierarchy process for regional landfill site selection in transitional countries: a case study from Serbia," *Environmental Management*, vol. 49, no. 2, pp. 445–458, 2012.

[49] A. Afzali, S. Sabri, M. Rashid, J. M. V. Samani, and A. N. M. Ludin, "Inter-municipal landfill site selection using analytic network process," *Water Resources Management*, vol. 28, no. 8, pp. 2179–2194, 2014.

[50] M. Sophocleous, "Interactions between groundwater and surface water: the state of the science," *Hydrogeology Journal*, vol. 10, no. 1, pp. 52–67, 2002.

[51] M. S. Reed, "Stakeholder participation for environmental management: a literature review," *Biological Conservation*, vol. 141, no. 10, pp. 2417–2431, 2008.

[52] V. Luyet, R. Schlaepfer, M. B. Parlange, and A. Buttler, "A framework to implement Stakeholder participation in environmental projects," *Journal of Environmental Management*, vol. 111, pp. 213–219, 2012.

[53] D. Maxwell and J. Parker, "Coordination in food security crises: a stakeholder analysis of the challenges facing the global food security cluster," *Food Security*, vol. 4, no. 1, pp. 25–40, 2012.

[54] Z. Chen, "The efficiency of ranked-set sampling relative to simple random sampling under multi-parameter families," *Statistica Sinica*, vol. 10, no. 1, pp. 247–264, 2000.

[55] A. Johari, H. Alkali, H. Hashim, S. I. Ahmed, and R. Mat, "Municipal solid waste management and potential revenue from recycling in Malaysia," *Modern Applied Science*, vol. 8, no. 4, p. 37, 2014.

[56] A. Pariatamby and M. Tanaka, *Municipal Solid Waste Management in Asia and the Pacific Islands*, Environmental Science, Springer, Singapore, 2014.

[57] J. S. Lim and P. Missios, "Does size really matter? Landfill scale impacts on property values," *Applied Economics Letters*, vol. 14, no. 10, pp. 719–723, 2007.

[58] M. Gardašević-Filipović and D. Z. Šaletić, "Multicriteria optimization in a fuzzy environment: the fuzzy analytic hierarchy process," *Yugoslav Journal of Operations Research*, vol. 20, no. 1, 2010.

Hindawi Publishing Corporation
Mathematical Problems in Engineering
Volume 2015, Article ID 362579, 16 pages
http://dx.doi.org/10.1155/2015/362579

Review Article

Solving Civil Engineering Problems by Means of Fuzzy and Stochastic MCDM Methods: Current State and Future Research

Jurgita Antucheviciene,[1] Zdeněk Kala,[2] Mohamed Marzouk,[3] and Egidijus Rytas Vaidogas[4]

[1]*Department of Construction Technology and Management, Faculty of Civil Engineering, Vilnius Gediminas Technical University, Saulėtekio Alėja 11, LT-10223 Vilnius, Lithuania*
[2]*Department of Structural Mechanics, Faculty of Civil Engineering, Brno University of Technology, Veveří Street 95, 602 00 Brno, Czech Republic*
[3]*Department of Structural Engineering, Faculty of Engineering, Cairo University, Giza 12613, Egypt*
[4]*Department of Labour Safety and Fire Protection, Faculty of Civil Engineering, Vilnius Gediminas Technical University, Saulėtekio Alėja 11, LT-10223 Vilnius, Lithuania*

Correspondence should be addressed to Jurgita Antucheviciene; jurgita.antucheviciene@vgtu.lt

Received 9 May 2015; Accepted 11 June 2015

Academic Editor: Peide Liu

The present review examines decision-making methods developed for dealing with uncertainties and applied to solve problems of civil engineering. Several methodological difficulties emerging from uncertainty quantification in decision-making are identified. The review is focused on formal methods of multiple criteria decision-making (MCDM). Handling of uncertainty by means of fuzzy logic and probabilistic modelling is analysed in light of MCDM. A sensitivity analysis of MCDM problems with uncertainties is discussed. An application of stochastic MCDM methods to a design of safety critical objects of civil engineering is considered. Prospects of using MCDM under uncertainty in developing areas of civil engineering are discussed in brief. These areas are design of sustainable and energy efficient buildings, building information modelling, and assurance of security and safety of built property. It is stated that before long the decision-making in civil engineering may face several methodological problems: the need to combine fuzzy and probabilistic representations of uncertainties in one decision-making matrix, the necessity to extend a global sensitivity analysis to all input elements of a MCDM problem with uncertainties, and an application of MCDM methods in the areas of civil engineering where decision-making under uncertainty is presently not common.

1. Introduction

Decision-making is applied in different areas of human activities. In the case of existence of at least two possible options, a person (i.e., a decision-maker) has to make a decision and to select the one which is best suited for his demands. Complex problems in science, engineering, technology, or management are characterised by multiple criteria. Usually they are hardly measurable, conflicting or interacting with each other. Decision-making (DM) problems based on multiple criteria are objects of MCDM.

MCDM is a discipline concerned with the theory and methodology for handling problems common in everyday life. They arise in such areas as business, engineering, social organisation, and so forth [1]. MCDM has grown as a part of operation research pertaining to the design of computational and mathematical tools for supporting the subjective evaluation of performance criteria by decision-makers [2].

As it is mentioned in a review paper [3], the origins of MCDM methods can be dated over 270 years ago. As an individual scientific discipline, MCDM has been widely spreading since the middle of the previous century. Numerous works on MCDM are summarized in a number of review papers [4]. Three main types of review papers related to MCDM can be distinguished: reviews of developments and extensions of a particular method (e.g., [5]) as well as its applications (e.g., [6, 7]); reviews of different approaches to modern MCDM methods (e.g., DM under uncertain and

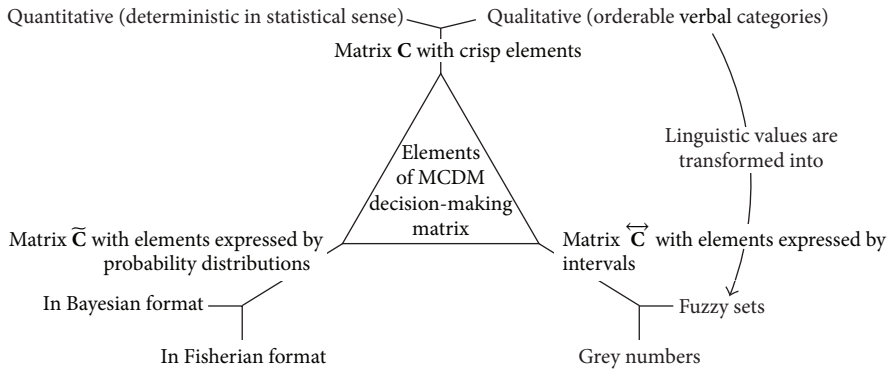

Figure 1: The main types of criteria used to construct the decision-making matrix of MCDM.

incomplete information and DM for groups of persons [2, 8]); reviews of applications of different MCDM methods for a particular problem [9–11].

Most, if not all, decisions in engineering are made under uncertainty. Accordingly, classical crisp methods, involving deterministic conditions under certain decision environments, are losing their relevance and new extensions for handling various types of uncertainties in MCDM problems appear. In most cases, uncertain elements of MCDM problems express subjective expert opinions and less often they represent stochastic nature of input data. Understanding the significance and impact of different types of uncertainties in input information and its relation to reality can increase the quality of DM process.

The present review strives to examine the current state of uncertainty modelling in MCDM and to identify several problems which decision-makers may face in the immediate future. The review is organized as follows. Section 2 presents the scope of the review and identifies several problems related to MCDM under uncertainty. Section 3 presents the latest references on applications of MCDM approaches in uncertain decision environments of civil engineering. Section 4 summarizes the applications of sensitivity analysis (SA) in fuzzy and stochastic MCDM techniques. Section 5 analyses published work on introducing measures of risk and reliability in the MCDM related to civil engineering. Section 6 attempts to identify the need for future research. This section presents a brief discussion on potential applications of MCDM under uncertainty in the areas which currently receive much attention in research and practice. Finally, conclusions and prospective research trends are presented in Section 7.

2. The Scope of the Review

Generally, a MCDM problem is defined as follows. Let $\mathbf{a} = (a_1, a_2, \ldots, a_i, \ldots, a_m)^{\mathrm{T}}$ be a vector of decision alternatives and $\mathbf{c} = (c_1, c_2, \ldots, c_j, \ldots, c_n)$ a set of criteria, according to which suitability of alternatives a_i is to be judged. The problem is stated as a $m \times n$ decision-making matrix $\mathbf{C}$ with the elements c_{ij}. The value c_{ij} expresses an impact of the criterion c_j on the alternative a_i. Values of $\mathbf{c}$ related to the alternatives a_i are the row vectors $\mathbf{c}_i = (c_{i1}, c_{i2}, \ldots, c_{ij}, \ldots, c_{in})$ and, with these vectors, the matrix $\mathbf{C}$ is formulated as $[\mathbf{c}_1, \mathbf{c}_2, \ldots, \mathbf{c}_j, \ldots, \mathbf{c}_m]^{\mathrm{T}}$. In many MCDM methods, the importance of the criteria c_j is expressed by the weights w_j which sum up to unity and are usually grouped into the vector $\mathbf{w} = (w_1, w_2, \ldots, w_j, \ldots, w_n)$. The purpose of DM is to determine the most preferable alternative among a_i with respect to all criteria or to rank the alternatives. The result of ranking is expressed by a preference sequence, for example, π: $a_x \succ a_y \succ a_z \succ \cdots$.

A large variety of MCDM methods have been developed to date. A universal and comprehensive classification of these methods does not exist. For the purposes of the present review, MCDM methods will be classified according to the nature of the criteria grouped into the decision-making matrix $\mathbf{C}$ (Figure 1). In the previous five decades, a development of MCDM was focused mainly on solving MCDM problems with crisp elements of $\mathbf{C}$. In parallel with this process, fuzzy MCDM methods have been developed since 1970s [12]. These methods allow solving MCDM problems with a decision-making matrix $\overleftrightarrow{\mathbf{C}}$, the elements of which are modelled by fuzzy sets. Development and application of fuzzy MCDM methods significantly increased during the last two-three decades. One of the possible representations of c_{ij} by fuzzy sets is grey numbers based on interval arithmetic. Several recent publications devoted to a use of grey numbers for decision-making in engineering can be cited here [13–15]. Finally, in the recent time, several MCDM methods were created and applied to a solution of decision-making problems, in which elements of $\mathbf{C}$ are modelled by means of probability distributions. Such a matrix will be denoted by the symbol $\widetilde{\mathbf{C}}$.

The fact that until now uncertainties in MCDM problems were expressed in several different ways generates a problem of choosing among these possibilities. Further problems related to handling uncertainties in decision-making are illustrated in Figure 2. A decision-maker having to rank the alternatives a_i in the presence of uncertainties may face the following problems:

(1) The problem of choice among different representations of uncertainty related to criteria values c_{ij} and weights w_j.

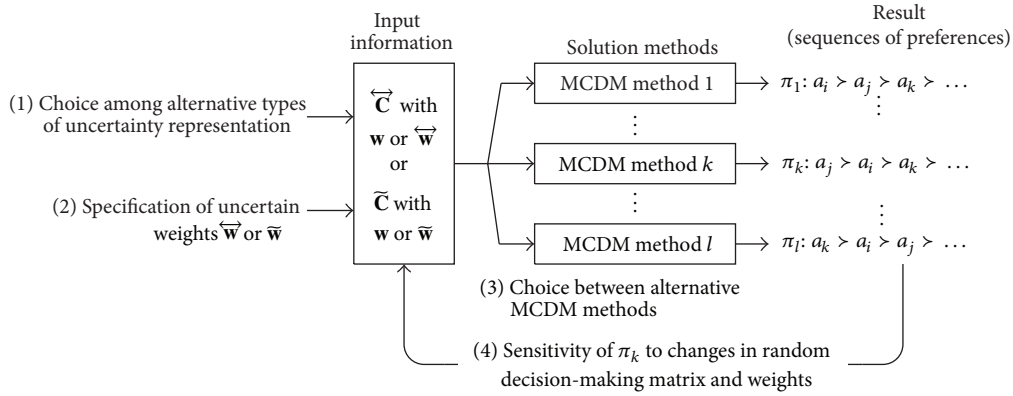

Figure 2: Four problems related to handling uncertainties in MCDM.

(2) Specification of the weights w_j in the case where they are uncertain quantities.

(3) The problem of choice among available MCDM methods for solving a problem with the decision-making matrices $\overleftrightarrow{\mathbf{C}}$ or $\widetilde{\mathbf{C}}$.

(4) Analysis of sensitivity of MCDM results to the changes in all elements of input data given by the matrices $\overleftrightarrow{\mathbf{C}}$ or $\widetilde{\mathbf{C}}$ and the vectors $\mathbf{w}$, $\overleftrightarrow{\mathbf{w}}$, or $\widetilde{\mathbf{w}}$. Input uncertainties can cause possible permutations in the sequences of preferences, π_k, obtained by means of a specific MCDM method k.

The first problem has its origin "outside" the domain of MCDM. Discussions of the type "fuzzy versus probabilistic" or "nonprobabilistic versus probabilistic" last many years and do not seem to be finished until now (e.g., [16]). In most applications of MCDM under uncertainty, authors do not trouble themselves to explain why a particular method of uncertainty quantification was preferred over others. The fuzzy logic prevails over probabilistic modelling by the number of MCDM methods developed to date and the number of MCDM applications to practical problems. Currently, one can state the obvious that probability distributions can be specified in Fisherian format for c_{ij} in the presence of sufficient amount of statistical data on c_{ij}. A representation of c_{ij} by fuzzy sets is better suited for c_{ij} expressing subjective expert opinions. However, it is important to remember that the Bayesian approach to probabilistic modelling has excellent means of quantifying and updating subjective judgments (e.g., [17]). This approach does not break down when data on c_{ij} is sparse or absent. MCDM problems can be solved when uncertainties in c_{ij} are represented in any of the aforementioned formats. A true problem will arise when the decision-making matrix will be a "mixture" of the elements c_{ij} expressed by different means of uncertainty quantification, probabilistic and nonprobabilistic.

The second problem of specifying elements of the vector of weights, $\mathbf{w}$, is obviously an "internal" problem of MCDM. There is a body of literature devoted to specifying values of w_j. Methods used to determine criteria weights are classified into subjective, objective, and hybrid or integrated ones [18–20]. However, the task of assigning specific values to the components w_j will always be subjective or at least partly subjective, no matter what is the degree of mathematical sophistication behind this assignment. A really intriguing question is how w_j can be interpreted as uncertain quantities. The experts who usually specify the values of w_j can be uncertain (vague) regarding their opinions on w_j. Should weights be modelled by a fuzzy vector $\overleftrightarrow{\mathbf{w}}$ or a vector $\widetilde{\mathbf{w}}$ with components expressed by probability distributions?

The third problem reflects the well-known decision-making paradox which was first identified by Triantaphyllou and Mann in 1989 [21]. The paradox was exhibited by many MCDM methods developed to deal with the crisp decision-making matrix $\mathbf{C}$. Switching to uncertain matrices $\overleftrightarrow{\mathbf{C}}$ or $\widetilde{\mathbf{C}}$ will not resolve this paradox. It will be likely to persist also in the field of decision-making under uncertainty. The present review will not address this tricky issue.

The fourth problem arises naturally, because a MCDM method is in essence a mathematical model relating the input information expressed by $\mathbf{C}$ and $\mathbf{w}$ to the output information given by the preference sequence π. A sensitivity of π to changes in elements of $\mathbf{C}$ and $\mathbf{w}$ can be estimated (analysed) by standard mathematical means of general use. However, a sensitivity analysis (SA) of a MCDM problem with uncertain matrices $\overleftrightarrow{\mathbf{C}}$ or $\widetilde{\mathbf{C}}$ and/or uncertain vectors $\overleftrightarrow{\mathbf{w}}$ or $\widetilde{\mathbf{w}}$ is a nontrivial task.

The four problems of MCDM under uncertainty listed and briefly discussed above are of methodological nature. This kind of DM can face also problems of different nature, namely, an application in such areas of civil engineering as development of sustainable and energy efficient buildings, building information modelling, assurance of security, and safety of built property. Solving MCDM problems in these areas will face the necessity to model uncertainties related to long-term predictions, vague information available in the process of building design, and possibility of rare but extremely damaging events. A particular need for modelling uncertainties in MCDM problems arises at a design of safety critical objects of civil engineering. Failures of such objects or damage to them can cause severe consequences to

society and environment. Many of safety critical objects are assessed (designed) by applying methods of reliability theory or probabilistic risk assessment. Measures of reliability and components of risk estimates can be uncertain quantities. An application of MCDM to the design of safety critical objects requires including these quantities into the decision-making matrix $\mathbf{C}$. In most cases, uncertainties related to reliably and risk are modelled by means of probability distributions. Therefore, the decision-making matrix will be formulated as the matrix $\widetilde{\mathbf{C}}$. A combination of SA and MCDM applied to the design of the safety critical objects will allow revealing the most important MCDM criteria related to safety.

The following sections of this review will consider the problems raised above in greater detail. The attention will be focused on both results achieved until now and problematic issues which may require attention in the future.

3. MCDM Techniques under Uncertainty in Civil Engineering

Decision-making in the field of civil engineering is increasingly complex and is associated with situations where robust decisions are required to be taken. These decisions are made in different stages of civil engineering projects. For example, decision-making takes place during feasibility study stage prior to design, procurement, and construction stages in order to determine the viability of project undertaken by an investor. Also it often faces the need to deal with hazardous phenomena, including industrial accidents able to damage built property, structural failures, extreme natural phenomena, and human acts affecting security. Proper decisions made by architects and civil engineers may reduce the risk posed by the aforementioned phenomena.

Decision-making in this field can be facilitated by an application of formal methods, such as methods of multiple criteria decision-making. Factors relevant to decisions can be identified using the methods of uncertainty and SA of mathematical model outputs.

The result of the evaluation of an alternative according to a given criteria is a single value (e.g., number or verbal expressions) for unambiguous deterministic information. For ambiguous information, the result of the evaluation of variants according to a given criteria is a random variable if the information is stochastic in nature or a fuzzy variable if the information is nonstochastic in nature. The stochastic nature of a phenomenon is associated with the unlimited repeatability of the phenomenon. Unrepeatable phenomena or phenomena with uncertain knowledge significance are nonstochastic in nature.

3.1. Fuzzy MCDM. The fuzzy framework is the most common approach to describe and handle uncertainty in MCDM. Considering the imprecisions and uncertainties, that is, fuzziness of the available data and the decision-making procedures, fuzzy set theory can be applied [22]. In a fuzzy MCDM, the elements c_{ij} of $\mathbf{C}$ are characterised by fuzzy sets. In what follows, such elements will be denoted by the symbol $\overleftrightarrow{c_{ij}}$ and a decision-making matrix containing fuzzy elements will be $\overleftrightarrow{\mathbf{C}}$. The fuzzy set theory can be used for a MCDM, whenever probability distributions of c_{ij} are unknown due to lack of statistical data or there is no wish to express subjective judgments about values of c_{ij} in a probabilistic way. The weights w_j can also be modelled as fuzzy variables $\overleftrightarrow{w_j}$ and so the vector $\mathbf{w}$ can be a fuzzy one, $\overleftrightarrow{\mathbf{w}}$.

In MCDM problems, three types of fuzziness can be observed: the ratings of each alternative with respect to each criterion are uncertain or imprecise and weights are crisp numbers ($\overleftrightarrow{c_{ij}}$, w_j); the ratings of alternatives are crisp numbers while fuzzy numbers are used to assess the weights of all criteria (c_{ij}, $\overleftrightarrow{w_j}$); both the ratings and the weights are fuzzy ($\overleftrightarrow{c_{ij}}$, $\overleftrightarrow{w_j}$). Each type of uncertainty has its own characteristics and is appropriate for special cases.

A lot of fuzzy extensions of MCDM methods have been proposed and applied in engineering, technology, or management. Fuzzy extensions of MCDM involve application of basic fuzzy logic, using triangular fuzzy numbers and arithmetic operations, also trapezoidal fuzzy numbers, as well as intuitionistic fuzzy relations, interval-valued intuitionistic fuzzy relations, type-2 fuzzy sets, and hesitant fuzzy sets concepts. Nonfuzzy uncertain decision methods include reliability theory and probabilistic and grey-valued formulations for handling incomplete or imprecise information. The most widely applied fuzzy extensions of MCDM methods are fuzzy AHP (analytic hierarchy process), with the origins dated to 1983 [23] and various numerous extensions of fuzzy TOPSIS (technique for order preference by similarity to ideal solution) [2, 24]. Several latest extensions of more recently developed methods are worth to be mentioned: extension of weighted aggregated sum product assessment in an interval-valued intuitionistic fuzzy environment (WASPAS-IVIF) [25], a complex proportional assessment method extended with interval-valued intuitionistic fuzzy numbers (COPRAS-IVIF), and suitable for group decision-making [26]. The most recent extended versions of MULTIMOORA (multiobjective optimization by ratio analysis plus full multiplicative form) utilize the basic fuzzy logic [27, 28] or are based on the interval 2-tuple linguistic variables [29], intuitionistic fuzzy numbers [30], or hesitant fuzzy numbers [31]. ARAS under fuzzy environment was also presented [32] and further applied [33, 34].

Numerous researches utilize not a single fuzzy MCDM (FMCDM) method but combine several of the methods. Two groups of researches can be distinguished: either integrating two or more available techniques and proposing so-called hybrid methods or employing several methods for a solution of a problem and comparing ranking results. The study [2] reviews papers on development and applications of MCDM during the last two decades by various aspects. The analysis covers 1081 papers related to MCDM and fuzzy MCDM. While a detailed survey is made on 403 papers published in peer review journals and entirely devoted to fuzzy decisions, involving 217 papers in a field of engineering, it is obvious that engineering applications cover over 50 percent of overall applications. Accordingly, it can be stated that fuzzy MCDM

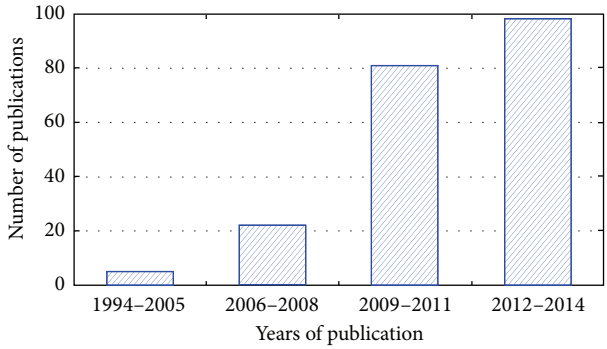

Figure 3: Increase of FMCDM applications in engineering.

is useful and applicable technique for complex decision-making in civil engineering under uncertainty.

The increasing importance of the methods can be based on the findings that the number of developments and applications is increasing every year. On the basis of collected data [2], annual distribution of papers in engineering field is explored. The period is divided into several stages. The first stage covers 1994–2005, when a number of papers are small or even absent in certain years. The later period starting from 2006, when a number of researches began increasing, is grouped in three years. A chart (Figure 3) shows increase of FMCDM applications in engineering, measured by a number of publications included in the review paper [2] on FMCDM techniques and applications during two decades.

The last period from the above four covers 46 percent of publications issued during 20 years. The largest number of researches on the whole is observed in 2014.

The latest FMCDM approaches are applied in various subfields of civil engineering field. Subfields which are the most numerously supported by considered approaches are related to sustainability and building lifecycle assessment, supply chain management in construction, technology and inventory selection in construction industries, location selection and infrastructure modelling, and knowledge management.

Environmental, social and economic aspects of sustainable building were incorporated when evaluating mining projects and their impact on environment [35], assessing building energy performance [36] or performance of pavements with emphasis on sustainability [37].

Supply chain management is handled through proper supplier selection considering multiple criteria simultaneously. Various approaches are applied for supplier evaluation and selection, starting from the most common fuzzy AHP and hybrid methods integrating AHP and TOPSIS [38], AHP and PROMETHEE [39], and so forth. Also novel extensions based on interval type-2 fuzzy sets [40] or intuitionistic fuzzy information [41] are utilized.

Selection of technologies, inventory, or materials in construction is also widely supported by FMCDM. Examples of the most recent applications are for selecting material handling equipment [42, 43], inventory classification [44], and selection of robots for automated technology operations [45].

Fuzzy decision-making methods are extremely important for handling vagueness in special-purpose building projects and their location. Fuzzy multiple criteria approaches successfully applied for nuclear power plant site selection [46], deep-water see port selection [47], and health monitoring of tunnels [48].

Regarding DM methodology in civil engineering applications, it can be concluded that the most common approach is observed to be fuzzy AHP-TOPSIS hybrid technique [38, 49], also combining fuzzy AHP with other classical methods as PROMETHEE [50] and DEMATEL [51, 52].

Another group of researches applies several FMCDM methods simultaneously and compares ranking results. An example can be provided of material selection applying a number of hybrid approaches, namely, FAHP-VIKOR, FAHP-PROMETHEE, FAHP-TOPSIS, and FAHP-ELECTRE [53], technology selection applying FAHP, TOPSIS-F, VIKOR-F, and COPRAS-G [45], and so forth.

3.2. Stochastic MCDM. The probabilistic framework is the second approach to describe and handle uncertainty in MCDM. In this framework, the elements c_{ij} of the decision-making matrix $\mathbf{C}$ are modelled by random variables $\widetilde{c}_{ij}$ expressing uncertainty in possible values of c_{ij}. The uncertainty is quantified by means of probability distributions which can be specified in the format Fisherian or Bayesian statistics. Presence of $\widetilde{c}_{ij}$ in $\mathbf{C}$ generates a matrix $\widetilde{\mathbf{C}}$, all or some elements of which are random. Stochastic MCDM methods are used to solve the decision problems with the matrix $\widetilde{\mathbf{C}}$.

MCDM solved with an emphasis on stochastic uncertainty (SMCDM) is focused on decision problems of the selection of alternatives from several criteria that are mathematically described neither as crisp numbers nor as fuzzy numbers or linguistic variables but as random variables [54]. Stochastic methods for the determination of weights from various types of information on the character of the significance of criteria are effectively implemented especially in the AHP method. The classical AHP method lacks probability values for the distinction of adjacent alternatives in the final ranking [55]. Vargas [56] considered the case where members of the pairwise comparison matrix were random variables.

It should be noted that although random variables are considered, purely stochastic uncertainty of input data and decision-making procedures is rare. The occurrence of a random phenomenon is almost always accompanied by a certain degree of personal belief; therefore, the term subjective probability is sometimes used. The reason for the implementation of random variables in MCDM is the attempt to use methods of the theory of probability and mathematical statistics for the analysis of uncertainty of the results of the decision-making process. Advanced methods of stochastic SA, the equivalent of which is unknown in fuzzy MCDM, are available for stochastic MCDM [57].

There are numerous SMCDM methods and applications in real world situations [58, 59]. The classical Monte Carlo (MC) method or its improved variants can be used to tackle most SMCDM problems [60, 61]. The theoretical application of the Monte Carlo method is very extensive; however,

the results of stochastic analysis are very sensitive to the laws of probability density functions and type of dependencies between input variables resulting in fuzzy (epistemic) uncertainty in decision-making tasks. Analysis of forecast uncertainty based on fuzzy stochastic approaches and its application to a number of problems in civil engineering and related fields is described in detail, for example, in the book [62]. However, the complexity of mathematical approaches and the interpretation of results limit the scientific ingenuity of the application of fuzzy stochastic SA methods.

4. Sensitivity Analysis Applied to MCDM

Two types of SA are most often mentioned in the literature: local SA and global SA (e.g., [63, 64]). Local SA determines a contribution of a given input parameter of a mathematical model to its output. Local methods do not attempt to fully explore the input parameter space. They examine small perturbations, usually one parameter at a time. Global SA examines a mathematical model in the presence of uncertain input parameters. SA of this type apportions output uncertainty to different sources of uncertainty in the input. Input and output uncertainties are expressed by probability distributions. Global SA applies perturbations of the entire space of input parameters. It is also argued that global SA should be used "in tandem" with uncertainty analysis and the latter should precede the former in practical applications [65, 66]. The aim of uncertainty analysis is to estimate variation in model output and SA apportions this variation to input parameters.

Local SA was applied in the recent past for better understanding of MCDM methods. Global SA was used for improving models which are related MCDM but do not fit strictly into its scheme. MCDM constitutes a special class of mathematical models. An application of SA to MCDM rises specific problems. However, any methodological specificity of performing SA for applications of MCDM in civil engineering is not known to us. In addition, combined applications of MCDM and SA to problems of civil engineering are few in number and deal mainly with selecting locations of buildings [67, 68]. A certain relation to civil engineering has applications of combined MCDM and SA to geographic information systems (see Malczewski and Rinner [69] and references cited therein). Therefore, the remainder of this section will be a general discussion on SA applications to a better understanding of MCDM methods.

4.1. Applications of SA in Deterministic MCDM and MCDM under Uncertainty. In the light of the aforementioned SA definitions, a deterministic (crisp) MCDM method can be interpreted as follows: elements of the matrix $\mathbf{C}$ and components of the vector $\mathbf{w}$ represent input parameters, the preference sequence π is model output, and the procedure relating π to $\mathbf{C}$ and $\mathbf{w}$ is a mathematical model. A sensitivity of π versus $\mathbf{C}$ and $\mathbf{w}$ is called ranking sensitivity or sensitivity to ranking stability (e.g., [70, 71]). With the deterministic input $\mathbf{C}$ and $\mathbf{w}$, a sensitivity of π versus $\mathbf{C}$ and $\mathbf{w}$ can be determined by means of local SA methods.

Triantaphyllou and Sánchez applied local SA to determine the criterion c_j and the decision matrix element c_{ij} which is most critical to the ranking expressed by π [72, 73]. They applied sensitivity measures based on minimum changes in the weights w_j and matrix elements c_{ij} which cause changes between ranks of the alternatives a_i. Bevilacqua and Braglia used a simple wide-range variation of the weights w_j to explore shifts in the ranking π obtained by means of a deterministic AHP [74]. Any numerical sensitivity measure or graphical representation of SA results was not suggested in this study. Chang et al. and Wu et al. carried out SA of AHP results based on increasing values of w_j up to 35% [67, 75]. They expressed SA results graphically. This approach was applied to SA of results obtained with fuzzy decision-making matrix $\overleftrightarrow{\mathbf{C}}$ [71]. The results were produced by means of fuzzy TOPSIS and fuzzy AHP methods.

Another kind of perturbations used to reveal sensitivity of π versus w_j is exchanging positions of the weights within the vector $\mathbf{w}$. Choudhary and Shankar used such perturbations for results obtained with a combined fuzzy AHP and TOPSIS method [76]. A total of n_p perturbations produces a set of preference sequences π_p $(p = 1, 2, \ldots, n_p)$ which are treated as SA result and expressed graphically. In a series of methodologically similar articles, Awasthi et al. suggested using the sequences π_p for a final ranking of the alternatives a_i [68, 77–79]. The sequences π_p were obtained for a problem with fuzzy weights $\overleftrightarrow{\mathbf{w}}$ and fuzzy matrix $\overleftrightarrow{\mathbf{C}}$. The alternatives a_i were ranked by counting scores for each a_i according to its position in π_p. These authors also tried to use this scoring for a qualitative assessment of ranking sensitivity. However, any quantitative sensitivity measure was not suggested.

A quantitative measure of ranking sensitivity used in several studies is known as an average shift in ranks (ASR). Some of these studies fit into the scheme of MCDM and some have common elements with this field. In line with the notations used herein, ASR is expressed as the mean $m^{-1} \sum_{i=1}^{m} |r_i^{\varsigma} - r_i^{\mathrm{ref}}|$, where r_i^{ς} is the rank of the alternative a_i related to a perturbation ς and r_i^{ref} is the rank of a_i in a reference (base) ranking. Saisana et al. used ASR as a model output for a global SA [80]. ASR was computed on the basis of a composite indicator. The reference ranks r_i^{ref} were obtained from one specific application of the indicator. Ben-Arieh used ASR in the format of MCDM for sort of a local SA [81]. ASR was applied to pairwise comparisons of alternative rankings obtained with different linguistic quantifiers (probabilities). They were used for calculating the weights w_j. The ranks r_i^{ς} and r_i^{ref} were obtained using pairs of different linguistic quantifiers. Later on, the same approach was used by other authors for assessing ranking sensitivity to fuzzy linguistic quantifiers [82–84]. ASR was applied also to a global SA related to MCDM. Ligman-Zielinska suggested using ASR as a scalar representation of output ranking and computing a sensitivity index based on variance of ASR [65]. Unfortunately, values of ASR depend on the choice of the reference ranks r_i^{ref} and this introduces certain arbitrariness in the process of SA. Apart from ASR, an alternative and well-elaborated scalar measure expressing a sensitivity of

permutations within π to input of MCDM models is not known to us.

4.2. Sensitivity to Model Selection. One of the key problems of MCDM is a selection of method (model) relating input information expressed by $\mathbf{C}$ and $\mathbf{w}$ to the output ranking sequence π. If the MCDM method requires normalisation of the initial matrix $\mathbf{C}$, the analyst will also face the problem of choosing among several normalisation rules (formulas) (e.g., [85]). Using different normalisation rules may also contribute to the variability of ranks within the sequence π.

An application of fuzzy numbers as elements of the matrix $\overleftrightarrow{\mathbf{C}}$ and components of the vector $\overleftrightarrow{\mathbf{w}}$ will introduce an additional problem of model selection. Membership functions of fuzzy numbers, $\mu_{\overleftrightarrow{w}_j}(w_j)$ and $\mu_{\overleftrightarrow{c}_{ij}}(c_{ij})$, may not necessarily be triangular as in the most fuzzy MCDM applications (Links 1 and 2, Figure 4). The choice of the type of fuzzy numbers in $\overleftrightarrow{\mathbf{C}}$ and components of the vector $\overleftrightarrow{\mathbf{w}}$ is a subjective exercise and introduces arbitrariness into MCDM process. Similar statements can be made about the use of random variables in $\widetilde{\mathbf{C}}$ and $\widetilde{\mathbf{w}}$. A specification of MCDM model input will require selecting specific types of probability densities $f_{\widetilde{c}_{ij}}(c_{ij} \mid \mu_{ij}, \sigma_{ij})$ and $f_{\widetilde{w}_j}(w_j \mid \alpha_j, \beta_j)$ for decision matrix elements $\widetilde{c}_{ij}$ and criteria weights $\widetilde{w}_j$ (Links 3 and 4, Figure 4). In case of $\widetilde{w}_j$, the selection of distribution type and then specification of its parameters α_j and β_j will be purely subjective task. However, in some cases, statistical data on the random components $\widetilde{c}_{ij}$ of $\widetilde{\mathbf{C}}$ can be available. In such cases, distribution type of $\widetilde{c}_{ij}$ will be dictated by this data. Consequently, we can speak about three SA problems:

(1) Sensitivity of the ranking sequence π to the selection of MCDM method.

(2) Sensitivity of π to the choice of normalisation rule.

(3) Sensitivity of π to the selection of membership function type in case of fuzzy MCDM and probability density type in case of stochastic MCDM.

The first two problems will be present in both deterministic MCDM and MCDM under uncertainty. The third problem will arise with the need to introduce uncertainties in MCDM process. To the best of our knowledge, a systematic, in-depth solution of these three problems is not available in the MCDM literature to date.

Apart from model selection problem, the use of the membership functions $\mu_{\overleftrightarrow{w}_j}(w_j)$ and $\mu_{\overleftrightarrow{c}_{ij}}(c_{ij})$ and the density functions $f_{\widetilde{c}_{ij}}(c_{ij} \mid \mu_{ij}, \sigma_{ij})$ and $f_{\widetilde{w}_j}(w_j \mid \alpha_j, \beta_j)$ will give rise to a problem of assessing sensitivity of the ranking sequence π to parameters of these functions (Links 5 to 8, Figure 4). An association of all or some w_j and c_{ij} with two or more parameters of membership function or density function may substantially increase the dimensionality of input space. This can encumber SA process, especially in case of global SA. It will be necessary to assign additional distributions to this parameter in order to carry out Monte Carlo analysis of a MCDM model under study.

5. Measures of Risk and Reliability in the MCDM Related to Civil Engineering

Civil engineering systems can be damaged by deliberate assaults, actions induced during industrial accidents and extremes of nature. Damage to components of civil engineering systems induces mechanical and thermal actions called often abnormal or accidental ones. Incidents with abnormal actions are relatively rare, short-lasting, and usually unexpected events. They can cause serious harm and sometimes catastrophic consequences [86]. In terms of civil engineering, such incidents are called "abnormal situations" or "accidental situations." The latter term is used in the widely known standards ISO 2394 and ENV 1991-1. An adequate design of civil engineering systems for abnormal situations will result in resilient buildings and infrastructure able to avoid or absorb damage without undergoing a complete failure [87–89].

5.1. MCDM and Safety in Civil Engineering. The design of components of safety critical civil engineering systems for abnormal situations requires, among other things, comparing alternative design solutions of these components. In terms of MCDM, they can be called alternative designs or simply alternatives a_i $(i = 1, 2, \ldots, m)$. Interalternative comparisons of a_i must include criteria c_{ij} expressing safety of a_i or, alternatively, risk posed by a_i. The row vector of criteria, $\mathbf{c}_i = (c_{i1}, c_{i2}, \ldots, c_{ij}, \ldots, c_{in})$, will include also elements which are not necessarily related to safety, for instance, economic, functional, and aesthetic criteria.

The adequacy of the design of critical objects of civil engineering for abnormal situations is assured by applying methods of reliability theory and probabilistic risk assessment (PRA) [90]. These two fields of engineering are closely related and the criteria c_{ij} can be specified by applying methods developed in each of them.

Values of c_{ij} can be probabilities of failure or quantitative estimates of risk related to the designs a_i [91]. Practical applications of MCDM to the design for abnormal situations will face the problem of uncertainty related to failure probabilities and risk estimates. Quantitative measures of this uncertainty can be introduced into MCDM problems. A well-established platform of uncertainty modelling in PRA is the Bayesian statistical theory or, in brief, the Bayesian approach [92]. In line with this approach, the uncertainty in potential safety-related criteria c_{ij} is divided into two kinds: stochastic (aleatory) and state-of-knowledge (epistemic) uncertainty [93–96]. Uncertainties of either kind can be accommodated in MCDM problems.

5.2. An Integration of Reliability Measures and Related Quantities into MCDM. A failure probability $p_{\mathrm{f}i}$ characterising a particular alternative design a_i can be used as a MCDM criterion c_{ij} [85, 91]. A value of the failure probability $p_{\mathrm{f}i}$ assigned to the alternative a_i accounts for the possibility of its potential failures. The probability $p_{\mathrm{f}i}$ can be "mechanically" included into a MCDM problem as one of components of the vector $\mathbf{c}_i$. However, in many cases the probabilities $p_{\mathrm{f}i}$ will be uncertain in the epistemic sense. The uncertainty in $p_{\mathrm{f}i}$

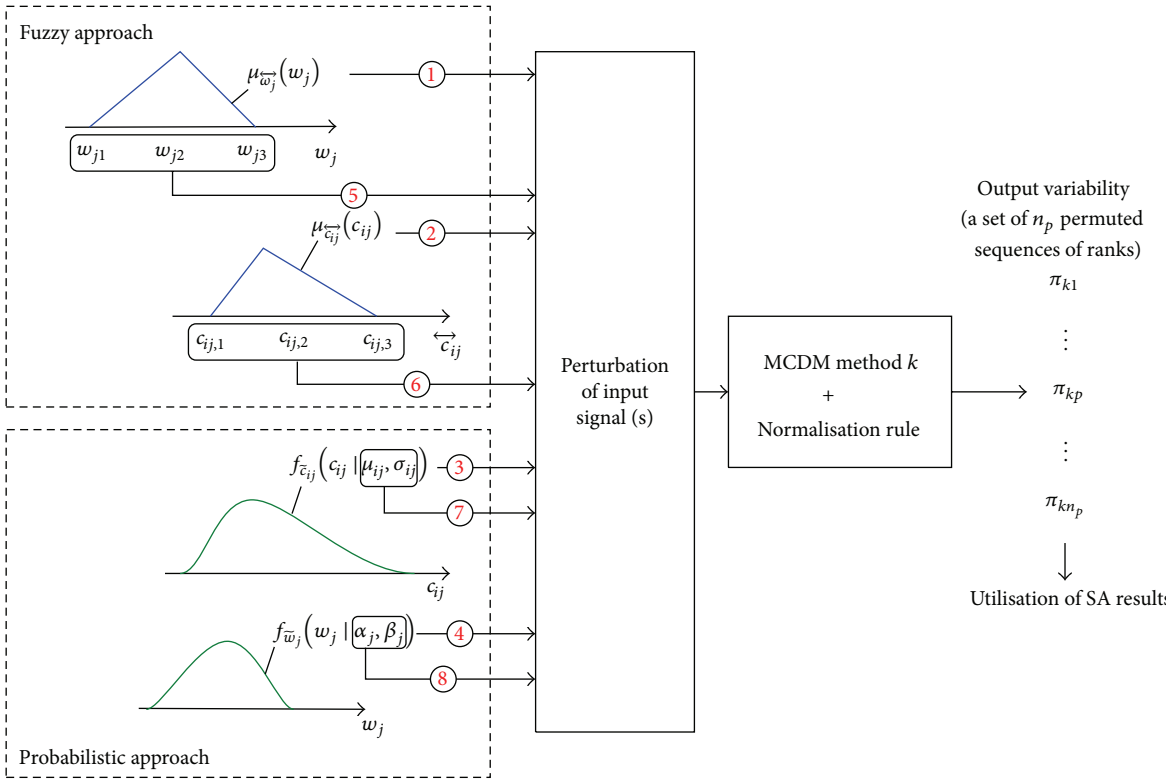

Figure 4: Possible SA links related to the input space of a MCDM problem and a specific MCDM method.

may stem primarily from sparse information on accidental actions. Quantitatively this uncertainty can be expressed by modelling the probabilities p_{fi} as epistemic random variables $\tilde{p}_{fi}$ [97]. If the uncertain failure probability $\tilde{p}_{fi}$ of a_i is taken as a MCDM criterion, the vectors $\mathbf{c}_i$ will contain at least one random component and can be replaced by the stochastic vectors $\tilde{\mathbf{c}}_i$ given by $(\tilde{p}_{fi1}, \tilde{p}_{fi2}, \ldots, \tilde{p}_{fik_i}, c_{k_i+1}, c_{k_i+2}, \ldots, c_{in})$, where k_i is the number of failure modes of a_i. Some or all criteria in the vector just mentioned can be uncertain in the stochastic (aleatory) sense. For instance, such criteria can be time of construction or cost of a_i. Uncertainty related to the stochastic components of $\tilde{\mathbf{c}}_i$ can be expressed by the random variables $\tilde{c}_{ij}$. With the random vectors $\tilde{\mathbf{c}}_i$, a MCDM problem will have to be solved by applying a decision-making matrix $\tilde{\mathbf{C}}$ some or all elements of which are random variables. Stochastic MCDM methods must be applied to deal with the matrix $\tilde{\mathbf{C}}$.

Vaidogas and Zavadskas suggested introducing the failure probabilities p_{fil} $(1 \leq l \leq k_i)$ into a MCDM problem indirectly, through comparison of the total (life-cycle) utilities $u_{\text{tot},i}$ related to the alternatives a_i [91]. The utility $u_{\text{tot},i}$ is expressed as a difference between expected benefit from a_i and a total cost of a_i. The failure probabilities p_{fil} are incorporated into the total cost of a_i through the cost of failures expressed by the sum $\sum_{l=1}^{k_i} p_{fil} c_{fl}$, where c_{fl} is the anticipated cost of failure according to the failure mode l.

Vaidogas et al. applied reliability-oriented MCDM for a selection among alternative construction projects of a building [85]. Reliability of the alternative projects a_i was expressed as a probability that a specified construction time will not be exceeded. A further application of MCDM was a ranking of designs of a reinforced concrete slab with different floorings. Probabilities of two failure modes of the slab were used as the criteria c_{ij}: probability of collapse and probability of excessive deflection.

5.3. An Integration of Risk Estimates into MCDM. The alternatives a_i can represent hazardous industrial objects which pose risk to people and environment in the form of industrial accidents. The magnitude of consequences of such accidents can range between minor and catastrophic consequences [98]. In the European Union, most of hazardous objects are regulated by Seveso Directives (currently Seveso III Directive) [99]. Such objects are assessed by means of formal methods developed in the field of PRA [93, 100].

A risk related to the design a_i is a very informative characteristic suitable for inclusion into a MCDM problem [98]. In line with PRA, the risk related to a_i is expressed by the set $\{(\lambda_{is}, c_{is}, \mathbf{m}_{is}), s = 1, 2, \ldots, n_{ai}\}$, in which λ_{is} and c_{is} are likelihood-consequence pairs, $\mathbf{m}_{is}$ are the vectors of magnitudes (severities) of c_{is}, and n_{ai} is the number of accident scenarios related to a_i. The vector $\mathbf{m}_{is}$ is given by a certain number n_s of magnitudes m_{isj} $(j = 1, 2, \ldots, n_s)$. Zavadskas and Vaidogas suggested expressing the criteria c_{ij} in the form of expected magnitudes $\overline{m}_{ij}$ [97]. The component c_{ij} of the decision-making matrix $\mathbf{C}$ represented by $\overline{m}_{ij}$ is computed as the sum $\sum_{s=1}^{n_{ai}} \lambda_{is} m_{isj}$.

As in the case of uncertain failure probabilities $\widetilde{p}_{fi}$, the likelihoods λ_{is} can be uncertain quantities modelled by epistemic random variables $\widetilde{\lambda}_{is}$. In most instances, the variables $\widetilde{\lambda}_{is}$ will represent uncertain annual frequencies of the consequences c_{is}. The presence of the random likelihood $\widetilde{\lambda}_{is}$ will stochastise the expected severities $\overline{m}_{ij}$ and they will turn into random variables, for example, $\widetilde{\overline{m}}_{ij}$. Consequently, a MCDM problem will turn into a stochastic one with a random decision-making matrix $\widetilde{\mathbf{C}}$. The row $\widetilde{\mathbf{c}}_i$ of $\widetilde{\mathbf{C}}$ will be expressed as $(\widetilde{\overline{m}}_{i1}, \widetilde{\overline{m}}_{i2}, \ldots, \widetilde{\overline{m}}_{in_s}, c_{i,n_s+1}, c_{i,n_s+2}, \ldots, c_{in})$ with $n - n_s \geq 1$, where the components denoted by the letter "c" can be either deterministic or stochastically uncertain quantities. With the vectors $\widetilde{\mathbf{c}}_i$ including the risk-related components $\widetilde{\overline{m}}_{ij}$, the matrix $\widetilde{\mathbf{C}}$ can be expressed as a two-block matrix $[\widetilde{\mathbf{C}}_1 \mid \mathbf{C}_2]$. The $m \times n_s$ matrix $\widetilde{\mathbf{C}}_1$ reflects risk estimates of the alternatives a_i, whereas the $m \times (n - n_s)$ matrix $\mathbf{C}_2$ includes criteria which are not directly related to the risk. Stochastic MCDM methods will be necessary to solve the MCDM problem with the matrix $[\widetilde{\mathbf{C}}_1 \mid \mathbf{C}_2]$.

Vaidogas and Šakėnaitė applied the risk-based MCDM to a choice among alternative sprinkler systems [101]. Zhou et al. used a safety-oriented MCDM for solving decision-making problems of hydropower construction project management [102]. Catrinu and Nordgård applied PRA and MCDM to a management of electricity distribution system asset [103].

In recent years, a fairly large number of publications considered an application of MCDM methods for handling managerial risk related to construction projects and running built facilities. Although risk of this type differs by nature from the "pure" risk posed by (to) physical objects, assessments of managerial and "pure" risk are related through a need to deal with uncertainties in risky objects or processes. Nieto-Morote and Ruz-Vila used fuzzy AHP method for assessing building projects and selection of contractors [104, 105]. Xiang et al. applied fuzzy AHP for assessing risk arising at a construction of submerged floating tunnels [106]. Wang et al. used AHP in combination with other decision-making methods to assess risk posed by exploitation of bridges [107]. El-Abbasy et al. applied AHP method together with Monte Carlo simulation for selecting contractors of a highway project [108]. The studies just listed involve elements of a nonprobabilistic uncertainty quantification based on fuzzy sets. As the "pure" risk is always a part of managerial risk, uncertain criteria $\widetilde{c}_{ij}$ specified by means of probabilistic methods of PRA can be included into the decision matrix $\mathbf{C}$ alongside with "fuzzy" criteria $\overleftrightarrow{c_{ij}}$. However, MCDM methods which allow a simultaneous juggling of "probabilistic" and "fuzzy" criteria $\widetilde{c}_{ij}$ and $\overleftrightarrow{c_{ij}}$ do not exist at present, to the best of our knowledge.

5.4. MCDM and Fire Protection of Civil Engineering Objects. Fire is a prevailing hazard in most objects of civil engineering. Fire accidents often occur on construction sites [109, 110]. As regards fire protection, MCDM methods were used until now mainly for ranking attributes expressing fire safety of completed buildings. AHP method was applied for developing weights of fire safety attributes in the so-called Edinburgh study [111]. A stochastic AHP was used by Zhao et al. to rank attributes of building fire safety [112]. Wong et al. used attributes of fire detection and alarm systems among a fairly large number of characteristics of an intelligent building. They applied two MCDM methods, AHP and ANP, to rank these characteristics [113, 114]. Vaidogas and Šakėnaitė formulated a number of MCDM problems, in which building fire safety is considered with respect to economics of fire protection: selection among existing buildings, building projects, and construction materials [115]. Vaidogas and Linkutė considered also problems of decision-making in the design of structures used for protection of built property against accidental explosions [116].

6. MCDM in Innovative Areas of Civil Engineering: A Look at Decision-Making under Uncertainty

6.1. Developing Sustainable and Energy Efficient Building. Sustainability is a natural subject of MCDM, because it automatically includes three subsets of criteria, involving economics, environmental, and social aspects. When solving problems of sustainable building, the fourth subset of criteria, involving engineering-technological dimensions, is also necessary. One of the innovative themes in sustainable construction is related to using materials of low embodied energy and energy efficient applications. However, such things as future and real building cost, environmental impact, and future social status of a constructed facility are very uncertain if considered in a long sight. For instance, large built areas in Hamburg (Germany) lost a lot of image due to a social downgrade of inhabitants. Also a lot of industrial and farming buildings having perfect infrastructure were left abandoned due to political and respective economic changes in post-Soviet states in Eastern Europe [117]. These buildings and territories make a great potential for further redevelopment as the recent trends in construction emphasize rehabilitation instead of occupying new territories, wasting building materials, and so forth. Building rehabilitation should be performed in accordance with principles of sustainable development, thus combining a number of usually conflicting and hardly measurable aspects.

The usefulness and even necessity of application of decision-making methods under uncertainty for aforementioned problems are summarized below. It is worth mentioning that DM under uncertainty is more characteristic to rehabilitation than to new construction. New construction is more regulated by technical norms, standards, and comprehensive planning. However, aspiration to redevelop a building in the most proper way is certainly a multiple criteria DM problem. Problem related to upgrading abandoned or depreciated buildings as well as physically and morally deteriorated built environment can generate several potential alternatives as demolishing depreciated building and building new structures (technically sound approach but contradicting to principles of sustainability), dismantling, reusing, or recycling of building materials (partly meeting principles of sustainability), renewal according to up-to-date requirements and using a building for previous purposes,

or upgrading a building with intention to use for other purpose (e.g., conversion of industrial buildings to commercial or apartments). When searching for the best alternative solution from several potential decision alternatives a_i, a set of criteria c_j should be defined and the matrix $\mathbf{C}$ can be formulated. The main challenge is in setting criteria values c_{ij} related to the alternatives a_i and criteria relative significances expressed by the weights w_j.

The four problems related to uncertainty measures could be identified. The first group of criteria has to assess features of building or surrounding environment, regional peculiarities using hardly measurable, vague, or incomplete data. Examples of criteria associated with vague, incomplete, or hardly measurable information, having no fixed values or expressed by linguistic scale, are architectural or historical value of a building (in terms of importance of preserving a building or its elements in a time of redevelopment), aesthetic appearance of a building and harmony with the environment after implementing a specific upgrading alternative, reflection of period norms, technologies, and so forth (in a case of upgrading vernacular buildings to contemporary building norms [14]). Examples of criteria associated with varying information, either related to a specific terms of a particular project or based on periodical or territorial measures, and expressed as interval data are building redevelopment costs (depending on particular material costs, labour costs in a locality, tax rates, etc.), energy savings (embodied energy, different technologies, and varying costs of energy), material and foreign investments in the area, changes in level of unemployment of local population or population activity index, and characterising social-economic value of a civil engineering project. The aforementioned uncertainty could be determined as fuzziness and managed with the help of fuzzy sets. Then, the elements c_{ij} of $\mathbf{C}$ are characterised by fuzzy sets and denoted as $\overleftrightarrow{c_{ij}}$. In that case, a decision-making matrix containing fuzzy elements $\overleftrightarrow{\mathbf{C}}$ could be composed.

Another group of criteria should assess development possibilities and should be able to reflect probable changes over the time, involving long-term prediction. Examples of criteria could be risk related to political and respective economic changes, technology innovations in civil engineering and related areas, state/region business foresights, cash flow and net present value of a potential civil engineering project, life quality parameters and a real value of a building, state income from business, and property taxes, and so forth. In the current case, risk factors should be taken into account and probabilistic modelling should be applied when the elements c_{ij} of the decision-making matrix $\mathbf{C}$ are modelled by random variables $\widetilde{c}_{ij}$ expressing uncertainty in criteria values, usually in Fisherian or Bayesian format. A matrix $\widetilde{\mathbf{C}}$ is subject to stochastic DM.

The third problem is based on combination of rather different criteria into a single solution. Combination of criteria is analysed in two senses. At first, a problem is in establishing relative significances of criteria in a particular task, based on decision-makers' preferences and peculiarities of the analysed problem. It is usually rather subjective and uncertain process. How could you compare significance of a local (e.g., cost of thermal insulation material) and a global criterion (e.g., energy savings, CO_2 emissions, and their impact on global warming) for different stakeholders? How could you express uncertain or linguistic decision-makers' preferences in a numerical format? What could be better specification of the weights w_j in the case they are of uncertain quantities: $\overleftrightarrow{\mathbf{w}}$ or $\widetilde{\mathbf{w}}$?

The next issue as the fourth problem is combining fuzzy and stochastic uncertainties in a single task. Based on the above assumptions on criteria $\overleftrightarrow{c_{ij}}$ and $\widetilde{c}_{ij}$ as well as relative significances of criteria ($\overleftrightarrow{\mathbf{w}}$ or $\widetilde{\mathbf{w}}$), there is the need to combine fuzzy and probabilistic representation of uncertainties in one initial decision-making matrix. Next comes the problem of choice among available MCDM methods or their extensions to be able to deal with fuzzy and stochastic data simultaneously. Thus, development of sustainable construction can be solved adequately by combining fuzzy and probabilistic representation of uncertainties, applying MCDM methods able to deal with fuzzy and stochastic input data, and including SA, that is, analysing effect related to the input data on the optimal solution of a MCDM problem.

6.2. Possibilities to Apply MCDM Methods within BIM Process. Building information modelling (BIM) goes through a series of levels of development (LODs) which represent an increasing level of detailing [118, 119]. The "fuzzy" detailing in such levels as LOD100 or LOD200 naturally introduces uncertainties in a DM process. They must be taken into account as long as MCDM is applied in this early design stage.

In the context of building design organised as a successive passing of LODs, a comparison of the alternatives a_i will make sense if a_i will represent the same LOD. In principle, branching of the design process into the alternatives a_i is possible on the conceptual level LOD100, as long as it is possible to characterise the vague information expressed by conceptual designs by some qualitative or quantitative criteria c_j. Most of them will express subjective opinions of architect and client, because very little can be measured quantitatively and objectively at this stage. This may require to express the opinions by fuzzy numbers or probability distributions and to solve a MCDM problem with respective matrices $\overleftrightarrow{\mathbf{C}}$ and $\widetilde{\mathbf{C}}$.

Higher levels of detail represented by LODs from 200 to 400 give better opportunity to formulate and solve a MCDM problem. Branching of the design process into the alternatives a_i can be done on each of these levels. However, uncertainties may still be present because the designs will not be fully finished. Some characteristics of a_i will be uncertain independently of available LOD. For instance, the final and precise construction cost and duration related to a_i will be known only after completion of construction process.

A development of a large number of the alternatives a_i and characteriation of each of them by the criteria c_j can encumber the design process. In essence, a solution of a MCDM problem will require to prepare m different designs of building related to the LOD reached in the design process. Thus, one can say that there is a "mega-uncertainty" related to

the number of LODs at which an application of MCDM will be most efficient.

6.3. Deciding on Security and Safety of Buildings. Security and safety are things and activities which are done in order to keep people and organisation safe from attack, harm, and damage. Three primary areas of security are physical security, information security, and personnel security [120]. Safety is achieved by protecting objects of civil engineering against fire, lightning, earthquakes, extreme winds, and contamination events which can negatively affect indoor air quality.

Measures and procedures of physical security are used to improve protection of an organisation against threats and vulnerabilities. Physical security of built property includes elements related to civil engineering: access control, barriers, doors, fencing, perimeter security, vaults, walls, and windows. Physical security is also interrelated with safety of built property. Malicious acts of people committed outside or inside perimeters of built objects may not only induce structural damage but also cause severe harm to their occupants. Examples of such acts are bombings, shootings, deliberate vehicular impacts, and arsons. The saddest events of this kind are September 11 attacks on the world trade centre in New York.

A higher investment in security systems may reduce damaging potential of malicious acts. If such acts will happen in spite of all security measures, damage caused by them can be limited by a better design for safety. Such design involves architectural and structural solutions enhancing safety and provision of better safety systems (alarms, fire and evacuation control systems, monitors of indoor air, etc.). Effectiveness of security and safety can be characterised by at least two MCDM criteria (one for security and one for safety). Further criteria related to them may be costs of security and safety systems. We can add criteria which measure impact of architectural and structural solutions on security and safety. Presence of a number of criteria makes out a case for an application of MCDM to design of buildings with respect to security and safety.

In a MCDM oriented towards security and safety, the alternatives a_i may represent different configurations of physical security systems and different solutions of safety systems. The alternatives a_i can also represent different architectural and structural solutions influencing security and safety. New structural solutions of tall buildings suggested since September 11 can serve as an example [121]. The architectural and structural solutions may seriously influence security and safety. For instance, a low-rise building provides better opportunities for escape from fire and firefighting than a tall one. However, a low-rise building will have much longer external perimeter to be guarded than a tall building with the same floor area. On the other hand, a tall building is a better target for shooting or an attack by a plane.

A simultaneous consideration of security and safety as well as architectural and structural aspects in the same MCDM problem may pose also several problems at generating the set of a_i. The number of a_i can be large due to a wide variety of security and safety systems available on the market. This number can be also increased by a large number of architectural and design solutions of the same building. A generation of the alternatives a_i can be influenced by legal and regulatory restrictions which must be regarded simultaneously at a formulation of the designs represented by a_i.

The criteria c_j used for evaluating the alternative triplets security-safety-architecture can be simple: amount and cost security equipment, number of security personnel, number of escape roots, minimum distance from a guarded object at which unauthorised persons must be stopped, and so forth. Such criteria are obvious and their values can be specified with relative ease. However, they do not reflect in-depth effectiveness of security and safety systems.

The effectiveness of safety systems can be expressed by applying methods of PRA as discussed in Section 5.2. Safety related criteria c_j can be either likelihood or expected severities of accident scenarios. These accidents can be initiated by security breaches. For instance, an arsonist, after an unauthorised access to secured areas of a building, can initiate fires in different places. They will lead to different fire scenarios. The higher is an estimated level of safety and robustness of the building represented by a_i, and the smaller should be likelihood and consequences of potential accidents. The possibility of different accident scenarios does not allow to measure the level of safety by a single MCDM criterion.

The effectiveness of a physical security system can also be expressed by several criteria c_j reflecting different identifiable scenarios of security breach. Examples of such scenarios are unauthorised access to secured areas, armed attack from outside of object perimeter, an attempt to hit a protected object with a vehicle, external disruption of power supply, and gas attack from outside the building. As in the case of PRA, likelihood measures can be estimated and consequences of security breaches assessed. The likelihood and consequence severities can be used as MCDM criteria c_j. The higher is level of physical security, and the smaller must be values of such criteria.

Attacks and adverse physical events impairing security and safety of built property are in most cases rare events. Data on such events is generally sparse. Therefore, estimating the likelihood of security and safety events will almost inevitably face the problem of quantifying epistemic uncertainties in the manner of PRA. This will lead to an inclusion of uncertain criteria into MCDM which are uncertain in the epistemic sense. In other words, problems of MCDM, in which security and safety of built property are regarded, can be solved adequately by composing the random decision-making matrix $\widetilde{\mathbf{C}}$.

7. Conclusions

In this review, methods developed for making decisions under uncertainty in civil engineering were examined. Along with this examination, several problems arising from dealing with uncertainties in decision-making were identified. The decision-making based on formal methods of MCDM was in the focus of the review. The prevailing two types of uncertainty quantification in MCDM rest on fuzzy logic and

probabilistic modelling. The need to introduce uncertainty modelling into MCDM exists in many areas of civil engineering. A proper handling of such uncertainties will require solving several methodological problems: specification of fuzzy and random decision-making matrices, analysis of sensitivity of MCDM results to changes in all elements of an initial MCDM problem, and the need to combine fuzzy and random criteria in the same decision-making task. MCDM under uncertainty is quite flexible methodology. It can be applied in areas of civil engineering which are currently under development and receive much attention in research.

A certain challenge to MCDM is sensitivity analysis. Various techniques of local sensitivity analysis were applied until now to explore MCDM methods applied in various fields. These applications deal mainly with sensitivity of MCDM output versus values of weights. Applications of global sensitivity analysis to MCDM are not numerous, despite the fact that analysis of this type is very popular in general science. These applications deal mainly with geographic information systems.

A partially unresolved issue in applications of sensitivity analysis to MCDM is how to represent sequences of alternative rankings by scalar variables. Currently, the only suggestion is to use for this purpose a quantity known as average shift in ranks. MCDM raises a sensitivity analysis problem characteristic to this methodology, namely, sensitivity to model selection. Ranking of alternatives could vary at choosing different MCDM methods and normalisation formulas. An additional model selection problem will arise at choosing the type of fuzzy numbers and probability distributions used for modelling input variables of a MCDM problem. At present, a clear and comprehensive answer to the issue of sensitivity to model selection in MCDM does not exist.

The need for modelling uncertainties can be particularly high in applications of MCDM to a design of safety critical objects. Damage to such objects may cause severe consequences. Safety critical objects can be assessed by means of reliability theory and probabilistic risk analysis. Measures of reliability and risk estimates are usually uncertain quantities. In terms of risk analysis, this uncertainty is called epistemic (state-of-knowledge) uncertainty. Epistemic uncertainties related to reliability and risk are modelled by means of probability distributions. An application of MCDM to the design of safety critical objects will require including epistemic random variables into a decision-making matrix of a MCDM problem. Probabilistic risk estimates can be elements of a broader class of risk known as business or managerial risk. A decision-making with respect to this kind of risk may require formulating and solving MCDM problems involving two types of uncertainties. Decision-making matrices of such problems will involve elements modelled by both fuzzy sets and probability distributions. Therefore, there is a need to develop MCDM methods allowing dealing with two different types of uncertainty in one decision-making problem.

MCDM under uncertainty has prospects to be intensively applied in such areas as development of sustainable and energy efficient buildings, building information management, and assurance of security and safety of built property. Decision-making in these areas faces large uncertainties related to long-term predictions, vague information on buildings under design, and rare and unexpected extreme events. Methods of fuzzy and stochastic MCDM can facilitate making decisions in the areas just mentioned.

Conflict of Interests

The authors declare that there is no conflict of interests regarding the publication of this paper.

Acknowledgment

The part of the paper done by the author from Czech Republic has been worked out under Project no. LO1408 "AdMAs UP."

References

[1] M. M. Wiecek, M. Ehrgott, G. Fadel, and J. R. Figueira, "Multiple criteria decision making for engineering," *Omega*, vol. 36, no. 3, pp. 337–339, 2008.

[2] A. Mardani, A. Jusoh, and E. K. Zavadskas, "Fuzzy multiple criteria decision-making techniques and applications—two decades review from 1994 to 2014," *Expert Systems with Applications*, vol. 42, no. 8, pp. 4126–4148, 2015.

[3] J. J. H. Liou and G.-H. Tzeng, "Comments on 'Multiple criteria decision making (MCDM) methods in economics: an overview'," *Technological and Economic Development of Economy*, vol. 18, no. 4, pp. 672–695, 2012.

[4] E. K. Zavadskas, Z. Turskis, and S. Kildiene, "State of art surveys of overviews on MCDM/MADM methods," *Technological and Economic Development of Economy*, vol. 20, no. 1, pp. 165–179, 2014.

[5] T. Baležentis and A. Baležentis, "A survey on development and applications of the multi-criteria decision making method MULTIMOORA," *Journal of Multi-Criteria Decision Analysis*, vol. 21, no. 3-4, pp. 209–222, 2014.

[6] M. Behzadian, R. B. Kazemzadeh, A. Albadvi, and M. Aghdasi, "PROMETHEE: a comprehensive literature review on methodologies and applications," *European Journal of Operational Research*, vol. 200, no. 1, pp. 198–215, 2010.

[7] M. Behzadian, S. Khanmohammadi Otaghsara, M. Yazdani, and J. Ignatius, "A state-of the-art survey of TOPSIS applications," *Expert Systems with Applications*, vol. 39, no. 17, pp. 13051–13069, 2012.

[8] R. Ureña, F. Chiclana, J. A. Morente-Molinera, and E. Herrera-Viedma, "Managing incomplete preference relations in decision making: a review and future trends," *Information Sciences*, vol. 302, no. 1, pp. 14–32, 2015.

[9] J. Chai, J. N. K. Liu, and E. W. T. Ngai, "Application of decision-making techniques in supplier selection: a systematic review of literature," *Expert Systems with Applications*, vol. 40, no. 10, pp. 3872–3885, 2013.

[10] G. Kabir, R. Sadiq, and S. Tesfamariam, "A review of multi-criteria decision-making methods for infrastructure management," *Structure and Infrastructure Engineering: Maintenance, Management, Life-Cycle Design and Performance*, vol. 10, no. 9, pp. 1176–1210, 2014.

[11] D. Jato-Espino, E. Castillo-Lopez, J. Rodriguez-Hernandez, and J. C. Canteras-Jordana, "A review of application of multi-criteria decision making methods in construction," *Automation in Construction*, vol. 45, pp. 151–162, 2014.

[12] C. Kahraman, "Multi-criteria decision making methods and fuzzy sets," in *Fuzzy Multi-Criteria Decision Making*, C. Kahraman, Ed., vol. 16 of *Springer Optimization and Its Applications*, pp. 1–18, Springer, New York, NY, USA, 2008.

[13] J. Tamošaitiene and E. Gaudutis, "Complex assessment of structural systems used for high-rise buildings," *Journal of Civil Engineering and Management*, vol. 19, no. 2, pp. 305–317, 2013.

[14] E. Šiožinyte, J. Antuchevičiene, and V. Kutut, "Upgrading the old vernacular building to contemporary norms: multiple criteria approach," *Journal of Civil Engineering and Management*, vol. 20, no. 2, pp. 291–298, 2014.

[15] J. L. Hougaard and T. Baležentis, "Fuzzy efficiency without convexity," *Fuzzy Sets and Systems*, vol. 255, pp. 17–29, 2014.

[16] L. A. Zadeh, "Fuzzy set theory and probability theory: what is the relationship?" in *International Encyclopedia of Statistical Science*, pp. 563–566, Springer, 2014.

[17] D. Kelly and C. Smith, *Bayesian Inference for Probabilistic Risk Assessment: A Practitioner's Guidebook*, Springer, New York, NY, USA, 2011.

[18] J.-J. Wang, Y.-Y. Jing, C.-F. Zhang, and J.-H. Zhao, "Review on multi-criteria decision analysis aid in sustainable energy decision-making," *Renewable and Sustainable Energy Reviews*, vol. 13, no. 9, pp. 2263–2278, 2009.

[19] Y.-M. Wang and Y. Luo, "Integration of correlations with standard deviations for determining attribute weights in multiple attribute decision making," *Mathematical and Computer Modelling*, vol. 51, no. 1-2, pp. 1–12, 2010.

[20] C. Fu and Y. Wang, "An interval difference based evidential reasoning approach with unknown attribute weights and utilities of assessment grades," *Computers and Industrial Engineering*, vol. 81, pp. 109–117, 2015.

[21] E. Triantaphyllou and S. H. Mann, "An examination of the effectiveness of multi-dimensional decision-making methods: a decision-making paradox," *International Journal of Decision Support Systems*, vol. 5, no. 3, pp. 303–312, 1989.

[22] L. A. Zadeh, "Fuzzy sets," *Information and Control*, vol. 8, no. 3, pp. 338–353, 1965.

[23] P. J. M. van Laarhoven and W. Pedrycz, "A fuzzy extension of Saaty's priority theory," *Fuzzy Sets and Systems*, vol. 11, no. 3, pp. 229–241, 1983.

[24] C. Kahraman, S. C. Onar, and B. Oztaysi, "Fuzzy multicriteria decision-making: a literature review," *International Journal of Computational Intelligence Systems*, vol. 8, no. 4, pp. 637–666, 2015.

[25] E. K. Zavadskas, J. Antucheviciene, S. H. R. Hajiagha, and S. S. Hashemi, "Extension of weighted aggregated sum product assessment with interval-valued intuitionistic fuzzy numbers (WASPAS-IVIF)," *Applied Soft Computing*, vol. 24, pp. 1013–1021, 2014.

[26] S. H. Razavi Hajiagha, S. S. Hashemi, and E. K. Zavadskas, "A complex proportional assessment method for group decision making in an interval-valued intuitionistic fuzzy environment," *Technological and Economic Development of Economy*, vol. 19, no. 1, pp. 22–37, 2013.

[27] H.-C. Liu, X.-J. Fan, P. Li, and Y.-Z. Chen, "Evaluating the risk of failure modes with extended MULTIMOORA method under fuzzy environment," *Engineering Applications of Artificial Intelligence*, vol. 34, pp. 168–177, 2014.

[28] H.-C. Liu, J.-X. You, C. Lu, and Y.-Z. Chen, "Evaluating health-care waste treatment technologies using a hybrid multi-criteria decision making model," *Renewable and Sustainable Energy Reviews*, vol. 41, pp. 932–942, 2015.

[29] H.-C. Liu, J.-X. You, Ch. Lu, and M.-M. Shan, "Application of interval 2-tuple linguistic MULTIMOORA method for health-care waste treatment technology evaluation and selection," *Waste Management*, vol. 34, no. 11, pp. 2355–2364, 2014.

[30] T. Balezentis, S. Z. Zeng, and A. Balezentis, "MULTIMOORA-IFN: a MCDM method based on intuitionistic fuzzy number for performance management," *Economic Computation and Economic Cybernetics Studies and Research*, vol. 48, no. 4, pp. 85–102, 2014.

[31] Z.-H. Li, "An extension of the MULTIMOORA method for multiple criteria group decision making based upon hesitant fuzzy sets," *Journal of Applied Mathematics*, vol. 2014, Article ID 527836, 16 pages, 2014.

[32] Z. Turskis and E. K. Zavadskas, "A new fuzzy additive ratio assessment method (ARAS-F). Case study: the analysis of fuzzy Multiple Criteria in order to select the logistic centers location," *Transport*, vol. 25, no. 4, pp. 423–432, 2010.

[33] M. Zamani, A. Rabbani, A. Yazdani-Chamzini, and Z. Turskis, "An integrated model for extending brand based on fuzzy ARAS and ANP methods," *Journal of Business Economics and Management*, vol. 15, no. 3, pp. 403–423, 2014.

[34] A. S. Ghadikolaei, S. K. Esbouei, and J. Antucheviciene, "Applying fuzzy MCDM for financial performance evaluation of Iranian companies," *Technological and Economic Development of Economy*, vol. 20, no. 2, pp. 274–291, 2014.

[35] N. Rikhtegar, N. Mansouri, A. A. Oroumieh, A. Yazdani-Chamzini, E. K. Zavadskas, and S. Kildienė, "Environmental impact assessment based on group decision-making methods in mining projects," *Economic Research-Ekonomska Istraživanja*, vol. 27, no. 1, pp. 378–392, 2014.

[36] M. Kabak, E. Köse, O. Kirilmaz, and S. Burmaoğlu, "A fuzzy multi-criteria decision making approach to assess building energy performance," *Energy and Buildings*, vol. 72, pp. 382–389, 2014.

[37] M. Kucukvar, S. Gumus, G. Egilmez, and O. Tatari, "Ranking the sustainability performance of pavements: an intuitionistic fuzzy decision making method," *Automation in Construction*, vol. 40, pp. 33–43, 2014.

[38] A. H. Azadnia, M. Z. M. Saman, and K. Y. Wong, "Sustainable supplier selection and order lot-sizing: an integrated multi-objective decision-making process," *International Journal of Production Research*, vol. 53, no. 2, pp. 383–408, 2015.

[39] S. M. Hashemian, M. Behzadian, R. Samizadeh, and J. Ignatius, "A fuzzy hybrid group decision support system approach for the supplier evaluation process," *The International Journal of Advanced Manufacturing Technology*, vol. 73, no. 5–8, pp. 1105–1117, 2014.

[40] M. K. Ghorabaee, M. Amiri, J. S. Sadaghiani, and G. H. Goodarzi, "Multiple criteria group decision-making for supplier selection based on COPRAS method with interval type-2 fuzzy sets," *The International Journal of Advanced Manufacturing Technology*, vol. 75, no. 5–8, pp. 1115–1130, 2014.

[41] S. Zeng, T. Balezentis, J. Chen, and G. Luo, "A projection method for multiple attribute group decision making with intuitionistic fuzzy information," *Informatica*, vol. 24, no. 3, pp. 485–503, 2013.

[42] S. M. Mousavi, B. Vahdani, R. Tavakkoli-Moghaddam, and N. Tajik, "Soft computing based on a fuzzy grey group compromise

solution approach with an application to the selection problem of material handling equipment," *International Journal of Computer Integrated Manufacturing*, vol. 27, no. 6, pp. 547–569, 2014.

[43] A. Hadi-Vencheh and A. Mohamadghasemi, "A new hybrid fuzzy multi-criteria decision making model for solving the material handling equipment selection problem," *International Journal of Computer Integrated Manufacturing*, vol. 28, no. 5, pp. 534–550, 2015.

[44] S. Kiris, "Multi-criteria inventory classification by using a fuzzy analytic network process (ANP) approach," *Informatica*, vol. 24, no. 2, pp. 199–217, 2013.

[45] B. Bairagi, B. Dey, B. Sarkar, and S. Sanyal, "Selection of robot for automated foundry operations using fuzzy multi-criteria decision making approaches," *International Journal of Management Science and Engineering Management*, vol. 9, no. 3, pp. 221–232, 2014.

[46] Ü. Kurt, "The fuzzy TOPSIS and generalized Choquet fuzzy integral algorithm for nuclear power plant site selection—a case study from Turkey," *Journal of Nuclear Science and Technology*, vol. 51, no. 10, pp. 1241–1255, 2014.

[47] E. K. Zavadskas, Z. Turskis, and V. Bagočius, "Multi-criteria selection of a deep-water port in the Eastern Baltic Sea," *Applied Soft Computing Journal*, vol. 26, pp. 180–192, 2014.

[48] W. Zhang, K. Sun, C. Lei, Y. Zhang, H. Li, and B. F. Spencer, "Fuzzy analytic hierarchy process synthetic evaluation models for the health monitoring of shield tunnels," *Computer-Aided Civil and Infrastructure Engineering*, vol. 29, no. 9, pp. 676–688, 2014.

[49] S. Avikal, R. Jain, and P. K. Mishra, "A Kano model, AHP and M-TOPSIS method-based technique for disassembly line balancing under fuzzy environment," *Applied Soft Computing Journal*, vol. 25, pp. 519–529, 2014.

[50] S. Avikal, P. K. Mishra, and R. Jain, "A fuzzy AHP and PROMETHEE method-based heuristic for disassembly line balancing problems," *International Journal of Production Research*, vol. 52, no. 5, pp. 1306–1317, 2014.

[51] C. H. Wang and H. S. Wu, "A novel framework to evaluate programmable logic controllers: a fuzzy MCDM perspective," *Journal of Intelligent Manufacturing*, 10 pages, 2014.

[52] T.-M. Yeh, F.-Y. Pai, and C.-W. Liao, "Using a hybrid MCDM methodology to identify critical factors in new product development," *Neural Computing and Applications*, vol. 24, no. 3-4, pp. 957–971, 2014.

[53] L. Anojkumar, M. Ilangkumaran, and V. Sasirekha, "Comparative analysis of MCDM methods for pipe material selection in sugar industry," *Expert Systems with Applications*, vol. 41, no. 6, pp. 2964–2980, 2014.

[54] C. Tan, W. H. Ip, and X. Chen, "Stochastic multiple criteria decision making with aspiration level based on prospect stochastic dominance," *Knowledge-Based Systems*, vol. 70, pp. 231–241, 2014.

[55] T. L. Saaty, "A scaling method for priorities in hierarchical structures," *Journal of Mathematical Psychology*, vol. 15, no. 3, pp. 234–281, 1977.

[56] L. G. Vargas, "Reciprocal matrices with random coefficients," *Mathematical Modelling*, vol. 3, no. 1, pp. 69–81, 1982.

[57] A. Saltelli, K. Chan, and E. M. Scott, *Sensitivity Analysis*, Wiley Series in Probability and Statistics, John Wiley & Sons, New York, NY, USA, 2004.

[58] Y. Zhang, Z.-P. Fan, and Y. Liu, "A method based on stochastic dominance degrees for stochastic multiple criteria decision making," *Computers and Industrial Engineering*, vol. 58, no. 4, pp. 544–552, 2010.

[59] J. Ren, Y. Gao, and C. Bian, "Multiple criteria decision making based on discrete linguistic stochastic variables," *Mathematical Problems in Engineering*, vol. 2013, Article ID 546508, 11 pages, 2013.

[60] M. D. McKay, R. J. Beckman, and W. J. Conover, "A comparison of three methods for selecting values of input variables in the analysis of output from a computer code," *Technometrics*, vol. 21, no. 2, pp. 239–245, 1979.

[61] R. L. Iman and W. J. Conover, "Small sample sensitivity analysis techniques for computer models with an application to risk assessment," *Communications in Statistics—Theory and Methods*, vol. 9, no. 17, pp. 1749–1842, 1980.

[62] B. Möller and U. Reuter, *Uncertainty Forecasting in Engineering*, Springer, Berlin, Germany, 2007.

[63] A. Saltelli, M. Ratto, T. Andres et al., *Global Sensitivity Analysis: the Primer*, John Wiley & Sons, Chichester, UK, 2008.

[64] A. Saltelli, S. Tarantola, F. Campolongo, and M. Ratto, *Sensitivity Analysis in Practice: A Guide to Assessing Scientific Models*, John Wiley & Sons, Chichester, UK, 2004.

[65] A. Ligmann-Zielinska, "Spatially-explicit sensitivity analysis of an agent-based model of land use change," *International Journal of Geographical Information Science*, vol. 27, no. 9, pp. 1764–1781, 2013.

[66] A. Ligmann-Zielinska and P. Jankowski, "Spatially-explicit integrated uncertainty and sensitivity analysis of criteria weights in multicriteria land suitability evaluation," *Environmental Modelling & Software*, vol. 57, pp. 235–247, 2014.

[67] C.-R. Wu, C.-T. Lin, and H.-C. Chen, "Optimal selection of location for Taiwanese hospitals to ensure a competitive advantage by using the analytic hierarchy process and sensitivity analysis," *Building and Environment*, vol. 42, no. 3, pp. 1431–1444, 2007.

[68] A. Awasthi, S. S. Chauhan, and S. K. Goyal, "A multi-criteria decision making approach for location planning for urban distribution centers under uncertainty," *Mathematical and Computer Modelling*, vol. 53, no. 1-2, pp. 98–109, 2011.

[69] J. Malczewski and C. Rinner, *Multicriteria Decision Analysis in Geographic Information Science*, Springer, New York, NY, USA, 2015.

[70] A. Shanian and O. Savadogo, "A methodological concept for material selection of highly sensitive components based on multiple criteria decision analysis," *Expert Systems with Applications*, vol. 36, no. 2, pp. 1362–1370, 2009.

[71] G. Büyüközkan and G. Çifçi, "A novel fuzzy multi-criteria decision framework for sustainable supplier selection with incomplete information," *Computers in Industry*, vol. 62, no. 2, pp. 164–174, 2011.

[72] E. Triantaphyllou and A. Sánchez, "A sensitivity analysis approach for some deterministic multi-criteria decision-making methods," *Decision Sciences*, vol. 28, no. 1, pp. 151–194, 1997.

[73] E. Triantaphyllou, *Multi-Criteria Decision Making: A Comparative Study*, Kluwer Academic Publishers, Dordrecht, The Netherlands, 2000.

[74] M. Bevilacqua and M. Braglia, "The analytic hierarchy process applied to maintenance strategy selection," *Reliability Engineering and System Safety*, vol. 70, no. 1, pp. 71–83, 2000.

[75] C.-W. Chang, C.-R. Wu, C.-T. Lin, and H.-C. Chen, "An application of AHP and sensitivity analysis for selecting the best

slicing machine," *Computers & Industrial Engineering*, vol. 52, no. 2, pp. 296–307, 2007.

[76] D. Choudhary and R. Shankar, "An STEEP-fuzzy AHP-TOPSIS framework for evaluation and selection of thermal power plant location: a case study from India," *Energy*, vol. 42, no. 1, pp. 510–521, 2012.

[77] A. Awasthi, S. S. Chauhan, H. Omrani, and A. Panahi, "A hybrid approach based on SERVQUAL and fuzzy TOPSIS for evaluating transportation service quality," *Computers & Industrial Engineering*, vol. 61, no. 3, pp. 637–646, 2011.

[78] A. Awasthi, S. S. Chauhan, and H. Omrani, "Application of fuzzy TOPSIS in evaluating sustainable transportation systems," *Expert Systems with Applications*, vol. 38, no. 10, pp. 12270–12280, 2011.

[79] A. Awasthi and S. S. Chauhan, "A hybrid approach integrating Affinity Diagram, AHP and fuzzy TOPSIS for sustainable city logistics planning," *Applied Mathematical Modelling*, vol. 36, no. 2, pp. 573–584, 2012.

[80] M. Saisana, A. Saltelli, and S. Tarantola, "Uncertainty and sensitivity analysis techniques as tools for the quality assessment of composite indicators," *Journal of the Royal Statistical Society Series A: Statistics in Society*, vol. 168, no. 2, pp. 307–323, 2005.

[81] D. Ben-Arieh, "Sensitivity of multi-criteria decision making to linguistic quantifiers and aggregation means," *Computers and Industrial Engineering*, vol. 48, no. 2, pp. 289–309, 2005.

[82] G. Büyüközkan and G. Çifçi, "A combined fuzzy AHP and fuzzy TOPSIS based strategic analysis of electronic service quality in healthcare industry," *Expert Systems with Applications*, vol. 39, no. 3, pp. 2341–2354, 2012.

[83] M. Zarghami, "Soft computing of the Borda count by fuzzy linguistic quantifiers," *Applied Soft Computing Journal*, vol. 11, no. 1, pp. 1067–1073, 2011.

[84] M. Zarghami and F. Szidarovszky, "On the relation between compromise programming and ordered weighted averaging operator," *Information Sciences*, vol. 180, no. 11, pp. 2239–2248, 2010.

[85] E. R. Vaidogas, E. K. Zavadskas, and Z. Turskis, "Reliability measures in multicriteria decision making as applied to engineering projects," *International Journal of Management and Decision Making*, vol. 8, no. 5-6, pp. 497–518, 2007.

[86] B. J. Garrick, *Quantifying and Controlling Catastrophic Risks*, Elsevier, Amsterdam, The Netherlands, 2008.

[87] L. F. Gay and S. K. Sinha, "Resilience of civil infrastructure systems: literature review for improved asset management," *International Journal of Critical Infrastructures*, vol. 9, no. 4, pp. 330–350, 2013.

[88] B. J. Jennings, E. D. Vugrin, and D. K. Belasich, "Resilience certification for commercial buildings: a study of stakeholder perspectives," *Environment Systems and Decisions*, vol. 33, no. 2, pp. 184–194, 2013.

[89] G. Lizarralde, K. Chmutina, L. Bosher, and A. Dainty, "Sustainability and resilience in the built environment: the challenges of establishing a turquoise agenda in the UK," *Sustainable Cities and Society*, vol. 15, pp. 96–104, 2015.

[90] M. Rausand, *Reliability of Safety-Critical Systems: Theory and Applications*, Wiley, Chichester, UK, 2014.

[91] E. R. Vaidogas and E. K. Zavadskas, "Introducing reliability measures into multi-criteria decision making," *International Journal of Management and Decision Making*, vol. 8, no. 5-6, pp. 475–496, 2007.

[92] N. D. Singpurwalla, *Reliability and Risk. A Bayesian Perspective*, Wiley, Chichester, UK, 2006.

[93] E. R. Vaidogas, "On applying sparse and uncertain information to estimating the probability of failure due to rare abnormal situations," *Information Technology and Control*, vol. 38, no. 2, pp. 135–146, 2009.

[94] J. C. Helton and W. L. Oberkampf, "Alternative representations of epistemic uncertainty," *Reliability Engineering & System Safety*, vol. 85, no. 1–3, pp. 1–10, 2004.

[95] C. J. Roy and W. L. Oberkampf, "A comprehensive framework for verification, validation, and uncertainty quantification in scientific computing," *Computer Methods in Applied Mechanics and Engineering*, vol. 200, no. 25–28, pp. 2131–2144, 2011.

[96] M. C. M. Troffaes, G. Walter, and D. Kelly, "A robust Bayesian approach to modeling epistemic uncertainty in common-cause failure models," *Reliability Engineering and System Safety*, vol. 125, no. 1, pp. 13–21, 2014.

[97] E. K. Zavadskas and E. R. Vaidogas, "Multiattribute selection from alternative designs of infrastructure components for accidental situations," *Computer-Aided Civil and Infrastructure Engineering*, vol. 24, no. 5, pp. 346–358, 2009.

[98] S. Mannan, Ed., *Lees's Loss Prevention in the Process Industries*, Elsevier, Amsterdam, The Netherlands, 2005.

[99] E. Versluis, M. van Asselt, T. Fox, and A. Hommels, "The EU Seveso regime in practice: from uncertainty blindness to uncertainty tolerance," *Journal of Hazardous Materials*, vol. 184, no. 1–3, pp. 627–631, 2010.

[100] L. T. Ostrom and C. A. Wilhelmsen, *Risk Assessment. Tools, Techniques, and Their Applications*, Wiley, Hoboken, NJ, USA, 2012.

[101] E. R. Vaidogas and J. Šakėnaitė, "Protecting built property against fire disasters: multi-attribute decision making with respect to fire risk," *International Journal of Strategic Property Management*, vol. 14, no. 4, pp. 391–407, 2010.

[102] J.-L. Zhou, Z.-H. Bai, and Z.-Y. Sun, "A hybrid approach for safety assessment in high-risk hydropower-construction-project work systems," *Safety Science*, vol. 64, pp. 163–172, 2014.

[103] M. D. Catrinu and D. E. Nordgård, "Integrating risk analysis and multi-criteria decision support under uncertainty in electricity distribution system asset management," *Reliability Engineering & System Safety*, vol. 96, no. 6, pp. 663–670, 2011.

[104] A. Nieto-Morote and F. Ruz-Vila, "A fuzzy approach to construction project risk assessment," *International Journal of Project Management*, vol. 29, no. 2, pp. 220–231, 2011.

[105] A. Nieto-Morote and F. Ruz-Vila, "A fuzzy multi-criteria decision-making model for construction contractor prequalification," *Automation in Construction*, vol. 25, pp. 8–19, 2012.

[106] Y. Xiang, C. Liu, K. Zhang, and Q. Wu, "Risk analysis and management of submerged floating tunnel and its application," *Procedia Engineering*, vol. 4, pp. 107–116, 2010.

[107] Y.-M. Wang, J. Liu, and T. M. S. Elhag, "An integrated AHP-DEA methodology for bridge risk assessment," *Computers & Industrial Engineering*, vol. 54, no. 3, pp. 513–525, 2008.

[108] M. S. El-Abbasy, T. Zayed, M. Ahmed, H. Alzraiee, and M. Abouhamad, "Contractor selection model for highway projects using integrated simulation and analytic network process," *Journal of Construction Engineering and Management*, vol. 139, no. 7, pp. 755–767, 2013.

[109] L. Hui, W. Yongqing, S. Shimei, and S. Baotie, "Study on safety assessment of fire hazard for the construction site," *Procedia Engineering*, vol. 43, pp. 369–373, 2012.

[110] M. A. Alqassim and N. N. Daeid, "Fires and related incidents in Dubai, United Arab Emirates (2006–2013)," *Case Studies in Fire Safety*, vol. 2, pp. 28–36, 2014.

[111] D. J. Rasbash, G. Ramachandran, B. Kandola, J. M. Watts, and M. Law, *Evaluation of Fire Safety*, John Wiley & Sons, Chichester, UK, 2004.

[112] C. M. Zhao, S. M. Lo, J. A. Lu, and Z. Fang, "A simulation approach for ranking of fire safety attributes of existing buildings," *Fire Safety Journal*, vol. 39, no. 7, pp. 557–579, 2004.

[113] J. Wong, H. Li, and J. Lai, "Evaluating the system intelligence of the intelligent building systems—part 1: development of key intelligent indicators and conceptual analytical framework," *Automation in Construction*, vol. 17, no. 3, pp. 284–302, 2008.

[114] J. Wong, H. Li, and J. Lai, "Evaluating the system intelligence of the intelligent building systems. Part 2: construction and validation of analytical models," *Automation in Construction*, vol. 17, no. 3, pp. 303–321, 2008.

[115] E. R. Vaidogas and J. Šakėnaitė, "Multi-attribute decision-making in economics of fire protection," *Engineering Economics*, vol. 22, no. 3, pp. 262–270, 2011.

[116] E. R. Vaidogas and L. Linkutė, "Sitting the barrier aimed at protecting roadside property from accidental fires and explosions on road: a pre-optimisation stage," *The Baltic Journal of Road and Bridge Engineering*, vol. 7, no. 4, pp. 277–287, 2012.

[117] E. K. Zavadskas and J. Antucheviciene, "Multiple criteria evaluation of rural building's regeneration alternatives," *Building and Environment*, vol. 42, no. 1, pp. 436–451, 2007.

[118] E. Krygiel and B. Nies, *Green BIM: Successful Sustainable Design with Building Information Modeling*, Wiley, Indianapolis, Ind, USA, 2008.

[119] AIA, *Guide, Instructions and Commentary to the 2013 AIA Digital Practice Documents*, The American Institute of Architects, Washington, DC, USA, 2013.

[120] B. A. Wayland, *Security for Business Professionals. How to Plan, Implement, and Manage your Company's Security Program*, Elsevier, Amsterdam, The Netherlands, 2014.

[121] D. Drengenberg and G. Corley, "Evolution of building code requirements in a post 9/11 world," *CTBUH Journal*, no. 3, pp. 32–35, 2011.

Hindawi Publishing Corporation
Mathematical Problems in Engineering
Volume 2015, Article ID 357981, 12 pages
http://dx.doi.org/10.1155/2015/357981

Research Article

Performance Requirements on Remodeling Apartment Housing and TOPSIS Evaluation

Jaeho Cho and Jaeyoul Chun

Department of Architectural Engineering, Dankook University, 126 Jukjeon-dong, Yongin-si, Gyeonggi-do 448-701, Republic of Korea

Correspondence should be addressed to Jaeyoul Chun; jaeyoul@dankook.ac.kr

Received 8 April 2015; Accepted 18 May 2015

Academic Editor: Jurgita Antucheviciene

Functional improvement needed in remodeling projects is determined by users in a complex manner since remodeling projects require performance improvement against deterioration. This study defines fundamental Remodeling Performance Criteria (RPC) for apartment housing by referring to performance criteria of both domestic and international performance-related systems. In this case study, performance evaluation of Construction Element Method (CEM) for remodeling projects was conducted based on RPC. For the objective evaluation of CEM, performance scores were calculated and normalized by using the Technique for Order of Preference by Similarity to Ideal Solution (TOPSIS) model, which is used in a multicriteria decision-making method. The TOPSIS evaluation model allows for a comprehensive and comparative analysis on the performance of the remodeling solution. The TOPSIS model in this study suggests a standard logic of performance evaluation for aged buildings as it analyzes the degree of deterioration at the prior remodeling phase and predicts the performance improvement level for CEM at the remodeling planning phase.

1. Introduction

Recently, as the domestic housing supply rate is reaching over 100% nationally, demand for remodeling related to functional improvement has been increasing due to the deterioration of existing apartment housing which was built earlier [1]. Regardless of whether new construction or remodeling is carried out, the users' requirements are determined with functional improvement in a specific manner.

The international standardization of building performance is currently in progress and is being led by the International Organization for Standardization (ISO).

In Japan, a study has been conducted to establish both the Evaluation Index of Performance (EIP) of building elements and an accreditation system for remodeling housing components [2].

Users' requests should be clearly defined since they are continually made and changed in all phases of a building life cycle, including planning, design, construction, maintenance, and destruction phases [3]. Therefore, a review of housing performance should be conducted according to the users' criteria, which are physical, psychological, physiological, and so forth [4].

In Korea, despite the availability of a design guide for housing performance that has been recommended by the Ministry of Land, Transport and Maritime Affairs, it has not been effectively utilized for the evaluation of CEM.

In the case of remodeling projects, in particular, studies on the performance evaluation of building elements have not been sufficiently performed. The study of EIP should be carried out as a priority in order to facilitate the continuous development of construction techniques in remodeling and to induce the extension of a building life cycle.

Constructability in remodeling projects is regarded as an important criterion for performance evaluation due to the structural constraints of remodeling. Constructability can be defined as the degree of ease in the measurement of the degree of difficulty for construction works [5]. Construction methods for remodeling are classified according to techniques for addition, component relocation, additional installation, exchange, layout change, and scale change [6]. Constructability is evaluated in order to select the most effective method through the comprehensive measurement of safety, environmental feasibility, and economic feasibility in the construction phases.

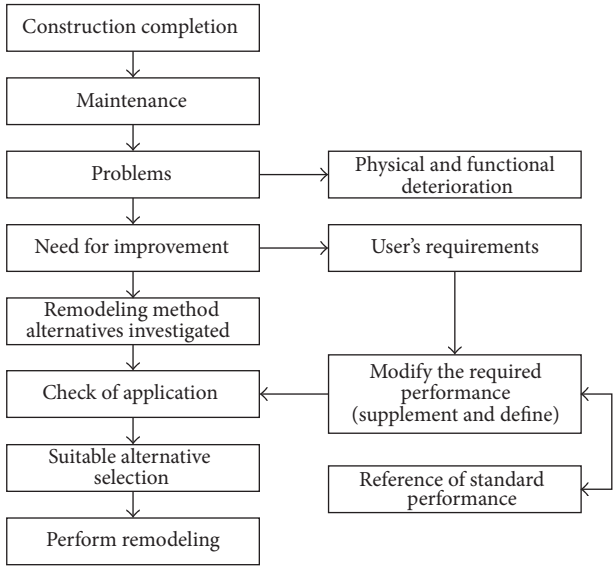

Figure 1: Remodeling procedures.

The basic procedures for remodeling projects are shown in Figure 1.

In this study, the fundamental criterion for the performance evaluation of domestic apartment housing is redetermined to ensure successful quality in remodeling projects.

Furthermore, an evaluation method of CEM is proposed by using the Technique for Order of Preference by Similarity to Ideal Solution (TOPSIS) model, which is a multicriteria decision-making method based on various attributes. TOPSIS is continuously redefined and extended so that it handles multiple extreme criteria (PIS: positive ideal solution; NIS: negative ideal solution), by which a decision maker can provide more than one pair of extreme points [7]. The Ordered Weighted Averaging (OWA) operator was suggested to solve the problem of multiple extreme criteria in TOPSIS [7].

The standardized score of the performance evaluation using TOPSIS can be effectively utilized in comparative analysis between different design solutions. In addition, extreme criteria PIS and NIS in TOPSIS are well coped with multicriteria decision related problems in construction performance evaluation. Many other kinds of methods in a multicriteria decision analysis (MCDA) or a multiattribute utility theory (MAUT) require complex ways: they usually combine other theories, such as fuzzy environment, analytic hierarchy process (AHP), and OWA. These approaches have limitations when applied in industrial engineering. The TOPSIS model will be an extremely simple method in performance evaluation in this study. A performance property in CEM must have only one pair of extreme criteria points. CEM has multiple performances that can be classified into one pair of extreme criteria by generating the other performance item. Figure 2 below presents a concept diagram regarding 1 : 1 relationship between function and performance for CEM evaluation.

Therefore, the TOPSIS evaluation model can be easily used as a user's decision-making tool because it analyzes the degree of deterioration and measures the performance improvement level for remodeling CEM. The performance definition in this study was cited from a master's thesis [1].

2. Methods and Scopes

The original purpose of building structures is regarded as being achieved when the performance of a certain construction method is sufficiently obtained compared to the performance criteria of certain elements of building structures.

The contents of this study are described in the following procedures for quality evaluation of CEM for remodeling:

(1) Existing studies on the definition of performance criteria and quality evaluation of CEM were investigated.

(2) Problems found in CEM evaluation for remodeling were analyzed.

(3) Various items of performance criteria were determined through the analysis of international and domestic systems related to housing performance and the requirements were reorganized to match the domestic status of remodeling the apartment housing.

(4) An EIP for each requirement was set to the relevant regulations.

(5) An evaluation method for remodeling constructability was proposed, considering the concept of constructability used in new construction works.

(6) The feasibility of this study was proposed through case analysis.

3. Literature Review

Studies on the performance criteria of apartment housing have been continuously conducted since the late 1990s and the "Study on Development of Performance Grade Indication System for Remodeling of Deteriorated Apartment Housing [8]" was recently conducted. In addition, studies on the quality evaluation of product performance are being conducted in various fields of Architecture, Engineering, and Construction (AEC). The findings obtained through the investigation of the existing studies are described by dividing them into "the definition of performance criteria" and "the method of quality evaluation of CEM."

3.1. Studies on the Definition of Performance Criteria. Housing Research Institute (HRI) has conducted numerous studies related to housing performance including the "Analysis and Prevention Countermeasure for Major Defect of Apartment Houses [9]," "Performance Guideline for Dry Construction Type-Heating Panel System of Apartment Houses [10]," "The Establishment of the Thermal Performance Standard of Exterior Windows in the Extended Balcony [11]," and "Customizing Remodeling Items for Deterioration Apartment Houses [12]."

The Ministry of Construction & Transportation published "Checklist of Design Criteria of Building Structures in Consideration of Remodeling [13]" and "Safety Inspection Manual for Housing Reconstruction Projects (2003)." In regard to green energy saving policies, the Ministry of Land,

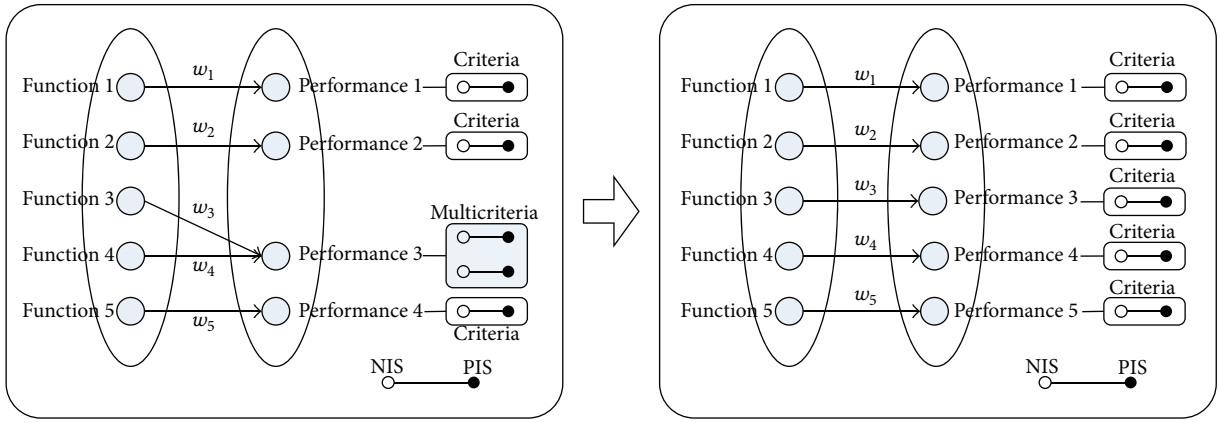

Figure 2: 1 : 1 relationship of function and performance with unique extreme criteria for CEM evaluation.

Transport and Maritime Affairs has been gradually reinforcing the performance criteria with the introduction of energy saving design criteria for building structures since 2009.

Korea Institute of Construction Technology (KICT) conducted the studies entitled "Study on Apartment Housing Performance Grade Indication System [4]," "Development of Performance Insurance System in Construction New Technology [14]," "Study on Strategy for Development of Apartment Housing Performance Grade Indication System [15]," "Study on Establishment of Guideline for Construction of General Building Structures (RC Structures) Preparing for Remodeling," and "Study on Development of Performance Grade Indication System for Remodeling of Deteriorated Apartment Housing [8]."

In addition, a study provided an acoustic performance for life in apartments [16]. All these studies have proposed the physical criteria required for housing performance evaluation and expanded enough to include the coping strategies like the warranty for defects in apartment housing.

3.2. Researches on the Evaluation of Element Technique. Researches were made on a multicriteria decision-making method in Value Engineering (VE) evaluation using the TOPSIS model [17]. A study was performed for quality evaluation on design solutions based on performance criteria by utilizing House of Quality (HOQ) technique of Quality Function Deployment (QFD) [18].

Singhaputtangkul et al. proposed a QFD-based knowledge management system for building envelopes [19]. Li et al. suggested another QFD-based knowledge management system combining itself with a fuzzy-TOPSIS that is used in a multicriteria decision-making method [20].

Despite the sustained studies on QFD till present, the focus of the reviews on its literatures has been made on the difficulties in the utilization of QFD in quality plans and benchmarking [21]. One of the findings is that the majority, up to 80%, of the methodological difficulties are related to the stage of elaborating quality matrix such as "interpreting the customer's voice" [22]. Another finding is that reducing the methodological difficulties in developing the quality matrix is a key factor in encouraging and expanding the use of QFD [21].

A study was conducted to see quality evaluation by using the AHP technique as a MCDA method to select appropriate building exterior materials [23]. Lee and Chun [24] utilized a FDD/IWDM method for the evaluation of alternatives. A feature of the FDD/IWDM method is to evaluate the relative priorities of multirequirement functions. Lee and Chun [25, 26] also focused on the design change and proposed a quantitative assessment method for alternative designs from the perspectives of cost, performance, and constructability. Cho [27] evaluated technologies to ensure green performance of apartment houses. Lee et al. [28] evaluated constructability items in terms of limitations to improve in the insulation performance on remodeling projects. Yin et al. proposed a decision support framework for building renovation strategies [29]. Yau suggested a multicriteria decision-making method for homeowners' participation in building maintenance [30]. Zhang and Lei studied environmental multiassessment for renovating residential buildings [31], adopting the principles of environmental efficiency in proposing an assessment framework for existing residential buildings that simultaneously reflects functionality and sustainability. The study demonstrated that the proposed framework provided useful information for prioritizing critical renovation issues, leading to notable improvements in functionality and sustainability.

Due to the word limit in this study, many other further studies on MCDA have been omitted.

4. Problems in Evaluation System for CEM

In order to evaluate the performance of CEM, the users' required functions should be systematically determined. The performance is related to the functions, performance targeting, and an evaluation scale.

Designers and engineers can easily obtain the title, adoption field, adopted building elements, the major effects of CEM, and the characteristics of CEM from the summaries of the technique information. The basic specifications to see the performance of CEM can be given by including representative plans or images in the introduction information. However, it does not present the suitable outcomes as the evaluation of the CEM about the adoption into building elements based on the Requirement Performance Criteria

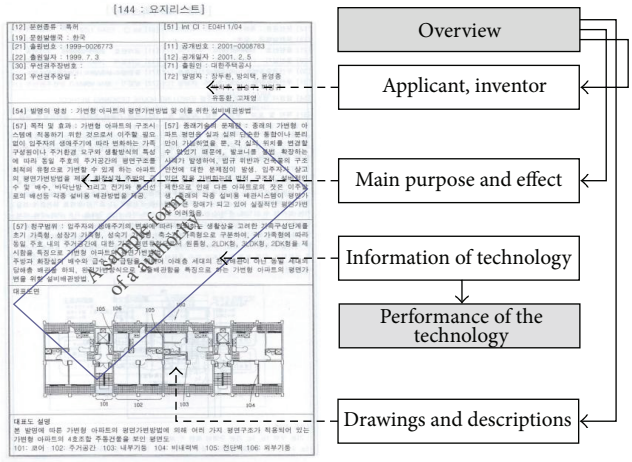

Figure 3: Composition of a CEM summary list.

(RPC). Even though information on the original performance of CEM has been additionally proven, the information usually includes the experimental evaluation obtained from an on-site test.

The objective evaluation of CEM and the comparison of performance between different construction element techniques are extremely difficult since the current performance evaluation system is not required to use any standard performance grade. Moreover, items for the evaluation of constructability are not specifically proposed in CEM evaluation.

Figure 3 presents a case of CEM information on the remodeling of a domestic building structure proposed by a certification institute.

5. TOPSIS

The Value Engineering (VE) technique is generally used in the manufacturing industry as a method of determining the ways to realize the function more economically by reviewing the function of materials systematically. In the VE technique, the total score for the function is calculated by using a weighted value and the evaluation grade of the function.

The TOPSIS technique, used as a multicriteria decision-making method, is able to analyze a preference by considering the positive ideal solution and negative ideal solution simultaneously. The TOPSIS method was originally proposed by Hwang and Yoon [32] to identify solutions from a finite set of alternatives. The detailed traditional TOPSIS solution can be found in Li et al. [20].

The VE technique evaluates the quality based on both the evaluation of each item for multiple functions and the total summed scores for a product evaluation. On the other hand, the TOPSIS method analyzes the product preference by considering the multiple properties of a product. Currently, a preference refers to the score obtained from the quality evaluation of a product and its ranges are distributed between 0 and 1. The quality is assumed to improve as the preference score approaches closer to 1.

Although both the VE technique and the TOPSIS method allow quality comparison amongst multiple alternatives, their evaluation methods differ. The VE technique generally specifies 3 or 5 grades for the evaluation of function while the TOPSIS method performs evaluation based on the distance after setting a positive ideal solution and a negative ideal solution. For the TOPSIS evaluation, the product quality value is divided by the total distance scale and then normalized in the ranges between 0 and 1. Hence, the value score calculated by the distance based the TOPSIS model can be generally used for making a decision in the AEC industry.

The preference value of TOPSIS allows comparison evaluation to be made among multiple alternatives and can be reused by many users as knowledge-based information.

In the TOPSIS evaluation model, the weighted value of the performance property is determined by the user. The performance property defines the evaluation criteria based on the positive ideal solution (PIS) and the negative ideal solution (NIS). Every single performance property must possess a PIS and a NIS; these two criteria neither contradict nor conflict with each other in terms of function description. In other words, every performance property has one PIS and one NIS, respectively. Therefore, the TOPSIS evaluation model will result in an objective evaluation on CEM purely due to performance measurement.

The procedures of TOPSIS can be expressed in the following steps.

Step 1. Calculate the normalized decision matrix. The normalized value n_{ij} is calculated as

$$n_{ij} = \frac{x_{ij}}{\max\left(x_{ij}\right)} \quad \left(i = 1, \ldots, m \;\; j = 1, \ldots, n\right). \tag{1}$$

In this study, the value n_{ij} was normalized to the absolute values rather than the relative values of the TOPSIS model.

Step 2. Calculate the weighted normalized decision matrix. The weight w_j is defined by a 10-point scale priority:

$$v_{ij} = w_j n_{ij} \quad \left(i = 1, \ldots, m \;\; j = 1, \ldots, n\right), \tag{2}$$

where w_j is the weight of the ith criterion.

The total sum of w_j in the original TOPSIS theory is 1. However, a user's subjective decision is always in priority involved for performance in all cases; thus, the user weighting definition is required to be as simple as possible. Extensive numbers of methodology and researches on the weighting approach have been conducted. Calculation of the weight is out of the range of this study. The 10-point scale priority is applied for the TOPSIS weight in this study in order to allow a reflection of a user's intuitive decision.

Step 3. Define the positive ideal solution (PIS) and negative ideal solution (NIS) as

$$\begin{aligned} &A^{+}\left\{V_1^{+}, \ldots, V_n^{+}\right\}, \\ &A^{-}\left\{V_1^{-}, \ldots, V_n^{-}\right\}, \end{aligned} \tag{3}$$

where, for benefit criterion,

$$v_j^+ = \max_i \left\{v_{ij}\right\}, \quad j = 1, 2, \ldots, n,$$
$$v_j^- = \min_i \left\{v_{ij}\right\}, \quad j = 1, 2, \ldots, n, \tag{4}$$

and, for cost criterion,

$$v_j^- = \max_i \left\{v_{ij}\right\}, \quad j = 1, 2, \ldots, n,$$
$$v_j^+ = \min_i \left\{v_{ij}\right\}, \quad j = 1, 2, \ldots, n. \tag{5}$$

Step 4. Calculate the distances of each alternative from both PIS and NIS using the following equations, respectively:

$$d_i^+ = \sum_{j=1}^{n} \operatorname{dis}\left(v_{ij} - v_j^+\right), \quad i = 1, \ldots, m,$$
$$d_i^- = \sum_{j=1}^{n} \operatorname{dis}\left(v_{ij} - v_j^-\right), \quad i = 1, \ldots, m, \tag{6}$$

where $\operatorname{dis}(v_{ij} - v_j^+)$ is the distance between the rating of alternative i and PIS on the jth criterion and $\operatorname{dis}(v_{ij} - v_j^-)$ is the distance between the rating of alternative i and NIS on the jth criterion.

Step 5. Calculate the relative closeness to the ideal solution. The relative closeness of alternative A_i with respect to A^+ is defined as

$$R_i = \frac{d_i^-}{d_i^+ + d_i^-}, \quad i = 1, \ldots, m. \tag{7}$$

According to the relative closeness degree R_i, the ranking order of all alternatives can be determined. Any alternative with the highest R_i is the most desirable alternative.

In this study, R_i values from the TOPSIS model are in the ranges between 0 and 1; the solution is classified as a higher performance as R_i values approach closer to 1.

6. Analysis of Performance Requirements

In this section, the original performance of CEM for remodeling is defined by analyzing the domestic and international performance evaluation systems to improve the performance of the building structures.

6.1. Analysis of the Domestic Performance Evaluation System. The domestic Housing Performance Grading Indication System was introduced in the 2005 Housing Act in order to provide accurate information for consumers and improve the quality of housing. This system has been made compulsory for apartment housing with 1,000 or more households since 2008; it includes items comprising 20 categories that belong to 5 sections, including noise, structure, energy environment, living environment, and firefighting. The Housing Performance Grading Indication System helps consumers to choose the housing type with the desired performance when planning or purchasing, since the system provides easy indication of housing performance together with standard grades and performance values.

6.2. Analysis on the International Performance Evaluation System. Housing Quality Indicator (HQI) of United Kingdom as an index used for evaluation of housing quality was designed to evaluate the quality of housing by assigning scores for characteristics of not only inside the housing but also outside the housing. The original purpose of the HQI evaluation system was to evaluate the quality of new construction apartment housing. However, it has been used for evaluation of housing quality with extensive ranges intending for public/private deteriorated housing of which revision was done.

HQI is composed of 10 indices including approximately 340 detailed Evaluation Indices of Performance (EIP) of quality in 3 major items including location, design, and performance. Furthermore, it is unique that the IPE can be adjusted to satisfy new environment or various social requirements with those 340 detailed HQI indices.

The Housing Performance Grading Indication System in Japan was designed based on the "Housing Quality Secure Facilitation Law." This system aims to promote the organization to systematically seek for the solutions for defect disputes related to housing and to support the market conditions that help consumers to safely purchase their houses. The primary content of the system is about a 10-year compulsory term to guarantee against the housing defects. Housing performance evaluation items are composed of 9 subcategories with 28 detailed items.

Quality Association (Association Qualitel) is a public service cooperation established by the Minister of Housing of the French government in 1974. The Qualitel Label System which was initiated in 1986 provides users with the outcomes of performance evaluation of building structures. At the time of its establishment, it aimed for the evaluation of design in new construction housing. The Qualitel Label is composed of 7 evaluation items and determines whether the design holds certain labels of quality [33]. In each item, the scores from 1 to 5 are given and the Qualitel Label is assigned when the score is 3 or more for all items.

6.3. Analysis Outcomes. Requirement performance criteria must be first defined in order to exchange and to repair building elements to achieve a certain level of housing performance. This is because an environment enables the user to select the appropriate CEM with the standard performance.

As a result of the comparison on the domestic and international performance evaluation systems, many similarities between the items were observed in terms of performance subjects, such as (1) durability and safety, (2) habitability and sanitation, (3) maintainability, (4) eco-friendliness, (5) energy saving, (6) aesthetic aspects, and (7) consideration for elderly people. However, the domestic performance evaluation system was shown to be insufficient in the detailed evaluation for the consideration of elderly people, crime prevention, energy saving, and aesthetic aspects compared to those of the international performance evaluation system. Therefore, the performance items of remodeling that would cope with the domestic system were defined by referring to the items of the international performance evaluation in Table 1.

Table 1: Requirement performance criteria (RPC) for remodeling projects.

Requirements (sections)	Requirements (categories)	Durability and safety					Habitability and sanitation					Consideration for elderly and weak people	Maintainability		Crime prevention	Eco-friendliness	Energy saving		Aesthetic aspects
		Durability of structural materials	Durability of planning	Design-related safety	Fire safety	Safety for natural disaster	Safety for use	Functionality of space	Gait, texture	Durability of structural materials	Durability of planning	Design-related safety	Fire safety	Safety against natural disaster	Safety for use	Functionality of space	Gait, texture	Durability of structural material	Durability of planning	Design-related safety	Fire safety	Safety from natural disaster	Safety for use
(1) Housing Performance Grading Indication System (domestic)		●	●	●	●	—	●	●	—	●	●	●	●	●	●	●	●	—	●	×	●	—	—
(2) Green Building Certification System (domestic)		—	—	●	—	●	●	●	●	—	●	—	●	—	—	—	—	—	●	—	●	●	●
(3) Building Energy Rating System (domestic)		—	—	—	—	—	●	—	—	●	●	—	●	—	—	●	—	—	●	—	●	●	—
(4) Housing Quality Indicator (HQI) of United Kingdom		●	●	●	—	—	●	●	●	●	—	●	●	●	●	●	—	—	●	—	●	●	—
(5) Housing Performance Grading Indication System in Japan		●	●	●	●	●	●	●	●	●	●	●	●	●	—	●	—	—	●	—	●	●	—
(6) Qualitel Label System in France		●	—	●	●	—	●	●	—	●	●	●	—	—	—	●	—	—	●	—	●	●	—
Adoption		o	×	o	o	o	o	o	o	o	o	o	o	o	×	o	×	o	o	×	o	o	o

Table 2: Evaluation index of performance for remodeling and PIS/NIS.

Sections	Number	Items	Evaluation Index	
			T/F	Grade
Durability and safety	1.1	Maintenance/repair of initial performance	●	
	1.2	Extension of structural life		Gr. 3
	1.3	Improvement in seismic performance	●	
	1.4	Improvement in bending or deformation performance	●	
	1.5	Improvement in collapse and destruction prevention	●	
	1.6	Improvement in impact resistance performance	●	
	1.7	Improvement in local compressive load performance	●	
	1.8	Improvement in load resistance performance	●	
	1.9	Improvement in distribution pressure resistance	●	
	1.10	Improvement in fire detection and alert performance		Gr. 3
	1.11	Improvement in smoke control and evacuation		Gr. 3
	1.12	Improvement in fireproof and noncombustion		Gr. 3
	1.13	Improvement in safety against natural disasters	●	
	1.14	Prevention against slip, collapse, and fall	●	
Habitability and sanitation	2.1	Expansion and secure area	●	
	2.2	Secure ceiling height	●	
	2.3	Impact absorption, noise-proof		Gr. 3
	2.4	Secure view		Gr. 3
	2.5	Secure natural lighting		Gr. 4
	2.6	Improvement in artificial lighting		Gr. 3
	2.7	Prevention for visual fatigue and secure visibility	●	
	2.8	Improvement in noise absorbing performance	●	
	2.9	Improvement in light weighted impact sound-proof		Gr. 4
	2.10	Improvement in heavy weighted impact sound-proof		Gr. 4
	2.11	Improvement in bathroom noise-proof performance		Gr. 4
	2.12	Improvement in boundary noise-proof performance		Gr. 3
	2.13	Reduction in self-noise occurrence	●	
	2.14	Improvement in thermal insulating performance		Gr. 3
	2.15	Improvement in dew-proof performance	●	
	2.16	Reduction in release of interior hazardous air pollutant		Gr. 3
	2.17	Improvement in ventilating and wind flowing		Gr. 3
Consideration for the weak	3.1	Consideration for people with visual impairment	●	
	3.2	Consideration for people with hearing disabilities	●	
	3.3	Consideration for the handicapped and the weak	●	
Maintainability	4.1	Reinforcement of fouling resistance	●	
	4.2	Variability of space planning (plane)		Gr. 4
	4.3	Facility variability	●	
	4.4	Easiness of conservation and repair		Gr. 4
	4.5	Easiness of replacement and repair	●	
Crime prevention	5.1	Performance of trespassing prevention	●	
	5.2	Reinforcement of surveillance function	●	
Eco-friendliness	6.1	Recyclability, renewability, and reusability of wastes at destruction	●	
	6.2	Prevention for air pollution while handling wasted materials	●	
	6.3	Prevention for soil pollution while handling wasted materials	●	
	6.4	Prevention for water pollution while handling wasted materials	●	
Energy conservation	7.1	Utilization of natural energy	●	
	7.2	Improvement in thermal insulation		Gr. 3
	7.3	Improvement in air tightness		Gr. 3
	7.4	Improvement in performance and function of facility		Gr. 3
	7.5	Improvement in facility efficiency (energy and water)		Gr. 3
	7.6	Extension of facility life		Gr. 3
Aesthetics	8.1	Improvement in aesthetics for indoor common area	●	
	8.2	Improvement in aesthetics for indoor private area	●	
	8.3	Improvement in external wall aesthetics	●	
	8.4	Improvement in rooftop aesthetics	●	
	8.5	Improvement in outdoor aesthetics	●	

Table 3: Constructability evaluation index for remodeling and PIS/NIS.

Performance sections	Number	Categories and items	Evaluation index	
			T/F	Grade
Constructability (manufacturability-workability)	9.1	Duration of design (unit: days)		Gr. 3
	9.2	Duration of the initiation of manufacturing (unit: days)		Gr. 3
	9.3	Duration per construction unit (unit: days)		Gr. 3
	9.4	Demanding crews (unit: crews/unit)		Gr. 3
	9.5	Demanding hypothesis per construction unit (hypothesis/unit)		Gr. 3
	9.6	Quality safety (reliability)	●	
	9.7	Easiness of clamping to and removal from existing elements	●	
	9.8	Level of difficulty for curing		Gr. 3
	9.9	Workability and capacity for fine-tuning at work site	●	
	9.10	Work compatibility	●	
Work safety	10.1	Safety for construction work		Gr. 3
	10.2	Safety for maintenance		Gr. 3
Energy conservation	11.1	Energy consumption at production stage		Gr. 3
	11.2	Water consumption at production stage		Gr. 3
Eco-friendliness	12.1	Release of hazardous volatile substances		Gr. 3
	12.2	Dust at production stage		Gr. 3
	12.3	Noise at production stage		Gr. 3

7. Evaluation Index of Performance (EIP)

In this section, detailed requirements and the Evaluation Index of Performance (EIP) will be established based on the defined performance items for remodeling that were proposed in Section 6. EIP is equivalent to the existing performance criteria used for newly constructed buildings. It is used to ensure the performance prior to remodeling as well as the performance after remodeling. Users can confirm and compare the degree of improvement in performance achieved in the subject building structures by using EIP.

EIP is applied differently for each CEM according to the characteristics regarding the diverse levels of the performance including durability, variability, noise protection function, solar protection, fire protection, and firefighting. EIP measurements are categorized either by criteria grading or by certain performance presence. In case of grading the criteria, grading is assigned according to the grades from 3 to 5. In case of the binary type, two types are assigned as true (value: 1) or false (value: 0). A grading scale is applied to the TOPSIS model after standardization in the ranges between 0 and 1 since the RPC is not standardized in the same scale.

Table 2 shows a list of detailed requirements and EIP for remodeling. The contents of EIP are carefully described in the study performed by Lee [1] and the study entitled "Study on Development of Performance Grade Indication System for Remodeling of Deteriorated Apartment Housing" by KICT [8].

Constructability is considered in order to minimize the issues that may occur in the construction phases such as economic feasibility, safety, environmental feasibility, and space-workability. In this study, the Evaluation Index for Constructability (EIC) was established by combining the constructability items that are generally applied for new construction work, which is shown in Table 3. The details of EIC are described in the study performed by Lee [1].

8. Case Analysis

Remodeling is composed of "nonchangeable elements" and "improvable elements." Nonchangeable elements which include a floor-to-ceiling height limit and a core position because the majority of apartment housing have wall type structure. Some examples of improvable elements are replacement of sanitary pipelines, change of shaft layout, change of access doors, and so forth. In this case study, design alternatives which are to be improved are selected in consideration of the remodeling constraints when new pipelines are installed in an aged bathroom space. The degree of performance improvement will be measured using the TOPSIS model by comparing respective design solutions before and after remodeling of the aged bathroom.

The shaft layout prior to the remodeling had a structure constraint that did not allow regular inspection. The structure is subjected to change in order to allow regular inspection with reshaping of the shaft. In the existing deteriorated space in the apartment housing, a noise occurs since a sewage pipeline is installed in the ceiling where the down surface of the floor of the upstairs household is. Getting a sewage pipeline buried in the bathroom floor with the additional 80 mm thick flooring is planned as the first alternative method for troubleshooting. For the second alternative method, the noise will be completely blocked by getting both sewage and waste water pipelines buried in a noise-proof wall.

The status prior to the remodeling, summary of the applied CEM, and performance evaluation of the applied CEM were reorganized by referring to EIP for remodeling, which are shown in Tables 4 and 5. Figure 4 presents the

Table 4: Summary of remodeling design solutions.

Items	The subject status for remodeling	Alternative method—CEM A	Alternative method—CEM B
Sectional view of the installed pipe	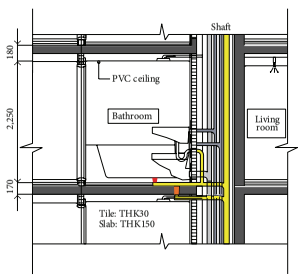	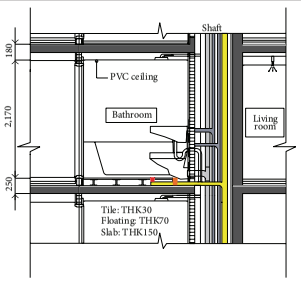	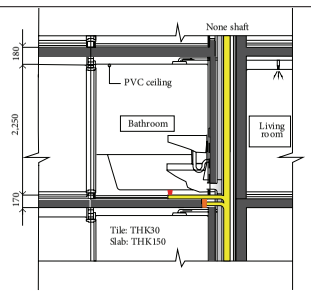
Features of the construction method	A sewage pipeline is installed on the ceiling of the household in downstairs	Repair of existing shaft space; piping the sewage pipeline in subject floor by constructing the additional 50 mm thick flooring	Shaft removal; sewage pipeline buried in a noise-proof wall
Major limitations of the technique	Difficulty in maintenance and issue of noise occurrence	Easy maintenance and relatively less noise	Easy maintenance, perfect noise blocking, and increase of useful workspace due to reduction in shaft space

Table 5: Performance evaluation of the design solutions.

Item	Weighting	Evaluation standard performance			Weighted standard performance		
		Deteriorated status	Alternative method-A	Alternative method-B	Deteriorated status	Alternative method-A	Alternative method-B
2.01	**10**	**0**	**0**	**1**	**0.00**	**0.00**	**10.00**
2.02	10	1	1	3	3.33	3.33	10.00
2.08	10	0	1	1	0.00	10.00	10.00
2.11	10	0	2	4	0.00	5.00	10.00
2.16	9	0	3	3	0.00	9.00	9.00
4.01	9	0	1	1	0.00	9.00	9.00
4.03	**7**	**1**	**1**	**0**	**0.00**	**7.00**	**7.00**
4.05	7	0	1	1	0.00	7.00	7.00
6.01	4	0	1	1	0.00	4.00	0.00
6.02	4	0	1	0	0.00	4.00	0.00
6.03	4	0	1	0	0.00	4.00	0.00
6.04	4	0	1	0	0.00	4.00	0.00
7.04	7	0	1	1	0.00	7.00	7.00
7.06	7	0	2	3	0.00	4.67	7.00
8.02	10	0	1	1	0.00	10.00	10.00
9.03	10	—	2	3	—	6.67	10.00
9.04	10	—	2	3	—	6.67	10.00
9.06	10	—	1	1	—	10.00	10.00
9.07	8	—	0	1	—	0.00	8.00
9.09	8	—	0	1	—	0.00	8.00
10.01	10	—	2	3	—	6.67	10.00
11.01	10	—	2	1	—	6.67	3.33
12.01	10	—	1	3	—	3.33	10.00

analyzed data obtained from the performance evaluation on the applied TOPSIS model.

In the case study, the performance improvement before remodeling and after the application of the CEM was analyzed for the bathroom space. The weight of EIP was defined by the user's subjective needs. The weight is different in all projects in terms of user's requirements. In the case study, 10-point scale priority was applied. The weight was obtained by 3 users in average since performance evaluation differs by user's determination on the weight.

EIP (2.01) and EIP (4.03) have the same performance property with each different function description. However, these outcomes of EIP have different extreme criteria (PIS: true; NIS: false). Alternatives A and B show the contradicting performance evaluation score by the different criteria.

The composite performance of alternative A was analyzed as 0.79 and that of alternative B was analyzed as 0.83. In terms of constructability, the performance of alternative A and that of alternative B were evaluated as 0.53 and 0.91, respectively. Alternative B was excellent in both the required performance and the constructability compared to those of alternative A. In future study, total composite value of performance improvement will be possibly calculated if the performance before and after remodeling is compared in one housing project.

9. Conclusions

Both personal- and national-wide interests in the housing remodeling rather than in the new construction are increasing as a trend. This study selected fundamental RPC for remodeling through research investigation on housing performance for new housing construction in domestic and international housing construction markets. With the increasing demand for remodeling, performance evaluation that is related to functional improvement is expected to facilitate successful management of design and product development. This case study contributes to TOPSIS utilization as a standard method for the performance evaluation on aged apartment housing. Major conclusions of this study are summarized as follows:

(1) Required performance for remodeling of apartment houses was categorized as 8 sections with 56 detailed items. For constructability, 4 sections with 17 detailed items were presented. For the establishment of EIP, domestic related criteria were referred to.

(2) The TOPSIS method was used to measure the performance improvement degree on remodeling design solutions before and after remodeling and to present composite performance scores with multiperformance properties, including constructability.

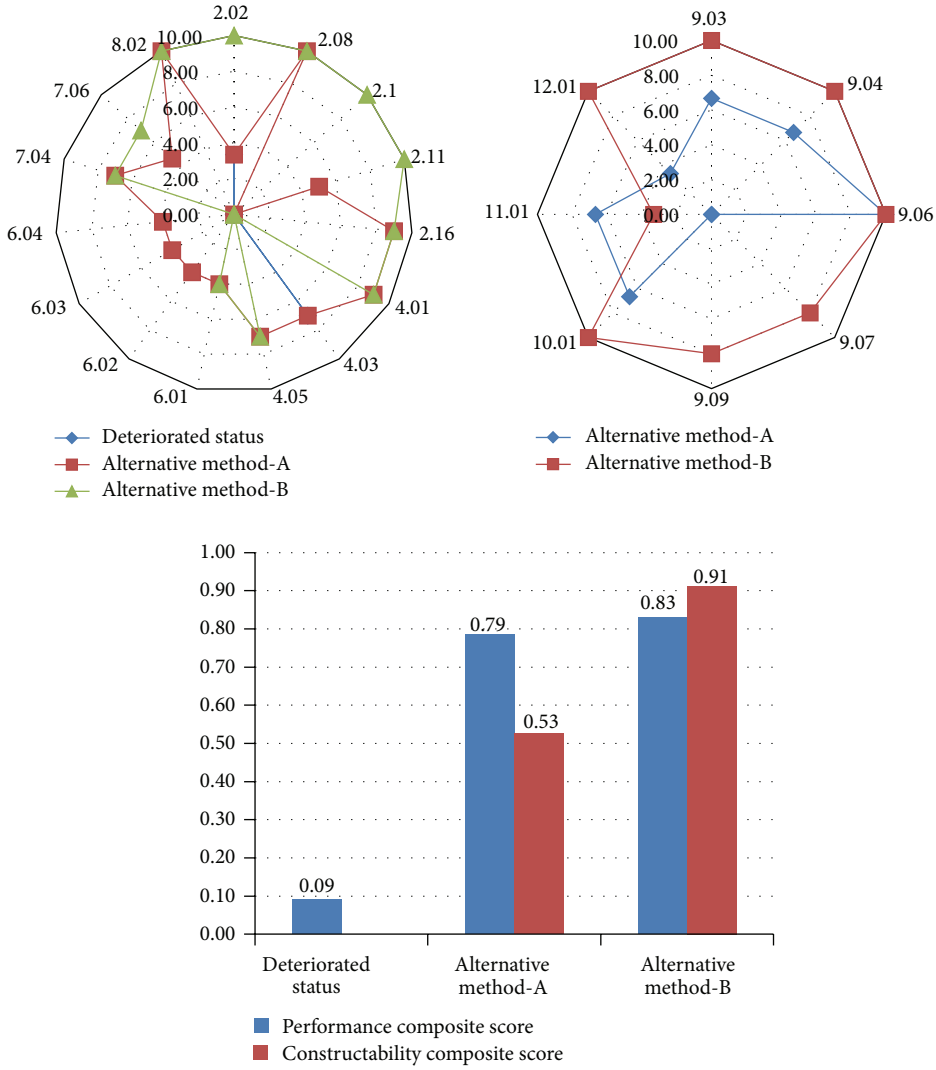

Figure 4: TOPSIS evaluation on performance and constructability for each alternative.

(3) PIS and NIS of the TOPSIS method provided objective performance evaluation scores for CEM by defining a unique performance property that can be related to one or more function requirements.

(4) Users' environment of remodeling projects was considered in the TOPSIS evaluation since it allowed the users to decide the weight for performance.

(5) Research on standardization of remodeling EIP is required since EIP varies by each research institution.

For future study, it is recommended to make an elaborated survey on the industrial utilization and verification of users' objectivity evaluation through the comparison with the existing performance evaluation methods such as VE and QFD.

Conflict of Interests

The authors declare that there is no conflict of interests regarding the publication of this paper.

Acknowledgment

This research was supported by the National Research Foundation of Korea (NRF) (no. NRF-2012R1A1A2043186).

References

[1] Y. H. Lee, *A study on evaluation system of elemental techniques for remodeling building [M.S. thesis]*, Dankook University, 2009.

[2] Housing Performance Evaluation and Certification Association, 2009, http://www.hyoukakyoukai.or.jp/seido/info.html.

[3] S. Isaac and R. Navon, "Feasibility study of an automated tool for identifying the implications of changes in construction projects," *Journal of Construction Engineering and Management*, vol. 134, no. 2, pp. 139–145, 2008.

[4] KICT, "Study on apartment housing performance grade indication system," KICT Report, 2005.

[5] W. C. Cha, B. W. Lim, C. H. Shin, B. H. Shin, J. S. Lee, and J. Y. Chun, "Availability evaluation system for remodeling of existing apartment houses," *Korea Journal of Construction Engineering and Management*, vol. 9, no. 5, pp. 204–213, 2008.

[6] Korean Intellectual Property Office (KIPO), "Remodeling technology of building structures," Technology Trends Survey Report, 2004.

[7] Y. Chen, K. W. Li, and S.-F. Liu, "An OWA-TOPSIS method for multiple criteria decision analysis," *Expert Systems with Applications*, vol. 38, no. 5, pp. 5205–5211, 2011.

[8] KICT, "Study on development of performance grade indication system for remodeling of deteriorated apartment housing," KICT Report, 2013.

[9] S. B. Lee, J. S. Ko, H. W. Paeng, and J. H. Oh, "Analysis and prevention countermeasure for major defect of apartment houses," *House Research Institute*, vol. 71, pp. 144–158, 2001.

[10] D. H. Lee, M. H. Cheon, and J. M. Choei, "Performance Guideline for Dry Construction Type-Heating Panel System of Apartment Houses," *House Research Institute*, vol. 73, no. partment, pp. 107–128, 2002.

[11] J. Y. Kim, H. J. Hwang, G. S. Ahn, J. C. Yoo, and J. H. Huh, "The establishment of the thermal performance standard of exterior windows in the extended balcony," Tech. Rep., House Research Institute, 2007.

[12] I. G. Lee, "Customizing remodeling items for deterioration apartment houses," House Research Institute Report, 2013.

[13] "Checklist of design criteria of building structures in consideration of remodeling," Ministry of Construction and Transportation Report, 2001.

[14] KICT, "Development of performance insurance system in construction new technology," KICT Report, 2007.

[15] KICT, "Study on strategy for development of apartment housing performance grade indication system," KICT Report, 2008.

[16] Y. K. Oh, "An assessment model for the indoor noise environment of aged apartment houses," *Journal of Asian Architecture and Building Engineering*, vol. 13, no. 2, pp. 445–451, 2014.

[17] G. S. Kim and S. Y. Jung, "Value evaluation using quantitative attribute in VE," *Quality Innovation*, vol. 2, no. 1, pp. 15–22, 2001.

[18] S. Y. Yoo and J. S. Yi, *A Basic Study on the Application of QFD at Architectural Design Phase*, Korea Institute of Construction Engineering and Management, 2005, Academic Annual Conference Proceedings.

[19] N. Singhaputtangkul, S. P. Low, A. L. Teo, and B.-G. Hwang, "Knowledge-based decision support system quality function deployment (KBDSS-QFD) tool for assessment of building envelopes," *Automation in Construction*, vol. 35, pp. 314–328, 2013.

[20] M. Li, L. Jin, and J. Wang, "A new MCDM method combining QFD with TOPSIS for knowledge management system selection from the user's perspective in intuitionistic fuzzy environment," *Applied Soft Computing*, vol. 21, pp. 28–37, 2014.

[21] J. A. Carnevalli and P. C. Miguel, "Review, analysis and classification of the literature on QFD-Types of research, difficulties and benefits," *International Journal of Production Economics*, vol. 114, no. 2, pp. 737–754, 2008.

[22] D. Ginn and M. Zairi, "Best practice QFD application: an internal/external benchmarking approach based on Ford Motors' experience," *International Journal of Quality and Reliability Management*, vol. 22, no. 1, pp. 38–58, 2005.

[23] J. S. Jeong, I. W. Ryoo, and Y. W. Lee, "A study on the choice of the curtain-wall type and the exterior material according to commercial building images by using the AHP," *Architectural Society: Planning Section*, vol. 22, no. 11, pp. 89–96, 2006.

[24] J. Lee and J. Chun, "Risk response analysis model for construction method using the forced-decision method and binary weighting analysis," *Journal of Asian Architecture and Building Engineering*, vol. 8, no. 1, pp. 205–212, 2009.

[25] J. S. Lee and J. Y. Chun, "Decision-making process for alternative selection of proper design change in construction project," *Korean Journal of Construction Engineering and Management*, vol. 11, no. 2, pp. 74–82, 2010.

[26] J. S. Lee and J. Y. Chun, "A numerical value evaluation model for the optimum design selection," *Journal of Asian Architecture and Building Engineering*, vol. 11, no. 2, pp. 283–290, 2012.

[27] K. M. Cho, "Evaluation of technologies ensuring green performance in multi-family housing projects in Korea," *Journal of Asian Architecture and Building Engineering*, vol. 13, no. 1, pp. 133–139, 2014.

[28] H. H. Lee, S. I. Kim, J. H. Lim, and S. Y. Song, "Case study of thermal insulation remodeling projects and analysis of restrictions," *Architecture Institute of Korea Conference Proceedings*, vol. 34, no. 1, pp. 231–232, 2014.

[29] H. Yin, P. Stack, and K. Menzel, "Decision support for building renovation strategies," in *Proceedings of the ASCE International Workshop on Computing in Civil Engineering*, pp. 834–841, June 2011.

[30] Y. Yau, "Multicriteria decision making for homeowners' participation in building maintenance," *Journal of Urban Planning and Development*, vol. 138, no. 2, pp. 110–120, 2012.

[31] H. Zhang and S. L. Lei, "An assessment framework for the renovation of existing residential buildings regarding environmental efficiency," *Procedia—Social and Behavioral Sciences*, vol. 68, pp. 549–563, 2012.

[32] C. L. Hwang and K. Yoon, *Multiple Attribute Decision Making: Methods and Applications*, vol. 186 of *Lecture Notes in Economics and Mathematical Systems*, Springer, Berlin, Germany, 1981.

[33] Qualitel, 2010, http://www.qualite-logement.org/accueil.html.

Hindawi Publishing Corporation
Mathematical Problems in Engineering
Volume 2015, Article ID 404926, 25 pages
http://dx.doi.org/10.1155/2015/404926

Research Article

Service Station Evaluation Problem in Catering Service of High-Speed Railway: A Fuzzy QFD Approach Based on Evidence Theory

Xin Wu,[1,2] Lei Nie,[1,2] and Meng Xu[2]

[1] *School of Traffic and Transportation, Beijing Jiaotong University, Beijing 100044, China*
[2] *State Key Laboratory of Rail Traffic Control and Safety, Beijing Jiaotong University, Beijing 100044, China*

Correspondence should be addressed to Lei Nie; lnie@bjtu.edu.cn

Received 10 April 2015; Revised 17 June 2015; Accepted 24 June 2015

Academic Editor: Zdeněk Kala

Catering Service of High-Speed Railway (CSHR) starts at suppliers, includes distribution centers and service stations in cities, and ends at cabinets in high-speed trains. In Distribution System Design (DSD) Problem for CSHR, it is critical to evaluate the alternatives of service stations, which is termed as Service Station Evaluation Problem in Catering Service of High-speed Railway (SSEP-CSHR). As a preparation work for DSD, SSEP-CSHR needs to be solved without detailed information and being accompanied with uncertainty. Fuzzy Quality Function Deployment (F-QFD) has been given in the literatures to deal with vagueness in Facility Location Evaluation (FLE). However, SSEP-CSHR that includes identifying and evaluating stations requires not only dealing with the vague nature of assessments but also confirming them. Based on evidence theory, this paper introduces the framework to give the truth of proposition "x is **A**." Then it is incorporated into a two-phase F-QFD with an approximate reasoning to enable the truth of the decisions to be measured. A case study that refers to 85 alternative stations on Chinese high-speed railway will be carried out to verify the proposed method. Analysis shows that the proposed evaluation method enhances scientific credibility of FLE and allows decision makers to express how much is known.

1. Introduction

In China, the significance of Catering Service of High-Speed Railway (CSHR) has emerged with the rapid development of high-speed passenger rail line's construction. The process of the service starts at suppliers, includes distribution centers and service stations in various cities, and ends at cabinets in high-speed trains (see Figure 1). Service stations, that is, places to catering foods, play an essential role as link-ups between suppliers and trains in food distribution system. The performance of each station for catering is extremely important for CSHR to maintain a continuous supply and rapid distribution. Hence for a new institute to establish a distribution system to support CSHR, it is an inevitable decision to evaluate alternative sites of service station as a preliminary work for other further decisions in CSHR. Service station Evaluation Problem (SSEP-CSHR) thus becomes a critical issue in CSHR.

The evaluation of alternative locations is a Multi-Criteria Decision-Making (MCDM) problem referring to qualitative criteria. Under this situation, the values referred in MCDM are often imprecisely defined for the decision-makers. So a fuzzy perspective is adopted naturally in related literatures to deal with above uncertainty. Kuo et al. [1] develop a decision support system in basis of Fuzzy Analytic Hierarchy Process (F-AHP) to assess new stores. Chen [2] proposes a MCDM approach to solve a distribution center evaluation problem under fuzzy environment. Kahraman et al. [3] solve Facility Location Evaluation (FLE) problem by four different fuzzy group decision-making methods, including a fuzzy model proposed by Blin [4], fuzzy synthetic evaluation, weighted goals method [5], and Extent Analysis by Chang [6]. Kulak et al. [7] develop an MCDM based on axiomatic design and Analytic Hierarchy Process (AHP) to select transportation companies. Guo [8] proposes a Fuzzy Data Envelopment Analysis (F-DEA) model for a case involving a new restaurant

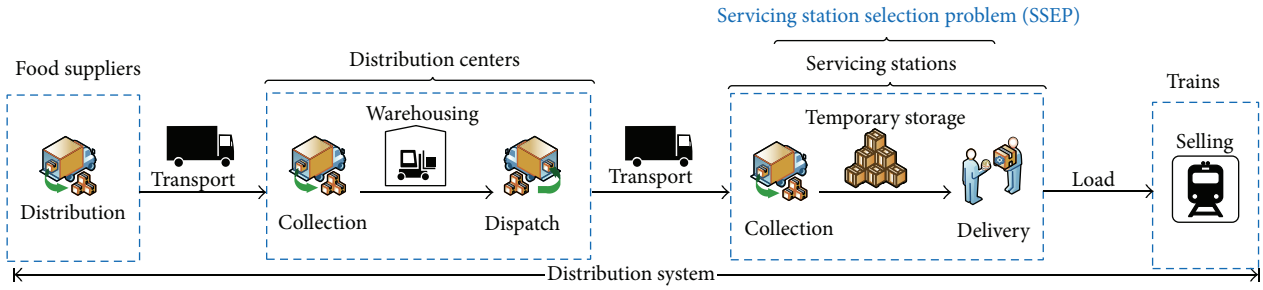

Figure 1: The process of catering service for High-Speed Railway (CSHR).

location. Like other MCDM problems, SSEP-CSHR is also required to be done without detailed information and thus is always accompanied with different types of uncertainty.

Service stations in CSHR are also required to satisfy some Basic Requirements, for example, accessibility to trains and, meanwhile, enough time for catering food. Quality Function Deployment (QFD) is one of coherent systems widely used to translate Basic Requirements into actionable alternatives [9]. A typical QFD contains info about "WHATs" and "HOWs," the relations between "WHATs" and "HOWs," and the correlations between "WHATs"/"HOWs" themselves. All above information can be presented by Houses of Quality (HOQ) [10].

Jamalnia et al. [11] have attempted to develop a Fuzzy Quality Function Deployment (F-QFD) approach for FLE. they proposed some facility locations requirements and then use alternative location to realize them. It follows that F-QFD methodology is capable of solving SSEP-CSHR as a special case of FLE problems. But one of challenges that FLE-F-QFD is encountering when it is utilized in SSEP-CSHR is accountability. Because expensive cost will be spent if a decision-maker plans to establish a cold chain for CSHR and SSEP-CSHR that involves identifying, evaluating alternative service stations requires not only handling the vague nature of assessments but also confirming them, that is, professing what decision makers do know and what they do not know [12]; It means that decision makers lead the truth of the outputs to be measured. Furthermore CSHR is a new field in logistic management, experts are far from having general agreement about the importance of certain Basic Requirements. So the results provided by FLE-F-QFD are indispensable to be crosschecked through various experts to ensure its credibility.

It leads to some important problems in related studies about uncertainty management in F-QFD. Kim et al. [13] conclude the uncertainty in QFD mainly arising from the following sources, *Fuzziness*, *Fluctuation*, and *Heterogeneity*.

(1) *Fuzziness* accounts for the imprecise nature or vagueness of the linguistic terms used in QFD. In fact, QFD teams usually do not have sufficient knowledge about the values taken in a HOQ due to the lack of clarity. It makes the application of fuzzy sets theory in QFD (i.e., F-QFD) significant in many problems; fuzzy sets are used to describe natural language-based criteria. F-QFD is one of extended version of typical QFD approaches, which have been widely used in many field [11, 14–20]. In F-QFD, (Fuzzy) AHP approaches [6, 21–25] are always used to generate the inputs.

(2) *Fluctuation* is associated with the change of Basic Requirements over time. SSEP-CSHR is placed on the early stage of SCD problem, so the Fluctuation of the requirements is inevitable. The framework of Robust QFD was presented by Kim et al. [13, 26] to accommodate this uncertainty and to prevent QFD teams obtaining misleading outputs.

(3) *Heterogeneity* comes from the different viewpoints of multiple experts. Hence it is required to justify the outputs obtained by a QFD team by other experts' opinions.

To achieve justifications to cope with the *Heterogeneity*, evidences from questionnaires must be referred to. Evidences from questionnaires are generally related to the occurrence of deterministic or stochastic events and treat crisp values or probability distributions as their paradigm. However sometimes the evidences involve nonrandom events, such as "an estimated strength of one passenger demand," and thus are biased by perception or even guess [12]. SSEP-CSHR apparently refers to subjective experience or uncertain considerations. In this case, evidences are represented by possibility distributions, or mixed evidences consist of both probability and possibility distribution. In regard to the above-mentioned status, FLE-F-QFD should be improved to adapt above complicated evidences in order to solve SSEP-CSHR.

Recently, great advances have been made in the field of evidence theory. Then complicated empirical evidence is utilized to confirm propositions "x is $\mathbf{A}$" in evidence theory. Various types of proofs are thus defined by the way of an evidence x proving its membership in any set $\mathbf{A}$ [27]. The objective of this paper is to introduce evidence theory to make an approximating reasoning possible in a modified QFD to dampen the effects of both *Fuzziness* and *Heterogeneity*.

Figure 2 concludes the relations among application background, motivations, existing versions of QFD, and our proposed method. In the paper, we firstly present the essence of evidence theory including its concepts and formulas to measure the truth of "x is $\mathbf{A}$." Meanwhile we propose two measures which will be used in our modified F-DFD. Further two-phase F-QFD is introduced. Based on the two-phase F-QFD method, we devote ourselves to incorporate evidence theory into SSEP-CSHR by a procedure of approximate reasoning and form an effective approach to determine alternatives in CSHR with respect to certain qualitative criteria.

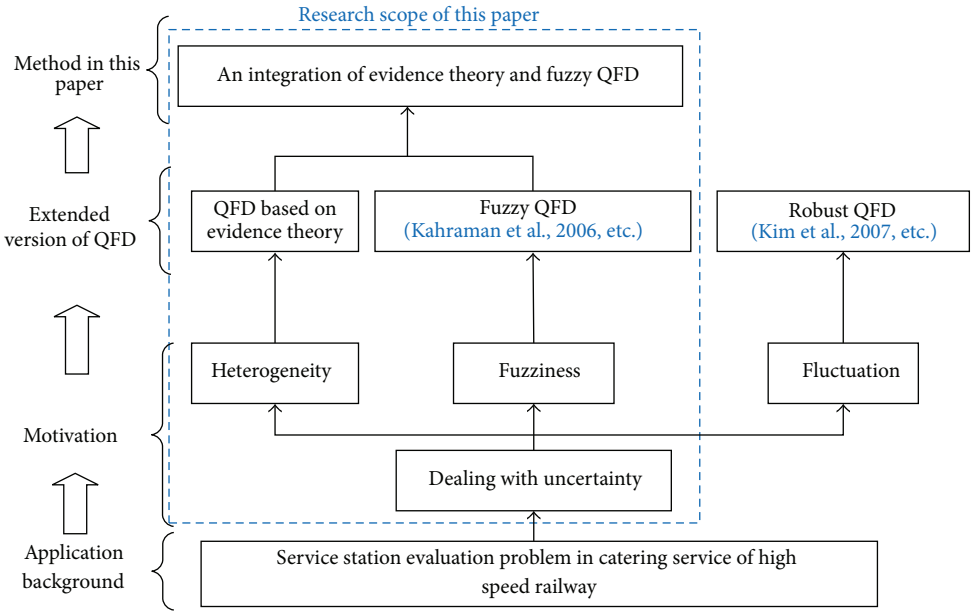

Figure 2: The precedence relationship among background, motivations, various QFDs, and our method.

This paper is organized as follows. In Section 2, a framework for determining the truth of "x is $\mathbf{A}$" in basis of evidence theory is introduced. In Section 3.2, a two-phase F-QFD methodology will be described briefly and in Section 3.2 HOQs in the context of SSEP-CSHR will be discussed in detail. Further, in Section 3.3, a procedure of approximate reasoning based on evidence theory is incorporated into FLE-F-QFD for SSEP-CSHR. In Section 4, a case study in the context of CSHR will be done to verify our methodology. The analysis shows that the proposed method enhances scientific credibility of FLE-F-QFD in CSHR and allows decision makers to express how much is known. Figure 3 illustrates the precedence relationship between our sections.

2. Framework for Determining the Truth of "x Is A" Based on Evidence Theory

2.1. Proposition. The canonical form of a proposition is "x is $\mathbf{A}$," where subject x refers to the condition of an object and $\mathbf{A}$ is a set that represents a predicate of x. The following are examples [12].

Example 1. Constructions Costs (CC) are very important.

x = Constructions Costs (CC); $\mathbf{A}$ = very important.

Example 2. Proximity to trains (PT) is quite important.

x = proximity to trains (PT); $\mathbf{A}$ = quite important.

$\mathbf{A}$ is represented by fuzzy sets. Truth of a proposition is evaluated by the degree of x supporting $\mathbf{A}$.

2.2. Set $\mathbf{A}$ *in "x Is* $\mathbf{A}$*".* The predicate $\mathbf{A}$ is a description of a situation and is treated as either crisp or fuzzy sets.

Given $\widetilde{\mathbf{A}} = \{(x, \widetilde{\mathbf{A}}(x)) \mid x \in \mathbf{U}\}$ is a fuzzy set, where $\widetilde{\mathbf{A}}(x)$ denotes normalized membership function, $\mathbf{U}$ is a universal set. According to the first decomposition theorem:

$$\widetilde{\mathbf{A}} = \bigcup_{\alpha \in [0,1]} \alpha \cdot \mathbf{A}_\alpha. \tag{1}$$

And sets called α-cut of the fuzzy set are defined as follows:

$$\mathbf{A}_\alpha = \left\{x \in \mathbf{U} \mid \widetilde{\mathbf{A}}(x) \geq \alpha\right\} = \left[(A)_\alpha^L, (A)_\alpha^U\right] \quad \forall \alpha \in [0,1]. \tag{2}$$

We set $\alpha \in \{1/K, 2/K, \ldots, 1\}$. K is the number of α-cut considered in $[0,1]$. For brevity, in this paper, we use Triangular Fuzzy Numbers (TFNs) $a/b/c$ to denote a fuzzy number on an x-α graph; say $\alpha = 1$ with $x = b$, and say $\alpha = 0$ with x in $[a, c]$ [27].

A membership function is a graphical expression about decision makers' opinions. For example, a group of decision makers is asked to express "the strength degree of the relation between CP and PT" by fuzzy scores. Each decision maker draws two lines on an x-y graph to describe the feeling about the strength, x-axis being the score, and y-axis being the membership level between 0 and 1 (like a triangle or a trapezoid). As shown in Figure 4(a), two lines will both start from $y = 1$ at $x = 5$, which means that "the strength of the relation between CP and PT is 5" is with the most certainty, and end at two points, respectively, on left and right side of score 5, where the scores are totally uncertain for the decision maker (thus $y = 0$ at the points). Many similar lines are drawn by different decision makers and a membership function can be obtained by combining them as shown in Figure 4(a). In Figure 4(b), we take $K = 5$; α-cuts of the fuzzy set are used to fit the depicted membership function. The larger the parameter K is, the better the α-cuts fit the function.

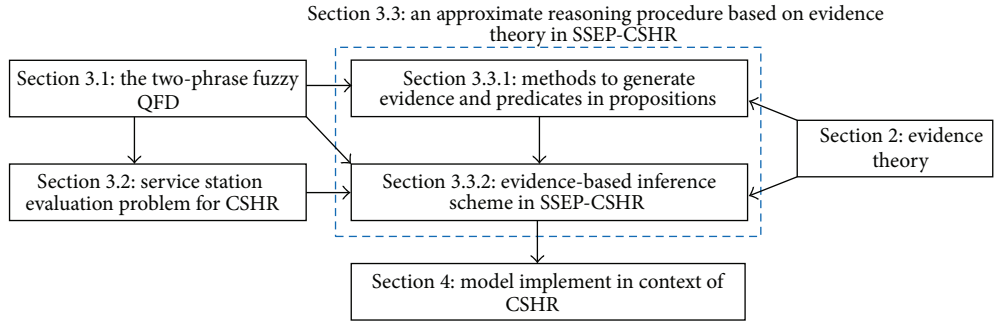

Figure 3: The precedence relationship between sections.

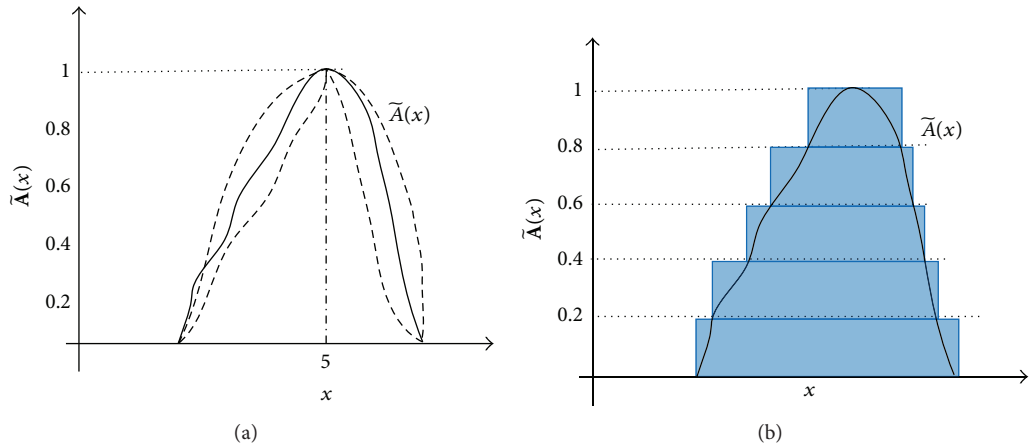

Figure 4: An illustration of the development of predicate A.

2.3. Evidence about x. Let a universal set be $\mathbf{U}$. The family of all subsets of a given set $\mathbf{A}$ is called the power set of $\mathbf{A}$, and it is denoted by $\mathscr{P}(\mathbf{A})$. The following function is called basic probability assignment of evidences:

$$m: \mathscr{P}(\mathbf{U}) \longrightarrow [0,1] \tag{3}$$

such that $m(\varnothing) = 0$ and

$$\sum_{A \in \mathscr{P}(\mathbf{U})} m(\mathbf{A}) = 1. \tag{4}$$

Every set $\mathbf{A}$ in $\mathscr{P}(\mathbf{U})$ for which $m(\mathbf{A}) > 0$ is usually named a focal element of m that is a subset of $\mathbf{U}$ on which the available evidence focuses. The pair $(\mathbf{F}, m)$ is termed as a body of evidence (BOE), where $\mathbf{F}$ denotes a set of focal elements and m denotes the associated basic assignment. Moreover, because m can be fully characterized by a list of focal elements $\mathbf{F} = \{\mathbf{f}_1, \mathbf{f}_2, \ldots, \mathbf{f}_M\}$; therefore in the paper $\mathbf{F}$ is used instead of $(\mathbf{F}, m)$ for short [27].

According to the properties of a BOE, the evidence about x is divided into three types.

(1) Conflicting Evidence (C-BOE). The BOE represents a random situation that each focal element is conflicting with one another, that is, for each $i \neq j \in \{1, 2, \ldots, M\}$:

$$\mathbf{f}_i \cap \mathbf{f}_j = \varnothing. \tag{5}$$

Each event yields a piece of evidence pointing to distinct focal elements. Based on the frequency at which pieces of evidence focuse on each focal element, a probability distribution is developed.

(2) Nested Evidence (N-BOE). In this type of BOE, pieces of evidence point to a range of nested sets. Nested sets indicate the focal elements in $\mathbf{F}$ which can be sorted as follows:

$$\mathbf{f}_{(1)} \subseteq \mathbf{f}_{(2)} \cdots \subseteq \mathbf{f}_{(M)}. \tag{6}$$

This is a situation that one faces in the data that describes estimated quantities. The distribution of this type is termed the possibility distribution.

(3) Mixed Evidence (M-BOE). This type is a generalization of C-BOE and N-BOE. In this case, some pieces of evidence point to sets that are nested and some to mutually exclusive sets.

By Venn Diagram, above types of BOEs are illustrated in Figure 5. Figure 5(a) is a C-BOE. Figure 5(b) is a N-BOE. Figure 5(c) is a M-BOE. All the BOEs satisfy $m(\mathbf{f}_1) + m(\mathbf{f}_2) + m(\mathbf{f}_3) + m(\mathbf{f}_4) + m(\mathbf{f}_5) + m(\mathbf{f}_6) = 1$.

A further question is how to develop the BOEs in SSEP-CSHR context. For example, a statement proposed by decision makers is "Cost performance (CP) is important." How do we generate a BOE to support the statement?

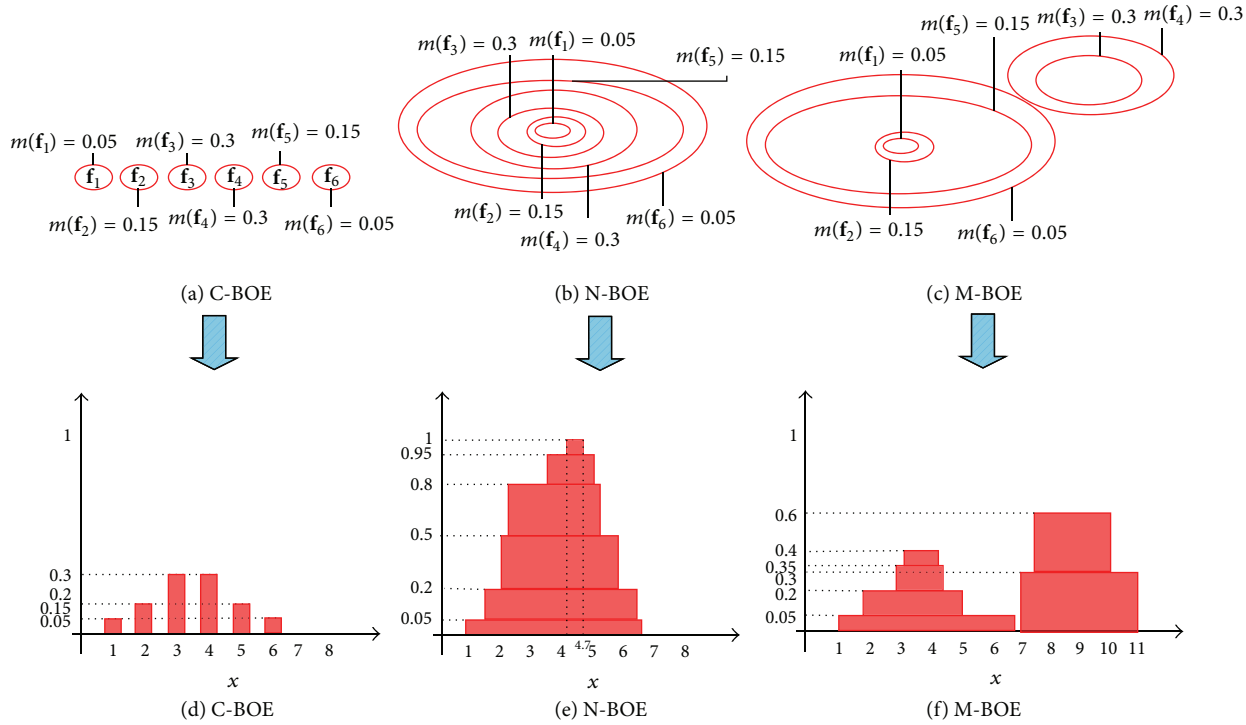

Figure 5: Three illustrative examples of body of evidence (BOE).

A C-BOE is often developed by choice questions with mutually exclusive options in questionnaires. Each interviewee is asked to select only one option from options. The accumulative frequency of each option gives a probability distribution. For example, in Figure 5(d) each interviewee is asked to select a score from the set $\{1, 2, 3, 4, 5, 6, 7, 8\}$.

An approach to develop N-BOE or M-BOE is to ask each interviewee to indicate the range of her agreeable score, and the enquirer draws a horizontal line corresponding to the range, and finally stacks the responses. If M people are asked during our survey, the height of one horizontal line is $1/M$. If a representation of the set of opinions is in general agreement, the evidence can be viewed as a possibility distribution (i.e., N-BOE) [12]. The differences among the opinions are only boundaries of the agreeable ranges. For instance, in Figure 5(e), we assume an "ideal" score ranging from 4 to 4.7 exists, which every interviewee agrees on, and interviewees give their acceptable closeness to the "ideal" score range. Sometimes evidences from questionnaires are without any general agreement. Then the evidence is an M-BOE. As shown in Figure 5(f), M-BOE needs no requirements of an "ideal" score range, so M-BOE can be used to describe the opinions without any consensus. Owing to info deficiency during solving SSEP-CSHR, sometimes SSEP-CSHR is required to deal with M-BOE.

2.4. Measuring the Truth of "x Is $\mathbf{A}$". How BOE and set $\mathbf{A}$ are combined dictates the framework for determining the truth of "x is $\mathbf{A}$."

Given a fuzzy set $\widetilde{\mathbf{A}}(x)$ and a BOE $(\mathbf{F}, m)$ on $\mathbf{U}$, where $\mathbf{F} = \{\mathbf{f}_1, \ldots, \mathbf{f}_M\}$, a framework to determine the truth of "x is $\mathbf{A}$" is based on two dual measures: Belief (Bel) and Plausibility (Pl) as follows:

$$\mathrm{Bel}\left(\mathbf{F}, \widetilde{\mathbf{A}}\right) = \frac{1}{K}\sum_{i=1}^{M} m\left(\mathbf{f}_i\right) \sum_{\alpha\in[0,1]} I_{\{\mathbf{f}_i \subset [(A)_\alpha^L, (A)_\alpha^U]\}}, \tag{7}$$

$$\mathrm{Pl}\left(\mathbf{F}, \widetilde{\mathbf{A}}\right) = \frac{1}{K}\sum_{i=1}^{M} m\left(\mathbf{f}_i\right) \sum_{\alpha\in[0,1]} I_{\{\mathbf{f}_i \cap [(A)_\alpha^L, (A)_\alpha^U] \neq \varnothing\}} \tag{8}$$

such that if $\widetilde{\mathbf{A}} = \varnothing$, then $\mathrm{Bel}(\mathbf{F}, \widetilde{\mathbf{A}}) = \mathrm{Pl}(\mathbf{F}, \widetilde{\mathbf{A}}) = 0$ and if $\widetilde{\mathbf{A}} = \mathbf{U}$, $\mathrm{Bel}(\mathbf{F}, \widetilde{\mathbf{A}}) = \mathrm{Pl}(\mathbf{F}, \widetilde{\mathbf{A}}) = 1$. In addition,

$$\begin{aligned} \mathrm{Bel}\left(\mathbf{F}, \widetilde{\mathbf{A}}\right) &= 1 - \mathrm{Pl}\left(\mathbf{F}, \overline{\widetilde{\mathbf{A}}}\right); \\ \mathrm{Pl}\left(\mathbf{F}, \widetilde{\mathbf{A}}\right) &= 1 - \mathrm{Bel}\left(\mathbf{F}, \overline{\widetilde{\mathbf{A}}}\right). \end{aligned} \tag{9}$$

In (7) and (8), K is the number of α-cuts considered in $[0, 1]$; $I_{\{p\}}$ is a Boolean function.

While, for every $i \in \{1, 2, \ldots, M\}$, $m(\mathbf{f}_i)$ characterizes the frequency of pieces of evidence focusing on exactly focal elements $\mathbf{f}_i$ alone, equation (7) represents the total evidence that each focal element belongs to every α-cut of the fuzzy set. Equation (8) represents not only the evidence that each focal element belongs to every α-cut, but also the additional evidence associating with the focal element overlapping every α-cut. Hence, the Bel is a conservative measure and the Pl is an optimistic one. Then the truth of "x is $\mathbf{A}$" can be defined by following weighted summation:

$$T\left(\mathbf{F}, \widetilde{\mathbf{A}}\right) = w_1 \mathrm{Bel}\left(\mathbf{F}, \widetilde{\mathbf{A}}\right) + w_2 \mathrm{Pl}\left(\mathbf{F}, \widetilde{\mathbf{A}}\right). \tag{10}$$

Based on the above discussion, the types of BOE are divided into C-BOE, N-BOE, and M-BOE. The types of set for **A** that we are mainly concerned with are the crisp set and the fuzzy set. Hence there are six cases of the proposition, "x is **A**," corresponding to the combination of the type of BOE and the type of set **A**. We give an illustrative example to illustrate the two measures.

Let $w_1 = w_2 = 0.5$ and $K = 5$. Let $m(\mathbf{f}_1) = 0.05; m(\mathbf{f}_2) = 0.15; m(\mathbf{f}_3) = 0.3; m(\mathbf{f}_4) = 0.3; m(\mathbf{f}_5) = 0.15; m(\mathbf{f}_6) = 0.05$ (the same as the values in Figure 5). All the six cases are illustrated in Figure 6 and the truth of each case is shown in Table 1.

To sum up, Figure 7 depicts different frameworks corresponding to different cases (Cases 1–6).

Case 1. C-BOE + crisp set.

Case 2. C-BOE + fuzzy set.

Case 3. N-BOE + crisp set.

Case 4. N-BOE + fuzzy set.

Case 5. M-BOE + crisp set.

Case 6. M-BOE + fuzzy set.

Firstly, Figure 7 displays that Cases 1-2 are traditionally expressed based on probability theory, while possibility theory is used to deal with Cases 3-4; secondly, Cases 1–4 are special cases of Cases 5-6, in that M-BOE is a mix of C-BOE and N-BOE. Evidence theory is a generalized form to measure the truth of "x is **A**" which suits for Cases 1–6 all [27].

3. An Integration of Evidence Theory and SSEP-CSHR

3.1. The Two-Phase F-QFD. In practice, series of HOQs can be integrated into a multiphase QFD. Each phase is closely correlated in a multiphase QFD since the inputs of one phase needs to apply the outputs of the previous phase [17, 18]. In the paper, we focused on QFD whose procedure has been thoroughly described by Mazur [10]. This approach consists of solving some successive HOQs. Among these HOQs, two HOQs named as Quality Deployment (QD) and Functional Deployment (FD) which is of the most essential are applied here to develop our MCDM model for SSEP-CSHR.

Quality Deployment (QD). It translates some Basic Requirements to certain quality attributes.

Functional Deployment (FD). It realized the quality attributes by specific alternatives.

At the beginning of the process, Demanded Qualities (DQs) have to be identified. The elements are gathered from surveys or experts' interviews. They are "WHATs" in QD phase:

$$\mathbf{L}_1 = \left\{R_1, \ldots, R_i, \ldots, R_{N_1}\right\}. \tag{11}$$

We determine the fuzzy importance ratings of DQs ($\mathbf{L}_1$). The fuzzy importance ratings are usually obtained by subjective method discussed in Section 2.2. F-AHP, for example, Extent Analysis (EA) or Lambda-Max Method (LMM) can also be used to capture the fuzzy ratings [6, 25]:

$$\widetilde{\mathbf{W}}^{\mathbf{L}_1} = \left(\widetilde{\mathbf{W}}_1^{\mathbf{L}_1}, \ldots, \widetilde{\mathbf{W}}_i^{\mathbf{L}_1}, \ldots, \widetilde{\mathbf{W}}_{N_1}^{\mathbf{L}_1}\right). \tag{12}$$

DQs are translated into "Quality Attributes" (QAs). QAs ($\mathbf{L}_2$) are assessment criteria that are related to the accomplishment of above DQs. Then QAs are "HOWs" in QD phase. And QFD team then generates the QAs as follows:

$$\mathbf{L}_2 = \left\{C_1, \ldots, C_i, \ldots, C_{N_2}\right\}. \tag{13}$$

Similarly, some Functional Techniques (FTs) ($\mathbf{L}_3$), that is, our alternatives to realize above QAs, are further defined by panel of experts. Here QAs are "WHATs" for FD and FTs are "HOWs" for FD:

$$\mathbf{L}_3 = \left\{F_1, \ldots, F_i, \ldots, F_{N_3}\right\}. \tag{14}$$

The core elements of F-QFD are "relationships matrices" in QD and FD, respectively:

(1) The relationship matrix between DQs ($\mathbf{L}_1$) and QAs ($\mathbf{L}_2$) to express how a quality attribute to meet a requirement;

(2) The relationship matrix between QAs ($\mathbf{L}_2$) and FTs ($\mathbf{L}_3$) to express how an alternative to realize an attribute;

(3) The correlation matrix between DQs ($\mathbf{L}_1$), QAs ($\mathbf{L}_2$), and FTs ($\mathbf{L}_3$) themselves.

To sum up, Table 2 defines all fuzzified inputs and outputs in the two-phase F-QFD.

All inputs and outputs are described by linguistic terms and defined as the fuzzy sets. A fuzzy set is fully and uniquely represented by its α-cuts (see Table 3).

Chen and Ko [17, 18] gave a formulation to implement multiphase F-QFD. Wang et al. [20, 28] have demonstrated that the method is not proper and provided a set of nonlinear programming (NLP) models to do F-QFD.

Let $\widetilde{\mathbf{A}}$ and $\widetilde{\mathbf{B}}$ be two fuzzy numbers; operations on two fuzzy numbers are defined as

$$\begin{aligned}\widetilde{\mathbf{A}} * \widetilde{\mathbf{B}} &= \bigcup_{\alpha\in[0,1]} \alpha\,(\mathbf{A} * \mathbf{B})_\alpha = \bigcup_{\alpha\in[0,1]} \alpha\,(\mathbf{A}_\alpha * \mathbf{B}_\alpha) \\ &= \bigcup_{\alpha\in[0,1]} \alpha\left\{ff * \in g\mathbf{A}_\alpha, g \in \mathbf{B}_\alpha\right\}.\end{aligned} \tag{15}$$

Let $*$ denote any of the four basic arithmetic operations. $\mathbf{A}_\alpha * \mathbf{B}_\alpha$ follows arithmetic operations on closed intervals [27]. Then based on Chen et al. [17, 18], and Wang and Chin [20], an algorithm to solve the two-phase F-QFD is introduced.

Table 1: The truth of each case in illustrative example in Figure 5.

BOE	**A**	Bel(**F**, **A**)	Pl(**F**, **A**)	T(**F**, **A**)	Example
C-BOE	Crisp	$= 0.2 \times (0.3 + 0.3 + 0.15 + 0.05) \times 5 = 0.8$	$= 0.3 + 0.3 + 0.15 + 0.05 = 0.8$	0.8	Figure 6(a)
C-BOE	Fuzzy	$= 0.2 \times (0.3 \times 1 + 0.3 \times 3 + 0.15 \times 4 + 0.05 \times 5) = 0.41$	$= 0.2 \times (0.3 \times 1 + 0.3 \times 3 + 0.15 \times 4 + 0.05 \times 5) = 0.41$	0.41	Figure 6(b)
N-BOE	Crisp	$= 0.2 \times (0.05 + 0.15) \times 5 = 0.2$	$= 0.2 \times (0.05 + 0.15 + 0.3 + 0.3 + 0.15 + 0.05) \times 5 = 1$	0.6	Figure 6(c)
N-BOE	Fuzzy	$= 0$	$= 0.2 \times (0.3 + 0.15 + 0.05) \times 5 = 0.5$	0.25	Figure 6(d)
N-BOE	Fuzzy	$= 0.2 \times (0.05 + 0.15) = 0.04$ (Equation (7)) $= 1-0.2\times(0.05\times5+0.15\times5+0.3\times5+0.3\times5+0.15\times4+0.05\times4) = 0.04$ (Equation (9))	$= (0.05 \times 5 + 0.15 \times 5 + 0.3 \times 4 + 0.3 \times 3 + 0.15 \times 2 + 0.05 \times 2) = 0.7$	0.37	Figure 6(e) Figure 6(f)
M-BOE	Crisp	$= 0.2 \times (0.05 + 0.15) \times 5 = 0.2$	$= 0.2 \times (0.05 + 0.15 + 0.3 + 0.3 + 0.15 + 0.05) \times 5 = 1$	0.6	Figure 6(g)
M-BOE	Fuzzy	$= 0.2 \times (0.05 + 0.15) = 0.04$	$= 0.2 \times (0.05 \times 5 + 0.15 \times 5 + 0.3 \times 2 + 0.3 + 0.15 \times 2 + 0.05 \times 2) = 0.46$	0.25	Figure 6(h)

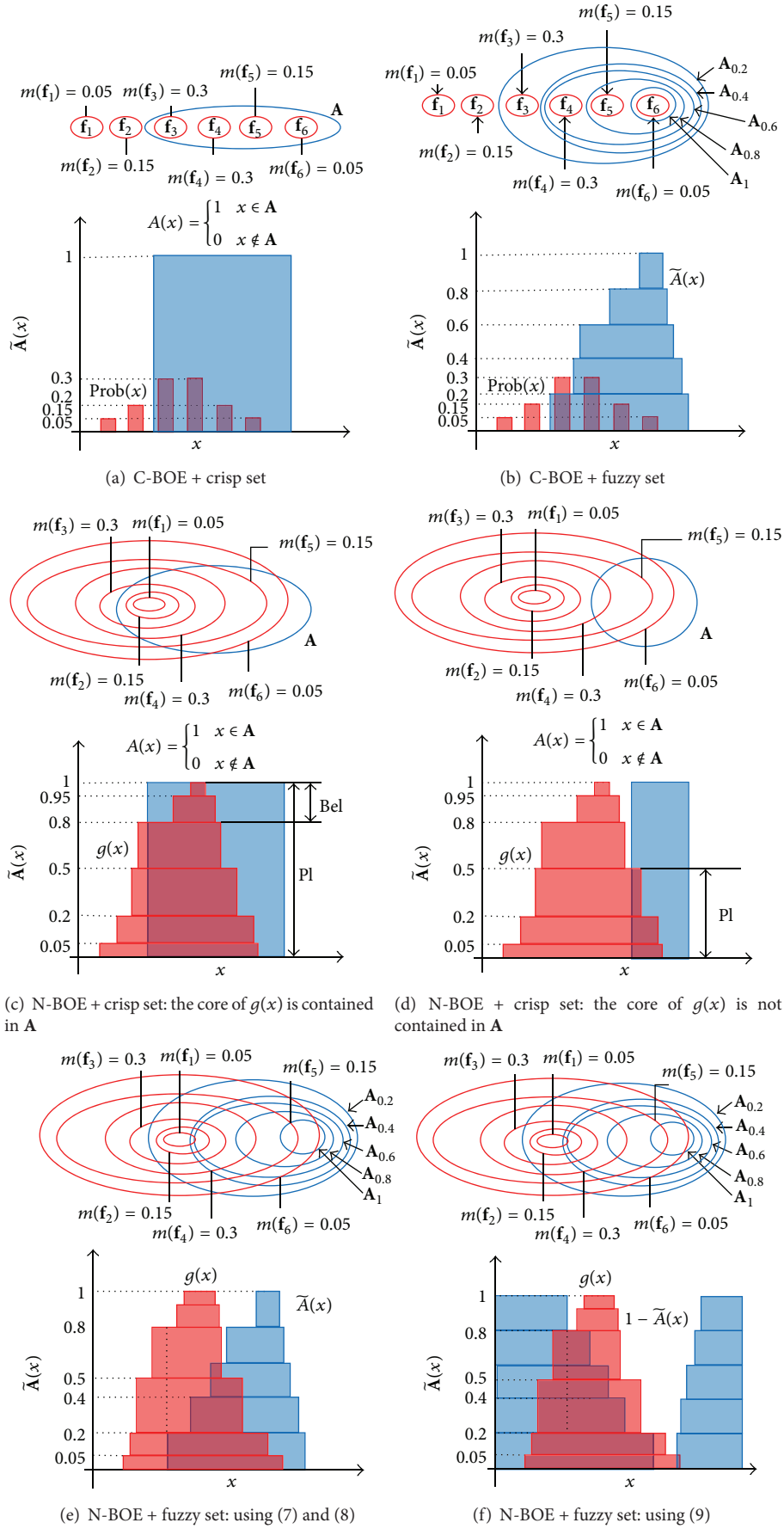

Figure 6: Continued.

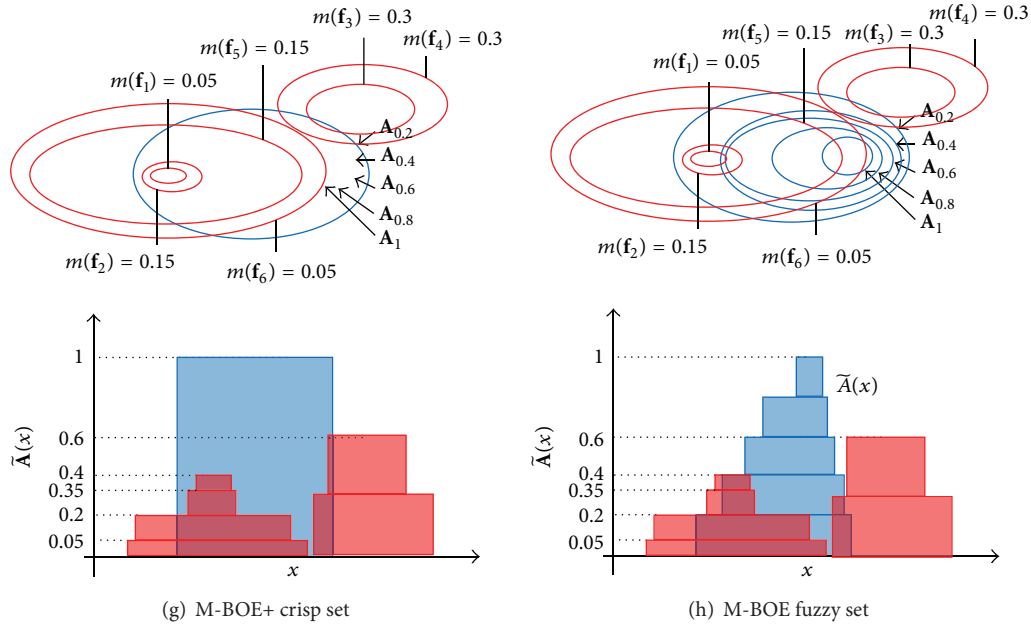

(g) M-BOE+ crisp set (h) M-BOE fuzzy set

Figure 6: Illustrative example of Belief and Plausibility measures.

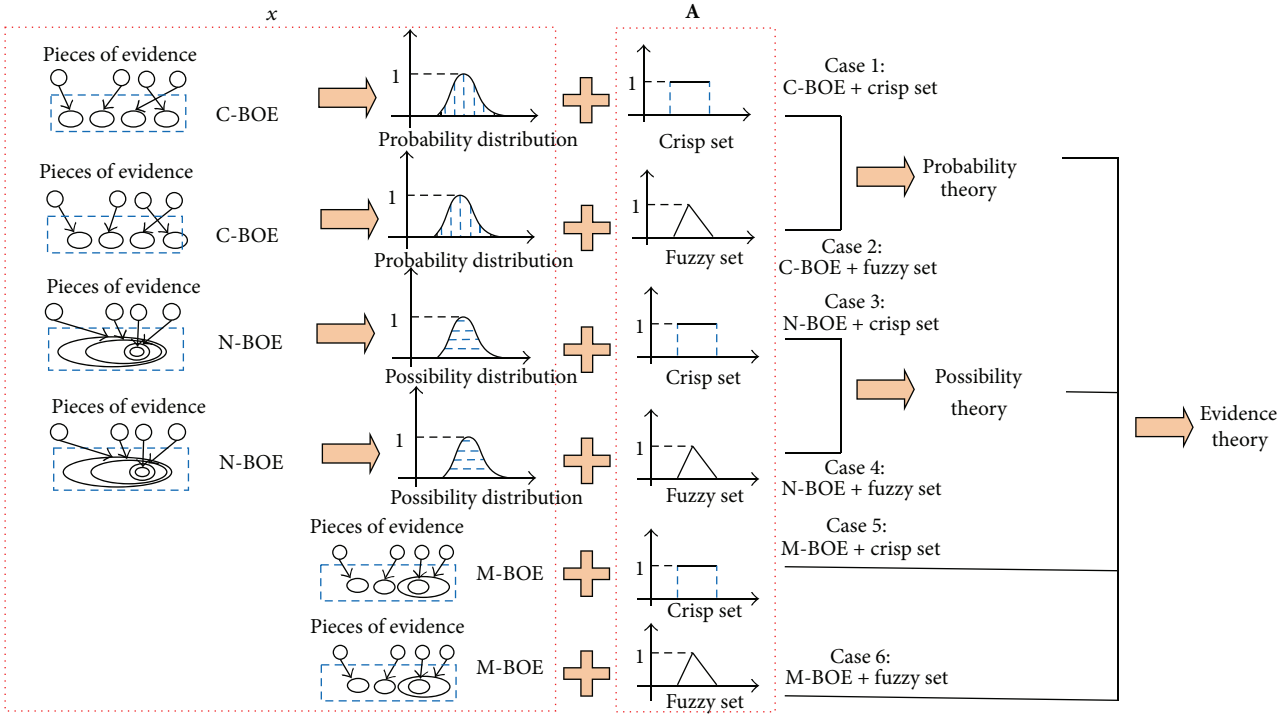

Figure 7: Different theory corresponding to the combination of the type of BOE and the type of set A.

Table 2: Inputs and outputs in HOQs of the two-phase F-QFD.

Inputs	Descriptions
$\widetilde{\mathbf{W}}_i^{\mathbf{L}_1}$	The fuzzy important ratings of R_i where $i = 1, 2, \ldots, N_1$
$\widetilde{\mathbf{B}}_{ij}^{\mathbf{L}_2}$	The fuzzy relationship score between R_i and C_j, where $i = 1, 2, \ldots, N_1$; $j = 1, 2, \ldots, N_2$
$\widetilde{\mathbf{B}}_{ij}^{\mathbf{L}_3}$	The fuzzy relationship score between C_i and F_j, where $i = 1, 2, \ldots, N_2$; $j = 1, 2, \ldots, N_3$
$\widetilde{\mathbf{A}}_{ij}^{\mathbf{L}_1}$	The fuzzy correlation score between R_i and R_j, where $i = 1, 2, \ldots, N_1$; $j = 1, 2, \ldots, N_1$
$\widetilde{\mathbf{A}}_{ij}^{\mathbf{L}_2}$	The fuzzy correlation score between C_i and C_j, where $i = 1, 2, \ldots, N_2$; $j = 1, 2, \ldots, N_2$
$\widetilde{\mathbf{A}}_{ij}^{\mathbf{L}_3}$	The fuzzy correlation score between F_i and F_j, where $i = 1, 2, \ldots, N_3$; $j = 1, 2, \ldots, N_3$
Outputs	Descriptions
$\widetilde{\mathbf{W}}_i^{\mathbf{L}_2}$	The fuzzy important ratings of C_i where $i = 1, 2, \ldots, N_2$
$\widetilde{\mathbf{W}}_i^{\mathbf{L}_3}$	The fuzzy important ratings of F_i where $i = 1, 2, \ldots, N_3$

Table 3: The α-cuts of the fuzzy sets in the two-phase F-QFD.

Notations	Descriptions
$\widetilde{\mathbf{W}}_{i\alpha}^{\mathbf{L}_1} = \left[\left(W_i^{\mathbf{L}_1}\right)_\alpha^L, \left(W_i^{\mathbf{L}_1}\right)_\alpha^U\right]$	The α-cuts of fuzzy important ratings $\widetilde{\mathbf{W}}_i^{\mathbf{L}_1}$
$\widetilde{\mathbf{B}}_{ij\alpha}^{\mathbf{L}_2} = \left[\left(B_{ij}^{\mathbf{L}_2}\right)_\alpha^L, \left(B_{ij}^{\mathbf{L}_2}\right)_\alpha^U\right]$	The α-cuts of fuzzy relationship $\widetilde{\mathbf{B}}_{ij}^{\mathbf{L}_2}$
$\widetilde{\mathbf{B}}_{ij\alpha}^{\mathbf{L}_3} = \left[\left(B_{ij}^{\mathbf{L}_3}\right)_\alpha^L, \left(B_{ij}^{\mathbf{L}_3}\right)_\alpha^U\right]$	The α-cuts of fuzzy relationship $\widetilde{\mathbf{B}}_{ij}^{\mathbf{L}_3}$
$\widetilde{\mathbf{A}}_{ij\alpha}^{\mathbf{L}_1} = \left[\left(A_{ij}^{\mathbf{L}_1}\right)_\alpha^L, \left(A_{ij}^{\mathbf{L}_1}\right)_\alpha^U\right]$	The α-cuts of fuzzy correlations $\widetilde{\mathbf{A}}_{ij}^{\mathbf{L}_1}$
$\widetilde{\mathbf{A}}_{ij\alpha}^{\mathbf{L}_2} = \left[\left(A_{ij}^{\mathbf{L}_2}\right)_\alpha^L, \left(A_{ij}^{\mathbf{L}_2}\right)_\alpha^U\right]$	The α-cuts of fuzzy correlation $\widetilde{\mathbf{A}}_{ij}^{\mathbf{L}_2}$
$\widetilde{\mathbf{A}}_{ij\alpha}^{\mathbf{L}_3} = \left[\left(A_{ij}^{\mathbf{L}_3}\right)_\alpha^L, \left(A_{ij}^{\mathbf{L}_3}\right)_\alpha^U\right]$	The α-cuts of fuzzy correlation $\widetilde{\mathbf{A}}_{ij}^{\mathbf{L}_3}$
$\widetilde{\mathbf{W}}_{i\alpha}^{\mathbf{L}_2} = \left[\left(W_i^{\mathbf{L}_2}\right)_\alpha^L, \left(W_i^{\mathbf{L}_2}\right)_\alpha^U\right]$	The α-cuts of fuzzy important ratings $\widetilde{\mathbf{W}}_{i\alpha}^{\mathbf{L}_2}$
$\widetilde{\mathbf{W}}_{i\alpha}^{\mathbf{L}_3} = \left[\left(W_i^{\mathbf{L}_3}\right)_\alpha^L, \left(W_i^{\mathbf{L}_3}\right)_\alpha^U\right]$	The α-cuts of fuzzy important ratings $\widetilde{\mathbf{W}}_{i\alpha}^{\mathbf{L}_3}$

Algorithm 3 (the algorithm to implement the two-phase F-QFD). Consider the following.

Step 1. Set α-cuts of the fuzzy set equal to $1/K, \ldots$, and 1 respectively. K is the number of α-cut in $[0, 1]$. Then the fuzzy importance ratings of FTs are obtained by following substeps.

Step 1.1. Let $k = 1$.

Step 1.2. The fuzzy correlations between $\mathbf{L}_k$ can be normalized by formula:

$$\widetilde{\omega}_i^{\mathbf{L}_k} = \frac{\sum_{n=1}^{N_k} \widetilde{W}_n^{\mathbf{L}_k} \otimes \widetilde{A}_{ni}^{\mathbf{L}_k}}{\sum_{n=1}^{N_k}\sum_{m=1}^{N_k} \widetilde{W}_n^{\mathbf{L}_k} \otimes \widetilde{A}_{nm}^{\mathbf{L}_k}} \quad \forall i \in \{1, 2, \ldots, N_k\}. \tag{16}$$

The formula can be achieved by the following Nonlinear Programming (NLP) models.

For all $i \in \{1, 2, \ldots, N_k\}$, $\alpha \in [0, 1]$, determine interval $[(\omega_i^{\mathbf{L}_k})_\alpha^L, (\omega_i^{\mathbf{L}_k})_\alpha^U]$ by models:

(Model 1)

$$\left(\omega_i^{\mathbf{L}_k}\right)_\alpha^L = \min \quad \frac{\sum_{n=1}^{N_k} \omega_n^{\mathbf{L}_k} a_{ni}^{\mathbf{L}_k}}{\sum_{n=1}^{N_k}\sum_{m=1}^{N_k} \omega_n^{\mathbf{L}_k} a_{nm}^{\mathbf{L}_k}},$$

$$\left(\omega_i^{\mathbf{L}_k}\right)_\alpha^U = \max \quad \frac{\sum_{n=1}^{N_k} \omega_n^{\mathbf{L}_k} a_{ni}^{\mathbf{L}_k}}{\sum_{n=1}^{N_k}\sum_{m=1}^{N_k} \omega_n^{\mathbf{L}_k} a_{nm}^{\mathbf{L}_k}},$$

$$\text{s.t} \quad \left(W_i^{\mathbf{L}_k}\right)_\alpha^L \le \omega_i^{\mathbf{L}_k} \le \left(W_i^{\mathbf{L}_k}\right)_\alpha^U \quad \forall i \in \{1, 2, \ldots, N_k\},$$

$$\left(A_{ij}^{\mathbf{L}_k}\right)_\alpha^L \le a_{ij}^{\mathbf{L}_k} \le \left(A_{ij}^{\mathbf{L}_k}\right)_\alpha^U \quad \forall i, j \in \{1, 2, \ldots, N_k\}. \tag{17}$$

Step 1.3. Furthermore, the fuzzy relationship between $\mathbf{L}_k$ and $\mathbf{L}_{k+1}$ can be defined by

$$\widetilde{\mathbf{Y}}_i^{\mathbf{L}_{k+1}} = \frac{\sum_{\eta=1}^{N_{k+1}} \widetilde{\mathbf{B}}_{i\eta}^{\mathbf{L}_{k+1}} \otimes \widetilde{\mathbf{A}}_{\eta j}^{\mathbf{L}_{k+1}}}{\sum_{l=1}^{N_{k+1}}\sum_{\eta=1}^{N_{k+1}} \widetilde{\mathbf{B}}_{i\eta}^{\mathbf{L}_{k+1}} \otimes \widetilde{\mathbf{A}}_{\eta l}^{\mathbf{L}_{k+1}}} \quad \forall i \in \{1, 2, \ldots, N_k\}. \tag{18}$$

Then we calculate the importance rating of $\mathbf{L}_{k+1}$ as the fuzzy weighted average of the normalized fuzzy relationships:

$$\widetilde{\mathbf{W}}_j^{\mathbf{L}_{k+1}} = \frac{\sum_{i=1}^{N_k} \widetilde{\mathbf{W}}_i^{\mathbf{L}_k} \otimes \mathbf{Y}_{ij}^{\mathbf{L}_{k+1}}}{\sum_{i=1}^{N_k} \widetilde{\mathbf{W}}_i^{\mathbf{L}_k}} \quad \forall j \in \{1, 2, \ldots, N_{k+1}\}. \tag{19}$$

The above two formulas can be achieved by following NLP models.

For all $i \in \{1, 2, \ldots, N_k\}$, $\alpha \in [0, 1]$, we can determine interval:

(Model 2)

$$\left(W_j^{\mathbf{L}_{k+1}}\right)_\alpha^L = \min \quad \frac{\sum_{\eta=1}^{N_k}\left(w_i^{\mathbf{L}_k}\sum_{\eta=1}^{N_{k+1}} b_{i\eta}^{\mathbf{L}_{k+1}} a_{\eta j}^{\mathbf{L}_{k+1}} / \sum_{l=1}^{N_{k+1}}\sum_{\eta=1}^{N_{k+1}} b_{i\eta}^{\mathbf{L}_{k+1}} a_{\eta l}^{\mathbf{L}_{k+1}}\right)}{\sum_{i=1}^{N_k} w_i^{\mathbf{L}_k}}$$

$$\left(W_j^{\mathbf{L}_{k+1}}\right)_\alpha^U = \max \quad \frac{\sum_{i=1}^{N_k}\left(w_i^{\mathbf{L}_k}\sum_{\eta=1}^{N_{k+1}} b_{i\eta}^{\mathbf{L}_{k+1}} a_{\eta j}^{\mathbf{L}_{k+1}} / \sum_{l=1}^{N_{k+1}}\sum_{\eta=1}^{N_{k+1}} b_{i\eta}^{\mathbf{L}_{k+1}} a_{\eta l}^{\mathbf{L}_{k+1}}\right)}{\sum_{i=1}^{N_k} w_i^{\mathbf{L}_k}} \tag{20}$$

$$\text{s.t} \quad \left(A_{ij}^{\mathbf{L}_{k+1}}\right)_\alpha^L \le a_{ij}^{\mathbf{L}_{k+1}} \le \left(A_{ij}^{\mathbf{L}_{k+1}}\right)_\alpha^U \quad \forall i, j \in \{1, 2, \ldots, N_{k+1}\} \tag{21}$$

$$\left(\omega_i^{\mathbf{L}_k}\right)_\alpha^L \le w_i^{\mathbf{L}_k} \le \left(\omega_i^{\mathbf{L}_k}\right)_\alpha^U \quad \forall i \in \{1, 2, \ldots, N_k\} \tag{22}$$

$$\left(B_{ij}^{\mathbf{L}_{k+1}}\right)_\alpha^L \le b_{ij}^{\mathbf{L}_{k+1}} \le \left(B_{ij}^{\mathbf{L}_{k+1}}\right)_\alpha^U \quad \forall i \in \{1, 2, \ldots, N_k\} \;\; j \in \{1, 2, \ldots, N_{k+1}\}. \tag{23}$$

Step 1.3. By (1), the fuzzy importance ratings of $\mathbf{L}_{k+1}$ are obtained:

$$\widetilde{\mathbf{W}}^{\mathbf{L}_{k+1}} = \left(\widetilde{\mathbf{W}}_1^{\mathbf{L}_{k+1}}, \ldots, \widetilde{\mathbf{W}}_i^{\mathbf{L}_{k+1}}, \ldots, \widetilde{\mathbf{W}}_{N_{k+1}}^{\mathbf{L}_{k+1}}\right). \tag{24}$$

Step 1.4. If $k + 1 = 3$, go to Step 2; else $k = k + 1$ return to Step 1.2.

Step 2. Fuzzy importance rating can be ranked by different methods. In the paper, the fuzzy importance ratings are compared with each other by method developed in Wang [29]:

$$\mathbf{W}_i^{\mathbf{L}_{k+1}} = \frac{1}{K}\sum_{\alpha\in[0,1]} \frac{\left(W_i^{\mathbf{L}_{k+1}}\right)_\alpha^L + \left(W_i^{\mathbf{L}_{k+1}}\right)_\alpha^U}{2} \quad \forall i \in \{1, 2, \ldots, N_k\}. \tag{25}$$

Step 3. END

Based on the method proposed in Wang and Chin [20], Models 1 and 2 can be linearized and solved optimally.

3.2. Service Station Evaluation Problem for CSHR. SSEP-CSHR is based on a reinterpretation of above two-phase F-QFD. In SSEP-CSHR, DQs in terms of Basic Requirements ($\mathbf{L}_1$) are translated into QAs in terms of Assessment Criteria ($\mathbf{L}_2$). And then service stations ($\mathbf{L}_3$), that is, specific alternatives to realize above Assessment Criteria, are served as FTs. Figure 8 gives the corresponding relationship between the two-phase F-QFD and SSEP-CSHR.

Basic Requirements ($\mathbf{L}_1$) in SSEP-CSHR are comprised of two aspects of requirements: Firstly, it contains some requirements used in FLE-F-QFD. These demands have been extensively described by the literatures about facility location and supply chain management [11, 19]. Moreover, it involves some distinct requirements because of special CSHR background. For the sake of clarity, all those requirements are shown in Table 4.

Basic Requirements ($\mathbf{L}_1$) are some requirements described by broad nature language. However, the set of Assessment Criteria ($\mathbf{L}_2$) usually use more specific descriptions. Similarly Assessment Criteria ($\mathbf{L}_2$) also consist of two parts: some criteria that are derived from relevant literatures [11, 19] and other ones that are gathered from experts' comments under certain background. All the criteria are presented in Table 5.

By solving the steps of the two-phase F-QFD (Algorithm 3), the importance ratings of alternative Service stations satisfying above requirements and criteria can be determined. Figure 9 provides the basic structure of two essential HOQs (QD and FD) used in SSEP-CSHR.

3.3. An Approximate Reasoning Procedure in SSEP-CSHR. Approximate reasoning is related to the appropriate processing of uncertain knowledge, given in a rule based manner. Deductive inference can be performed by means of classical logic modus ponens (MP). For using linguistic variables expressed fuzzy sets, a generalized MP has been proposed by Zadeh [30]. It enables an approximate deductive reasoning with the following general scheme:

$$\begin{aligned} &\text{Facts}: \; x \text{ is } \widetilde{\mathbf{A}}' \text{ AND } y \text{ is } \widetilde{\mathbf{B}}' \\ &\text{Rule 1}: \; \text{IF } x \text{ is } \widetilde{\mathbf{A}}_1 \text{ AND } y \text{ is } \widetilde{\mathbf{B}}_1 \text{ THEN } z \text{ is } \widetilde{\mathbf{C}}_1 \\ &\underline{\text{Rule 2}: \; \text{IF } x \text{ is } \widetilde{\mathbf{A}}_2 \text{ AND } y \text{ is } \widetilde{\mathbf{B}}_2 \text{ THEN } z \text{ is } \widetilde{\mathbf{C}}_2} \\ &\text{Conclusions}: \; z \text{ is } \widetilde{\mathbf{C}}'. \end{aligned} \tag{26}$$

Let us proceed one step further and provide a generalization of the two-phase F-QFD based on the generalized MP. We find that the situation of "WHATs" in QD and "HOWs" in FD can all be described by propositions "x is $\mathbf{A}$." The fundamental idea in our paper is to obtain the truth of the propositions about Basic Requirements by evidence theory to infer the truth of the propositions about service stations by implication "if x is $\mathbf{A}$, then y is $\mathbf{B}$."

Table 4: List of $\mathbf{L}_1$ for SSEP-CSHR.

Basic requirements	Description
Proximity to trains (PT)	Proximity to demands; number of trains that can be served; cost of serving trains
Sound catering condition (SC)	Space and time condition for delivery
Labor availability (LA)	Availability of required professional and nonprofessional workforce; wage rates; quality of workforce; and so forth
Availability of foods (AF)	Closeness to food suppliers or distributional centers; freight costs of transportation
Government incentives (GI)	Convenience provided by government or railway authorities
Constructions costs (CC)	Construction costs of building cold stores at the station and also availability of space for future expansion

Table 5: List of $\mathbf{L}_2$ for SSEP-CSHR.

Assessment criteria	Description
Quality and location of neighboring suppliers (QL)	Proximity to suppliers; alternative suppliers; and speed and responsiveness of suppliers
Accessibility to trains (AT)	Number of train that can be served (number of trains departing from the city; number of trains stopping at the city, the ratio of the above two)
Available catering time (AC)	Average available catering time
Physical catering conditions (PC)	The platform area
Human resource conditions (HR)	Labor costs; attitudes toward works and labor turnover, economical growths, and declines effects
Economics related factors (EF)	Urban economic development, tax incentives, and business climate; interest rates
Political issues (PI)	Availability and size of government; aids attitude of government to inward investment

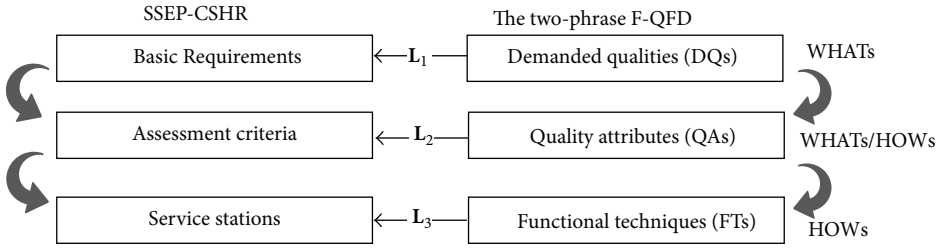

Figure 8: Corresponding relationship between the two-phase F-QFD and SSEP-CSHP.

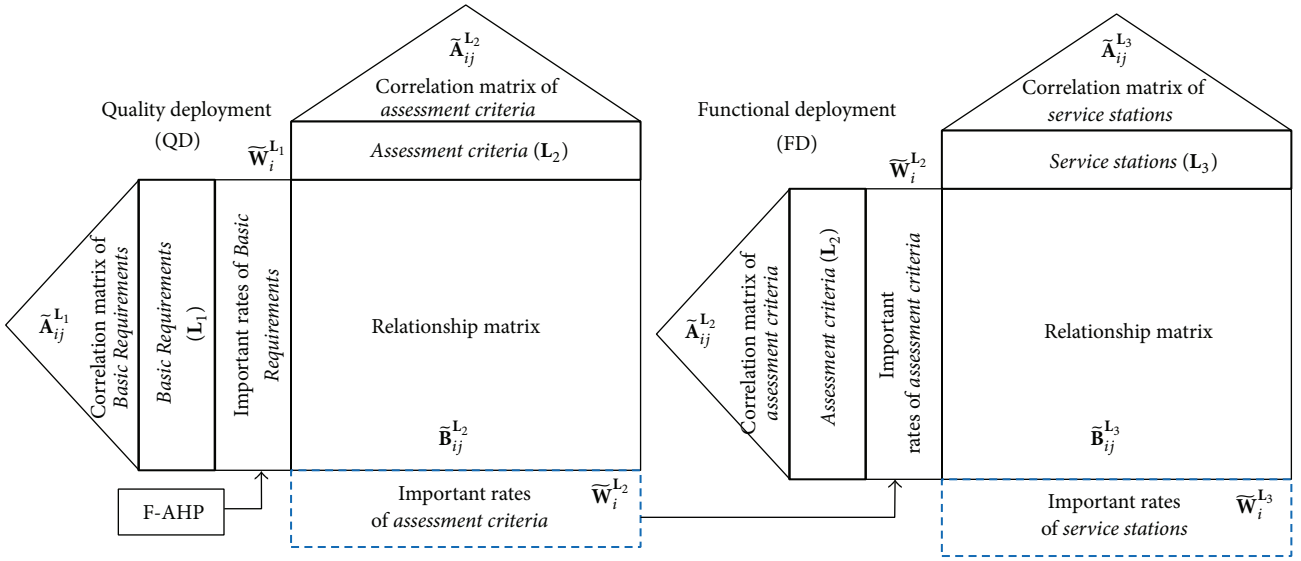

Figure 9: Basic structure of HOQs for SSEP-CSHR.

The methods to generate the evidences x and the linguistic terms of predicates in SSEP-CSHR are analyzed in Section 3.3.1. In Section 3.3.2, the expression of an *if-then* production rules and a general scheme of a multiconditional approximate reasoning in SSEP-CSHR are discussed.

3.3.1. Methods to Generate Evidence and Predicates. Figure 9 has provided the basic structure of two essential HOQs (QD and FD) used in SSEP-CSHR. Here we propose a method to generate the predicates of propositions incorporated in HOQs.

(1) Propositions about Basic Requirements $\mathbf{L}_1$. Column vector $\widetilde{\mathbf{W}}_i^{\mathbf{L}_1}$ in Figure 9 in QD shows the importance ratings of each R_i, that is, the following.

Proposition 4. *R_i is $\widetilde{\mathbf{W}}_i^{\mathbf{L}_2}$* $\forall i \in \{1, 2, \ldots, N_1\}$.

Proposition 4 can be truth-qualified by a canonical form "x is $\mathbf{A}$ is T," where T is a truth qualifier represented by crisp values. We should do the following analysis on truth-qualified proposition "x is $\mathbf{A}$ is T" [27] to capture the truth of "x is $\mathbf{A}$."

Algorithm 5 (the Algorithm to capture the truth of "x is $\mathbf{A}$"). Consider the following

Step 1. The evidences about R_i (that might be C-BOE, N-BOE, or M-BOE) are collected from many experts by questionnaires (the method to generate BOE has been discussed in Section 2.3).

For each $i \in \{1, 2, \ldots, N_1\}$, a list of focal elements with basic probability distribution is then generated from the questionnaires (the list of focal elements is expressed by $(\mathbf{F}_i^{\mathbf{L}_1}, m_i^{\mathbf{L}_1})$).

Step 2. The predicates in Proposition 4 are the same as the fuzzy importance ratings of $\mathbf{L}_1$ obtained by the two-phase F-QFD (see Algorithm 3 Step 2).

Step 3. Then the truth of Proposition 4 is calculated by the following formulas:

$$T\left(\mathbf{F}_i^{\mathbf{L}_1}, \widetilde{\mathbf{W}}_i^{\mathbf{L}_1}\right) = w_1 \mathrm{Bel}\left(\mathbf{F}_i^{\mathbf{L}_1}, \widetilde{\mathbf{W}}_i^{\mathbf{L}_1}\right) + w_2 \mathrm{Pl}\left(\mathbf{F}_i^{\mathbf{L}_1}, \widetilde{\mathbf{W}}_i^{\mathbf{L}_1}\right) \quad \forall i \in \{1, 2, \ldots, N_1\}, \tag{27}$$

where $T(\mathbf{F}_i^{\mathbf{L}_1}, \widetilde{\mathbf{W}}_i^{\mathbf{L}_1})$ is the truth qualifier of proposition "R_i is $\widetilde{\mathbf{W}}_i^{\mathbf{L}_2}$" that is; "$R_i$ is $\widetilde{\mathbf{W}}_i^{\mathbf{L}_2}$" is $T(\mathbf{F}_i^{\mathbf{L}_1}, \widetilde{\mathbf{W}}_i^{\mathbf{L}_1})$.

Step 4. End.

Table 6 shows the steps to analyze a truth-qualified proposition.

"'Construction Cost is important' is true":

(i) The predicate "important" is given by a fuzzy set $\widetilde{\mathbf{W}}_i^{\mathbf{L}_2}$ (see Column 2).

(ii) The evidences about x are generated from questionnaires (see Column 1).

(iii) The predicate "true" is expressed by a crisp number on $T(\mathbf{F}_i^{\mathbf{L}_1}, \widetilde{\mathbf{W}}_i^{\mathbf{L}_1}) \in [0, 1]$ (see Column 3).

(2) Propositions about Service Stations ($\mathbf{L}_3$). Row vector $\widetilde{\mathbf{W}}_i^{\mathbf{L}_2}$ in FD of Figure 9 shows the importance ratings of each F_i (i.e., each station).

Proposition 6. *F_i is $\widetilde{\mathbf{W}}_i^{\mathbf{L}_3}$* $\forall i \in \{1, 2, \ldots, N_3\}$.

Here an approximate reasoning is demanded to infer the truth of Proposition 6 based on the truth of Proposition 4 (see Section 3.3.2).

3.3.2. Evidence-Based Inference Scheme in SSEP-CSHR. The evidence-based inference schema of multiconditional approximate reasoning in the two-phase F-QFD has the following form:

Facts: R_1 is $\mathbf{F}_1^{\mathbf{L}_1}$ AND R_2 is $\mathbf{F}_2^{\mathbf{L}_1}$ AND $\ldots R_{N_1}$ is $\mathbf{F}_{N_1}^{\mathbf{L}_1}$

Rule 1: IF R_1 is $\widetilde{\mathbf{W}}_{11}^{\mathbf{L}_1}$ AND R_2 is $\widetilde{\mathbf{W}}_{12}^{\mathbf{L}_1}$ AND $\ldots R_{N_1}$ is $\widetilde{\mathbf{W}}_{1N_1}^{\mathbf{L}_1}$ THEN F_1 is $\widetilde{\mathbf{W}}_{11}^{\mathbf{L}_3}$ AND F_2 is $\widetilde{\mathbf{W}}_{12}^{\mathbf{L}_3}$ AND $\ldots F_{N_3}$ is $\widetilde{\mathbf{W}}_{1N_3}^{\mathbf{L}_3}$

Rule 2: IF R_1 is $\widetilde{\mathbf{W}}_{21}^{\mathbf{L}_1}$ AND R_2 is $\widetilde{\mathbf{W}}_{21}^{\mathbf{L}_1}$ AND $\ldots R_{N_1}$ is $\widetilde{\mathbf{W}}_{2N_1}^{\mathbf{L}_1}$ THEN F_1 is $\widetilde{\mathbf{W}}_{21}^{\mathbf{L}_3}$ AND F_2 is $\widetilde{\mathbf{W}}_{22}^{\mathbf{L}_3}$ AND $\ldots F_{N_3}$ is $\widetilde{\mathbf{W}}_{2N_3}^{\mathbf{L}_3}$

$\vdots$

Rule N: IF R_1 is $\widetilde{\mathbf{W}}_{N1}^{\mathbf{L}_1}$ AND R_2 is $\widetilde{\mathbf{W}}_{N1}^{\mathbf{L}_1}$ AND $\ldots R_{N_1}$ is $\widetilde{\mathbf{W}}_{NN_1}^{\mathbf{L}_1}$ THEN F_1 is $\widetilde{\mathbf{W}}_{N1}^{\mathbf{L}_3}$ AND F_2 is $\widetilde{\mathbf{W}}_{N2}^{\mathbf{L}_3}$ AND $\ldots F_{N_3}$ is $\widetilde{\mathbf{W}}_{NN_3}^{\mathbf{L}_3}$

Conclusions: F_1 is $\widetilde{\mathbf{W}}_1^{\mathbf{L}_3\prime}$ AND F_2 is $\widetilde{\mathbf{W}}_2^{\mathbf{L}_3\prime}$ AND $\ldots F_{N_3}$ is $\widetilde{\mathbf{W}}_{N_3}^{\mathbf{L}_3\prime}$. (28)

Above inference schema developed to infer the truth of Proposition 6 consists of the following parts:

(1) The IF part of a rule consists of (i) some expressions (Proposition 4) linked by AND, and (ii) the fuzzy sets expressing the importance of the Basic Requirements in Rule n, for example:

$\widetilde{\mathbf{W}}_{ni}^{L_1}$ is the predicates describing the situation of R_i by Rule n,

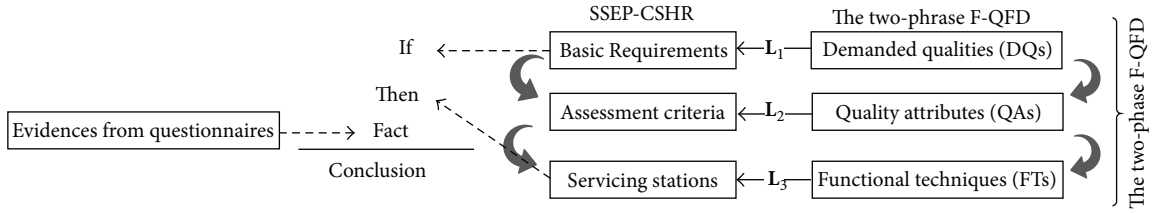

Figure 10: Corresponding relationship between SSEP-CSHR and proposed reasoning.

Table 6: An analysis on a truth-qualified proposition.

	Column 1		Column 2		Column 3
Canonical form	x	is	$\mathbf{A}$	is	$\mathbf{T}$
Example	Construction cost	is	important	is	true
Description	BOE expressing evidence about x		Fuzzy sets expressing predicates		The truth of "x is $\mathbf{A}$"
Math expression	$(\mathbf{F}_i^{\mathbf{L}_1}, m_i^{\mathbf{L}_1})$		$\widetilde{\mathbf{W}}_i^{\mathbf{L}_2}$		$T(\mathbf{F}_i^{\mathbf{L}_1}, \widetilde{\mathbf{W}}_i^{\mathbf{L}_1})$
Methods	By organizing questionnaires from experts		By estimation from QFD team (see Algorithm 3)		By (10) in evidence theory
Analysis step	Step 1 in Algorithm 5		Step 2 in Algorithm 5		Step 3 in Algorithm 5

(2) the THEN part of a rule consists of (i) some expressions linked by AND, and (ii) the fuzzy sets corresponding to the importance of the service stations in Rule n, for example,

$\widetilde{\mathbf{W}}_{ni}^{L_3}$ is the predicates describing the situation of F_i by Rule n,

(3) given N *if-then* rule, rules 1 though N, and Facts, Conclusions will be obtained,

$\mathbf{F}_i^{\mathbf{L}_1}$ is the evidences (BOE) describing the score range of R_i obtained by questionnaires,

$\widetilde{\mathbf{W}}_i^{\mathbf{L}_3\prime}$ is a new predicate for F_i, which is modified by the truth of Proposition 6.

Figure 10 explicates the corresponding relationship between SSEP-CSHR and the above reasoning.

The most common way to determine conclusions in the above reasoning is referred to as a method of *interpolation* [27]. The *interpolation* method is actually a special case of the max-min compositional rule of inference that uses operations:

(1) intersection operation: minimization;

(2) implication operation: minimization;

(3) aggregations operation: maximization.

Based on the operations, we propose an algorithm as follows.

Algorithm 7 (the Algorithm to do approximate reasoning in SSEP-CSHR). Consider the following.

Step 1. Use Algorithm 3 to implement the two-phrase F-QFD in SSEP-CSHR.

Step 2. For each $i \in \{1, 2, \ldots, N_1\}$, develop a BOE for R_i by the method proposed in Section 2.3.

Step 3. For each $i \in \{1, 2, \ldots, N_1\}$, $k \in \{1, 2, \ldots, n\}$, by Algorithm 5, we calculate the truth of propositions:

$$T\left(\mathbf{F}_i^{\mathbf{L}_1}, \widetilde{\mathbf{W}}_{ni}^{\mathbf{L}_1}\right) = w_1 \mathrm{Bel}\left(\mathbf{F}_i^{\mathbf{L}_1}, \widetilde{\mathbf{W}}_{ni}^{\mathbf{L}_1}\right) + w_2 \mathrm{Pl}\left(\mathbf{F}_i^{\mathbf{L}_1}, \widetilde{\mathbf{W}}_{ni}^{\mathbf{L}_1}\right) \quad \forall i \in \{1, 2, \ldots, N_1\},\ n \in \{1, 2, \ldots, N\}. \tag{29}$$

The truth value here is a generalization of the concept of *the degree of consistency* in the *interpolation* method of multiconditional approximate reasoning [27].

Step 4. Calculate the degree of truth between the given facts and the antecedent of each *if-then* rule n in terms of the fuzzy *intersection operation*:

$$T_n = \min_{i \in \{1,2,\ldots,N_1\}} \left(T\left(\mathbf{F}_i^{\mathbf{L}_1}, \widetilde{\mathbf{W}}_{ni}^{\mathbf{L}_1}\right)\right) \quad \forall n \in \{1, 2, \ldots, N\}. \tag{30}$$

Step 5. By *implication* and *aggregation operations* above, we can calculate the Conclusions. That is,

$$\widetilde{\mathbf{W}}_j^{L_3\prime}(x) = \sup_{n \in \{1,2,\ldots,N\}} \min\left[T_n, \widetilde{\mathbf{W}}_{nj}^{L_3}(x)\right] \quad \forall j \in \{1, 2, \ldots, N_3\}. \tag{31}$$

for all $x \in \mathbf{U}$.

Step 6. End.

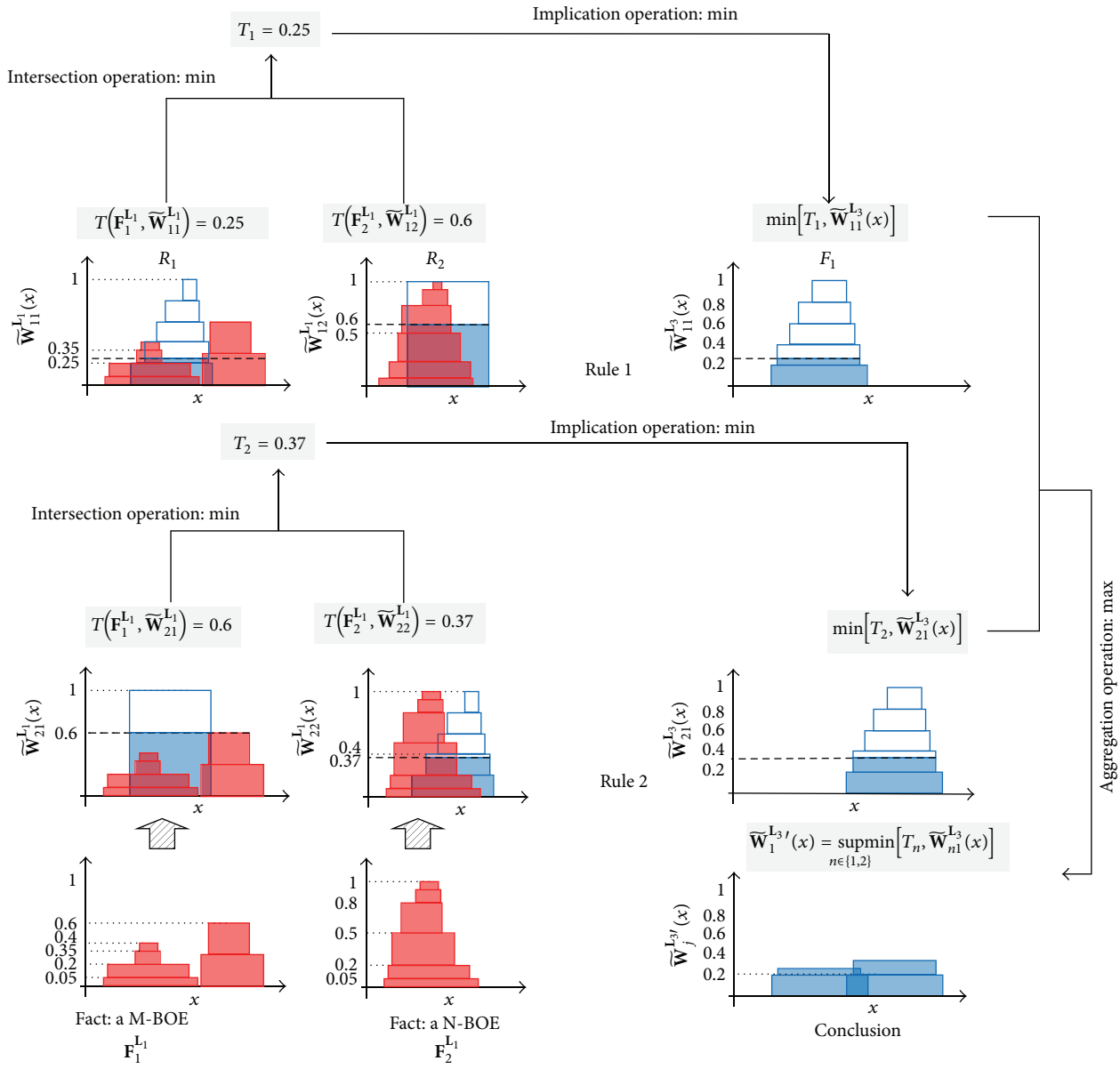

Figure 11: Illustration of approximate reasoning procedure in SSEP-CSHR.

An self-explanatory example of above approximate reasoning for two *if-then* rules with two Basic Requirements (R_1, R_2) and a service station (F_1) is given in Figure 11. In Figure 11 the fuzzy set, crisp set, and evidences about both R_1 and R_2 (a M-BOE and a N-BOE) have all been discussed in Section 2.4.

When BOE for each i in $\{1, 2, \ldots, N_1\}$ is a crisp number a_i,

$$T\left(a_i, \widetilde{\mathbf{W}}_{ni}^{\mathbf{L}_1}\right) = \widetilde{\mathbf{W}}_{ni}^{\mathbf{L}_1}(a_i) \quad \forall i \in \{1, 2, \ldots, N_1\},\ n \in \{1, 2, \ldots, N\}. \tag{32}$$

Then Algorithm 7 becomes a normal *interpolation* for a multiconditional approximate reasoning [27]. Figure 12 manifests this vestigial form.

The general steps of our integrated approach for SSEP-CSHR are summarized in Figure 13.

It is noted that not only Proposition 4 but also any other propositions (of course containing the relation propositions abstract from Relation Matrices and Correlation Matrices in Figure 9) might serve as "cause" to affect the predicates of Proposition 6. However, in the above approximate reasoning we did not consider these "causes" for the following two reasons: Firstly, adding more "causes" did not influence the basic schema of above evidence-based reasoning. Secondly, the relationship between a "WHAT" and a "HOW" and the correlations of "WHATs" and "HOWs" are usually more "objective" (and thus truer) than the importance ratings of "WHATs." It means that the corresponding propositions of them are usually accompanied with higher truth value. If

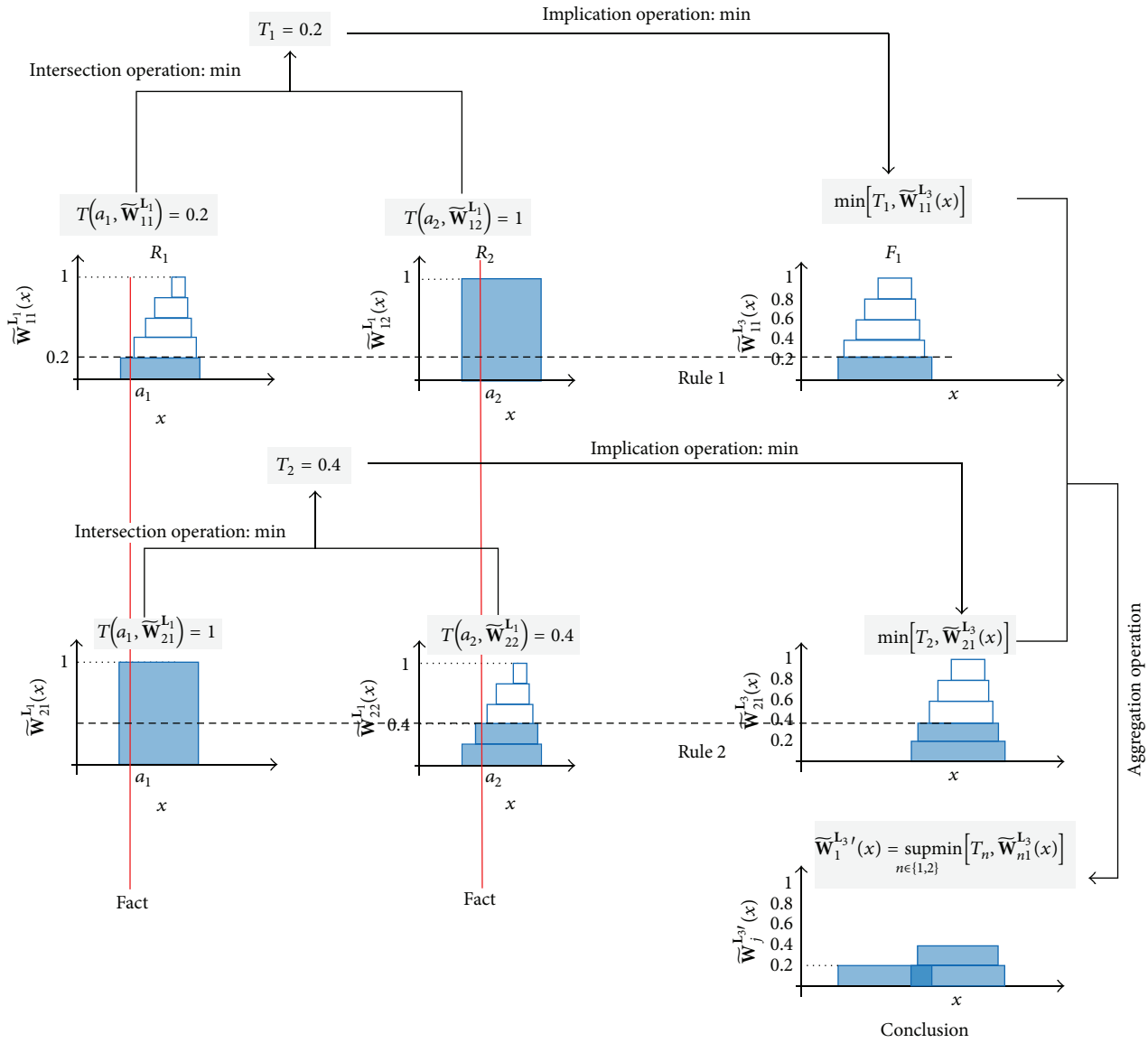

Figure 12: Illustration of normal *interpolation* for multiconditional approximate reasoning procedure.

standard fuzzy operations are used (as in Algorithm 7), these propositions only have little impact on the predicates of Conclusions.

4. Model Implementation

In this section, the integrated evidence theory and F-QFD for SSEP-CSHR will be applied to a practical case study, which refers to 85 alternative service stations on Chinese high-speed rail network. The set of service stations ($\mathbf{L}_3$) is generated based on the real timetables of high-speed trains on April in 2014 in China (see Figure 14). The stations are selected from the rail stations with plenty of starting train lines and stations at which trains usually stop. Table 7 presents names of the stations and their indexes.

Tables 4 and 5 have presented $\mathbf{L}_1$ and $\mathbf{L}_2$ by details. Further QFD team expresses the opinions about the relationship between $\mathbf{L}_1$ and $\mathbf{L}_2$ in Table 8 (i.e., the relationship matrix in QD). The relationship between $\mathbf{L}_2$ and $\mathbf{L}_3$ is expressed in Appendix ((i.e., the relationship matrix in FD)). Correlation degrees between $\mathbf{L}_1$, $\mathbf{L}_2$, and $\mathbf{L}_3$ themselves are not considered in this study for simplification. In all the following matrices, $a/b/c$ means a triangle fuzzy number on an x-α graph; say $\alpha = 1$ with $x = b$, and say $\alpha = 0$ with $x \in [a, c]$.

Table 9 is a pairwise comparison matrix of F-AHP used here to give the importance ratings of Basic Requirements. Three F-AHPs are used to determine the importance rating of Basic Requirements $\mathbf{L}_1$ including Extent Analysis (EA) [6], Modified Extent Analysis (MEA) [24], and Lambda-Max Method (LMM) [25]. Different QFD teams might generate

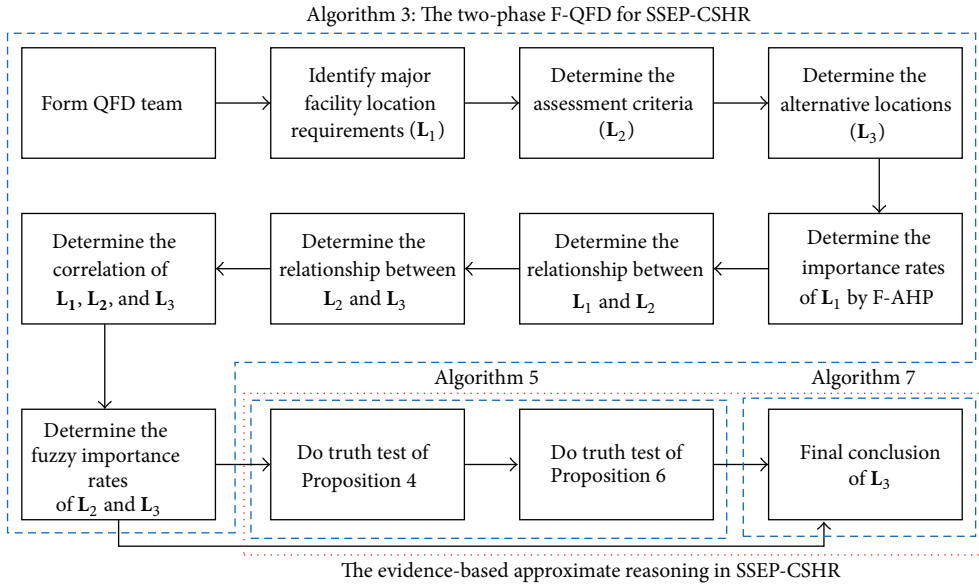

Figure 13: General steps of proposed approach.

different comparison matrix of F-AHP and thus generate different production rules in approximate reasoning. In this case, only one QFD team has made our decision.

Table 10 shows the fuzzy importance ratings of requirements in $\mathbf{L}_1$ obtained by EA, MEA, and LMM. By using (25) to defuzzify the fuzzy importance ratings, all three methods obtain the crisp results that signify "SC > PT > CC > LA > GI > AF". We also find that the fuzzy importance ratings obtained by LMM are "narrower" than the ratings from MEA and EA. Klir and Yuan [27] characterize this nature as nonspecificity (Non). Then we get $\text{Non}_{\text{EA}} > \text{Non}_{\text{MEA}} > \text{Non}_{\text{LMM}}$.

N-BOEs are generated randomly with 20,000 samples corresponding to each R_i in $\mathbf{L}_1$. Based on the N-BOE and the fuzzy importance ratings in Table 10, we can measure the truth between the evidences about Basic Requirements and the predicates of Proposition 4 (which are obtained by fuzzy importance ratings of $\mathbf{L}_1$). In our experiment, N-BOEs are used instead of M-BOE for the purpose of easy presentation. Table 11 shows that fuzzy importance ratings calculated by LMM have lower truth than the results by EA and MEA, that is $\text{Truth}_{\text{EA}} > \text{Truth}_{\text{MEA}} > \text{Truth}_{\text{LMM}}$. It is just the opposite of the state of nonspecificity. It follows that vagueness usually leads propositions more difficult to be falsified.

Figure 15 explicitly illustrates the relationship between the fuzzy important ratings (or the predicates of Proposition 4) obtained by EA, MEA, and LMM and the N-BOE of PT. Apparently, the predicates obtained by LMM are too strict to be proved by our evidences (Bel measure is 0 and Pl measure is 1). The fuzzy important rate of PT from EA although hardly provides any precision information, in this case, but the proposition "R_1 is $\widetilde{\mathbf{W}}_1^{\mathbf{L}_1}$" is truer from the view of the N-BOE. The values of "Min Truth" in Table 11 are important for that they determine the truth of our results of SSEP-CSHR when we only have one Rule in evidence-based inference schema.

Figure 16 displays the trade-off between nonspecificity and truth of fuzzy important ratings in F-QFD by a fitting curve based on all the fuzzy important ratings obtained by the above three methods. It actually shows an inclination that truer propositions are usually accompanied with more Fuzziness. It is noted that Klir and Yuan [27] treat fuzziness and nonspecificity as different conceptions; however, in many researches, nonspecificity is actually used the same as Fuzziness, such as Csutora and Buckley [25], and in fact, in general case nonspecificity is normally directly proportional to fuzziness.

It leads to some interesting conclusions in the field of "uncertainty management." In many existing literatures, minimizing Fuzziness usually serves as a basic principle in MCDM problems. For example, Csutora and Buckley [25] designed LMM in basis of the principle of minimizing Fuzziness. Wang et al. [20, 24] criticized the normalization methods in Chang's [6] EA and Chen et al.'s (2011) fuzzy linear programming because they did not generate the narrowest interval and fuzzy weights.

Our experiments partly justify a diversity of "uncertainty management," just as Klir and Yuan discussed in their book [27]. In F-QFD, when we use precise predicates to describe the situation of $\mathbf{L}_1$, it is possible (not necessary) to result in less truth Conclusions in reasoning and thus decrease the credibility of our evaluation.

Using the results of LMM as inputs, then we execute our two-phase F-QFD methods. Let K be the number of α-cut in $[0, 1]$. When solving the NLPs, that is, (15)–(19), we define $K = 10$. Above algorithms are all coded in MATLAB and executed by using a desktop with CPU Intel-Core i7-4700MQ and 8 G RAM. Finally using about 15 min we get the fuzzy important ratings of 85 stations.

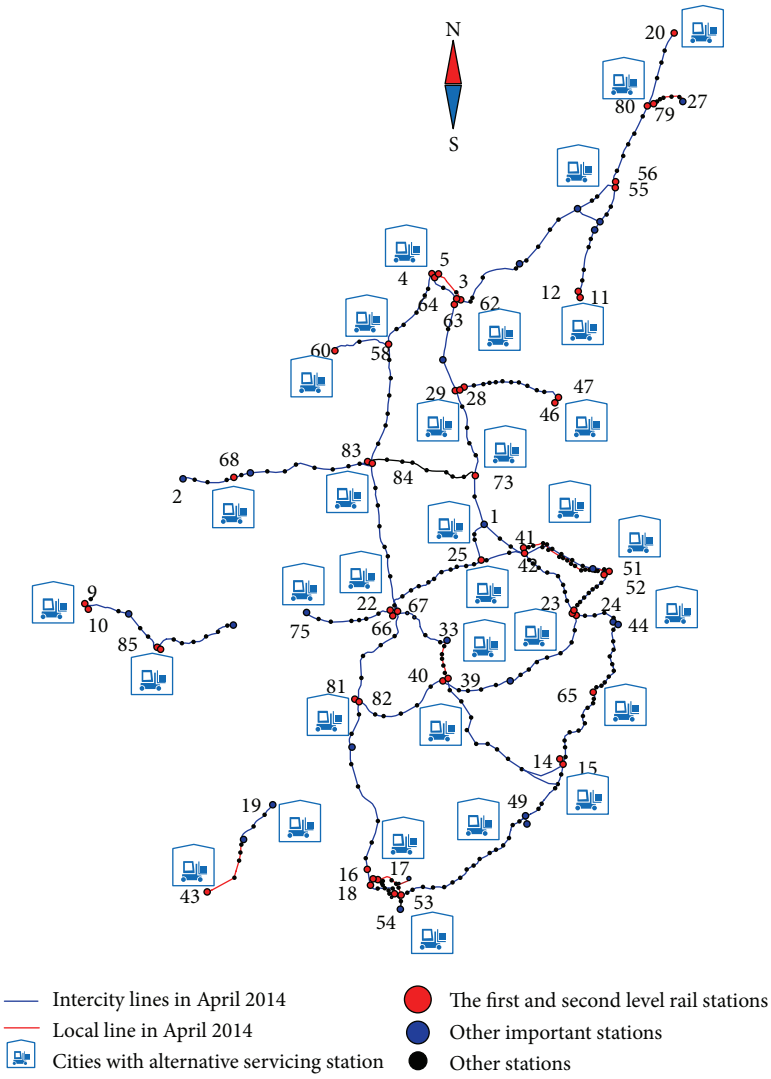

FIGURE 14: Alternative service stations considered in our case study.

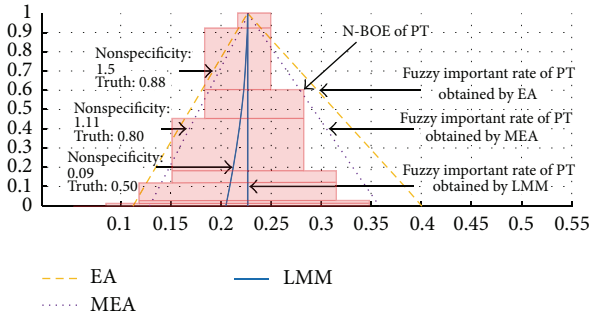

FIGURE 15: Fuzzy important rate of PT in $\mathbf{L}_1$ by three different methods.

4.1. Small Scale Example. We use the data in Appendix (ID: 1, 5, 9, 18, 22, 42, 52, 68) to construct a 7 ∗ 8 relationship matrix between QAs and these eight service stations. Then by Algorithm 3, based on the outputs of phase 1, we determine the fuzzy important rating of stations. Due to large amount of outputs, only eight stations' important ratings at certain α-cuts ($\alpha = 0$ and $\alpha = 1$) are displayed in Table 12. The fuzzy sets which are used to express the fuzzy important ratings are shown in Figure 17(a). Figure 17(b) shows the Conclusions obtained by proposed approximate reasoning.

Figure 18 gives all fuzzy important ratings of above eight service stations (with lower and upper bounds when $\alpha = 0$, as well as the core of the fuzzy sets) based on all the above three types of F-AHPs (i.e., EA, MEA, and LMM). We find that the Conclusions obtained based on LMM provide the most precision information, but with only "truth value = 0.25." The Conclusions obtained from EA provide the most vague outputs, however, with "truth value = 0.48."

4.2. Large Scale Example. Figure 19 utilizes a boxplot to display all the fuzzy important ratings of above 85 stations ($\mathbf{L}_3$) ($a/b/c$, the minimum of a box is a in fuzzy triangle number $a/b/c$; the median of a box is b in fuzzy triangle number

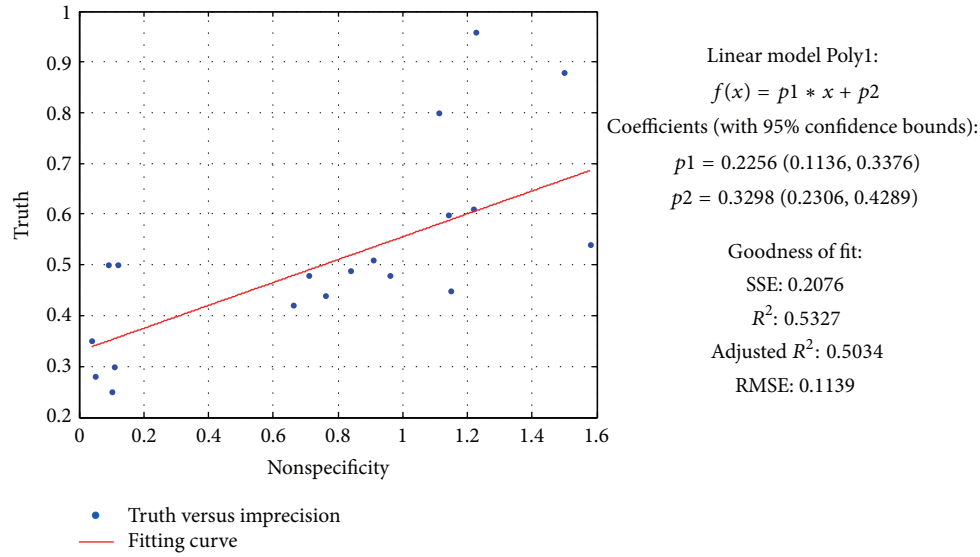

Figure 16: Trade-off between *imprecision* and truth of fuzzy important ratings.

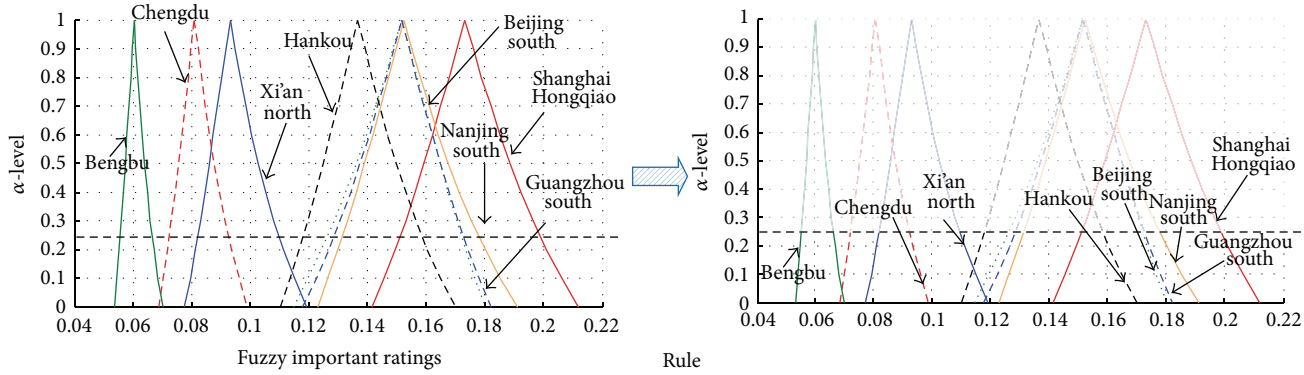

Figure 17: Fuzzy important ratings of the eight service stations and the conclusions after reasoning.

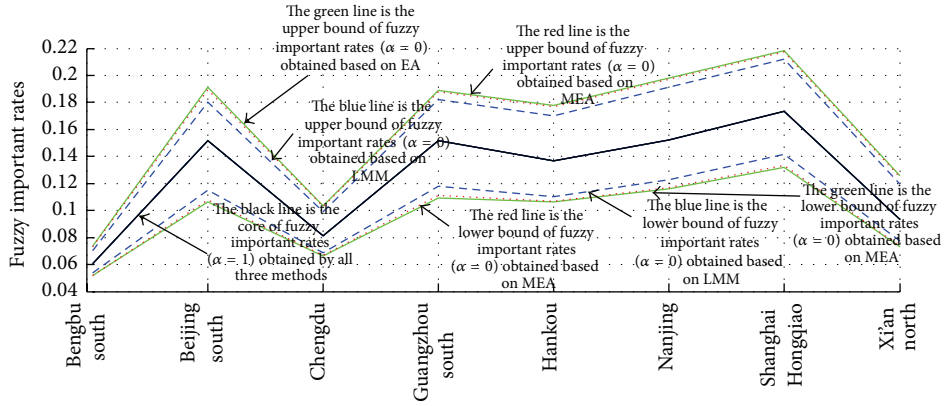

Figure 18: Fuzzy important ratings of service stations based on different F-AHPs.

Table 7: Alterative service rail stations and their IDs in example network.

ID	Station
1	Bengbu south
2	Baoji south
3	Beidaihe
4	Beijing
5	Beijing south
6	Beijing west
7	Cangnan
8	Changzhou
9	Chengdu
10	Chengdu east
11	Dalian
12	Dalian north
13	Fuding
14	Fuzhou
15	Fuzhou south
16	Guangzhou
17	Guangzhou east
18	Guangzhou south
19	Guilin
20	Harbin west
21	Handan east
22	Hankou
23	Hangzhou
24	Hangzhou east
25	Hefe
26	Huainan east
27	Jilin
28	Jinan
29	Jinan west
30	Jiangshan
31	Jinhua west
32	Jingzhou
33	Jiujiang
34	Lichuan
35	Lingbao west
36	Liu'an
37	Longyan
38	Luoyang longmen
39	Nanchang
40	Nanchang west
41	Nanjing
42	Nanjing south
43	Nanning
44	Ningbo
45	Qinhuangdao
46	Qingdao
47	Qingdao north
48	Sanming north
49	Xiamen north
50	Shangqiu
51	Shanghai
52	Shanghai Hongqiao
53	Shenzhen
54	Shenzhen north
55	Shenyang
56	Shenyang north
57	Shiyan
58	Shijiazhuang
59	Suzhou
60	Taiyuan
61	Taining
62	Tianjin
63	Tianjin south
64	Tianjin west
65	Wenzhou south
66	Wuchang
67	Wuhan
68	Xi'an north
69	Xiangyang
70	Xinxiang east
71	Xinyang east
72	Xuzhou
73	Xuzhou east
74	Yan'an
75	Yichang east
76	Yiwu
77	YueYangDong
78	Zhangzhou
79	Changchun
80	Changchun west
81	Changsha
82	Changsha south
83	Zhengzhou
84	Zhengzhou east
85	Chongqing north

Table 7: Continued.

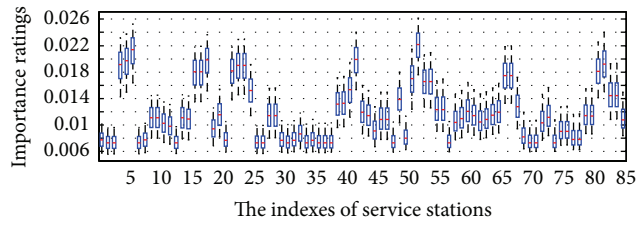

Figure 19: Boxplots to express the fuzzy important ratings for service stations.

Table 8: Relation matrices of QD (between $\mathbf{L}_1$ and $\mathbf{L}_2$).

	QL	AT	AC	PC	HR	EF	PI
PT	0.08/0.09/0.1	0.29/0.29/0.29	0.1/0.12/0.14	0.11/0.12/0.15	0.08/0.09/0.1	0.11/0.12/0.15	0.16/0.17/0.19
SC	0.07/0.08/0.08	0.07/0.08/0.08	0.24/0.25/0.25	0.24/0.25/0.26	0.07/0.08/0.09	0.13/0.14/0.15	0.13/0.14/0.15
LA	0.08/0.09/0.11	0.11/0.14/0.16	0.08/0.09/0.12	0.09/0.09/0.12	0.31/0.31/0.31	0.11/0.14/0.16	0.12/0.14/0.17
AF	0.3/0.3/0.3	0.08/0.09/0.11	0.1/0.13/0.15	0.11/0.13/0.16	0.08/0.09/0.11	0.11/0.13/0.16	0.11/0.13/0.17
GI	0.13/0.15/0.17	0.13/0.15/0.18	0.08/0.09/0.11	0.08/0.09/0.12	0.06/0.07/0.08	0.26/0.26/0.26	0.18/0.2/0.23
CC	0.15/0.17/0.18	0.15/0.17/0.19	0.1/0.12/0.13	0.1/0.12/0.14	0.08/0.08/0.09	0.22/0.23/0.23	0.11/0.12/0.14

Table 9: Pairwise comparison matrix of F-AHP.

	PT	SC	LA	AF	GI	CC
PT	1/1/1	0.5/1/1.5	1/1.5/2	1.5/2/2.5	1.5/2/2.5	1/1.5/2
SC	0.67/1/2	1/1/1	1/1.5/2	1.5/2/2.5	1.5/2/2.5	1/1.5/2
LA	0.5/0.67/1	0.5/0.67/1	1/1/1	1/1.5/2	1/1.5/2	0.5/1/1.5
AF	0.4/0.5/0.67	0.4/0.5/0.67	0.5/0.67/1	1/1/1	0.5/1/1.5	0.5/0.67/1
GI	0.4/0.5/0.67	0.4/0.5/0.67	0.5/0.67/1	0.67/1/2	1/1/1	0.5/0.67/1
CC	0.5/0.67/1	0.5/0.67/1	0.67/1/2	1/1.5/2	1/1.5/2	1/1/1

Table 10: Fuzzy importance ratings of $\mathbf{L}_1$ obtained from EA, MEA, and LMM.

	Importance ratings of $\mathbf{L}_1$ by different F-AHP					
	EA	Equation (25)	MEA	Equation (25)	LMM	Equation (25)
PT	0.12/0.23/0.4	0.25	0.13/0.23/0.34	0.23	0.21/0.23/0.23	0.223
SC	0.13/0.23/0.41	0.26	0.14/0.23/0.35	0.24	0.22/0.23/0.24	0.230
LA	0.08/0.16//0.29	0.18	0.09/0.16/0.26	0.17	0.14/0.15//0.17	0.157
AF	0.06/0.11/0.2	0.12	0.07/0.11/0.18	0.12	0.11/0.11/0.12	0.111
GI	0.07/0.11/0.22	0.13	0.07/0.11/0.20	0.13	0.11/0.11/0.12	0.114
CC	0.09/0.16/0.31	0.19	0.10/0.16/0.27	0.18	0.15/0.16/0.18	0.161

Table 11: Comparison analysis between truth and nonspecificity.

$\mathbf{L}_1$	*Nonspecificity* by different F-AHPs			$\mathbf{L}_1$	*Truth* of $\mathbf{L}_1$ by different F-AHPs		
	EA	MEA	LMM		EA	MEA	LMM
PT	1.5	1.11	**0.09**	PT	**0.88**	0.80	0.5
SC	1.58	1.15	**0.1**	SC	**0.54**	0.45	0.25
LA	1.14	0.91	**0.11**	LA	**0.6**	0.51	0.30
AF	0.76	0.66	**0.04**	AF	**0.44**	0.42	0.35
GI	0.84	0.71	**0.05**	GI	**0.49**	0.48	0.28
CC	1.22	0.96	**0.12**	CC	**0.61**	0.48	0.5
Max nonspecificity	1.58	1.15	**0.18**	*Min truth*	**0.44**	0.42	0.25

Table 12: Fuzzy important ratings of some service stations.

α-cut	Bengbu south	Beijing south	Chengdu	Guangzhou south	Hankou	Nanjing south	Shanghai Hongqiao	Xi'an north
$(\widetilde{A})_0^L$	0.054	0.114	0.069	0.118	0.110	0.123	0.142	0.078
$(\widetilde{A})_1^L$	0.060	0.152	0.081	0.152	0.136	0.152	0.173	0.093
$(\widetilde{A})_0^U$	0.070	0.180	0.099	0.182	0.170	0.191	0.212	0.119

Table 13: Relation matrices of FD (between $\mathbf{L}_2$ and $\mathbf{L}_3$).

	QL	AT	AC	PC	HR	EF	PI
1	0.006/0.007/0.007	0.008/0.009/0.011	0.006/0.007/0.008	0.006/0.007/0.008	0.007/0.008/0.009	0.007/0.008/0.01	0.007/0.008/0.009
2	0.006/0.007/0.007	0.006/0.007/0.008	0.006/0.007/0.008	0.006/0.007/0.008	0.007/0.008/0.009	0.007/0.008/0.01	0.007/0.008/0.009
3	0.006/0.007/0.007	0.006/0.007/0.008	0.006/0.007/0.008	0.006/0.007/0.008	0.007/0.008/0.009	0.007/0.008/0.01	0.007/0.008/0.009
4	0.022/0.023/0.023	0.008/0.009/0.011	0.017/0.019/0.02	0.017/0.019/0.02	0.014/0.016/0.017	0.02/0.021/0.023	0.026/0.027/0.027
5	0.022/0.023/0.023	0.012/0.013/0.015	0.018/0.019/0.02	0.017/0.019/0.02	0.014/0.016/0.017	0.02/0.021/0.023	0.026/0.027/0.027
6	0.022/0.023/0.023	0.012/0.013/0.015	0.024/0.025/0.025	0.024/0.025/0.025	0.014/0.016/0.017	0.02/0.021/0.023	0.027/0.027/0.027
7	0.006/0.007/0.007	0.006/0.007/0.008	0.006/0.007/0.008	0.006/0.007/0.008	0.007/0.008/0.009	0.007/0.008/0.01	0.007/0.008/0.009
8	0.006/0.007/0.007	0.008/0.009/0.011	0.006/0.007/0.008	0.006/0.007/0.008	0.007/0.008/0.009	0.007/0.008/0.01	0.007/0.008/0.009
9	0.008/0.009/0.01	0.012/0.013/0.015	0.009/0.01/0.011	0.012/0.014/0.016	0.007/0.008/0.009	0.009/0.011/0.013	0.009/0.011/0.013
10	0.008/0.009/0.01	0.012/0.013/0.015	0.009/0.01/0.011	0.012/0.014/0.016	0.007/0.008/0.009	0.009/0.011/0.013	0.009/0.011/0.013
11	0.011/0.013/0.014	0.008/0.009/0.011	0.012/0.014/0.015	0.009/0.01/0.011	0.01/0.011/0.013	0.007/0.008/0.01	0.007/0.008/0.009
12	0.008/0.009/0.01	0.008/0.009/0.011	0.009/0.01/0.012	0.012/0.014/0.016	0.01/0.011/0.013	0.007/0.008/0.01	0.007/0.008/0.01
13	0.006/0.007/0.007	0.006/0.007/0.008	0.006/0.007/0.008	0.006/0.007/0.008	0.007/0.008/0.009	0.007/0.008/0.01	0.007/0.008/0.01
14	0.011/0.013/0.014	0.012/0.013/0.015	0.009/0.01/0.012	0.012/0.014/0.016	0.007/0.008/0.009	0.009/0.011/0.013	0.007/0.008/0.01
15	0.011/0.013/0.014	0.012/0.013/0.015	0.009/0.01/0.012	0.012/0.014/0.016	0.01/0.011/0.013	0.007/0.008/0.01	0.007/0.008/0.01
16	0.022/0.023/0.023	0.017/0.018/0.019	0.012/0.014/0.016	0.012/0.014/0.016	0.021/0.022/0.022	0.014/0.016/0.018	0.02/0.021/0.022
17	0.022/0.023/0.023	0.017/0.018/0.019	0.012/0.014/0.016	0.012/0.014/0.016	0.021/0.022/0.022	0.014/0.016/0.018	0.02/0.021/0.022
18	0.022/0.023/0.023	0.023/0.024/0.024	0.018/0.019/0.02	0.012/0.014/0.016	0.014/0.016/0.017	0.02/0.021/0.023	0.02/0.021/0.022
19	0.008/0.009/0.01	0.008/0.009/0.011	0.006/0.007/0.008	0.009/0.01/0.011	0.01/0.011/0.013	0.01/0.011/0.014	0.007/0.008/0.01
20	0.008/0.009/0.01	0.008/0.009/0.011	0.012/0.014/0.016	0.012/0.014/0.016	0.014/0.016/0.017	0.01/0.011/0.014	0.007/0.008/0.01
21	0.006/0.007/0.007	0.006/0.007/0.008	0.006/0.007/0.008	0.006/0.007/0.008	0.01/0.011/0.013	0.007/0.008/0.01	0.007/0.008/0.01
22	0.016/0.017/0.018	0.023/0.024/0.024	0.018/0.019/0.02	0.018/0.019/0.02	0.014/0.016/0.017	0.014/0.016/0.018	0.014/0.016/0.017
23	0.016/0.017/0.018	0.017/0.018/0.019	0.024/0.025/0.025	0.018/0.019/0.02	0.014/0.016/0.017	0.02/0.021/0.023	0.014/0.016/0.017
24	0.016/0.017/0.018	0.017/0.018/0.019	0.024/0.025/0.025	0.018/0.019/0.02	0.014/0.016/0.017	0.02/0.021/0.023	0.014/0.016/0.017
25	0.011/0.013/0.014	0.012/0.013/0.015	0.018/0.019/0.02	0.012/0.014/0.016	0.014/0.016/0.018	0.014/0.016/0.018	0.014/0.016/0.018
26	0.006/0.007/0.007	0.006/0.007/0.008	0.006/0.007/0.008	0.006/0.007/0.008	0.007/0.008/0.009	0.007/0.008/0.01	0.007/0.008/0.01
27	0.006/0.007/0.008	0.006/0.007/0.008	0.006/0.007/0.008	0.006/0.007/0.008	0.007/0.008/0.009	0.007/0.008/0.01	0.007/0.008/0.01
28	0.008/0.009/0.01	0.017/0.018/0.019	0.012/0.014/0.016	0.012/0.014/0.016	0.007/0.008/0.009	0.007/0.008/0.01	0.007/0.008/0.01
29	0.008/0.009/0.01	0.017/0.018/0.019	0.012/0.014/0.016	0.012/0.014/0.016	0.007/0.008/0.009	0.007/0.008/0.01	0.007/0.008/0.01
30	0.006/0.007/0.008	0.006/0.007/0.008	0.006/0.007/0.008	0.006/0.007/0.008	0.01/0.011/0.013	0.007/0.008/0.01	0.007/0.008/0.01
31	0.006/0.007/0.008	0.006/0.007/0.008	0.007/0.007/0.009	0.006/0.007/0.008	0.007/0.008/0.009	0.007/0.008/0.01	0.007/0.008/0.01
32	0.006/0.007/0.008	0.006/0.007/0.008	0.009/0.01/0.012	0.006/0.007/0.008	0.007/0.008/0.009	0.007/0.008/0.01	0.007/0.008/0.01
33	0.006/0.007/0.008	0.008/0.009/0.011	0.009/0.01/0.012	0.006/0.007/0.008	0.007/0.008/0.009	0.007/0.008/0.01	0.009/0.011/0.013
34	0.006/0.007/0.008	0.006/0.007/0.008	0.007/0.007/0.009	0.007/0.007/0.008	0.007/0.008/0.009	0.007/0.008/0.01	0.007/0.008/0.01
35	0.006/0.007/0.008	0.006/0.007/0.008	0.007/0.007/0.009	0.007/0.007/0.009	0.01/0.011/0.013	0.007/0.008/0.01	0.007/0.008/0.01
36	0.006/0.007/0.008	0.006/0.007/0.008	0.007/0.007/0.009	0.007/0.007/0.009	0.007/0.008/0.009	0.007/0.008/0.01	0.007/0.008/0.01
37	0.006/0.007/0.008	0.006/0.007/0.008	0.007/0.007/0.009	0.007/0.007/0.009	0.007/0.008/0.009	0.007/0.008/0.01	0.007/0.008/0.01
38	0.006/0.007/0.008	0.006/0.007/0.008	0.007/0.007/0.009	0.007/0.007/0.009	0.007/0.008/0.009	0.007/0.008/0.01	0.007/0.008/0.01
39	0.011/0.013/0.014	0.008/0.009/0.011	0.012/0.014/0.016	0.012/0.014/0.016	0.014/0.016/0.018	0.01/0.011/0.014	0.014/0.016/0.018
40	0.011/0.013/0.014	0.012/0.013/0.015	0.009/0.01/0.012	0.012/0.014/0.016	0.014/0.016/0.018	0.014/0.016/0.018	0.009/0.011/0.013
41	0.016/0.017/0.018	0.023/0.024/0.024	0.013/0.014/0.016	0.012/0.014/0.016	0.014/0.016/0.018	0.01/0.011/0.014	0.009/0.011/0.013
42	0.016/0.017/0.018	0.023/0.024/0.024	0.018/0.019/0.02	0.024/0.025/0.025	0.014/0.016/0.018	0.02/0.021/0.023	0.014/0.016/0.018
43	0.011/0.013/0.014	0.012/0.013/0.015	0.009/0.01/0.012	0.012/0.014/0.016	0.014/0.016/0.018	0.007/0.008/0.01	0.009/0.011/0.013
44	0.016/0.017/0.019	0.012/0.013/0.015	0.009/0.01/0.012	0.009/0.01/0.011	0.01/0.011/0.013	0.007/0.008/0.01	0.009/0.011/0.013
45	0.008/0.009/0.01	0.006/0.007/0.008	0.007/0.007/0.009	0.007/0.007/0.009	0.01/0.011/0.013	0.01/0.011/0.014	0.01/0.011/0.013
46	0.011/0.013/0.014	0.012/0.013/0.015	0.007/0.007/0.009	0.007/0.007/0.009	0.007/0.008/0.01	0.01/0.011/0.014	0.014/0.016/0.018
47	0.012/0.013/0.014	0.012/0.013/0.015	0.007/0.007/0.009	0.007/0.007/0.009	0.007/0.008/0.01	0.01/0.011/0.014	0.014/0.016/0.018

Table 13: Continued.

	QL	AT	AC	PC	HR	EF	PI
48	0.006/0.007/0.008	0.006/0.007/0.008	0.007/0.007/0.009	0.007/0.007/0.009	0.007/0.008/0.01	0.007/0.008/0.011	0.007/0.008/0.01
49	0.016/0.017/0.019	0.012/0.013/0.015	0.013/0.014/0.016	0.012/0.014/0.017	0.01/0.011/0.013	0.014/0.016/0.018	0.01/0.011/0.013
50	0.008/0.009/0.01	0.006/0.007/0.008	0.007/0.007/0.009	0.007/0.007/0.009	0.01/0.011/0.013	0.007/0.008/0.011	0.007/0.008/0.01
51	0.022/0.023/0.023	0.023/0.024/0.024	0.018/0.019/0.021	0.018/0.019/0.021	0.014/0.016/0.018	0.01/0.011/0.014	0.007/0.008/0.01
52	0.022/0.023/0.023	0.017/0.018/0.019	0.024/0.025/0.025	0.025/0.025/0.025	0.014/0.016/0.018	0.02/0.021/0.023	0.027/0.027/0.027
53	0.016/0.017/0.019	0.012/0.013/0.015	0.018/0.019/0.021	0.018/0.019/0.021	0.014/0.016/0.018	0.014/0.016/0.018	0.014/0.016/0.018
54	0.016/0.017/0.019	0.012/0.013/0.015	0.013/0.014/0.016	0.012/0.014/0.017	0.021/0.022/0.022	0.014/0.016/0.018	0.02/0.021/0.022
55	0.008/0.009/0.01	0.008/0.009/0.011	0.013/0.014/0.016	0.009/0.01/0.011	0.01/0.011/0.013	0.014/0.016/0.018	0.014/0.016/0.018
56	0.008/0.009/0.011	0.008/0.009/0.011	0.009/0.01/0.012	0.013/0.014/0.017	0.01/0.011/0.013	0.014/0.016/0.018	0.014/0.016/0.018
57	0.006/0.007/0.008	0.006/0.007/0.008	0.007/0.007/0.009	0.007/0.007/0.009	0.007/0.008/0.01	0.007/0.008/0.011	0.007/0.008/0.01
58	0.008/0.009/0.011	0.008/0.009/0.011	0.013/0.014/0.016	0.013/0.014/0.017	0.01/0.011/0.013	0.007/0.008/0.011	0.007/0.008/0.01
59	0.008/0.009/0.011	0.008/0.009/0.011	0.013/0.014/0.016	0.009/0.01/0.012	0.014/0.016/0.018	0.01/0.011/0.014	0.007/0.008/0.01
60	0.008/0.009/0.011	0.012/0.013/0.016	0.009/0.01/0.012	0.013/0.014/0.017	0.015/0.016/0.018	0.01/0.011/0.014	0.01/0.011/0.014
61	0.012/0.013/0.014	0.012/0.013/0.016	0.013/0.014/0.016	0.009/0.01/0.012	0.01/0.011/0.013	0.007/0.008/0.011	0.01/0.011/0.014
62	0.012/0.013/0.014	0.009/0.009/0.011	0.009/0.01/0.012	0.013/0.014/0.017	0.007/0.008/0.01	0.01/0.011/0.014	0.007/0.008/0.011
63	0.012/0.013/0.014	0.009/0.009/0.011	0.009/0.01/0.012	0.009/0.01/0.012	0.015/0.016/0.018	0.01/0.011/0.014	0.007/0.008/0.011
64	0.012/0.013/0.014	0.009/0.009/0.011	0.009/0.01/0.012	0.009/0.01/0.012	0.01/0.011/0.013	0.01/0.011/0.014	0.014/0.016/0.018
65	0.016/0.017/0.019	0.009/0.009/0.011	0.009/0.01/0.012	0.009/0.01/0.012	0.015/0.016/0.018	0.01/0.011/0.014	0.01/0.011/0.014
66	0.016/0.017/0.019	0.023/0.024/0.024	0.018/0.019/0.021	0.018/0.019/0.021	0.015/0.016/0.018	0.01/0.011/0.014	0.014/0.016/0.018
67	0.016/0.017/0.019	0.023/0.024/0.024	0.018/0.019/0.021	0.018/0.019/0.021	0.015/0.016/0.019	0.01/0.011/0.014	0.014/0.016/0.018
68	0.012/0.013/0.015	0.017/0.018/0.02	0.013/0.014/0.016	0.013/0.014/0.017	0.01/0.011/0.013	0.007/0.008/0.011	0.01/0.011/0.014
69	0.008/0.009/0.011	0.007/0.007/0.008	0.007/0.007/0.009	0.007/0.007/0.009	0.007/0.008/0.01	0.01/0.011/0.014	0.007/0.008/0.011
70	0.006/0.007/0.008	0.007/0.007/0.008	0.007/0.007/0.009	0.007/0.007/0.009	0.007/0.008/0.01	0.007/0.008/0.011	0.007/0.008/0.011
71	0.006/0.007/0.008	0.007/0.007/0.008	0.007/0.007/0.009	0.007/0.007/0.009	0.007/0.008/0.01	0.007/0.008/0.011	0.007/0.008/0.011
72	0.006/0.007/0.008	0.009/0.009/0.011	0.007/0.007/0.009	0.009/0.01/0.012	0.01/0.011/0.013	0.015/0.016/0.019	0.01/0.011/0.014
73	0.008/0.009/0.011	0.012/0.013/0.016	0.009/0.01/0.012	0.009/0.01/0.012	0.01/0.011/0.013	0.015/0.016/0.019	0.007/0.008/0.011
74	0.006/0.007/0.008	0.007/0.007/0.008	0.007/0.007/0.009	0.007/0.007/0.009	0.008/0.008/0.01	0.007/0.008/0.011	0.007/0.008/0.011
75	0.006/0.007/0.008	0.009/0.009/0.012	0.009/0.01/0.012	0.009/0.01/0.012	0.008/0.008/0.01	0.007/0.008/0.011	0.01/0.011/0.014
76	0.006/0.007/0.008	0.009/0.009/0.012	0.009/0.01/0.012	0.009/0.01/0.012	0.008/0.008/0.01	0.007/0.008/0.011	0.01/0.011/0.014
77	0.006/0.007/0.008	0.007/0.007/0.008	0.007/0.007/0.009	0.007/0.007/0.009	0.008/0.008/0.01	0.007/0.008/0.011	0.01/0.011/0.014
78	0.006/0.007/0.008	0.007/0.007/0.008	0.007/0.007/0.009	0.007/0.007/0.009	0.008/0.008/0.01	0.007/0.008/0.011	0.01/0.011/0.014
79	0.012/0.013/0.015	0.012/0.013/0.016	0.009/0.01/0.012	0.009/0.01/0.012	0.01/0.011/0.014	0.01/0.011/0.014	0.01/0.011/0.014
80	0.012/0.013/0.015	0.009/0.009/0.012	0.013/0.014/0.016	0.009/0.01/0.012	0.01/0.011/0.014	0.01/0.011/0.015	0.01/0.011/0.014
81	0.016/0.017/0.019	0.017/0.018/0.02	0.018/0.019/0.021	0.013/0.014/0.017	0.021/0.022/0.022	0.02/0.021/0.023	0.014/0.016/0.018
82	0.016/0.017/0.019	0.017/0.018/0.02	0.018/0.019/0.021	0.013/0.014/0.017	0.015/0.016/0.019	0.027/0.027/0.027	0.02/0.021/0.022
83	0.016/0.017/0.019	0.012/0.013/0.016	0.013/0.014/0.017	0.018/0.019/0.021	0.015/0.016/0.019	0.01/0.011/0.015	0.01/0.011/0.014
84	0.016/0.017/0.019	0.012/0.013/0.016	0.013/0.014/0.017	0.018/0.019/0.021	0.015/0.016/0.019	0.01/0.011/0.015	0.01/0.011/0.014
85	0.012/0.013/0.015	0.009/0.009/0.012	0.009/0.01/0.012	0.009/0.01/0.012	0.01/0.011/0.014	0.01/0.011/0.015	0.01/0.011/0.014

$a/b/c$; the maximum of a box is c in fuzzy triangle number $a/b/c$). Based on LMM inputs and the approximate reasoning procedure in SSEP-CSHR, we know that the outputs only have truth value 0.25 (see Table 11).

5. Conclusions

QFD is a method to specify the customer wants and needs and then to evaluate each alternative in terms of its impact on meeting those needs. This paper is an effort to improve the scientific credibility and practicability of F-QFD and to offer a qualitative approach for SSEP-CSHR based on the two-phase F-QFD with an approximate procedure based on evidence theory. Belief and Plausibility are two types of measures in the view of evidence theory. Using the two measures, a framework to determine the truth of "x is $\mathbf{A}$" is investigated in Section 2 and then is used to deal with different types of BOE that might be met in CSHR's survey. The contribution of Section 3 is twofold. Firstly, this paper offers a MCDM

approach for SSEP-CSHR based on the two-phase F-QFD to select potential service stations for CSHR with regard to series of practical criteria and Basic Requirements in context of CSHR. Secondly, this paper illustrates that the usage of evidence theory allows an approximate reasoning based on various types of BOE to be incorporated into F-QFD. In our case study, the proposed method is implemented in a high-speed rail network of China referring to 85 railway stations. The application, on the one hand, presents the fuzzy importance ratings for 85 service stations; on the other hand, it shows the truth of our Conclusions to be assessed by using proposed evidence-based inference schema. It demonstrated that the proposed method enhances scientific credibility of F-QFD in SSEP-CSHR and allows decision makers to express how much they know. By deep analysis, we realize an interesting trade-off between nonspecificity and truth in F-QFD. Hence our experiments partly justify a diversity of "uncertainty management."

Appendix

See Table 13.

Conflict of Interests

The authors declare that there is no conflict of interests regarding the publication of this paper.

Acknowledgments

This research was supported by the following funds: evaluation and system research about line planning of high-speed railway (China Railway Corporation) (Grant no. 2014X010-A); National Natural Science Foundation of China (U1434207); Fundamental Research Funds for the Central Universities (Beijing Jiaotong University) (Grant no. 2014JBZ008).

References

[1] R. J. Kuo, S. C. Chi, and S. S. Kao, "A decision support system for locating convenience store through fuzzy AHP," *Computers & Industrial Engineering*, vol. 37, no. 1, pp. 323–326, 1999.

[2] C.-T. Chen, "A fuzzy approach to select the location of the distribution center," *Fuzzy Sets and Systems*, vol. 118, no. 1, pp. 65–73, 2001.

[3] C. Kahraman, D. Ruan, and I. Doğan, "Fuzzy group decision-making for facility location selection," *Information Sciences*, vol. 157, no. 1–4, pp. 135–153, 2003.

[4] J. M. Blin, "Fuzzy relations in group decision theory," *Journal of Cybernetics*, vol. 4, pp. 17–22, 1974.

[5] R. R. Yager, "Fuzzy decision-making including unequal objectives," *Fuzzy Sets and Systems*, vol. 1, no. 2, pp. 87–95, 1978.

[6] D.-Y. Chang, "Applications of the extent analysis method on fuzzy AHP," *European Journal of Operational Research*, vol. 95, no. 3, pp. 649–655, 1996.

[7] O. Kulak and C. Kahraman, "Fuzzy multi-attribute selection among transportation companies using axiomatic design and analytic hierarchy process," *Information Sciences*, vol. 170, no. 2–4, pp. 191–210, 2005.

[8] P. J. Guo, "Fuzzy data envelopment analysis and its application to location problems," *Information Sciences*, vol. 179, no. 6, pp. 820–829, 2009.

[9] Y. Akao, "QFD: past, present and future," in *Proceedings of the International Symposium on QFD*, pp. 1–12, Linköping, Sweden, October 1997.

[10] G. H. Mazur, "QFD for service industries—from voice of customer to task deployment," in *Proceedings of the 5th Symposium on Quality Function Deployment*, pp. 1–17, Novi, Mich, USA, June 1993.

[11] A. Jamalnia, H. A. Mahdiraji, M. R. Sadeghi, S. H. R. Hajiagha, and A. Feili, "An integrated fuzzy QFD and fuzzy goal programming approach for global facility location-allocation problem," *International Journal of Information Technology & Decision Making*, vol. 13, no. 2, pp. 263–290, 2014.

[12] S. Kikuchi and P. Chakroborty, "Place of possibility theory in transportation analysis," *Transportation Research Part B: Methodological*, vol. 40, no. 8, pp. 595–615, 2006.

[13] K.-J. Kim, D.-H. Kim, and D.-K. Min, "Robust QFD: framework and a case study," *Quality and Reliability Engineering International*, vol. 23, no. 1, pp. 31–44, 2007.

[14] C. Temponi, J. Yen, and W. A. Tiao, "House of quality: a fuzzy logic-based requirements analysis," *European Journal of Operational Research*, vol. 117, no. 2, pp. 340–354, 1999.

[15] C. K. Kwong and H. Bai, "Determing the importance weights for the customer requirements in QFD using a fuzzy AHP with an extent analysis approach," *IIE Transactions*, vol. 35, pp. 619–626, 2003.

[16] C. Kahraman, T. Ertay, and G. Büyüközkan, "A fuzzy optimization model for QFD planning process using analytic network approach," *European Journal of Operational Research*, vol. 171, no. 2, pp. 390–411, 2006.

[17] L.-H. Chen and W.-C. Ko, "Fuzzy linear programming models for new product design using QFD with FMEA," *Applied Mathematical Modelling*, vol. 33, no. 2, pp. 633–647, 2009.

[18] L.-H. Chen and W.-C. Ko, "Fuzzy linear programming models for NPD using a four-phase QFD activity process based on the means-end chain concept," *European Journal of Operational Research*, vol. 201, no. 2, pp. 619–632, 2010.

[19] E. Bottani and A. Rizzi, "Strategic management of logistics service: a fuzzy QFD approach," *International Journal of Production Economics*, vol. 103, no. 2, pp. 585–599, 2006.

[20] Y.-M. Wang and K.-S. Chin, "Technical importance ratings in fuzzy QFD by integrating fuzzy normalization and fuzzy weighted average," *Computers & Mathematics with Applications*, vol. 62, no. 11, pp. 4207–4221, 2011.

[21] T. L. Saaty, "A scaling method for priorities in hierarchical structures," *Journal of Mathematical Psychology*, vol. 15, no. 3, pp. 234–281, 1977.

[22] J. J. Buckley, T. Feuring, and Y. Hayashi, "Fuzzy hierarchical analysis," in *Proceedings of the IEEE International Fuzzy Systems Conference Proceedings (FUZZ-IEEE '99)*, vol. 2, pp. 1009–1013, IEEE, Seoul, Republic of Korea, August 1999.

[23] K.-J. Zhu, Y. Jing, and D.-Y. Chang, "Discussion on extent analysis method and applications of fuzzy AHP," *European Journal of Operational Research*, vol. 116, no. 2, pp. 450–456, 1999.

[24] Y.-M. Wang, Y. Luo, and Z. Hua, "On the extent analysis method for fuzzy AHP and its applications," *European Journal of Operational Research*, vol. 186, no. 2, pp. 735–747, 2008.

[25] R. Csutora and J. J. Buckley, "Fuzzy hierarchical analysis: the Lambda-Max method," *Fuzzy Sets and Systems*, vol. 120, no. 2, pp. 181–195, 2001.

[26] D.-H. Kim and K.-J. Kim, "Robustness indices and robust prioritization in QFD," *Expert Systems with Applications*, vol. 36, no. 2, pp. 2651–2658, 2009.

[27] G. J. Klir and B. Yuan, *Fuzzy Sets and Fuzzy Logic—Theory and Application*, Prentice Hall PTR, Upper Saddle River, NJ, USA, 1995.

[28] Y.-M. Wang and T. M. Elhag, "On the normalization of interval and fuzzy weights," *Fuzzy Sets and Systems*, vol. 157, no. 18, pp. 2456–2471, 2006.

[29] Y.-M. Wang, "Centroid defuzzification and the maximizing set and minimizing set ranking based on alpha level sets," *Computers & Industrial Engineering*, vol. 57, no. 1, pp. 228–236, 2009.

[30] L. A. Zadeh, "Outline of a new approach to the analysis of complex systems and decision processes," *IEEE Transactions on Systems, Man and Cybernetics*, vol. 3, no. 1, pp. 28–44, 1973.

Hindawi Publishing Corporation
Mathematical Problems in Engineering
Volume 2015, Article ID 892549, 9 pages
http://dx.doi.org/10.1155/2015/892549

Research Article

A Novel Model of Set Pair Analysis Coupled with Extenics for Evaluation of Surrounding Rock Stability

Mingwu Wang, Xinyu Xu, Jian Li, Juliang Jin, and Fengqiang Shen

School of Civil and Hydraulic Engineering, Hefei University of Technology, Hefei 230009, China

Correspondence should be addressed to Mingwu Wang; wanglab307@foxmail.com

Received 3 May 2015; Accepted 5 July 2015

Academic Editor: Jurgita Antucheviciene

The evaluation of surrounding rock stability is a complex problem involving numerous uncertainty factors. Here, based on set pair analysis (SPA) coupled with extenics, a novel model, considering incompatibility, certainty, and uncertainty of evaluation indicators, was presented to analyze the surrounding rock stability. In this model, extension set was first utilized to describe the actual problem of surrounding rock stability. Then, the connectional membership degree of the set pair was introduced to compare the measured values with classification standards from three aspects embracing identity, discrepancy, and contrary. Also, according to identity-discrepancy-contrary (IDC) analysis in the universe of the extension set, the connection numbers were proposed to specify the connectional membership degree of an evaluation indicator to each class. Combined with the weights of evaluation indicators, integrated connectional membership degrees were calculated to determine their classes of rock stability. Finally, a case study and comparison with variable fuzzy set method, triangular fuzzy number method, and basic quality (BQ) grading method were performed to confirm the validity and reliability of the proposed model. The results show that this model can effectively and quantitatively express the differences within a group, transformation of different groups, and uncertainty of complex indicators as a whole.

1. Introduction

Urbanization development and economic growth result in the rapid expansion of transport systems and hydropower and energy construction projects. To ensure the safety of large-scale construction projects and provide useful quantitative information, the rational classification of surrounding rock stability has become increasingly complex because more and more parameters have to be considered. At the same time, it is also a critical engineering question for the crisis management of hazards. Therefore, scholars and engineers pay much attention to this issue.

Rock mass classification schemes have been developing for over 140 years since Ritter tried to formalize an empirical approach to tunnel design in 1879 [1]. The first practicable method of rock load classification system was put forward by Terzaghi [2]. And stand-up time classification method proposed by Lauffer [3] contributed to the development and application of the New Austrian Tunneling method in soft or poor rock mass. To provide a quantitative estimate of rock mass quality from drill hole core, Deere et al. [4] introduced a rock quality designation (RQD) index method, but the influences of joint tightness, orientation, continuity, and infilling were neglected before. Then, some quantitative classification methods including rock structure rating (RSR) system [5], Q-system [6, 7], and rock mass rating (RMR) method [8–11], were proposed on the basis of case histories. All of these systems have limitations, but they are valuable tools if applied properly with care. Because of ease and versatility of use, RMR and Q system methods have been widely accepted at present. In addition, although other numerous organizations have suggested different guidelines for surrounding rock classification, there was little consistency among these guidelines, and they had not found a wide variety of practical applications. In China, basic quality (BQ) grading standard in engineering rock mass classification (GB 50218-94) [12] is often used to evaluate the surrounding rock stability. However, surrounding rock stability involves various uncertainties and other variable and fuzzy factors [13, 14]. With the increasing complexity of construction

environment, conventional methods may result in trouble in decision-making due to the uncertainty and changeable features of indicators. And these approaches cannot describe the relativity of the system assessment from the view of information utilization [15]. Thus, conventional methods have some inadequacies and cannot meet the needs of practical engineering. There is an urgent need for development and perfection on the surrounding rock stability rating which can take into account fuzzy variation, incompatibility, and uncertainty of evaluation indicators.

As mentioned above, previous classification schemes for rock mass only considered single type of uncertainty (e.g., fuzziness, variability). However, for problems in real rock engineering, the uncertainty of evaluation indicators shows incompatibility, complexity, and diversity, and they are often fused with each other. Various improved methods, such as the fuzzy sets method [16, 17], the fuzzy analytical hierarchy process [18], the distance discriminate analysis method [19, 20], the support vector machine method [21, 22], the automated rock classification system [23], and the cloud approach [24], have been proposed to overcome those problems. Overall, whereas considerable research has been performed to improve the techniques for analyzing the surrounding rock stability, rock quality evaluation is still not well resolved nowadays. Besides, those analytical methods are mainly dependent on indicators of single type of uncertainty. Conventional methods consider the degree that an object has certain nature as being unchangeable because they lay particular emphasis on the static status on the nature of objects. They are not characterized by addressing the issue of incompatibility and dynamic uncertainty. The true state of surrounding rock stability in specified conditions is changeable, and truthfulness or falseness of the classification may be different in degree. Thus, changes of the nature have to be taken into consideration in the quantitative analysis of the surrounding rock stability. Unfortunately, uncertainty and incompatibility of evaluation indicators cannot be well described by conventional methods. To develop a rational classification method for the engineering practice, uncertainty and incompatibility nature of evaluation indicators of surrounding rock stability should be deeply investigated.

The main objective of this work is to treat the evaluation of surrounding rock stability as a decision-making problem of uncertainty and incompatibility. A novel method using set pair analysis coupled with extenics is introduced to analyze the above issue. This method can effectively and quantitatively take account of certainty and uncertainty, compatibility and incompatibility of indicators as a whole, and make the evaluation results apply in practical engineering more accurately.

2. Theory and Methodology

The newly emerging methodologies of extenics and SPA show their advantages in dealing with contradictory and uncertainty problems [25–30]. They can provide a novel coupling method to know and analyze stability of surrounding rock from a new perspective.

2.1. Introduction of Extension Theory. In practice, things are solvable through the transformation between quality and quantity of the study objects. The Chinese famous ancient story "Cao Chong weighed the elephant" is just a good example. By transformation, Cao turned an elephant into stones and succeeded in weighing the elephant. However, the classic cantor set and fuzzy set both describe mainly static properties of matters and cannot take care of incompatible problems. The extenics proposed by Cai [25] helps people break away from the shackles of traditional fields and reflects the inherent relations of research objects with symbols.

In extenics, the objective world is a world of elements. Matter-element and extension set are basic concepts of extenics. Relation and transformation of quality and quantity can be considered together in the extension theory. Their definitions are illustrated as follows.

An ordered triple $R = (N, C, V)$ is a fundamental element to describe a matter and is called matter-element. In matter-element, R, N, and V stand for the name of an object and the measure N of the nature C, respectively. The extensibility of matter-element strongly provides a tool to solve contradictory problems and presents reversed and conjugate thinking modes [25–28].

Let $\mathbf{U}$ be a universe of discourse and let k be mapping of $\mathbf{U}$ to the real field; there is a real number $k(x_0) \in (-\infty, +\infty)$ corresponding to an element $x_0 \in \mathbf{U}$. Then, call $A = \{(x_0, y) \mid x_0 \in \mathbf{U}, y = k(x_0) \in (-\infty, +\infty)\}$ as an extension set on the discourse universe $\mathbf{U}$. Here, $y = k(x_0)$ is the dependent function of A, and $k(x_0)$ is the dependent degree of x_0 to A. The mathematical model of dependent function is written as follows:

$$k(x_0) = \frac{\rho(x_0, X_0)}{\rho(x_0, X) - \rho(x_0, X_0)}, \quad \rho(x_0, X_0) \neq \rho(x_0, X),$$
$$\rho(x_0, X_0) = \left| x_0 - \frac{m+n}{2} \right| - \frac{n-m}{2}, \tag{1}$$
$$\rho(x_0, X) = \left| x_0 - \frac{p+q}{2} \right| - \frac{q-p}{2},$$

where $\rho(x_0, X)$ and $\rho(x_0, X_0)$ are the extension distances between point x_0 and intervals X and X_0, respectively. m and n are limits of interval X_0. p and q are limits of interval X. $\rho(x_0, X) - \rho(x_0, X_0)$ denotes the place value of point x_0 about the nest of the interval composed of intervals X and X_0, which are used to describe the relation between x_0 and two intervals.

The positive field, zero, and negative field of an extension set are just right to express transformations between "yes" and "no" and depict quantitative and qualitative changes. Zero point is a criticality of "Both A and B." Suppose certain attribute of the study object is divided into K real intervals; the universe of extension set is presented as showed in Figure 1. In Figure 1, F_k is the limit of the class k ($k = 1, 2, \ldots, K$). The intervals $[F_k, F_{k+1})$ and $[F_1, F_{K+1}]$ denote the intervals X_0 and X, respectively.

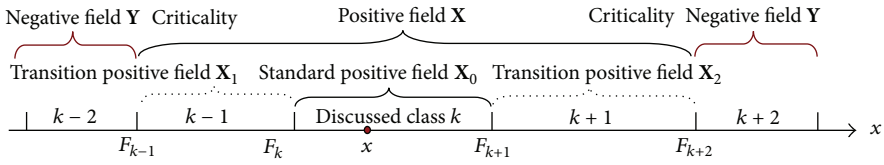

Figure 1: The universe of extension set.

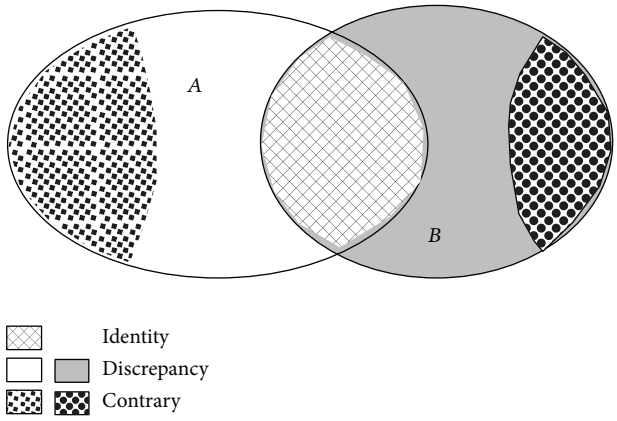

Figure 2: Sketch of identity, discrepancy, and contrary of set pair.

As mentioned above, extension distance achieves a quantitative description of the internal differences within a group or class. The extension set makes dynamic classification and recognition more suitable to people's thinking modes and actual situation. The extenics provides a new formalized and quantified tool for contradictory problems encountered in practice and enriches the uncertainty analysis theory.

2.2. Brief of SPA Theory. SPA theory is a novel analytical method for systematic problems of uncertainty [28–32]. Both the dialectical law of the unity of opposites in philosophy and principle of universal connection are given consideration to depict uncertainty problems. Set pair and connection number are pillars of the SPA theory. Connection number is used to express the interaction and transformation of attributes in multiple scales for a set pair consisting of two related sets. The fundamental procedure of a set pair analysis is to quantitatively express uncertainty problem from identity, discrepancy, and contrary aspects (Figure 2). And the definition of the connection number is given as follows.

Letting a set pair $H = (A, B)$ consisting of set A and set B, there are total attributes N, identical terms S, and contrary attributes P in the H, respectively. So residual attributes $F = N-S-P$ are discrepancy attributes. Uncertainty relation of the two sets can be represented by a connection number of three elements. The Equation of the connection number is written as follows:

$$\mu_{(A,B)} = \frac{S}{N} + \frac{F}{N}i + \frac{P}{N}j = a + bi + cj, \tag{2}$$

where $\mu_{(A,B)}$ is the connection number. a, b, and c are identity degree, discrepancy degree, and contrary degree, respectively, and $a + b + c = 1$. i is the discrepancy coefficient within $[-1, 1]$. j is the contrary coefficient and generally specified as -1. This analytical method is therefore of advantage for the representation of certainty and uncertainty in a unified way and can present transformation of discrepancy.

For problems of evaluation and risk analysis, much attention is usually paid to the relation between a point and a standard interval. The identity-discrepancy-contrary relationships of the discussed point relative to given interval are presented as showed in Figure 3. Namely, when the point x locates in the given standard set $[F_k, F_{k+1})$, it is considered as an identity relationship. Connection number is given as 1 when we do not take account of internal differences in a group. When x is in the separated interval, it is defined as a contrary relationship, and $\mu_{(A,B)} = -1$. When x is in the interval next to the given interval, the relationship is of uncertainty and called discrepancy, $\mu \in [-1, 1]$. However, the connection number in $[0, 1]$ sometimes may not describe the transformation of study objects [28–30]. Here, the connectional membership degree is introduced to expand the connection number in order to satisfy the laws of the unity of opposites and the transformation process of quality and quantity. The mathematical model is written as

$$\mu(x,k) = \begin{cases} -\left|\dfrac{x - F_k}{M_{k-1} - M_k}\right|, & F_{k-1} \le x < F_k \\ \dfrac{2(x - F_k)}{F_{k+1} - F_k}, & F_k \le x < \dfrac{F_k + F_{k+1}}{2} \\ \dfrac{2(F_{k+1} - x)}{F_{k+1} - M_k}, & \dfrac{F_k + F_{k+1}}{2} \le x < F_{k+1} \\ -\left|\dfrac{x - F_{k+1}}{F_{k+1} - F_{k+2}}\right|, & F_{k+1} \le x < F_{k+2} \\ -1, & \text{other,} \end{cases} \tag{3}$$

where $\mu(x, k)$ is a connectional membership degree and $\mu(x, k) \in [-1, 1]$. M_{k-1}, M_k, M_{k+1}, and M_{k+2} are limits of intervals, respectively.

The connection membership degree displays IDC relations in SPA, but it differs from the fuzzy membership degree. Its value is of wide range, which overcomes the defects of the traditional concept "all are the same within the class." Namely, it can point out differences in degree that point qualities for the given interval; meanwhile, even when points were found in the same group, reflect the difference and transformation of different intervals. It also describes the transformation of certainty and uncertainty. In general, the SPA can express the dynamic change of objects embodied in the certainty of "Either A or B" and uncertainty of "Both A and B."

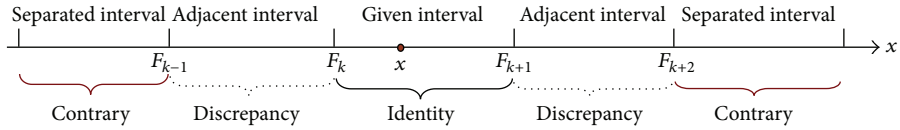

Figure 3: IDC relations between the point and intervals.

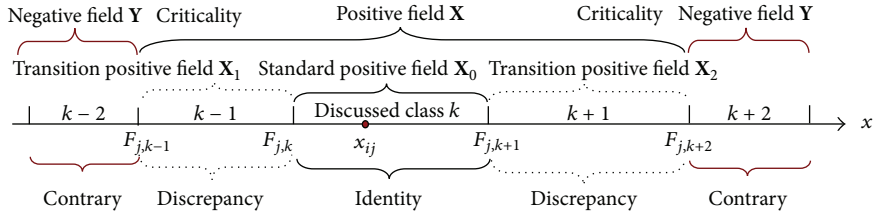

Figure 4: Relationship between the IDC of set pair and the universe of extension set.

2.3. Extension Set and IDC Analysis. As we all know, the analysis of cantor set, fuzzy set, and rough set always regards the attributes of objects as invariable from the static perspective. The traditional set theory is incapable of revealing the dialectical transformation from quantitative and qualitative aspects. Unfortunately, in fact, the membership to a certain attribute is changeable. As noted above, the dependent degree in the extension theory was introduced to quantify the change in quality and quantity of objects. Extenics provides a new way for microanalysis of set pair discrepancy. Hence, extenics and SPA are of advantage in depicting the development from "all are the same in the same group" to a quantitative differences in the same group. To couple SPA with extenics, corresponding theoretical basis will be further analyzed as below.

Uncertainty and certainty of interaction and transformation can be treated dialectically by IDC analysis as a whole in SPA. This demonstrates the close relation and similarity between the outlook on uncertainty transformation of extenics and that of SPA. Namely, the measured data may locate in positive field, zero, or negative field of an extension set, which is similar to IDC relationships in SPA. Figure 4 exhibits relationship between the IDC relationship of set pair and the universe of extension set.

Based on the SPA theory, when the measured point locates in the discussed standard positive field, it is defined as identity. And the discrepancy and contrary are defined when measured point locates in the transition positive field and negative field, respectively. To properly specify the discrepancy degree is the key point during the SPA. Unfortunately, up to date, this problem is still controversial. Herein, coupling SPA with extenics, it can make full use of extension transformation and calculation and provides a new idea to overcome the specification of discrepancy coefficient and attempts to establish a valid connection for the two uncertainty analytical theories.

3. Development of a Model of SPA Coupled with Extenics

3.1. Evaluation Procedures. The evaluation procedure with the model of SPA coupled with extenics is as follows.

First, identify evaluation indexes and classification standard, and establish matter-elements based on the measured values of samples.

Then, set up the corresponding set pairs, and conduct IDC analysis of extension universe between the evaluations of samples and standard sets.

Next, based on SPA analysis of extension universe, determine the function of connectional membership degree. Combine indicator weights to calculate evaluation samples' connectional membership degree to each class.

Finally, specify class of samples according to integrated value of connectional membership degree.

The concrete flowchart of the evaluation procedure is shown in Figure 5.

3.2. Development of Evaluation Model. Evaluation of surrounding rock stability is a complex system issue since it links to changes and interaction of evaluation indicators. Besides, evaluation indicators are of contradiction and coexistence of qualitative and quantitative changes and fuzzy characteristic [33]. Here, a new attempt is made to couple SPA and extenics with the aim of analyzing certainty and uncertainty, compatible and incompatible problems from an integral and unified perspective. Assuming $N_1, N_2, \ldots, N_k, \ldots, N_K$ ($k = 1, 2, \ldots, K$) is an evaluation class vector, C_j is jth ($j = 1, 2, \ldots, m$) nature and v_{ik} is the measure of C_i. Then the matter-element model for the class N_k is

$$R_k = \left(N_k, C_j, V_k\right) = \begin{bmatrix} N_k & C_1 & V_{1k} \\ & C_2 & V_{2k} \\ & \vdots & \vdots \\ & C_m & V_{mk} \end{bmatrix}, \tag{4}$$

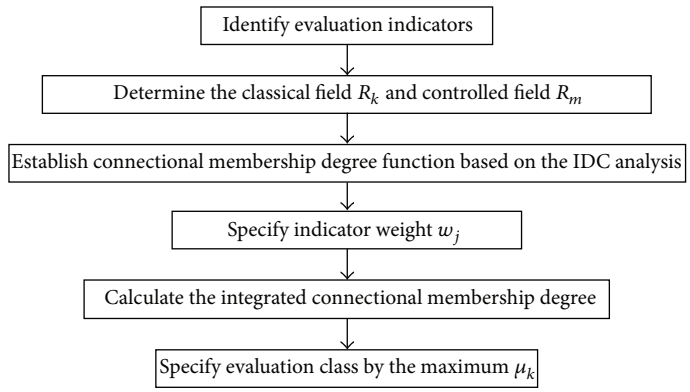

Figure 5: Evaluation flowchart based on the model of SPA coupled with extenics.

where $V_k = \langle a_{jk}, b_{jk} \rangle$ is the range of nature C_i for the evaluation class N_k. And the corresponding expression of matter-element model by means of the classical field and controlled field is depicted in formulas (5) and (6), respectively. Consider

$$R_K = \begin{bmatrix} N & N_1 & N_2 & \cdots & N_K \\ C & V_1 & V_2 & \cdots & V_K \end{bmatrix} = \begin{bmatrix} N & N_1 & N_2 & \cdots & N_K \\ C_1 & \langle a_{11}, b_{11} \rangle & \langle a_{12}, b_{12} \rangle & \cdots & \langle a_{1K}, b_{1K} \rangle \\ C_2 & \langle a_{21}, b_{21} \rangle & \langle a_{22}, b_{22} \rangle & \cdots & \langle a_{2K}, b_{2K} \rangle \\ \vdots & \vdots & \vdots & \ddots & \vdots \\ C_m & \langle a_{m1}, b_{m1} \rangle & \langle a_{m2}, b_{m2} \rangle & \cdots & \langle a_{mK}, b_{mK} \rangle \end{bmatrix}, \quad (5)$$

$$R_m = \begin{bmatrix} N & C_1 & V_{1d} \\ & C_2 & V_{2d} \\ & \vdots & \vdots \\ & C_m & V_{md} \end{bmatrix} = \begin{bmatrix} N & C_1 & \langle a_{1d}, b_{1d} \rangle \\ & C_2 & \langle a_{2d}, b_{2d} \rangle \\ & \vdots & \vdots \\ & C_m & \langle a_{md}, b_{md} \rangle \end{bmatrix}, \quad (6)$$

where N is the class and $\langle a_{1d}, b_{1d} \rangle$ is the total range of nature C_i under a certain condition.

Similarly, matter-element model R_P ($p = 1, 2, 3, \ldots, P$) of all evaluation samples is given as follows:

$$R_P = \begin{bmatrix} P & p_1 & p_2 & \cdots & p_P \\ C_1 & v_{11} & v_{12} & \cdots & v_{1P} \\ C_2 & v_{21} & v_{22} & \cdots & v_{2P} \\ \vdots & \vdots & \vdots & \ddots & \vdots \\ C_m & v_{m1} & v_{m2} & \cdots & v_{mP} \end{bmatrix}. \quad (7)$$

According to the above analysis, IDC relation can be applied to describe the universe of extension set. If the measured value x_{ij} is in the given interval of class k ($k = 1, 2, \ldots, K$), which consists of limits of indicator j, the relation between x_{ij} and k is called identity. And the discussed interval of class k is treated as a standard positive field of an extension set, $\mathbf{X}_0 = \langle F_{j,k}, F_{j,k-1} \rangle$; the corresponding computation model of connectional membership degree is

$$\mu_k(x_{ij}) = \begin{cases} \dfrac{2(F_{j,k+1} - x_{ij})}{F_{j,k+1} - F_{j,k}}, & x_{ij} \geq \dfrac{F_{j,k} + F_{j,k+1}}{2} \\ \dfrac{2(x_{ij} - F_{j,k})}{F_{j,k+1} - F_{j,k}}, & x_{ij} < \dfrac{F_{j,k} + F_{j,k+1}}{2}, \end{cases} \quad (8)$$

where $F_{j,k}$ and $F_{j,k+1}$ are limits of the class and $\mu_k(x_{ij})$ is the connectional membership degree of index j for sample i to the class k.

When index j locates in the class $k - 1$ ($k > 2$) or $k + 1$ and its value still belongs to transition positive field $\mathbf{X}_1 = \langle F_{j,k-1}, F_{j,k} \rangle$ or $\mathbf{X}_2 = \langle F_{j,k+1}, F_{j,k+2} \rangle$, it is defined as discrepancy. And connectional membership degree is calculated by formulas (9), (10), and (11). Consider

$$\mu_k(x_{ij}) = \begin{cases} \dfrac{\rho(x_{ij}, X_0)}{\rho(x_{ij}, X) - \rho(x_{ij}, X_0)} & \rho(x_{ij}, X_0) \neq \rho(x_{ij}, X) \\ -\rho(x_{ij}, X_0) & \rho(x_{ij}, X_0) = \rho(x_{ij}, X),\ x_{ij} \in X_0 \\ -1 & \rho(x_{ij}, X_0) = \rho(x_{ij}, X),\ x_{ij} \notin X_0,\ x_{ij} \in X \end{cases} \quad (9)$$

$$\rho\left(x_{ij}, X_0\right) = \left|x_{ij} - \frac{F_{j,k} + F_{j,k+1}}{2}\right| - \frac{F_{j,k+1} - F_{j,k}}{2} \tag{10}$$

$$\rho\left(x_{ij}, X\right) = \left|x_{ij} - \frac{F_{j,k-1} + F_{j,k+2}}{2}\right| - \frac{F_{j,k+2} - F_{j,k-1}}{2}, \tag{11}$$

where $F_{j,k-1}$ and $F_{j,k+2}$ are limits of the class. $\rho(x_{ij}, \mathbf{X})$ and $\rho(x_{ij}, \mathbf{X}_0)$ are the distances of x_{ij} (the measured value of the sample i for index j) to extension positive field and standard positive field, respectively. In formula (11), while $k = 1$ and $k = K$, get $F_{j,k-1} = F_{j,k}$ and $F_{j,k+2} = F_{j,K}$, respectively.

When index j is not in the extension set positive field $X = \langle F_{j,k-1}, F_{j,k+2}\rangle$ but in extension set negative field $\mathbf{Y}$ including the intervals of classes $k - 2$ and $k + 2$ ($k > 2$), this relation can be specified as contrary, and connectional membership degree is

$$\mu_k\left(x_{ij}\right) = -1. \tag{12}$$

Combining the evaluation index weights, the integrated connectional membership degrees can be calculated by the following formula:

$$\mu_k = \sum_{j=1}^{M} w_j \mu_k\left(x_{ij}\right), \tag{13}$$

where w_j are weights of indicators.

Finally, the class is determined by the maximum integrated connectional membership degree. The criteria can be given as

$$k = \max\left\{\mu_1, \mu_2, \ldots, \mu_m\right\}, \tag{14}$$

where k is the evaluated class.

4. Case Study

4.1. Evaluation Indicator System Identification of Surrounding Rock Stability. Classification of surrounding rock stability is substantially dependent on the indicator selection. Generally, the selection process of evaluation indicators is primarily from geological and engineering aspects including rock mass characteristics, underground water, the state of stress, and joint plane. Herein, based on the design codes in China, previous research, and literature reviews, we selected rock mass quality, uniaxial compressive strength, integrality degree of rock mass, groundwater percolation capacity, and joint as the evaluation indicators. Rock mass quality, uniaxial compressive strength, and integrality degree of rock mass all reflect rock mass characteristics. The joints condition reveals geological structure effect on rock mass stability, and groundwater percolation capacity indicates activity of underground water. Here, stability of surrounding rock is divided into five classes named as very good (I), good (II), fair (III), poor, (IV) and very poor (V) by the orders of stability from the highest to the lowest.

To confirm the reliability and the validity of this presented model, data of the references [16, 34] were used to conduct a case study. The classification standard and the indicator values measured from the samples are listed in Tables 1 and 2.

4.2. Model Validation and Discussion. According to Tables 1 and 2, the extension model of the surrounding rock stability and corresponding control field R_m can be written as

$$R_K = \begin{bmatrix} N & N_1 & N_2 & N_3 & N_4 & N_5 \\ C_1 & \langle 0, 0.10\rangle & \langle 0.10, 0.25\rangle & \langle 0.25, 0.40\rangle & \langle 0.40, 0.60\rangle & \langle 0.60, 1.00\rangle \\ C_2 & \langle 200, 300\rangle & \langle 100, 200\rangle & \langle 50, 100\rangle & \langle 25, 50\rangle & \langle 0, 25\rangle \\ C_3 & \langle 0.75, 1.00\rangle & \langle 0.55, 0.75\rangle & \langle 0.30, 0.55\rangle & \langle 0.15, 0.30\rangle & \langle 0.0, 0.15\rangle \\ C_4 & \langle 0, 5\rangle & \langle 5, 10\rangle & \langle 10, 25\rangle & \langle 25, 125\rangle & \langle 125, 250\rangle \\ C_5 & \langle 9, 10\rangle & \langle 7, 9\rangle & \langle 4, 7\rangle & \langle 2, 4\rangle & \langle 0, 2\rangle \end{bmatrix}, \tag{15}$$

$$R_m = \begin{bmatrix} N & C_1 & \langle 0, 1.00\rangle \\ & C_2 & \langle 0, 300\rangle \\ & C_3 & \langle 0, 1.00\rangle \\ & C_4 & \langle 0, 250\rangle \\ & C_5 & \langle 0, 10\rangle \end{bmatrix}. \tag{16}$$

Table 1: Classification standard to surrounding rock stability.

Stability class	Rock mass quality	Uniaxial compressive strength (MPa)	Integrality degree of rock mass	Groundwater percolation capacity (L/(min·10 m))	Joint
Very good I	0–0.10	200–300	0.75–1.00	0–5	9-10
Good II	0.10–0.25	100–200	0.55–0.75	5–10	7–9
Fair II	0.25–0.40	50–100	0.30–0.55	10–25	4–7
Poor IV	0.40–0.60	25–50	0.15–0.30	25–125	2–4
Very poor V	0.60–1.00	0–25	0–0.15	125–250	0–2

Table 2: Measured values of evaluation indicators.

Samples	Rock mass quality	Uniaxial compressive strength (MPa)	Integrality degree of rock mass	Groundwater percolation capacity (L/(min·10 m))	Joint
1	0.12	185.5	0.89	6	8
2	0.27	176.4	0.80	8	7
3	0.08	158.2	0.94	6	7
4	0.04	201.1	0.97	5	9
5	0.24	181.9	0.92	9	8

Table 3: Results of case study and comparison.

Samples	Integrated connectional membership degree					Proposed model	Basic quality grading method	Variable fuzzy set method [34]	Triangular fuzzy number method [16]
	μ_1	μ_2	μ_3	μ_4	μ_5				
1	−0.0844	0.3383	−0.7903	−1.0000	−1.0000	II	II	II	II
2	−0.5669	0.1899	−0.5298	−0.9679	−1.0000	II	II	II	II
3	−0.1752	0.0859	−0.8778	−1.0000	−1.0000	II	II	II	II
4	0.2320	−0.2744	−1.0000	−1.0000	−1.0000	I	I	I	I
5	−0.4351	0.3030	−0.4721	−1.0000	−1.0000	II	II	II	II

And the evaluated matter-element model R_P will be

$$R_P = \begin{bmatrix} P & p_1 & p_2 & p_3 & p_4 & p_5 \\ C_1 & 0.12 & 0.27 & 0.08 & 0.04 & 0.24 \\ C_2 & 185.5 & 176.4 & 158.2 & 201.1 & 181.9 \\ C_3 & 0.89 & 0.80 & 0.94 & 0.97 & 0.92 \\ C_4 & 6 & 8 & 6 & 5 & 9 \\ C_5 & 8 & 7 & 7 & 9 & 8 \end{bmatrix}. \quad (17)$$

The weights of the indexes were from the literature [34]. The discussed coupling method was utilized to conduct classification of surrounding rock stability. Results of the evaluation samples were listed in Table 3. The results evaluated from triangular fuzzy number method [16], basic quality method, and variable fuzzy set method [34] were also taken to confirm the validity and reliability of the proposed method.

It was found from Table 3 that the results determined were in a good agreement with the original data assessed by the BQ grading standards and other methods. It suggests that this proposed model presents the validity in surrounding rock stability evaluation, reveals uncertainty during the evaluation process, and lessens judgmental bias. This method may offer a more quantitative measure of surrounding rock stability because it can depict the degree that an object has certain nature and the change of truthfulness or falseness of position.

5. Conclusions

The classification of rock mass stability is often used in rock engineering and design; meanwhile, the surrounding rock instabilities are major hazards for human activities, causing injuries or fatalities, property damage, and maintenance costs. So it has received wide attention from engineers and scholars. However, previous studies of surrounding rock stability on position and reasoning are performed from a static perspective. It is obvious that those methods cannot depict the changeable and uncertainty features of various overlapping variable and uncertainty factors. This work

presents a novel method of SPA coupled with extenics to analyze surrounding rock stability. Some conclusions are drawn as follows.

(1) The results show that this novel method is reliable and acceptable for evaluating the surrounding rock stability and convenient for practical applications. This proposed model may be an alternative effective method for the classification of other problems.

(2) The idea of connectional membership degree brings to light transformation among classes and differences in degree within the class from the transformational perspective and overcomes the drawback of fixed nature expressed by conventional methods. It can be viewed as concise and quantitative expressions of certainty and uncertainty of surrounding rock stability in a unified way.

(3) This coupling method provides a new idea to specify discrepancy coefficient for SPA and sets up a valid bridge connecting the two uncertainty analytical theories, SPA and extenics. And it enables us to express variability of surrounding rock stability due to uncertainty or incompatibility of evaluation indicators.

(4) Although our examination method has provided a useful basis for introducing dynamic uncertainty analysis from three aspects embracing identity, discrepancy, and contrary, into surrounding rock stability, the effects of other evaluation indicators on the prediction are required to clarify in future, and applications in practice will still involve a considerable amount of work both in the laboratory and in the field.

Conflict of Interests

The authors declare that there is no conflict of interests regarding the publication of this paper.

Acknowledgments

Financial support provided by the National Natural Sciences Foundation, China (nos. 41172274 and 71273081) is gratefully acknowledged. The authors would also like to express their sincere thanks to the reviewers for their thorough reviews and useful suggestions.

References

[1] Z. T. Bieniawski, *Engineering Rock Mass Classifications*, John Wiley & Sons, New York, NY, USA, 1989.

[2] K. Terzaghi, "Rock defects and loads on tunnel supports," in *Rock Tunneling with Steel Supports*, vol. 1, pp. 17–99, Commercial Shearing and Stamping Company, Youngstown, Ohio, USA, 1946.

[3] H. Lauffer, "Gebirgsklassifizierung für den Stollenbau," *Geologie und Bauwesen*, vol. 24, no. 1, pp. 46–51, 1958.

[4] D. U. Deere, A. J. Hendron, F. D. Patton, and E. J. Cording, "Design of surface and near-surface construction in rock," in *Proceedings of the 8th US Symposium on Rock Mechanics (USRMS '66)*, pp. 237–302, Society for Mining Engineers/American Institute Mining, Metallurgical and Petroleum Engineers, Minneapolis, Minn, USA, September 1966.

[5] G. E. Wickham, H. Tiedemann, and E. H. Skinner, "Support determination based on geologic predictions," in *Proceedings of the 1st North American Rapid Excavation Tunneling Conference*, pp. 43–64, AIME, New York, NY, USA, 1972.

[6] N. R. Barton, R. Lien, and J. Lunde, "Engineering classification of rock masses for the design of tunnel support," *Rock Mechanics*, vol. 6, no. 4, pp. 189–236, 1974.

[7] A. Palmstrom and E. Broch, "Use and misuse of rock mass classification systems with particular reference to the Q-system," *Tunnelling and Underground Space Technology*, vol. 21, no. 6, pp. 575–593, 2006.

[8] Z. T. Bieniawski, "Engineering classification of jointed rock masses," *Transactions of the South African Institution of Civil Engineers*, vol. 15, pp. 335–344, 1973.

[9] Z. Şen and B. H. Bahaaeldin, "Modified rock mass classification system by continuous rating," *Engineering Geology*, vol. 67, no. 3-4, pp. 269–280, 2003.

[10] L. Pantelidis, "Rock slope stability assessment through rock mass classification systems," *International Journal of Rock Mechanics and Mining Sciences*, vol. 46, no. 2, pp. 315–325, 2009.

[11] Z.-X. Liu and W.-G. Dang, "Rock quality classification and stability evaluation of undersea deposit based on M-IRMR," *Tunnelling and Underground Space Technology*, vol. 40, pp. 95–101, 2014.

[12] The National Standards Compilation Group of People's Republic of China, *GB/T50218-2014, Standard for Engineering Classification of Rock Masses*, China Planning Press, Beijing, China, 2015 (Chinese).

[13] S. Y. Choi and H. D. Park, "Comparison among different criteria of RMR and Q-system for rock mass classification for tunnelling in Korea," *Tunnelling and Underground Space Technology*, vol. 17, no. 4, pp. 391–401, 2002.

[14] Z. Şen, "Rock quality designation-fracture intensity index method for geomechanical classification," *Arabian Journal of Geosciences*, vol. 7, no. 7, pp. 2915–2922, 2014.

[15] T. Ramamurthy, "A geo-engineering classification for rocks and rock masses," *International Journal of Rock Mechanics and Mining Sciences*, vol. 41, no. 1, pp. 89–101, 2004.

[16] M.-W. Wang, G.-Y. Chen, and J.-L. Jin, "Risk evaluation of surrounding rock stability based on stochastic simulation of multi-element connection number and triangular fuzzy numbers," *Chinese Journal of Geotechnical Engineering*, vol. 33, no. 4, pp. 643–647, 2011.

[17] A. Aydin, "Fuzzy set approaches to classification of rock masses," *Engineering Geology*, vol. 74, no. 3-4, pp. 227–245, 2004.

[18] Y.-C. Liu and C.-S. Chen, "A new approach for application of rock mass classification on rock slope stability assessment," *Engineering Geology*, vol. 89, no. 1-2, pp. 129–143, 2007.

[19] F. Q. Gong and X. B. Li, "Application of distance discriminant analysis method to classification of engineering quality of rock masses," *Chinese Journal of Rock Mechanics and Engineering*, vol. 26, no. 1, pp. 190–194, 2007 (Chinese).

[20] W. Zhang, X.-B. Li, and F.-Q. Gong, "Stability classification model of mine-lane surrounding rock based on distance discriminant analysis method," *Journal of Central South University of Technology*, vol. 15, no. 1, pp. 117–120, 2008.

[21] A.-N. Jiang and X.-T. Feng, "Case-based SVM method for maximal deformation forecasting of surrounding rocks of tunnels," *Journal of Northeastern University (Natural Science)*, vol. 25, no. 8, pp. 793–795, 2004 (Chinese).

[22] D. Qiu, S. Li, L. Zhang, and Y. Xue, "Application of GA-SVM in classification of surrounding rock based on model reliability examination," *Mining Science and Technology*, vol. 20, no. 3, pp. 428–433, 2010 (Chinese).

[23] R. Huang, J. Huang, N. Ju, and Y. Li, "Automated tunnel rock classification using rock engineering systems," *Engineering Geology*, vol. 156, pp. 20–27, 2013.

[24] J. Li, M.-W. Wang, P. Xu, and P.-C. Xu, "Classification of stability of surrounding rock using cloud model," *Chinese Journal of Geotechnical Engineering*, vol. 36, no. 1, pp. 83–87, 2014 (Chinese).

[25] W. Cai, *The Matter-Element Model and Its Application*, Science and Technology Literature Publishing House, Beijing, China, 1994 (Chinese).

[26] W. Cai, "Extension theory and its application," *Chinese Science Bulletin*, vol. 44, no. 17, pp. 1538–1548, 1999.

[27] W. Cai, C. Y. Yang, and W. C. Lin, *The Extension Engineering Method*, Science and Technology Press, Beijing, China, 1997 (Chinese).

[28] K. Q. Zhao, *Set Pair Analysis and Its Preliminary Application*, Zhejiang Science and Technology Press, Hangzhou, China, 2000 (Chinese).

[29] W.-S. Wang, J. L. Jin, J. Ding, and Y. Q. Li, "A new approach to water resources system assessment—set pair analysis method," *Science in China Series E: Technological Sciences*, vol. 52, no. 10, pp. 3017–3023, 2009.

[30] M. W. Wang, J. L. Jin, and Y. L. Zhou, *Set Pair Analysis Based Coupling Methods and Applications*, Science Press, Beijing, China, 2014 (Chinese).

[31] M. Wang and G. Chen, "A novel coupling model for risk analysis of swell and shrinkage of expansive soils," *Computers and Mathematics with Applications*, vol. 62, no. 7, pp. 2854–2861, 2011.

[32] M.-W. Wang, P. Xu, J. Li, and K.-Y. Zhao, "A novel set pair analysis method based on variable weights for liquefaction evaluation," *Natural Hazards*, vol. 70, no. 2, pp. 1527–1534, 2014.

[33] M.-W. Wang, J.-L. Jin, and L. Li, "Application of extension method to the evaluation of the grade of shrinkage and expansion for the expansive soil," *Chinese Journal of Geotechnical Engineering*, vol. 25, no. 6, pp. 754–757, 2003 (Chinese).

[34] S. Chen and X. Han, "Engineering method of variable fuzzy set for assessment of surrounding rock stability," *Chinese Journal of Rock Mechanics and Engineering*, vol. 25, no. 9, pp. 1857–1861, 2006 (Chinese).

Hindawi Publishing Corporation
Mathematical Problems in Engineering
Volume 2015, Article ID 980619, 8 pages
http://dx.doi.org/10.1155/2015/980619

Research Article

Predicted Thermal Sensation Index for the Hot Environment in the Spinning Workshop

Rui-Liang Yang,[1] Lei Liu,[2] and Yi-De Zhou[2]

[1]*School of Mechanical Engineering, Tianjin Polytechnic University, Tianjin 300387, China*
[2]*School of Energy and Environment, Zhongyuan University of Technology, Zhengzhou 450007, China*

Correspondence should be addressed to Rui-Liang Yang; yangruiliang2001@sina.com

Received 17 March 2015; Revised 15 June 2015; Accepted 16 June 2015

Academic Editor: Jurgita Antucheviciene

The spinning workshop is the most typical cotton textile workshop in the textile mill and is characterized by the feature of high temperature all the year. To effectively evaluate the general thermal sensation of the textile worker exposed to the hot environment in the spinning workshop, a new heat index named predicted thermal sensation (PTS) index was proposed in this paper. The PTS index based on the heat balance equation can be derived by the empirical equations of air temperature and heat imbalance. A one-month-long continuous research was carried out to investigate the actual thermal condition and judge the validity of the PTS index. Actual workshop temperatures in the spinning workshop during the measuring period were all above 32°C, belonging to extreme hot environment. The calculated thermal sensation by the PTS index is very close to the actual thermal sensation, which means that the PTS index can accurately estimate the actual thermal sensation of the textile workers exposed to the hot environment in the spinning workshop. Compared to other indices, the PTS index can more effectively predict the mean thermal response of a large group of textile workers exposed to the hot environment in the spinning workshop.

1. Introduction

The spinning workshop is the most typical cotton textile workshop in the textile mill and is characterized by the feature of high temperature all the year. According to Chinese national standard "code for design of cotton spinning and weaving factory" (GB 50481-2009) [1], summer temperature of the spinning workshop should range from 30°C to 32°C, much exceeding the acceptable operative temperature range from 23°C to 26°C by ISO 7730 [2]. In fact, the temperature of the spinning workshop may often be higher than 32°C, especially in the summer. Obviously, higher temperature of the spinning workshop can decrease energy consumption and capitalized cost but results in deteriorating working conditions and poor thermal comfort. Furthermore, working in the spinning workshop with high temperature has physiological and psychological effects on workers: it reduces their productivity and increases their irritability and loss of their enthusiasm for their work [3].

Evidence about risks in a hot environment and the related health consequences have increased dramatically in the past few decades [4]. Extreme hot environment, in which the temperature is above 35°C for living and above 32°C for working [5], is prevalent in the spinning workshop. Several methods have been proposed to estimate the heat stress in an extreme hot environment. The wet-bulb globe temperature (WBGT) index [6], predicted heat strain (PHS) model [7], and the predicted mean vote (PMV) index [8] are standard methods and remain the choice by most researchers. The WBGT index is a composite temperature used to estimate the effect of temperature, humidity, and solar radiation on humans, which is regarded as the most accepted index representing the heat stress to which an individual is exposed in an industrial environment [9]. But the WGBT index should be regarded as an exploratory method, with the drawback of being longer and more difficult to undertake [6]. The most serious limitation of the WBGT index is that environments at a given level of the index are more stressful when the evaporation of sweat is restricted (by high humidity, such as the spinning workshop) than when evaporation is free [10]. Thus, it is encouraged immediately to define a new index or method instead of the WGBT index to be used

in an industrial environment [6]. The PHS model evaluates the thermal stress in the hot climate and determinates the maximum allowable exposure time (such as Dlimtre index) with which the physiological strain is acceptable. The PHS model only considers standard subjects in good health and fit for the work they perform; it is therefore intended to be used to evaluate working conditions, and it does not predict the physiological response of individual subjects [7]. Although PHS can evaluate the exposure limit for various situations, it has a limitation when considering the cases in which humans exercise moderately [11] such as the work in the spinning workshop. The PMV index based on the heat balance of the human body can be used to predict the general thermal sensation and degree of discomfort of people exposed to moderate thermal environments, and it should be used only for values of PMV between −2 and +2 and when the main parameters are within the specified range, such as air temperature between 10°C and 30°C [2]. Except for three standard methods, there are a number of indices that have been proposed to measure the heat stress in the hot environment, such as the equivalent temperature (ET) index [12], the temperature-humidity index (THI) [13], and the environmental stress index (ESI) [14]. But these indices are mostly constructed based on several simple environmental variables, not including the personal variables and comprehensive environmental information, which makes these indices unreliable and ambiguous in the special environment such as the spinning workshop. Furthermore, most indices except the PMV index [2, 8] are used to evaluate the thermal condition in the hot environment instead of predicting the physiological response of individual subjects.

The textile industry plays an irreplaceable role in the Chinese economy [15] and poor workshop environment in the spinning workshop is particularly important to the health of workers [16], but there is no appropriate index used to predict the general thermal sensation of the textile worker nowadays. To effectively evaluate the general thermal sensation of the textile worker exposed to the hot environment in the spinning workshop, a heat index named predicted thermal sensation (PTS) index was proposed in this paper. The PTS index, an objective index based on the heat balance equation, can effectively predict the mean thermal response of a large group of textile workers exposed to the hot environment in the spinning workshop.

2. Model

The thermal balance equation of the body may be written as [17]

$$M - W = (C + R + E_{sk}) + (C_{res} + E_{res}) + S. \quad (1)$$

The sensible heat loss from skin ($C + R$), describing the heat exchanges between the clothing and the environment, is estimated by [7]

$$C + R = f_{cl} \times \left[h_{cdyn} \times (t_{cl} - t_a) + 3.96 \times 10^{-8} \times (t_{cl} + 273)^4 - (t_r + 273)^4\right], \quad (2)$$

where the clothing area factor f_{cl} may be estimated from the following equation [18]:

$$f_{cl} = 1 + 0.28 I_{cl}. \quad (3)$$

The dynamic convective heat exchange h_{cdyn} can be estimated as [7]

$$h_{cdyn} = \max\left\{2.38\left|t_{sk} - t_o\right|^{0.25}, 3.5 + 5.2 v_a, 8.7 {v_a}^{0.6}\right\}. \quad (4)$$

The sensible heat loss from skin ($C + R$), also describing the heat exchanges between the skin and the clothing surface, is estimated by [7]

$$C + R = \frac{t_{sk} - t_{cl}}{I_{cldyn}}, \quad (5)$$

where dynamic clothing insulation, I_{cldyn}, can be derived as [7]

$$I_{cldyn} = I_{totdyn} - \frac{I_{adyn}}{f_{cl}}, \quad (6)$$

where

$$I_{totdyn} = C_{orr,tot} \times \left(I_{cl} + \frac{I_{ast}}{f_{cl}}\right), \qquad I_{adyn} = C_{orr,Ia} \times I_{ast}. \quad (7)$$

For $I_{cl} \geq 0.6$ clo,

$$C_{orr,tot} = C_{orr,cl} = e^{0.043 - 0.398 v_a + 0.066 {v_a}^2 - 0.378 v_w + 0.094 {v_w}^2}. \quad (8)$$

For nude person ($I_{cl} = 0$ clo),

$$C_{orr,tot} = C_{orr,Ia} = e^{-0.472 v_a + 0.047 {v_a}^2 - 0.342 v_w + 0.117 {v_w}^2}. \quad (9)$$

For $0 \leq I_{cl} \leq 0.6$ clo,

$$C_{orr,tot} = \frac{(0.6 - I_{cl})\, C_{orr,Ia} + I_{cl} \times C_{orr,cl}}{0.6} \quad (10)$$

with $C_{orr,tot}$ limited to 1, v_a limited to 3 m/s, and v_w limited to 1.5 m/s. I_{ast} is the static boundary layer thermal insulation (= 0.7 clo) [18].

In the hot environment, the worker's body finally reaches steady state [7, 11] and the steady state mean skin temperature t_{sk} can be estimated as a function of the parameters of the working situation, using the following empirical expressions [7]:

$$t_{sk} = \begin{cases} t_{sk,nu} & \text{for } I_{cl} \le 0.2\,\text{clo} \\ t_{sk,cl} & \text{for } I_{cl} \ge 0.6\,\text{clo} \\ t_{sk,nu} + 2.5 \times (t_{sk,cl} - t_{sk,nu}) \times (I_{cl} - 0.2) & \text{for } 0.2\,\text{clo} < I_{cl} < 0.6\,\text{clo}, \end{cases} \tag{11}$$

$$t_{sk,nu} = 7.19 + 0.064t_a + 0.061t_r - 0.348v_a + 0.198p_a + 0.616t_{co},$$

$$t_{sk,cl} = 12.17 + 0.020t_a + 0.044t_r - 0.253v_a + 0.194p_a + 0.005346M + 0.51274t_{co}.$$

The actual evaporation rate E_{sk} is given by [19]

$$E_{sk} = \begin{cases} \lambda S_r & \dfrac{\lambda S_r}{E_{max}} < 0.46 \\ \lambda S_r \exp\left[-0.4127 \times \left(\dfrac{1.8\lambda S_r}{E_{max}} - 0.46\right)^{1.168}\right] & 0.46 \le \dfrac{\lambda S_r}{E_{max}} \le 1.7 \\ E_{max} & \dfrac{\lambda S_r}{E_{max}} > 1.7, \end{cases} \tag{12}$$

where λ is the latent heat of evaporation of sweat = 657 W·hr/kg at 30°C. Sweat rate S_r is a function of the thermoregulatory signal and can be adequately described by [19]

$$S_r = 0.42 + 0.44 \tanh\left[1.16 \times (0.1t_{sk} + 0.9t_{co} - 37.4)\right]. \tag{13}$$

The maximum evaporative heat flow at the surface is given by [7]

$$E_{max} = \frac{0.38 \times (p_{sk} - p_a) \times \left(2.6{C_{orr,tot}}^2 - 6.5C_{orr,tot} + 4.9\right)}{16.7 \times C_{orr,tot} \times (I_{cl} + I_{ast}/f_{cl})}. \tag{14}$$

The saturated water vapor pressure at skin temperature p_{sk} can be estimated as a function of the skin temperature t_{sk}.

The heat transfer from the deep body core to the skin H can be expressed as [19]

$$H = \{84 + 72 \times \tanh\left[1.3 \times (0.1t_{sk} + 0.9t_{co} - 37.9)\right]\} \times (t_{co} - t_{sk}). \tag{15}$$

For a heat balance in the body, heat flow core to skin equals heat flow skin to environment:

$$H = E_{sk} + C + R. \tag{16}$$

If t_a, t_r, p_a, M, v_a, v_w, and I_{cl} are known, all terms in Expressions (2)~(16) including H and t_{co} can be solved iteratively by Expressions (2)~(16).

The heat flow by respiratory convective C_{res} can be estimated by the following empirical expression [7]:

$$C_{res} = 0.00152M\left(28.56 + 0.885t_a + 0.641p_a\right). \tag{17}$$

The heat flow by respiratory evaporative E_{res} can be estimated by the following empirical expression [7]:

$$E_{res} = 0.00127M\left(59.34 + 0.53t_a - 11.63p_a\right). \tag{18}$$

Taking Expressions (5), (12), (17), and (18) into Expression (1) yields

$$S = M - W - \left(C + R + E_{sk}\right) - \left(C_{res} + E_{res}\right). \tag{19}$$

The heat storage S is solved as the difference between internal heat production and heat loss to the actual environment at the steady state in the hot environment for a person hypothetically kept at the empirical equations of t_{sk}, S_r, and H. In most industrial situations including the spinning workshop, the effective mechanical power W is small and can be neglected [7]. To more effectively predict the mean thermal response of a large group of textile workers exposed to the hot environment in the spinning workshop, the relationship of heat storage S and TSV value was researched by linear analysis based on a large number of previous experiments. Then, a new heat index named predicted thermal sensation (PTS) index was proposed as follows:

$$\text{PTS} = \left(0.0025t_a - 0.0657\right) \times \left[M - \left(C + R + E_{sk}\right) - \left(C_{res} + E_{res}\right)\right]. \tag{20}$$

The PTS index was derived by the empirical equations of air temperature and heat imbalance between internal heat production and heat loss to the actual environment at the steady state in the hot environment. Similarly to the PMV index, the PTS index can predict the mean thermal sensation of a large group of people on the seven-point thermal sensation scale. The difference is that the PTS index was proposed to be used in the hot environment in the spinning

Table 1: Anthropometric data of subjects.

Gender	Number	Seniority (years)	Height (cm)	Weight (kg)
Male	310	20.3 ± 8.9[a]	171.2 ± 7.2	71.1 ± 7.5
Female	513	18.1 ± 8.6	160.1 ± 6.2	60.6 ± 7.6
Total	823	19.0 ± 8.8	164.3 ± 8.5	64.5 ± 9.1

[a]Standard deviation.

workshop, but the PMV index cannot be used to the hot environment in the spinning workshop due to temperature above 30°C.

3. Experiment

To investigate the actual thermal condition in the spinning workshop and judge the validity of the PTS index, a one-month-long continuous research was carried out in the spinning workshop of Zhengzhou Hongye Textile Co. Ltd., one of the largest cotton companies in Henan Province (the central part of China, the most populous province with over 103 million people). Experiments were conducted from July 1 to July 31 of 2014 in the spinning workshop with area of 4985 m^2. The selected workers with years of work experience (see Table 1) were the most typical representative of Chinese textile workers. All investigated subjects recommended by the workshop director have more than 2-year work experience and were responsible for their work, which ensures that the investigated subjects fully adapt to the thermal environment of the spinning workshop. Front-line workers with 2/3 of dayshifts and 1/3 of nightshifts were chosen in the survey. Atypical workers such as those with less cohesive strength or bad work were excluded from this survey to ensure that participators are typical representative. Participating workers were investigated near their workstations during the experimental process. 823 sets of data were collected in this experiment, with about 20 to 40 sets of data in one day.

The PTS index was deduced by four physical variables (temperature t_a, air velocity v_a, mean radiant temperature t_r, and relative humidity RH) and three personal variables (clothing insulation I_{cl}, activity level M, and walking speed v_w). Temperature (±0.5°C for 0~400°C), relative humidity (±3 for 10% ~95%), air velocity (±0.02 m/s for 0~0.99 m/s, ±3% F.S for 1~5 m/s), and globe temperature (±1°C for 0~80°C) were measured by using the laboratory-grade instruments. Mean radiant temperature was calculated by temperature, air velocity, and global temperature according to ISO 7726 [20]. Measurements for workers were made in workstations where workers were known to spend their time [8]. The measuring positions were selected to be close to the participant within a distance of 0.2 m and at three heights (0.1 m, 1.1 m, and 1.7 m). Clothing values adopted garment insulation values from ISO 9920 [18]. A time-average metabolic rate [2, 8] for the worker with activities was used since the worker's activity consists of a combination of work/investigation periods. Worker's miscellaneous occupational activities should be classified as "light machine work," while investigation activities should be classified as "standing, relaxed." Thus, every worker who typically spent 50 minutes out of each hour "light machine work" with metabolic rate of 128 W/m^2 and 10 minutes "standing, relaxed" with metabolic rate of 70 W/m^2 had an average metabolic rate of $128 \times 50/60 + 70 \times 10/60 = 118\ W/m^2$. p_a was estimated by the air temperature t_a and relative humidity RH. Due to the work characteristics of the investigated workers, the walking speed is supposed to be 0.5 m/s. Once four physical variables and three personal variables were determined, the PTS index can be calculated by Expression (20).

Analogously, the PHS model can be solved by four physical variables (temperature t_a, air velocity v_a, mean radiant temperature t_r, and relative humidity RH) and five personal variables (clothing insulation I_{cl}, activity level M, walking speed v_w, weight, and height) [7]. The PMV index can be obtained by temperature t_a, air velocity v_a, mean radiant temperature t_r, relative humidity RH, clothing insulation I_{cl}, and activity level M [2, 8]. The WGBT index can be estimated by temperature t_a, globe temperature t_g, and relative humidity RH [6]. Because the spinning workshop belongs to indoor hot and humid environments, solar radiation term in the ESI index can be neglected [12]. Equivalent temperature (ET) [12], the temperature-humidity index (THI) [13], and the environmental stress index (ESI) [14] were all obtained by the temperature t_a and relative humidity RH. The Actual Mean Vote (AMV) was obtained by thermal sensation vote recorded on the ASHRAE seven-point scale [8] during the survey.

4. Results and Discussion

4.1. Outdoor and Workshop Temperature during the Measuring Period. To investigate actual air temperature in the spinning workshop, a one-month-long continuous monitoring was carried out by using the laboratory-grade instruments, with eight o'clock in the morning and two o'clock in the afternoon, from July 1 to July 31 of 2014, and five measured points were distributed evenly in the spinning workshop. The average temperature of five measured points was used as the workshop temperature. The outdoor temperature was obtained from local meteorological records.

Figure 1 shows the outdoor temperature and workshop temperature during the measuring period (i.e., from July 1 to July 31, 2014), respectively. It can be found from Figure 1 that the workshop temperatures were all above 32°C, exceeding the acceptable operative temperature range from 23°C to 26°C by ISO 7730 [5], required temperature range from 30°C to 32°C by GB 50481-2009, and upper limit 30°C of PMV application range. Thus, the workshop environment in the spinning workshop during the measuring period belongs to extreme hot environment [5]. Due to the risks in hot environment and related health consequences, it is necessary to present an objective evaluation instead of subjective evaluation of thermal sensation for the textile worker exposed to the hot environment in the spinning workshop. The PTS index was an appropriate index to predict the thermal sensation for the textile work, which is helpful

Table 2: Measured parameters around the textile worker.

Gender	Male ($n = 310$)	Female ($n = 513$)	Total ($n = 823$)
Temperature t_a (°C)	33.9 ± 1.0[a]	34.1 ± 1.0	34.0 ± 1.0
Air velocity v_a (m/s)	0.42 ± 0.23	0.42 ± 0.22	0.42 ± 0.22
Mean radiant temperature t_r (°C)	34.0 ± 1.7	34.0 ± 1.8	34.0 ± 1.8
Relative humidity RH (%)	59.2 ± 7.6	60.1 ± 7.7	59.8 ± 7.7
Clothing insulation I_{cl} (clo)	0.47 ± 0.03	0.47 ± 0.02	0.47 ± 0.03

[a]Standard deviation.

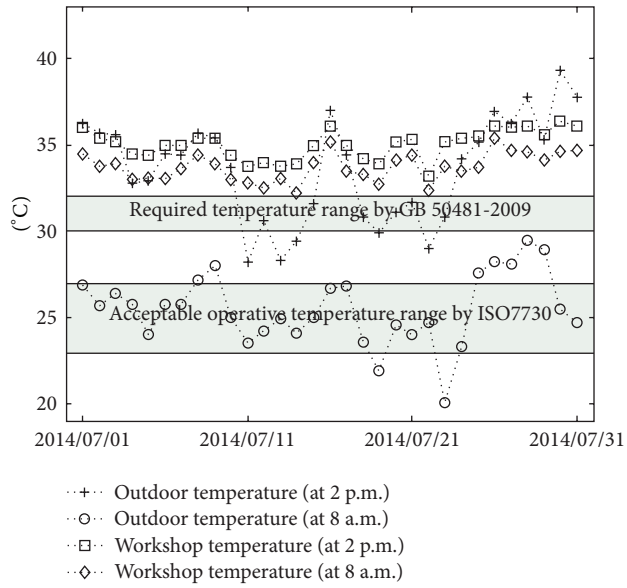

Figure 1: Outdoor temperature and mean workshop temperature during the measuring period.

for taking effective strategies to prevent the health risk to the worker.

4.2. Comparison of the PTS and the Actual Thermal Sensation. Table 2 shows the measured parameters around the textile worker during the measuring period, which were used to derive the PTS index. Figure 2 shows the actual thermal sensation (AMV) against the PTS index. The PTS value was obtained by Expression (20), representing the calculated thermal sensation of the worker, while the AMV value was obtained by thermal sensation vote record during the survey, representing the actual thermal sensation of the worker. Most of the AMV values were 1 (denoting "slightly warm") and 2 (denoting "warm"). In Figure 2 a trend line is shown with the corresponding R^2 value ($n = 823$, $p < 0.001$), representing AMV changes with PTS. The dotted line in Figure 2 shows PTS = AMV, so ideally all values would be on this line. The reality is that calculated thermal sensation is very close to the actual thermal sensation.

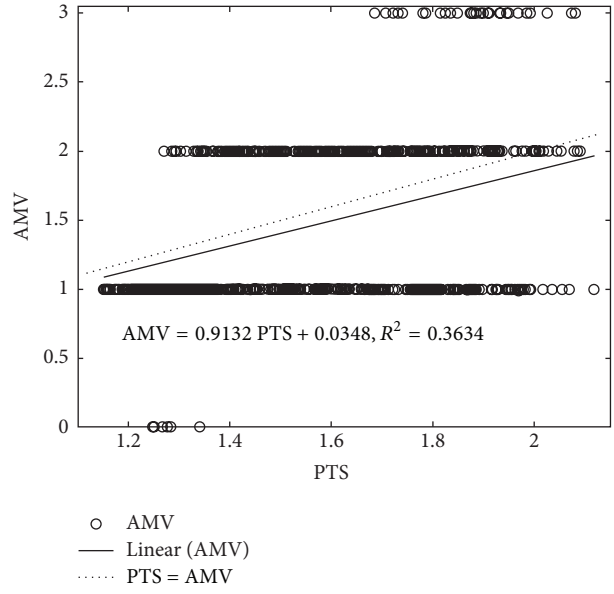

Figure 2: AMV versus PTS.

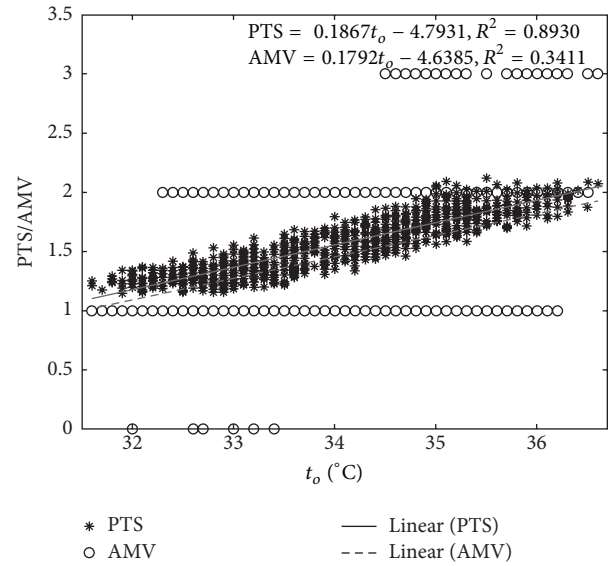

Figure 3: PTS/AMV versus operative temperature t_o.

Figure 3 shows the PTS/AMV against the operative temperature t_o. The operative temperature t_o is the common temperature in the thermal research field and can be solved by the temperature t_a, air velocity v_a, and mean radiant temperature t_r [2, 8]. There are two trend lines with corresponding R^2 value in Figure 3, representing PTS/AMV changes with the operative temperature t_o. Two trend lines ($n = 823$, $p < 0.001$) are very close, which means that calculated thermal sensation is very close to the actual thermal sensation. The fact that the PTS index is very close to the actual thermal sensation means that the PTS index can accurately estimate the actual thermal sensation of the textile workers in the spinning workshop.

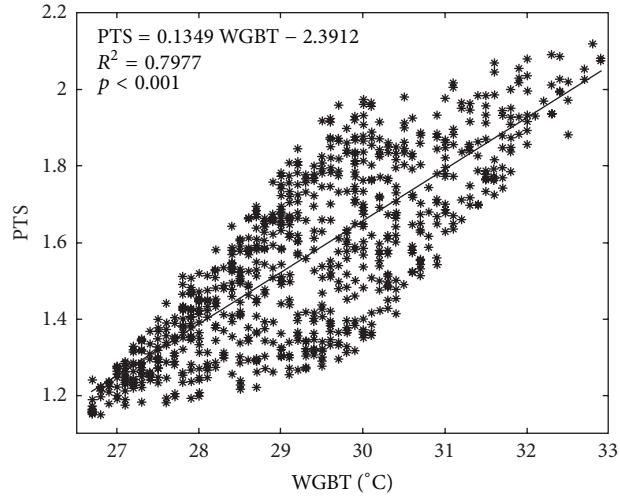

Figure 4: PTS versus WGBT.

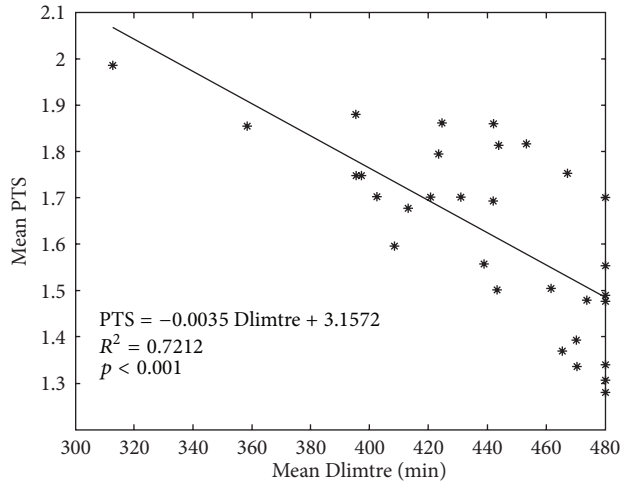

Figure 5: Mean PTS versus mean Dlimtre of each day during the measuring period.

4.3. Comparison of the PTS Index and Other Indices. In order to test the validity of this new index, the PTS index is compared with the commonly used indices (WBGT [6] and Dlimtre [7]) in these experiments. The WBGT index and the PHS model should be used for evaluating working conditions instead of predicting the physiological response of individual subjects. However, due to the lack of appropriate reference index, here the WGBT value and the Dlimtre index in the PHS model were used as the reference object to compare with the PTS index. The analysis between PTS and WBGT value is presented in Figure 4 for correlation. Dlimtre represents the maximum allowable exposure time for heat storage in PHS model [7], and mean Dlimtre of each day during the measuring period was calculated to compare with the mean PTS in Figure 5. The linear regression equations and the bivariate correlation results calculated by SPSS software are also shown in Figures 4 and 5. The correlations between PTS and WBGT (n = 823, p < 0.001) and mean PTS and mean Dlimtre (n = 31, p < 0.001) are statistically significant.

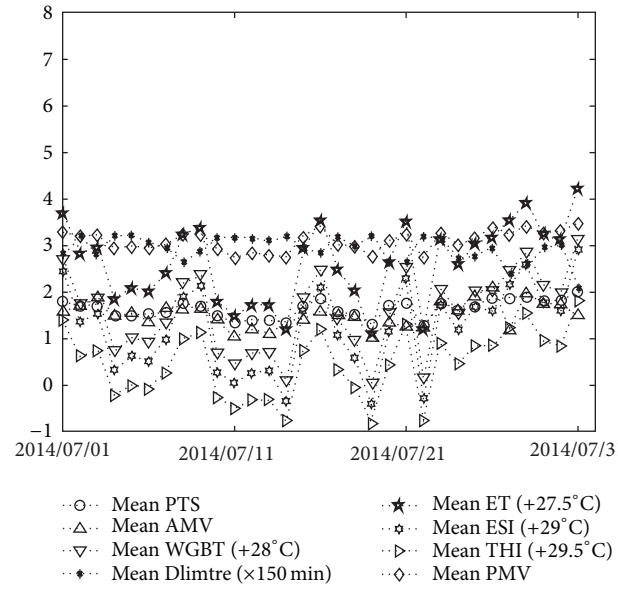

Figure 6: Comparison of mean PTS and other indices in each day during the measuring period. PTS: (20); AMV: thermal sensation vote; WGBT: $0.7t_w + 0.3t_g$ [6]; ET: $0.38t_a + 0.63t_g$ [12]; Dlimtre: maximum allowable exposure time for heat storage in PHS model [7]; PMV: PMV index [2, 8]; ESI: $0.63t_a - 0.03\text{RH} + 0.0054(t_a \cdot \text{RH}) - 0.73$ [14]; THI: $t_a - (0.55 - 0.0055\text{RH}) \times (t_a - 14.5)$ [13].

Therefore, the PTS (mean PTS) index is linearly related to the WBGT (mean Dlimtre) index.

Figure 6 shows comparison of mean PTS index and other indices in each day during the monitoring period. It can be seen from Figure 6 that the mean PTS index is much closer to the mean actual thermal sensation than other indices. Dlimtre [7], ET [12], ESI [14], and THI [13] may be used to evaluate the thermal condition in the hot environment, but they cannot be used to predict the physiological response of individual subjects. The mean PMV index much exceeded the valid PMV range of −2 to 2 in each day, meaning a large amount of thermal dissatisfied people, which is not a fact according to the AMV. Thus, compared to other indices, the PTS index can more effectively predict the mean thermal response of a large group of textile workers exposed to the hot environment in the spinning workshop.

4.4. Nonthermal Factors. Figure 7 shows AMV versus PTS of different gender (female: n = 513; male: n = 310). There are 4, 287, 199, and 23 female workers voting 0, 1, 2, and 3 in the AMV inquiry, respectively, while there are 3, 181, 115, and 11 male workers in the AMV inquiry. The results show that female worker and male worker have almost the same PTS and the actual thermal sensation. There are two trend lines with corresponding R^2 value in Figure 7, representing AMV of different genders change with the PTS. Two trend lines are both very close to the line of PTS = AMV, which means that calculated PTS values of different genders are both close to the actual thermal sensation.

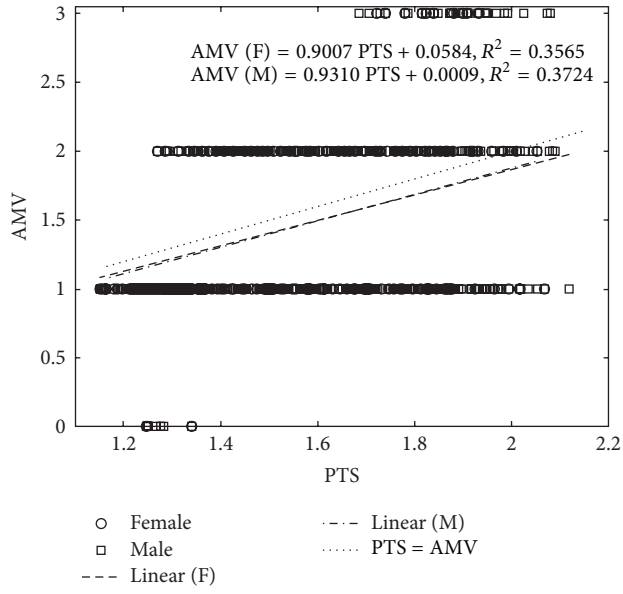

Figure 7: AMV versus PTS of different gender.

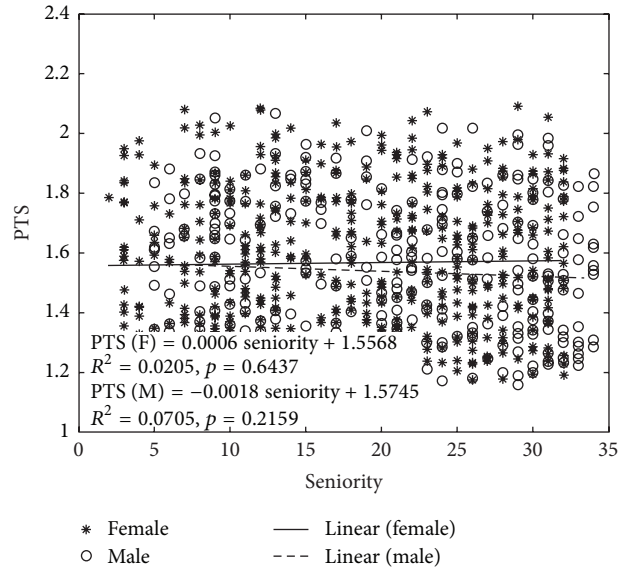

Figure 8: The PTS index of different gender versus seniority.

Figure 8 shows that the PTS index of the worker changes with worker's seniority. No significant differences (female: $n = 513$, $p = 0.6437$; male: $n = 310$, $p = 0.2159$) were observed in PTS following the seniority, which means that the thermal sensation of the textile worker has little relationship with the seniority. Reference [17] points that the young and old people are equally sensitive to cold or heat, which is confirmed with this conclusion.

5. Conclusions

The predicted thermal sensation (PTS) index was proposed to predict the mean thermal response of a large group of textile workers exposed to the hot environment in the spinning workshop. Actual workshop temperatures in the spinning workshop during the measuring period were all above 32°C, exceeding the acceptable operative temperature range from 23°C to 26°C by ISO 7730 and required temperature range from 30°C to 32°C by GB 50481-2009, belonging to extreme hot environment.

Higher temperature of the cotton textile workshop may result in deteriorating working conditions and poor thermal comfort. The PTS index was an appropriate index to predict the thermal sensation for the textile work, which is helpful for taking effective strategies to prevent the health risk to the worker. Comparison of the PTS index and the AMV shows that the PTS index is very close to the actual thermal sensation, which means that the PTS index can accurately estimate the actual thermal sensation of the textile workers exposed to the hot environment in the spinning workshop. Compared to other indices, the PTS index can more effectively predict the mean thermal response of a large group of textile workers according to the ASHRAE thermal sensation scale. Furthermore, the calculated PTS values of different genders are both very close to the actual thermal sensation. No significant differences were observed in PTS following the seniority, which means that the thermal sensation of the textile worker has little relationship with the seniority.

Nomenclature

C: Convective heat loss from skin (W/m^2)
$C_{\mathrm{orr,cl}}$: Correction for the dynamic total dry thermal insulation at or above 0.6 clo (dimensionless)
$C_{\mathrm{orr},Ia}$: Correction for the dynamic total dry thermal insulation at 0 clo (dimensionless)
$C_{\mathrm{orr,tot}}$: Correction for the dynamic clothing insulation as a function of the dimensionless actual clothing (dimensionless)
C_{res}: Heat flow by respiratory convection (W/m^2)
E_{max}: Maximum evaporative heat flow at the skin surface (W/m^2)
E_{res}: Heat flow by respiratory evaporative (W/m^2)
E_{sk}: Total rate of evaporative heat loss from skin (W/m^2)
f_{cl}: Clothing area factor (dimensionless)
H: Heat transfer from the deep body core to the skin (W/m^2)
h_{cdyn}: Dynamic convective heat exchange (W/(m^2·K))
I_{ast}: Static boundary layer thermal insulation (= 0.7 clo)
I_{adyn}: Dynamic boundary layer thermal insulation
I_{cl}: Static clothing insulation (clo)
I_{cldyn}: Dynamic clothing insulation (clo)
I_{totdyn}: Total dynamic clothing insulation (clo)

M: Activity level (W/m^2)
p_a: Water vapor partial pressure (Pa)
p_{sk}: Saturated water vapor pressure at skin temperature (Pa)
R: Radiative heat loss from skin (W/m^2)
RH: Relative humidity (%)
S: Heat storage (W/m^2)
S_r: Sweat rate (kg/(m^2·hr))
t_a: Air temperature (°C)
t_{cl}: Clothing surface temperature (°C)
t_{co}: Core temperature (°C)
t_g: Globe temperature (°C)
t_o: Operative temperature (°C)
t_r: Mean radiant temperature (°C)
t_{sk}: Temperature of skin compartment (°C)
$t_{sk,nu}$: Steady state mean skin temperature for nude subject (°C)
$t_{sk,cl}$: Steady state mean skin temperature for clothed subject (°C)
t_w: Wet-bulb temperature (°C)
v_a: Air velocity (m/s)
v_w: Walking speed (m/s)
W: Effective mechanical power (W/m^2)
λ: Latent heat of evaporation of sweat, 657 W·hr/kg at 30°C (W·hr/kg).

Conflict of Interests

The authors declare that there is no conflict of interests regarding the publication of this paper.

Acknowledgments

This research was supported by the NSFC (the Natural Science Foundation of China) no. 51208527 and Funding Scheme for Young Teachers of Higher School in Henan Province (2012GGJS-124).

References

[1] GB 50481, "Code for design of cotton design spinning and weaving factory," 2009.

[2] ISO, "Ergonomics of the thermal environment—analytical determination and interpretation of thermal comfort using calculation of the PMV and PPD indices and local thermal comfort criteria," ISO 7730, 2005.

[3] J. Zhao, N. Zhu, and S. Lu, "Productivity model in hot and humid environment based on heat tolerance time analysis," *Building and Environment*, vol. 44, no. 11, pp. 2202–2207, 2009.

[4] M. Ilangkumaran, M. Karthikeyan, T. Ramachandran, M. Boopathiraja, and B. Kirubakaran, "Risk analysis and warning rate of hot environment for foundry industry using hybrid MCDM technique," *Safety Science*, vol. 72, pp. 133–143, 2015.

[5] Z. Tian, N. Zhu, G. Zheng, and H. Wei, "Experimental study on physiological and psychological effects of heat acclimatization in extreme hot environments," *Building and Environment*, vol. 46, no. 10, pp. 2033–2041, 2011.

[6] ISO, "Hot environments—estimation of the heat stress on working man, based on the WBGT-index (wet bulb globe temperature)," ISO 7243, 1989.

[7] ISO, "Ergonomics of the thermal environment—analytical determination and interpretation of heat stress using calculation of the predicted heat strain," ISO 7933, 2004.

[8] ANSI/ASHRAE Standard 55, "Thermal environment conditions for human occupancy," 2013.

[9] R. Kralikovaa, H. Sokolovaa, and E. Wessely, "Thermal environment evaluation according to indices in industrial workplaces," *Procedia Engineering*, vol. 69, pp. 158–167, 2014.

[10] G. M. Budd, "Wet-bulb globe temperature (WBGT)-its history and its limitations," *Journal of Science and Medicine in Sport*, vol. 11, no. 1, pp. 20–32, 2008.

[11] R. Ooka, Y. Minami, T. Sakoi, K. Tsuzuki, and H. B. Rijal, "Improvement of the sweating model in 2-node model and its application to thermal safety for hot environment," *Building and Environment*, vol. 45, no. 7, pp. 1565–1573, 2010.

[12] C. Liang, G. Zheng, N. Zhu, Z. Tian, S. Lu, and Y. Chen, "A new environmental heat stress index for indoor hot and humid environments based on Cox regression," *Building and Environment*, vol. 46, no. 12, pp. 2472–2479, 2011.

[13] J. Unger, "Comparisons of urban and rural bioclimatological conditions in the case of a Central-European city," *International Journal of Biometeorology*, vol. 43, no. 3, pp. 139–144, 1999.

[14] D. S. Moran, K. B. Pandolf, Y. Shapiro et al., "An environmental stress index (ESI) as a substitute for the wet bulb globe temperature (WBGT)," *Journal of Thermal Biology*, vol. 26, no. 4-5, pp. 427–431, 2001.

[15] J. Ruan and X. Zhang, ""Flying geese" in China: The textile and apparel industry's pattern of migration," *Journal of Asian Economics*, vol. 34, pp. 79–91, 2014.

[16] R. Yang, L. Liu, and Z. Long, "Research on workshop environment in the textile company using analytic hierarchy process," *Energy Education Science and Technology*, vol. 33, no. 3, pp. 1581–1594, 2015.

[17] *ASHRE Handbook-Fundamental*, American Society of Heating, Refrigerating and Air-Conditioning Engine, 2009.

[18] ISO, "Estimation of thermal insulation and water vapour resistance of a clothing ensemble," ISO 9920, 2007.

[19] C. H. Wyndham and A. R. Atkins, "A physiological scheme and mathematical model of temperature regulation in man," *Pflügers Archiv European Journal of Physiology*, vol. 303, no. 1, pp. 14–30, 1968.

[20] International Organization for Standardization (ISO), *ISO 2276, Ergonomics of the Thermal Environment—Instruments for Measuring Physical Quantities*, International Organization for Standardization (ISO), London, UK, 1998.

Hindawi Publishing Corporation
Mathematical Problems in Engineering
Volume 2015, Article ID 851303, 13 pages
http://dx.doi.org/10.1155/2015/851303

Research Article

QFD Based Benchmarking Logic Using TOPSIS and Suitability Index

Jaeho Cho,[1] Jaeyoul Chun,[1] Inhan Kim,[2] and Jungsik Choi[2]

[1]*Department of Architectural Engineering, Dankook University, 126 Jukjeon-dong, Yongin-si, Gyeonggi-do 448-701, Republic of Korea*
[2]*Department of Architecture, Kyung Hee University, 1732 Deogyeong-daero, Giheung-gu, Yongin-si, Gyeonggi-do 446-701, Republic of Korea*

Correspondence should be addressed to Jungsik Choi; jungsikchoi@gmail.com

Received 10 April 2015; Accepted 26 July 2015

Academic Editor: Mohamed Marzouk

Users' satisfaction on quality is a key that leads successful completion of the project in relation to decision-making issues in building design solutions. This study proposed QFD (quality function deployment) based benchmarking logic of market products for building envelope solutions. Benchmarking logic is composed of QFD-TOPSIS and QFD-SI. QFD-TOPSIS assessment model is able to evaluate users' preferences on building envelope solutions that are distributed in the market and may allow quick achievement of knowledge. TOPSIS (Technique for Order of Preference by Similarity to Ideal Solution) provides performance improvement criteria that help defining users' target performance criteria. SI (Suitability Index) allows analysis on suitability of the building envelope solution based on users' required performance criteria. In Stage 1 of the case study, QFD-TOPSIS was used to benchmark the performance criteria of market envelope products. In Stage 2, a QFD-SI assessment was performed after setting user performance targets. The results of this study contribute to confirming the feasibility of QFD based benchmarking in the field of Building Envelope Performance Assessment (BEPA).

1. Introduction

(1) Theory of QFD and Benchmarking. Various ways of utilizing QFD have been continuously studied in the construction industry. QFD is one of Quality Management's techniques to deal with customer needs and expectations more systematically for achieving the most important objective of a construction company, satisfaction of clients [1, 2]. Today, QFD has been widely adopted not only by the manufacturing industry, but also among various other disciplines [3].

A lot of QFD tools have been made to examine decision-making tools as a comparison analysis between performance of products and experience knowledge gained from the current project [4]. Application of benchmarking in QFD is one of many utilization purposes and can be used at the final stage. A QFD after design stage can be used as a tool to make comparisons between competitors and to gain knowledge of the expectations of end users to be used in forthcoming projects [2].

Benchmarking has been defined as a systematic approach of measuring one's performance against that of recognized leaders with the purpose of determining best practices for continuous improvement [5]. It is used to measure performance using a specific indicator resulting in a metric of performance that is then compared to others [6]. Modern industries are increasingly integrating benchmarking in businesses with their strategic planning initiatives in order to gain a competitive edge in the global market, maintain their market shares, and acquire world-class standards and recognition [7, 8].

A benchmarking process should contain at least three steps: collect a reasonably large database, obtain performance information, and conduct comparison analysis [9]. Performance assessment of the market product and storage of such assessment information is a basic procedure for preparation of benchmarking based on QFD.

(2) State of the BEPE (Building Envelope Performance Evaluation). There is a global trend in understanding and evaluating

the overall performance of buildings. In several countries (Japan, United States, Canada, EU countries, etc.) such programs have been or are being developed in an attempt to assess the issues that influence the performance of the building [10]. The goal of BPE (Building Performance Evaluation) is to improve the quality of decisions made at every phase of the building life cycle, that is, from strategic planning to programming, design, and construction, all the way to facility management [11].

The performance assessment, including environmental elements and sustainability, should be reflected in the field of BPE as well. Building envelopes, as the interface between interior space and exterior environment, serves the function of weather and pollution exclusion and thermal and sound insulation [12]. Building envelope has multiple performance items. The designer and the user should make design decisions by considering the priority of multiple performance items. For this reason, the product of building envelope is a very appropriate subject on QFD.

The fundamental performance required for building envelopes is defined by the following criteria: (1) thermal performance, (2) moisture protection, (3) visual, (4) sound, (5) safety, (6) maintenance access, (7) health and indoor air quality, (8) durability and service life expectancy, (9) maintainability and repairability, and (10) sustainability [13].

High-performance sustainable facades can be defined as exterior enclosures that use the least possible amount of energy to maintain a comfortable interior environment, which promotes the health and productivity of the building's occupants [14]. Although there is a wide selection of optimal designs the performance of their multiattributes should be taken into account. This requires decision making process involving project stakeholder to compromise requirements [15].

Lack of communication and integration has been recognized as a crucial problem during the design stage. Poor communication and integration render the achievement of an optimal design difficult, as well as a time-consuming process [16, 17]. This problem tends to lead to unclear instructions, additional work, progress delay, project delay, and poor quality of design solutions [18, 19].

(3) Current QFD Barriers and Proposed Approach. Currently implemented QFD is recognized as an excellent tool that allows comprehensive assessment on quality in consideration of multiattributes for performance and gathers project stakeholder requirements [2]. However, there are still limitations for users in assessing performance by using QFD, reutilizing the results from such assessments and analyzing users' quality satisfaction [20]. In terms of benchmarking, recommendations on suitable solutions for projects depend on the empirical decision of designers and professional engineers. Mohsini pointed out a problem that is ignoring interdependency relationship of the individual evaluation systems in a matter of performance assessment [21].

The market's subjective assessment on novel technology and unfamiliar usability excludes new chance to improve the performance [22]. Moreover, performance criteria, as user satisfaction, have not been proposed. Stakeholder's satisfaction is a key factor in project success, and a project cannot be deemed as successful until it is completed [23]. Since satisfaction is subjective measurement, it is rarely used in the performance measurement of stakeholders [24].

Abovementioned problems are also applied in building envelope solutions. In the designing stage, benchmarking an environment for the best, good, better, and standard technology in the market has not been established when users take into consideration multiattribute performances for building envelopes. Also, user satisfaction in current projects has been evaluated in a subjective manner.

For this, firstly, this study normalizes and standardizes the quality information on envelope in the market based on QFD. Such information on quality assessment allows designers and users to facilitate the benchmarking process to survey envelope design solutions in market. Performance assessment for market products should be preceded above all in order to establish the benchmarking environment. Then, the users can set target performance criteria through the benchmarking of the market solution.

Secondly, this study, analyzes the Suitability Index (SI), which presents the level of user satisfaction calculated by comparison between products and required performance criteria (RPC). The Similarity Index is able to recommend the better solution to users through confirmation of satisfaction level.

2. Research Object, Scope, and Procedures

The purpose of this study is to propose QFD based benchmarking logic for building envelope solutions. QFD-TOPSIS performs the performance assessment and the performance benchmarking for the market product by defining users' order of function priority; QFD-SI analyzes the quality suitability based on users' requirement.

The range of this study includes investigation on validity and applicability of benchmarking logic through a simple case study. Establishment of QFD knowledge management systems for Building Envelope Performance Assessment is subjected to future study. The study was conducted in the following procedure.

(1) Set the approach and purpose of the study.

(2) Investigate studies related to decision-making methods and benchmarking application in QFD.

(3) Propose the fundamental theory of QFD.

(4) Establish benchmarking logic based QFD.

(5) Propose QFD-TOPSIS model in which TOPSIS is combined to QFD.

(6) Propose QFD-SI model in which SI is applied to QFD in order to analyze users quality suitability.

(7) Validity of benchmarking logic through case analysis.

(8) Draw conclusion of this study.

3. Literature Review

QFD has been recognized as a useful tool for technical realization of clients' subjective requirements and measurement of clients' satisfaction [2, 25]. Today, QFD has been widely adopted not only by the manufacturing industry, but also among various other disciplines [3]. The extent of areas where QFD has been researched has become so exhaustive that Carnevalli and Miguel investigated the research done in QFD as a research topic itself [20].

Harding et al. suggested an information model connecting the market product and users' requirement by utilizing QFD [26]. The study has become the concept model of QFS-based benchmarking logic. Singhaputtangkul et al. proposed a QFD assessment system for a building envelope [22]. Li et al. suggested a QFD system combining a fuzzy-TOPSIS that is used in multicriteria decision-making [27].

Furthermore, QFD has been studied in combination with various decision-making models. The following studies are examples: the decision-making model combining QFD and fuzzy theory [28–32], the decision-making model of fuzzy based QFD combined with ANP [33], the decision-making model combining QFD and ANP [33, 34], in addition to the Kano model [35], DEA model [36], Rough Set model [37], SMART (Simple Multiattribute Rating Technique) [38], conjoint analysis [39], MAV [40], and FAHP (Fuzzy Analytic Hierarchy Process) model [32], which were all utilized in QFD as quality assessment methods.

Such assessment methods have focused on relative comparisons among products and thereby carry a weakness of difficulty in utilization in the market benchmarking. In addition, the evaluation methods involving complex calculation processes are becoming a fundamental problem to lower the utilization of QFD.

Meanwhile, the benchmarking studies using QFD were being conducted. Benchmarking the application of QFD is a system engineering approach for continuously evaluating and measuring current operations (system, process, product, or service) and comparing them to "best-in-class" operations [7]. In particular, with respect to a rapidly changing market, the incorporation of the new product development risk, the competitors' benchmarking information, and the feedback information into the network model may be considered as a novel contribution in QFD literature [34].

The benchmarking approach with QFD was studied in the automobile industry [41]. Benchmarking on QFD requires information collection, information analysis, and update of recent products. Hence, QFD based knowledge management systems and decision-making methods are expected to be closely related in QFD based benchmarking.

Despite of the continuous studies up to date on QFD, reviews on the literature have noted that there are difficulties in utilization of quality planning and benchmarking by QFD [20]. It was found that the major methodological difficulties are related to the stage of elaborating quality matrixes (almost 80% of the mentions) such as "interpreting the customer' voice" [41], "identifying the most important customer demands" [42], and "project decision-making, since correlations among the demands are not clear" [43]. It was noted that reducing the methodological difficulties in developing the quality matrix is a key factor in encouraging and expanding the use of QFD [20]. The detail of those difficulties in utilization of QFD has been described in [20, 41, 42].

In particular, there is an issue of having different results from quality assessments depending on the kinds of decision-making model applied for HOQ. Therefore, following several demands are required to be considered in order to improve QFD usability in benchmarking. First, the quality assessment in QFD should be excluded subjectively and obtained objectively. Second, the decision-making model for QFD should be as simple as possible, considering users usability. Third, the comparison on the performance upon the users' priority for function should be practicable since the market products carry multiattribute performances. Forth, the quality suitability should be confirmed based on users' RPC. Sections 5, 6, and 7 in this study propose QFD based benchmarking logic and formula model in consideration of above the 4 improvement demands.

4. QFD Theory

Quality function deployment (QFD) is a technique that deals with customer needs and expectations in a more systematic nature in order to achieve the most important objectives of a construction company and satisfaction of clients [2]. The core of the QFD method is a matrix base commonly referred to as the "house of quality" (HOQ), a 2D matrix that displays customer's needs, also referred to as the WHAT, and the organization's technical responses to these needs, also referred to as the HOW.

Each of the customer needs for the WHAT can be cross-checked against the related design and product response elements of the HOW. The core matrix of QFD or HOQ is illustrated in Figure 1 [44].

A flow chart depicting the steps involved in QFD is provided in Figure 2 [3].

(1) WHATs: the primary input in the HOQ is a prioritized list of basic customer demands (requirements and needs).

Each demand is documented as a WHAT and prioritized as represented by WHAT-1, . . . , WHAT-n in Figure 2.

(2) HOWs: HOWs are the design (or technical or product) characteristics that serve to meet the WHATs. For each WHAT, a corresponding HOW is identified as represented by HOW-1, . . . , HOW-n in Figure 2.

(3) Relationship matrix: it indicates how product characteristics or decisions affect the satisfaction of each customer need. It consists of relationships existing between each WHAT and each HOW attribute.

(4) Absolute weights and ranking of HOWs: it contains results of the prioritization of product characteristics to satisfy customer requirements.

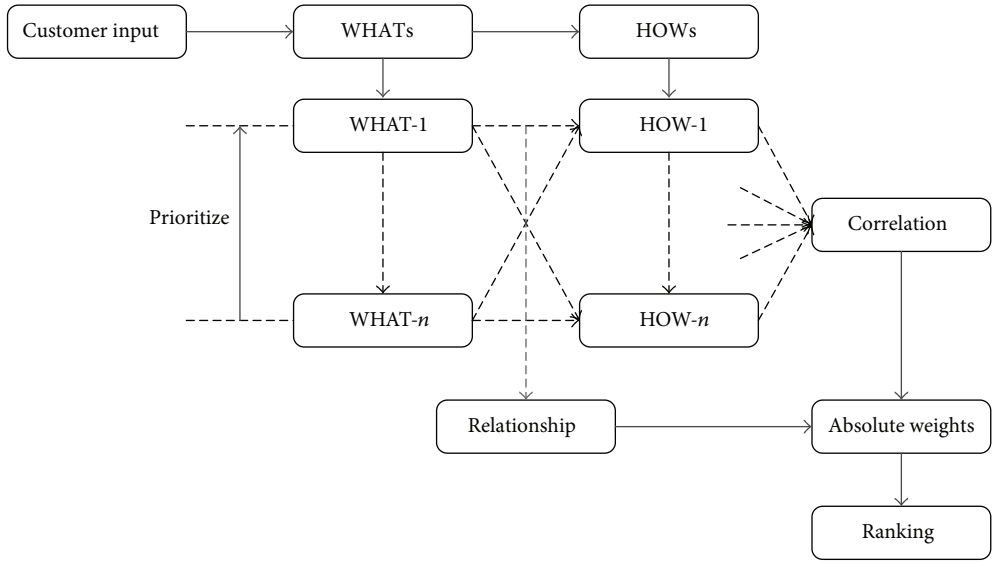

Figure 1: QFD matrix chart.

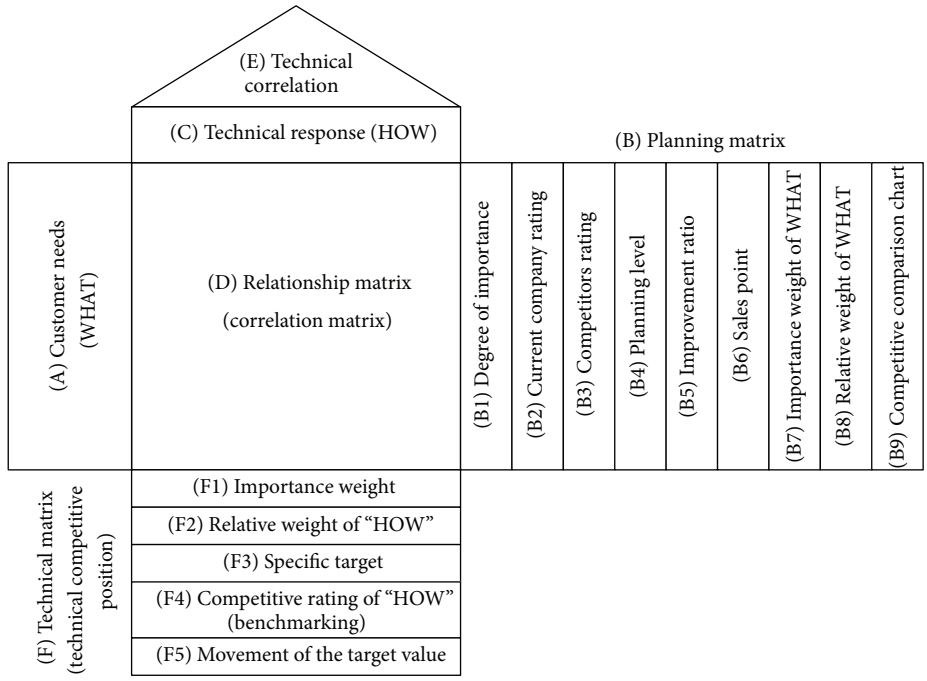

Figure 2: QFD-HOQ concept model.

It represents the impact of each HOW attribute on the WHATs and is the final step before ranking of the weights for decision-making as shown in Figure 2.

(5) Correlation matrix: it is the roof of the HOQ and represents the interdependencies among HOWs as shown in Figure 2.

5. Benchmarking Logic Based QFD

QFD benchmarking logic generates state of performance distribution on market products in order to improve performance of current solution. Performance criteria of products are determined by technical characteristics of "HOW" in HOQ matrix. Designers and users can ensure an improvement possibility of performance through comparison on multiattribute performance of HOQ-HOW.

The subject for quality comparison is products or the latest solutions that are currently used in the market. Benchmarking on new technology provides a good opportunity for raising improvement of performance. An important advantage of the benchmarking process is that it allows the users to confirm the level of improvement for performance beyond the simple copycat performance. Figure 3 presents benchmarking logic for users' quality planning in this study.

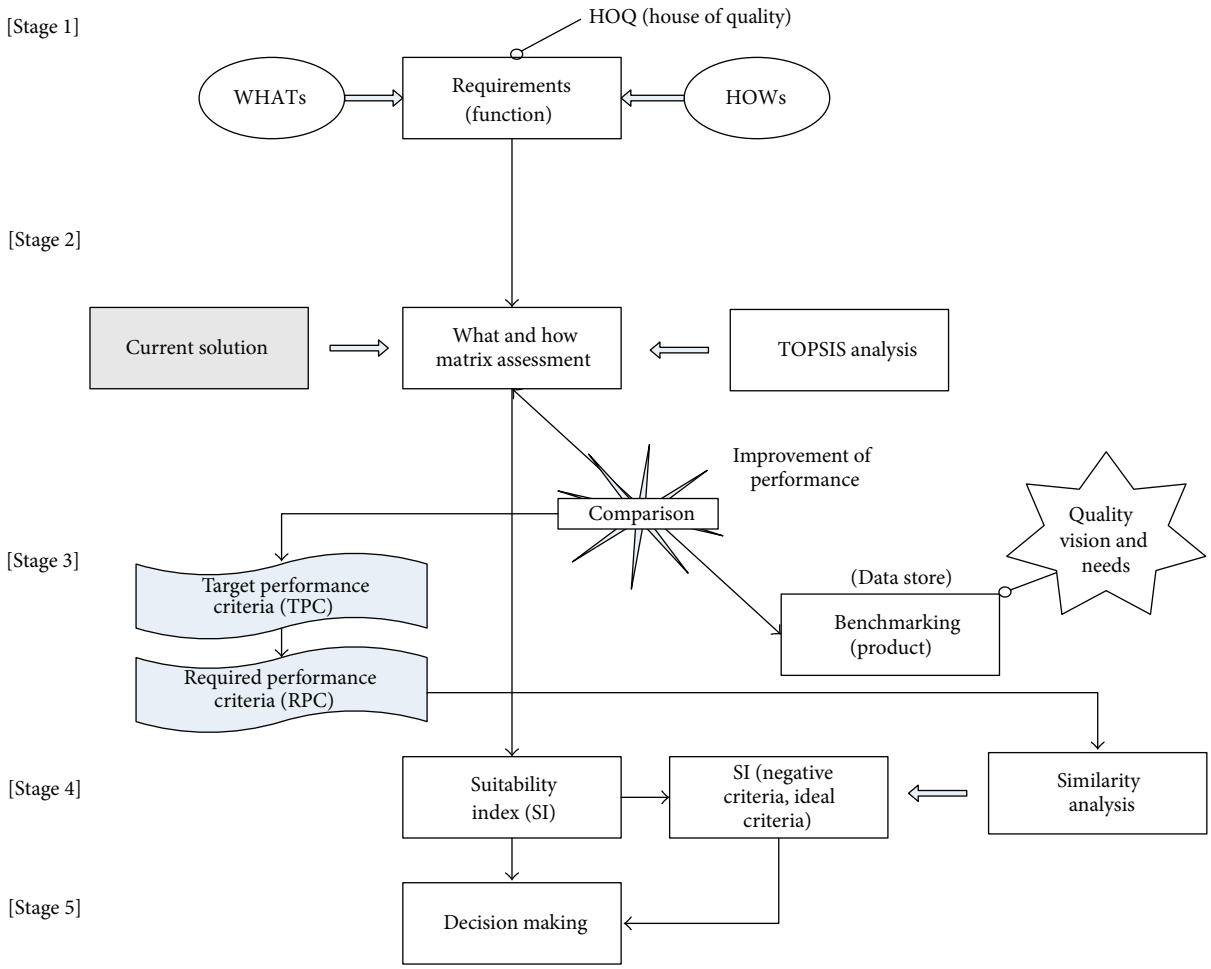

Figure 3: Benchmarking logic based on QFD and TOPSIS.

The benchmarking process is performed by following procedure.

(1) Requirements of designers and users (WHATs) are defined and the priority for technical characteristics (HOWs) is set.

(2) A product solution that is currently considered as standard quality is compared with products in market by using QFD-TOPSIS model.

(3) Designers and users set performance target with benchmarking of a product in the market that is higher than the current solution. This will be the required performance criteria (RPC).

(4) SI of the market products is calculated by similarity of RPC and product actual performance (PAP).

(5) Users select the most suitable solution for the current project: the solution with its total SI that is the nearest to 0, with lower SI-NC and higher SI-IC.

6. QFD-TOPSIS

The overall customer satisfaction level is derived from multiple customer attributes that are generally conflicting with one another. Therefore a multiattribute value (MAV) function is very well suited for mathematical formulations in QFD [45].

TOPSIS technique uses a multicriteria decision-making method to analyze preferences among alternatives. TOPSIS is usually employed to analyze the relative comparison of alternatives [46, 47]. It calculates scores that are a distance between a positive ideal solution (PIS) and negative ideal solution (NIS). Hwang and Yoon [48] originally proposed the TOPSIS method in order to identify solutions from a finite set of alternatives. The detailed traditional TOPSIS solution can be found in Chan and Wu [29].

TOPSIS analyzes the product preference in consideration of the multiproperties of a product, service, system, and so forth. Currently, the preference can refer to scores obtained from the quality evaluation. The score range is distributed between 0 and 1. The quality is more improved as the preference score approaches closer to 1.

In this study, value N_{ij} is normalized to an absolute value while original TOPSIS models use relative values. Product quality can be defined as a grade and the value in turn normalized to between 0 and 1 by dividing the total distance. Figure 4. presents the concept of normalization for product performances possessing different measurements for evaluations.

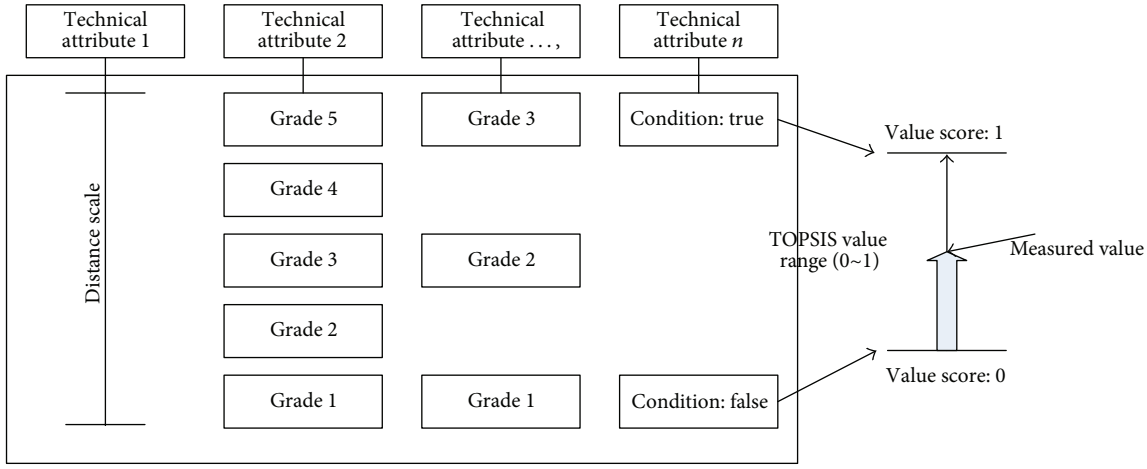

Figure 4: TOPSIS evaluation model in multicriteria decision-making.

"WHATs" and "HOWs" possess 1 : 1 relationship in QFD-TOPSIS model. When one "WHAT" has two more "HOWs," 1 : 1 relationship is kept by accepting duplication of "WHAT." When one "HOW" has two more "WHATs," a statement is made by summarizing "WHAT" as one "WHAT." One of the reasons why keeping 1 : 1 relationships between "WHAT" and "HOW" in an independent manner is because QFD-TOPSIS evaluation models only evaluate product performance.

Unlike the existing QFD studies used in function evaluation methods, performance evaluation is solely one of the best approaches securing the objectivity measurement. Furthermore, the relationship with $1 : n$ or $n : 1$ between "WHAT" and "HOW" carries a risk intervention of subjective evaluation, the most challenging issue in terms of QFD utilization.

In the practical environment, one requirement (WHAT) can have one or more technical characteristics (HOWs). Another case, one technical characteristic (HOW) can have one or more requirements (WHATs). The first step for securing the objectiveness is to get rid of the subjective matrix relationship between WHATs and HOWs and to recognize a technical characteristic as a unique being.

Technical characteristic must have PIV and NIV. This is indeed an objective fact in terms of engineering. Therefore, the technical characteristics can be changed as a unique being in relation to the functional requirements. A technical characteristic can be matched to a functional requirement; however, the functional requirement here is allowed to be defined with multiple subfunctions.

As a result, technical characteristics have distinct functional requirement, and the PIV and the NIV are defined based on the corresponding functional requirement. All technical characteristics present the objective fact of PIV and NIV based on 1 : 1 relationship between WHATs and HOWs. The assessment results will always be consistent regardless of the replacement of the field expert since they are based on the objective fact.

The next step following the 1 : 1 relationship is to define the priority of functional requirements with technical characteristics. Ranking the priority of technical characteristics is the domain of a user's subjective judgement.

The procedure of QFD-TOPSIS is expressed in the following steps.

Step 1 (generate technical measurement criteria (HOWs)). This step defines performance criteria (H_j, $j = 1, \ldots, n$) for evaluation of products quality. The performance criteria are the technical characteristics for realization of users' requirements.

Step 2 (identify customer requirements (WHATs)). This step defines the users' functional requirements.

The requirements (W_x) are described as technical "HOW" of the products.

The definition of "WHAT" may go through repetitive revision in order to keep a 1 : 1 relationship between "WHATs" and "HOWs."

Step 3 (define the importance rating of customer requirements (r_x)). Users and designers measure the priority of "WHAT" from a scale of 1 to 10 points.

In turn, align in order according to the priority of "WHAT."

Step 4 (determine initial technical performance ratings of HOWs). The actual measurement of the product is determined by using a standardized scale that is currently used in the market. The type of performance measurement is one of distance scale, ordinal scale (9, 7, 5, and 3 point), ratio scale, and a binary value (True/False). Initial technical performance rating is T_{ij}, (product ID: $i = 1, \ldots, m$, technical attribute: $j = 1, \ldots n$). In turn, the Positive Ideal Value (PIV) and Negative Ideal Value (NIV) are defined as

$$\begin{aligned} \mathrm{PIV}_i^+ &= \left\{T_{i1}^+, \ldots, T_{ij}^+\right\}, \\ \mathrm{NIV}_i^- &= \left\{T_{i1}^-, \ldots, T_{ij}^-\right\}, \end{aligned} \tag{1}$$

where $T_{ij}^+ = \max_i\{T_{ij}\}$, $j = 1, 2, \ldots, n$, and $T_{ij}^- = \min_i\{T_{ij}\}$, $j = 1, 2, \ldots, n$.

Step 5 (weight of the technical characteristics HOWs). The performance is compared with each pair item referring to the priority of "WHAT" that is determined in Step 3. The value of pair comparison is determined in scores for relative advantage regarding H_1 and H_2, H_1 and $H_3, \ldots H_1$, and H_n (i.e., 1 point is added when the priority is the same; 2 points are added when the priority is higher by 1 point; 3 points are added when the priority is higher by 2 points). The weight for H_j is calculated by the following:

$$w_j = \frac{\sum_{j=1}^{n} a_j}{\max_j \sum_{j=1}^{n} a_j} \times 10. \tag{2}$$

Step 6 (determine the relationship between WHATs and HOWs). T_{ij}, the actual performance values of products, are matched in a 1 : 1 relationship of "WHATs" and "HOWs."

Step 7 (competitive rating HOWs). The performance evaluation on market product is recorded. The decision-making matrix V for the (j)th technical characteristic HOW of the (i)th product is shown in the following:

$$V = \begin{bmatrix} v_{11} & \cdots & v_{1n} \\ \vdots & \ddots & \vdots \\ v_{m1} & \cdots & v_{mn} \end{bmatrix} \tag{3}$$

($i = 1, \ldots, m$, m is the number of the product).

($j = 1, \ldots, n$, n is the number of the technical characteristic).

The v_{ij} is multiplied by weight to normalize the value, as follows:

$$v_{ij} = w_j N_{ij}. \tag{4}$$

The N_{ij} is normalized as the unit vector in which the maximum value is 1.

The normalized value (N) is calculated as follows:

$$N_{ij} = \sqrt[2]{\frac{T_{ij} - T_{ij}^{-}}{T_{ij}^{+} - T_{ij}^{-}}}. \tag{5}$$

Step 8 (analysis preference and benchmarking). In turn, calculate P_i that is the sum of distance between the value (v_{ij}) and NIV (Negative Ideal Value: 0) using the following equation:

$$P_i = \sum_{j=1}^{n} \left(v_{ij} - 0\right). \tag{6}$$

Finally, calculate the closeness to the ideal solution.

The closeness C_i of product P_i is defined as

$$C_i = \frac{P_i}{\sum_{i=1}^{n} w}. \tag{7}$$

The closer C_i of a product to 1, the higher the users' preference. Users confirm the difference in preference between the current solution and market products by referring the preference score. Furthermore, users will benchmark the products with relatively higher preference compared to the current solution.

Step 9 (product performance targeting). Users set feasible targets to improve the performance comparing the current solution and benchmarking product.

7. QFD-SI

QFD-SI recommends the most suitable products for users through a similarity analysis between RPC and product actual performance (PAP) in the market. SI becomes closer to 0 as the similarity between RPC and PAP increases. Suitability is composed of Total Suitability Index (TSI), Suitability Index based on negative criteria (SI-NC), and Suitability Index based on ideal criteria (SI-IC). Users can consider the product as the most suitable solution when TSI and SI-NC are close to 0 and SI-IC is close to 1.

After the QFD-TOPSIS procedures is complete, the process of QFD-SI is expressed in the following steps.

Step 10 (TSI (Total Suitability Index)). Assign Suitability Index (SI_i) by measuring differential value between RPC and PAP.

TSI (Total Suitability Index) for a product is estimated by the following:

$$\mathrm{TSI}\,(i) = \frac{\mathrm{SI}_i}{\sum_{j=1}^{n} w_j}, \quad \mathrm{SI}_i = \sum_{j=1}^{n} \left(v_{ij}^{\mathrm{PAP}} - v_{ij}^{\mathrm{RPC}}\right). \tag{8}$$

Step 11 (SI-NC (Suitability Index based on negative criteria)). SI-NC is the sum of SI^{-} when it is less than 0 divided by the absolute negative maximum as a total of SI^{-}:

$$\text{SI-NC} = \frac{\mathrm{SI}_i^{-}}{\sum_{j=1}^{n} v_{ij}^{\mathrm{RPC}}}, \quad \left\{\mathrm{SI}_i^{-} < 0\right\}, \; -1 \le \text{SI-NC} < 0 \tag{9}$$

Step 12 (SI-IC (Suitability Index based on ideal criteria)). SI-IC is the sum of SI^{+} when it is greater than 0 divided by the ideal maximum as a total of SI^{+}:

$$\text{SI-IC} = \frac{\mathrm{SI}_i^{+}}{\sum_{j=1}^{n} \left(w_j - v_{ij}^{\mathrm{RPC}}\right)}, \quad \left\{\mathrm{SI}_i^{+} \ge 0\right\}, \; 0 \le \text{SI-NC} \le 1. \tag{10}$$

Step 13 (improvement performance ratio). The ratio represents performance improvement that is the difference between the current alternative TSI and the base alternative TSI. Figure 5 shows the concept of QFD-TOPSIS and QFD-SI models in this study.

8. Numerical Examples

In case study, the performance evaluation data of a building envelope is utilized in order to verify QFD-TOPSIS and QFD-SI models. Targeting performance criteria (TPC) is set based on 10 sample data, in turn the quality suitability is analyzed based on RPC.

8.1. Curtain Wall Performance Evaluation. The evaluation criteria on performance of a curtain wall in this study are

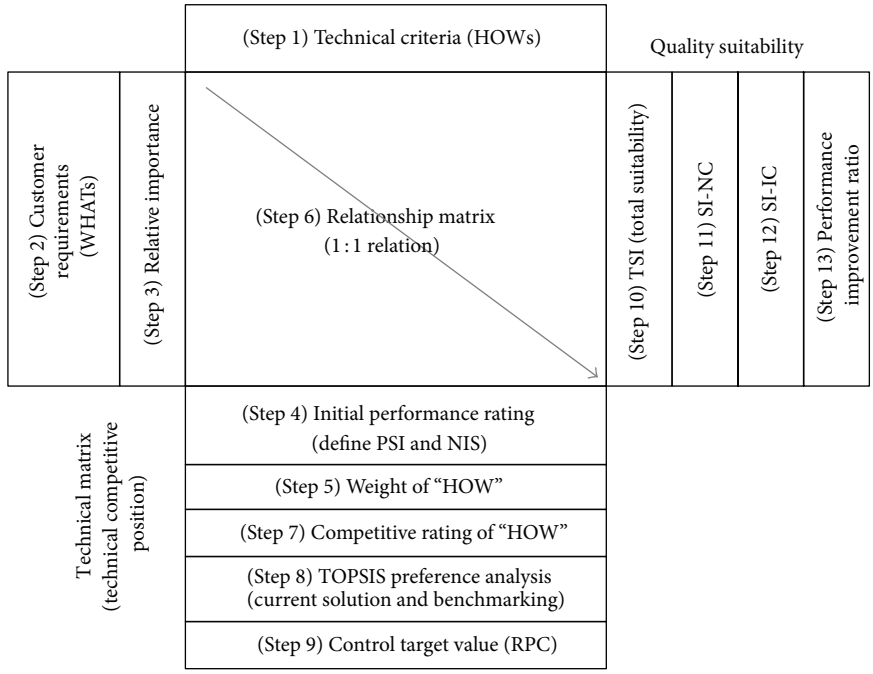

Figure 5: QFD-TOPSIS, QFD-SI model.

composed of the following 10 items. (1) U value (glazing): distance scale, (2) U value (total): distance scale, (3) SHGC (summer): distance scale, (4) SHGC (winter): distance scale, (5) VT: distance scale, (6) CR: distance scale, (7) AT: distance scale, (8) Aesthetic: ordinal scale, (9) WS: ordinal scale, and (10) WT: binary scale.

The U value is the measure of how much heat is transferred through the window. A lower U value has a better thermal insulation performance. The performance of the U value can be classified into glass itself and the glass curtain wall including the frame.

Solar Heat Gain Coefficient (SHGC) is a measure of how much solar radiation passes through the window. SHGC is expressed as a number between 0 and 1. The lower a window's SHCG is, the less solar heat it transmits. In terms of users' functional requirement, SHGC can be classified into SHGC (summer) and SHGC (winter). The ideal values for SHGC (summer) and SHGC (winter) are 1 and 0, respectively.

Visible transmittance is the amount of light in the visible portion of the spectrum that passes through a glazing material. A higher VT means there is more daylight in a space, which if designed properly can offset electric lighting and its associated cooling loads.

Condensation Resistance (CR) measures how well a product resists the formation of condensation. CR is expressed as a number between 1 and 100. The higher the number is, the better a product is able to resist condensation.

Air-tightness (AT) can be defined as the resistance to inward or outward air leakage through unintentional leakage points or areas in the building envelope. The amount of air leakage must be lower than the acceptable standards, 0.06 cfm/ft2, based on the ASTM E283 standards test.

The aesthetics means user aesthetic function of the envelope. Measurement on the aesthetics is flexible in relation to an individual's subjectivity and culture. In this study, a 5-grade ordinal scale was applied to the aesthetics performance (i.e., grade 5: the best).

Wind safety (WS) is the safety of the windows against wind. Safety measurement follows standards test of ASTM E330. In this study, WS adopts 3-grade scale (i.e., grade 3: the most excellent) since a domestic standardized scale for WS is not available yet.

Water tightness (WT) is windows' resistance against water leakage. The amount of water leakage must be 0 based on standard tests of ASTME 331. In this study, the evaluation of WT is determined as 1 (no leakage) or 0 (leakage) based on the test results.

8.2. Users' Requirement on Curtain Wall. The weight of technical characteristics is calculated upon interactive comparisons of the performance properties. The weight is calculated by relative comparison based on users' priority score for "WHATs." Figure 6 is a comparison matrix and the weight of performance.

A–J means that A and J have the same importance. B-2 means that B is more important than F by 2. (In F column) For the performance items (A~J), the sum of each importance is calculated. Then, the importance of those performance items were normalized by using the scale of 10. The item A has the highest value of importance as 10. Each of B, C, D, and E has an importance of 4.2. Each of F, G, H, I, and J has an importance of 1.5.

The intercomparison in between performance has an advantage of securing user's consistency in setting the

	U value (total)	*U* value (glazing)	AT	WS	WT	SHGC (summer)	SHGC (winter)	Aesthetic	VT	CR	
	A	B	C	D	E	F	G	H	I	J	Weight
A	A-3	A-3	A-3	A-3	A-4	A-4	A-4	A-4	A-4	10.0
B	B-C	B-D	B-E	B-2	B-2	B-2	B-2	B-2	4.2
C	C-D	C-E	C-2	C-2	C-2	C-2	C-2	4.2
D	D-E	D-2	D-2	D-2	D-2	D-2	4.2
E	E-2	E-2	E-2	E-2	E-2	4.2
F	F-G	F-H	F-I	F-J	1.5
G	G-H	G-I	G-J	1.5
H	H-I	H-J	1.5
I	V-J	1.5
J	1.5

Importance
5 point: 4 higher
4 point: 3 higher
3 point: 2 higher
2 point: 1 higher
1 point: same

Figure 6: Weighting matrix for users performance requirements.

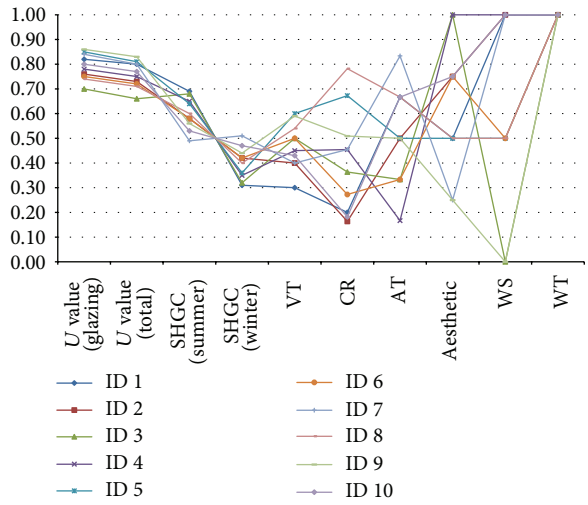

Figure 7: Normalized data for 10 curtain wall products.

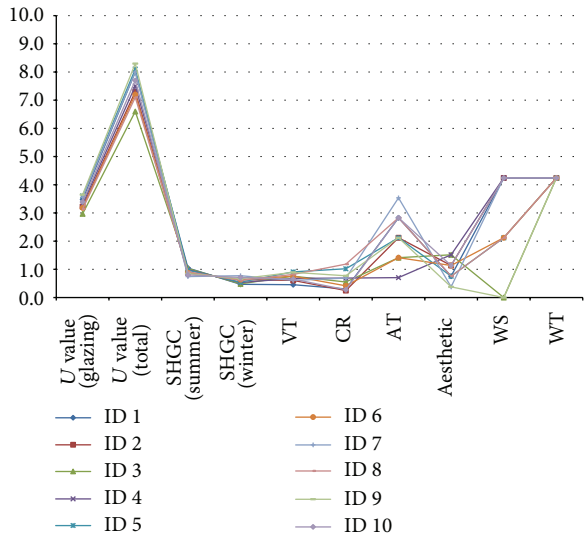

Figure 8: Weighted data for users' preference.

priority. However, compensation for distortion of the priority score is required. This is out of the range of this study.

8.3. Preference Analysis. The 10 samples of the windows in building envelope were chosen for validation of case study. Table 1 shows a sample of the performance data for the curtain wall products. Product ID 8 was selected for the solution for the current project. Table 2 is the performance data that are normalized (see also Figure 7). The normalized performance has the value between 0 and 1. Table 3 is the results of the preference analysis based on TOPSIS. Among 10 products, the product ID 7 has the preference of 0.77 that is the nearest value to 1 (see also Figure 8). Hence, users can select the product ID 7 as the benchmarking solution.

8.4. Benchmarking and Setting Up TPC (RPC). The product ID 11 is a new TPC that was set in this study. The TPC was set to compare the performance between the benchmarking product ID 7 and the current product ID 8. The subject for performance improvement was targeted to insulation performance for energy saving in this case study by the authors; the *U* value and AT become a key with regard to energy saving. User's requirement and subjects of interest differ by the project environment. Therefore, the *U* value and AT of the benchmarking product (ID 7) were set as TPC (ID 11). In Table 4, the product ID 11 solution presented the RPC that adjusted the performance criteria through users' benchmarking. In Table 5, the product ID 11 solution presented the RPC in which the weight was applied.

8.5. Suitability Index. SI of the 10 products was calculated based on the RPC of the product ID 11. It represents TSI, SI-NC, and SI-IC of the 10 products in Table 6 and Figure 9. The product ID 1 was analyzed as the solution that is the closest to 0 as the TSI presents 0.00. TSI of the product 1 has as a value of 0.00.

RPC and PAC are considered to completely match up together if TSI has a value of 0.00. However, such result will be occasionally obtained because the values of SI-NC and SI-IC

Table 1: Initial performance data for 10 curtain wall products.

Product	U value (glazing)	U value (total)	SHGC (summer)	SHGC (winter)	VT	CR	AT	Aesthetic	WS	WT
	Distance scale	Distance scale	Distance scale	Distance scale	Distance scale	Distance scale	Distance scale	Ordinal scale (5)	Ordinal scale (3)	Binary scale
Max	0.00	0.00	0.00	1.00	100	80	0.00	5	3	1
Min	1.00	1.00	1.00	0.00	0	25	0.06	1	1	0
1	0.18	0.20	0.31	0.31	30	36	0.02	3	3	1
2	0.24	0.27	0.42	0.42	40	34	0.03	4	3	1
3	0.30	0.34	0.32	0.32	50	45	0.04	5	1	1
4	0.22	0.25	0.35	0.35	45	50	0.05	5	3	1
5	0.15	0.19	0.36	0.36	60	62	0.03	3	2	1
6	0.25	0.28	0.42	0.42	50	40	0.04	4	2	1
7	0.16	0.20	0.51	0.51	40	50	0.01	2	3	1
8	0.26	0.29	0.40	0.40	54	68	0.02	3	2	1
9	0.14	0.17	0.44	0.44	59	53	0.03	2	1	1
10	0.20	0.23	0.47	0.47	43	35	0.02	4	3	1

Product ID (8): current solution.

Table 2: Normalized data for 10 curtain wall products.

Product	U value (glazing)	U value (total)	SHGC (summer)	SHGC (winter)	VT	CR	AT	Aesthetic	WS	WT
	Distance scale	Distance scale	Distance scale	Distance scale	Distance scale	Distance scale	Distance scale	Ordinal scale (5)	Ordinal scale (3)	Binary scale
Max	1.00	1.00	1.00	1.00	100	80	0.00	5	3	1
Min	0.00	0.00	0.00	0.00	0	25	0.06	1	1	0
1	0.82	0.80	0.69	0.31	0.30	0.20	0.67	0.50	1.00	1
2	0.76	0.73	0.58	0.42	0.40	0.16	0.50	0.75	1.00	1
3	0.70	0.66	0.68	0.32	0.50	0.36	0.33	1.00	0.00	1
4	0.78	0.75	0.65	0.35	0.45	0.45	0.17	1.00	1.00	1
5	0.85	0.81	0.64	0.36	0.60	0.67	0.50	0.50	0.50	1
6	0.75	0.72	0.58	0.42	0.50	0.27	0.33	0.75	0.50	1
7	0.84	0.80	0.49	0.51	0.40	0.45	0.83	0.25	1.00	1
8	0.74	0.71	0.60	0.40	0.54	0.78	0.67	0.50	0.50	1
9	0.86	0.83	0.56	0.44	0.59	0.51	0.50	0.25	0.00	1
10	0.80	0.77	0.53	0.47	0.43	0.18	0.67	0.75	1.00	1

Product ID (8): current solution.

are offset each other. For product 1, SI-NC is −0.08 and SI-IC is 0.26. Offset of these values yields the final value of TSI as 0.00 due to the weighted value.

This study proposed the feasibility of TSI, SI-NC, and SI-IC in case study. TSI, SI-IC, and SI-NC enable suitability analysis, automatic product search, optimal decision-making, and risk review based on requirement.

For this, development of the computer program using logic of TSI, SI-IC, and SI-NC is required.

8.6. Summary of Case Study. Multiple performances were analyzed by using 10 sample data. The performance items were redefined as the unique technical characteristic based on the functional requirement. The 10 samples were evaluated based on the corresponding performance criteria since performance has both PIS and NIS. In turn, benchmarking based on performance item was conducted under assumption of the project's characteristics and user's requirement.

TPC in relation to the envelope performance was defined, and TSI, SI-IC, and SI-NC of the 10 samples were analyzed with the TPC. The product ID 1 was selected as the most optimal alternative based on the requirements.

Therefore, this study validated the benchmarking logic in QFD by using TOPSIS and SI.

Table 3: Weighted data for users' preference.

Product	U value (glazing)	U value (total)	SHGC (summer)	SHGC (winter)	VT	CR	AT	Aesthetic	WS	WT	Preference and rank	
	Distance scale	Distance scale	Distance scale	Distance scale	Distance scale	Distance scale	Distance scale	Ordinal scale (5)	Ordinal scale (3)	Binary scale		
Max	4.2	10.0	1.5	1.5	1.5	1.5	4.2	1.5	4.2	4.2		
Min	0.0	0.0	0.0	0.0	0.0	0.0	0.0	0.0	0.0	0.0		
1	3.5	8.0	1.0	0.5	0.5	0.3	2.8	0.8	4.2	4.2	0.75	2
2	3.2	7.3	0.9	0.6	0.6	0.2	2.1	1.1	4.2	4.2	0.71	3
3	3.0	6.6	1.0	0.5	0.8	0.6	1.4	1.5	0.0	4.2	0.57	7
4	3.3	7.5	1.0	0.5	0.7	0.7	0.7	1.5	4.2	4.2	0.71	3
5	3.6	8.1	1.0	0.5	0.9	1.0	2.1	0.8	2.1	4.2	0.71	3
6	3.2	7.2	0.9	0.6	0.8	0.4	1.4	1.1	2.1	4.2	0.64	5
7	3.6	8.0	0.7	0.8	0.6	0.7	3.5	0.4	4.2	4.2	0.77	1
8	3.1	7.1	0.9	0.6	0.8	1.2	2.8	0.8	2.1	4.2	0.69	4
9	3.6	8.3	0.8	0.7	0.9	0.8	2.1	0.4	0.0	4.2	0.63	6
10	3.4	7.7	0.8	0.7	0.7	0.3	2.8	1.1	4.2	4.2	0.75	2

Product ID (8): current solution; product ID (7): benchmarking solution.

Table 4: Comparison in initial performance data.

Product	U value (glazing)	U value (total)	SHGC (summer)	SHGC (winter)	VT	CR	AT	Aesthetic	WS	WT
	Distance scale	Distance scale	Distance scale	Distance scale	Distance scale	Distance scale	Distance scale	Ordinal scale (5)	Ordinal scale (3)	Binary scale
7	0.16	0.20	0.51	0.51	40	50	0.01	2	3	1
8	0.26	0.29	0.40	0.40	54	68	0.02	3	2	1
11	0.16	0.20	0.40	0.40	54	68	0.01	3	2	1

Product ID (8): current solution; product ID (7): benchmarking solution; product ID (11): RPC.

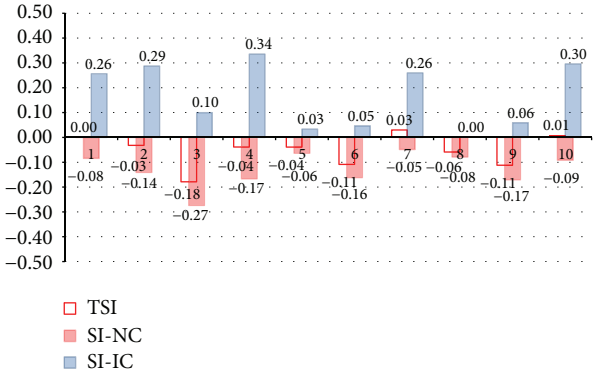

Figure 9: Suitability Index for market product.

9. Conclusions

Current new technology in the market is the best subject for benchmarking for performance improvement of buildings. Designers and users can define TPC by conducting investigations on the performance status of market products. QFD benchmarking methods proposed in existing studies have been limitedly used in benchmarking utilization due to subjective evaluations on users' requirements and functions. In this study, TOPSIS was adopted for multicriteria decision in order to improve industrial utility of QFD and secure the objectiveness of the product evaluation.

(1) This case study confirmed the feasibility of benchmarking based on QFD-TOPSIS and QFD-SI in field of BEPA.

(2) QFD-TOPSIS assessment model evaluates users' preference and provides performance improvement criteria result from benchmarking of market products.

(3) QFD-SI proposes suitability information that is generated to compare with users' RPC and PAP in the market.

(4) QFD based TOPSIS and SI logic in this study was confirmed to be eligible for application to the multicriteria decision-making problems that occur in broad range of the engineering industry.

For future studies, a web-based QFD knowledge system in which project stakeholders can share performance information will be studied.

Table 5: Comparison in weighted data.

Product	U value (glazing)	U value (total)	SHGC (summer)	SHGC (winter)	VT	CR	AT	Aesthetic	WS	WT
	Distance scale	Distance scale	Distance scale	Distance scale	Distance scale	Distance scale	Distance scale	Ordinal scale (5)	Ordinal scale (3)	Binary scale
7	3.6	8.0	0.7	0.8	0.6	0.7	3.5	0.4	4.2	4.2
8	3.1	7.1	0.9	0.6	0.8	1.2	2.8	0.8	2.1	4.2
11	3.6	8.0	0.9	0.6	0.8	1.2	3.5	0.8	2.1	4.2

Product ID (8): current solution; product ID (7): benchmarking solution; product ID (11): RPC.

Table 6: Suitability Index.

Product ID	1	2	3	4	5	6	7	8	9	10
TSI	0.00	−0.03	−0.18	−0.04	−0.04	−0.11	0.03	−0.06	−0.11	0.01
SI-NC	−0.08	−0.14	−0.27	−0.17	−0.06	−0.16	−0.05	−0.08	−0.17	−0.09
SI-IC	0.26	0.29	0.10	0.34	0.03	0.05	0.26	0.00	0.06	0.30

Disclosure

The first author is Jaeho Cho.

Conflict of Interests

The authors declare that there is no conflict of interests regarding the publication of this paper.

Acknowledgments

This research was supported by a grant (15AUDP-C067809-03) from Architecture & Urban Development Research Program funded by Ministry of Land, Infrastructure and Transport of Korean government. This research was supported by the National Research Foundation of Korea (NRF) (no. NRF-2012R1A1A2043186).

References

[1] R. M. Fifer, "Cost benchmarking functions in the value chain," *Strategy & Leadership*, vol. 17, no. 3, pp. 18–19, 1989.

[2] I. Dikmen, M. Talat Birgonul, and S. Kiziltas, "Strategic use of quality function deployment (QFD) in the construction industry," *Building and Environment*, vol. 40, no. 2, pp. 245–255, 2005.

[3] A. Bolar, S. Tesfamariam, and R. Sadiq, "Management of civil infrastructure systems: QFD-based approach," *Journal of Infrastructure Systems*, vol. 20, no. 1, Article ID 04013009, 2014.

[4] J. Chun and J. Cho, "QFD model based on a suitability assessment for the reduction of design changes in unsatisfactory quality," *Journal of Asian Architecture and Building Engineering*, vol. 14, no. 1, pp. 113–120, 2015.

[5] P.-C. Liao, W. J. O'Brien, S. R. Thomas, J. Dai, and S. P. Mulva, "Factors affecting engineering productivity," *Journal of Management in Engineering*, vol. 27, no. 4, pp. 229–235, 2011.

[6] C. E. Bogan and M. J. English, *Benchmarking for Best Practices: Winning Through Innovative Adaptation*, Best Practices, LLC, New York, NY, USA, 1994.

[7] B. Ghahramani and A. Houshyar, "Benchmarking the application of quality function deployment in rapid prototyping," *Journal of Materials Processing Technology*, vol. 61, no. 1-2, pp. 201–206, 1996.

[8] A. Kumar, J. Antony, and T. S. Dhakar, "Integrating quality function deployment and benchmarking to achieve greater profitability," *Benchmarking*, vol. 13, no. 3, pp. 290–310, 2006.

[9] L. Pérez-Lombard, J. Ortiz, R. González, and I. R. Maestre, "A review of benchmarking, rating and labelling concepts within the framework of building energy certification schemes," *Energy and Buildings*, vol. 41, no. 3, pp. 272–278, 2009.

[10] P. Fazio, H. S. He, A. Hammad, and M. Horvat, "IFC-based framework for evaluating total performance of building envelopes," *Journal of Architectural Engineering*, vol. 13, no. 1, pp. 44–53, 2007.

[11] W. F. E. Preiser and J. C. Vischer, *Assessing Building Performance*, Routledge, 2012, First published by: Elsevier 2005.

[12] C. J. Kibert, *Sustainable Construction: Green Building and Delivery*, John Wiley & Sons, Hoboken, NJ, USA, 2nd edition, 2008.

[13] WBDG, "Building Envelope Design Guide-Curtain Walls," http://www.wbdg.org/design/env_fenestration_cw.php.

[14] A. Aksamija, *Perkins+Will, Sustainable Facades*, John Wiley & Sons, Hoboken, NJ, USA, 2013.

[15] J. Lee and J. Chun, "A numerical value evaluation model for the optimum design selection," *Journal of Asian Architecture and Building Engineering*, vol. 11, no. 2, pp. 283–290, 2012.

[16] L. Sui Pheng and D. L. L. T'ng, "Factors influencing design development time of commercial properties in Singapore," *Facilities*, vol. 16, no. 1/2, pp. 40–51, 1998.

[17] J. Marsot, "QFD: a methodological tool for integration of ergonomics at the design stage," *Applied Ergonomics*, vol. 36, no. 2, pp. 185–192, 2005.

[18] M. Kagioglou, R. Cooper, G. Aouad, and M. Sexton, "Rethinking construction: the generic design and construction process protocol," *Engineering Construction and Architectural Management*, vol. 7, no. 2, pp. 141–153, 2000.

[19] S. Austin, A. Newton, J. Steele, and P. Waskett, "Modelling and managing project complexity," *International Journal of Project Management*, vol. 20, no. 3, pp. 191–198, 2002.

[20] J. A. Carnevalli and P. C. Miguel, "Review, analysis and classification of the literature on QFD—types of research, difficulties

and benefits," *International Journal of Production Economics*, vol. 114, no. 2, pp. 737–754, 2008.

[21] R. A. Mohsini, "Performance and building: problems of evaluation," *Journal of Performance of Constructed Facilities*, vol. 3, no. 4, pp. 235–242, 1989.

[22] N. Singhaputtangkul, S. P. Low, A. L. Teo, and B.-G. Hwang, "Knowledge-based decision support system quality function deployment (KBDSS-QFD) tool for assessment of building envelopes," *Automation in Construction*, vol. 35, pp. 314–328, 2013.

[23] S. O. Ogunlana, "Construction professional's perception of critical success factors for large-scale construction projects," *Construction Innovation*, vol. 9, no. 2, pp. 149–167, 2009.

[24] P. Rashvand and M. Z. Abd Majid, "Critical criteria on client and customer satisfaction for the issue of performance measurement," *Journal of Management in Engineering*, vol. 30, no. 1, pp. 10–18, 2014.

[25] M. Xie, K. C. Tan, and T. N. Goh, *Advanced QFD Applications*, ASQ Quality Press, Milwaukee, Wis, USA, 2003.

[26] J. A. Harding, K. Popplewell, R. Y. K. Fung, and A. R. Omar, "Intelligent information framework relating customer requirements and product characteristics," *Computers in Industry*, vol. 44, no. 1, pp. 51–65, 2001.

[27] M. Li, L. Jin, and J. Wang, "A new MCDM method combining QFD with TOPSIS for knowledge management system selection from the user's perspective in intuitionistic fuzzy environment," *Applied Soft Computing*, vol. 21, pp. 28–37, 2014.

[28] Y. Q. Yang, S. Q. Wang, M. Dulaimi, and S. P. Low, "A fuzzy quality function deployment system for buildable design decision-makings," *Automation in Construction*, vol. 12, no. 4, pp. 381–393, 2003.

[29] L.-K. Chan and M.-L. Wu, "A systematic approach to quality function deployment with a full illustrative example," *Omega*, vol. 33, no. 2, pp. 119–139, 2005.

[30] L.-H. Chen and W.-C. Ko, "Fuzzy approaches to quality function deployment for new product design," *Fuzzy Sets and Systems*, vol. 160, no. 18, pp. 2620–2639, 2009.

[31] R. Y. Fung, Y. Chen, and J. Tang, "Estimating the functional relationships for quality function deployment under uncertainties," *Fuzzy Sets and Systems*, vol. 157, no. 1, pp. 98–120, 2006.

[32] S. Yousefie, M. Mohammadi, and J. H. Monfared, "Selection effective management tools on setting European Foundation for Quality Management (EFQM) model by a quality function deployment (QFD) approach," *Expert Systems with Applications*, vol. 38, no. 8, pp. 9633–9647, 2011.

[33] Y. Lin, H.-P. Cheng, M.-L. Tseng, and J. C. C. Tsai, "Using QFD and ANP to analyze the environmental production requirements in linguistic preferences," *Expert Systems with Applications*, vol. 37, no. 3, pp. 2186–2196, 2010.

[34] H. Raharjo, A. C. Brombacher, and M. Xie, "Dealing with subjectivity in early product design phase: a systematic approach to exploit quality function deployment potentials," *Computers & Industrial Engineering*, vol. 55, no. 1, pp. 253–278, 2008.

[35] C. Garibay, H. Gutiérrez, and A. Figueroa, "Evaluation of a digital library by means of quality function deployment (QFD) and the kano model," *Journal of Academic Librarianship*, vol. 36, no. 2, pp. 125–132, 2010.

[36] M. Azadi and R. Farzipoor Saen, "A combination of QFD and imprecise DEA with enhanced Russell graph measure: a case study in healthcare," *Socio-Economic Planning Sciences*, vol. 47, no. 4, pp. 281–291, 2013.

[37] Y.-L. Li, J.-F. Tang, K.-S. Chin, Y. Han, and X.-G. Luo, "A rough set approach for estimating correlation measures in quality function deployment," *Information Sciences*, vol. 189, pp. 126–142, 2012.

[38] T. Park and K.-J. Kim, "Determination of an optimal set of design requirements using house of quality," *Journal of Operations Management*, vol. 16, no. 5, pp. 569–581, 1998.

[39] M. E. Pullman, W. L. Moore, and D. G. Wardell, "A comparison of quality function deployment and conjoint analysis in new product design," *The Journal of Product Innovation Management*, vol. 19, no. 5, pp. 354–364, 2002.

[40] H. Moskowitz and K. J. Kim, "QFD optimizer: a novice friendly quality function deployment decision support system for optimizing product designs," *Computers and Industrial Engineering*, vol. 32, no. 3, pp. 641–655, 1997.

[41] D. Ginn and M. Zairi, "Best practice QFD application: an internal/external benchmarking approach based on ford motors' experience," *International Journal of Quality and Reliability Management*, vol. 22, no. 1, pp. 38–58, 2005.

[42] W. Yan, L. P. Khoo, and C.-H. Chen, "A QFD-enabled product conceptualisation approach via design knowledge hierarchy and RCE neural network," *Knowledge-Based Systems*, vol. 18, no. 6, pp. 279–293, 2005.

[43] R. Y. K. Fung, Y. Chen, and J. Tang, "Estimating the functional relationships for quality function deployment under uncertainties," *Fuzzy Sets and Systems*, vol. 157, no. 1, pp. 98–120, 2006.

[44] S. M. Ahmed, L. P. Sang, and Ž. M. Torbica, "Use of quality function deployment in civil engineering capital project planning," *Journal of Construction Engineering and Management*, vol. 129, no. 4, pp. 358–368, 2003.

[45] H. Moskowitz and K. J. Kim, "QFD optimizer: a novice friendly quality function deployment decision support system for optimizing product designs," *Computers & Industrial Engineering*, vol. 32, no. 3, pp. 641–655, 1997.

[46] C. L. Hwang and K. P. Yoon, *Multiple Attribute Decision Making: Methods and Appli-Cations*, Springer, New York, NY, USA, 1981.

[47] Z. Xu and R. R. Yager, "Dynamic intuitionistic fuzzy multi-attribute decison making," *International Journal of Approximate Reasoning*, vol. 48, no. 1, pp. 246–262, 2008.

[48] C. L. Hwang and K. P. Yoon, *Multiple Attribute Decision Making: Methods and Applications*, vol. 186 of *Lecture Notes in Economics and Mathematical Systems*, Springer, New York, NY, USA, 1981.

Hindawi Publishing Corporation
Mathematical Problems in Engineering
Volume 2015, Article ID 710264, 7 pages
http://dx.doi.org/10.1155/2015/710264

Research Article

Cross-Efficiency Evaluation Method with Compete-Cooperate Matrix

Qiang Hou and Xue Zhou

School of Management, Shenyang University of Technology, Shenyang, Liaoning 110870, China

Correspondence should be addressed to Xue Zhou; 15998806313@163.com

Received 26 April 2015; Accepted 5 July 2015

Academic Editor: Jurgita Antucheviciene

Cross-efficiency evaluation method is an effective and widespread adopted data envelopment analysis (DEA) method with self-assessment and peer-assessment to evaluate and rank decision making units (DMUs). Extant aggressive, benevolent, and neutral cross-efficiency methods are used to evaluate DMUs with competitive, cooperative, and nontendentious relationships, respectively. In this paper, a symmetric (nonsymmetric) compete-cooperate matrix is introduced into aggressive and benevolent cross-efficiency methods and compete-cooperate cross-efficiency method is proposed to evaluate DMUs with diverse (relative) relationships. Deviation maximization method is applied to determine the final weights of cross-evaluation to enhance the differentiation ability of cross-efficiency evaluation method. Numerical demonstration is provided to illustrate the reasonability and practicability of the proposed method.

1. Introduction

Data envelopment analysis (DEA) is a nonparametric programming method for evaluating the relative efficiencies of a group of decision making units (DMUs) with multiple inputs and outputs. Since Charnes et al. [1] proposed the CCR model in 1978 and Banker et al. [2] proposed the BCC model in 1984, DEA is widely used in various fields. The traditional DEA models, including the CCR and BCC model, are based on self-assessment system; the obtained input and output weights of evaluated DMUs take the aim at maximizing their own efficiency, which will cause problems in three aspects. (1) The traditional DEA models can only distinguish the efficient and inefficient DMUs but cannot rank the merits and with a lower degree of differentiation on CCR-efficient DMUs. (2) The obtained efficiency weights are only beneficial to the single DMU, which is easy to exaggerate its own advantages in some inputs and outputs angles, but circumvent its disadvantages in other input and output angles, resulting in lip-deep efficient phenomena. (3) Each DMU selects its own favorable weighting scheme, lacking comparability among DMUs.

In response to these problems, scholars have proposed a number of improvements [3–5]; the typical methods include cross-efficiency evaluation method [6], public-weight method [7], superefficient DEA method [8], and other DEA methods, wherein the cross-efficiency evaluation method has been applied repeatedly, which is proposed by Sexton et al. [9] in 1986, as an expansion and improvement of traditional DEA model. The essence of the method is the introduction of peer-assessment system, using self-assessment and peer-assessment system to evaluate the efficiencies of DMUs. The cross-efficiency method is possible to get complete ranks and comparable evaluated scores, which has a higher degree of differentiation on CCR-efficient DMUs. Therefore, this method has been widespread and widely used to deal with specific problems in academic fields [10–13].

But the cross-efficiency method may fall into a predicament of multiple solutions, so many scholars have been keen on the improvement of the traditional cross-efficiency model. The typical treatments to avoid the problem include Doyle and Green's [14] aggressive and benevolent cross-efficiency evaluation methods, which introduce secondary objective functions to cross-efficiency evaluation method and can select the optimal weights to minimize and maximize the sum of the outputs of other DMUs, respectively. Later Wang and Chin [15], based on the aggressive and benevolent

methods, propose the neutral DEA model, which has effectively reduced the number of zero outputs' weights. Wu et al. [16] introduce secondary goals in cross-efficiency evaluation to avoid multiple solutions, they propose a novel model to determine the final cross-efficiency and optimize the ranking order, they indicate that pursuing the best ranking is more important than maximizing the individual score, and this model is able to draw the best ranking. Jahanshahloo et al. [17] also introduce secondary goals to cross-efficiency and select symmetric weights and propose the symmetric weight assignment technique (SWAT) method to effectively select weights from multiple optimal solutions. Wu et al. [18] propose a weight-balanced DEA method to deal with the nonunique cross-efficiency scores resulting from the presence of alternate optima in traditional DEA models. This method can effectively lessen the differences in weighted data and reduce the zero weights. Wang et al. [19] introduce a virtual ideal DMU (IDMU) and a virtual antideal DMU (ADMU) to cross-efficiency evaluation method, propose several new DEA models, and result in neutral cross-evaluation scores, which enhance the theory and methodology of cross-efficiency evaluation method and can be more neutral and logical. Wang et al. [20] introduce neutral input and output weights for each DMU, replace the aggressive or benevolent ones, thus minimize the virtual disparity in cross-efficiency evaluation, and reduce the number of zero weights.

In this paper, we mainly aim for the improvement on the practicality and application of cross-efficiency evaluation method. The benevolent, aggressive, and neutral cross-efficiency evaluation methods suppose that the relationships of DMUs are absolutely partnership, competitive, and nontendentious, respectively. But in practical applications, the following two situations generally exist. (1) The relationships of evaluated DMUs are complex; they not only involve partnership relationships but also involve competitive relationships. (2) The relationship of a pair of DMUs is relativity. A DMU regards another DMU as friend and partner, while another DMU regards the DMUs as enemies and rivals. Focusing on the two situations, we introduce a compete-cooperate matrix into aggressive and benevolent cross-efficiency methods and build compete-cooperate cross-efficiency model. Our method can effectively evaluate the efficiencies of DMUs which has complex relationships compared to extant cross-efficiency methods. In addition, extant cross-efficiency methods obtain the final scores of DMUs by calculating the average of self-assessment scores and peer-assessment scores. This method sets all DMUs on equal status, with lower degree of differentiation on self-assessment and peer-assessment. In this paper, we apply the deviation maximization method [21] to calculate the weights of each model, which give different evaluated scores with different importance and can effectively widen the gap of scores of DMUs.

The paper is arranged as follows. Section 2 introduces the CCR model, aggressive model, benevolent model, and neutral model. Section 3 introduces the proposed compete-cooperate cross-efficiency model and the deviation maximization method. Section 4 provides a numerical example. Section 5 finally shows the conclusion.

2. Traditional Cross-Efficiency Models

Let there be n DMUs, where DMU_j $(j = 1, 2, \ldots, n)$ uses m kind of resources to produce s kind of outputs. The input and output vectors can be denoted as $x_j = (x_{1j}, x_{2j}, \ldots, x_{mj})$ and $y_j = (y_{1j}, y_{2j}, \ldots, y_{sj})$. Then, for a given DMU_d $(1 \le d \le n)$, its efficiency score of E_{dd} can be determined by the CCR model as follows:

$$\begin{aligned} \max \quad & E_{dd} = \sum_{r=1}^{s} \mu_{rd} y_{rd} \\ \text{s.t.} \quad & \sum_{i=1}^{m} v_{id} x_{id} = 1 \\ & \sum_{i=1}^{m} v_{id} x_{ij} - \sum_{r=1}^{s} \mu_{rd} y_{rj} \ge 0, \quad j = 1, 2, \ldots, n \\ & \mu_{rd} \ge 0, \ v_{id} \ge 0, \ r = 1, 2, \ldots, s; \ i = 1, 2, \ldots, m, \end{aligned} \tag{1}$$

where v_{id} $(i = 1, 2, \ldots, m)$ and μ_{rd} $(r = 1, 2, \ldots, s)$ are the weights assigned to x_{ij} and y_{ij}, respectively. Let E^*_{dd} be the CCR-efficiency score of DMU_d and reflect its self-assessment and let $v^*_{1d}, \ldots, v^*_{md}, \mu^*_{1d}, \ldots, \mu^*_{sd}$ be the optimal solutions to model (1). Then the cross-efficiency model where we can obtain the cross-efficiency scores of all the DMUs with self-assessment score and peer-assessment scores can be presented as

$$\begin{aligned} \theta^*_{jd} &= \frac{\sum_{r=1}^{s} \mu^*_{rj} y_{rd}}{\sum_{i=1}^{m} v^*_{rj} x_{id}}, \quad j = 1, \ldots, n; \ j \ne d \\ \overline{\theta}^*_d &= \frac{1}{n} \left(\sum_{j=1, j \ne d}^{n} \theta^*_{jd} + E^*_{dd} \right). \end{aligned} \tag{2}$$

Using the average cross-efficiency scores, we can compare and rank all the DMUs. However, the cross-efficiency scores may not be unique because of the existence of alternate optimal weights, which reduce the usefulness of the cross-efficiency evaluation method. To resolve the problem, the most representative and most applied model and the aggressive and benevolent cross-efficiency models are proposed by Doyle and Green, which can be shown as follows:

$$\begin{aligned} \text{min or max} \quad & \sum_{r=1}^{s} \left(\mu_{rd} \sum_{j=1, j \ne d}^{n} y_{rj} \right) \\ \text{s.t.} \quad & \sum_{i=1}^{m} v_{id} \left(\sum_{j=1, j \ne d}^{n} x_{ij} \right) = 1 \\ & \sum_{r=1}^{s} \mu_{rd} y_{rd} - E^*_{dd} \sum_{i=1}^{m} v_{id} x_{id} = 0 \\ & \sum_{i=1}^{m} v_{id} x_{id} - \sum_{r=1}^{s} \mu_{rd} y_{rd} \ge 0 \end{aligned}$$

$$
\begin{aligned}
&j = 1, 2, \ldots, n;\ \ j \neq d \\
&\mu_{rd} \geq 0,\ \ v_{id} \geq 0, \\
&r = 1, 2, \ldots, s;\ \ i = 1, 2, \ldots, m,
\end{aligned} \tag{3}
$$

where E^*_{dd} is the CCR-efficiency score of DMU_d obtained from model (1). The aggressive efficiency model, with a min-objective function in model (3), is given to minimize the other DMUs' cross-efficiency on the promise of unchanged CCR-efficiency value, and the benevolent efficiency model, with a max-objective function, is given to maximize the cross-efficiency of other DMUs. Then Wang and Chin, based on aggressive and benevolent models, proposed a neutral DEA model for cross-efficiency evaluation; the model is presented as

$$
\begin{aligned}
\max \quad & \delta = \min_{r \in \{1, \ldots, s\}} \left(\frac{\mu_{rd} y_{rd}}{\sum_{i=1}^{m} v_{id} x_{id}} \right) \\
\text{s.t.} \quad & \sum_{r=1}^{s} \mu_{rd} y_{rj} - \sum_{i=1}^{m} v_{rd} x_{ij} \leq 1 \\
& \sum_{r=1}^{s} \mu_{rd} y_{rd} - E_{dd} \sum_{i=1}^{m} v_{id} x_{id} = 0 \\
& j = 1, 2, \ldots, n;\ \ j \neq d \\
& \mu_{rd} \geq 0,\ \ r = 1, 2, \ldots, s \\
& v_{id} \geq 0,\ \ i = 1, 2, \ldots, m,
\end{aligned} \tag{4}
$$

where $\mu_{rd} y_{rd} / \sum_{i=1}^{m} v_{id} x_{id}$ is the efficiency of the DMU_d of the rth output. Compared with the aggressive and benevolent methods, there is no difficulty for DMUs to make a subjective choice and determine the input and output weights just from their own perspective in neutral DEA method.

3. Compete-Cooperate Cross-Efficiency Model

3.1. Compete-Cooperate Matrix and Compete-Cooperate Cross-Efficiency Model. In actual application of cross-efficiency method, we often encounter the following two situations. (1) The relationships of DMUs are complex; there not only exist partner related DMUs, but also involve competitive related DMUs. (2) The relationship between two DMUs is relativity. Some DMU_j ($j = 1, 2, \ldots, n$) reckons DMU_g ($g = 1, 2, \ldots, n$, $g \neq j$) as a cooperative partner, while DMU_g ($g = 1, 2, \ldots, n$, $g \neq j$) reckons DMU_j ($j = 1, 2, \ldots, n$) as a competitor. In these cases, we cannot simply use aggressive or benevolent cross-efficiency model to calculate the values of DMUs.

In this paper, we introduce a cross-efficiency model with compete-cooperate matrix to resolve these problems. First of all, we should build the compete-cooperate matrix. For the first situation, we argue that if two DMUs are cooperative partners, set the coefficient of the matrix as 1. However, if the relationship between two DMUs is competition, then set the coefficient of the matrix as −1. The coefficient of self-assessment will be 0. For the second situation, we argue that if DMU_j ($j = 1, 2, \ldots, n$) reckons DMU_g ($g = 1, 2, \ldots, n$, $g \neq j$) as a cooperative friend, set the coefficient of the matrix as 1. If DMU_g ($g = 1, 2, \ldots, n$, $g \neq j$) reckons DMU_j ($j = 1, 2, \ldots, n$) as a competitor, set the coefficient of the matrix as −1 and set the coefficient of self-assessment as 0. For the first situation, the compete-cooperate matrix is a symmetric matrix and for the second situation, the matrix is a nonsymmetric matrix. Then the compete-cooperate cross-efficiency model is built as follows:

$$
\begin{aligned}
\max \quad & \sum_{r=1}^{s} \mu_{rd} \left(\sum_{j=1}^{n} g_{rj} y_{rj} \right) \\
\text{s.t.} \quad & \sum_{i=1}^{m} v_{id} \sum_{j=1}^{n} x_{ij} = 1 \\
& \sum_{i=1}^{m} v_{id} x_{id} - \sum_{r=1}^{s} \mu_{rd} y_{rd} \geq 0 \\
& \sum_{r=1}^{s} \mu_{rd} y_{rd} - E^*_{dd} \sum_{i=1}^{m} v_{id} x_{id} = 0 \\
& j = 1, 2, \ldots, n \\
& \mu_{rd} \geq 0,\ \ v_{id} \geq 0, \\
& r = 1, 2, \ldots, s;\ \ i = 1, 2, \ldots, m,
\end{aligned} \tag{5}
$$

where g_{rj} is the compete-cooperate relationship matrix, determined by the relationship of DMUs, and E^*_{dd} is the CCR-efficiency value of DMU_d obtained from model (1). Obviously, the compete-cooperate cross-efficiency model can effectively evaluate the efficiencies of DMUs with complex and relative relationship. It is the biggest advantage of the compete-cooperate cross-efficiency model.

3.2. Deviation Maximization Method. Extant cross-efficiency evaluation methods, like aggressive, benevolent, and neutral methods, generally seek the final cross-efficiency scores by calculating the average after determining the self- and peer-assessment scores of each DMU; then each of the evaluated scores participates in the evaluation on the equal weights. Generally speaking, when we evaluate the m index of n DMUs, we usually want to widen the gap of DMUs' efficiency values, in order to pull the grade, facilitate the sorting, and enhance the ability of differentiation. So we need to choose the best weight coefficient index to widen the gap of the efficiency values of the DMUs. Assuming $\omega = (\omega_1, \omega_2, \ldots, \omega_m)^T$ is the weight coefficient vector and $x_i = (x_{i1}, x_{i2}, \ldots, x_{im})^T$ is m vectors of the i evaluation object, the scoring matrix

$$
A = \begin{bmatrix}
x_{11} & x_{12} & \cdots & x_{1m} \\
x_{21} & x_{22} & \cdots & x_{2m} \\
\vdots & \vdots & \vdots & \vdots \\
x_{n1} & x_{n2} & \cdots & x_{nm}
\end{bmatrix}. \tag{6}
$$

Table 1: Description of the inputs and outputs of 30 provinces.

	Indices	Description	Unit	Average	Median
Inputs	x_1	R&D expenditure	10^9 yuan	343.22	258.38
	x_2	R&D personnel FTE	10^4 man	10.82	8.05
	x_3	Amount of technical inflow contract	10^9 yuan	187.58	122.45
Outputs	y_1	Number of accepted domestic patents	Piece	38115.53	20025
	y_2	Output value for new products	10^9 yuan	852.30	201.94
	y_3	Amount of contract deals in technical markets	10^9 yuan	194.70	63.54

Table 2: Stage of economic development division (unit: yuan).

Stage of economic development	Primary	Industrialization I	Industrialization II	Industrialization III	Industrialization IV	Advanced
Per capita income limit	4742.39	9471.364	18949.44	36684.77	71048.65	113683.2
Per capita income ceiling	9471.364	18949.44	36684.77	71048.65	113683.2	170524.8

Then the final scores of n DMUs can be presented as

$$Y = A\omega, \tag{7}$$

where $y = (y_1, y_2, \ldots, y_n)^T$ is the final score vector of n DMUs and y_i is the efficiency value of DMU$_j$ $(j = 1, 2, \ldots, n)$; in order to widen the gap between DMUs' efficiency values, we need to make the variance of efficiency values as large as possible, which can be presented as

$$\max s^2 = \frac{1}{n-1}\sum_{i=1}^{n}\left(y_i - \overline{y}\right)^2. \tag{8}$$

Put (7) into (8), and normalize the raw data; the following equation will be obtained:

$$ns^2 = \omega^T A^T A\omega = \omega^T H\omega, \tag{9}$$

where $H = A^T A$ is a real symmetric matrix. ω is the weight vector; so $\omega^T\omega = 1$. Therefore, the way to make the variance can be described as

$$\begin{aligned} \max \quad & \omega^T H\omega \\ \text{s.t.} \quad & \omega^T\omega = 1 \\ & \omega > 0, \end{aligned} \tag{10}$$

where ω is the eigenvector for the maximum eigenvalue of H, and (10) gets its maximum value. Then normalize ω to obtain the optimal weight coefficient vector. Consider $\omega^* = (\omega_1^*, \omega_2^*, \ldots, \omega_n^*)^T$. In this paper, the deviation maximization method is applied to obtain the final weight factor for aggressive, benevolent, neutral, and proposed compete-cooperate cross-efficiency methods.

4. An Illustrative Example

In this section, we use a specific example to illustrate our method. The example aims at evaluating the technology innovation efficiency of domestic 31 provinces (DMUs). Each province has to be evaluated in terms of three inputs (x_1, x_2, x_3) and three outputs (y_1, y_2, y_3). Because of the incomplete data of the Tibet Autonomous Region, we choose the remaining 30 provinces as DMUs. We use the data of the 30 provinces in 2012, obtained from *China Statistical Yearbook on Science and Technology* 2013 and economy prediction system. Table 1 shows the specific description of the inputs and outputs of 30 provinces.

In this paper, we only choose the first situation as an example, since the calculating process of the two situations is only different in the data of compete-cooperate matrix g_{rj}. We apply the CCR-efficiency method and the aggressive, benevolent, and neutral cross-efficiency methods and report their scores in this section to be compared with the proposed compete-cooperate cross-efficiency model for some necessary analysis. First of all, we need to give certain values to the compete-cooperate matrix g_{rj}. This paper, according to regional GDP in 2012, divides GDP amount of 30 provinces into 6 stages; Table 2 shows the specific stage of each section. We argue that the relationship of two provinces whose GDP amount belongs to the same interval is partnership; set the coefficient of the matrix as 1. The relationship of two provinces whose GDP amount belongs to different intervals is competition; set the coefficient of the matrix as −1. Set the coefficient of self-assessment as 0.

In this paper, we apply the deviation maximization method to get the optimal weights. Table 3 shows the weights for aggressive, benevolent, neutral, and proposed compete-cooperate cross-efficiency models. Table 4 shows the final efficiency scores and ranks of the 30 provinces in CCR, aggressive, benevolent, neutral, and proposed DEA models.

It can be seen from the example scores and ranks that the traditional CCR-efficiency model has lower differentiation on CCR-efficient DMUs; there are a number of CCR-efficient provinces, including Zhejiang, Anhui, Beijing, Guangdong, and Jiangsu provinces, while using the cross-efficiency evaluation method did not get such a result. Therefore,

Table 3: Optimal weights of aggressive, benevolent, neutral, and proposed models.

Benevolent		Aggressive		Neutral		Compete-cooperate	
0.0529	0.0207	0.0499	0.0234	0.0449	0.0264	0.0480	0.0226
0.0087	0.0316	0.0331	0.0297	0.0146	0.0315	0.0330	0.0298
0.0203	0.0271	0.0186	0.0241	0.0176	0.0353	0.0186	0.0245
0.0199	0.0539	0.0183	0.0441	0.0188	0.0488	0.0184	0.0444
0.0289	0.0119	0.0270	0.0141	0.0266	0.0077	0.0274	0.0135
0.0249	0.0200	0.0234	0.0203	0.0241	0.0407	0.0236	0.0203
0.0211	0.0448	0.0201	0.0377	0.0203	0.0514	0.0199	0.0388
0.0488	0.0400	0.0521	0.0373	0.0472	0.0362	0.0519	0.0377
0.0383	0.0392	0.0342	0.0406	0.0376	0.0428	0.0345	0.0399
0.0539	0.0360	0.0607	0.0361	0.0445	0.0353	0.0609	0.0365
0.0552	0.0477	0.0607	0.0406	0.0382	0.0470	0.0591	0.0407
0.0452	0.0452	0.0444	0.0448	0.0428	0.0381	0.0437	0.0454
0.0366	0.0377	0.0348	0.0407	0.0307	0.0397	0.0333	0.0420
0.0267	0.0148	0.0276	0.0151	0.0251	0.0183	0.0276	0.0151
0.0231	0.0248	0.0236	0.0229	0.0365	0.0312	0.0254	0.0234

Table 4: Scores and ranks of the 30 provinces of the 5 DEA models.

Province	CCR	Cross-efficiency methods			Proposed
		Benevolent	Aggressive	Neutral	
Beijing	1.0000 (1)	0.9416 (2)	0.7782 (3)	0.9327 (2)	0.8874 (3)
Tianjin	0.8812 (6)	0.5220 (12)	0.4479 (13)	0.5261 (12)	0.4920 (13)
Hebei	0.3069 (27)	0.2814 (25)	0.2495 (25)	0.2794 (25)	0.2656 (25)
Shanxi	0.2826 (29)	0.2268 (28)	0.1883 (28)	0.2180 (27)	0.2022 (27)
Inner Mongolia	0.4851 (22)	0.3209 (23)	0.2529 (24)	0.2906 (24)	0.2756 (24)
Liaoning	0.5161 (21)	0.3615 (22)	0.3014 (21)	0.3542 (21)	0.3279 (21)
Jilin	0.3683 (24)	0.2996 (24)	0.2619 (23)	0.2965 (23)	0.2853 (23)
Heilongjiang	0.8715 (7)	0.7100 (6)	0.6060 (6)	0.7008 (6)	0.6705 (6)
Shanghai	0.6940 (14)	0.5823 (9)	0.4968 (11)	0.5880 (9)	0.5523 (10)
Jiangsu	1.0000 (1)	0.9727 (1)	0.8931 (1)	0.9697 (1)	0.9264 (1)
Zhejiang	1.0000 (1)	0.9344 (3)	0.8648 (2)	0.9175 (3)	0.8886 (2)
Anhui	1.0000 (1)	0.7753 (4)	0.7222 (4)	0.7805 (4)	0.7686 (4)
Fujian	0.7333 (12)	0.4688 (15)	0.3962 (15)	0.4403 (16)	0.4054 (16)
Jiangxi	0.4506 (23)	0.4109 (19)	0.3554 (18)	0.4072 (19)	0.3844 (17)
Shandong	0.8549 (8)	0.5422 (10)	0.5489 (8)	0.5666 (10)	0.5720 (9)
Henan	0.7968 (11)	0.4887 (14)	0.4813 (12)	0.4980 (14)	0.5096 (12)
Hubei	0.5486 (20)	0.4540 (16)	0.3871 (16)	0.4544 (15)	0.4309 (15)
Hunan	0.8088 (10)	0.5188 (13)	0.5135 (10)	0.5329 (11)	0.5404 (11)
Guangdong	1.0000 (1)	0.7737 (5)	0.7203 (5)	0.7688 (5)	0.7407 (5)
Guangxi	0.2911 (28)	0.2352 (26)	0.2232 (26)	0.2319 (26)	0.2285 (26)
Hainan	0.3165 (26)	0.1747 (29)	0.1283 (29)	0.1463 (29)	0.1295 (29)
Chongqing	0.6921 (15)	0.4354 (18)	0.3542 (19)	0.4100 (18)	0.3682 (19)
Sichuan	0.6977 (13)	0.6131 (8)	0.5539 (7)	0.6175 (8)	0.5899 (8)
Guizhou	0.6456 (18)	0.4534 (17)	0.3698 (17)	0.4192 (17)	0.3830 (18)
Yunnan	0.5494 (19)	0.4026 (20)	0.3217 (20)	0.3770 (20)	0.3491 (20)
Shanxi	0.8268 (9)	0.6435 (7)	0.5300 (9)	0.6463 (7)	0.6132 (7)
Gansu	0.6540 (17)	0.5332 (11)	0.4226 (14)	0.5093 (13)	0.4782 (14)
Qinghai	0.6727 (16)	0.3920 (21)	0.2994 (22)	0.3367 (22)	0.3208 (22)
Ningxia	0.2377 (30)	0.1548 (30)	0.1209 (30)	0.1390 (30)	0.1259 (30)
Xinjiang	0.3669 (25)	0.2335 (27)	0.1884 (27)	0.2160 (28)	0.1953 (28)

Table 5: The results of Spearman correlation analysis for the five models.

Correlation coefficient	CCR	Benevolent	Aggressive	Neutral	Proposed
CCR	1.000	0.939	0.943	0.936	0.935
Benevolent	0.939	1.000	0.990	0.996	0.992
Aggressive	0.943	0.990	1.000	0.994	0.997
Neutral	0.936	0.996	0.994	1.000	0.996
Proposed	0.935	0.992	0.997	0.996	1.000

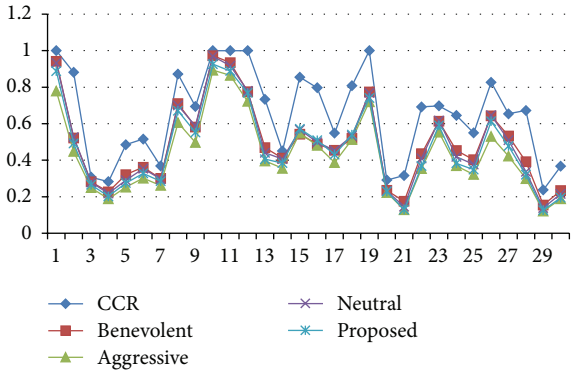

Figure 1: Efficiency scores of the five models.

the traditional CCR method which relies solely on self-assessment system has certain drawbacks compared with cross-efficiency evaluation method.

Table 4 shows the scores and ranks of 30 provinces from CCR, aggressive, benevolent, neutral, and proposed compete-cooperate DEA methods, which are different in some provinces, but there are still the same parts. Compared with CCR model, the 5 CCR-efficient provinces are top-ranked in proposed model, but there are also some provinces, such as Tianjin, which is ranked 6 in CCR model but ranked 13 in proposed model. Thus, the result of the analysis of proposed model is more flexible. Compared with aggressive, benevolent, and neutral cross-efficiency methods, provinces top-ranked from top 1 to top 6 are the same, including Jiangsu, Zhejiang, Beijing, Anhui, Guangdong, and Heilongjiang province, but there are still subtle differences on the ranking of individual provinces, such as Shanghai and Jiangxi province.

In this paper, Spearman method is used to analyze the correlation among CCR model, aggressive, benevolent, and neutral cross-efficiency model, and proposed compete-cooperate cross-efficiency method. Table 5 shows the results of Spearman correlation analysis for the five models. Correlation coefficients r_s are all between 0.9 and 1, which shows that the efficiency scores and ranks of the five methods are significantly correlated and highly consistent, but relatively speaking, the results of proposed method and aggressive method are highly consistent.

Figure 1 shows the efficiency scores of CCR, aggressive, benevolent, neutral, and proposed compete-cooperate DEA methods. It can be seen that the efficiency scores evaluated by traditional CCR model, benevolent model, and neutral model can be higher than other methods' scores; efficiency scores calculated by aggressive cross-efficiency method can be lower than other methods' scores. However, the scores of the 30 provinces calculated by proposed method are lower than CCR, benevolent, and neutral methods but higher than aggressive model. Although the extant cross-efficiency models, use self-assessment and peer-assessment system, can avoid the problem of appearing multiple CCR-efficient provinces in CCR model, complete competitive relationships in the aggressive model cause the lower scores, complete friendly relationships in the benevolent model cause the higher scores. The relationships of the provinces are non-tendentious in neutral model, while the proposed compete-cooperate cross-efficiency method takes the relationship of cooperation and competition of the provinces into account and produces more rational evaluated scores and more reliable ranks.

5. Conclusions

Cross-efficiency evaluation method is a method for assessing and evaluating the efficiency scores of DMUs, with self-assessment and peer-assessment system, avoiding low degree of differentiation of CCR-efficient DMUs in traditional CCR model. However, the aggressive, benevolent, and neutral cross-efficiency evaluation methods can only resolve the problem of DMUs with competitive, partnership, and non-tendentious relationships, respectively. But in practice, the relationships of DMUs are not absolute; there may exist two situations: (1) Some DMUs are cooperative partnership, but others are competitive relationship. (2) There exists relative relationship between two or several DMUs. Namely, some DMU_1 regards DMU_2 as a partner, while DMU_2 regards DMU_1 as a competitor. For these cases, this paper introduced a compete-cooperate matrix into aggressive and benevolent cross-efficiency models, built compete-cooperate cross-efficiency model, and applied deviation maximization method to obtain the final weight factor for cross-efficiency evaluation methods to widen the gap between the efficiency values of the DMUs. Furthermore, we use an example of technological innovation efficiency evaluation of the 30 provinces to analyze and interpret the proposed model. The results showed that proposed compete-cooperate cross-efficiency model has significant consistency with CCR, aggressive, benevolent, and neutral model; it can effectively evaluate the efficiency of DMUs with complex and relative relationship issues and enhance the stability and practicality of cross-efficiency evaluation. Future work may focus on determining the degree of authority of DMUs, namely, the weight of each DMU.

Conflict of Interests

There is no conflict of interests regarding the publication of this paper.

Acknowledgment

This paper is supported by Liaoning Education Department fund item "regional innovation efficiency evaluation and promotion strategy of Liaoning province" (serial no.: W2014026).

References

[1] A. Charnes, W. W. Cooper, and E. Rhodes, "Measuring the efficiency of decision making units," *European Journal of Operational Research*, vol. 2, no. 6, pp. 429–444, 1978.

[2] R. D. Banker, A. Charnes, and W. W. Cooper, "Some models for estimating technological and scale inefficiences in data envelopment analysis," *Management Science*, vol. 30, no. 9, pp. 1078–1092, 1984.

[3] R. G. Thompson, P. S. Dharmapala, and R. M. Thrall, "Importance for DEA of zeros in data, multipliers, and solutions," *Journal of Productivity Analysis*, vol. 4, no. 4, pp. 379–390, 1993.

[4] T. Entani and H. Tanaka, "Improvement of efficiency intervals based on DEA by adjusting inputs and outputs," *European Journal of Operational Research*, vol. 172, no. 3, pp. 1004–1017, 2006.

[5] P. Grösche, "Measuring residential energy efficiency improvements with DEA," *Journal of Productivity Analysis*, vol. 31, no. 2, pp. 87–94, 2009.

[6] R. H. Green, J. R. Doyle, and W. D. Cook, "Preference voting and project ranking using DEA and cross-evaluation," *European Journal of Operational Research*, vol. 90, no. 3, pp. 461–472, 1996.

[7] W. D. Cook and J. Zhu, "Within-group common weights in DEA: an analysis of power plant efficiency," *European Journal of Operational Research*, vol. 178, no. 1, pp. 207–216, 2007.

[8] J. Zhu, "Super-efficiency and DEA sensitivity analysis," *European Journal of Operational Research*, vol. 129, no. 2, pp. 443–455, 2001.

[9] T. R. Sexton, R. H. Silkman, and A. J. Hogan, "Data envelopment analysis: critique and extensions," in *Measuring Efficiency: An Assessment of Data Envelopment Analysis*, R. H. Silkman, Ed., vol. 32, pp. 73–105, Jossey-Bass, San Francisco, Calif, USA, 1986.

[10] J. Du, W. D. Cook, L. Liang, and J. Zhu, "Fixed cost and resource allocation based on DEA cross-efficiency," *European Journal of Operational Research*, vol. 235, no. 1, pp. 206–214, 2014.

[11] S. Lim, K. W. Oh, and J. Zhu, "Use of DEA cross-efficiency evaluation in portfolio selection: an application to Korean stock market," *European Journal of Operational Research*, vol. 236, no. 1, pp. 361–368, 2014.

[12] H. Tsai, J. Wu, and J. Sun, "Cross-efficiency evaluation of Taiwan's international tourist hotels under competitive and cooperative relationships," *Journal of China Tourism Research*, vol. 9, no. 4, pp. 413–428, 2013.

[13] X. Zhang, G. H. Huang, Q. Lin, and H. Yu, "Petroleum-contaminated groundwater remediation systems design: a data envelopment analysis based approach," *Expert Systems with Applications*, vol. 36, no. 3, pp. 5666–5672, 2009.

[14] J. Doyle and R. Green, "Efficiency and cross-efficiency in DEA: derivations, meanings and uses," *The Journal of the Operational Research Society*, vol. 45, no. 5, pp. 567–578, 1994.

[15] Y.-M. Wang and K.-S. Chin, "A neutral DEA model for cross-efficiency evaluation and its extension," *Expert Systems with Applications*, vol. 37, no. 5, pp. 3666–3675, 2010.

[16] J. Wu, L. Liang, Y. Zha, and F. Yang, "Determination of cross-efficiency under the principle of rank priority in cross-evaluation," *Expert Systems with Applications*, vol. 36, no. 3, pp. 4826–4829, 2009.

[17] G. R. Jahanshahloo, F. H. Lotfi, Y. Jafari, and R. Maddahi, "Selecting symmetric weights as a secondary goal in DEA cross-efficiency evaluation," *Applied Mathematical Modelling*, vol. 35, no. 1, pp. 544–549, 2011.

[18] J. Wu, J. Sun, and L. Liang, "Cross efficiency evaluation method based on weight-balanced data envelopment analysis model," *Computers & Industrial Engineering*, vol. 63, no. 2, pp. 513–519, 2012.

[19] Y.-M. Wang, K.-S. Chin, and Y. Luo, "Cross-efficiency evaluation based on ideal and anti-ideal decision making units," *Expert Systems with Applications*, vol. 38, no. 8, pp. 10312–10319, 2011.

[20] Y.-M. Wang, K.-S. Chin, and S. Wang, "DEA models for minimizing weight disparity in cross-efficiency evaluation," *The Journal of the Operational Research Society*, vol. 63, no. 8, pp. 1079–1088, 2012.

[21] Y. Guo, *Theory, Methodology and Application of Synthesis Evaluation*, Science Press, Beijing, China, 2007.

Hindawi Publishing Corporation
Mathematical Problems in Engineering
Volume 2015, Article ID 797953, 8 pages
http://dx.doi.org/10.1155/2015/797953

Research Article

Planning Tunnel Construction Using Markov Chain Monte Carlo (MCMC)

Juan P. Vargas,[1] Jair C. Koppe,[2] Sebastián Pérez,[1] and Juan P. Hurtado[1]

[1]*Departamento de Ingeniería en Minas, Universidad de Santiago de Chile, Santiago, Chile*
[2]*Departamento de Engenharia de Minas, Universidade Federal do Rio Grande do Sul, Porto Alegre, Brazil*

Correspondence should be addressed to Juan P. Vargas; juan.vargas@usach.cl

Received 10 April 2015; Revised 9 June 2015; Accepted 14 June 2015

Academic Editor: Zdeněk Kala

Tunnels, drifts, drives, and other types of underground excavation are very common in mining as well as in the construction of roads, railways, dams, and other civil engineering projects. Planning is essential to the success of tunnel excavation, and construction time is one of the most important factors to be taken into account. This paper proposes a simulation algorithm based on a stochastic numerical method, the Markov chain Monte Carlo method, that can provide the best estimate of the opening excavation times for the classic method of drilling and blasting. Taking account of technical considerations that affect the tunnel excavation cycle, the simulation is developed through a computational algorithm. Using the Markov chain Monte Carlo method, the unit operations involved in the underground excavation cycle are identified and assigned probability distributions that, with random number input, make it possible to simulate the total excavation time. The results obtained with this method are compared with a real case of tunneling excavation. By incorporating variability in the planning, it is possible to determine with greater certainty the ranges over which the execution times of the unit operations fluctuate. In addition, the financial risks associated with planning errors can be reduced and the exploitation of resources maximized.

1. Introduction

Underground mining represents a fundamental pillar of ore production in Chile. It is assumed that in the coming years the proportion of underground mining compared with open-cast mining will increase as mineral resources accessible to surface exploitation become progressively exhausted.

One of the main activities involved in underground mining is tunnel construction, or, more generally, horizontal works, because this produces the infrastructure that provides access to the ore for extraction. Here, a "tunnel" should be understood as any underground excavation whose purpose is to join two points.

Given the importance of tunnels for mining, it is evident that there is a need to have a methodology that allows accurate planning of their excavation. To achieve this goal, the Markov chain Monte Carlo (MCMC) method is appropriate, since the construction of a tunnel is a cycle of activities consisting of unit operations, each of which exhibits a variability that can be represented in terms of a probability distribution function (PDF). Furthermore, the success or failure of the construction cycle is related to its actual duration compared with what was planned, which also depends on the time at which the cycle begins within the day's work shift. Thus, the construction cycle of a tunnel is dependent on the success or failure of the immediately preceding cycle, and therefore the event's probability of success is related to its predecessor, constituting an MCMC relation [1].

2. Tunnel Construction

There are several methods of tunnel excavation. This paper will focus on the construction of tunnels by drilling and blasting [2]. This technique involves an excavation or work cycle comprising a number of different activities. Suorineni et al. [3] mention the following unit operations: drilling of the tunnel surface, loading of explosives and blasting, ventilation (considered as an interference within the cycle), scaling and

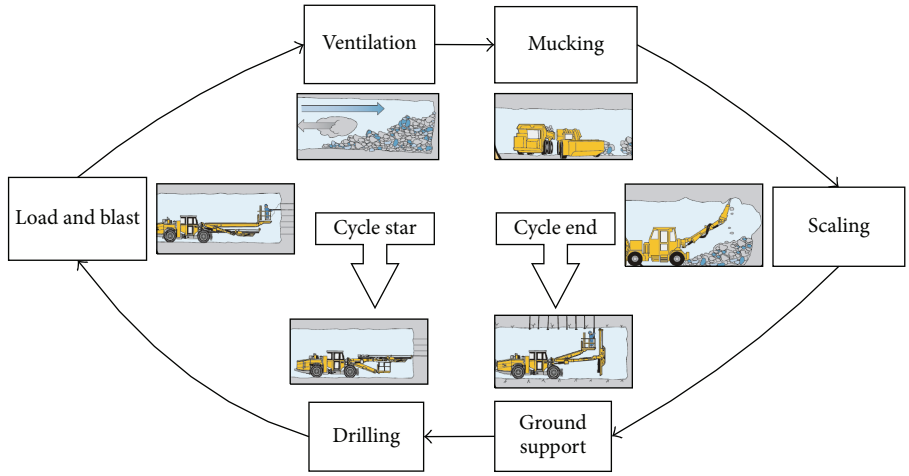

Figure 1: The drilling and blasting cycles in tunneling.

loading of the blasted material, and fortification (bolts, nets, and shotcrete, among others). Figure 1 illustrates the drilling and blasting cycles involved in tunneling.

The aim of the excavation cycle is to break up the rock with explosives, giving the required cross-sectional shape while the tunnel advances proportionally to the length of the drilling in the tunnel face. In this way, with successive cycles, the infrastructure is built gradually until the tunnel has been completed. However, even with knowledge of the number of unit operations in each cycle, and the time generally taken to perform each one, it is very difficult to determine exactly the total time required to complete the construction of the tunnel, mainly because all of the operations are subject to variations that depend on unforeseen events (although they can be associated with a probability of occurrence).

On the other hand, the work cycles, and therefore each of the unit operations, are executed within well-defined time periods (work shifts), which are framed within a 24-hour period. Usually, mining operates in continuous time periods without stoppages in production, and therefore tunnel construction proceeds in the same continuous manner. This is particularly important because the relation between the duration of the construction cycle and the period defined for the work shift will affect the efficiency of the cycle. Some of these inefficiencies result from changes in work shift that interfere with the working cycle. That is why Chilean law [4] specifies several types of work shifts, with various configurations as shown in Table 1. The choice among these is made on the basis of the estimated duration of the tunnel's construction cycle. For example, if the cycle time is estimated as less than 8 hours, the work shift that fits this best should be used, in this case T1 (Table 1), because this allows three cycles per day and thus a more rapid advance of the tunnel.

Table 1: Configuration of evaluated shifts.

Shift ID	Shifts per day	Hour per shift	Effective hours per day
T1	3	8	24
T2	2	10	20
T3	2	12	24

3. Planning of Tunnel Construction

Currently, to plan the construction of a tunnel, whatever its purpose, fixed values of the relevant parameters are used, giving consistent results. This is reflected in the following equation, which gives the construction speed of the tunnel in days related to the drilling length unit (RA) in terms of the drilling length (Lp), weighted by the effectiveness of the blasting (Ed), divided by the sum of the times for the unit operations in hours (Tp), and divided in turn by a factor that involves the unproductive times (Ti) in relation to the 24 hours of the day:

$$RA = \frac{Lp \times Ed}{\left[\left(\sum_{i=1}^{n} Tp_i\right) / \left(24 - \sum_{p=1}^{m} Ti_p\right)\right]}. \quad (1)$$

Then, with knowledge of the length of the tunnel (Lt), the execution time (D) is given by

$$D = \frac{Lt}{RA}. \quad (2)$$

The results obtained with this approach have until now always been used to plan this type of construction, but they can be improved by including the variability of each of the unit operations involved.

4. Monte Carlo Method and Tunnel Construction Planning

As already mentioned, tunnel construction involves excavation cycles consisting of unit operations that can be represented by PDFs, and it is clear that this process can

be simulated using a Monte Carlo method [5]. With this approach, an excavation cycle (De) is simulated as follows:

$$De = F_{op(1)}^{-1}\left(r\#_{(1)}\right) + F_{op2}^{-1}\left(r\#_{(2)}\right) + \cdots + F_{op(n)}^{-1}\left(r\#_{(n)}\right),$$
$$De = \sum_{i=1}^{n} F_{op(i)}^{-1}\left(r\#_{(i)}\right), \tag{3}$$

where F_{op}^{-1} is the inverse probability function of each of the n unit operations and $r\#$ is a pseudorandom number between 0 and 1.

Assuming that the number of excavation cycles required to construct the total length of the tunnel is known, since the advance achieved in each cycle is determined by the drilling length, which remains unchanged throughout the construction, the theoretical time taken for construction (Ds) is given by the following equation:

$$Ds = \sum_{j=1}^{k}\sum_{i=1}^{n} F_{op(i)}^{-1}\left(r\#_{(i)}\right), \tag{4}$$

where k is the number of cycles. For the model presented in (4) to represent reality, it is necessary to include in the construction of the PDFs the unproductive times and inefficiencies associated with each activity.

However, the duration of tunnel construction cannot be estimated using the Monte Carlo method alone, because this method does not take account of an aspect that is extremely important, namely, the fact that the probability of success of a cycle depends on the preceding cycle.

5. Application of Markov Chains

As already mentioned, the use of Markov chain theory is appropriate in this context, considering the characteristics of tunnel construction. Construction in mining takes place continuously 24 hours per day, and in general the working day is broken up into two or three periods (shifts), depending on the chosen workday (see Table 1) and as permitted by Chilean law [4]. Taken into account this work structure, tunnel construction in mining is faced with some particular problems that are mainly the result of inefficiencies due to changes of work teams and their transfer to the working areas.

In underground mining, owing to the specific characteristics of the work, excavation cycles are generally kept as multiples of working shifts, for a duration of less than 8 hours, for example, with preference being given to a T1 type of shift over T2 or T3 (Table 1), so that three cycles per day can be run.

It is possible that, owing to particular aspects of operational interference or inefficiency, an excavation cycle will not fit the established workday, increasing the duration of the cycle and affecting the next cycle. On the other hand, if success in the execution of an excavation cycle is represented by its completion within the established work shift or group of work shifts (with the cycle otherwise being considered a failure), then this condition in turn reduces the possibility of success of the following shift, because it takes time away from the latter and furthermore adds unproductive time due to activities interrupted as a result of the change of work. These situations can be considered as processes that can be modeled using Markov chain theory [1].

The algorithm presented in (4) cannot model such behavior, because it is unable to determine the simulation time of an excavation cycle as a function of the duration of the work shift. Therefore, to incorporate this behavior, it is necessary to have an algorithm for evaluating this simulation time.

6. Simulation Algorithm

To predict tunnel construction time, the Monte Carlo method appears to be an appropriate tool to use together with the Markov chain principle, given that it is a stochastic simulation that allows analysis of complex systems with several degrees of freedom. The Monte Carlo method [5] has become one of the most common ways to solve complex mathematical problems by random sampling [6–10]. It consists in generating random or pseudorandom numbers that are entered into an inverse distribution function, delivering as a result as many scenarios as the number of simulations performed [11]. The estimation will be the more precise the greater the number of iterations that can be done.

To use the Monte Carlo method, the unit operations are identified and each is assigned a PDF that depends on its nature and on the results of field sampling.

If the inverse functions of the PDFs of each unit operation of the excavation cycle are fed with random numbers, they will give as a result the duration of each operation. If the times thus obtained are added, this gives the total duration of the excavation cycle.

Once we know the duration of the excavation cycle, we must also consider another very important variable, namely, the distance advanced, or the real advance, after blasting (Le). This distance can also be described by a PDF, since it corresponds to the drilling distance (Lp) as affected by the blasting efficiency (Ed), as shown in (1). The drilling distance is a fixed value that depends on the characteristics of the drilling equipment, but the efficiency of the blast depends on the condition of the rock, variations in geological structure, and the characteristics of the explosive used, among other things, making this parameter vary from one blast to another.

Thus, if the durations of all the excavation cycles and the corresponding distances advanced are known, it is possible to determine the time taken for tunnel construction. Simulating this as many times as possible, a large number of scenarios are produced, generating a PDF of the time taken for tunnel construction.

The algorithm (see Algorithm 1) is composed of three loops, which control the number of simulations required, the required tunnel length, and the existing relation between the duration of the work shift and that of the tunnel excavation cycle. This point is fundamental for this work, being very important when it comes to choosing the best shift configuration to use. All these items are necessary to allow the simulation of the total construction time.

The proposed scheme consists of three inclusive loops dependent on each other. The operating form is that the first

```
BEGIN
i ← 1
WHILE (i ≤ nsim)
        dev ← 0
        operation ← op.1
        shift ← 1
        t ← 0
                WHILE (dev ≤ ltunnel)
                        av ← 0
                        WHILE (t ≤ (dt − tol))
                                CASE operation
                                        op.1
                                                t ← t + DI.op.1(rand#)
                                                operation ← op.2
                                        op.2
                                                t ← t + DI.op.2(rand#)
                                                operation ← op.3
                                                ⋮
                                        op.n
                                                t ← t + DI.op.n(rand#)
                                                operation ← op.1
                                                av ← Le ∗ DI.rec(rand#) + av
                                END CASE
                        END WHILE
                        IF (t > dt)
                                t ← t − dt + beg
                           ELSE
                                t ← 0
                        END IF
                        shift ← shift + 1
                        dev ← dev + av
                END WHILE
        s(i) ← shift
        i ← i + 1
END WHILE
END
Variables:
nsim: number of simulation
ltunnel: lenght of tunnel (meters)
DI.op.m: inverse distribution of operation unit "m"
DI.rec: inverse distribution of efficiency of the blast
Le: lenght of the drilling
dt: during of the work shift (minutes)
rand#: random number.
```

Algorithm 1: Algorithm to simulate tunnel excavation time.

loop, which contains the other two, controls the number of required simulations, on the basis that each simulation is the construction of a tunnel with specified length.

The second loop imposes the condition that the construction does not exceed the defined tunnel length, with every advance being estimated by the PDF of the performance of the blast multiplied by the drilling length. The drilling length is a fixed value, and is added consecutively until the required tunnel length is achieved.

Finally, the third loop has the function of adding consecutively the times for the unit operations in each cycle and comparing this total time with the established work shift, a fundamental aspect of this work.

This last loop is the key to the simulation, because it constructs the cycle within the shift. This procedure is carried out using the Monte Carlo method, where the inverses of the PDFs associated with the execution times of the unit operations are applied. The times obtained from this simulation are added, and it is determined whether the cycle can finish during the operating shift.

The proposed simulation algorithm is detailed in the following section.

6.1. Control of the Number of Simulations. As already mentioned, the function of the first loop is to control the number of simulations required, taking into account that each simulation estimates the time required to build a tunnel with an already defined length. This loop, which contains the other two, starts with the variable "*i*," which represents the number of the simulation under way and is initially assigned the value 1. The first loop is "*WHILE* ($i \leq nsim$)," where "*nsim*" corresponds to the number of required simulations.

Some variables are then defined to start the execution of the algorithm. The variable "*dev*" is an auxiliary adder that is assigned an initial value of 0 and is increased in relation to the advances per blasting at the end of the second loop. The purpose of this variable is to control the simulation in relation to the tunnel length built, executing the second loop until the desired length "*WHILE* ($dev \leq ltunnel$)" is achieved, where "*ltunnel*" represents the length of the tunnel to be built.

In the first loop, there is the variable "*operation,*" whose purpose is to identify the operations that will be performed in the third loop and that are adapted according to the operations of the construction cycle described by Suorineni et al. [3]. It should be noted that this is the only alphanumeric variable. The value assigned by default in this location is "*op.1,*" since it indicates the first operation of the cycle, which is represented by the suffix 1. Every time that we begin simulating the construction of the tunnel, we will start with drilling, the first operation of the cycle.

On the other hand, the variable "*shift*" defines the work shifts required for the construction of the tunnel, and it is a counter that is modified at the end of the second loop, storing the data in a matrix "*S*" that is of dimension equal to the number of required simulations and that will provide the data for later analysis.

Finally, the variable "*t*," an auxiliary variable used for storing the sum of the times of the operations required for the tunnel construction, is set equal to zero every time the tunnel construction starts, but it can also be initialized, depending on conditions that will be explained later, within the second loop.

6.2. Control of the Simulated Construction Advance. The second loop imposes the condition that the simulated construction advance does not exceed the proposed length, and to that end the construction takes place in the third loop, whose purpose is to control the duration of the cycle in terms of the duration of the work shift "*WHILE* ($t \leq (dt - tol)$)."

The verification expression is true as long as the sum of the times of the cycle's operations "*t*" is less than the duration of the shift "*dt*" minus a tolerance time "*tol.*" This last variable is an operational parameter that indicates if it is possible to continue with the next unit operation within the shift or if the operation is to be passed to the following shift.

6.3. Calculation of the Time for Each of the Unit Operations. The cycle's duration in the work shift is built successively in a selection routine "CASE" that adds the time for each operation until the end of the cycle; then, the following cycle can start again within the same shift or stop the execution to retake it on the following shift, and this depends on the operational tolerance "*tol*" that is estimated for the execution of the tunnel. We will go into this point more deeply when we apply the algorithm.

The "CASE" routine in the third loop has the function of arranging the operations so they take place one after the other and also of evaluating the time taken under the loop's condition, in order to see if this is still within the duration of the chosen shift.

The times for each operation belong to the probability distributions used to represent the process. In our case, the variable "*DI.op.n*" corresponds to the inverse distribution of the operation specified in the suffix, in this case "*n*," and this variable is a function of random numbers between 0 and 1.

By means of the variable "*rand#,*" which represents random numbers between 0 and 1, the values of the operation are generated and fitted to the distribution used, as pointed out by Sobol [11]. Once the operation has been executed, the variable "*operation*" stores the value of the following operation so that, in the next iteration, as a result of "CASE," it keeps advancing.

At the end of the third loop, there is a conditioning routine depending on whether the cycle ends together with the shift or is interrupted. This routine evaluates whether "*t*" is greater than "*dt,*" telling the algorithm whether the next shift should add an activity restarting time "$t \leftarrow t - dt + beg$," where "*beg*" corresponds to the restarting time, which is not included in any of the unit operations. If the shift ends cutting an activity, this restarting time is added. In the opposite case, where the activity ends within the shift, it is not necessary to add the restarting time. If appropriate, this restarting time will be added to the next sequence of the loop in the corresponding operation.

Also, at the end of the second loop, a work shift is added in the variable "*shift,*" and the advance is added in the variable "*dev*" only if it has gone through the last operation where the advance caused by the blasting, "$av = Le * DI.rec(r\#) + average$," is found, where "*av*" reflects the advance of the tunnel (in meters) and "*DI.rec(r#)*" is the inverse distribution of the percentage efficiency of the advance caused by the blast.

In this way, the successive simulations are constructed, delivering the time taken for each simulated tunnel, and accounted for in work shifts.

Taking in account the possibility of iterating as many times as necessary, we will have a representative sample of the population from which we can infer the most probable duration of the tunnel's construction.

7. Application of the Algorithm to Tunnel Construction

Minera San Pedro Limitada (MSP) has several copper ore deposits in the Lohpan Alto district, located in the Coastal Range of Central Chile. One of these deposits is Mina Romero, where the ore will be removed by underground mining [12].

To gain access and prepare the mineralized body for its exploitation, MSP has planned the construction of a 560 m access tunnel with no slope and in a straight line, with a cross section of approximately 3.5 m × 3.0 m.

The equipment used for drilling is an electrohydraulic drill of 45 mm diameter and the explosives are ammonium nitrate-fuel oil (ANFO) and Tronex (a derivative of dynamite), initiated by a nonelectrical shock tube detonator (NONEL). The mucking equipment is a load haul dump (LHD) of 6 yd^3.

To estimate the duration of construction of this tunnel, MSP, based on its experience in similar projects, has considered that, for every three work shifts with a duration of 9 actual hours each, it is able to carry out four cycles with a drilling length of 1.8 m, giving a rate of advance of 2.4 m per shift, so, with two work shifts per day, an advance of 4.8 m/day would be achieved.

Taking the above figures into account, MSP has estimated that the project should take 117 days, although previous experience in mines close to Mina Romero has shown that this estimate is not precise, because there are often delays that have not been considered at the time of planning.

To apply the proposed methodology, data from areas with similar geological and operational characteristics to those that will be faced in Mina Romero have been used. For that purpose, exploratory tunnels have been made in the upper part of the deposit, with the same cross section of the one that will be built and in rocks with similar characteristics to those of the Mina Romero access tunnel.

The cycle has been divided into five activities: drilling, loading and blasting, ventilation, scaling, and mucking. Support is not considered, because of the good quality of the rock. The rock mass rating (RMR) geomechanical classification of the rock mass [13] carried out by MSP indicates that the rock mass in the tunnel section can be classified as very good rock, with RMR over 85 points (class 1), and so no support is required.

After measurements had been made of the operational times of the cycle in the exploratory activities with characteristics similar to those that will be simulated, under the guidance of the Engineering Department of MSP, each of the activities was characterized in a statistical analysis that allowed determination of the probability distribution that best fitted the performance of each of the unit operations. Table 2 shows a summary of the statistical analysis, with the corresponding assigned PDFs.

Ventilation was kept constant in time, because MSP provides lunch for workers at the same time, and the duration of both lunch and ventilation is 90 min.

The distributions shown in Table 2 are those that were used to produce the algorithm and will be used in the Monte Carlo simulation of the tunnel construction time.

In general, the analysis presented in Table 2 is based on data obtained from field sampling, and the fitting was made by MSP, who are solely responsible for the data handling, but it should be noted that the fitting of the probability distribution curves was done by the Anderson-Darling method.

The simulation is involved between 10^5 and 10^6 iterations. It was found that the variability between the first and last simulations from this interval was not significant, considering the mean and the mode of the results (see Table 3), so it is believed that all the results delivered by simulation beyond 10^5 iterations are good.

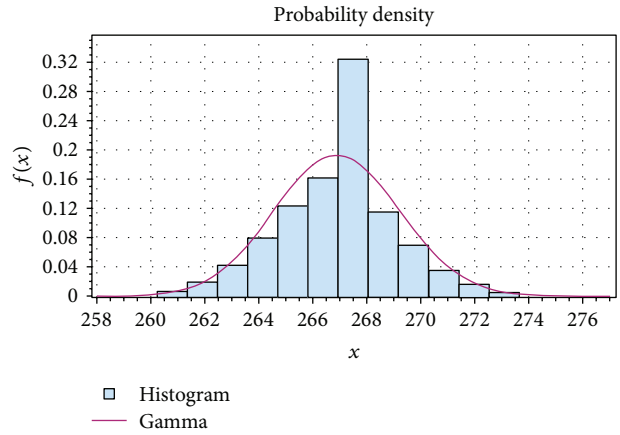

Figure 2: Probability distribution for the simulation in Mina Romero.

As stated in the model, every simulated event involves the construction of a tunnel with the specified length, taking into account the duration of the shift and the tolerance ("Tolerance" in Table 3) to ending the activities within the cycle. This means that less time is left rather than stipulated in this item to end the shift, so the activities are suspended and are taken up by the following shift.

Finally, it is also necessary to consider the restarting time ("Reset" in Table 3) of the activities, which corresponds to the time required to resume activities if the operation is interrupted by the end of the shift.

Both the tolerance and the restarting time can be modeled as Markov chain processes [1], because the success or failure of an event has an effect on the following one.

For the simulation, a tunnel of 3.5 m × 3.0 m with a length of 560 m is considered, with two work shifts per day, each of 540 min duration, with a tolerance of 60 min, which represents the time between the end of a cycle and the end of the shift. If the tolerance time is less than 60 min, the activities are finished and service or other activities related to the operation, such as cleaning, are carried out.

A 30 min time is considered for resumption of activities, implying that if the cycle time is longer than the shift time, this value is added to the cycle time, because all the distributions presented in Table 1 consider the starting time of the activity, but not a restart caused by a shift change. The considered values correspond to expert data coming from the experience of MSP in the operations area.

8. Analysis of the Results

According to the data presented in Table 3, and considering a simulation with 10^5 iterations (the difference compared with a simulation with 10^6 iterations is negligible and the shorter simulation is easier to handle with the available statistical software), Figure 2 shows the probability distribution obtained for the simulation in Mina Romero.

Table 2: Summary of statistical adjustment for unit operation.

Unit operation	Used data	Parameters							Probability Distribution
		Mean	Median	Mode	Standard deviation	Coefficient of variability	Minimum	Maximum	
Drilling	137	195.45	193.89	190.23	38.08	0.19	70.98	392.79	**Beta**
Load and blasting	133	56.09	55.76	54.98	11.64	0.20	14.77	113.51	**Beta**
Ventilation	136	90.00	90.00	90.00	0	—	—	—	**Constant**
Scaling	135	26.08	25.24	23.54	6.77	0.25	8.04	—	**Lognormal**
Mucking	135	70.03	65.66	58.33	20.22	0.28	30.95	—	**Gamma**

Table 3: Sensitivity analysis for iteration determination for the simulation.

Number of iterations	Tunnel length (m)	Shift duration (min)	Tolerance (min)	Reset (min)	Average (shifts)	Mode (shifts)	Standard deviation (shifts)	Min. (shifts)	Max. (shifts)
$1.0E+05$	560	540	60	30	266.89	267	2.31	257	277
$2.0E+05$	560	540	60	30	266.88	267	2.31	256	277
$3.0E+05$	560	540	60	30	266.89	267	2.31	256	278
$4.0E+05$	560	540	60	30	266.89	267	2.31	256	279
$5.0E+05$	560	540	60	30	266.89	267	2.31	256	277
$1.0E+6$	560	540	60	30	266.89	267	2.31	256	279

In contrast to the conventional planning method, which determines one value for the required number of shifts, one of the advantages offered by the simulation method presented here is that it is possible to have both pessimistic and optimistic scenarios with respect to the number of shifts required for carrying out the work. These scenarios can be considered as the lower and upper limits of the confidence interval that describes the construction time for the tunnel under study in shifts.

The simulation produces a histogram with a mean of 266.89 shifts, a mode of 267 shifts, a median of 267 shifts (with a minimum of 257 and a maximum of 277), and a standard deviation of 2.31, with a distribution that is symmetric in form. This histogram is fitted into a gamma distribution (Figure 2) with parameters $\alpha_1 = 7.4145$, $\alpha_2 = 8.4196$, $a = 257$ (minimum), and $b = 277$ (maximum). The curve was fitted using the Anderson-Darling method, as mentioned earlier.

For the case in question, 267 shifts, which is the value of the mean as well as the median and the mode, were considered. It was decided to use this value because it is a good representation of the simulated case and is the most repeated value. Figure 3 shows the probability distribution for the simulation in Mina Romero, and from this curve, it is possible to obtain the probability of success, in this case 0.6 (60%).

The gamma distribution is not of symmetrical type, but in this case is the best fit to the simulation data using the Anderson-Darling method—this is why the mean probability of success is 60% rather than 50%. Figure 2 shows that the mean is not in the middle of the curve, and this is confirmed by Figure 3.

Once the tunnel construction, which took 133 days, was finished, the means resulting from the simulation could be compared with the MSP plans and with the actual data (Table 4), revealing an error of 0.37% compared with the real time, while with the conventional planning method used by MSP the error was 12.28% with respect to the actual construction time. This difference is significant because, when it is translated into execution days, it can be seen that the conventional planning method used by MSP underestimated by 16.5 days the time required, whereas the simulation gave a mean differing by only one day from the real execution time. When the standard deviation is considered, we have a quite precise tool for planning, because the value considered is 267 ± 3 shifts.

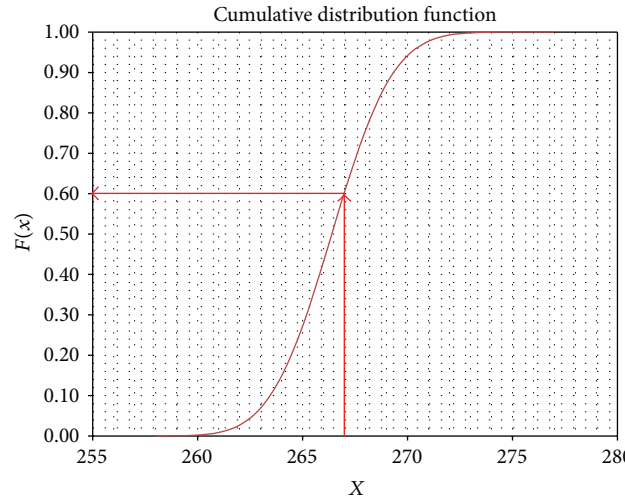

Figure 3: Cumulative distribution function of simulated data.

Table 4: Summary of real data, planned data, and simulation data.

Description	Cycles per shift	Advance rate [m/shift]	Daily advance rate [m/day]	Planned time [days]	Average shifts	% Error with real case
Planning	1.33	2.4	4.8	117	233	12.28%
Simulation	1.16	2.1	4.2	134	267	0.37%
Real	1.18	2.1	4.2	133	266	

It should be mentioned that the plan made by the Engineering Department of MSP is not represented in the histogram shown here. A more careful analysis would show that there is no event similar to what was planned and indeed that it would be very difficult for the event planned by the mining company to occur.

As can be seen, this simulation methodology based on the Monte Carlo method can estimate the time required for the construction of a tunnel used in underground mining.

9. Conclusions

The data analysis performed at MSP shows that this kind of stochastic simulation is a very effective tool for planning the construction time of a tunnel.

Beyond the accuracy of the means, the range of minima and maxima obtained by the simulation is interesting, because it delivers a potentially useful parameter for establishing planning criteria.

Based on the minimum and maximum values obtained from the simulation, optimistic and/or pessimistic scenarios can be proposed that they can serve as background information for making mine planning decisions.

Because of the random nature of the execution times of the operations involved in mining construction, it has been determined that a planning methodology based on the Monte Carlo method provides a better fit to real conditions than a conventional approach, because, with its use of probability distributions, it incorporates the variability inherent in the planning process.

By incorporating variability into planning, it is possible to determine with greater certainty the ranges over which the execution times of the different operations fluctuate. It is thereby possible to reduce the financial risks due to planning errors while maximizing the exploitation of resources.

Conflict of Interests

The authors declare that there is no conflict of interests regarding the publication of this paper.

Acknowledgments

This work was supported by DICYT/Universidad de Santiago de Chile, USACH (code 051515VN), and PPGE3M Universidade Federal do Rio Grande do Sul.

References

[1] F. S. Hillier and G. Lieberman, "Markov chain," in *Introduction to Operations Research*, pp. 675–682, McGraw-Hill, 9th edition, 2010.

[2] S. P. Singh and P. Xavier, "Causes, impact and control of overbreak in underground excavations," *Tunnelling and Underground Space Technology*, vol. 20, no. 1, pp. 63–71, 2005.

[3] F. T. Suorineni, P. K. Kaiser, and J. G. Henning, "Safe rapid drifting—support selection," *Tunnelling and Underground Space Technology*, vol. 23, no. 6, pp. 682–699, 2008.

[4] Gobierno de Chile, *Código del Trabajo, Capítulo IV 'De la jornada de trabajo'*, Gobierno de Chile, 2012.

[5] N. Metropolis and S. Ulam, "The Monte Carlo method," *Journal of the American Statistical Association*, vol. 44, no. 247, pp. 335–341, 1949.

[6] H. T. Chiwaye and T. R. Stacey, "A comparison of limit equilibrium and numerical modelling approaches to risk analysis for open pit mining," *Journal of the Southern African Institute of Mining and Metallurgy*, vol. 110, no. 10, pp. 571–580, 2010.

[7] E. Ghasemi, K. Shahriar, M. Sharifzadeh, and H. Hashemolhosseini, "Quantifying the uncertainty of pillar safety factor by Monte Carlo simulation—a case study," *Archives of Mining Sciences*, vol. 55, no. 3, pp. 623–635, 2010.

[8] R. Khalokakaie, P. A. Dowd, and R. J. Fowell, "Incorporation of slope design into optimal pit design algorithms," *Transactions of the Institution of Mining and Metallurgy Section A: Mining Technology*, vol. 109, no. 2, pp. A70–A76, 2000.

[9] M. A. Morin and F. Ficarazzo, "Monte Carlo simulation as a tool to predict blasting fragmentation based on the Kuz-Ram model," *Computers & Geosciences*, vol. 32, no. 3, pp. 352–359, 2006.

[10] M. Sari, C. Karpuz, and C. Ayday, "Estimating rock mass properties using Monte Carlo simulation: ankara andesites," *Computers and Geosciences*, vol. 36, no. 7, pp. 959–969, 2010.

[11] I. M. Sobol, *A Primer for the Monte Carlo Method*, CRC Press, Boca Raton, Fla, USA, 1994.

[12] X. Chen, "Resuing shrinkage stoping," *Engineering & Mining Journal*, vol. 199, no. 10, pp. 34–36, 1998.

[13] Z. R. Bieniawski, "Rock mass classification in rock engineering," in *Proceedings of the Exploration for Rock Engineering*, pp. 97–106, A.A. Balkema, Cape Town, South Africa, 1976.

Hindawi Publishing Corporation
Mathematical Problems in Engineering
Volume 2015, Article ID 978040, 5 pages
http://dx.doi.org/10.1155/2015/978040

Research Article

A Straight-Line Method for Analyzing Residual Drawdowns at an Observation Well

Mesut Çimen

Department of Civil Engineering, Faculty of Engineering, Süleyman Demirel University, 32260 Isparta, Turkey

Correspondence should be addressed to Mesut Çimen; mesutcimen@sdu.edu.tr

Received 20 March 2015; Revised 21 May 2015; Accepted 25 May 2015

Academic Editor: Zdeněk Kala

Determination of the hydraulic parameters (transmissivity and storage coefficients) of a confined aquifer is important for effective groundwater resources. For this purpose, the residual drawdowns have been in use to estimate the aquifer parameters by the classical Theis recovery method. The proposed method of this paper depends on a straight-line through the field data and it helps to calculate the parameters quickly without any need for long-term pumping data. It is based on the expansion series of the Theis well function by consideration of three terms, and this approach is valid for the dimensionless time factor $u' = S'r^2/4Tt' \leq 0.2$. The method can be applied reliably to extensive and homogeneous confined aquifers resulting in different storage coefficients during the pumping and recovery periods ($S \neq S'$). It presents a strength methodology for the parameters decision making from the residual data in the groundwater field of civil engineering.

1. Introduction

One of the practical ways to estimate the aquifer parameter is to measure the water level rise by time in the production or observation wells after the pumping test stoppage. This is referred to as the recovery test which starts just after the pump shut. The recovery method serves as a check and alternative to the pumping test. The parameters' estimations from both tests are practically equal to each other if the Theis [1] assumptions are satisfied.

The residual drawdown measurement at any time during the recovery period is the difference between the observed water level and the prepumping static water level. The recovery drawdown is known as the difference between the total drawdown at the end of pumping and the residual drawdown [2, 3]. With the Theis recovery method, the transmissivity can be estimated easily using pumping well recovery data, but the storage coefficient cannot be calculated due to wellbore storage effects, unknown effective radius, and difficulty in finding the time of zero recovery as needed for the application of Cooper and Jacob [4] method. However, in cases of measurements from the observation wells there will not be such restrictive effects. The Theis recovery method considers the late-time residual drawdowns with the Cooper and Jacob formulations and it estimates the transmissivity and the ratio of storativity values during pumping and recovery periods. Theis [1] observed that a straight-line through the residual drawdowns (s') *versus* t/t' plot (t indicates the total time since pump start while t' is the time since pump shut). This plot on the semilogarithmic graph paper passes below the origin ($t/t' = 1, s' = 0$) giving the value of $t/t' > 1$ for a zero residual drawdown and that is the reason why different storage coefficient estimations are valid for the pumping and recovery periods. On the other hand, Jacob [5] observed that the storage coefficient estimation is generally greater during the pumping period than the recovery period.

Bruin and Hudson [6] proposed the time-recovery drawdown graph to find the time of zero recovery. The method depends on the extension of the time-drawdown pumping test data, which can also be applied to the time-recovery graph. Later, USDI [7] gave an alternative method for determining the storage coefficient (S) as follows:

$$S = \frac{2.25Tt'/r^2}{\log^{-1}\left[\left(s_p - s'\right)/\Delta\left(s_p - s'\right)\right]}, \quad (1)$$

where T is the transmissivity, s_p is pumping period drawdown projected to time t' at any radial distance, r, s' is residual

drawdown at time t', $(s_p - s')$ is recovery at time t', and $\Delta(s_p - s')$ is slope of the time-recovery graph. In this formulation $\log^{-1}[x]$ corresponds to the antilogarithm as 10^x.

The recovery analysis is also investigated by many researchers. For instance, Case et al. [8] developed convenient equations in the forms of a series based on the Theis recovery equation using the residual drawdown data. Agarwal [9] developed a method for recovery test analysis which is widely used by petroleum engineers. Through a simple transformation of the data from a recovery test, Agarwal method allows one to apply the same diagnostic principles and type curves used for drawdown analysis in the interpretation of recovery data. Ramey [10] presented the type curves for drawdown during the pumping and recovery periods, where the recovery times are plotted as large times. Mishra and Chachadi [11] obtained the recovery type curves for large-diameter pumping wells by discrete kernel approach while Şen [12] presented an analytical solution and a set of type curves for the drawdown distribution in a large-diameter well recovery. Later, Yeh and Wang [13] developed a mathematical model for describing the residual drawdown by taking into consideration the pumping drawdown distribution in addition to the effects of well radius and wellbore storage. They obtained the Laplace domain solution for the residual drawdown. Goode [14] proposed a set of graphical recovery type curves based on Theis' [1] exact well-function solution. These type curves depend on the dimensionless duration of pumping. Ballukraya and Sharma [15] proposed an approach derived from the Cooper-Jacob equation for estimating storativity by using residual drawdown measurements. Banton and Bangoy [16] presented a graphical method with the first three terms of the Theis series approximation. The method involves three separate plots with the equality of the storage coefficients in pumping and recovery periods ($S = S'$), but this approach requires at least two observation wells. Singh [17] proposed a numerical method by considering the derivative of the Theis recovery equation. Zheng et al. [18] suggested a straight-line method based on the Cooper-Jacob approximation for the extended pumping period and the first three terms in the expansion are from the well function for the recovery period. The method considers that $S = S'$. Singh [19] presented an optimization method based on nonlinear least-squares for the identification of the transmissivity and the storage coefficients in the pumping and recovery periods. Samani et al. [20] used a derivative analysis of pumping and recovery test data to estimate the hydraulic parameters in a heterogeneous aquifer. They showed that the drawdown-derivative analysis improves estimation of aquifer parameters and identification of different forms of heterogeneity. Kambhammettu and King [21] estimated the transmissivity and storage coefficient using a generalized MATLAB code with the conventional Levenberg-Marquardt algorithm. They considered the residual drawdowns measurements from a single observation well. Ashjari [22] determined the transmissivity and storage coefficients from residual data in case of $S \neq S'$ by using a modified version of Banton and Bangoy [15] method. This method is basically fitting a straight-line to a plot of residual drawdown *versus* square of radial distance at the same time.

In this study, another straight-line method is proposed using the first three terms from the expansion of the well function for the pumping and recovery periods. The method offers the use of spreadsheet for the inequality $S \neq S'$, which implies different storage coefficients during pumping and recovery periods. The procedure involves a linear regression line and its coefficients' estimations based on a set of recovery data from a single observation well. It is valid for the dimensionless time factor, $u' \leq 0.2$.

2. Proposed Method

In a homogeneous isotropic confined aquifer with infinite domain without the well storage, Theis [1] gave the residual drawdown expression for an observation well as follows:

$$s\left(r, t'\right) = \frac{Q}{4\pi T}\left[\int_u^\infty \frac{e^{-x}}{x}dx - \int_{u'}^\infty \frac{e^{-x}}{x}dx\right], \tag{2}$$

where $s(r, t')$ is the residual drawdown at any distance r and at any recovery time t', Q is the constant rate (discharge) towards the pumping well during the pumping and recovery periods, T is the transmissivity, $u = r^2S/4Tt$ is the dimensionless time factor for the pumping period, $u' = r^2S'/4Tt'$ is another dimensionless time factor for the recovery period, S and S' are the storage coefficients of aquifer during the pumping and recovery periods, $t = t_p + t'$, and t_p is the time of pumping. This expression can be considered after the first three terms of the exponential function series as follows:

$$\begin{aligned} s\left(r, t'\right) = \frac{Q}{4\pi T}&\left[(-0.5772 - \ln u + u)\right. \\ &\left. - \left(0.5772 - \ln u' + u'\right)\right], \end{aligned} \tag{3a}$$

$$s\left(r, t'\right) = \frac{Q}{4\pi T}\left[\ln\left(\frac{S'}{S}\frac{t}{t'}\right) + \frac{r^2S'}{4T}\left(\frac{S}{S'}\frac{1}{t} - \frac{1}{t'}\right)\right]. \tag{3b}$$

The error involved in adopting (3b) instead of (2) is less than 1% for $u' \leq 0.2$. Theis [1] proposed the first two terms of the series in (2) by considering that $S/S' = 1$ in order to estimate the aquifer transmissivity only. Theis approach is valid for $u' \leq 0.01$. Hence, (3b) considers more recovery data than Theis method. Equation (3b) can be rewritten to estimate the aquifer parameters as

$$W = a\tau - b, \tag{4}$$

$$W = \frac{s\left(r, t'\right)}{1/t' - \left(S/S'\right)(1/t)}, \tag{5}$$

$$a = \frac{Q}{4\pi T}, \tag{6}$$

$$\tau = \frac{\ln\left(\left(S'/S\right)\left(t/t'\right)\right)}{1/t' - \left(S/S'\right)(1/t)}, \tag{7}$$

$$b = a\frac{r^2S'}{4T}. \tag{8}$$

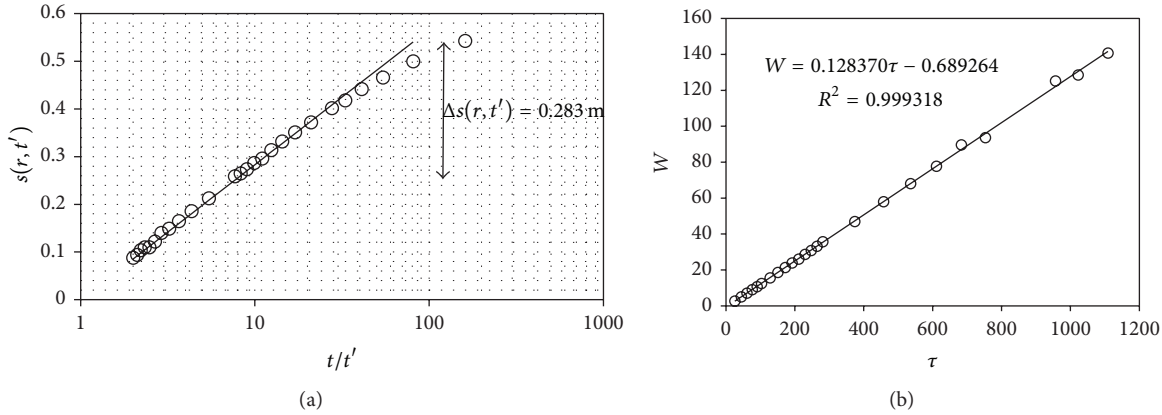

Figure 1: Straight-line fit to recovery data: (a) Theis recovery method and (b) proposed method.

Equation (4) presents a straight-line between τ and W. The first approximation of the aquifer parameter estimations can be obtained from the time residual drawdown data on a spreadsheet with the exception of a few early time instances, and the aquifer parameters can be estimated after fitting a straight-line to the field data and the coefficients of the regression line result from (6) and (8). By considering the calculated parameters, the dimensionless time factors, u', should be determined especially for the first data values. If u' is greater than 0.2, then the straight-line should be rearranged. Furthermore, the ratio of S/S' may be easily investigated with various straight-lines.

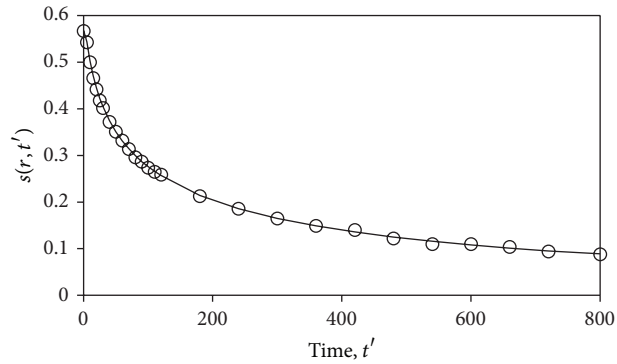

Figure 2: Observed and simulated residual drawdowns.

3. Application and Discussion

Two data sets are used to illustrate the application of the proposed method. The first set of data is taken from the USDI [7]. The data is recorded in an observation well located at 30.48 m from the pumping well. The well is pumped during 800 min with a constant discharge rate of 4.613 m^3/min, and the recovery period is also recorded as 800 min after the pump is turned off. The last record of pumping data is 0.567 m at 800 min. USDI [7] estimated the transmissivity as 2.982 m^2/min with the Theis recovery method (for $S = S'$ and $u' \leq 0.01$) and the storage coefficient as 0.07 according to (1) (for $(s_p - s') = 0.533$ m and $\Delta(s_p - s') = 0.302$ m). Figure 1(a) explicitly shows a difficulty at fitting a straight-line to the data on a semilogarithmic graph plot between residual drawdown and t/t'. By the application of (5) and (7) for $S/S' = 1$ to the observed recovery data except for the data at $t' = 0$, 540, and 600 min and after fitting a straight-line, a relationship similar to (4) is obtained (Figure 1(b)). From the straight-line parameters, the transmissivity and the storage coefficients are calculated as 2.8596 m^2/min and 0.0661, respectively. For $u' = 0.2$, the recovery time, t', is determined as 26.8 min from these estimations. For this reason, the data after 26.8 min is reconsidered, and the transmissivity and the storage coefficients are recalculated as 2.8594 m^2/min and 0.0666 (for $a = 0.12838$ and $b = 0.694922$), respectively. These parameters yield 0.568 m as a close value to 0.567 m, which is the last drawdown at $t = 800$ min during the pumping period. According to USDI's [7] parameter values, the last drawdown is 0.544 m, which is far away from 0.567 m. Zheng et al. [18] method ($T = 2.855$ m^2/min and $S = 0.0696$) which uses a straight-line similar to the proposed methodology produces 0.563 m. The reason of the difference between the values of Zheng et al. [18] and the methodology of this paper may be due to the lack of $S/S't$ in the right-side of (3b). Figure 2 shows the measured and simulated residual drawdowns *versus* time.

The second set of recovery data is produced synthetically for $Q = 3$ m^3/min, $r = 50$ m, $t_p = 70$ min, $s(r, t_p) = 0.396$ m, $T = 1$ m^2/min, $S = 0.0055$, and $S' = 0.005$. Table 1 shows the residual drawdowns for this data. Figure 3(a) presents a nonlinear relation between τ and W for $S = S'$, while Figure 3(b) shows a linear relation for $S/S' = 1.1$. Figure 3(a) implies that the rate of S/S' has a big effect on the late-time residual drawdowns during the recovery period. From the straight-line parameters at Figure 3(b), the transmissivity and the storage coefficients during the recovery and pumping periods are calculated as 1.0 m^2/min from (6), 0.0048 from (8), and 0.0053 from $S/S' = 1.1$, respectively. For $u' = 0.2$, the recovery time, t', is determined as 14.99 min from these estimations (T and S'). For this reason, the data after 14.99 min

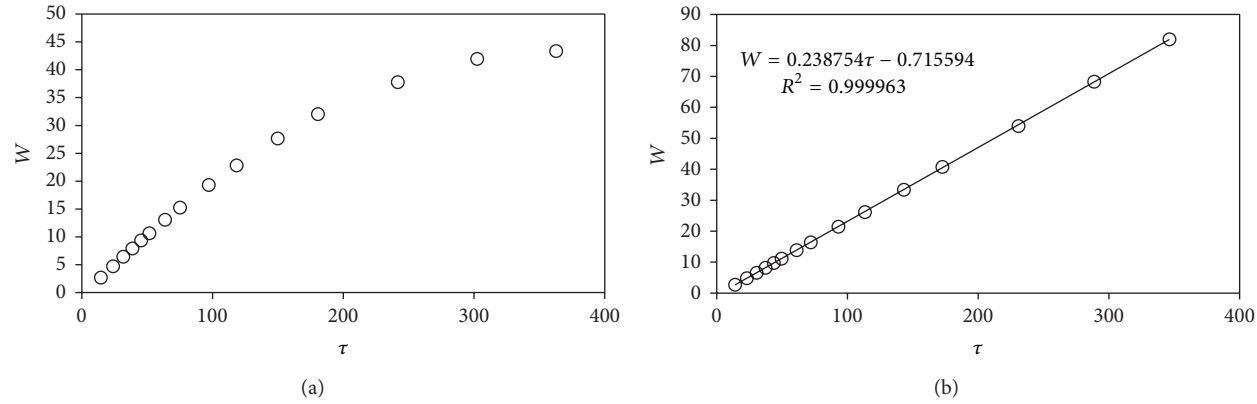

Figure 3: Plots of W *versus* τ of the synthetic data: (a) for $S = S'$ and (b) straight-line fit to recovery data for $S/S' = 1.1$ and fitting parameters.

Table 1: Synthetic residual drawdowns.

t' (min)	$s(r, t')$ (m)
0	0.593
5	0.506
10	0.415
15	0.354
20	0.309
25	0.276
30	0.249
40	0.208
50	0.178
70	0.138
90	0.111
120	0.085
150	0.068
210	0.045
270	0.032
330	0.023

is reconsidered, and the transmissivity and storage coefficients are found as 1.0 m^2/min, 0.00494, and 0.00543 (for $a = 0.238856$ and $b = 0.737662$), respectively. The errors in the obtained storage coefficients with respect to the other storage coefficients are due to the rounded recovery values, which are calculated from (2).

4. Conclusion

An effective method has been proposed for decision making to the transmissivity and storage coefficients estimations from the residual drawdowns during the recovery period. The methodology is valid for the confined aquifers and considers the expanding series of Theis well function with the first three terms and the maximum dimensionless time as $u' \leq 0.2$. This approach considers a lot of residual drawdown data than the classical Theis recovery method. The procedure depends on a straight-line through the field data and calculates rather easily the aquifer parameters without the pumping data (if it is unavailable). Validity of the procedure is presented by considering actual field data, while the Theis recovery method has some difficulties at fitting a straight-line to a given field data. This method of this paper is very effective for the aquifer parameters estimation and it can be reliably applied to the residual data at an observation well in the extensive and homogeneous confined aquifers with different storage coefficients during the pumping and recovery periods ($S \neq S'$).

Conflict of Interests

The author declares that there is no conflict of interests regarding the publication of this paper.

References

[1] C. V. Theis, "The relation between the lowering of the piezometric surface and the rate and duration of discharge of a well using ground-water storage," *Transactions, American Geophysical Union*, vol. 16, no. 2, pp. 519–524, 1935.

[2] Z. Şen, *Applied Hydrogeology for Scientists and Engineers*, CRC Press, New York, NY, USA, 1995.

[3] V. Batu, *Aquifer Hydraulics: A Comprehensive Guide to Hydrogeologic Data Analysis*, John Wiley & Sons, New York, NY, USA, 1998.

[4] H. H. Cooper and C. E. Jacob, "A generalized graphical method for evaluating formation constants and summarizing well-field history," *Transactions, American Geophysical Union*, vol. 27, no. 4, pp. 526–534, 1946.

[5] C. E. Jacob, "The recovery method for determining the coefficient of transmissibility," in *Methods of Determining Permeability, Transmissibility and Drawdown*, USGS Water Supply Paper 1536-I, pp. 283–292, 1963.

[6] J. Bruin and H. E. Hudson, *Selected Methods for Pumping Test Analysis*, Report of Investigation no. 25, Illinois State Water Survey, Champaign, Ill, USA, 1955.

[7] USDI, *Ground Water Manual*, US Department of Interior, Bureau of Reclamation, Washington, DC, USA, 1981.

[8] C. M. Case, W. W. Pidcoe, and P. R. Fenske, "Theis equation analysis of residual drawdown data," *Water Resources Research*, vol. 10, no. 6, pp. 1253–1256, 1974.

[9] R. G. Agarwal, "A new method to account for producing time effects when drawdown type curves are used to analyze pressure buildup and other test data," in *Proceedings of the 55th Annual Fall Technical Conference and Exhibition of the Society of Petroleum Engineers*, SPE Paper 9289, 1980.

[10] H. J. Ramey, "A drawdown and build-up type curve for interference testing," in *Proceedings of the 3rd Invitational Well-Testing Symposium*, T. W. Doc and W. J. Schwarz, Eds., pp. 130–134, Berkeley, Calif, USA, 1980.

[11] G. C. Mishra and A. G. Chachadi, "Analysis of flow to a large-diameter well during the recovery period," *Ground Water*, vol. 23, no. 5, pp. 646–651, 1985.

[12] Z. Şen, "Drawdown distribution during recovery around a large diameter well," *Nordic Hydrology*, vol. 22, no. 4, pp. 253–264, 1991.

[13] H.-D. Yeh and C.-T. Wang, "A semianalytical solution for residual drawdown at a finite diameter well in a confined aquifer," *Journal of the American Water Resources Association*, vol. 49, no. 4, pp. 966–972, 2013.

[14] D. J. Goode, "Composite recovery type curves in normalized time from Theis' exact solution," *Ground Water*, vol. 35, no. 4, pp. 672–678, 1997.

[15] P. N. Ballukraya and K. K. Sharma, "Estimation of storativity from recovery data," *Ground Water*, vol. 29, no. 4, pp. 495–498, 1991.

[16] O. Banton and L. M. Bangoy, "A new method to determine storage coefficient from pumping test recovery data," *Ground Water*, vol. 34, no. 5, pp. 772–777, 1996.

[17] S. K. Singh, "Storage coefficient and transmissivity from residual drawdowns," *Journal of Hydraulic Engineering*, vol. 129, no. 8, pp. 637–644, 2003.

[18] L. Zheng, J.-Q. Guo, and Y. Lei, "An improved straight-line fitting method for analyzing pumping test recovery data," *Ground Water*, vol. 43, no. 6, pp. 939–942, 2005.

[19] S. K. Singh, "Identification of aquifer parameters from residual drawdowns: an optimization approach," *Hydrological Sciences Journal*, vol. 51, no. 6, pp. 1139–1148, 2006.

[20] N. Samani, M. Pasandi, and D. A. Barry, "Characterizing a heterogeneous aquifer by derivative analysis of pumping and recovery test data," *Journal of Geological Society of Iran*, vol. 1, pp. 29–41, 2006.

[21] B. V. N. P. Kambhammettu and J. P. King, "Estimation of aquifer parameters from residual drawdowns," *Proceedings of the Institution of Civil Engineers: Water Management*, vol. 163, no. 7, pp. 361–365, 2010.

[22] J. Ashjari, "Determination of storage coefficients during pumping and recovery," *GroundWater*, vol. 51, no. 1, pp. 122–127, 2013.

Hindawi Publishing Corporation
Mathematical Problems in Engineering
Volume 2015, Article ID 301241, 8 pages
http://dx.doi.org/10.1155/2015/301241

Research Article

Three-Dimensional Numerical Analysis of the Tunnel for Polyaxial State of Stress

Wenge Qiu, Chao Kong, and Kai Liu

Key Laboratory of Transportation Tunnel Engineering, Ministry of Education, School of Civil Engineering, Southwest Jiaotong University, Chengdu 610031, China

Correspondence should be addressed to Chao Kong; 394757022@qq.com

Received 10 May 2015; Accepted 8 June 2015

Academic Editor: Jurgita Antucheviciene

The aim of this study is to have a comprehensive understanding of the mechanical behavior of rock masses around excavation under different value of intermediate principal stress. Numerical simulation was performed to investigate the influence of intermediate principal stress using a new polyaxial strength criterion which takes polyaxial state of stress into account. In order to equivalently substitute polyaxial failure criterion with Mohr-Coulomb failure criterion, a mathematical relationship was established between these two failure criteria. The influence of intermediate principal stress had been analyzed when Mohr-Coulomb strength criterion and polyaxial strength criterion were applied in the numerical simulation, respectively. Results indicate that intermediate principal stress has great influence on the mechanical behavior of rock masses; rock strength enhanced by intermediate principal stress is significant based on polyaxial strength criterion; the results of numerical simulation under Mohr-Coulomb failure criterion show that it does not exert a significant influence on rock strength. Results also indicate that when intermediate principal stress is relatively small, polyaxial strength criterion is not applicable.

1. Introduction

With respect to underground engineering, rock strength is one of the most important factors that affect stability of underground structure. Among the factors that affect rock strength, cohesion, internal friction angle, fissures, joints, and stress state of rock mass have a significant influence on rock strength [1].

When the ratio of the spacing of discontinuities is far smaller than the excavation dimension, the effect that discontinuities exert on excavation is also relatively small. Moreover, this effect brought by discontinuities is deemed to be acting on the whole rock mass and the whole underground structure rather than on partial rock mass and partial supporting structure system. As a result, discontinuity rock mass can be thought of as continuum. At the same time, Mohr-Coulomb failure criterion is presented that only cohesion and internal friction angle are considered to describe strength of rock mass. With the rapid development of numerical simulation brought by superior performance of computer, Mohr-Coulomb failure criterion is widely applied as a simple and practical form in numerical simulation of geotechnical field.

Under Mohr-Coulomb failure criterion, major principal stress σ_1 can be predicted if minor principal stress σ_3 is determined. Major principal stress σ_1 is written as

$$\sigma_1 = f(\sigma_3, k), \tag{1}$$

where k are "material constants" that could depend, among other factors, on rock type and quality, weathering, loading history, or strain [2]. In Mohr-Coulomb failure criterion, both major principal stress σ_1 and minor principal stress σ_3 are considered. Note that Mohr-Coulomb failure criterion does not take into account intermediate principal stress σ_2. According to Wang and Kemeny [3], however, intermediate principal stress σ_2 has a significant influence on σ_1 even if σ_3 equals zero. Senent et al. [2] thought that although enhancement of rock strength by intermediate principal stress σ_2 was seriously affected by the defeats in the rock mass, rock mass could also be modeled as homogeneous media with reduced strength property.

In general, under both deep-buried and squeezing geoenvironment, rock mass is always in polyaxial stress state, shown in Figure 1, where longitudinal stress was intermediate principal stress (σ_2). Excavation will bring about stress redistribution in rock mass. σ_3/σ_1 is called lateral pressure coefficient K; it can influence the failure mode of tunnel during excavation [4]. When K is smaller, the initial damage appears in arch foot and arch; when K is bigger, the initial damage appears in sidewall and arch; tensile damage is the main failure mode. But intermediate principal stress σ_2 is not relaxed significantly with advance of excavation [5, 6]. Polyaxial strength criterion has been introduced by Singh et al. [5]. They initiated a large number of studies on the polyaxial constitutive models to prove the applicability of underground engineering in severe squeezing conditions, explaining the differences between what was predicted by traditional elastoplasticity theory and that by observations. Back analysis of the data obtained from field reveals that rock masses around the excavation have a strength enhancement owing to the effect of intermediate principle stress σ_2. Singh et al. [5] proposed a semiempirical approach that incorporates the effect of intermediate principal stress σ_2 in the conventional formula of Mohr-Coulomb failure criterion by substituting σ_3 with the average value of σ_2 and σ_3 at the second term:

$$\text{Mohr-Coulomb: } \sigma_1 - \sigma_3 = \sigma_{cr} + \sigma_3 A, \tag{2}$$

$$\text{polyaxial criterion: } \sigma_1 - \sigma_3 = \sigma_{cr} + \frac{\sigma_3 + \sigma_2}{2} A, \tag{3}$$

where $A = 2\sin\varphi/(1 - \sin\varphi)$.

Yield curves of the two failure criteria on π-plane are shown in Figure 2.

Polyaxial failure criterion has gradually been accepted by scholars and engineers. Scussel and Chandra [7] verified the precision and validity of this failure criterion through actual project [8]. Scussel and Chandra [9] used Fish computer language of Flac^{3D} [10] to establish the constitutive model of polyaxial failure criterion with satisfactory results. However, due to limitations of Fish computer language itself, this failure criterion is not widely applied into the commercial software. When polyaxial failure criterion is applied into commercial software, relatively poor efficiency of calculation is another factor that may explain its unpopularity.

This paper begins with the effect of intermediate principal stress σ_2 on the behavior of rock masses using Mohr-Coulomb failure criterion in Flac^{3D}. Then, according to the established mathematic relationship between Mohr-Coulomb failure criterion and polyaxial failure criterion, polyaxial failure criterion is equivalently substituted with Mohr-Coulomb failure criterion. As a result, polyaxial failure criterion is introduced in Flac^{3D}. Meanwhile numerical simulation is conducted using polyaxial failure criterion to investigate the effect of intermediate principal stress σ_2 on the behavior of rock masses. In the end, comparisons of numerical results between these two failure criteria are made and applicability of these two failure criteria is discussed.

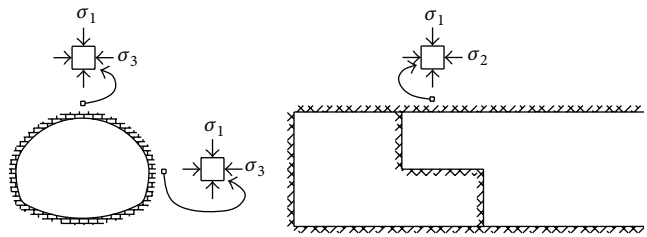

Figure 1: Stress state of rock mass during tunneling.

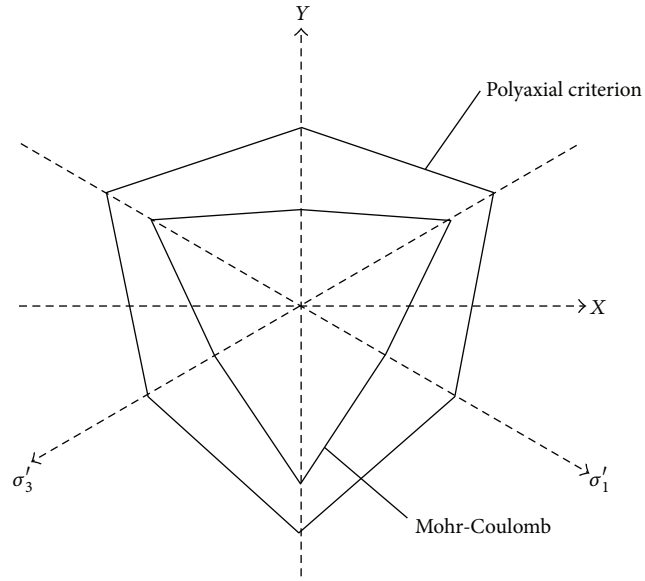

Figure 2: Yield curves on π-plane.

Table 1: Property of rock mass.

ϕ	c	P_v	P_h	P_0
30	0.2 MPa	15 MPa	15 MPa	15 MPa
UCS	E	ν	λ	r_i
1.89 MPa	3 Gpa	0.3	1	3.2 m

2. Analysis of σ_2 Using MOHR-Coulomb Failure Criterion

2.1. Description of Numerical Model. The typical example of deep-buried circular tunnel subjected to a hydrostatic in situ stress field shown in Figure 3 has been selected. Property of geomaterials is shown in Table 1 [11].

Numerical simulation is performed using Mohr-Coulomb failure criterion of Flac^{3D} [10]. The X-axis and Y-axis are in the cross section perpendicular to the tunnel longitudinal direction (Z-axis). The model size is 60 m × 60 m × 40 m ($X \times Y \times Z$). As shown in Figure 3, the normal (vertical) displacement is fixed at the model base. For the lateral boundary condition, stress boundary is applied. In order to simulate the effect of intermediate principal stress well and eliminate other factors affecting the results, numerical simulation adopts 3D model with full excavation

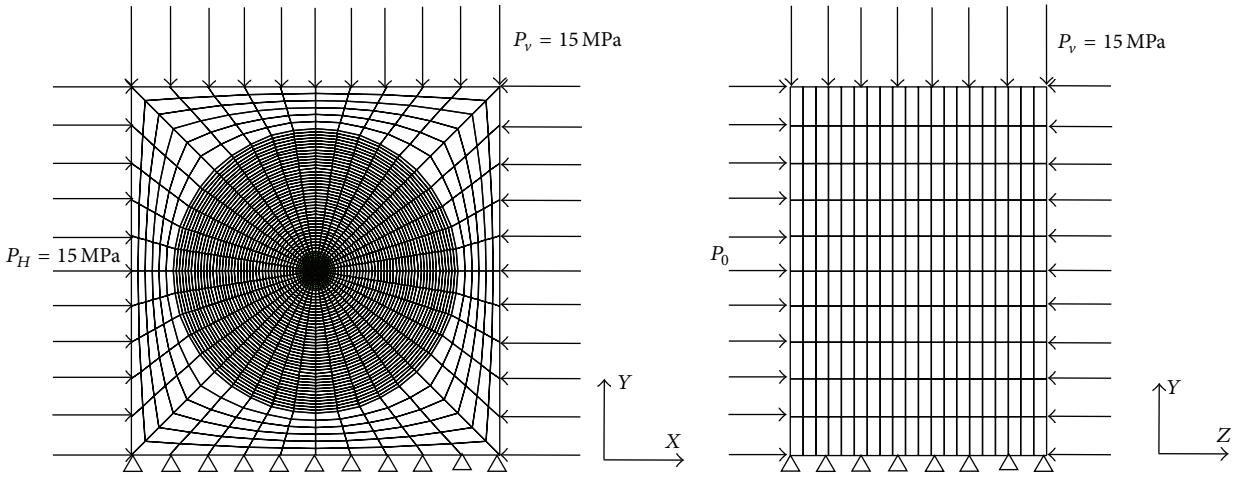

(a) Front view (b) Lateral view

Figure 3: Numerical simulation.

method. During the process of simulation, blasting cycle is 1 m and support system is not installed.

The research includes two cases. Case I: intermediate principle stress $\sigma_2 = 15$ MPa; case II: intermediate principle stress $\sigma_2 = 10$ MPa.

2.2. Numerical Results. In order to minimize boundary effect, the central plane (perpendicular to tunnel longitudinal direction, $z = -20$ m) of the model is selected as the analysis plane. As displacement and size of plastic zone as well as stress distribution can well reflect the effect on the mechanical behavior of rock masses, this research analyzes the results mainly from three aspects mentioned above. In the two cases above, displacement, size of plastic zone, and stress distribution are shown, respectively, in Figures 4~6.

As shown in Figures 4 and 5, value of crown displacement in Figure 4(a) is approximate to that in Figure 4(b); radius of plastic zone in Figure 5(a) is close to that in Figure 5(b). Specifically, the result indicates that when $\sigma_2 = 10$ MPa, displacement of crown and radius of plastic zone are 26.97 cm and 12.64 m, respectively. When $\sigma_2 = 15$ MPa, displacement of crown and radius of plastic zone are 27.75 cm and 12.64 m, respectively. As shown in Figure 6, when intermediate principal stresses are 10 MPa and 15 Mpa, respectively, the distribution of tangential stress shares the same characteristics and distribution of radial stress also shares the same characteristics. As a result, effect of intermediate principal stress σ_2 on rock strength enhancement is not well reflected by deformation and stress and by area of plastic zone when Mohr-Coulomb failure criterion is applied in the numerical simulation. For squeezing geocondition (when sigma-2 is much bigger), applying Mohr-Coulomb failure criterion to simulate rock strength enhancement brought by σ_2 cannot be realized.

3. Analysis of σ_2 Using Polyaxial Failure Criterion

3.1. Establishment of Mathematic Relationship between Mohr-Coulomb and Polyaxial Criterion. A mathematic relationship between Mohr-Coulomb failure criterion and polyaxial failure criterion is established. This relationship is well reflected by the equivalent mechanical parameters inputted into Mohr-Coulomb failure criterion in Flac^{3D} to equivalently substitute polyaxial failure criterion [11] (equivalent Mohr-Coulomb failure criterion). The established mathematic relationship is written as

$$\text{polyaxial: } \sigma_1 = N'_\phi \sigma_3 + \sigma'_{cr}, \tag{4}$$

$$\text{Mohr-Coulomb: } \sigma_1 = N_\phi \sigma_3 + \sigma_{cr}, \tag{5}$$

where $N_\phi = (1 + \sin\varphi)/(1 - \sin\varphi)$, $N'_\phi = 1/(1 - \sin\varphi)$, $\sigma_{cr} = 2c\cos\varphi/(1 - \sin\varphi)$, $\sigma'_{cr} = (\text{UCS} + \sigma_2(A/2))$, $A = 2\sin\varphi/(1 - \sin\varphi)$.

Equivalent Mohr-Coulomb failure criterion is expressed as follows:

$$\text{Equivalent Mohr: } \sigma_1 = N'_{\phi(eq)} \sigma_3 + \sigma'_{cr(eq)}, \tag{6}$$

where $N'_{\varphi(eq)} = (1 + \sin\varphi')/(1 - \sin\varphi')$ and $\sigma'_{cr(eq)} = 2c\cos\varphi'/(1 - \sin\varphi')$.

If (3) is equal to (5), (6) and (7) have to be met:

$$N'_\phi = N'_{\phi(eq)}, \tag{7}$$

$$\sigma'_{cr} = \sigma'_{cr(eq)}. \tag{8}$$

Equivalent internal friction angle is expressed as

$$\varphi' = 2\tan^{-1} \frac{\sin\varphi/(2 - \sin\varphi)}{1 + \sqrt{1 + (\sin\varphi/(2 - \sin\varphi))^2}}. \tag{9}$$

Equivalent cohesion is expressed as

$$c' = \left(\text{UCS} + \sigma_2 \frac{A}{2}\right) B, \tag{10}$$

where $A = 2\sin\varphi/(1 - \sin\varphi)$ and $B = (1 - \sin\varphi)/(2 - \sin\varphi)\cos(\sin^{-1}(\sin\varphi/(2 - \sin\varphi)))$.

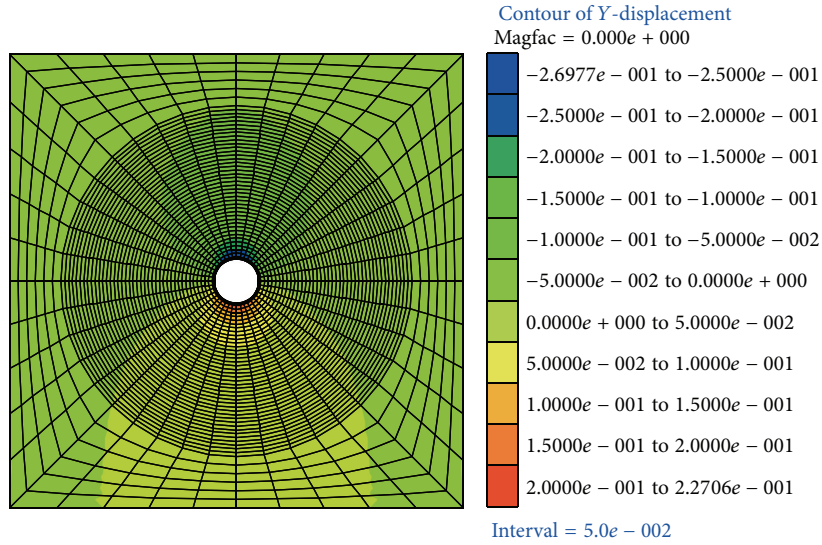

(a) $\sigma_2 = 15$ MPa

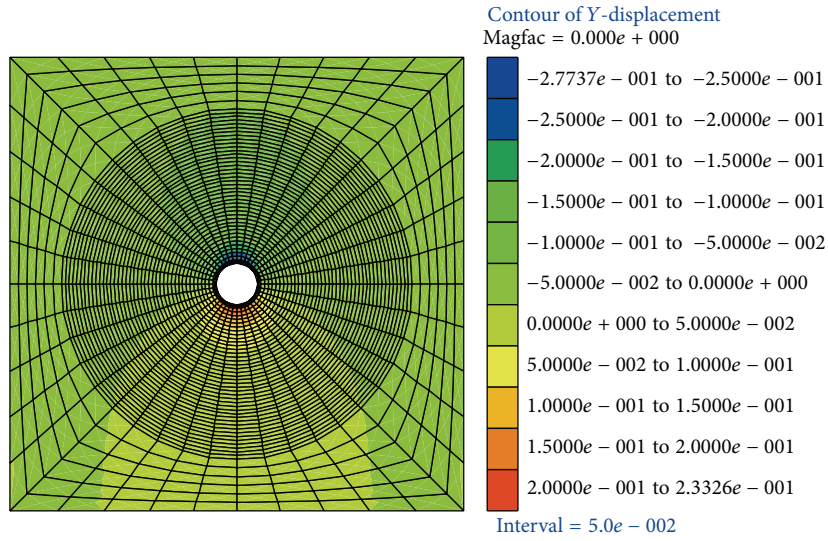

(b) $\sigma_2 = 10$ MPa

Figure 4: Vertical displacement (m).

φ', c' are equivalent internal friction angle and equivalent cohesion, respectively, in equivalent Mohr-Coulomb failure criterion. φ and c are internal friction angle and cohesion, respectively, in Mohr-Coulomb failure criterion.

3.2. Description of Numerical Model. Properties of geomaterials are shown in Table 2. The numerical simulation employs the equivalent Mohr-Coulomb failure criterion (polyaxial failure criterion). According to the established relationship as shown in (8) and (9) between Mohr-Coulomb failure criterion and polyaxial failure criterion, polyaxial failure criterion can be equivalently substituted in the numerical simulation by inputting equivalent cohesion and equivalent internal friction angle into Mohr-Coulomb failure criterion. This numerical simulation includes six cases: case I: $\sigma_2 = 5$ MPa; case II: $\sigma_2 = 10$ MPa; case III: $\sigma_2 = 15$ MPa; case IV: $\sigma_2 = 20$ MPa; case V: $\sigma_2 = 25$ MPa; case VI: $\sigma_2 = 50$ MPa.

The model mainly adopts stress boundary, except the base of the model and boundaries perpendicular to Z-axis, both of which employ the displacement boundary condition. Based on actual requirements, stress boundary is specified on the rest of boundaries as shown in Figure 7. In order to simulate the effect of intermediate principal stress well and eliminate the influence of other factors affecting numerical results, this research adopts 3D (three-dimensional) model with full excavation method. During the simulating process, blasting cycle is 1 m and support system is not installed.

3.3. Numerical Results

3.3.1. Analysis on Displacement. In the six cases above, crown displacement curve, horizontal convergence curve, and invert uplift curve are shown in Figure 8.

Table 2: Equivalent parameters under equivalent Mohr-Coulomb failure criterion.

σ_2	5 Mpa	10 Mpa	15 Mpa	20 Mpa	25 Mpa	50 Mpa
c_{eq}	2.436 MPa	4.204 MPa	5.972 MPa	7.739 MPa	9.507 MPa	18.346 MPa
φ_{eq}	19.47°	19.47°	19.47°	19.47°	19.47°	19.47°

Note: c, φ are 0.2 MPa and 30°, respectively, under Mohr-Coulomb failure criterion.

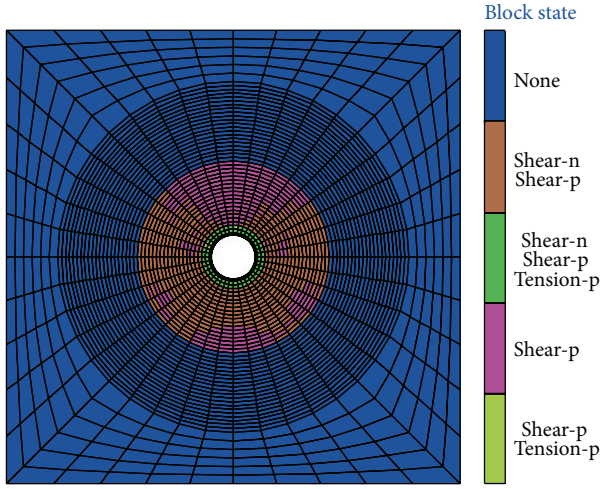

(a) σ_2 = 15 MPa

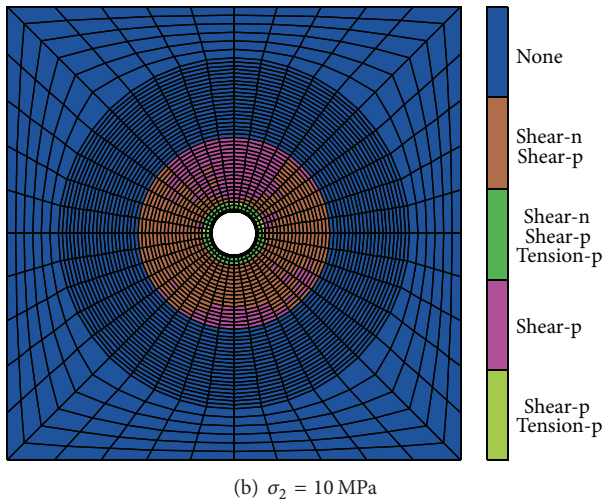

(b) σ_2 = 10 MPa

Figure 5: Plastic zone (m).

Figure 8 shows that deformation value tends to decrease with increment of intermediate principal stress and represents a nonlinear characteristic. When $\sigma_2 \geqslant 20$ MPa, deformation of the rock mass tends to be constant; when $\sigma_2 \geqslant 20$ MPa, rock strength enhancement brought by σ_2 is not significant. It is worth noting that since support structure system is not installed during the numerical simulation, minor principal stress σ_3 equals 0 MPa on the tunnel surface; it is also worth noting that when the intermediate principal stress $\sigma_2 \geqslant 20$ MPa, displacement controller of the rock mass begins to become minor principal stress σ_3 instead of intermediate principal stress σ_2.

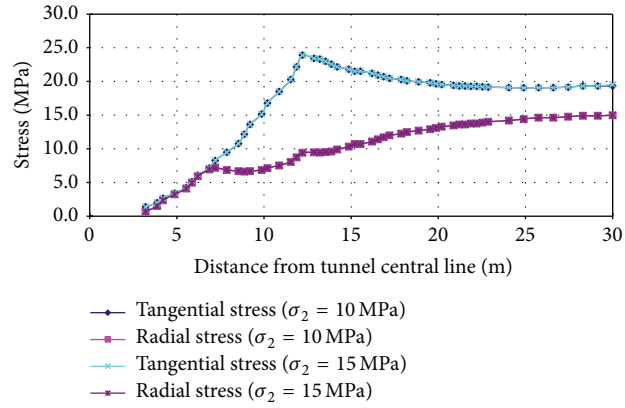

Figure 6: Stress distribution of rock mass.

3.3.2. Analysis on Plastic Zone. The plastic zone with different intermediate principal stress is shown in Figures 9~11. Curve of plastic zone radius shares the same characteristics as displacement curve. Figure 12 shows that effect of intermediate principal stress on the area of plastic zone decreases with the increment of intermediate principal stress.

3.3.3. Analysis of Stress Distribution. After excavation, rock masses around the excavation may fall into plastic state if stress of rock is greater than rock strength, resulting in plastic and shear slip or plastic flow of the rock mass. According to rock mechanics [12], when rock masses fall into plastic state, deformation increases without the change of stress. Based on the rock stress redistribution theory of unsupported tunnel, excavation produces a limited stress concentration at tangential direction. In other words, tangential stress σ_θ continues to increase within a certain distance; if the distance to the tunnel surface is greater than the distance, tangential stress σ_θ decreases. When σ_θ reaches the maximum value, the corresponding distance to the tunnel surface represents the maximum size of the plastic zone.

The results show that radial stress and tangential stress share the same distribution characteristics. With the increment of intermediate principal stress σ_2, the maximum tangential stress also tends to increase, shown in Figures 13~15. Specifically, the maximum tangential stresses are 22.3 MPa (σ_2 = 5 MPa), 23.4 MPa (σ_2 = 10 MPa), 25.1 MPa (σ_2 = 15 MPa), 25.7 MPa (σ_2 = 20 MPa), 28.2 MPa (σ_2 = 25 MPa), and 28.2 MPa (σ_2 = 30 MPa), respectively. Besides, the results indicate that with the increment of intermediate principal stress σ_2 area of stress redistribution tends to be smaller gradually.

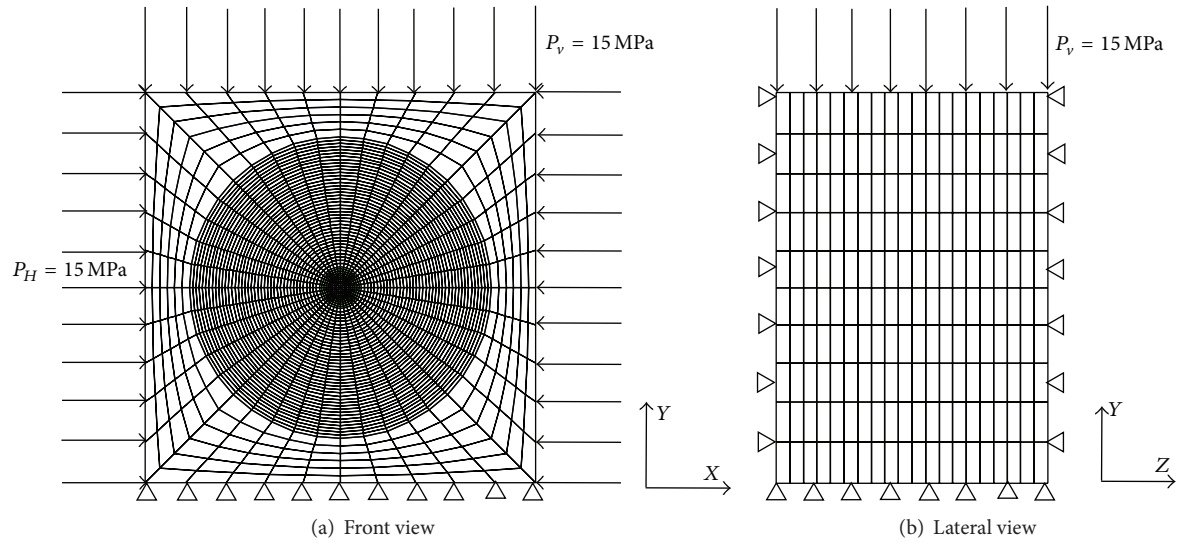

(a) Front view (b) Lateral view

Figure 7: Numerical simulation.

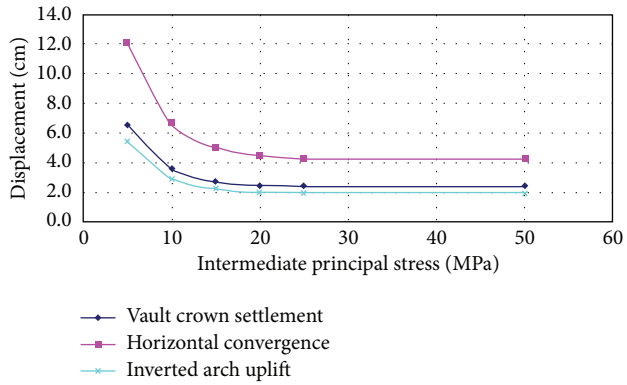

Figure 8: Displacement with increment of intermediate principal stress.

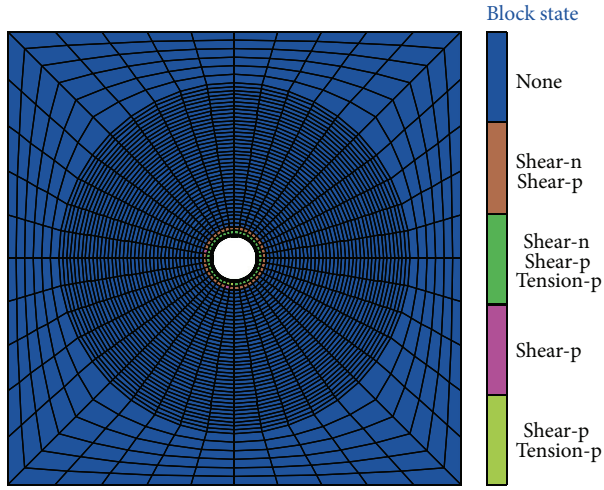

Figure 10: Plastic zone, σ_2 = 15 MPa (radius: 4.20 m).

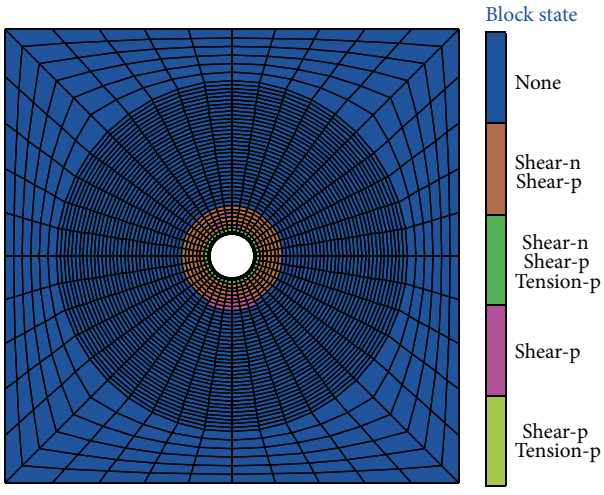

Figure 9: Plastic zone, σ_2 = 5 MPa (radius: 6.70 m).

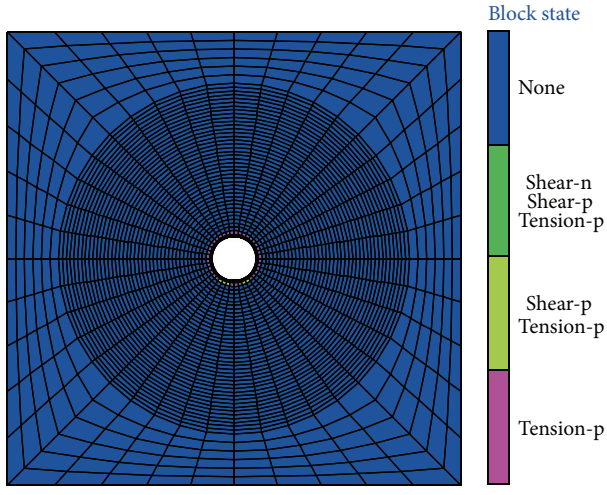

Figure 11: Plastic zone, σ_2 = 25 MPa (radius: 3.60 m).

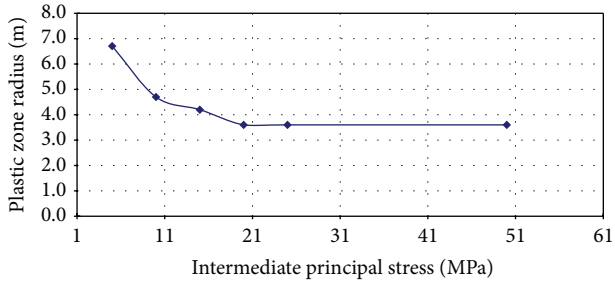

Figure 12: Plastic zone radius with increment of intermediate principal stress.

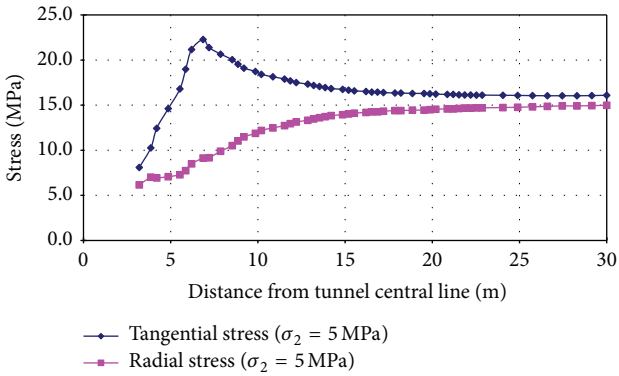

Figure 13: Stress distribution of rock mass (σ_2 = 5 MPa).

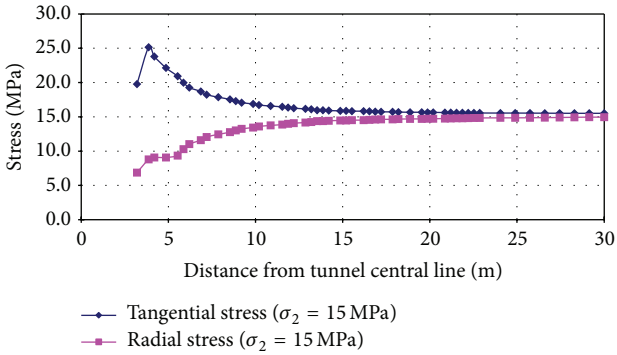

Figure 14: Stress distribution of rock mass (σ_2 = 15 MPa).

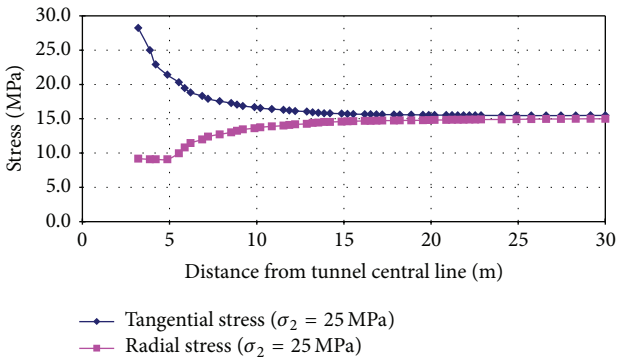

Figure 15: Stress distribution of rock mass (σ_2 = 25 MPa).

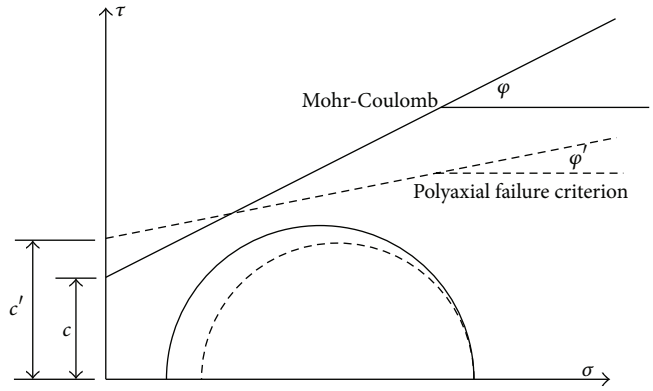

Figure 16: Mohr-Coulomb envelope and polyaxial envelope.

Table 3: Internal friction angle φ and equivalent internal friction angle φ'.

φ (°)	15	20	25	30	35	40
φ' (°)	8.55	11.90	15.54	19.47	23.71	28.27

Table 4: Cohesion c and equivalent cohesion c'.

c (MPa)	15	20	25	30	35	40
c' (MPa)	2.44	4.20	5.97	7.74	9.51	11.27

Table 5: Results of numerical simulation.

Failure criterion	Settlement at crown	Radius of plastic zone
M-C	26.97 cm	12.64 m
Ploy	70.63 cm	24.16 m

4. Discussions

The relationship between cohesion c and equivalent cohesion c' and the relationship between internal friction φ and equivalent internal friction φ' are written as (8) and (9), respectively. According to (8)~(9), equivalent cohesion and equivalent internal friction used in the numerical simulation are shown in Tables 3 and 4, respectively.

From (8) and (9), Mohr-Coulomb failure criterion envelope and polyaxial failure criterion envelope on τ-σ coordinate system are shown in Figure 16.

Figure 16 shows that, for polyaxial failure criterion, effect of intermediate principal stress on rock strength is explained that internal friction is reduced and meanwhile cohesion is increased. Equations (2)~(3) indicate that the effect of σ_3 under Mohr-Coulomb failure criterion is smaller than that under polyaxial failure criterion, when intermediate principal stress σ_2 is = 0. As a result, when intermediate principal stress σ_2 = 0 or rock strength enhancement brought by σ_2 can be ignored (such as tunnel portal), it is improper that numerical simulation is executed using polyaxial failure criterion. Table 5 shows settlement of the crown and radius of plastic zone when Mohr-Coulomb failure criterion and polyaxial failure criterion are applied, respectively, in the numerical simulation.

5. Conclusions

(1) The results of numerical simulation under Mohr-Coulomb failure criterion show that the intermediate principal stress σ_2 does not exert a significant influence on stress redistribution and displacement at crown as well as the size of plastic zone in numerical simulation.

(2) Intermediate principal stress has a significant enhancement on rock strength. Specifically, greater σ_2 not only significantly reduces the displacement at the crown and excavation disturbance area as well as the size of plastic zone but also improves the bearing capacity of rock mass. Particularly for the squeezing condition, effect of σ_2 is significant. As a result, for squeezing geocondition where lateral pressure coefficient K is greater than 0.5 Mohr-Coulomb is not applicable to analyze the mechanical behavior of rock mass.

(3) For polyaxial failure criterion, effect of intermediate principal stress on rock strength enhancement is explained that internal friction angle is reduced and meanwhile cohesion is increased.

(4) The effect of σ_3 under Mohr-Coulomb failure criterion is smaller than that under polyaxial failure criterion, when intermediate principal stress σ_2 is = 0 or is small. As a result, when in tunnel portal (σ_2 is much smaller than other principal stresses), using polyaxial failure criterion in numerical simulation is not proper.

Conflict of Interests

The authors declare that there is no conflict of interests regarding the publication of this paper.

Acknowledgments

The authors gratefully acknowledge the financial support to this study from NSFC (Natural Science Foundation of China) (U1434206, 51378321, and 51208437) and the Fundamental Research Funds for the Central Universities (2682015CX095).

References

[1] E. Hoek, P. K. Kaiser, and W. F. Bawden, *Support of Underground Excavations in Hard Rock*, Funding by Mining Research Directorate and Universities Research Incentive Fund, A.A. Balkema Publishers, 1993.

[2] S. Senent, R. Jimenez, and A. Reyes, "Numerical simulation of the influence of small-scale defects on the true-triaxial strength of rock samples," *Computers and Geotechnics*, vol. 53, pp. 142–156, 2013.

[3] R. Wang and J. M. Kemeny, "A new empirical failure criterion under polyaxial compressive stresses," in *Proceedings of the 35th U.S. Symposium on Rock Mechanics*, J. J. K. Daemen and R. A. Schultz, Eds., pp. 453–459, Reno, Nev, USA, 1995.

[4] Z.-H. Li, W.-C. Zhu, X.-T. FenG, S.-J. Li, H. Zhou, and B.-R. Chen, "Effect of lateral pressure coefficients on damage and failure process of horseshoe-shaped tunnel," *Rock and Soil Mechanics*, vol. 31, pp. 434–461, 2010 (Chinese).

[5] B. Singh, R. K. Goel, V. K. Mehrotra, S. K. Garg, and M. R. Allu, "Effect of intermediate principal stress on strength of anisotropic rock mass," *Tunnelling and Underground Space Technology*, vol. 13, no. 1, pp. 71–79, 1998.

[6] B. Singh and R. K. Goel, *Tunnelling in Weak Rocks*, vol. 5 of *Geo-Engineering*, Elsevier Science, 2006.

[7] D. Scussel and S. Chandra, "New approach to the design of tunnels in squeezing ground," *International Journal of Geomechanics*, vol. 14, no. 1, pp. 110–117, 2014.

[8] N. Barton, R. Lien, and J. Lunde, "Engineering classification of rock masses for the design of tunnel support," *Rock Mechanics Felsmechanik Mécanique des Roches*, vol. 6, no. 4, pp. 189–236, 1974.

[9] D. Scussel and S. Chandra, "Polyaxial stress analysis of underground openings using FLAC," *Journal of Rock Mechanics and Tunnel Technologies*, vol. 18, no. 1, pp. 41–54, 2012.

[10] *Itasca User's Guide for FLAC3D*, Version 3.0, 2005.

[11] D. Scussel and S. Chandra, "A new approach to obtain tunnel support pressure for polyaxial state of stress," *Tunnelling and Underground Space Technology*, vol. 36, pp. 80–88, 2013.

[12] G. Baoshu, *Tunnel Mechanics*, Southwest Jiaotong University Press, 1993.

Hindawi Publishing Corporation
Mathematical Problems in Engineering
Volume 2015, Article ID 157129, 13 pages
http://dx.doi.org/10.1155/2015/157129

Research Article

Sustainability-Related Decision Making in Industrial Buildings: An AHP Analysis

Jesús Cuadrado, Mikel Zubizarreta, Eduardo Rojí, Harkaitz García, and Marcos Larrauri

Department of Mechanical Engineering, University of the Basque Country (UPV/EHU), Alameda Urquijo s/n, 48013 Bilbao, Spain

Correspondence should be addressed to Mikel Zubizarreta; m.zubizarreta@ehu.es

Received 5 March 2015; Accepted 20 May 2015

Academic Editor: Jurgita Antucheviciene

Few other sectors have such a great impact on sustainability as the construction industry, in which concerns over the environmental dimension have been growing for some time. The sustainability assessment methodology presented in this paper is an AHP (Analytic Hierarchy Process) based on Multicriteria Decision Making (MCDM) and includes the main sustainability factors for consideration in the construction of an industrial building (environmental, economic, and social), as well as other factors that greatly influence the conceptual design of the building (employee safety, corporate image). Its simplicity is well adapted to its main objective, to serve as a sustainability-related decision making tool in industrial building projects, during the design stage. Accompanied by an economic valuation of the actions to be undertaken, this tool means that the most cost-effective solution may be selected from among the various options.

1. Introduction

The environmental footprint of construction activity is immense. The building sector in the developed countries of the European Union consumes 40% of their total energy consumption [1]. The building industry consumes a somewhat similar percentage of all materials in the global economy. In the typical "life cycle" of a building (building, maintenance, and demolition), the building is "responsible" for 50% of total energy consumption and for 50% of total CO_2 atmospheric emissions [2]. The focal area of this study looks at the important area of nonresidential buildings and more specifically industrial buildings, which represent roughly 15% of all buildings.

The "ICLEI-Annual Sustainability Report 2011-2012" affirmed once again that sustainable development should be high on the agenda [3]. Up until its publication, the environmental requirement had been the focus of most studies, databases, design guides, and assessment tools on sustainable construction [4–7]. However, the number of research papers and assessment tools that also incorporate economic and/or social requirements [8–10] as well as the first standards which legislate social aspects [11, 12] has recently begun to emerge.

These tools may be described as follows:

(i) Life Cycle Analysis (LCA): tools that process complex data sets such as ECOQUANTUM and ENVEST [13].

(ii) Scientific standards: less complex but also accurate tools, such as DGNB, LEED, and BREEAM [14, 15].

(iii) Checklists: very simple tools based on best practice, such as IHOBE Guides [16].

Specific modules that are part of LEED, BREEAM, and DGNB, for example, exist for the evaluation of industrial buildings.

The methodology advanced in this paper sets a sustainability value for industrial buildings, by applying a limited number of easily quantifiable evaluation criteria, so as to assist decision making in relation to sustainability during the design stage of industrial building projects.

The Integrated Value Model for Sustainable Assessment (Modelo Integrado de Valor para una Evaluación Sostenible, MIVES), a Multicriteria Decision Making (MCDM) tool based on AHP (Analytic Hierarchy Process), is central to this assessment process. MIVES is applied in the Spanish structural concrete standards [17] and the Spanish structural

Table 1: Criteria in relation to the different requirements according to their stage of its life cycle.

Study scope	Life cycle			
	Conception	Materialization	Use	Reintegration
Safety	Cr_{SC1}	Cr_{SM1}	Cr_{SU1}	Cr_{SR1}
	Cr_{SC2}	Cr_{SM2}	Cr_{SU2}	Cr_{SR2}
	⋮	⋮	⋮	⋮
Society	Cr_{SoC1}	Cr_{SoM1}	Cr_{SoU1}	Cr_{SoR1}
	Cr_{SoC2}	Cr_{SoM2}	Cr_{SoU2}	Cr_{SoR2}
	⋮	⋮	⋮	⋮
Environment	Cr_{EC1}	Cr_{EM1}	Cr_{EU1}	Cr_{ER1}
	Cr_{EC2}	Cr_{EM2}	Cr_{EU2}	Cr_{ER2}
	⋮	⋮	⋮	⋮
Economy	Cr_{EcC1}	Cr_{EcM1}	Cr_{EcU1}	Cr_{EcR1}
	Cr_{EcC2}	Cr_{EcM2}	Cr_{EcU2}	Cr_{EcR2}
	⋮	⋮	⋮	⋮
Functionality	Cr_{FC1}	Cr_{FM1}	Cr_{FU1}	Cr_{FR1}
	Cr_{FC2}	Cr_{FM2}	Cr_{FU2}	Cr_{FR2}
	⋮	⋮	⋮	⋮
Corporate image	Cr_{CIC1}	Cr_{CIM1}	Cr_{CIU1}	Cr_{CIR1}
	Cr_{CIC2}	Cr_{CIM2}	Cr_{CIU2}	Cr_{CIR2}
	⋮	⋮	⋮	⋮

steel standards [18] as well as in many other areas [19]. As with the sustainable design of residential or office buildings [20, 21], in this study, the impact of the production process is not considered in the sustainable design of the industrial building.

2. Sustainability in Industrial Buildings

Our definition of a factory or an industrial building is as follows: "an area in which industrial production takes place as well as storage. The term factory as an alternative to industrial building covers generic aspects of industrial production. Nevertheless, both terms imply the existence of constructions, that is, areas of human design completed with the use of natural and artificial products, elements and construction systems within a controlled environment" [22].

In the past, the design of an industrial building was limited to its envelope, four walls, and a roof, under which productive activities took place. Today, their sustainable aspects refer mainly to the production processes that take place inside it. Attention centres on aspects such as pollution from the productive activity at all stages of the building life cycle (air, noise, water, etc.), as well as waste disposal and recycling, while very few resources are dedicated to research on the actual building [23, 24].

2.1. Sustainability Requirements and the Life Cycle of an Industrial Building. Factories may be perceived in terms of architectural elements interacting with sustainability requirements [15]. This innovative vision entails certain macro criteria or "sustainable requirements" in the design of an industrial building. So, the building should comply with sustainable global aspects, defined in terms of targets and needs. These should be identified at all stages of the building life cycle: that is, design, construction, usage, and reintegration.

In conventional terms, three basic, interrelated pillars constitute sustainability: the environment, the economy, and the society [25]. As with all constructions, the factors that comprise these three basic pillars of sustainability have to be strengthened in industrial buildings. However, the characteristics of industrial constructions emphasize design and construction functionality (factors linked to plant performance), worker safety throughout all the phases of life cycle, and the public image of the firm in the building (factors linked to marketing and economics). Even though they might form part of three basic requirements in other sorts of buildings, these requirements are of great importance in this type of buildings and should be considered independently [26, 27].

A total of six scopes of study or requirements are therefore defined around these 3 basic pillars for the sustainability assessment of a factory. Further 3 requirements were separately defined, due to their relevance to industrial production, as shown in Table 1.

Each of the headings set out below relate to one of the various requirements.

Safety and Industrial Risk Prevention. Safety implies an accident prevention programme that protects the physical integrity of anyone in or near the building, particularly during construction and demolition processes and maintenance works. The main purpose of these programmes is the prevention of industrial accidents. Consideration should also

be given to structural safety, should the building be exposed to explosions or fires, as well as security and the protection of products, equipment, and the know-how.

Society. An industrial building provides employment and brings positive economic advantages at a local level. In this area, working relationships, the quality of the environment, and mobility within the building should also be considered. Travel between the home and the workplace should also be highlighted here, including the offer of alternative modes of transport to the private vehicle and health alternatives such as travel on foot and by bike. Workers on a building site should also have access to services that fulfill basic human needs for hygiene and rest (changing rooms, wash rooms, rest areas, meeting rooms...).

Environment. Various alternative locations for industrial buildings should be compared. Moreover, the use of "ecological" materials with a lower environmental impact should be assessed to reduce the energy consumption of the plant with a view to the reduction of energy. The use of recycled materials may also be studied. The end of the building life cycle involves selective demolition and waste management that can also mitigate the overall environmental impact. Throughout its useful life, an industrial building can accumulate a series of waste products, disposal of which requires management and planning of storage space within the installations. Total energy consumption, which is significant throughout the life of the building, can be reduced by means of cogeneration techniques and the introduction of renewable energies.

Economy. Careful consideration must be given to the economic requirement of the building at the construction stage and to maintenance and preservation actions in the course of its useful life. In terms of sustainability, coordination of consumption patterns throughout the useful life of the building is of great importance. Where possible, contractual arrangements for construction work should refer to sustainability-related issues (material origin and quality) and any completion dates should be within an economically viable period so that the investment may be recovered within the shortest possible time.

Functionality. A functional design implies that certain activities may be easily performed without any problems that relate to the building. The space available in the building for the process must be assessed in case future economic growth may require further plant expansion, reducing any future need for new materials, lowering economic costs and any waste that may be generated. The interior working conditions and ambient setting can affect the performance of employees and, in consequence, plant productivity. Various parts of the building may contain aggressive agents that affect its useful life and generate further maintenance needs that can have serious economic consequences. Expert knowledge will help locate the necessary services for production, planning enough room for auxiliary and storage facilities, and loading and unloading bays, which are essential components in the smooth management of the plant.

Corporate Image. Building image and aesthetics is a further aspect to recall. An architectural asset can contribute to the built environment of the city and industrial area and specifically to the company image. The company that owns the building often promotes its own corporate image in the construction, with higher associated costs and impacts.

All of these sustainable requirements have clear roles in the different phases of the building life cycle, from the design and throughout its useful life to its demolition and the management of any waste products. A list of 31 study criteria was composed, connected to the 6 requirements described above for sustainability evaluation in industrial buildings.

3. Materials and Methods

The MIVES [28] assessment methodology, as explained, was combined with a simplified Life Cycle Assessment (LCA). MIVES is a Multicriteria Decision Making (MCDM) with added AHP-based value functions. Their incorporation makes it possible to add homogeneity to different indicators which have different measurement units (economy is measured in €; environmental impact is measured in CO_2 kg). A reliable assessment requires a relevant evaluation model with a suitable requirement tree, with a balanced number of indicators [29].

The hierarchical structure of the requirement tree defines the assessment object, scopes of study, criteria, and indicators. Following the definition of this requirement tree, the methodology is used to calculate the Industrial Building Sustainability Index (IBSI), as shown in (Figure 1).

The following requirements are also known as the scopes of study (SS): safety, society, environment, economy, functionality, and corporate image. These can be divided into more specific criteria (CR): external mobility, safety measures in the construction process, use of ecological materials, cost of supplies, durability, brand image of the firm, and so forth. In turn, each criterion can be subdivided into indicators (ID), estimated with quantifiable values.

The key aspect in the definition of the indicators is that, apart from allowing quantification and simplification of the study phenomena, they must reflect the changes that occur in the system. Moreover, the utility of the indicators varies greatly with the context, which suggests that they have to be very carefully selected. The available information on the processes, functions, and study factors is a further key point in the selection of the indicators. All these points have an effect on the indicators, on their development, and on the development of their defining variables.

3.1. Sustainability Assessment. The following steps have to be completed, to prepare the sustainability assessment.

Step 1. Prepare an evaluation tree consisting of scopes of study, criteria, and indicators. A requirement tree that has a balanced number of criteria is of great importance.

Step 2. Calculate the weights to attach to each different stage in the evaluation; each criterion with its indicators, the requirement with its set of criteria, and the requirements that

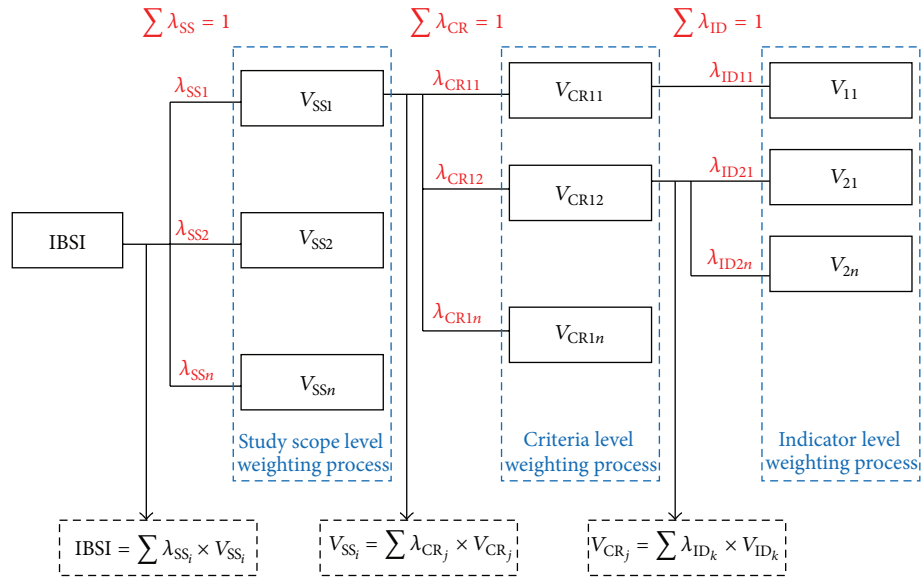

Figure 1: Hierarchical structure of the requirement tree.

comprise the "Industrial Building Sustainability Index" are all assigned to different levels of the evaluation tree.

Step 3. The value function of each indicator between a minimum value of "0" (the worst solution) and the maximum value of "1" (the best solution) offers a range of possible solutions, a set score or an output register.

Step 4. The requirements yield partial results, as well as the value of the "Industrial Building Sustainability Index," when the set of output registers are added, on the basis of the proposed system of weighting at each stage. All these values are in turn defined at some point between 0 and 1.

3.2. The Expert Panel and Selection of the Criteria. The most important criteria were selected using the Delphi method. This method addresses a complex problem through a group of individuals (Expert Panel) [30]. The group members followed this systematic process by choosing the evaluation criteria to assess the sustainability of industrial buildings. The first phase of this method began with open-ended questions, from which the items and issues were extracted for the continuation of the work. In a second phase, the questions were directed towards the evaluation, ranking, or comparison of the items. These successive questionnaires were intended to reduce the range of opinions and to clarify the consensus average opinion.

In the first phase, the Expert Panel obtained a total of 185 criteria, through an open-ended questionnaire. Following the initial collection of the criteria, the Expert Panel ranked these criteria, in the course of several successive meetings, and allocated a relative weight to each one, grouped under the requirements. These results were unified in the final phase, eliminating those with a relative weight of less than 5%. A total of 154 criteria were filtered out with this process, to arrive at 31 final evaluation criteria.

The Delphi method was selected for this study, because it offers the following advantages [30–32]:

(i) Group knowledge will always be superior to the knowledge of an individual participant who is better prepared than others, as the knowledge of each of the participants is complementary.

(ii) The opinions of each of its members may be contrasted.

(iii) The number of factors under study is higher, as each expert contributes a general idea of the topic from their specific knowledge domain to the discussion.

Using this method, it is necessary to avoid the dominant influence of any member of the group over the rest, in order to achieve an effective communication process. Many authors have pointed out that the Delphi method can minimize this aspect [33–35]. It is therefore necessary for each participant to remain unaware of the identity of the other participants.

An essential key to carry this process through successfully is the appropriate selection of panel members, selected for their skills, knowledge, and independence. The members of the Expert Panel comprised construction sector professionals (experts in raw materials, construction products, construction, engineering, and health and safety as well as researchers at technology centres and universities). Various panel member selection methods can be used. The criteria defined by Hallowell and Gambatese [36] require each expert to score at least 11 points in relation to categories of achievements or experience needed to sit on the panel. These authors considered an ideal panel in terms of a varied and a highly qualified group of between 8 and 16 individuals. The experts were chosen from a construction sector database of 72 professionals, employed by 31 different organizations at a national level (companies, technological

Table 2: Breakdown of the scopes of study.

Industrial Building Sustainability Index (IBSI)				
Scope of study	Weight	Criterion	Designation	Weight
SS1 Safety	16.67%	CR1.1	Structural safety against fire	19%
		CR1.2	Safety and health in the execution procedure	37%
		CR1.3	Safety measures in the construction process	19%
		CR1.4	Maintenance and conservation of the industrial plant	10%
		CR1.5	Safety against intruders	5%
		CR1.6	Safety and health during deconstruction	10%
SS2 Society	16.67%	CR2.1	External mobility	43%
		CR2.2	Respect for the urban environment	14%
		CR2.3	Auxiliary services for personnel	43%
SS3 Environment	16.67%	CR3.1	Integration in the natural environment	6%
		CR3.2	Environmental impact during construction	17%
		CR3.3	Use of ecological materials	10%
		CR3.4	Environmental impact during utilization	34%
		CR3.5	Waste management during utilization	10%
		CR3.6	Impact of materials from demolition	23%
SS4 economy	16.67%	CR4.1	Cost of executing the work	17%
		CR4.2	Construction timeframe	12%
		CR4.3	Cost of supplies	32%
		CR4.4	Cost of maintenance	32%
		CR4.5	Cost of building demolition	7%
SS5 Functionality	16.67%	CR5.1	Performance of the building in use	6%
		CR5.2	Constructability of ease of construction	11%
		CR5.3	Quality of internal environment	23%
		CR5.4	Durability	16%
		CR5.5	Flexibility	23%
		CR5.6	Ease of maintenance	11%
		CR5.7	Auxiliary production services	4%
		CR5.8	Deconstructibility	6%
SS6 corporate image	16.67%	CR6.1	Integration in the urban environment	20%
		CR6.2	Brand image of the firm	60%
		CR6.3	Aesthetic maintenance of the building	20%

centres, and universities). They have all taught on the Master's Degree in Construction Engineering at the University of the Basque Country (UPV/EHU). The details of the project were shared with professionals and the different stakeholder groups in workshops at the University of the Basque Country (UPV/EHU), where the content of the master's course are imparted. Following the selection process, the Expert Panel comprised 11 members.

Table 2 presents the selected scopes of study and criteria in the calculation of the IBSI, together with their relative weights.

Certain tangible and therefore directly measurable criteria were selected. Other more subjective and intangible criteria as in the case of "quality of internal environment" had also to be considered. In these cases, quantifiable indicators were used to assess the criteria. Measurement of the "quality of internal environment" was quantified through an evaluation of the following 5 indicators: "light level," "interior ventilation," "temperature in the work area," "noise present in the building," and "electromagnetic pollution." The relevant weights were attached to the indicators that constituted each criterion for its quantification.

3.3. Assignment of the Relative Weights. Initially, sustainability priorities or weights have to be attached to the respective hierarchical levels of the assessment model (λ_i, λ_{CR}, and λ_{SS}).

In recent years, various studies have examined the preferential assignment of some criteria in relation to others, based on attributes wherever complete information is missing [37–42]. The "Analytic Hierarchy Process (AHP)" Decision Method [43, 44] was used for calculating the sustainability weights.

Following this method, the relative priority of each alternative is placed on a quantifiable scale. It thereby emphasizes the intuitive criteria of the decision-makers and the reliability of their comparisons when rating different options. The methodology incorporates the principle that knowledge and experience guide the judgments of decision-makers.

It also organizes both tangible and intangible factors in a systematic manner, to arrive at a simple structured solution. As explained, this methodology constitutes a numerical assessment of alternatives based on the systematic assessment of a set of decision alternatives [45].

3.4. The Industrial Building Sustainability Index (IBSI). The addition of each dimensionless value (V_{SS}) of the 6 requirements or scopes of study yields the Industrial Building Sustainability Index (IBSI). These values have previously been corrected according to their own final weight (λ_{SS}), as shown in

$$\text{IBSI} = \sum_{i=1}^{j} \lambda_{SS_i} \times V_{SS_i}, \tag{1}$$

where IBSI is Industrial Building Sustainability Index. λ_{SS_i} is weight of the study scope i. V_{SS_i} represents value of the study scope i. j is total number of study scopes.

The addition of the specific dimensionless values (V_{CR}) of the 3-to-8 criteria of each requirement yielded the dimensionless values (V_{SS}) of each of the 6 requirements. These values were previously corrected according to their own final weight (λ_{CR}), as shown in

$$V_{SS_k} = \sum_{i=1}^{j} \lambda_{CR_{i,k}} \times V_{CR_{i,k}}, \tag{2}$$

where V_{SS_k} is study scope k value. $\lambda_{CR_{i,k}}$ represents criterion weight i of study scope k. $V_{CR_{i,k}}$ is criterion value i of study scope k. j represents number of criteria hanging from study scope k.

Each of the dimensionless values (V_{CR}) of the 31 criteria was obtained by adding up the dimensionless value functions ($V_{i,k}$) of the 1-to-4 indicators of each criterion. These values were previously corrected according to their own final weight ($\lambda_{i,k}$), as shown in

$$V_{CR_k} = \sum_{i=1}^{j} \lambda_{i,k} \times v_{i,k}\left(x_{alt}\right), \tag{3}$$

where V_{CR_k} is criterion k value. $\lambda_{i,k}$ represents indicator weight i of criterion k. $v_{i,k}(x_{alt})$ is indicator value i of criterion k. j represents number of indicators hanging from criterion k.

The value functions ($v_{i,k}$) range from 0 to 1, which are the minimum and the maximum level of satisfaction with each indicator. Each value function is defined by 5 parameters. The function shape and, consequently, the variation in each indicator value may be defined with these parameters in relation to the dimensionless scale. Function (4) assigns a numerical value to the different coefficients and parameters to model the physical behaviour of the indicator:

$$v_i = A + \frac{1}{B} X \left[1 - e^{-k_i X(|x_{alt} - x_{min}|/C_i)^{P_i}}\right], \tag{4}$$

where x_{min} is minimum reference point on the indicator scale under consideration. Response to the indicator generates a value equal to 0. x_{max} represents maximum reference point on the indicator scale under consideration. Response to the indicator generates a value equal to 1. x_{alt} is response to the assessed alternative regarding the indicator under consideration, which will lie between the values x_{min} and x_{max}. Response to the indicator generates a value equal to $v_i(x_{alt})$, which is sought. P_i is a form factor defining whether the curve is concave, convex, lineal, or "S" shaped, where concave curves are obtained for $P_i < 1$ values, convex or "S" shaped curves if $P_i > 1$, and lineal if $P_i \approx 1$. k_i defines the ordinate value of point C_i. A represents value of response "x_{min}," $A = 0$, or $A = 1$ (generally $A = 0$). B is a factor enabling maintenance of the value function in the range (0.00; 1.00) and the best response always has a value equal to 1. This factor is defined by

$$B = \frac{1}{1 - e^{-k_i X(|x_{max} - x_{min}|/C_i)^{P_i}}}. \tag{5}$$

By entering different values in the 5 variables of the expression, we can get different modes of adaptation to the nature of the study variable (indicator). Thus, the obtained values can vary from a linear response (ascending or descending), to concave shaped responses, convex shaped responses, or even "S" shaped responses, as seen in Figure 2.

3.5. Example of a Criteria Evaluation Process. In the following section, only the example of the evaluation of the indicator associated to "safety measures in the construction process (CR 1.3)" criterion will be described, due to limitations on the length of the paper.

The input values that are taken into account to assess this specific indicator are shown in Table 3.

As an evaluation example, Case Study 1 (oil mill housing) has been selected, which is described in more detail in the next section (Section 4). Based on this case and once all points have been checked, the score obtained in the indicator associated with criterion CR 1.3 was 40 points. By entering this score in the value function associated with this indicator (Figure 3), which is a lineal function in this case, a dimensionless value of 0.4 is obtained. The next step in the evaluation consists in multiplying this value by the corresponding relative weight of criterion 1.3, which has been defined in Table 2, in this case 19%. Thus, the final value of Criterion 1.3 for the Case Study 1 is 0.077, as can be seen in Table 4.

4. Results and Discussion

Three case studies of industrial buildings were performed with the methodology: a building housing an oil mill, another housing slag pits at a steel plant, and a construction materials storage depot and showroom. The three examples have very different characteristics, so as to test the responsiveness of the proposed methodology and its behaviour. These characteristics reflect different locations, from rural to highly urbanized zones with large-scale public communications infrastructure. Steel and precast concrete were the main construction materials found in the buildings. The various

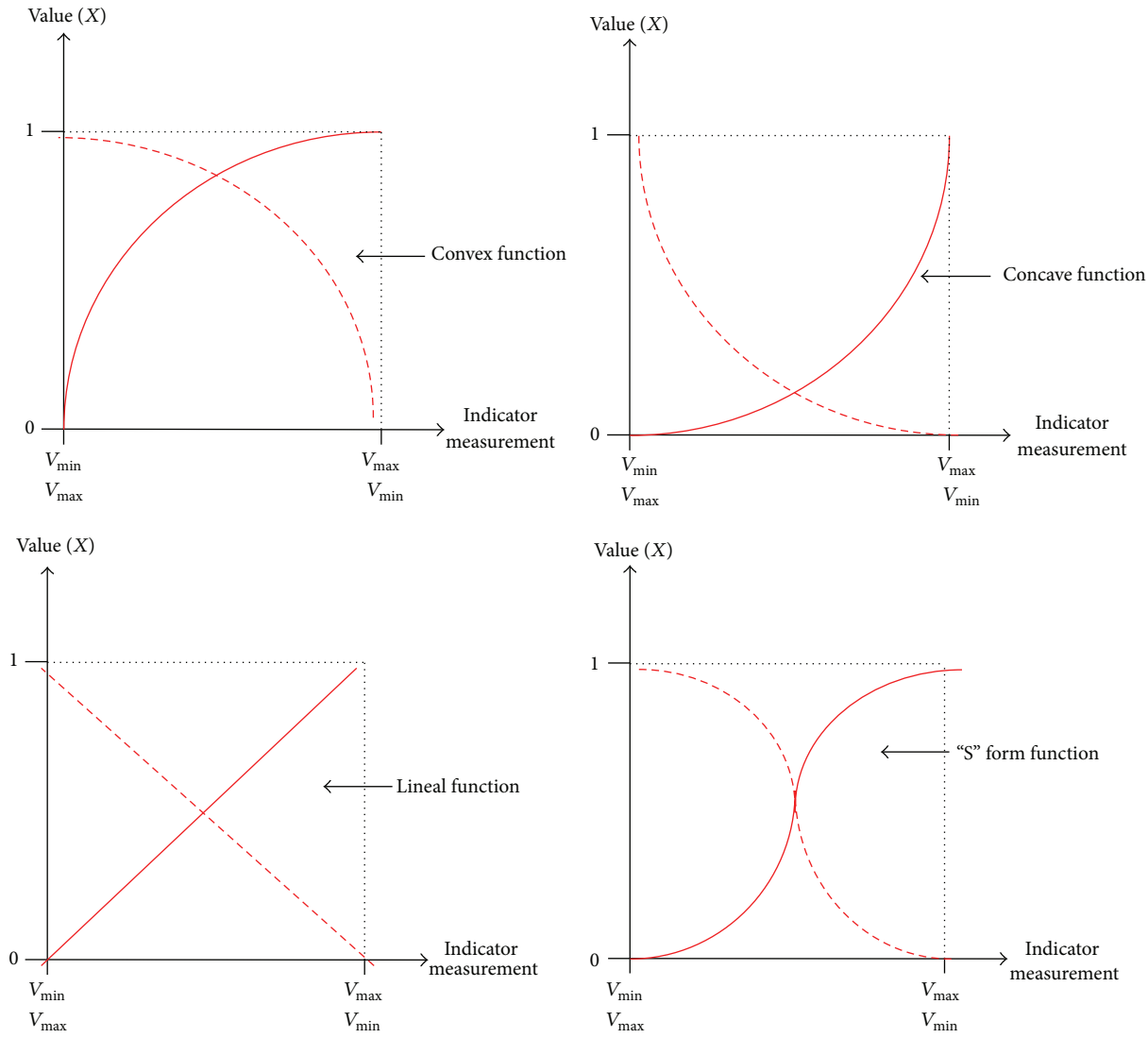

Figure 2: Modes of adaptation to the nature of the indicator.

Table 3: Input values of the indicator associated with criterion CR1.3.

Number	Input value	Satisfied	Not satisfied	Case Study 1
1	Strict compliance with the safety rules in force	0	Evaluation is not allowed	0
2	Existence of a health and safety coordinator, which has to belong to the construction company and must not be outsourced	30 points	0 points	0
3	In the technical specifications, the existence of the requirement that all personal and collective protection systems must have the CE marking	30 points	0 points	0
4	Promotion of the use of collective protection measures, rather than individual protective equipment, which are only used when it is essential	40 points	0 points	40 points
	Total			**40 points**

Table 4: Breakdown of "safety" study scope at its different hierarchical levels.

Study scope	Criterion (CR)	Oil mill housing $V_{CR1,k}$	Slag pit housing $V_{CR1,k}$	Storage depot $V_{CR1,k}$
Safety (SS1)	Structural safety against fire (CR1.1)	0.000	0.000	0.087
	Safety and health in the execution procedure (CR1.2)	0.037	0.257	0.184
	Safety measures in the construction process (CR1.3)	0.077	0.193	0.135
	Maintenance and conservation of the industrial plant (CR1.4)	0.036	0.051	0.068
	Safety against intruders (CR1.5)	0.051	0.051	0.051
	Safety and health during deconstruction (CR1.6)	0.098	0.098	0.065

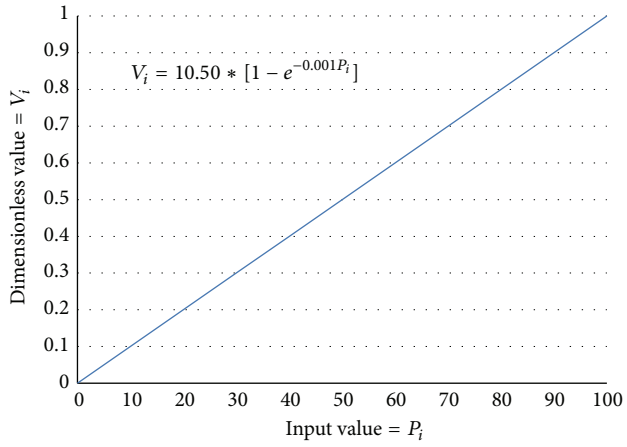

Figure 3: Value function of the indicator associated with criterion CR1.3.

agents who intervened in the construction held different quality and environmental certifications. The processes that take place inside them differ and, in consequence, so do their environmental requirements. The proposed sustainability assessment methodology is applied to the different practical case studies in the following sections.

4.1. Case Study 1: Oil Mill Housing. The manufacturing process of pressing olive oil takes place regularly at the same time of year in this building. Throughout the rest of the year the building remains open to sell and to distribute the product. The oil mill is near a rural agglomeration of 4,000 inhabitants, without any public transport links. The building occupies an area of 1,092 m^2, on a shallow foundation, poured with 105.94 m^3 of concrete. Its metallic frameworks are finished off with laminated profiles (38,542.47 Kg) and it has a 70 m^2 mezzanine floor. The warehouse is enclosed with panels made of two sheets joined by a 100 mm thick polyurethane foam core, with a total area of 802.40 m^2. This same system of panels covers the gable roof at an inclination of 15%, occupying a total area of 1,122 m^2. The facade covering the hallway that leads to the different work areas has large windows to take in natural light and for ventilation, with a total glass area of 74.11 m^2. The building has standard installations, with a mixed boiler partially fuelled by the waste from the oil extraction process. A small engineering firm, with no quality or environmental certification, completed the design. The same may be said of the construction firm and the promoter and owner of the plant. The industrial activity of the firm according to Spanish legislation is an activity that is classified as unpleasant, unhealthy, or dangerous, which also generates toxic waste.

4.2. Case Study 2: Slag Pit Housing. This industrial building houses one part of the steel coil production process. Its industrial site is nearby two large urban areas, with reliable public transport links via interurban train and bus networks. The built area of the building is 3,175 m^2. It has a continuous shallow foundation, poured with 610 m^3 of concrete. It supports a concrete wall with 6 mm sacrificial shuttering in the form of steel sheets that also serve as a means of fire protection. The main structure is covered with oversized laminated profiles to counter the risk of explosions (245,788 Kg). The walls and roof consist of simple sheet metal, painted with the corporate image of the firm, over a total surface area of 2,905 m^2. The sewer system collects industrial waters and moves them to the sewage network for further treatment. The project was designed by a large engineering consultancy firm that, along with the construction firm, has ISO 9001 and ISO 14001 accreditation. The corporate promoter and owner of the installation have gained the following four accreditations: ISO 9001, ISO 14.001, EMAS, and OHSAS 18001.

The firm carries out an unpleasant, unhealthy, or dangerous activity under Spanish legislation that involves a risk of explosions. Moreover, slag vapours can involve short-term damage to the metal sheeting on the walls and roof and the metallic structure. All parts of the roof are accessible for inspection purposes, to ensure good repair that will reduce the dangers associated with explosions.

4.3. Case Study 3: Storage Depot for Construction Materials. This building stores construction material for retail and wholesale business. It is located in an urban area with widespread business and industrial activity. Public transport links the industrial zone to the rest of the city with frequent services. The building is not precisely an industrial one, as its serves as a storage depot for the retail sale of construction material to the general public and the building trade, so it is usually clean and well arranged. Its built area occupies 1,584 m^2 and the foundation was poured (112.5 m^3 concrete) with 30 separate footings, joined by a perimeter

Table 5: Breakdown of "social" study scope at its different hierarchical levels.

Study scope (SS)	Criterion (CR)	Oil mill housing $V_{CR2,k}$	Slag pit housing $V_{CR2,k}$	Storage depot $V_{CR2,k}$
Society (SS2)	External mobility (CR2.1)	0.080	0.428	0.428
	Respect for the urban environment (CR2.2)	0.057	0.057	0.028
	Auxiliary services for personnel (CR2.3)	0.172	0.086	0.258

Table 6: Breakdown of "environment" study scope at its different hierarchical levels.

Study scope (SS)	Criterion (CR)	Oil mill housing $V_{CR3,k}$	Slag pit housing $V_{CR3,k}$	Storage depot $V_{CR3,k}$
Environment (SS3)	Integration in the natural environment (CR3.1)	0.017	0.033	0.025
	Environmental impact during construction (CR3.2)	0.087	0.066	0.167
	Use of ecological materials (CR3.3)	0.000	0.000	0.000
	Environmental impact during utilization (CR3.4)	0.127	0.042	0.212
	Waste management during utilization (CR3.5)	0.000	0.099	0.099
	Impact of materials from demolition (CR3.6)	0.000	0.000	0.235

Table 7: Breakdown of "economic" study scope at its different hierarchical levels.

Study scope (SS)	Criterion (CR)	Oil mill housing $V_{CR4,k}$	Slag pit housing $V_{CR4,k}$	Storage depot $V_{CR4,k}$
Economy (SS4)	Cost of executing the work (CR4.1)	0.117	0.089	0.121
	Construction timeframe (CR4.2)	0.076	0.098	0.092
	Cost of supplies (CR4.3)	0.054	0.051	0.065
	Cost of maintenance (CR4.4)	0.116	0.198	0.234
	Cost of building demolition (CR4.5)	0.075	0.075	0.000

Table 8: Breakdown of "functionality" study scope at its different hierarchical levels.

Study scope (SS)	Criterion (CR)	Oil mill housing $V_{CR5,k}$	Slag pit housing $V_{CR5,k}$	Storage depot $V_{CR5,k}$
Functionality (SS5)	Performance of the building in use (CR5.1)	0.064	0.064	0.064
	Constructability of ease of construction (CR5.2)	0.098	0.078	0.101
	Quality of internal environment (CR5.3)	0.085	0.103	0.194
	Durability (CR5.4)	0.049	0.098	0.131
	Flexibility (CR5.5)	0.153	0.076	0.153
	Ease of maintenance (CR5.5)	0.000	0.080	0.053
	Auxiliary production services (CR5.6)	0.038	0.017	0.033
	Deconstructibility (CR5.7)	0.059	0.050	0.045

beam brace that supports the facade panels. The structure of the building was designed with prefabricated concrete. Its structural elements contain 148.5 m^3 of concrete volume. Its mezzanine floor consists of precast hollow core slabs. The facade enclosures are concrete panels with an interior insulation core, covering an area of 1,442 m^2. The gable roof, with an inclination of 5%, is covered with steel panels and a 50 mm thick mineral-blanket core, with an area of 1,317 m^2. Uniformly distributed skylights occupy an area of 233 m^2 on the roof, which is in addition to the overhead lighting inside the building. There are various security systems to prevent intruders from illegal entry. Both the engineering consultancy and the promoter have gained the ISO 9001 and ISO 14001 quality and environmental certifications.

Tables 4, 5, 6, 7, 8, and 9 present the hierarchical breakdown of each requirement or study scope in the three case studies.

Table 10 shows the final values of the different requirements and the final value of the Industrial Building Sustainability Index (IBSI) in the three case studies.

These results can be represented in a bar diagram, for better observation of the strong and the weak points in each

Table 9: Breakdown of "corporate image" study scope at its different hierarchical levels.

Study scope (SS)	Criterion (CR)	Oil mill housing $V_{CR6,k}$	Slag pit housing $V_{CR6,k}$	Storage depot $V_{CR6,k}$
Corporate image (SS6)	Integration in the urban environment (CR6.1)	0.066	0.033	0.000
	Brand image of the firm (CR6.2)	0.000	0.451	0.451
	Esthetic maintenance of the building (CR6.3)	0.147	0.100	0.196

Table 10: Values of the different requirements and IBSI values.

Study scope (SS)	Oil mill housing $V_{SS,k}$	Slag pit housing $V_{SS,k}$	Storage depot $V_{SS,k}$
Safety (SS1)	0.298	0.650	0.590
Society (SS2)	0.308	0.571	0.714
Environment (SS3)	0.231	0.240	0.737
Economy (SS4)	0.439	0.510	0.513
Functionality (SS5)	0.545	0.566	0.773
Corporate image (SS6)	0.213	0.584	0.647
IBSI	**0.339**	**0.520**	**0.662**

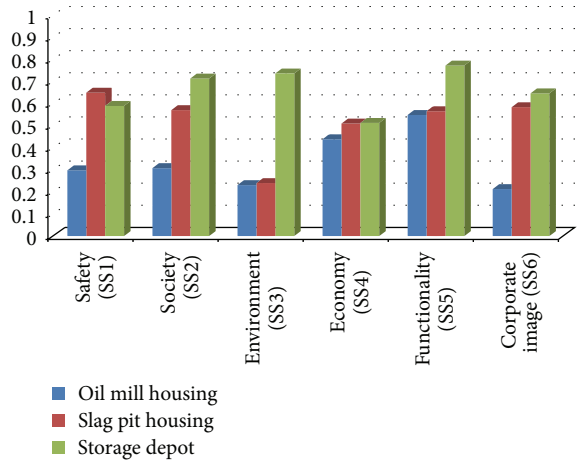

Figure 4: Results of the 3 case studies.

case study, so as to facilitate decision making regarding the selection of the best improvement measures to take, as shown in Figure 4.

5. Practical Relevance and Potential Applications

The proposed methodology is capable of improving the sustainability level of a construction project during the design stage. Its application incorporates features of interest: it gives aggregated global and partial indexes as a result and quantifies each indicator, criteria, requirements, and results and it has been configured and specially adapted for this area of study. Thus, the proposed modifications at the design stage may be studied to see how they would affect the different requirements. Therefore, at this stage, the proposed solution may be improved in terms of its sustainability, because the changes at the design stage have less economic impact than the changes at the construction phase and in subsequent phases.

5.1. Improvement of the IBSI Rate in Case Study 1: Oil Mill. This section describes how the methodology can help decision making in relation to the sustainability value of a construction project. Consequently, we may see how the decisions taken at the design phase modify the final sustainability values of the construction project. Case Study 1 has been selected for this purpose because it has the lowest IBSI rate. In Table 11, a series of improvements are described to visualize how changes affect each criterion and, consequently, the level of sustainability of the plant. The improvement actions were introduced through requirements and those with the lowest economic impact were selected.

With this set of actions taken in the case study of the oil mill, the IBSI rose from an initial value of 0.339 to a final value of 0.581.

Figure 5 presents the results of the IBSI, before and after the improvement proposals.

6. Conclusions

The advanced vision of the sustainable construction concept that has been described in this paper focuses on the following requirements in the context of industrial building: safety and industrial health, functionality, and corporate image. These requirements may be added to generic ones—environmental, economic, and social requirements—which are standard in all construction work. The noncommercial MIVES methodology that we have proposed has been used to calculate a global sustainability index and partial indicators of an industrial building. It has meant that we can now ascertain the strengths and weaknesses of a project, at the design stage, identifying those indicators and criteria in need of

Table 11: Improvement proposals.

		Previous value	Improved value
	SS1: safety		
CR 1.1	The introduction of fire detection systems and alarms	**0.000**	**0.019**
CR 1.2	The existence of a health & safety coordinator The construction company must be responsible for its own preventive activity, so that this activity is not outsourced	**0.037**	**0.220**
CR 1.3	The inclusion of the requirement that all personal and collective protection systems must have the "EC" label in the tender specifications The health & safety coordinator must belong to the construction company and must not be outsourced	**0.077**	**0.135**
CR 1.4	Placing anchoring systems and lifelines, in order to facilitate maintenance and cleaning under safe conditions, throughout the life of the building	**0.036**	**0.070**
	SSS2: Society		
CR 2.1	Changes to the planned location of the plant to an industrial estate closer to the town centre, with access to public transport lines, improving worker access to the plant	**0.080**	**0.153**
CR 2.2	The introduction of a budget heading on water spraying systems to reduce the generation of dust in the environment	**0.057**	**0.085**
CR 2.3	An increased level of hygiene above the legal minimum, because the plant has an area dedicated to the sale of olive oil products to the public	**0.172**	**0.258**
	SS3: environment		
CR 3.1	The installation of solar photovoltaic panels on the roof, with the aim of reducing external energy consumption and therefore CO_2 emissions The promotion and the encouragement of public transport among workers, leading to reductions in CO_2 emissions	**0.017**	**0.033**
	SS4: economy		
CR 4.2	The imposition of clauses threatening economic sanctions, in case of delays, in order to ensure compliance with deadlines	**0.076**	**0.094**
CR 4.3	Rain water collection tanks for subsequent reuse of rainwater in other applications, thereby reducing resource consumption The use of energy produced in the solar photovoltaic system, for own consumption or for sale to the electric network	**0.054**	**0.106**
	SS5: functionality		
CR 5.3	The implementation of a system to regulate the use of lighting, to reduce energy consumption The installation of a forced ventilation system for the circulation of air The installation of acoustically insulated panels in equipment that generates noise	**0.085**	**0.137**
CR 5.4	The requirement that quality accreditation must be held by the engineering company that bids for the design of the project	**0.049**	**0.065**
CR 5.6	The implementation of security systems, in order to facilitate access to the roof and in consequence, to enable operators to perform maintenance work safely	**0.000**	**0.080**
	SS6: corporate image		
CR 6.1	Reduction of the visual impact of the parking of the factory, considering the trees growing on the plot where it is located	**0.100**	**0.133**
CR 6.2	The requirement that the company should hold quality and environmental management accreditations	**0.000**	**0.451**
	Total value of IBSI	**0.339**	**0.581**

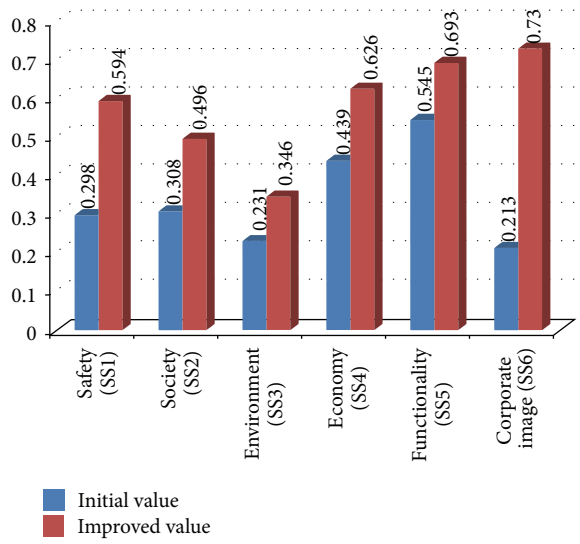

Figure 5: Initial results and improved results.

improvement, and facilitating sustainability-related decision making.

In the 3 case studies that were contrasted, the storage and sale of construction materials, which is not strictly a productive process, obtained the highest scores for the environmental, economic, societal, functional, and corporate image requirements. The presence of this firm in the tertiary or service sector influenced this assessment, where there is greater contact with the general public. New and improved images are sought to improve sales, along with better communications systems and proximity to significant residential areas, as it is a nonpolluting process.

Functional and economic requirements were given greater priority in the two specifically industrial processes. As firm size grows, concerns for other requirements also grow such as security and the social factor, above all when the firm has a brand image, which also leads to increased environmental awareness. From this comparison, it may also be seen that the scores of the smallest firm are lower than the scores of the larger firms, principally due to their having fewer available economic resources. A number of improvement proposals have been proposed for the case study of the oil mill, which has the lowest sustainability index. In this way, the IBSI has increased from an initial value of 0.339 to a final value of 0.581.

The development of this methodology was made possible thanks to the work of the Expert Panel, comprising qualified professionals in the construction sector, who defined the evaluation tree, identifying criteria, indicators, and the specific weights for each one, following Delphi methodology guidelines, which has proved itself suitable in these types of problems.

Conflict of Interests

The authors declare that there is no conflict of interests regarding the publication of this paper.

Acknowledgments

The authors of the paper gratefully acknowledge funding from the Basque Regional Government through IT781-13 and from the UPV/EHU under Program UFI 11/29. They also acknowledge the Ph.D. Grant received from the Vice-Rectorate of Basque Language of the University of the Basque Country (UPV/EHU).

References

[1] C. A. Balaras, A. G. Gaglia, E. Georgopoulou, S. Mirasgedis, Y. Sarafidis, and D. P. Lalas, "European residential buildings and empirical assessment of the Hellenic building stock, energy consumption, emissions and potential energy savings," *Building and Environment*, vol. 42, no. 3, pp. 1298–1314, 2007.

[2] C. Bob, T. Dencsak, and L. Bob, *Sustainability of Buildings*, 2010.

[3] ICLEI, "Local governments for sustainability," Annual Sustainability Report 2011–2012, ICLEI, Bonn, Germany, 2013.

[4] R. J. Cole, "Building environmental assessment methods: clarifying intentions," *Building Research and Information*, vol. 27, no. 4-5, pp. 230–246, 1999.

[5] J. A. Todd, D. Crawley, S. Geissler, and G. Lindsey, "Comparative assessment of environmental performance tools and the role of the Green Building Challenge," *Building Research and Information*, vol. 29, no. 5, pp. 324–335, 2001.

[6] T. Häkkinen, "Assessment of indicators for sustainable urban construction," *Civil Engineering and Environmental Systems*, vol. 24, no. 4, pp. 247–259, 2007.

[7] R.-Y. Huang and W.-T. Hsu, "Framework development for state-level appraisal indicators of sustainable construction," *Civil Engineering and Environmental Systems*, vol. 28, no. 2, pp. 143–164, 2011.

[8] S. Sartori, F. L. da Silva, and L. M. de Souza Campos, "Sustainability and sustainable development: a taxonomy in the field of literature," *Ambiente e Sociedade*, vol. 17, no. 1, pp. 1–22, 2014.

[9] R. Hoogmartens, S. Van Passel, K. Van Acker, and M. Dubois, "Bridging the gap between LCA, LCC and CBA as sustainability assessment tools," *Environmental Impact Assessment Review*, vol. 48, pp. 27–33, 2014.

[10] J. Pope, D. Annandale, and A. Morrison-Saunders, "Conceptualising sustainability assessment," *Environmental Impact Assessment Review*, vol. 24, no. 6, pp. 595–616, 2004.

[11] International Organization for Standardization (ISO), *ISO 26000: Guidance on Social Responsibility*, International Organization for Standardization (ISO), 2010.

[12] H. Wallbaum, Y. Ostermeyer, C. Salzer, and E. Zea Escamilla, "Indicator based sustainability assessment tool for affordable housing construction technologies," *Ecological Indicators*, vol. 18, pp. 353–364, 2012.

[13] A. Haapio and P. Viitaniemi, "A critical review of building environmental assessment tools," *Environmental Impact Assessment Review*, vol. 28, no. 7, pp. 469–482, 2008.

[14] L. de Santoli and G. Felici, "Use of an expert system rating for the energy performance of a building," *Building Services Engineering Research and Technology*, vol. 26, no. 4, pp. 349–360, 2005.

[15] E. Conte and V. Monno, "Beyond the buildingcentric approach: a vision for an integrated evaluation of sustainable buildings," *Environmental Impact Assessment Review*, vol. 34, pp. 31–40, 2012.

[16] IHOBE (Department of the Environment and Territorial Policy of the Basque Government), *Guide Books on Ecodesign*, IHOBE (Department of the Environment and Territorial Policy of the Basque Government), 2010.

[17] Spanish Ministry of Development, *EHE—08: Appendix 13 of the Spanish Structural Concrete Code (EHE)*, Spanish Ministry of Development, 2008.

[18] Spanish Ministry of Development, *EAE—11: Appendix 11 of the Spanish Structural Steel Code (EAE)*, 2011.

[19] J. Cuadrado, M. Zubizarreta, B. Pelaz, and I. Marcos, "Methodology to assess the environmental sustainability of timber structures," *Construction and Building Materials*, vol. 86, pp. 149–158, 2015.

[20] M. S. O. Ilha, L. H. Oliveira, and O. M. Gonçalves, "Environmental assessment of residential buildings with an emphasis on water conservation," *Building Services Engineering Research and Technology*, vol. 30, no. 1, pp. 15–26, 2009.

[21] B. Vučićević, M. Stojiljković, N. Afgan, V. Turanjanin, M. Jovanović, and V. Bakić, "Sustainability assessment of residential buildings by non-linear normalization procedure," *Energy Build*, vol. 58, pp. 348–354, 2013.

[22] E. Rojí, R. Losada, and J. Cuadrado, "The sustainability assessment in industrial buildings," in *Integrated Value Model for Sustainable Buildings*, 2007.

[23] D. Katunský, M. Lopušniak, M. Bagoňa, E. Dolníková, J. Katunská, and M. Vertal', "Simulations and measurements in industrial building research," *Journal of Theoretical and Applied Information Technology*, vol. 44, no. 1, pp. 40–50, 2012.

[24] P. O. Akadiri and P. O. Olomolaiye, "Development of sustainable assessment criteria for building materials selection," *Engineering, Construction and Architectural Management*, vol. 19, no. 6, pp. 666–687, 2012.

[25] A. Morrison-Saunders, J. Pope, A. Bond, and F. Retief, "Towards sustainability assessment follow-up," *Environmental Impact Assessment Review*, vol. 45, pp. 38–45, 2014.

[26] J.-T. San José, I. Garrucho, and J. Cuadrado, "The first sustainable industrial building projects," *Proceedings of the Institution of Civil Engineers: Municipal Engineer*, vol. 159, no. 3, pp. 147–153, 2006.

[27] J. P. Reyes, J. T. San-José, J. Cuadrado, and R. Sancibrian, "Health & Safety criteria for determining the sustainable value of construction projects," *Safety Science*, vol. 62, pp. 221–232, 2014.

[28] B. Alarcon, A. Aguado, R. Manga, and A. Josa, "A value function for assessing sustainability: application to industrial buildings," *Sustainability*, vol. 3, no. 1, pp. 35–50, 2011.

[29] H. ALwaer and D. J. Clements-Croome, "Key performance indicators (KPIs) and priority setting in using the multi-attribute approach for assessing sustainable intelligent buildings," *Building and Environment*, vol. 45, no. 4, pp. 799–807, 2010.

[30] H. A. Linstone and M. Turoff, *The Delphi Method: Techniques and Applications*, 2002.

[31] J. Landeta, *El método Delphi. Una Técnica de previsión para la incertidumbre*, 1999.

[32] N. K. Denzin and Y. S. Lincoln, *The SAGE Handbook of Qualitative Research*, SAGE Publications, 2011.

[33] P. K. Ray and S. Sahu, "Productivity management in India: a Delphi Study," *International Journal of Operations & Production Management*, vol. 10, no. 5, pp. 25–51, 1990.

[34] R. D. Klassen and D. C. Whybark, "Barriers to the management of international operations," *Journal of Operations Management*, vol. 11, no. 4, pp. 385–396, 1994.

[35] B. L. MacCarthy and W. Atthirawong, "Factors affecting location decisions in international operations—a Delphi study," *International Journal of Operations and Production Management*, vol. 23, no. 7-8, pp. 794–818, 2003.

[36] M. R. Hallowell and J. A. Gambatese, "Qualitative research: application of the delphi method to CEM research," *Journal of Construction Engineering and Management*, vol. 136, no. 1, pp. 99–107, 2010.

[37] B. Malakooti, "Ranking and screening multiple criteria alternatives with partial information and use of ordinal and cardinal strength of preferences," *IEEE Transactions on Systems, Man, and Cybernetics Part A: Systems and Humans*, vol. 30, no. 3, pp. 355–368, 2000.

[38] J. Gustafsson, A. Salo, and T. Gustafsson, "PRIME decisions: an interactive tool for value tree analysis," in *Multiple Criteria Decision Making in the New Millennium*, vol. 507 of *Lecture Notes in Economics and Mathematical Systems*, pp. 165–176, Springer, Berlin, Germany, 2001.

[39] S. Seo, T. Aramaki, Y. Hwang, and K. Hanaki, "Fuzzy decision-making tool for environmental sustainable buildings," *Journal of Construction Engineering and Management*, vol. 130, no. 3, pp. 415–423, 2004.

[40] Z. Chen, H. Li, and C. T. C. Wong, "EnvironalPlanning: analytic network process model for environmentally conscious construction planning," *Journal of Construction Engineering and Management*, vol. 131, no. 1, pp. 92–101, 2005.

[41] I. Garrucho, "Development of a methodology for the sustainable design of industrial buildings under environment requirements," 2006.

[42] R. Losada, E. Rojí, J. Cuadrado, and M. Larrauri, "Optimized regulation of production spaces via the integrating focus of planning, sustainability and economy," *DYNA Ingeniería e Industria*, vol. 83, pp. 61–68, 2008.

[43] O. Pons and A. de La Fuente, "Integrated sustainability assessment method applied to structural concrete columns," *Construction and Building Materials*, vol. 49, pp. 882–893, 2013.

[44] T. L. Saaty, *The Analytic Hierarchy Process*, McGraw-Hill, New York, NY, USA, 1980.

[45] A. del Caño, D. Gómez, and M. P. de La Cruz, "Uncertainty analysis in the sustainable design of concrete structures: a probabilistic method," *Construction and Building Materials*, vol. 37, pp. 865–873, 2012.

Hindawi Publishing Corporation
Mathematical Problems in Engineering
Volume 2015, Article ID 830781, 12 pages
http://dx.doi.org/10.1155/2015/830781

Research Article

Naïve Bayesian Classifier for Selecting Good/Bad Projects during the Early Stage of International Construction Bidding Decisions

Woosik Jang,[1] Jung Ki Lee,[1] Jaebum Lee,[2] and Seung Heon Han[1]

[1]*School of Civil and Environmental Engineering, Yonsei University, Seoul 120-749, Republic of Korea*
[2]*Department of Civil and infrastructure, Hyundai Engineering Co., Ltd., Seoul 140-2, Republic of Korea*

Correspondence should be addressed to Seung Heon Han; shh6018@yonsei.ac.kr

Received 11 April 2015; Revised 17 July 2015; Accepted 26 July 2015

Academic Editor: Mohamed Marzouk

Since the 1970s, revenues generated by Korean contractors in international construction have increased rapidly, exceeding USD 70 billion per year in recent years. However, Korean contractors face significant risks from market uncertainty and sensitivity to economic volatility and technical difficulties. As the volatility of these risks threatens project profitability, approximately 15% of bad projects were found to account for 74% of losses from the same international construction sector. Anticipating bad projects via preemptive risk management can better prevent losses so that contractors can enhance the efficiency of bidding decisions during the early stages of a project cycle. In line with these objectives, this paper examines the effect of such factors on the degree of project profitability. The Naïve Bayesian classifier is applied to identify a good project screening tool, which increases practical applicability using binomial variables with limited information that is obtainable in the early stages. The proposed model produced superior classification results that adequately reflect contractor views of risk. It is anticipated that when users apply the proposed model based on their own knowledge and expertise, overall firm profit rates will increase as a result of early abandonment of bad projects as well as the prioritization of good projects before final bidding decisions are made.

1. Introduction

In 2013, the international construction industry generated USD 8.9 trillion in annual construction spending [1]. The compound annual growth rate is predicted to reach 4.1% by 2021, suggesting future steady growth and thus implying that more contractors will enter the international construction market. Korean contractors have attained the highest revenues in this market, in which total international revenues over the last five decades have reached USD 600 billion [2]. In recent years, this volume has reached more than USD 70 billion per year, placing Korea sixth among countries generating the highest international revenues. In achieving this level of success, large Korean contractors have aggressively entered the international market, competing against other contractors from around the world.

However, given the presence of market volatility and other forms of uncertainty, particularly in developing and underdeveloped countries, international construction projects still carry a high degree of risk exposure, which affects the overall financial soundness of the contractor. Korean international construction profit rate data show that the average dropped from 4.7% to 3.8% and then to 3.2% from 2010 to 2012. As Korean contractors have actively penetrated several countries and won bids for several international projects, the number of loss projects has also simultaneously increased, causing contractors to experience financial instability. According to actual data related to Korean contractors, as shown in Figure 1, 15% of approximately 300 projects were severely underperforming projects, and these projects accounted for 74% of all losses [2], demonstrating that a small portion of loss projects causes the majority of financial losses among international projects. For instance, Samsung Engineering's annual report [3] showed an increase in total revenues of KRW 9.8 trillion. However, the report revealed operating profit losses of KRW 1.03 trillion in 2013, which was mainly the result of a few major construction projects such as the UAE refinery project, Saudi gas projects, and the aluminum project. Despite the successful bidding that increases firms' overall revenues, a small number of projects

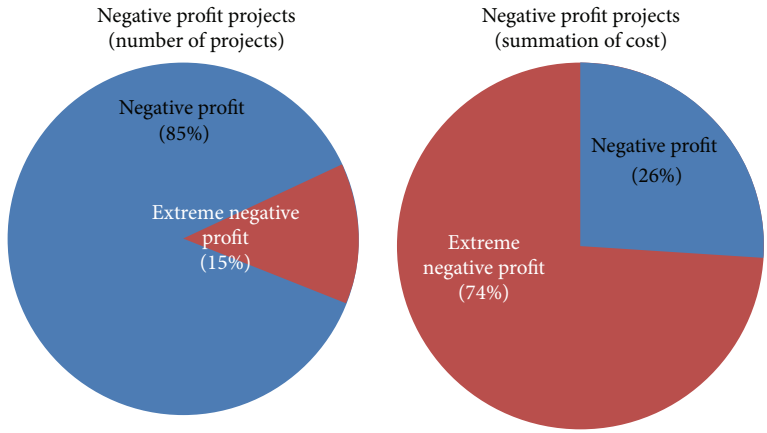

Figure 1: Distribution of bad projects in international construction.

such as these which cause negative profits after construction are completed. Other Korean firms have also experienced significant earnings shocks in recent years, illustrating the importance of screening projects that cause such losses.

Risk management has become central to successful project management, particularly in an uncertain international construction environment [4–7]. However, approaches to risk management focus primarily on the engineering and construction phases, that is, after a bidding decision has been made [8–12]. Moreover, these approaches are often limited by a reliance on historical data, which largely rely on the subjective judgments of users and hence do not provide comprehensive support for all levels of industry [13, 14]. To overcome these limitations, this paper examines retrospective data to elicit implicit meaning from the actual performance of previous cases. The paper also identifies risk factors that affect the profitability of international projects and examines the relationship between these factors and project profitability. To this end, the authors employ the Naïve Bayesian classifier using binomial variables, which improve practical applicability and thus the burden of screening out bad projects through simple yet accurate methodology and results for industry practitioners that are similar to actual project performances. Through the lens of this relationship, the proposed model evaluates whether a project is likely to be good or bad based on limited information available before final bidding decisions are made.

The procedure for developing a project classification model is shown schematically in Figure 2. First, the content of previous research is examined to enhance the theoretical aspects of this study. Based on a review of previous approaches, the limitations of existing strategies are also identified.

Second, risk attributes that affect the soundness of construction projects in the early stages are identified in interviews with relevant experts; risk types are categorized based on this information. Third, case-based surveys are conducted to relate risk attributes with project profitability. Case projects were performed from 1999 to 2010 by Korean international contractors. Questionnaires assessed risk attributes of a given project and actual levels of profitability, forming the basis of the proposed model.

Third, the correlations between each risk attribute level and project profitability are analyzed using a probabilistic classification model. To enhance the practical applicability of the model, the Naïve Bayesian classifier is used as a proper probabilistic tool to support the screening of good/bad projects in the early stages of a project. The advantages and detailed structure of this approach are also described.

Finally, cross validation is employed to test its usability. To validate the project classification model, actual project data are used to compare results obtained from the model with actual performance data, testing the accuracy and reliability of the proposed model.

2. Research Background

Risk management has been widely investigated by various researchers focusing on different phases of construction for the management scope. For example, Hastak and Shaked [15] developed a model based on country, firm, and risk assessment projects. Han et al. [16] also developed a fully integrated risk management system (FIRMS) that considers the enterprise and individual risk management project level. Furthermore, various methodologies have been used to develop risk management systems, including case based reasoning [17], artificial neural networks [18], the total risk index [19, 20], and the fuzzy analytic hierarchy process [4, 21].

As international construction volumes have grown rapidly in recent decades, various studies have assessed project conditions based on the assumption that a full risk assessment of a given project can be performed prior to the bidding stage by analyzing the information collected. However, in reality, it is impossible for contractors to consider all of the risks that affect project profitability at this early stage. Accordingly, del Caño and de la Cruz [22] identified certain project characteristics, including complexity, size, and owner capabilities and suggested that risk analysis results should be derived based on project characteristics. The authors also emphasized that an appropriate risk management method

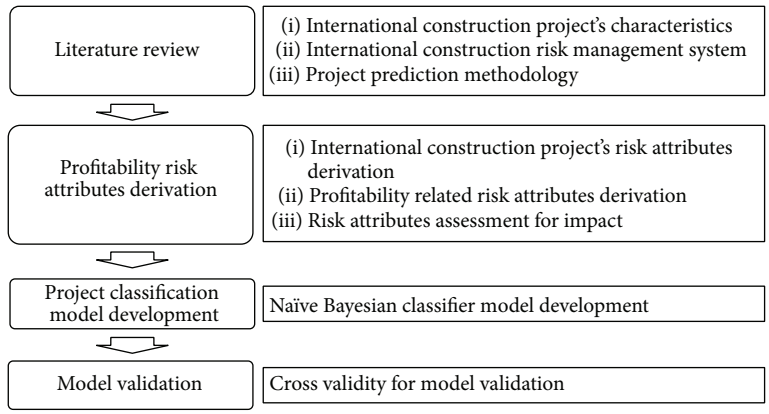

Figure 2: Research procedure.

based on representing attributes should be employed for effective project screening modeling. Thus, a systematic methodology that predicts project profitability during this early stage is imperative.

For developing the prediction models, the various theories and tools can be categorized as statistical or learning methods. Several researchers have used regression models, through which the impact of each risk attribute is assessed on a Likert scale by experts [23, 24]. However, such assessment is usually plagued by ambiguousness from maintaining consistency with different standards depending on expert's cognitive limitations or the cooperation cultures during surveys. In addition, input data usually include subjective assessments that often distort practitioner's decision-making and judgment [15, 25]. As such, previous studies that have attempted to classify profit levels by Likert or numeric scale have not yet reached a statistical level of significance in profit prediction due to their compound mechanism and a large number of inputs for understanding complicated project information [15, 26]. To develop a more reliable prediction model and improve its applicability for industry practitioners, expert assessments should be consistent, and a more simplified risk assessment model is imperative.

Data-based learning tools have also been widely applied to support the reliability of classifications such as Matlab for Artificial Neural Network (ANN), C5.0 for decision tree, and Linear Discriminant Analysis (LDA). ANN and C5.0 are considered representative data mining techniques for detecting dependent variables from the loads of input data with complex calculations [27, 28]. LDA utilizes the linear functions between various classes where the data can be categorized according to the appropriate number of classes and its relationships [29]. Unfortunately, these data-mining tools do not properly explain the underpinning rule of prediction results. In addition, these methods strictly require a large number of data for improved prediction. Hence, the Naïve Bayesian classifier is considered a suitable method for this research that uses a relatively small amount of historical data to determine whether a given project is likely to be bad or good.

To sum up, previous studies on profit prediction have been limited to simple Likert scale assessments based on experts' subjective judgments of contractor experience, potentially generating skewed results. These not only contain unrealistic assumptions and a high burden for practical applicability but also show limited accuracy when such complex calculations with a large number of input data are utilized [29]. The authors thus present a simple binary classification model based on the updated conditional probability data from the actual project's performance. This approach is expected to reduce bias while improving practical applicability.

3. Risk Attributes of Project Profitability

Project classification model development begins by incorporating overall risk attributes for international projects that are present prior to early bidding stages. Risks identified as important in previous studies were selected and analyzed via meta-analysis and frequency measurements. Studies by Hastak and Shaked [15], the American Construction Industry Institute [30], the International Construction Association of Korea [2], and Han et al. [16, 25] identified risk factors that affect construction project profitability. In addition to conducting a literature review, the authors performed interviews with eight industry experts; as a result, 20 risk factors were added to the analysis. Table 1 presents a total of 71 risk attributes derived from the aforementioned procedures.

A case-based questionnaire with refined risk attributes was designed to identify relevant information for the proposed model. The questionnaire measured the effect of 71 risk factors on profit levels on a 7-point Likert scale, in which −2 refers to a positive impact (in the sense of gain), 0 indicates no impact, 2 refers to a negative impact, and 4 refers to a critical impact on project profitability. Sample projects were chosen among actual international projects performed by the most prominent 20 Korean contractors since 2000. Approximately 900 projects were available; of these, 140 projects, which included sufficient data for prediction model development, were compiled for further analysis. The collected data were

Table 1: Risk attributes affecting project profitability.

Category	Risk code	Risk attribute	Cronbach's α value
Political and social risks	R1	High degree of corruption, collusion, and illegal transaction	0.787
	R2	Lack of familiarity with local cultures, customs, and traditions	
	R3	Frequent policy and postlegislative changes	
	R4	Insufficient legal system	
Economic and inflation risks	R5	High material unit price volatility	0.735
	R6	High equipment unit price volatility	
	R7	High local currency exchange rate volatility	
Owner risks	R8	Unsatisfactory owner management capabilities	0.869
	R9	Insufficient design information from the owner	
	R10	Lacking specifications and bidding documents provided by the owner	
	R11	Approval and permission delays on documentation and construction	
	R12	Illegal requirements without contracts	
Bidding and contract risks	R13	Insufficient time for bidding and construction quotation preparation	0.834
	R14	Inadequate consideration of variations in contract duration	
	R15	High-level local content requirements	
	R16	Complex tax and tariff regulations	
	R17	Low-level inflation compensation conditions	
	R18	Inadequate warranty-related conditions	
	R19	Inadequate payment regulations relative to international contracts	
	R20	Ineffective dispute resolution procedures and regulations	
Procurement risks	R21	Inadequate local labor supplies and procurement conditions	0.905
	R22	Inadequate local labor supplies and demand conditions	
	R23	Inadequate material production supplies and procurement conditions	
	R24	Inadequate material production supplies and demand conditions	
	R25	Inadequate material production from third-world-country supplies and demand conditions	
	R26	Inadequate equipment from local country supplies and procurement conditions	
	R27	Inadequate local equipment supply procurement and demand conditions	
	R28	Inadequate local subcontractor procurement conditions	
Geographic risks	R29	Inadequate geographical conditions of materials and equipment delivery	0.853
	R30	Inadequate logistical conditions (i.e., electricity, water, gas, and communication)	
	R31	Inadequate business environment and welfare conditions	
	R32	Inadequate weather conditions for construction	
	R33	Inadequate geological site conditions	
	R34	Severe complaints regarding construction throughout project implementation	

Table 1: Continued.

Category	Risk code	Risk attribute	Cronbach's α value
Construction performance risks	R35	Lacking design experience	0.917
	R36	Lacking bid estimation experience	
	R37	Unsatisfactory cash flow management capabilities	
	R38	Unsatisfactory site manager leadership and organization management capabilities	
	R39	Unsatisfactory site manager experience relative to similar construction projects	
	R40	Unsatisfactory international project planning and management capabilities	
	R41	Unsatisfactory quality management capabilities	
	R42	Unsatisfactory resource management capabilities	
	R43	Unsatisfactory conflict management capabilities	
	R44	Unsatisfactory contract management capabilities	
	R45	Lacking connectivity between sites and headquarters	
	R46	Unsatisfactory localization	
	R47	Lacking trust between project participants	
	R48	Poor communication between project participants	
	R49	Poor project management capabilities based on IT	
	R50	Inadequate construction methods for the specific project	
	R51	Insufficient subcontractor project performance	

first tested for reliability, stability, consistency, predictability, accuracy, and dependency [31]. Cronbach's coefficient alpha internal consistency method was employed, and results ranging from 0.8 to 0.9 were considered reliable. The PASW Statistics 21 program was used to analyze the data. As Table 1 shows, missing values in the raw data were excluded from the reliability test to increase reliability. As a result, a total of seven categories with 51 attributes were selected; an average reliability of 0.843 was obtained, indicating a high level of reliability. A total of 121 datasets for the 140 projects were used to develop the Naïve Bayesian classifier, indicating that approximately 20% of the responses were excluded due to data inconsistency.

4. Naïve Bayesian Classifier

A Naïve Bayesian classifier based on Bayes' theorem is employed to derive a probabilistic classification model from previously assessed attributes. It is most commonly used for antispam mail filtering, which trains the filter to automatically separate spam mail and legitimate messages in a binary manner [32, 33]. In doing so, each attribute corresponds with words included in the spam and legitimate mails, thus distinguishing between the two; in turn, the former are blocked by a trained filter.

4.1. Conceptual Structure of a Proposed Model. Because the objective of this research is to screen bad or good projects in the early stages of international construction projects, the result of the proposed model should also be binary (good or bad). Thus, the authors transformed the original conditions of each risk attribute (7-point Likert scale) into a binary scale to develop the Naïve Bayesian model. In addition, the early stages of the construction possess a high level of uncertainties which prohibit analysis of exact ranges of profit rates or detailed numeric classification of project conditions. Accordingly, a specific profit level or numeric number of each risk attribute is not essential, particularly during this early phase. To this end, authors consider the unity of the binary distribution of the dependent variable as well as the preassessed risk attributes to improve its practical application.

The benefits of employing the Naïve Bayesian classifier are the following [34–36]. First, the model is less sensitive to outliers. Generally, when an outlier exists in the data, the results may skew. The reduction of outlier effects is thus required for data analysis. Because the Naïve Bayesian classifier uses a probabilistic distribution, it enables minimizing the outlier effects of the original data and prediction results are less sensitive to outliers. Second, less data is required to predict the parameter. By using the utility function, relearning the probability of a given conditional probability is not strictly required in the Naïve Bayesian classifier, thus minimizing data collection efforts for risk prediction. Third, the classifier is more applicable to the industry practitioners by reducing the burden of data collection. Although the model utilizes simple assumptions and algorithms, the classification results are powerful even though the specified assumptions may contain errors. Finally, the models allow for the consideration of additional attributes by combining existing characteristics of the attributes, thus increasing the accuracy of the model's predictions. Based on the aforementioned benefits of the Naïve Bayesian method, the authors have chosen this

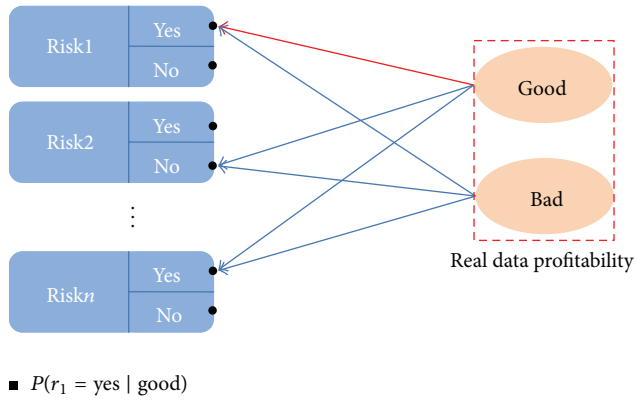

Figure 3: Conceptual model of the Naïve Bayesian classifier.

approach as the main mechanism for the proposed prediction model.

To structure the Naïve Bayesian classifier, we considered the unity of the binary distribution of the dependent variables. As mentioned earlier, the effect of each risk attribute on the level of profit is assessed by using a 7-point Likert scale (−2 to 4) to improve the model's practical application. In this study, a binary approach is used to identify the presence of risk, and final project profitability is predicted via the Naïve Bayesian classification. Because this research is focused on the early stages of the construction project, screening and recognizing a bad project are the priority rather than analyzing the specific value of the project. Therefore, the assessment range from −2 to 1 correlated with absence of risk or a "No" answer, and a score from 2 to 4 was correlated with the presence of risk or a "Yes" answer, as shown in Figure 3.

As the assessment approach is fairly simple, users perform fewer risk assessment tasks, increasing the accuracy of predictions. The benefit of a Naïve Bayesian classifier is the fact that all risk probabilities are assumed to be independent; according to Murphy [35], although these assumptions may not be correct, developing a model using the Naïve Bayesian classifier is feasible and generates highly reliable results for classification compared to other methodologies.

Equation (1) presents the classification group c set (i.e., good or bad project), where $r_1, r_2, r_3, \ldots, r_D$ are vectors ascribed to each independent risk variable in the Naïve Bayesian classifier. This categorization of attributes maximizes the probability of each classification result. Consider

$$P = \left(c \mid r_1, r_2, \ldots, r_D\right). \tag{1}$$

Equation (2) shows the prediction mode that applies (1) to Bayes' theorem. Consider

$$\frac{P(c) \times P\left(r_1, r_2, \ldots, r_D \mid c\right)}{P\left(r_1, r_2, \ldots, r_D\right)}. \tag{2}$$

As discussed above, the Naïve Bayesian classifier assumes that each attribute divided into each classification is independent; thus, (3) can be derived accordingly, where v is the target value of the group c set (i.e., the profit rate). Consider

$$\begin{aligned} P\left(r_2 \mid c, r_1\right) &= P\left(r_2 \mid c\right), \\ P\left(r \mid v = c\right) &= \prod_{i=1}^{D} P\left(r_i \mid v_j = c\right). \end{aligned} \tag{3}$$

Hence, the Naïve Bayesian classifier is considered a suitable method that uses a relatively small amount of historical data to determine whether projects are likely to be bad or good. The next section describes the proposed model, which uses the Naïve Bayesian classifier to examine the actual project data collected previously.

4.2. Naïve Bayesian Project Classification Model. In developing the Naïve Bayesian model, the aforementioned risk attributes were used as relevant independent variables for predicting good or bad projects. An overview of the model is presented in Figure 4.

The dependent variable was predicted over two or three classification intervals, and the two models are presented accordingly. The model with two intervals is based on a profitability of less than 0% for a bad project and more than 0% for a good project. The model with three intervals represents projects with less than 0% profitability—those generating a 0% to 4.5% rate of return—and a profit rate above 4.5%, which is considered a good project. A marginal profit rate of 4.5% was chosen because the average profit rate for good projects out of the total sample of projects was calculated at this range. Because projects with negative profitability are all considered "bad," "moderate" and "good" projects are differentiated based on the reference profit value of 4.5%. Table 2 represents intervals divided based on the results.

Using the training dataset, each risk attribute is categorized into a specific class to develop the project-screening model. Therefore, the conditional probability of each attribute

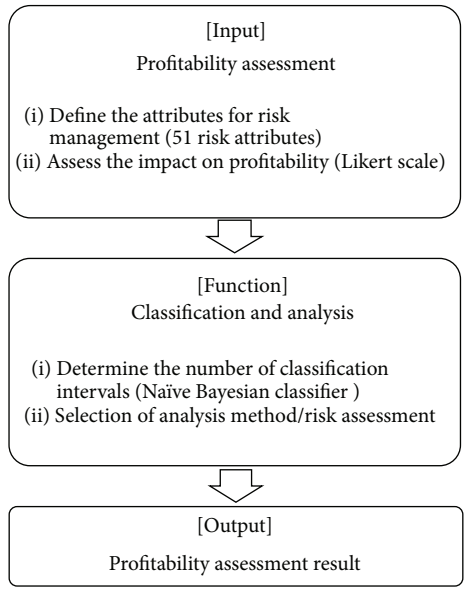

Figure 4: Overview of project classification model.

Table 2: Classification of profitability.

	Bad project	Moderate project	Good project
2 classification intervals	Below 0%	—	Above 0%
3 classification intervals	Below 0%	0%–4.5%	Above 4.5%

given to the bad project in advance is shown in the following equation:

$$P\left(r_i \mid v_j\right) = \frac{n_c}{n}, \tag{4}$$

P is estimated conditional probability, r_i is risk attributes i, v_j is the condition of profit rate on Bad or Good based on the training data (v = below 0), n_c is number of bad projects under the specific risk a_i in the training data ($v = v_j$ and $r = r_i$), and n is number of bad projects in the training data ($v = v_j$).

However, whereas this study examines 140 units of data, the number of training data is insufficient relative to the number of risk attributes. Unbalanced datasets also lead to an inappropriate result in the statistical analysis [37]. It is thus necessary to augment the small datasets in the training set which decreases the accuracy of the model. To overcome this, the authors borrowed the concept of the m-estimate from [38–40]. By setting the value of a suitable "m" number, the shifting of probability toward parameter "p" is controlled; this also further increases model accuracy as shown in the following equation:

$$P'\left(r_i \mid v_j\right) = \frac{n_c + mp}{n + m}, \tag{5}$$

P' is estimated conditional probability using m-estimate, m is equivalent data size, and p is prior probability based on training data (4).

Zadrozny and Elkan [38] recommend that the value of mp be set to less than 10, thus using a probabilistic equation to cross-validate 140 data units; 70 units are set as training data, and the remaining 70 units of m parameter are set to an equivalent data size to develop the project screening model. In turn, parameter p becomes 10/70 or 1/7 for (5). Of the 140 data units collected, 20 units were therefore classified as bad projects, and 120 were deemed good projects. Therefore, the two datasets—training and equivalent data size—consist of 10 bad projects and 60 good projects that are chosen via random selection.

Five different datasets are created randomly to develop and validate the model in view of cross validation. Random data are selected using Microsoft Excel, which generates data in a range from 0 to 1 for random probability. In addition, for the training dataset, the actual risk exposure level for each attribute in a given project is used to develop the model. In this paper, only one set of training data results out of five different datasets is presented in detail, as the other results were found to be almost equivalent.

The Naïve Bayesian classifier consists of an m-estimator parameter, which gives a random value of m to control the classification bias. This study uses m value from the "moderate" interval of project profitability, which had the highest error percentage, for further validation. According to the results of the first analysis, m value in the Naïve Bayesian classifier was reduced in the second analysis: by modifying m value, the moderate profitability project produces a more stable result. In addition, the weights given to the bad projects increased, which results in both increased stability of the classification and reduction of bad project's classification error. Therefore, the analysis of the moderate classification results was reanalyzed. To identify a suitable m value, a sensitivity analysis was also performed for the changes as m value decreases.

Table 3: Part of the conditional probability of Naïve Bayesian classifier model.

Category	Risk code	$P'(r_i \mid \text{BAD})$	$P'(r_i \mid \text{GOOD})$
Political and social risks	R1	35%	23.4%
	R3	15%	5.6%
Economic and inflation risks	R5	15%	8.9%
	R7	20%	24.2%
Bidding and contract risk	R15	10%	27.4%
	R19	15%	15.3%
Procurement risks	R22	30%	36.2%
	R24	5%	18.5%
Geographic risks	R29	40%	22.6%

By using the derived model using m-estimate, each risk factor is calculated for the conditional probability for Bad and Good. The two classification intervals model is used to analyze each risk factor. Table 3 shows the conditional probability of the key risk factors from each category that has a severely negative impact (assessed as 3 or 4 points) on the total sample data (140 projects). For example, the R24 risk had an 18.5% probability of occurring in a "Good" project and a 5% probability of occurring in a "Bad" project. To summarize Table 3, external (politic or economic) factors more frequently appear in the "bad" projects, while internal (bidding or procurement) factors more frequently occurr in the "good" projects.

5. Model Analysis and Validation

5.1. Model Validation. In employing the classifier model, two datasets (training and sample test datasets) for 70 projects were used to compare actual and predicted risk impacts on the dependent variable. Actual risk effects in a given project were used to determine the profitability of the 70 projects. In addition to evaluating the performance level of the model, the model's usability and accuracy were tested using a confusion matrix of Bayes' theorem. To determine the accuracy of the model, the dependent variable, profitability, included a sample test dataset of 70 projects for comparison with the actual project performance and predicted performance of a given project. The 2 and 3 classification intervals models were also tested by classification into bad (PB: Predicted Bad), moderate (PM: Predicted Moderate), and good (PG: Predicted Good) categories; the training dataset for the 70 projects also employs the actual profit level, which is classified as bad (AB: Actual Bad), normal (AM: Actual Moderate), or good (AG: Actual Good). Tables 4 and 5 present the results of the two models.

The aforementioned five models were randomly tested for cross validation. In the test models, a dataset of 70 projects was randomly selected to determine the model's accuracy. As an initial measure, each project was deemed bad or good. As shown in Table 4, the overall correct level is found to be 79.7% by dividing the bold numbers with the total number of samples. Other cross validation models also showed highly accurate levels of 78.6%, 77.1%, 82.7%, and 80%, respectively.

Table 4: Validation of profitability at 2 classification intervals.

Model 1 out of five cross validations	Classification level		Total
	Bad (PB)	Good (PG)	
Actual Level			
Bad (AB)	**5**	5	10
Good (AG)	9	**51**	60
Total	14	56	70

Table 5: Validation of profitability at 3 classification intervals.

Model 1 out of five cross validations	Classification level			Total
	Bad (PB)	Moderate (PM)	Good (PG)	
Actual Level				
Bad (AB)	**3**	5	2	10
Moderate (AM)	3	**16**	13	32
Good (AG)	3	13	**12**	28
Total	9	34	27	70

In contrast, the model with three classified intervals presented relatively low levels of 44.3%, 42.9%, 51.4%, 48.6%, and 50.0%, with a mean percentage of 44.8%, reflecting less accurate results (refer to Table 5). Models with 2 and 3 classification intervals showed standard deviations of 2.07 and 3.07, respectively; this suggests the presence of a few differences and consistent results between the two models. The 2 classification intervals model is considered an excellent vehicle for screening purposes, as it presents highly accurate results and less deviation. Although the 3 classification intervals model shows a relatively low level of accuracy, in a real business environment, the users also may apply the 3 classification intervals model for screening out a moderate range of projects by sacrificing the prediction accuracy.

Additional analysis to validate the Naïve Bayesian classification model is performed through comparing with linear regression model using SPSS 21. The authors used the same binary method of dividing the profit rate into good and bad (2 classification intervals). By utilizing the same 140 projects' units of data that is composed of 70 training units of data and 70 test units of data, the accuracy result of linear regression model is found to be 52.2%. This result shows a significantly lower accuracy than the 2 classification intervals Naïve Bayesian model (79.7%) and slightly higher accuracy than the 3 classification intervals model (44.8%).

In summary, this study proposed two types of models depending on the user's need and degree of risk exposure. The models were validated through comparing the accuracy of the prediction result with other learning methods. In addition, the user can flexibly select the proper model that best suited to a given firm, whether he or she requires an accurate classification between good and bad project or is contend to identify a moderate or good project.

Profitability assessment			
Method	1	Naïve Bayesian classifier	
Category	Risk code	Risk attributes	Risk
Country's political and social risk	R1	Country's corruption, collusion, and illegal transaction	O
	R2	Culture, customs, and tradition difference	X
	R3	Policy and postlegislative changes	X
	R4	Country's overall legal system's maturity	X
Country's economic and inflation risks	R5	Average material unit price change	X
	R6	Average equipment unit price change	X
	R7	Local currency exchange rate change	X
Stakeholder risks	R8	Stakeholder's understanding and management ability	O
	R9	Design error provided to stakeholder	O
	R10	Clarity of specifications and bidding documents provided to stakeholder	X
	R11	Stakeholder's administrative and construction consent delay	X
	R12	Requirements regardless of contract from stakeholder	X
Bidding and contract terms	R13	Bidding and quotation preparation time for construction	X
	R14	Contract of construction duration for construction	X
	R15	Required degree of local contents	X
	R16	Tax and tariff regulations	X
	R17	Inflation compensation conditions compared to international contract	X
	R18	Warranty-related conditions compared to international contract	X
	R19	Payment regulations compared to international contract	X
	R20	Dispute resolution procedures regulation compared to international contract	X

Figure 5: Excel-based risk assessments.

5.2. Excel-Based Model Development. Based on the aforementioned basic algorithm, the authors developed an Excel-based system that serves as a continuous risk management platform for project screening for the international construction sector. To initiate project screening, risk attributes related to a given project are assessed for their impact on project profit depending on the amount of information acquired. As shown in Figure 5, system inputs for risk assessment are based on two scenarios: the specified risk either affects the project or does not. In addition, users may select their model depending on their objectives: the more accurate Naïve Bayesian classifier with a higher project classification rate (2 classification intervals model) or the less accurate model with a more conservative classification rate (3 classification intervals model).

The authors present a sample case in which the developed program is utilized to test the project screening model through the user interface. This case considers a Korean contractor working on a harbor expansion project that lasts 22 months. Figure 5 shows step 1, which is the actual user interface of the program generated with case study data inputs for good/bad project screening. As shown in Figure 5, the user first evaluates the risk attribute using "O" for "risk exists," indicating the presence of a given risk, and "X" for "risk does not exist," indicating an absence of project risk. The user then selects a model, that is, the number of classification intervals. Depending on the model selected, the classification model categorizes projects as bad, moderate, or good. The model classifies the good projects as ranging from 0% to 4.5% of the profit rate. Project screening is conducted by selecting profit interval ranges depending on firm risk behavior. Model results are obtained from the training sample via random selection, through which classification results are selected from the highest predicted value from 100 prediction cycles. This process increases reliability, and the results are shown in percentage form for ease of comprehension.

Figure 6 shows the procedural steps in the process of the Excel-based model. Risk assessment is performed primarily in step 1. Then, in step 2, the model counts for the risk existence based on the historical dataset of 140 real projects.

2

		R1	R2	R3	R4	R5	R6	R7	R8	R9	R10
Bad	n	10	10	10	10	10	10	10	10	10	10
	n_c	1	1	0	0	2	3	1	0	0	0
	p	0.142857143	0.142857143	0.142857	0.142857	0.142857	0.142857	0.142857	0.142857	0.142857	0.142857
	m	0.01	0.01	0.01	0.01	0.01	0.01	0.01	0.01	0.01	0.01
	p (ai | bad)	0.1000	0.1000	0.0001	0.0001	0.1999	0.2998	0.1000	0.0001	0.0001	0.0001
	Select										
	Result	1	1	1	1	1	1	1	1	1	1
	p (bad)	0.142857143									
Moderate	n	31	31	31	31	31	31	31	31	31	31
	n_c	0	0	0	0	0	0	0	0	0	0
	p	0.442857143	0.442857143	0.442857	0.442857	0.442857	0.442857	0.442857	0.442857	0.442857	0.442857
	m	0.01	0.01	0.01	0.01	0.01	0.01	0.01	0.01	0.01	0.01
	p (ai | normal)	0.000142811	0.000142811	0.000143	0.000143	0.000143	0.000143	0.000143	0.000143	0.000143	0.000143
	Select	0	0	0	0	0	0	0	0	0	0
	Result	1	1	1	1	1	1	1	1	1	1
	p (normal)	0.442857143									
Good	n	29	29	29	29	29	29	29	29	29	29
	n_c	17	10	15	12	29	12	10	19	14	9
	p	0.414285714	0.414285714	0.414286	0.414286	0.414286	0.414286	0.414286	0.414286	0.414286	0.414286
	m	0.01	0.01	0.01	0.01	0.01	0.01	0.01	0.01	0.01	0.01
	p (ai | good)	0.586147634	0.344851529	0.517206	0.413793	0.999798	0.413793	0.344852	0.655089	0.482735	0.310381
	Select	0	0	0	0	0	0	0	0	0	0
	Result	1	1	1	1	1	1	1	1	1	1
	p (good)	0.414285714									

3

Result table	Bad	Good	Moderate
	$1.7238E-35$	$6.9489E-07$	$7.19685E-47$
Max	$6.9489E-07$		

4

Final result	Good

5

Profitability assessment result		
Project screening result		Good project
Top 5 risks to be managed		Probability
1	Average material unit price change	0.999
2	Country's local subcontractor's procurement conditions	0.704
3	Complaints from construction during the project	0.655
4	Stakeholder's administrative and construction consent delay	0.586
5	Clarity of specifications and bidding documents provided to stakeholders	0.555

Figure 6: Process for assessment result.

Through the sum of its risk existence, the conditional probability is calculated given each classification of a project (Good, Moderate, or Bad) separately.

Step 3 shows the result table for each classification that has been selected from the profitability assessment. This is the step in which users are to perform the risk assessment from Figure 6, where selected risks are calculated for conditional probability. The result is calculated from the product of each probability from the 51 risks attributes. Step 4 then shows the final result by selecting the highest probability from each classification. In the illustrative example, "Good" had the highest probability. In addition, as shown in step 5 in the user interface, the risks that most directly affect project profitability can be prioritized, which should be continuously monitored and controlled by the user. These five risk attributes serve as the basis of a risk response strategy.

The proposed model prioritizes the top 5 risks that affect overall construction profitability. According to Halawa et al. [41], construction projects are dramatically influenced by this financial evaluation and awareness of the financial status improves; it offers a better chance of determining project feasibility. Therefore, this study incorporates the Naïve Bayesian classifier with an Excel-based model to give practitioners a quantitative analysis result (statistical references) and qualitative analysis results (the top risk attributes to be managed). It should also be noted that although the result of the model shows an absolute value of bad, moderate, or good, it is up to the managers and decision-makers to make a bad project,

a moderate project, or even good project by careful and proactive risk management as presented in the illustrative case application.

6. Conclusions

This study predicted the profitability of early-stage international construction projects and identified good projects that may affect firm's financial stability. The current state of the international construction market was first analyzed; losses were shown to account for 73% of the entire market, reflecting the importance of predicting project profitability in advance. Risk attributes that affect project profitability were identified, and a risk management system was developed to manage, prioritize, and monitor higher impact risks. The Naïve Bayesian classifier method was used to improve the practical application of the project-screening model. When risk attribute assessments for determining risk exposure levels are completed, assessed risk exposure is classified into a binary parameter that presents an approach to risk management that is supported by a probabilistic methodology.

This study used case study data to create a model using Microsoft Excel. Depending on the Naïve Bayesian classifier m-estimator value of the weight application and the user's risk behaviors, users can choose the model that best suits a given firm. The results show that when a 70-unit training dataset and 70-unit sample dataset area are used (a 140-unit set in total) to cross-validate the Naïve Bayesian classifier, the model has on average a 79.7% prediction accuracy for the 2 classification intervals model and a 44.8% accuracy for the 3 classification intervals model. Additional analysis to validate the model is performed through linear regression analysis to show the higher precision result from the Naïve Bayesian classification model.

For project screening, conditional probability is used with information acquired during early project stages. Although risk attributes were largely derived in the model, risk attributes that more clearly affect projects can be further extracted, elucidating the effects of bad projects.

As for the limitations of this study, analytical results for the application of the developed program to a more diverse scenario will be essential; for example, different types of construction projects may be examined for superior results. In addition, if contract types were categorized as contractor, subcontractor, and joint ventures, this may have altered the profitability of each project. A new-entry market scenario will also be analyzed separately due to the unique characteristics of new markets. Given a range of unique construction project qualities, a more realistic and practical application can be obtained in future research. Furthermore, if additional data on both project risk assessment and the actual reliable profit rates are accumulated, a diverse segmentation of the intervals can be obtained to examine each project in a precise measure.

Conflict of Interests

The authors declare that there is no conflict of interests regarding the publication of this paper.

Acknowledgment

This research was supported by a grant (14IFIP-B089065-01) funded by Ministry of Land, Infrastructure and Transport of Korean government.

References

[1] Global Insight, *Global Construction Outlook*, Global Insight, Lexington, Mass, USA, 2014.

[2] International Contractors Association of Korea (ICAK), *International Construction Information Service. Construction Statistics*, 2013, http://www.icak.or.kr/sta/sta_0101.php.

[3] Samsung Engineering, *Business Results Report: Third Quarter of 2013*, Samsung Engineering, Seoul, Republic of Korea, 2013.

[4] M. Abdelgawad and A. R. Fayek, "Risk management in the construction industry using combined fuzzy FMEA and fuzzy AHP," *Journal of Construction Engineering and Management*, vol. 136, no. 9, pp. 1028–1036, 2010.

[5] G. Aydogan and A. Koksal, "An analysis of international construction risk factors on partner selection by applying ANP approach," in *Proceedings of the International Conference on Construction and Real Estate Management (ICCREM '13)*, pp. 658–669, Karlsruhe, Germany, October 2013.

[6] B.-G. Hwang, X. Zhao, and L. P. Toh, "Risk management in small construction projects in Singapore: status, barriers and impact," *International Journal of Project Management*, vol. 32, no. 1, pp. 116–124, 2014.

[7] A. E. Yildiz, I. Dikmen, M. T. Birgonul, K. Ercoskun, and S. Alten, "A knowledge-based risk mapping tool for cost estimation of international construction projects," *Automation in Construction*, vol. 43, pp. 144–155, 2014.

[8] O. Taylan, A. O. Bafail, R. M. S. Abdulaal, and M. R. Kabli, "Construction projects selection and risk assessment by fuzzy AHP and fuzzy TOPSIS methodologies," *Applied Soft Computing*, vol. 17, pp. 105–116, 2014.

[9] S. Mu, H. Cheng, M. Chohr, and W. Peng, "Assessing risk management capability of contractors in subway projects in mainland China," *International Journal of Project Management*, vol. 32, no. 3, pp. 452–460, 2014.

[10] F. Acebes, J. Pajares, J. M. Galán, and A. López-Paredes, "A new approach for project control under uncertainty. Going back to the basics," *International Journal of Project Management*, vol. 32, no. 3, pp. 423–434, 2014.

[11] Y. Zhang and Z.-P. Fan, "An optimization method for selecting project risk response strategies," *International Journal of Project Management*, vol. 32, no. 3, pp. 412–422, 2014.

[12] M. Rohaninejad and M. Bagherpour, "Application of risk analysis within value management: a case study in dam engineering," *Journal of Civil Engineering and Management*, vol. 19, no. 3, pp. 364–374, 2013.

[13] Q. Yang and Y. Zhang, "Application research of AHP in project risk management," *Advanced Materials Research*, vol. 785-786, pp. 1480–1483, 2013.

[14] O. Kapliński, "The utility theory in maintenance and repair strategy," *Procedia Engineering*, vol. 54, pp. 604–614, 2013.

[15] M. Hastak and A. Shaked, "ICRAM-1: model for international construction risk assessment," *Journal of Management in Engineering*, vol. 16, no. 1, pp. 59–69, 2000.

[16] S. H. Han, W. Jung, D. Y. Kim, and H. Park, "A study for the improvement of international construction risk management,"

Conference of Korean Society of Civil Engineering (KSCE), no. 10, pp. 791–794, 2009.

[17] V. Kumar and N. Viswanadham, "A CBR-based decision support system framework for construction supply chain risk management," in *Proceedings of the 3rd IEEE International Conference on Automation Science and Engineering (CASE '07)*, pp. 980–985, IEEE, Scottsdale, Ariz, USA, September 2007.

[18] B. Yang, L. X. Li, H. Ji, and J. Xu, "An early warning system for loan risk assessment using artificial neural networks," *Knowledge-Based Systems*, vol. 14, no. 5-6, pp. 303–306, 2001.

[19] P. Sanchez, "Neural-risk assessment system for construction projects," in *Proceedings of the Construction Research Congress*, pp. 1–11, San Diego, Calif, USA, April 2005.

[20] B. R. Fortunato III, M. R. Hallowell, M. Behm, and K. Dewlaney, "Identification of safety risks for high-performance sustainable construction projects," *Journal of Construction Engineering and Management*, vol. 138, no. 4, pp. 499–508, 2012.

[21] J. Li and P. X. W. Zou, "Fuzzy AHP-based risk assessment methodology for PPP projects," *Journal of Construction Engineering and Management*, vol. 137, no. 12, pp. 1205–1209, 2011.

[22] A. del Caño and M. P. de la Cruz, "Integrated methodology for project risk management," *Journal of Construction Engineering and Management*, vol. 128, no. 6, pp. 473–485, 2002.

[23] A. P. C. Chan, D. C. K. Ho, and C. M. Tam, "Design and build project success factors: multivariate analysis," *Journal of Construction Engineering and Management*, vol. 127, no. 2, pp. 93–100, 2001.

[24] D. J. Lowe and J. Parvar, "A logistic regression approach to modelling the contractor's decision to bid," *Construction Management and Economics*, vol. 22, no. 6, pp. 643–653, 2004.

[25] S. H. Han, D. Y. Kim, and H. Kim, "Predicting profit performance for selecting candidate international construction projects," *Journal of Construction Engineering and Management*, vol. 133, no. 6, pp. 425–436, 2007.

[26] A. S. Bu-Qammaz, I. Dikmen, and M. T. Birgonul, "Risk assessment of international construction projects using the analytic network process," *Canadian Journal of Civil Engineering*, vol. 36, no. 7, pp. 1170–1181, 2009.

[27] T. Hegazy and A. Ayed, "Neural network model for parametric cost estimation of highway projects," *Journal of Construction Engineering and Management*, vol. 124, no. 3, pp. 210–218, 1998.

[28] RuleQuest, Data mining tools, 2008, http://www.rulequest.com.

[29] W. Jung, *Three-Staged Risk Evaluation Model for Bidding on International Construction Projects*, Graduate School, Yonsei University School of Civil and Environmental Engineering, Seoul, Republic of Korea, 2011.

[30] Construction Industry Institute (CII), "Risk assessment for international projects," Research Report 181-11, Construction Industry Institute (CII), Austin, Tex, USA, 2003.

[31] G. Young, "Glossary and discussion of terms," in *Malingering, Feigning, and Response Bias in Psychiatric/Psychological Injury*, vol. 56 of *International Library of Ethics, Law, and the New Medicine*, pp. 777–795, Springer, Dordrecht, The Netherlands, 2014.

[32] M. Sahami, S. Dumais, D. Heckerman, and E. Horvitz, "A Bayesian approach to filtering junk e-mail," in *Learning for Text Categorization: Papers from the 1998 Workshop*, vol. 62, pp. 98–105, 1998.

[33] I. Androutsopoulos, J. Koutsias, K. V. Chandrinos, G. Paliouras, and C. Spyropoulos, "An evaluation of Naïve Bayesian anti-spam filtering," in *Proceedings of the Workshop on Machine Learning in the New Information Age, 11th European Conference on Machine Learning*, G. Potamias, V. Moustakis, and M. van Someren, Eds., pp. 9–17, Barcelona, Spain, 2000, http://arxiv.org/pdf/cs/0006013.pdf.

[34] H. Zhang, "The optimality of naïve Bayes," in *Proceedings of the 17th International Florida Artificial Intelligence Research Society Conference (FLAIRS '04)*, Miami Beach, Fla, USA, May 2004.

[35] K. P. Murphy, *Naive Bayes Classifiers*, University of British Columbia, Vancouver, Canada, 2006.

[36] R. R. Yager, "An extension of the naive Bayesian classifier," *Information Sciences*, vol. 176, no. 5, pp. 577–588, 2006.

[37] D. Lowd and P. Domingos, "Naive Bayes models for probability estimation," in *Proceedings of the 22nd International Conference on Machine Learning (ICML '05)*, pp. 529–536, ACM, Bonn, Germany, August 2005.

[38] B. Zadrozny and C. Elkan, "Learning and making decisions when costs and probabilities are both unknown," in *Proceedings of the 7th ACM SIGKDD International Conference on Knowledge Discovery and Data Mining*, pp. 204–213, ACM, August 2001.

[39] L. Jiang, H. Zhang, Z. H. Cai, and D. Wang, "Weighted average of one-dependence estimators," *Journal of Experimental and Theoretical Artificial Intelligence*, vol. 24, no. 2, pp. 219–230, 2012.

[40] J. Wu and Z. Cai, "A naive Bayes probability estimation model based on self-adaptive differential evolution," *Journal of Intelligent Information Systems*, vol. 42, no. 3, pp. 671–694, 2014.

[41] W. S. Halawa, A. M. K. Abdelalim, and I. A. Elrashed, "Financial evaluation program for construction projects at the pre-investment phase in developing countries: a case study," *International Journal of Project Management*, vol. 31, no. 6, pp. 912–923, 2013.

Hindawi Publishing Corporation
Mathematical Problems in Engineering
Volume 2015, Article ID 717095, 13 pages
http://dx.doi.org/10.1155/2015/717095

Research Article

Map Matching Based on Conditional Random Fields and Route Preference Mining for Uncertain Trajectories

Ming Xu,[1] Yiman Du,[2] Jianping Wu,[2] and Yang Zhou[2]

[1]*School of Computer Science, Beijing University of Posts and Telecommunications, Beijing 100876, China*
[2]*School of Civil Engineering, Tsinghua University, Beijing 100084, China*

Correspondence should be addressed to Yiman Du; ymducp@gmail.com

Received 14 January 2015; Revised 26 March 2015; Accepted 26 March 2015

Academic Editor: Jurgita Antucheviciene

In order to improve offline map matching accuracy of uncertain GPS trajectories, a map matching algorithm based on conditional random fields (CRF) and route preference mining is proposed. In this algorithm, road offset distance and the temporal-spatial relationship between the sampling points are used as features of GPS trajectory in a CRF model, which integrates the temporal-spatial context information flexibly. The driver route preference is also used to bolster the temporal-spatial context when a low GPS sampling rate impairs the resolving power of temporal-spatial context in CRF, allowing the map matching accuracy of uncertain GPS trajectories to get improved significantly. The experimental results show that our proposed algorithm is more accurate than existing methods, especially in the case of a low-sampling-rate.

1. Introduction

In recent years, the prevalence of GPS-enabled devices has resulted in incredible amounts of vehicle trajectory data, which records human mobility and reflects the dynamic characteristics of a city. In general, trajectory data consisting of time-stamped locations come from GPS sensors embedded vehicles or other mobile devices. However, the raw trajectory data are not completely reliable; that is, the locations indicated in such a trajectory are not the real accurate locations of vehicles or mobile devices, since the measurement errors of the device and the complex communication environment make the readings of GPS sensors frequently deviate from the actual positions. Therefore, map matching, that is, the process of adjusting the trajectory points to real road segments, is very important to some location-based services and applications and has got considerable attention by the researchers.

There are two types of map matching approaches, that is, online and offline map matching. For online map matching, real-time route navigation, for example, although accuracy is concerned, prompt speed of map matching is the most needed. For offline map matching, the most concerned is obtaining accurate matched paths which can be used for future works (e.g., knowledge mining); therefore instantaneity is not important for offline map matching while accuracy is required as much as possible.

Offline map matching is widely employed by many applications, such as pickup location recommendation [1], ridesharing services [2, 3], regional function analysis [4], urban planning analysis [5], abnormal event detection [6–8], travel time estimation [9, 10], real-time traffic flow prediction [11], and traffic guidance [12, 13]. One of the biggest challenges of offline map matching is the uncertainty caused by low-sampling-rates; that is, it is difficult to determine the best matching. In fact, low-sampling-rates are often encountered in map matching; for example, for energy consumption considerations, GPS sampling intervals of most vehicles are more than 30 seconds, and even a considerable number of trajectories' sampling intervals exceed two or three minutes. Consider the example in Figure 1, which compares two trajectories. The sampling interval of one is twenty seconds, while that of another one is three minutes. Obviously, the path of the high-sampling-rate trajectory can be identified clearly, while the path of the sparse trajectory is difficult to determine. In other words, the low-sampling-rate results in the uncertainty of map matching. Such uncertainty produces

(a) (b)

Figure 1: A comparison between high-sampling-rate and low-sampling-rate map matching.

severe effects on the abovementioned trajectory mining-based applications. However, some valuable pieces of information in the trajectories, such as temporal context and drivers' route preference, are neglected by most existing approaches of offline map matching. The instability of these approaches may be caused when dealing with low-sampling-rate trajectories.

In this paper, we explore a way that can reduce the map matching uncertainty to accurately determine a path for a low-sampling-rate trajectory. To achieve this, we make full use of available information, such as trajectory characteristics, road network topology, and driver route history. We treat offline map matching of GPS sampling points as a sequence-labeling problem [14] in machine learning and propose a conditional random field (CRF) [15] map matching algorithm employing spatial context and temporal context between sampling points. There also exist other probabilistic approaches suitable for the sequence-labeling problem, such as hidden Markov model (HMM) [16] and maximum entropy Markov model (MEMM) [17]. However, the HMM assumes that all trajectory points are conditionally independent, and the current state depends only on the previous state in the process of state transition. This assumption may lose some significant context and result in a "labeled bias" problem [18]; that is, the HMM model tends to match sampling points to long-distance road segments that have few intersections. Although the MEMM avoids the conditional independence assumptions on trajectory points by improving the structure of a probabilistic graphical model, it also suffers from the "labeled bias" problem. Therefore we select CRF to overcome the drawbacks of the HMM and the MEMM. CRF has obvious advantages in flexible integration of a variety of features and context information. In addition, we find that most drivers usually choose familiar paths to travel. Inspired by this, we employ driver route preferences to improve the quality of the algorithm. Specifically, if the GPS sampling frequency of given trajectory is too low to guarantee the effectiveness of CRF features, we extract the route preferences from historical well matched paths and superpose them on the features of CRF with appropriate weighting. We have conducted lots of experiments to verify that our algorithm can match the trajectory points to actual paths.

The contributions of our paper are threefold.

(1) We propose a CRF-based algorithm of map matching that combines spatial and temporal features effectively. Experimental results show that temporal features can boost the resolving power of existing CRF models that solely employ spatial features, especially in areas with similar spatial features, such as interaction-dense areas.

(2) We design a framework for mining the drivers' route preferences from historically matched paths to improve the effectiveness of our CRF-based algorithm, which can weaken the effect of the uncertainty caused by low-frequency-sampling.

(3) We perform extensive experiments on a real trajectory dataset collected from the physical world and labeled manually. Our algorithm is evaluated for matching accuracy. The results show that our algorithm outperforms previous methods significantly on low-sampling-rate trajectories.

The remainder of the paper is organized as follows. A review of some existing map matching methods is given in Section 2. Section 3 presents our map matching framework and problem definition. The algorithm is proposed with detailed discussion and analysis in Section 4. Section 5 presents the experimental evaluation. We conclude the paper in Section 6.

2. Related Work

Knowledge discovery in sets of moving objects attracts many researchers, and a large number of approaches have been proposed. These studies can be divided into two categories: (1) models of moving objects, which can move freely in Euclidean space [19]; (2) models of objects, whose movements are subject to spatial constraints, such as road networks. The method proposed by this paper is related to the second research category and can be applied in transportation, urban planning, location-based services, activity recognition [20, 21], and so forth. Indeed, if we know the geometry and the topology of the network, we can represent a trajectory by a list of traversed road segments; such a process

is called "map matching." Depending on the application scenario, these methods can be divided into two categories: online and offline.

Online algorithms mainly employ a greedy strategy to search for the optimal local matching from an existing solution. Greenfeld [22] proposes an incremental algorithm that considers only geometric information to evaluate each candidate edge. This information contains distance similarity and orientation similarity. Chawathe [23] proposes a segment-based method, in which a confidence score is defined and assigned to different sampling points. When a new trajectory appears, high-confidence edges are matched first, and then low-confidence edges are matched, according to already matched edges. Wenk et al. [24] propose an "adaptive clipping" approach that obtains the shortest path on a local free space graph. These kinds of methods can identify matching segments quickly due to using only a small part of the trajectory; for this reason, they are widely used for online applications, such as navigation systems. However, the accuracy of these algorithms drops sharply when sampling frequency decreases.

Offline algorithms handle the entire trajectory after completing a trip. Most studies detect the closest candidate roads from the current trajectory by means of Fréchet distance or its extended metrics; its underlying meaning is that continuity of curves is taken into account to search for corresponding paths. In the algorithm proposed by Alt et al. [25], the critical values are worked out in a parametric search process, and then the Fréchet distance is measured by finding a monotone path in the free space from the lower left corner to the upper right corner. In order to reduce the effect of anomalous sampling points in this work, Brakatsoulas et al. [26] propose an extended algorithm using average Fréchet distance; in addition, weak Fréchet distance is used in their work to reduce the time cost to $O(mn \log mn)$. Yin and Wolfson [27] model road networks using weight graphs, and their proposed algorithm is based on edit distance, which is similar to average Fréchet distance. However, these deterministic algorithms are susceptible to noise and perform worse with low-sampling-rates.

To deal with noise, low-sampling-rates, and other issues effectively, methods based on probabilities are widely used. Lou et al. [28] propose an ST-Matching algorithm that combines temporal and spatial contexts. At first, the candidate roads of each sampling point in the given trajectory are determined according to Euclidean distance between the current point and each candidate road, and then spatial and temporal analysis is used to calculate observation probability and transition probability. After accumulating probability scores, the path, which has the maximum joint probability, would be considered the matched path. However, this method does not take into account the weights of different factors and interaction between nonneighboring points, so the accuracy falls rapidly when the path is too long or when there are multiple lanes in the area. Newson and Krumm [16] propose a map matching algorithm for low-sampling-rate trajectories based on a hidden Markov model (HMM). In their work, observation probability matrix and transition probability matrix are inferred by learning from the training dataset, and then a Viterbi algorithm [15] is used to get the result. But HMM has a too strict independence assumption, ignoring the impact between points over long distances and with nonorthogonal features, so its accuracy is slightly lower than that of ST-Matching. Liao et al. [29] also suggest a CRF-based algorithm, but since it employs only the spatial context, the sampling points tend to match roads on the shortest path, and it is not suited for low-sampling-rate trajectories.

3. System Overview

3.1. Problem Definition. In this section, we give definitions of some terms used in this paper.

Definition 1. A *trajectory* θ is a sequence of GPS point which is generated by a vehicle in a trip. Formally, $\theta = o^{(1)} \rightarrow o^{(2)} \rightarrow \cdots \rightarrow o^{(T)}$, where T is the total number of sampling points in the GPS trajectory, the symbols $o^{(1)}$ and $o^{(T)}$ denote start point and end point, respectively. Each GPS point $o^{(t)}$ can be represented by a three-tuple $\langle x, y, t \rangle$, where x denotes latitude, y denotes longitude, and t denotes timestamp. Let Θ denote the collection of N trajectories.

Definition 2. A *trip* tr is an origin-destination pair (OD), which is represented by a two-tuple $\langle r_o, r_d \rangle$, where r_o denotes an origin road and r_d denotes a destination road. If the origin and destination roads of two trips, tr_A and tr_B, are the same, $\mathrm{tr}_A = \mathrm{tr}_B$ can be considered tenable.

Definition 3. A *path* γ is a road segments sequence which is traversed by a vehicle in one trip. $\gamma = r^{(1)} \rightarrow r^{(2)} \rightarrow \cdots \rightarrow r^{(T)}$, where $r^{(1)}$ denotes an origin road and $r^{(T)}$ denotes a destination road. For $r^{(t)} \in \{r_w\}_{w=1}^{W}$, the symbol w is the ID of a road segment, and W is total number of road segments in the road network. If any two neighboring road segments of a path are different and topologically connected, that path is called a *complete* path.

Map matching is equivalent to a sequence-labeled problem in machine learning. Given an observable GPS trajectory θ, a sampling points sequence o can be regarded as an observation sequence to be labeled; road set $\{r_w\}_{w=1}^{W}$ can be regarded as the label set. The objective is to find a path γ^* that is an optimal match for trajectory θ, where γ^* is essentially a maximum a posteriori probability path; that is, $\gamma^* = \mathrm{argmax}_\gamma p(\gamma \mid \theta)$.

3.2. System Framework. The framework of our proposed algorithm is presented in Figure 2. It consists of a training phase and a prediction phase. In the training phase, the parameters of the CRF model are inferred by learning from labeled trajectories. In the prediction phase, generative features and transition features are extracted from the given trajectory to establish the CRF model, and then the value of average sampling interval f is checked; if f is not lower than a given threshold, the matched path is obtained by using the CRF model directly. In detail, the conditional probability of matching a road segment given a sampling point equals

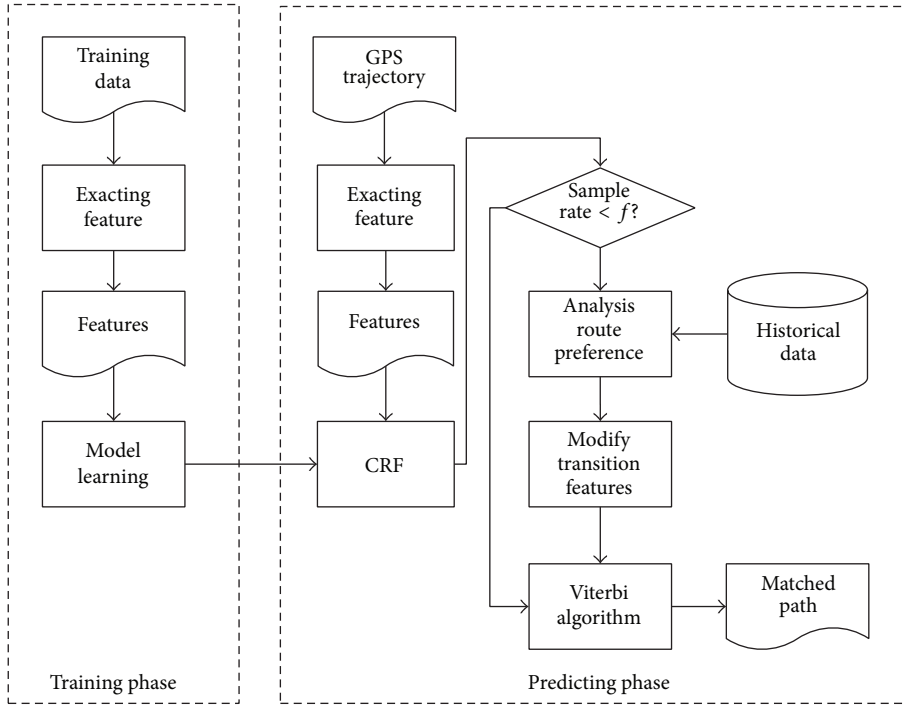

Figure 2: The framework of proposed map matching algorithm.

the sum value of all the features, and then the matched path with maximum joint conditional probability is worked out. Otherwise, the sampling rate is considered too low to capture the temporal and spatial correlation; in order to improve matching accuracy, route preference information is extracted from historical trajectories of the corresponding vehicle, and then it is superposed, with appropriate weighting, on transition features of CRF to generate new transition features.

4. Proposed Approach

4.1. CRF-Based Approach. As a special case of undirected graphical models, a conditional random field is developed on the basis of the maximum entropy model; this approach is widely used in sequence-labeled problems. It avoids the labeled bias problem in the maximum entropy model. Detailed information about CRF can be found in [18, 30].

Definition 4. Let X and Y be sets of observations and random variables, respectively, and $p(Y \mid X)$ the conditional probability of Y given X. If the set Y of random variables constitutes an undirected graph $G = (V, E)$ satisfying the Markov property, that is to say, $p(Y_v \mid X, Y_w, w \neq v) = p(Y_v \mid X, Y_w, w \sim v)$ is founded on any node v in the graph, where $w \sim v$ denotes all the nodes connecting node v in graph G, then $w \neq v$ denotes all the nodes except node v. The probability distribution $p(Y \mid X)$ is called *condition random fields*.

A sequence-labeled problem can be modeled using a linear CRF. If we denote the values assigned to observation sequence X by a vector x, the vector y assigned to labeled sequence Y has the following form:

$$p(y \mid x) = \frac{1}{Z(x)} \exp\left(\sum_{i+1 \in V}\left(\sum_j \mu_j \varphi_j(y_i, x) + \sum_k \lambda_k \delta_k(y_i, y_{i+1}, x)\right)\right), \tag{1}$$

where $Z(x)$ is the normalized factor, which is used to convert $p(y \mid x)$ to a valid probability and which is defined as the sum of exponential number of sequences:

$$Z(x) = \sum_y \exp\left(\sum_{i+1 \in V}\left(\sum_j \mu_j \varphi_j(y_i, x) + \sum_k \lambda_k \delta_k(y_i, y_{i+1}, x)\right)\right). \tag{2}$$

The function $p(y \mid x)$ belongs to an exponential family, which is a set of probability distribution functions of a common form. The function $\varphi(y_i, x)$ is the potential function defined for the nodes in the graph model. This function is also called a generative feature, which makes a different effect of observation sequence x on the probability that label sequence y occurs. If $\mu > 0$, the bigger the value $\varphi(y_i, x)$ is, the more the model prefers to label y_i for x_i. The function $\delta(y_i, y_{i+1}, x)$ is the potential function corresponding to the edges that link nodes and model the dependencies between two labels. It is

called a *transition feature*. That is to say, in labeling y_{i+1}, both x and previously labeled y_i would be considered. The vectors μ and λ are parameters of the CRF and control the weights of their potential functions. All the potential functions and parameters can take arbitrary real values, and the entire exp() function will be nonnegative. The local information of the graph is modeled using potential functions, and such context information can be propagated through the edges linking the nodes; therefore, CRF can integrate a wide range of context information.

With respect to the map matching problems, the road segment that is matched by current sampling point of a vehicle may depend on this vehicle's previous locations. In theory, a high-order CRF that integrates long-distance context dependencies should be used in the model to achieve high accuracy. However, inferring the parameters for a high-order CRF requires complicated computation. In this paper, we use a simple first-order linear CRF model, in which only the dependency between road segments of neighboring sampling points is considered. Our experiments verify the validity of modeling in this way.

4.2. Feature Selection. In this section, we give the concrete expression of each feature function. As mentioned in Definition 1, generative feature is determined only by the current GPS point without considering the effect of other road segments. According to [16, 28, 29], error of GPS points follows Gaussian distribution $N(0, \sigma^2)$. This is in accordance with our intuition that a GPS point is more likely to match to the nearest road segment. Therefore, the formula of generative feature is given by

$$\varphi\left(r_m^{(t)}, o^{(t)}\right) = \frac{1}{\sqrt{2\pi}\sigma} \exp\left(-\frac{d_p^2\left(r_m^{(t)}, o^{(t)}\right)}{2\sigma^2}\right), \quad (3)$$

where $r_m^{(t)}$ denotes mth candidate road segment of GPS point $o^{(t)}$ at sampling time t and $d_p(r_m^{(t)}, o^{(t)})$ denotes the projection distance from $o^{(t)}$ to $r_m^{(t)}$. This formula is based on the assumption that the standard deviation σ is constant over the road network. This is not true in practice, due to urban canyoning effects [31] and satellite occlusions, and [32] uses geographical clustering of the regions of interest to estimate σ. However, this method is more complex. In this paper, we still consider that σ is invariant and set it to 20 meters by measuring on the real dataset. The experimental results show that the effect of the model is ideal. The generative feature ignores the relation of neighborhood points. So it is insufficient to match GPS point based only on generative feature. An example is given in Figure 3. The GPS point $o^{(t)}$ would be matched to the nearest road segment r_3 without considering its neighboring points $o^{(t-1)}$ and $o^{(t+1)}$. In fact, the road segment r_2 is correct.

The transition features model the possibility of jumping between the candidate road segments of two neighboring points. In general, drivers are unlikely to choose a detour path, and the candidate road segments of neighborhood GPS points should be adjacent or close to one another in spatial topology. Therefore, the spatial transition feature δ_1 is defined as

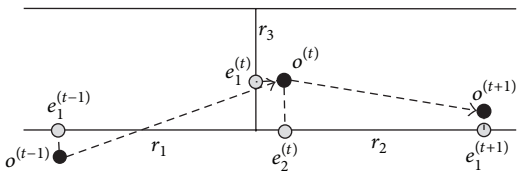

Figure 3: An example of mistake generated by merely matching the GPS points to the nearest road.

$$\delta_1\left(r_m^{(t)}, r_n^{(t+1)}\right) = \left[\frac{d\left(o^{(t)}, o^{(t+1)}\right)}{d_r\left(e_m^{(t)}, e_n^{(t+1)}\right)}\right]^2, \quad (4)$$

where $e_m^{(t)}$ is the projection point of $o^{(t)}$ on the mth candidate road. The functions $d()$ and $d_r()$ are used to calculate the Euclidean distance and path distance between two points, respectively. Obviously, $\delta_1() \in (0, 1)$, and the smaller is the value of $\delta_1()$, the more roundabout is the path. The function $\delta_1()$ reflects the spatial dependency of a GPS point on its neighboring points. However, in some cases, the spatial context cannot be sufficiently reliable to determine the actual path, as when, for example, in some dense parts of a road network, the spatial features of multiple candidate road segments may be similar. In order to distinguish the actual path from other candidates, other high-resolving-power features should be integrated into our model. Consider that the speed constraint of a road segment may be different from that of others, for example, an expressway or a bypass; even with respect to the same road, the average speed can be different at different times. A GPS point is unlikely to be matched to the road segments, on which the corresponding vehicle exceeds the speed limit. We therefore introduce the temporal feature. Assume that there are k road segments in a subpath between $e_m^{(t)}$ and $e_n^{(t+1)}$; the historical average time Δt_e of traversing from $e_m^{(t)}$ to $e_n^{(t+1)}$ can be calculated by

$$\Delta t_e = \sum_k \frac{r_k \cdot l}{r_k \cdot v}, \quad (5)$$

where $r_k \cdot l$ denotes the distance of traversing on road segment k and $r_k \cdot v$ denotes the historical average speed of traversing road segment k at the same time slot. The temporal transition feature δ_2 is given as

$$\delta_2\left(r_t^m, r_{t+1}^n\right) = \left(\frac{\min\left(\Delta t, \Delta t_e\right)}{\max\left(\Delta t, \Delta t_e\right)}\right)^2. \quad (6)$$

As with $\delta_1()$, the temporal transition feature $\delta_2() \in (0, 1)$. Due to taking the temporal feature into consideration, the model would give a higher probability of matching a GPS point to the candidate road whose average speed is closer to the speed of the trajectory.

In summary, the posterior probability of the matched path γ given a trajectory o can be presented as

$$p(\gamma \mid \theta) = \exp\left(\sum_{t\le T}\mu\varphi\left(r_m^{(t)}, o^{(t)}\right) + \sum_{t+1\le T}\left(\lambda_1\cdot\delta_1\left(r_m^{(t)}, r_n^{(t+1)}\right) + \lambda_2\cdot\delta_2\left(r_m^{(t)}, r_n^{(t+1)}\right)\right)\right). \tag{7}$$

The weighted coefficients μ, λ_1, and λ_2 are the model parameters, which are determined in the training phase.

4.3. Model Inference. The goal of model inference is to infer parameters $\omega = \{\mu, \lambda_1, \lambda_2\}$, which are independent of time t. A training set containing labeled trajectories is needed in this phase. Given the definition of conditional probability $p(\gamma \mid \theta)$, the optimization goal is to maximize the likelihood of the training data, and the logarithm likelihood function is given by $\ell(\omega) = \sum_l \log p(\gamma^{(l)} \mid \theta^{(l)}; \omega)$. A standard parameter learning process is to calculate the gradient of the objective function $\ell(\omega)$ and then use this gradient to search for the optimal solution. There are many algorithms for completing this task, and we use L-BFGS [33] in this paper.

In the actual process of parameter learning, if the number of candidate roads is not limited, every road in the city will be involved in the calculation, and this will lead to low efficiency. By preanalyzing on our real dataset, we find that the distance between a GPS point and its correctly matched road is unlikely more than 400 meters. Therefore, we can ignore roads that are more than 400 meters away from the GPS point so that the algorithm can be executed faster without reducing the accuracy. Maximum likelihood estimates of ω can be obtained after parameter learning; this is denoted by $\widehat{\omega}$. Map matching is the process of seeking the maximum a posteriori estimation of $p(\gamma \mid \theta, \omega)$. In this paper, we use a Viterbi algorithm [15], which can calculate a global optimal solution with low time complexity.

4.4. Map Matching Based on CRF and Route Preference Mining (RPM). The CRF model above can match a GPS trajectory to the corresponding path. However, when dealing with a low-sampling-rate trajectory, the accuracy is not satisfactory. The main reason is that the correlation between neighboring points decreases with increasing sampling intervals. As mentioned earlier, if the sampling rate is too low, the span of two neighborhood observations $o^{(t)}$ and $o^{(t+1)}$ may contain multiple candidate subpaths, whose length and speed limit are close to others, especially in the zone of dense interactions. Such an example was shown in Figure 1. To tackle this issue, some additional information is needed to supply the weakness of the resolving power of existing features. In previous research, Froehlich and Krumm [34] found that 60 percent of the paths of a driver are repeated, and most drivers select routes following their personal preferences. Motivated by this, we use personal route preference to enlarge the discrepancy in transition features. A natural way to quantify route preference is using the conditional probability $p_v(r_n^{(t+1)} \mid r_m^{(t)})$ that vehicle v traverses the nth candidate road at time $t+1$, given the condition that it traverses the mth candidate road at time t. This can be calculated as follows:

$$p_v\left(r_n^{(t+1)} \mid r_m^{(t)}\right) = \frac{p_v\left(r_n^{(t+1)}, r_m^{(t)}\right)}{p_v\left(r_m^{(t)}\right)} = \frac{\mathrm{Count}_v\left(r_m \longrightarrow r_n\right)}{\sum_{j=1}^{I_{t+1}}\mathrm{Count}_v\left(r_m \longrightarrow r_j\right) + 1}. \tag{8}$$

Here, $\mathrm{Count}_v(r_m \rightarrow r_n)$ denotes the number of trips of vehicle v, whose paths contain the road segments r_m and r_n following the order $r_m \rightarrow r_n$. The symbol I_t denotes the number of candidate roads at time t. The conditional probability $p_v(r_n^{(t+1)} \mid r_m^{(t)})$ can be obtained by counting in the database. However, after some thought, it is easy to find that $p_v(r_n^{(t+1)} \mid r_m^{(t)})$ cannot describe the personal route preference entirely, because if the historical records of a driver or a path are scarce, the value of $p_v(r_n^{(t+1)} \mid r_m^{(t)})$ is incredible. To tackle this issue, we introduce the function $f_v(r_m)$ that represents the driving experience of vehicle v on road r_m. In [12], the growth of driving experience is modeled using a sigmoid curve; this motivated us to give a similar definition:

$$f_v(r_m) = \frac{1}{1 + e^{-(ax_m^v + b)}}, \tag{9}$$

where x_m^v is the number of times that vehicle v traverses r_m, the expression $ax_m^v + b$ is the linear transformation mapping x_m^v from $[0, +\infty]$ to $[-5, +5]$, and a and b are coefficients. Obviously, the more times vehicle v traverses road r_m, the closer $f_v(r_m)$ is to 1. Based on the analysis above, the route preference $h_v(r_m^{(t)}, r_n^{(t+1)})$ of v vehicle is given as

$$h_v\left(r_m^{(t)}, r_n^{(t+1)}\right) = f_v(r_m)\, p_v\left(r_n^{(t+1)} \mid r_m^{(t)}\right). \tag{10}$$

The personal route preference is the reinforcement of the transition features. But the latter cannot be completely replaced by the former. Because although the resolving power of the transition features is weakened with decreases in the sampling rate, they do not completely disappear. In many cases, the transition features are still effective. Therefore, a reasonable way of using route preference is that, when matching low-sampling-rate observations, $h_v(r_m^{(t)}, r_n^{(t+1)})$ is superposed, appropriately weighted, on the transition features of CRF to generate a new transition feature, which is given by

$$\delta'\left(r_m^{(t)}, r_n^{(t+1)}\right) = \alpha\cdot h_i\left(r_m^{(t)}, r_n^{(t+1)}\right) + (1-\alpha)\cdot\left[\lambda_1\cdot\delta_1\left(r_m^{(t)}, r_n^{(t+1)}\right) + \lambda_2\cdot\delta_2\left(r_m^{(t)}, r_n^{(t+1)}\right)\right], \tag{11}$$

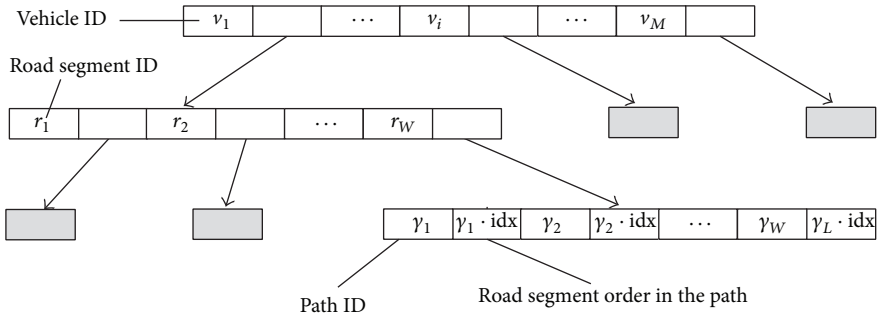

Figure 4: The structure of inverted-index table.

Input: a trajectory $o_{1:T}$ of vehicle v, CRF model, IDT of vehicles
Output: the matched path (road segment sequence)
(1) Check the average sampling interval of trajectory, if lower than threshold, **goto** (2); **otherwise goto** (9);
(2) **for** $t := 0$ to $T - 1$ **do**
(3) **for** each candidate road i in candidate road set of GPS observation of time t **do**
(4) Count the number C_i of paths passing through i
(5) **for** each candidate road j in candidate road set of GPS observation of time $t + 1$ **do**
(6) Count the number $C_{i \to j}$ of paths passing through i to j in order $i \to j$
(7) Calculate the route preference of driver v using formula (10)
(8) Calculate new transmission features using formula (11)
(9) Calculate the maximum posterior probability using Viterbi algorithm.

Algorithm 1: Map matching algorithm based on CRF and route preference mining.

where α is weighting factor, which is used to control the balance between the transition features in CRF and route preference, and which is determined by experiment. Specifically, we can set α to different values and observe accuracy changes in the results of applying our algorithm and then choose the value of α that makes the algorithm achieve higher performance.

When calculating the function, there are frequent queries for the number of a certain road or a certain path passed by a vehicle, which lead to the low efficiency. To reduce the response time, we design an inverted-index table (IDT), which is implemented in three layers of nested hash structure. Its structure is showed in Figure 4. The key of the first layer hash is the vehicle ID, and its value is a pointer, which points to the second-layer hash. The key of the second-layer hash is the ID of the road segment visited by the corresponding vehicle, and its value is a pointer pointing to the third-layer hash table. The key of the third-layer hash is the ID of the path that includes the road segments traversed by the corresponding vehicle, and the value of the third-layer hash is the road segment order in the corresponding path. It is used to determine the direction of the path.

In general, drivers adopt different route strategies at different time. For example, a detour is taken to guarantee the minimum travel time in morning peak hours, and the shortest path or habitual route is selected in normal times. Therefore, in order to calculate route preference accurately, we partition a day into three time slots: morning peak, from 7:30 to 9:30, evening peak, from 17:30 to 19:30, and a normal period of nonpeak hours. Each IDT is built in each time slot. When launching a query, the request is handled in the corresponding IDT according to the sampling time. Algorithm 1 shows our proposed algorithm combining CRF and route preference.

5. Experiments

5.1. Experimental Setting and Dataset Description. For our experiments, we construct a LAN consisting of three computers, which are used to provide GIS service, database, and algorithm execution. We implement our algorithm using C#, and the GIS server is set up with ArcGIS. The digital map mainly includes road network layers with "shape" format. The attributes of the road network include ID, name, level, and length. The network traffic flow information is derived from statistics on historical trajectory data. All information, such as original GPS, traffic flow, the path of each trip, and the IDT, is stored in SQL Server.

We use real trajectory data set generated by 720 Beijing taxis over a period of six months (from March 2012 to August 2012). The sampling interval is approximately 10 seconds. The entire dataset is labeled manually. To validate the regularity of the personal route, we define the repeated path γ_c of path γ_h, which can be computed as

$$\text{repeat}\left(\gamma_c \longrightarrow \gamma_h\right) = \frac{\text{Card}\left(\gamma_c \cap \gamma_h\right)}{\text{Card}\left(\gamma_c\right)}. \tag{12}$$

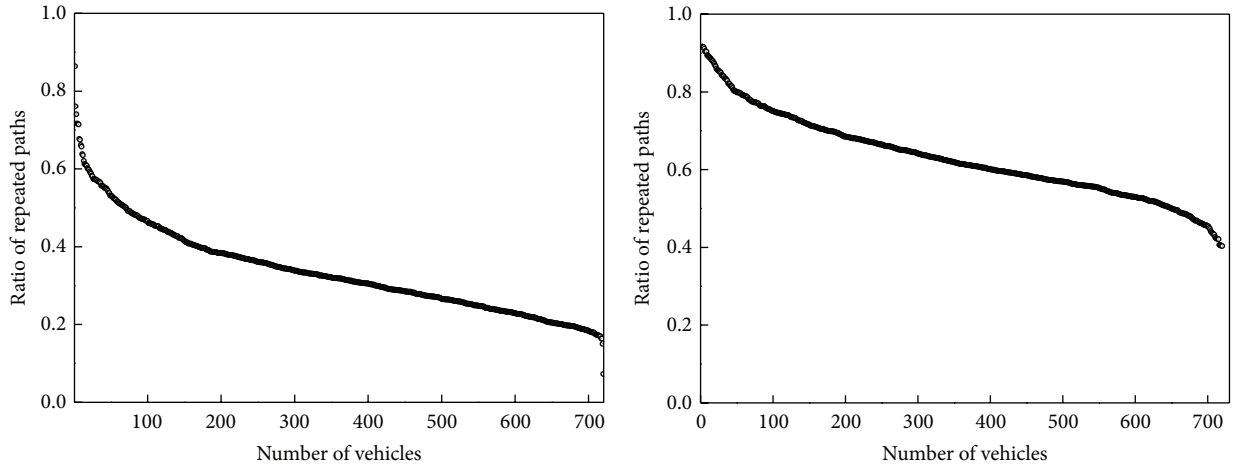

Figure 5: A comparison of the repeated paths ratio in two months (a) and five months (b) of the trajectories dataset.

When repeat($\gamma_c \rightarrow \gamma_h$) is greater than the threshold ζ, the path γ_c can be considered as a repeated path of γ_h; here ζ is set to 0.8. Note that γ_b is not necessarily the repeated path of γ_c. For example, γ_h is a path containing ten road segments, and γ_c is subpath of γ_h, which contains four road segments. The statistics of our dataset are shown in Figure 5. We find that the ratio of repeated paths increases with growth in the amount of data, and the taxi routes show the expected repetitiveness. When trajectories are accumulated over two months, an average 32.4% of paths are repeated. For 68 of these vehicles, the rate is 50%+. Only 47 vehicles have less than 20% repeated paths, since their daily trips are fewer than others. When data is gathered over five months, the average repeated paths rate grows to 63.2%, and 54 vehicles have 80%+ repeated paths, with all others reaching a minimum of 40.4% repeated paths.

We also validate that the number of repeated paths grows with more days of observation. Figure 6(a) presents the growth trend of one driver's repeated path ratio over a period of five months. At first, the ratio increases relatively slowly, and it is less than 20% when accumulating to the 40th day, which indicates that more obscure paths are generated in this period. Then the growth rate increases significantly as the number of days continues to grow; when accumulating to 90 days, the average repeated path ratio is 60%+. Thereafter, the growth rate seems to slow again; ultimately, the average of this ratio holds at approximately 70%. Furthermore, the regularity of route selection is verified. Figure 6(b) presents 387 paths derived from 6820 trips of a driver over five months. We find that the major path bears 235 trips, which is 3.4% of the total number; moreover, 1432 trips, 21% of the total, are distributed over the top 10 frequent paths. This inhomogeneity of path distribution confirms the existence of personal route preferences.

5.2. Experimental Result. The effectiveness of our proposed algorithm is evaluated using two accuracy metrics: accuracy by road segments (A_s) and accuracy by paths (A_r). These are defined as

$$A_s = \frac{\#\text{correctly matched road segments}}{\#\text{all road segments of the trajectories}}$$
$$A_r = \frac{\#\text{correctly matched paths}}{\#\text{all paths of the trajectories}}. \quad (13)$$

First, we estimate the effects of our CRF model (denoted as CRF^1) by comparing with other algorithms, such as incremental, HMM, and CRF [29] (denoted as CRF^2). We select any five months' trajectories as a training set and process the remaining one-month trajectories to generate a plurality of groups at different time intervals (by 30-second increments) for testing. Figure 7 shows the results of each algorithm.

As demonstrated in Figure 7, under the same conditions, A_r is much lower than A_s, due to the strict restriction of A_r. When the sampling interval is less than 30 seconds, all algorithms can achieve high accuracy. And as the sampling interval increases, the accuracy of all algorithms shows varying degrees of decline. All of these algorithms use the context information of the sampling points, and the effects of context information are weakened gradually with decreases in sampling frequency. Specifically, the accuracy of the incremental approach using the local geometric features drops most dramatically. Both HMM and CRF^2, which only consider the spatial context, exhibit similar performance to each other. And the accuracy of CRF^2 is slightly higher, since the CRF^2 model obtains the optimized weights of each feature by parameter learning and makes better use of the spatial context. As temporal correlation is considered, when the sampling interval is not too large, CRF^1 significantly outperforms CRF^2. We also find that, as the sampling interval continues to increase, the accuracy curve of CRF^1 drops sharply and gets close to CRF^2, which indicates that temporal correlation has

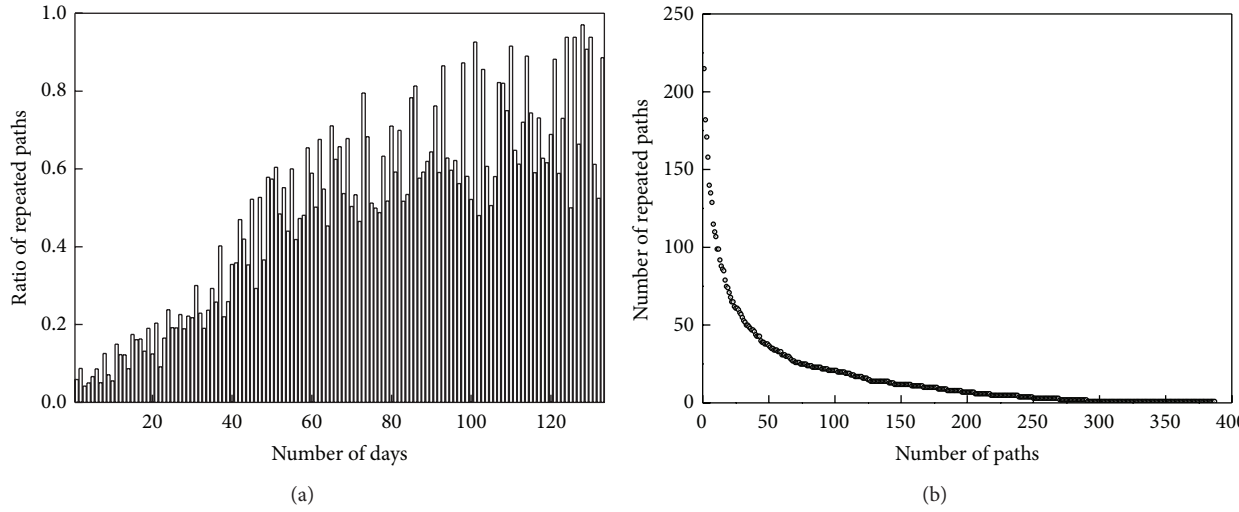

Figure 6: The relation between repeated paths ratio and days (a) and distribution of number of repeated paths (b) for a taxi.

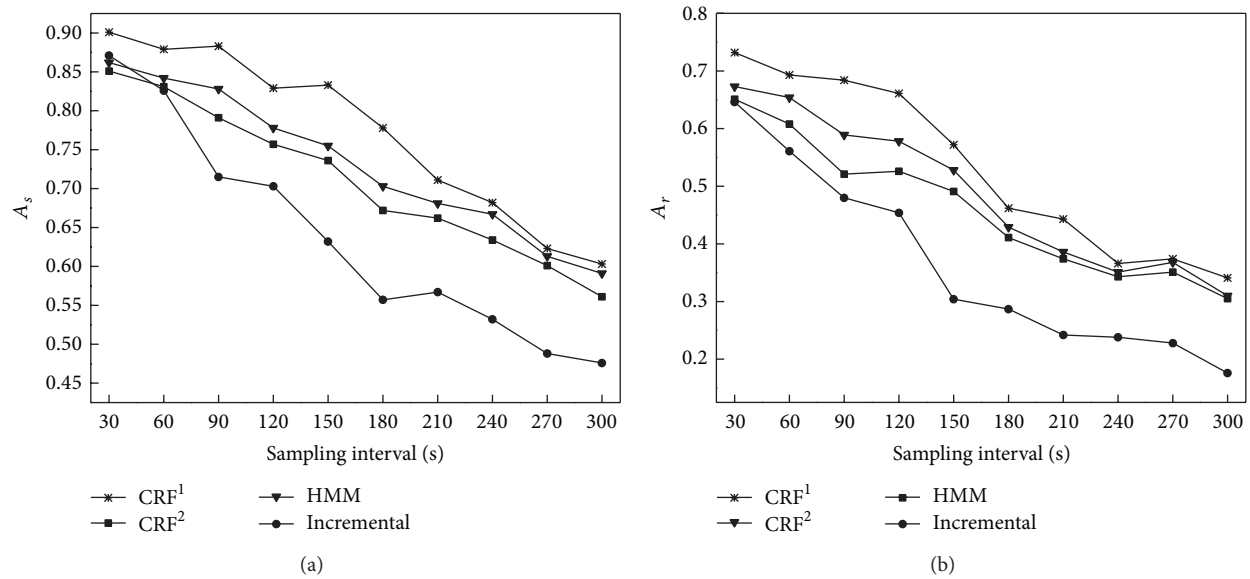

Figure 7: Comparison of HMM, incremental algorithm, CRF[1], and CRF[2].

a weaker effect when neighboring observations are far away from each other.

The parameter α in our proposed framework is used to balance the ratio of temporal-spatial constraints and route preference. We estimate α by analyzing the change in accuracy resulting from setting α to different values. We use any five months' matched trajectories to calculate route preference, and set up three groups of test sets according to different sampling intervals: 180 seconds, 300 seconds, and 420 seconds. Figure 8 shows the evaluation results. In the test set with a 180-second interval, with the value of α rising, A_s grows gradually first and reaches a maximum of 0.821 when α is 0.7; then A_s declines. The reason is that when the proportion of route preference is too high, its effect covers the effective temporal-spatial features. Although some GPS observations are matched to the correct road segments, more observations are mismatched to road segments, which the corresponding driver traverses frequently. Meanwhile, A_r exhibits a tendency toward stabilization after a time of rising. In test sets on 300-second and 420-second intervals, A_s and A_r exhibit a growth trend to different degrees, which implies that, under lower sampling frequencies, the temporal and spatial contexts have less effect, and route preference ought to dominate map matching. Considering that trajectories of higher sampling frequency are more valuable, it is necessary to ensure that the matching accuracy of these trajectories is as high as possible. According to evaluation results on different sampling intervals, the value of α is set to 0.7.

When the sampling interval exceeds 180 seconds, A_s and A_r drop lower than 80% and 50%, respectively. This

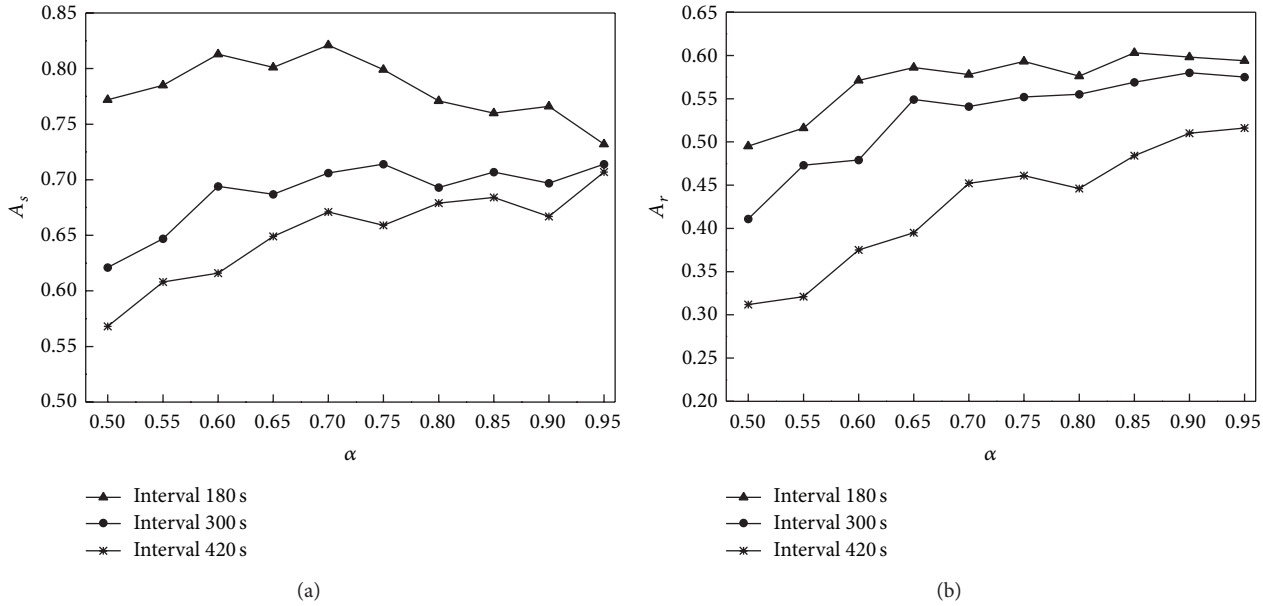

Figure 8: Evaluation of α under different sampling intervals.

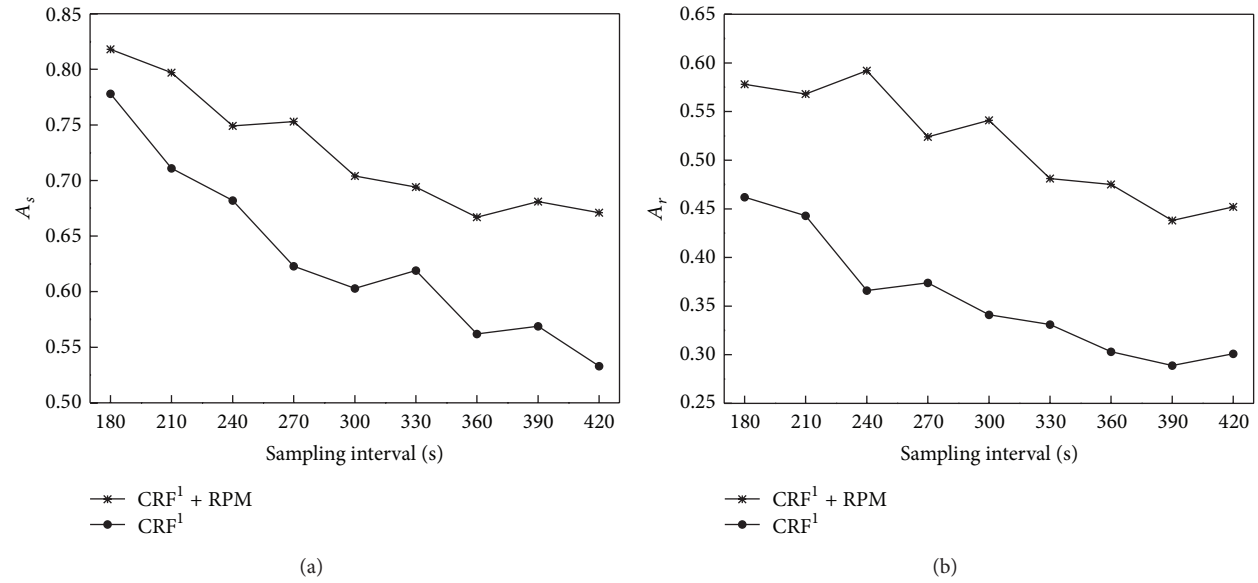

Figure 9: The results of CRF^1 and CRF^1 + RPM.

implies that CRF^1, which depends on temporal-spatial context, can hardly maintain a satisfying effectiveness of map matching. So we integrate route preference into the CRF-based algorithm to provide replenishment of context. Next, we compare our algorithm combining CRF^1 and RPM (CRF^1 + RPM) with CRF^1. As presented in Figure 9, with increasing sampling interval, A_s and A_r of these two algorithms drop at different rates. However, comparing with CRF^1, A_s of CRF^1 + RPM drops slowly and tends to become stable. This means that the improvement of A_s, which is attributed to route preference mining, is more significant with an increasing sampling interval, and the growth rate of A_r is more stable and exceeds 12%. This part of the experiment indicates that CRF^1 + RPM outperforms CRF^1 for all sampling rates significantly. Figure 10 presents a comparison of matching results of CRF^1 and CRF^1 + RPM. As shown in Figure 10, a trajectory with a 300-second sampling interval, consisting of four GPS observations, is matched to a wrong path using CRF^1, while we get the correct path using CRF^1 + RPM.

Finally, we validate the influence of the accumulation of data on effectiveness. Similar to the above, our algorithm is evaluated at different sampling intervals: 180 seconds, 300 seconds, and 420 seconds, and the amount of trajectory used for route preference analysis is increased successively, with

FIGURE 10: Matching results of CRF[1] before (a) and after (b) integrating route preference mining.

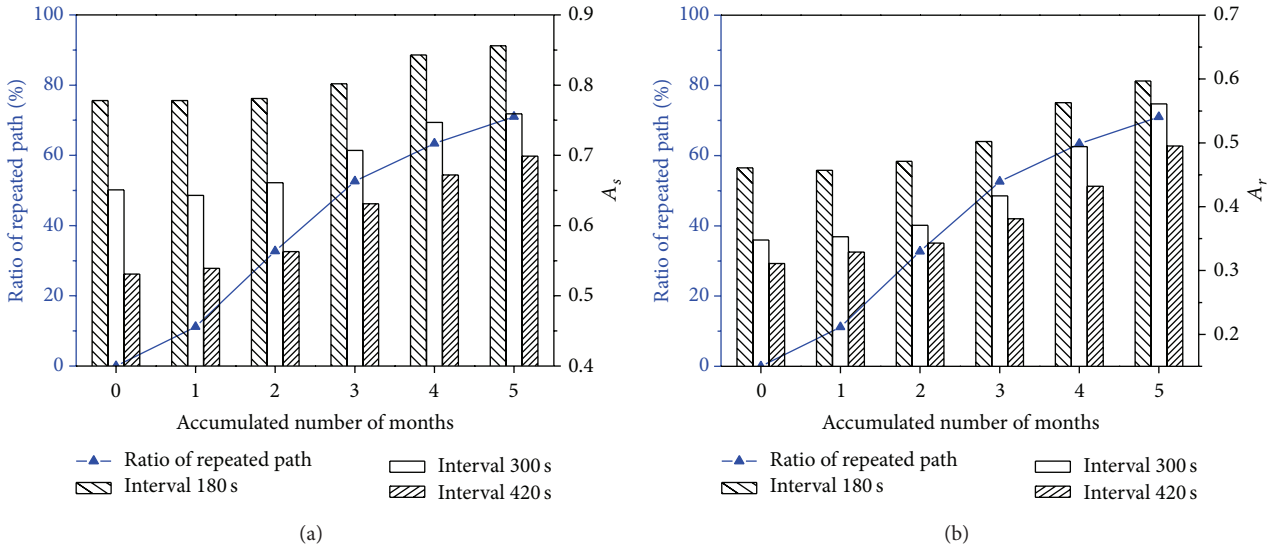

FIGURE 11: The evaluation of historical accumulation impact on accuracy.

increments of one month. Figure 11 presents the evaluation results. In the first two months, the proportion of repeated paths is so low that route preference mining cannot make a great contribution to improve performance, since this stage mainly reflects a period of generating rare paths. When three months' worth of data is accumulated, accuracy begins to grow sharply, following the rise of the repeated path ratio. And when the amount of data reaches five months, A_s and A_r are improved by nearly 10%+ and 15%+, respectively. In addition, we also find that RPM is more effective for the low-sampling-rate trajectories.

5.3. Discussion. Our proposed map matching algorithm is based on linear chain CRF, which can be regarded as the undirected graphical model version of HMM. However, compared with the HMM, CRF provides better support for modeling overlapping, nonindependent features of the output. Taking advantage of this, we introduce the temporal context of neighboring observations, which can boost the resolving power of the transition feature and integrate it with the spatial context. Experiments show that this combination achieves very good performance. In some regions of dense and diverse roads, many candidate paths of GPS observations have similar spatial context information, but their temporal features are quite different, as with, say, expressways and bypasses; thus we see that temporal correlation can heighten the divergence among the solutions to some extent.

When the sampling interval is too large (e.g., exceeding 240 seconds), the effect of temporal context diminishes sharply; so we remove the temporal feature from transition features in order to make the algorithm execute faster; meanwhile, we introduce route preference. These correct matched trajectories, resulting from consideration of route preference, are derived from the trips that mainly happen in the morning or evening peak hours. During these peak hours, probably, the shortest path is not the fastest path, due to traffic congestion, and drivers may choose a roundabout but habitual route. This may weaken the effect of the spatial feature and generate more mismatches under a low-sampling-rate. The addition of route preference maintains the accuracy of the algorithm at a relatively stable and high level. Further, it tends to correctly match or mismatch an entire trajectory. Once mismatching of an observation occurs, a considerable proportion of observations would be matched to incorrect road segments.

Note that the trajectories we used are derived from taxi trips, which are irregular, due to randomness of picking up passengers. If this technology was applied to private cars, it is likely that higher performance would be achieved.

6. Conclusions and Future Work

This paper proposes a CRF-based map matching algorithm, which has the advantage of integrating context information into features flexibly. The spatial and temporal correlations between neighborhood sampling points are chosen as features in order to improve distinguishability of the trajectory. To further improve the algorithm's performance, in the case of a low-sampling-rate, we discover and utilize the personal route preference information to supply the lack of effective features. Experimental results illustrate that this algorithm can accurately find the actual path on multiple sampling frequency datasets. Compared with other map matching methods, the performance is significantly improved. In the future, we will further study the impact of unexpected social events on the effectiveness of our method.

Conflict of Interests

The authors declare that there is no conflict of interests regarding the publication of this paper.

Acknowledgments

The research reported in this paper was conducted as part of the project "The research and application of the urban air environment regulation and control technology based on the Internet of Things," which is under the State High-Tech Development Plan (the 863 program), and funded by National Science Foundation of China (Project no. 2012AA063303) and National Science Foundation of China (Project no. 51408237) "Research on Modeling and Simulation of Bicycle Microscopic Behaviors at Nonsignalized Intersections Based on Information Fusion." In addition, the authors thank Dr. Ling Huang for her help in English improvement of their paper.

References

[1] J. Yuan, Y. Zheng, L. Zhang, X. Xie, and G. Sun, "Where to find my next passenger?" in *Proceedings of the 13th International Conference on Ubiquitous Computing (UbiComp '11)*, pp. 109–118, ACM, September 2011.

[2] W. He, D. Li, T. Zhang, L. An, M. Guo, and G. Chen, "Mining regular routes from GPS data for ridesharing recommendations," in *Proceedings of the ACM SIGKDD International Workshop on Urban Computing (UrbComp '12)*, pp. 79–86, ACM, 2012.

[3] S. Ma, Y. Zheng, and O. Wolfson, "T-share: a large-scale dynamic taxi ridesharing service," in *Proceedings of the 29th IEEE International Conference on Data Engineering (ICDE '13)*, pp. 410–421, IEEE, Brisbane, Australia, April 2013.

[4] J. Yuan, Y. Zheng, and X. Xie, "Discovering regions of different functions in a city using human mobility and POIs," in *Proceedings of the 18th ACM SIGKDD International Conference on Knowledge Discovery and Data Mining (KDD '12)*, pp. 186–194, ACM, August 2012.

[5] Y. Zheng, Y. Liu, J. Yuan, and X. Xie, "Urban computing with taxicabs," in *Proceedings of the 13th International Conference on Ubiquitous Computing*, pp. 89–98, ACM, September 2011.

[6] J. Zhang, "Smarter outlier detection and deeper understanding of large-scale taxi trip records: a case study of NYC," in *Proceedings of the ACM SIGKDD International Workshop on Urban Computing (UrbComp '12)*, pp. 157–162, ACM, Beijing, China, August 2012.

[7] C. Chen, D. Zhang, P. S. Castro et al., "iBOAT: isolation-based online anomalous trajectory detection," *IEEE Transactions on Intelligent Transportation Systems*, vol. 14, no. 2, pp. 806–818, 2013.

[8] S. Chawla, Y. Zheng, and J. Hu, "Inferring the root cause in road traffic anomalies," in *Proceedings of the 12th IEEE International Conference on Data Mining (ICDM '12)*, pp. 141–150, December 2012.

[9] D. Tong, W.-H. Lin, and A. Stein, "Integrating the directional effect of traffic into geostatistical approaches for travel time estimation," *International Journal of Intelligent Transportation Systems Research*, vol. 11, no. 3, pp. 101–112, 2013.

[10] Y. Wang, Y. Zheng, and Y. Xue, "Travel time estimation of a path using sparse trajectories," in *Proceedings of the 20th ACM SIGKDD International Conference*, pp. 25–34, ACM, August 2014.

[11] E. Jenelius and H. N. Koutsopoulos, "Travel time estimation for urban road networks using low frequency probe vehicle data," *Transportation Research Part B. Methodological*, vol. 53, pp. 64–81, 2013.

[12] J. Yuan, Y. Zheng, X. Xie, and G. Sun, "Driving with knowledge from the physical world," in *Proceedings of the 17th ACM SIGKDD International Conference on Knowledge Discovery and Data Mining (KDD '11)*, pp. 316–324, ACM, August 2011.

[13] J. Yuan, Y. Zheng, C. Zhang et al., "T-drive: driving directions based on taxi trajectories," in *Proceedings of the 18th SIGSPATIAL International Conference on Advances in Geographic Information Systems*, pp. 99–108, ACM, November 2010.

[14] N. Nguyen and Y. Guo, "Comparisons of sequence labeling algorithms and extensions," in *Proceedings of the 24th International Conference on Machine Learning*, pp. 681–688, ACM, June 2007.

[15] J. Lafferty, A. McCallum, and F. C. N. Pereira, "Conditional random fields: probabilistic models for segmenting and labeling sequence data," in *Proceedings of the 18th International Conference on Machine Learning (ICML '01)*, pp. 282–289, 2001.

[16] P. Newson and J. Krumm, "Hidden Markov map matching through noise and sparseness," in *Proceedings of the 17th ACM SIGSPATIAL International Conference on Advances in Geographic Information Systems (GIS '09)*, pp. 336–343, ACM, November 2009.

[17] A. McCallum, D. Freitag, and F. C. N. Pereira, "Maximum entropy Markov models for information extraction and segmentation," in *Proceedings of the 17th International Conference on Machine Learning (ICML '00)*, pp. 591–598, 2000.

[18] J. Lafferty, A. McCallum, and F. C. N. Pereira, "Conditional random fields: probabilistic models for segmenting and labeling sequence data," in *Proceedings of the 18th International Conference on Machine Learning (ICML '01)*, pp. 282–289, 2001.

[19] D. R. Brillinger, "Modeling spatial trajectories," in *Handbook of Spatial Statistics*, A. E. Gelfand, P. Diggle, P. Guttorp, and M. Fuentes, Eds., pp. 463–475, CRC Press, Boca Raton, Fla, USA, 2010.

[20] J. Gong, J. Tang, and A. C. M. Fong, "ACTPred: activity prediction in mobile social networks," *Tsinghua Science and Technology*, vol. 19, no. 3, pp. 265–274, 2014.

[21] X. Su, H. Tong, and P. Ji, "Activity recognition with smartphone sensors," *Tsinghua Science and Technology*, vol. 19, no. 3, pp. 235–249, 2014.

[22] J. S. Greenfeld, "Matching GPS observations to locations on a digital map," in *Proceedings of the Transportation Research Board 81st Annual Meeting*, 2002.

[23] S. S. Chawathe, "Segment-based map matching," in *Proceedings of the IEEE Intelligent Vehicles Symposium (IV '07)*, pp. 1190–1197, IEEE, June 2007.

[24] C. Wenk, R. Salas, and D. Pfoser, "Addressing the need for map-matching speed: localizing global curve-matching algorithms," in *Proceedings of the IEEE 18th International Conference on Scientific and Statistical Database Management*, pp. 379–388, 2006.

[25] H. Alt, A. Efrat, G. Rote, and C. Wenk, "Matching planar maps," *Journal of Algorithms. Cognition, Informatics and Logic*, vol. 49, no. 2, pp. 262–283, 2003.

[26] S. Brakatsoulas, D. Pfoser, and R. Salas, "On map-matching vehicle tracking data," in *Proceedings of the 31st International Conference on Very Large Data Bases (VLDB '05)*, pp. 853–864, VLDB Endowment, 2005.

[27] H. Yin and O. Wolfson, "A weight-based map matching method in moving objects databases," in *Proceedings of the16th International Conference on Scientific and Statistical Databse Management (SSDBM '04)*, pp. 437–438, IEEE, June 2004.

[28] Y. Lou, C. Zhang, Y. Zheng, X. Xie, W. Wang, and Y. Huang, "Map-matching for low-sampling-rate GPS trajectories," in *Proceedings of the 17th ACM SIGSPATIAL International Conference on Advances in Geographic Information Systems*, pp. 352–361, ACM, November 2009.

[29] L. Liao, D. Fox, and H. Kautz, "Extracting places and activities from GPS traces using hierarchical conditional random fields," *The International Journal of Robotics Research*, vol. 26, no. 1, pp. 119–134, 2007.

[30] F. Sha and F. Pereira, "Shallow parsing with conditional random fields," in *Proceedings of the 2003 Conference of the North American Chapter of the Association for Computational Linguistics on Human Language Technology*, vol. 1, pp. 134–141, Association for Computational Linguistics, May 2003.

[31] Y. Cui and S. S. Ge, "Autonomous vehicle positioning with GPS in urban canyon environments," *IEEE Transactions on Robotics and Automation*, vol. 19, no. 1, pp. 15–25, 2003.

[32] T. Hunter, P. Abbeel, and A. Bayen, "The path inference filter: model-based low-latency map matching of probe vehicle data," *IEEE Transactions on Intelligent Transportation Systems*, vol. 15, no. 2, pp. 507–529, 2014.

[33] J. Nocedal and S. J. Wright, *Numerical Optimization*, Springer, New York, NY, USA, 1999.

[34] J. Froehlich and J. Krumm, "Route prediction from trip observations," SAE Technical Paper, SAE International, 2008.

Hindawi Publishing Corporation
Mathematical Problems in Engineering
Volume 2015, Article ID 502121, 8 pages
http://dx.doi.org/10.1155/2015/502121

Research Article

Decision Making Method Based on Importance-Dangerousness Analysis for the Potential Risk Behavior of Construction Laborers

In-Hye Han,[1] Gi-Nam Yang,[1] Sangyong Kim,[2] Gwang-Hee Kim,[1] and Yoonseok Shin[1]

[1]*Department of Plant and Architectural Engineering, Kyonggi University, Gwanggyosan-ro 154-42, Yeongtong-gu, Suwon, Gyeonggi-do 443-760, Republic of Korea*
[2]*School of Architecture, Yeungnam University, 280 Daehak-ro, Gyeongsan-si, Gyeongbuk-do 712-749, Republic of Korea*

Correspondence should be addressed to Yoonseok Shin; shinys@kgu.ac.kr

Received 10 February 2015; Accepted 1 May 2015

Academic Editor: Egidijus Rytas Vaidogas

Unsafe behavior contributes to 90% of the causes of construction accidents. To prevent construction accidents, studies on existing unsafe behaviors have been regularly conducted. However, existing studies generally tend to average the survey results and conduct analyses thereon, and such a method cannot consider the potential risk as regards people's anxiety about a certain unsafe behavior. Thus, this research suggests an Importance-Dangerousness Analysis (IDA) technique so that potential risks due to unsafe behaviors of laborers working in the construction sector could be evaluated. In order to verify the applicability of the suggested technique, an actual survey was conducted, and the results of Importance-Performance Analysis (IPA) and IDA were compared with each other. It was found that, unlike IPA, unsafe behaviors that could pose potential risks were confirmed by IDA. Further, unsafe behaviors in the construction sector that should be urgently addressed were also studied. Finally, the IDA suggested in this research could contribute to effective construction safety management on-site by supporting the decisions of the safety manager based on the unsafe behavior analysis of construction laborers.

1. Introduction

Construction industry is highly accident-prone owing to the typical job characteristics such as outdoor production, workplace height, and high dependency on manpower. According to the revisions to the 2012 Census of Fatal Occupational Injuries counts, the total number of fatal work injuries in the United States was 4,628 in 2012, up from the preliminary estimate of 4,383 reported in August 2013. As per industry classification, among the 1,823 laborers in goods producing sectors, the number of accident victims in the agriculture, forestry, fishery, and hunting sectors was 509 (27.9%); the number of accident victims in the construction sector was 806 (44.2%); and the number of accident victims in the manufacturing sector was 327 (17.9%). The statistics indicate that the construction industry has the maximum number of accident victims [1]. According to a report from Korea Occupational Safety and Health Agency (KOSHA), the total number of industrial accident victims in Korea was 92,256 in 2012, wherein the number of accident victims in the construction sector was 23,349, thus, accounting for 25.3% of the total industrial accident victims. In particular, the death toll in industrial accidents in the construction sector was 557, which accounted for 38.8% of the total death toll of 1,435 in the entire industry. This represented the highest accident fatality rate in the industry. Further, the number of accident victims in the last 5 years (2008–2012) has increased from 20,835 in 2008 to 23,349 in 2012. Hence, urgent safety measures are needed for preventing accidents in the construction industry.

Unsafe behavior is a major feature of accidents. Heinrich et al. [2] suggested that about 90% of industrial accidents involve unsafe behavior; however, this does not mean that unsafe behavior is the cause of 90% of the accidents; rather, it is one of the many contributing factors, and, very often, it is the final "trigger" event. Unsafe behavior is also a major cause

of accidents in the construction sector [3]. Thus, audits and management of unsafe acts by encouraging safer behavior can be a means of accident prevention.

Recent studies on the causes of industrial accidents are moving away from the existing perception that accidents occur due to unsafe physical working conditions to the perspective of investigating the relationship between the personal characteristics (i.e., social, physical, and psychological factors, etc.) of the laborers and the causal factors of industrial accidents [4]. In the construction sector, various studies are being conducted to evaluate the background factors of unsafe behavior of construction field laborers, structural analysis of the influencing factors of safe behavior, and so forth. Generally, in existing studies, data are collected based on survey results, and analysis is then conducted using techniques such as one-way ANOVA [5], factor analysis [6], structural equation model [4, 7–9] analytic hierarchy process [10], and Importance-Performance Analysis [11]. However, like in most of the survey analysis, the average value has a significant implication in such methods, and, thus, this process is inherently inadequate in evaluating the potential risks of unsafe behavior. For example, in the case of a survey on a five-point scale, the result of 100 subjects marking three points has the same average value as the result of 50 subjects marking one point and the other 50 subjects marking five points. However, evaluation of the dangers of unsafe behavior should focus on the latter case where 50 subjects marked five points, not on how much the average value is. That is, when compared to the former case, 50 people assessed that a certain factor is dangerous in the latter case, and, thus, the factor has high potential risk. It is almost impossible to evaluate such potential risk in the existing analysis method. So, an appropriate decision making method and its application in the complicate problem are essentially needed. Thus, in this study, a method for analyzing the potential risk of unsafe behaviors of construction laborers is to be suggested. In Section 2, the existing research literature on unsafe behavior is reviewed. In Section 3, a methodology for analyzing the potential risk of unsafe behavior, that is, IDA, is suggested. And, the usefulness of the suggested methodology is verified by comparing the result obtained by using the existing IPA with the outcome achieved through the methodology suggested in this research. Lastly, in Section 4, the limitations of the study and the suggested direction of the future research are described.

2. Literature Review

The relationship between unsafe behavior and construction accidents has been verified through a number of existing studies. Dester and Blockley [3] suggest that poor safety culture is a significant factor in the unsatisfactory safety record of the construction industry and that unsafe behavior is a feature of this culture. The relationship between unsafe behavior and inappropriate culture was stressed conclusively. Langford et al. [6] tried to identify the important factors affecting the safe behavior of construction laborers. The research model of connecting the three themes, implementation strategies for safety management, attitudes of laborers about safety, and behavioral factors displayed by construction laborers, was used. Data was collected through survey, and five important factors were derived through factor analysis. In order to study the relationship between safety climate and laborers' safe behavior in the construction sector, Mohamed [7] established a structural equation model that has 10 independent variables, including commitment, safety rules and procedure, and laborers' involvement. According to the analysis result, safety climate and laborers' safe behavior showed a significant justice relationship. Safety climate plays the role of a mediator between the independent variables and laborers' safe behavior. Oliver et al. [4] examined the relationships between an individual's psychological state, work environment, organizational variables, and occupational accidents, using structural equation modeling. It was clearly established that the organizational involvement positively affects laborers' safe behavior. Choudhry and Fang [12] conducted interviews to analyze the reason for the construction laborers' unsafe behavior. As a result, the reason for the laborers' seven unsafe behavioral conducts, including ignorance and lack of safety knowledge, was identified. The research also identified 11 factors that affected the safe behavior of laborers.

Several studies on unsafe behavior have been actively conducted in Korea, where frequent construction accidents occur. Choi and Kim [8] tried to identify the relationship between the major safety climate factors and laborers' safe behavior in the Korean construction industry. With this objective, the researchers applied the structural equation model of Mohamed [7] to the Korean construction industry and drew the conclusion that "personal risk recognition" and "laborers' safety competence" were the major factors and that the safety climate positively affects laborers' safe behavior. Ryu and Her [10] recognized that safety accidents frequently occur in conditions where unsafe behavior and unsafe status were combined, and they suggested an AHP model as a systematic technique of analyzing the background of the cause of unsafe behavior. Consequently, a checklist that enabled the evaluation of unsafe behavioral factors was developed. Lee at al. [5] statistically analyzed the awareness per category regarding the accident experience of the construction laborers and, based thereon, tried to find a method to improve the safety management activities by improving the awareness levels. They conducted a survey on 36 items followed by an analysis using one-way ANOVA. Subsequently, factors including the major cause of accident occurrence and awareness of the construction laborers about the actual safety conditions in the construction sites were summarized. Shin and Lee [9] tried to reveal the causal relation among the variables affecting safe behavior. The safety climate and laborers' safe behavior were investigated, and the result was analyzed by using structural equation modeling. According to the result, the safe behavior of the construction laborers was directly affected by communication and educational training. Further, safe behavior is not confined merely to personal aspects but is also linked to the organizational climate regarding safety. Han et al. [11] attempted to identify the characteristics of unsafe behaviors of Korean and foreign laborers and prioritized the ones that required improvement by using Importance-Performance Analysis (IPA). As a result,

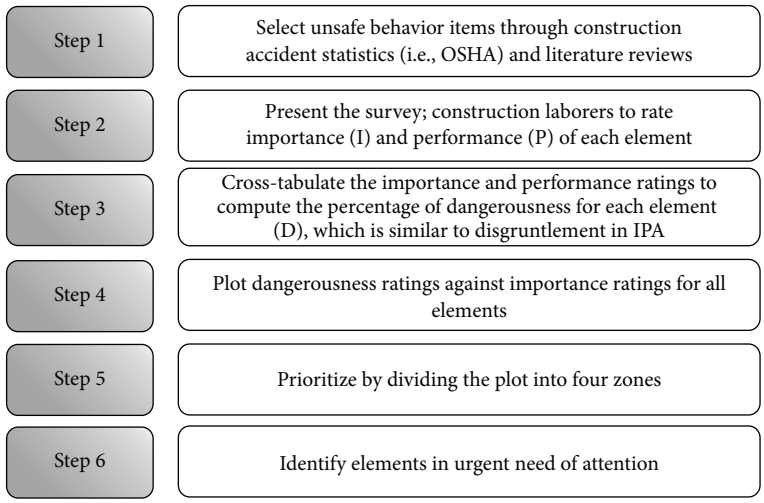

Figure 1: Six-step methodology.

among 19 items, 7 items requiring urgent improvement were derived, and the difference between unsafe behaviors of Korean and foreign laborers was identified.

Such studies indicate that personal psychology and behavior are important factors for preventing accident occurrence in the construction sector. Although such relevant studies have been regularly conducted, existing findings are not capable of considering the potential risk of unsafe behavior of laborers that can cause construction accidents. Thus, this research intends to suggest an improved analysis method that considers such potential risks.

3. Methodology

3.1. Importance-Dangerousness Analysis. The method of analyzing the potential risk of unsafe behavior of construction laborers, as suggested in this research, benchmarked the 6-step methodology suggested by Stradling et al. [13]. They suggested an analysis method that is more detailed than the IPA method, which is one of the existing methods for evaluating customer dissatisfaction. Instead of conducting an analysis by simply using the average value of the response results from the existing IPA, a new measure of "disgruntlement" was derived based on the proportion of respondents marking "quite important" or "very important" on the importance of certain items or "disagree" or "strongly disagree" on the performance of those items through cross-tabulation process.

By weighing performance ratings with importance ratings in this manner, disgruntlement gives a more plausible measure than performance alone on which to base remedial actions to improve user satisfaction with service. Rather than dealing with aggregate mean scores and discrepancies between them, this method identifies "how many" and, potentially, "which" respondents believe an aspect of a service important to them is not being delivered well [13]. Regarding unsafe behavior, the aspect of "how many" and potentially "which unsafe behaviors" do the laborers consider risky would be a more significant outcome in safety management than the aspect of how risky the laborers consider the behavior to be, on an average. The methodology suggested in this research, Importance-Dangerousness Analysis (hereafter IDA), is as shown in Figure 1.

3.2. Steps 1–3. Items related to unsafe behavior were selected in step 1. In that selection process, we referred to the items related to unsafe behavior in the "accident occurrence statistics" [14] of KOSHA and selected 19 items. Subsequently, through interviews with two safety managers who have over 10 years of experience in construction safety management, the appropriateness of the selected items was assessed. Finally, the questionnaire items were prepared, as shown in "Table 1."

Regarding the response method, importance (I) and performance (P) were adjusted to importance (I) and performance of management (P), and the respondents replied as per Likert's five-point scale (from 1 = "strongly disagree" to 5 = "strongly agree").

In step 2, a survey was conducted on construction laborers across five construction companies from March 15, 2014, to April 20, 2014 (for about a month). A total of 358 laborers participated and 279 questionnaire responses, except for 45 that were deemed to be invalid, were analyzed. The details of the respondents are shown in "Table 2."

To confirm the consistency of the survey results, a reliability analysis was conducted using Cronbach's alpha coefficient through SPSS 19.0 program. In general, if Cronbach's alpha value is over 0.6, the survey result is deemed to be reliable [15]. Cronbach's alpha for the survey results of this research was over 0.6 for every item, as shown in "Table 3," and, thus, the statistical value indicated acceptable level in this result.

Tables 4 and 5 show the ranking of the proportion of people who answered "agree" or "strongly agree" regarding the performance and importance of the 19 items of unsafe behavior.

In step 3, dangerousness per item was assessed. Dangerousness assessment is conducted by using cross-tabulation in accordance with the importance assessment per item. For example, Table 6 is the result of cross-tabulation of item

Table 1: Factors in construction cost estimation.

Number	Main item	Number	Subitem
A	Inadequate use of equipment, machineries, and materials	A-1	Inadequate use of protection management
		A-2	Inadequate use of vehicle
		A-3	Cleaning and repairing of working machines
		A-4	Inadequate handling of toxic substance
B	Neglect of dangerous structure	B-1	Neglect of dangerous structures
		B-2	Obstacles left alone on the ground
		B-3	Use of defective tools and materials
		B-4	Bad state of load
		B-5	Incognizance of obstacles at bottom
C	Careless working and breaking the procedure	C-1	Inappropriate method and procedure
		C-2	Inadequate supervision and management
D	Unsafe working posture	D-1	Unsafe working posture
E	Mistakes at working	E-1	Equipment malfunction
		E-2	Wrong handling of hand tools
		E-3	Miss of footing on the stairs
F	The reckless and unnecessary acts	F-1	Reckless acts
		F-2	Unnecessary acts
		F-3	Approach hazardous locations
G	Inadequate use of protective equipment	G-1	Inadequate use of protective equipment

Table 2: Summary of the questionnaire survey.

Factor	Category	Korean		Foreign	
		The number	Ratio (%)	The number	Ratio (%)
Sex	Male	130	97	123	95
	Female	4	3	6	5
Age	~29	3	2	3	2
	30–39	22	16	12	9
	40–49	53	40	60	47
	50~	56	42	54	42
Work	Steel-frame	20	15	40	31
	Bricklayers	7	5	2	2
	Plastering	5	4	9	7
	Heating system	2	1	1	1
	Waterproof	5	4	10	8
	Carpenter	14	10	15	12
	Metal	8	6	0	0
	Windows and doors	4	3	1	1
	Masonry	9	7	2	2
	Painting	0	0	1	1
	Insulation	4	3	3	2
	Interior finishing	2	1	3	2
	Frame	54	40	42	33
Career	~1 year	10	7	7	5
	1–5 years	28	21	60	47
	5–10 years	31	23	42	33
	10 years~	65	49	20	16

Table 3: Cronbach's alpha for Importance-Performance Analysis.

Main category	Number of questions	Cronbach's alpha			
		Korean		Foreign	
		Importance	Performance	Importance	Performance
A	4	0.777	0.749	0.888	0.771
B	5	0.812	0.672	0.876	0.798
C, D	3	0.749	0.626	0.885	0.831
E	3	0.787	0.722	0.887	0.736
F, G	4	0.775	0.816	0.907	0.856

Table 4: Performance ratings of 19 elements of unsafe behavior.

Number	Subitem	Performance (%): % strongly agree + % agree
B-2	Obstacles left alone on the ground	45
C-2	Inadequate supervision and management	50
E-2	Wrong handling of hand tools	52
A-4	Inadequate handling of toxic substance	52
B-1	Neglect of dangerous structures	52
E-1	Equipment malfunction	53
B-4	Bad state of load	54
F-2	Unnecessary acts	54
C-1	Inappropriate method and procedure	54
B-3	Use of defective tools and materials	55
A-1	Inadequate use of protection management	55
A-3	Cleaning and repairing of working machines	57
G-1	Inadequate use of protective equipment	57
F-3	Approach hazardous locations	58
E-3	Miss of footing on the stairs	58
D-1	Unsafe working posture	59
F-1	Reckless acts	62
B-5	Incognizance of obstacles at bottom	62
A-2	Inadequate use of vehicle	64

Table 5: Importance ratings of 19 elements of unsafe behavior.

Number	Subitem	Importance (%): % strongly agree + % agree
A-2	Inadequate use of vehicle	76
F-1	Reckless acts	76
E-3	Miss of footing on the stairs	75
B-3	Use of defective tools and materials	73
B-1	Neglect of dangerous structures	71
E-1	Equipment malfunction	71
A-1	Inadequate use of protection management	70
E-2	Wrong handling of hand tools	69
A-3	Cleaning and repairing of working machines	67
D-1	Unsafe working posture	67
F-3	Approach hazardous locations	67
B-5	Incognizance of obstacles at bottom	66
B-4	Bad state of load	65
C-1	Inappropriate method and procedure	64
A-4	Inadequate handling of toxic substance	63
F-2	Unsafe working posture	62
B-2	Unnecessary acts	61
C-2	Inadequate supervision and management	60
G-1	Inadequate use of protective equipment	60

"B-5." As per this result, 7% (0% + 2% + 4% + 1%) of the total respondents answered that item "B-5" presents high importance but shows low performance.

Using this process, the dangerousness of 19 unsafe behavior items is determined and is displayed in Table 7 in a descending order.

As shown in Table 4, item "B-5" presents significantly high performance. According to Table 8, however, the level of dangerousness turned out to be significantly higher, unlike the results of performance. Consequently, this item could be deemed to present high potential risk. Moreover, as shown in Table 8, items A-2, B-4, B-5, and F-3, for whom the rating of dangerousness has significantly risen when compared to that of performance, can be deemed to present high potential risk.

3.3. Steps 4–6. In steps 4–6, the priority list presenting high dangerousness and importance is identified. The result is shown in Figure 2. For easy identification of the items requiring urgent improvement, we made a classification of four zones by using the average of data as the standard as shown in Table 9.

Zone 1 is the area where both dangerousness and importance are high. The unsafe behavior belonging to this zone requires urgent improvement. Four items, including A-2, B-1, and E-1, belong to this zone. Zone 2 is the area where dangerousness is high whereas importance is low. This zone presents lower importance than Zone 1 but is deemed to present potential dangerousness and thus requires constant

Table 6: Cross-tabulation of performance and importance ratings for "B-5."

Performance (%)	Importance (%)					Row total
	Strongly disagree	Disagree	Neutral	Agree	Strongly agree	
Strongly disagree	<2	<2	<0	**0**	**5**	9
Disagree	<1	6	6	**11**	**3**	27
Neutral	<0	8	17	24	13	62
Agree	<1	10	22	42	31	106
Strongly agree	0	5	9	17	28	59
Column total	4	31	54	94	80	$N = 263$

Table 7: Dangerousness measures of 19 elements of unsafe behavior.

Number	Subitem	Dangerous (%): % strongly agree + % agree
B-1	Neglect of dangerous structures	11
B-4	Bad state of load	10
E-1	Equipment malfunction	9
A-4	Inadequate handling of toxic substance	9
F-3	Approach hazardous locations	8
B-2	Obstacles left alone on the ground	8
B-5	Incognizance of obstacles at bottom	7
C-1	Inappropriate method and procedure	7
E-2	Wrong handling of hand tools	7
A-2	Inadequate use of vehicle	7
E-3	Miss of footing on the stairs	6
G-1	Inadequate use of protective equipment	6
A-3	Cleaning and repairing of working machines	6
C-2	Inadequate supervision and management	6
A-1	Inadequate use of protection management	5
B-3	Use of defective tools and materials	5
D-1	Unsafe working posture	5
F-1	Reckless acts	5
F-2	Unnecessary acts	4

monitoring. Six items including A-4, B-2, and B-4 belong to this zone. Zone 3 is the area where both dangerousness and importance are low. For the sake of effective conduct of management tasks, it is justified to accord the lowest priority to the unsafe behavior in this zone. Four items, including A-3, C-1, and C-2, belong to this zone. Zone 4 is the area where dangerousness is low, whereas importance is high. Regarding unsafe behavior in this zone, it is deemed that the relevant items are under good management when compared to the other items, and, thus, it is necessary to maximize efforts to maintain the current condition. Four items including A-1, B-3, and E-3 belong to this zone.

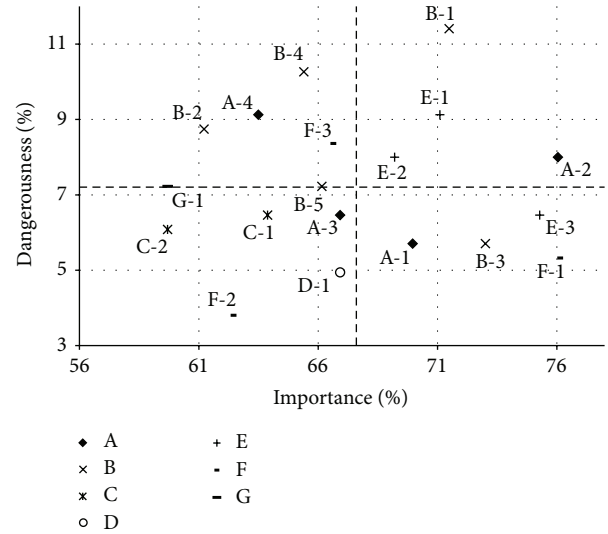

Figure 2: Scatter graph of dangerousness versus importance (IDA).

3.4. Analysis of Results. In this research, an IDA that can assess the potential risk of 19 items of unsafe behaviors of construction laborers is suggested, and the applicability thereof is assessed by using the actual survey results. As it can derive the potential risk, IDA has an advantage when compared to the existing analysis methods. To elaborate, items A-2, B-4, B-5, and F-3 received relatively favorable assessments in step 2. However, according to the dangerousness assessment results in step 3, the ratings are assessed to be relatively dangerous. The items that had been considered well-managed were actually evaluated to have potential dangerousness. This outcome cannot be seen in the IPA result based on average.

This feature is also displayed during the comparison of the final results of IDA and IPA. The results of IPA are shown in Figure 3. Five items belonging to the second quadrant in IPA, which is not well-managed, are A-1, B-1, B-3, E-1, and E-2. Four items belonging to first quadrant, which is important and dangerous in IDA, are A-2, B-1, E-1, and E-2. All these items require urgent improvement or treatment. The items of IPA and IDA that belong to the zone, where high dangerous or low performance but high importance is, are shown in Table 10.

In particular, item A-2 was assessed to be well-managed in IPA. However, according to the results of IDA, it was derived as an item that presents high dangerousness as it belonged to

Table 8: Potential risks items (in step 3).

Rating	Performance		Dangerousness	
1	B-2	44%	B-1	11%
2	A-4	52%	**B-4**	**10%**
3	C-2	52%	A-4	9%
4	E-2	53%	E-1	9%
5	B-1	54%	B-2	8%
6	E-1	54%	**F-3**	**8%**
7	F-2	55%	**A-2**	**7%**
8	A-1	55%	**B-5**	**7%**
9	B-3	55%	E-2	7%
10	**B-4**	**55%**	G-1	7%
11	C-1	56%	E-3	6%
12	A-3	58%	A-3	6%
13	G-1	58%	C-1	6%
14	**F-3**	**59%**	C-2	6%
15	E-3	60%	A-1	5%
16	D-1	61%	B-3	5%
17	F-1	62%	F-1	5%
18	**A-2**	**64%**	D-1	5%
19	**B-5**	**64%**	F-2	4%

Table 9: Definitions of Zones 1–4.

Zone 2 High dangerousness but low importance	Zone 1 High dangerousness + high importance
Zone 3 Low dangerousness + low importance	Zone 4 High importance but low dangerousness

Table 10: Comparison of results of IPA and IDA.

Methodology	Number	Subitem
IDA	A-2	Inadequate use of vehicle
	B-1	Neglect of dangerous structures
	E-1	Equipment malfunction
	E-2	Wrong handling of hand tools
IPA	A-1	Inadequate use of protection management
	B-1	Neglect of dangerous structures
	B-3	Use of defective tools and materials
	E-1	Equipment malfunction
	E-2	Wrong handling of hand tools

Zone 1. Here, it can be deemed that item A-2 is relatively well-managed in the perspective of average value, but it also means that a relatively high number of respondents answered that it is not being well-managed.

When compared to other management tasks of construction projects (i.e., cost management, quality management, scheduling, etc.), lack of management would be critical, as it not only affects the economic aspects but also can cause

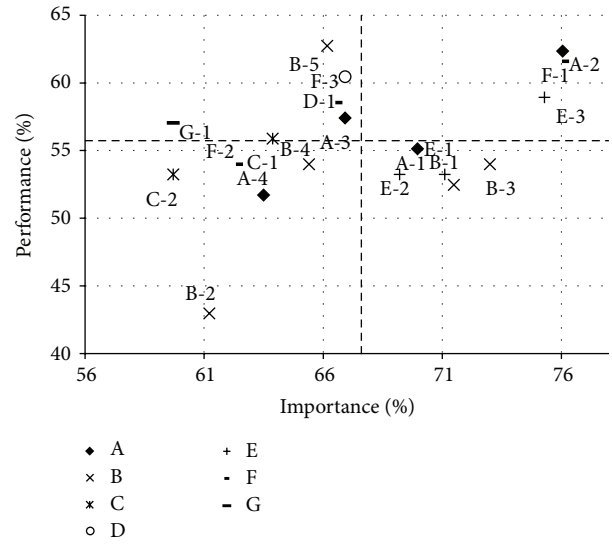

Figure 3: Scatter graph of IPA (reversion of the x-axis and y-axis).

casualties. Thus, when the factors in safety management such as unsafe behavior are considered, how many people find it dangerous may be a more adequate standard in assessing dangerousness than how dangerous it is on average. The IDA suggested in this research could conclusively help safety managers in deriving items that have potential risk. The results of IDA identify the areas that require urgent attention and support the decision making of the safety manager so that he/she could effectively conduct specific tasks within the limited resources and time. Additionally, IDA can be used in various dangerousness analyses of safety management, including assessment of unsafe behavior of construction laborers, analysis on the job stress of construction laborers, assessment of the construction equipment, and assessment of the safety management level in the construction sector.

4. Conclusion

The single most important factor among all direct causes of construction accidents is unsafe behavior. Although studies on unsafe behavior have been regularly conducted, they tend to average survey results and conduct analyses thereon. With that method, however, it is impossible to consider how many people feel anxious about certain unsafe behaviors. Thus, in this research, the IDA technique is suggested in order to assess the potential risks regarding unsafe behaviors of laborers in the construction sector. In order to verify the applicability of the suggested technique, the results obtained by the actual survey and application thereof were compared with the results obtained using the IPA technique. Consequently, unsafe behaviors posing potential risks that were not found in IPA were confirmed in IDA. Moreover, through IDA, it was possible to identify which unsafe behaviors required urgent measures. The IDA suggested in this research supports the decision making of the safety manager by assessing potential risks and highlighting the items that require urgent measures. Therefore, it is expected to help

the safety managers in effectively conducting safety management tasks in the construction sector.

In this research, an improved analysis method that can show up potential risks resulting from the unsafe behavior of construction laborers was suggested. However, the subject of the analysis in this research was limited to one factor, unsafe behavior, and, thus, it is difficult to confirm that the IDA suggested in this research is also effective in deriving potential risks in other areas. Therefore, future studies wherein IDA is applied to various subjects, including job stress and safety management level assessment in the sector, are necessary to verify the applicability of IDA.

Conflict of Interests

The authors declare that there is no conflict of interests regarding the publication of this paper.

Acknowledgment

This research was supported by Basic Science Research Program through the National Research Foundation of Korea (NRF) funded by the Ministry of Education (2012R1A1A1042693).

References

[1] Office of Occupational Safety and Health Statistics, *Revisions to the 2012 Census of Fatal Occupational Injuries Counts*, Office of Occupational Safety and Health Statistics, 2014, http://www.bls.gov/iif/oshcfoi1.htm.

[2] H. W. Heinrich, D. Petersen, and N. Roos, *Industrial Accident Prevention*, McGraw-Hill, New York, NY, USA, 1950.

[3] W. S. Dester and D. I. Blockley, "Safety—behaviour and culture in construction," *Engineering, Construction and Architectural Management*, vol. 2, no. 1, pp. 17–26, 1995.

[4] A. Oliver, A. Cheyne, J. M. Tomás, and S. Cox, "The effects of organizational and individual factors on occupational accidents," *Journal of Occupational and Organizational Psychology*, vol. 75, no. 4, pp. 473–488, 2002.

[5] H. Lee, S. Yeo, and S. Go, "A study on the improving safety management by analyzing safety consciousness of construction labors," *Journal of the Korea Institute of Building Construction*, vol. 9, no. 3, pp. 51–58, 2009.

[6] D. Langford, S. Rowlinson, and E. Sawacha, "Safety behaviour and safety management: its influence on the attitudes of workers in the UK construction industry," *Engineering, Construction and Architectural Management*, vol. 7, no. 2, pp. 133–140, 2000.

[7] S. Mohamed, "Safety climate in construction site environments," *Journal of Construction Engineering and Management*, vol. 128, no. 5, pp. 375–384, 2002.

[8] S. I. Choi and H. Kim, "A study on the safety climate and worker's safe work behavior in construction site," *Journal of The Korea Society of Safety*, vol. 21, no. 5, pp. 60–71, 2006.

[9] D. P. Shin and D. E. Lee, "The structural analysis between safety factors having an effect on the construction workers' behavior," *Journal of Korea Institute of Construction Engineering and Management*, vol. 14, no. 1, pp. 101–114, 2013.

[10] S. W. Ryu and D. G. Her, "A study on evaluating background factors of the unsafe behavior using AHP," in *Proceedings of the Autumn Annual Meeting for the Korean Safety Management and Science*, Seoul, Republic of Korea, November 2009.

[11] I. H. Han, G. N. Yang, H. G. Cho, G. H. Kim, and Y. S. Shin, "The analysis on the unsafe acts of laborers at domestic construction sites," *Journal of the Korean Society of Safety*, vol. 29, no. 4, pp. 132–139, 2014.

[12] R. M. Choudhry and D. Fang, "Why operatives engage in unsafe work behavior: investigating factors on construction sites," *Safety Science*, vol. 46, no. 4, pp. 566–584, 2008.

[13] S. G. Stradling, J. Anable, and M. Carreno, "Performance, importance and user disgruntlement: a six-step method for measuring satisfaction with travel modes," *Transportation Research Part A: Policy and Practice*, vol. 41, no. 1, pp. 98–106, 2007.

[14] Korea Occupational Safety & Health Agency, *The Statistics of Great Disaster of Construction Industry : KOSHA 2002–2010*, Korea Occupational Safety & Health Agency, 2014, http://www.kosha.or.kr/.

[15] H. S. Lee and J. H. Lim, *Basic SPSS Manual*, Jyphyunjae Publishing Co., Seoul, Republic of Korea, 2012.

Hindawi Publishing Corporation
Mathematical Problems in Engineering
Volume 2015, Article ID 105024, 14 pages
http://dx.doi.org/10.1155/2015/105024

Research Article

Structural Optimization of Steel Cantilever Used in Concrete Box Girder Bridge Widening

Qian Wang,[1] Wen-liang Qiu,[1] and Sheng-li Xu[2]

[1] *Faculty of Infrastructure Engineering, Bridge Science Research Institute, Dalian University of Technology, Dalian, Liaoning 116024, China*
[2] *School of Energy and Power Engineering, Dalian University of Technology, Dalian, Liaoning 116024, China*

Correspondence should be addressed to Sheng-li Xu; xusl@dlut.edu.cn

Received 3 April 2015; Revised 11 June 2015; Accepted 21 June 2015

Academic Editor: Zdeněk Kala

The structural optimization method of steel cantilever used in concrete box girder bridge widening is illustrated in this paper. The structural optimization method of steel cantilever incorporates the conceptual layout design of steel cantilever beam based on the topological theory and the determination of the optimal location of the transverse external prestressed tendons which connect the steel cantilever and the box girder. The optimal design theory and the analysis process are illustrated. The mechanical model for the prestressed steel cantilever is built and the analytical expression of the optimal position of the transverse external tendon is deduced. At last the effectiveness of this method is demonstrated by the design of steel cantilevers which are used to widen an existing bridge.

1. Introduction

Structural optimization is an important tool for structural designers because it allows the designers to tailor a structure to a specific performance level required by the owner. Structural optimization is nowadays common in mechanical and aeronautical engineering, and in recent years, it has been progressively adopted for structural engineering and bridges [1–10]; particularly in the aspects of generation of strut-and-tie patterns for reinforced concrete structures [11–13] and fiber-reinforcement retrofitting structures [14–16], the topology optimization is widely used. Aiming at different structures the corresponding optimization schemes should be proposed to help the designers to find structural forms that not only better exploit material but also give the structure greater aesthetic value.

In this paper, the structural optimization method of steel cantilever which is used in concrete box girder bridge widening is illustrated. Steel cantilever widening concrete box girder method is a new box girder widening method without piers, which has many advantages, such as shorter construction period, open clearance of span, lesser traffic interference, better traffic capacity, and better economic benefit [17, 18]. According to this method, the original bridge deck is widened by the orthotropic steel decks that are laid on the cantilevers (Figure 1). The cantilevers are connected to the original box girder by transverse external prestressed tendons. Pairs of steel cantilever beams are installed on both sides of the original box girder at regular distance (L, see Figure 2). As it is shown in Figure 3, postpouring concrete diaphragms are used to connect with the newly added steel cantilever beams. Concrete postpouring diaphragms are placed in pairs and their quantities and locations should be consistent with those of newly added steel cantilever beams.

The widened box girder is a special structure of steel and concrete combined transversely. Ensuring the reasonable stress on interface between the steel cantilever and the box girder is an important precondition to guarantee that the entire structures work together. Besides, the beautiful shape and reasonable function holes which are used to settle pipelines are essential to the steel cantilevers. The reasonable design of the steel cantilevers is the key problem. Although the conceptual design of the steel cantilevers depends on the designer's intuition and ability to recognize the role of steel

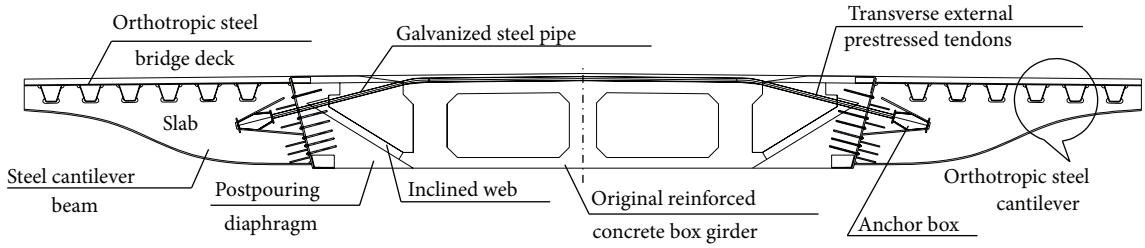

Figure 1: Sectional drawing of original box girder widened by steel cantilevers.

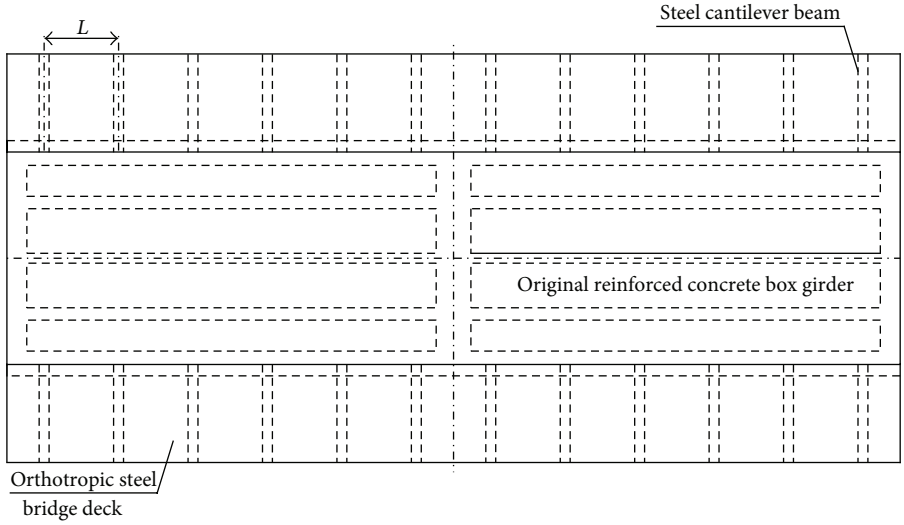

Figure 2: Plane figure of original box girder widened by steel cantilevers.

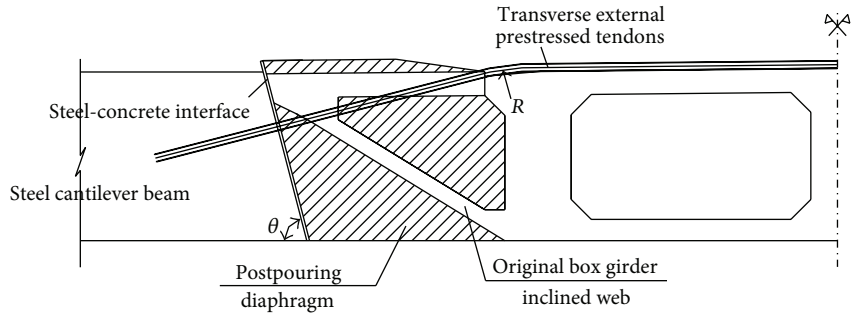

Figure 3: Diagram of interface between steel and concrete.

cantilevers in transferring weight and loads to the original box girder, currently, structural optimization may help the designer find the most suitable shape and layout of a steel cantilever from a structural and an architectural point of view [19, 20].

The topic of this paper is a structural optimization problem which incorporates the conceptual layout design of the steel cantilever and the determination of the optimal location of the transverse external prestressed tendons. The author applied the topological optimization theory to the shape and layout design of steel cantilever and builds the mechanical model for the prestressed steel cantilever. Then the analytical expression of the reasonable acting position of the transverse external prestressed tendons on the steel cantilever is deduced and the steel cantilever structural optimization scheme is proposed.

2. The Optimization Problem Statement

There are two key issues for optimization design of the steel cantilever.

The first one is the conceptual layout design of steel cantilever beam. The steel cantilever is newly added to the original box girder; the additional live load and dead load on the steel cantilever should be effectively transmitted to the original box girder. This requires the shape, layout of steel

cantilever, and the setting of function holes for the pipelines should not damage the structure stiffness; namely, the load path of steel cantilever should not be broken.

The second issue is the decision of the optimal location of the transverse prestressed tendons. The transverse external prestressed tendons which connected the original box girder and the steel cantilevers are key components of the widened structure, whose location influences the stress on the steel-concrete interface as shown in Figure 3 directly. In order to ensure that the steel cantilever is connected with original concrete box girder closely and the concrete at interface is not crushed, the optimal location of transverse prestressed tendons is an important prerequisite. The reasonable stress state of steel-concrete interface is that there should be no tensile stress on the key position of interface and the compressive stress should not exceed the compressive strength of the concrete at interface, which should be obeyed in deducing the optimal location of the prestressed tendons.

3. Topological Optimization of the Steel Cantilever

The aim of topological optimization is to find a conceptual layout of steel cantilever by distributing a given amount of material in a domain, thereby achieving the lightest and stiffest structure while satisfying certain specified design constraints.

Many innovative optimization methods and algorithms have been developed and reported [21–29]. In this paper, topological optimization was carried out through the SIMP method [30–33], due to its computational efficiency and conceptual simplicity.

3.1. Numerical Model. Steel-concrete interface is the key position for this composite structure. While pursuing optimization design of the entire steel cantilever beam to make it light, convenient to be processed, and well-formed, it should be premised on that the vehicle load and dead load on steel cantilevers could be transmitted to the interface effectively. The dead load here is the weight of orthotropic steel bridge deck and the bridge deck pavement including concrete paving layer and asphalt concrete paving layer.

In order to get the optimal transmitting path of load on the steel cantilever from which to the interface, the interface of steel cantilever is considered as consolidated from the perspective of model simplification. Because the orthotropic bridge deck slab should be set at top of steel cantilever actually, U-shaped slots need to be reserved for placing bridge deck slab, as it is shown in Figure 4. Thus, single-ended consolidated structure with U-shaped slots is the basic structure for topological optimization of steel cantilever.

The load on steel cantilever involves dead load and motor vehicle wheel load. The uniform force "q_0" of dead load as shown in Figure 5 is the weight of orthotropic bridge deck and deck pavement equally distributed on each steel cantilever. According to the regulations of *General Code for Design of Highway Bridges and Culverts* [34], the most unfavorable wheel load distribution is arranged. Setting widening one lane

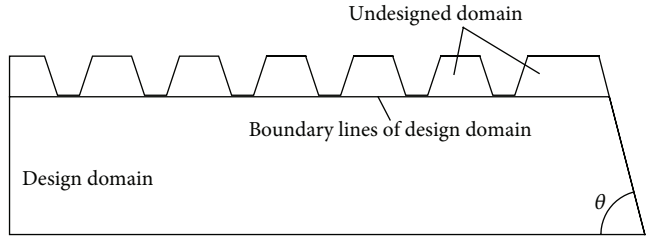

Figure 4: Actual structure for topological optimization.

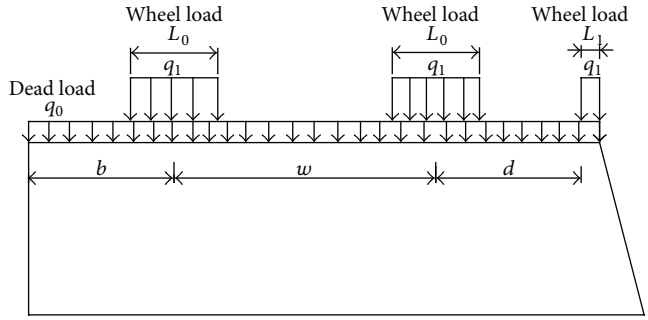

Figure 5: Topological optimization structural under Load Case 1.

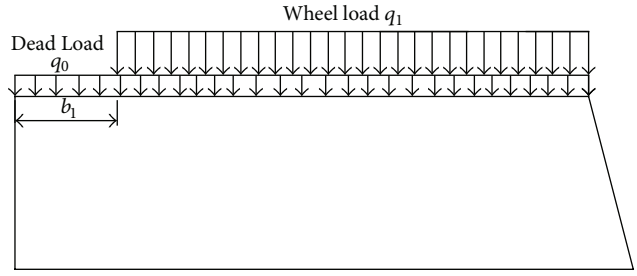

Figure 6: Topological optimization structure under Load Case 2.

unilaterally as an example, within widening range of steel cantilever, two wheels and part of one wheel may be arranged. Wheel uniform load "q_1" could be calculated according to the vehicle axle load and wheel action range. Optimization analysis for Load Case I refers to the combined action of dead load uniform force "q_0" and actual most unfavorable wheel load, as it is shown in Figure 5.

The position of wheel load is random and not fixed within the range of the motor vehicle possible passing. Thus, besides the above most unfavorable loading case, wheel load also has other various loading cases. In order to make optimization results widely suitable for various loading conditions, wheel load is hereby fully distributed within the range that wheel load may appear conservatively, which is Load Case 2 as shown in Figure 6. Besides the dead load and wheel load on the steel cantilever, the self-weight of the steel cantilever also should be considered during the topological optimization process.

3.2. Mathematical Model. In this paper, minimum compliance of the system is regarded as objective function of

the structure optimization. In similar design area, when boundary conditions and load are certain, the smaller the compliance is, the larger the stiffness is [33, 35].

Suppose external force exerted on the system as F, then its strain energy could be expressed as

$$E_s = \frac{1}{2}\int_{\Omega} \varepsilon(u)^T D\varepsilon(u)\, d\Omega = \frac{1}{2}F^T U. \tag{1}$$

In the equation, Ω is given design area; $\varepsilon(u)$ is strain under load F; u is elastic deformation of any point in design area under load F; D is elastic matrix; F is load vector; and U is displacement vector.

Equilibrium equation of the system is expressed as

$$KU = F, \tag{2}$$

wherein K represents the stiffness matrix of the system and $K^T = K$. Joining (1) and (2) together, it could be concluded that

$$E_s = \frac{1}{2}U^T K^T U = \frac{1}{2}U^T KU. \tag{3}$$

Compliance of the system could be expressed as $C = F^T U$. Compared with (1), it could be concluded that if compliance of the system is minimum, its strain energy is minimum.

Mathematical model for topological optimization of steel cantilever structure is established as

$$\begin{aligned} \rho(x) &= x_i \rho_0, \\ E(x) &= x_i^P E_0; \end{aligned} \tag{4}$$

wherein ρ_0 and E_0 represent density and elastic matrix of cantilever after subdivision, respectively; x_i represents relative density of the element; and P represents penalty factor.

As it is illustrated in Section 3.1, actual topological structure is mainly designed according to two load cases (see Figures 5 and 6). Making stiffness of steel cantilever the largest, the best material distribution results can be calculated. In order to ensure that the steel cantilever can transmit the loads to the interface effectively, Load Case 1 and Load Case 2 are considered together to confirm the boundary and layout of steel cantilever. The multiload approach [36, 37], which considers multiload cases by using the weight coefficient, can be used to perform the optimization boundary and layout of steel cantilever.

Considering two load cases, the topology optimization problem to minimize the compliance of the steel cantilever structure while it is subjected to a limited amount of material in the design domain can be written as

$$\begin{aligned} \text{Find} \quad & X = [x_1, x_2, x_3, \ldots, x_n]^T \\ \text{Minimize:} \quad & C(X) = c_1 U_1^T KU_1 + c_2 U_2^T KU_2 \\ & = c_1 \sum_{i=1}^{n} (x_i)^P U_{1e}^T KU_{1e} \\ & + c_2 \sum_{i=1}^{n} (x_i)^P U_{2e}^T KU_{2e} \\ \text{Subjected to:} \quad & \sum_{i=1}^{n} x_i \le f \\ & KU_1 = F_1 \\ & KU_2 = F_2 \\ & 0 < x_{\min} < x_i < 1. \end{aligned} \tag{5}$$

In the equation, relative density of the element x_i is design variable; f represents volume coefficient; $KU_1 = F_1$ is the equilibrium equation for Load Case 1, and $KU_2 = F_2$ is the equilibrium equation for Load Case 2; c_1 and c_2 are the weight coefficients for Load Case 1 and Load Case 2. In this case, the mathematical model could be described as finding density distribution of each element to make the stiffness of the steel cantilever the largest in certain combination of load weight coefficients.

In this paper, the optimization analysis is performed using the topological optimization module in ANSYS.

In design domain of steel cantilever, function holes which are used to settle pipelines should be placed in the area that does not need to arrange materials. Leading the obtained optimization results into cartographic software, the shape and function holes of the steel cantilever that do not damage the structure stiffness could be designed according to material distribution results, which means the shape and layout of the function holes design are designed on the premise of ensuring not to damage load transmission path and maintaining the structure stiffness. The specific design procedure will be described later in the application of an actual bridge example.

4. Determination of Optimal Location of the Transverse External Tendon

4.1. Mechanical Model. While analyzing the stress on the interface between steel cantilever and concrete postpouring diaphragm, we suppose that there is no elastic deformation caused to steel cantilever, but only rigid body moves and rotates. The counterforce on concrete interface is in straight-line distribution, as it is shown in Figures 7 and 8.

The key issue for ensuring that the special composite structures work cooperatively refers to the fact that newly added steel cantilever should contact with concrete box girder closely and the concrete at interface will not be crushed, which means tensile stress will not happen to the interface and compressive stress should not exceed the compressive strength of the concrete at interface.

Combined with actual project, from construction stage to application stage, the stress at steel-concrete interface involves two critical cases. Critical Case I is in construction stage. When steel cantilever is well installed, transverse prestressed tendons are stretched, while orthotropic bridge deck slab and bridge deck pavement are not constructed. During this period, the prestress load takes the main role. The compressive stress on top edge of steel-concrete interface is maximum and the stress on bottom edge of interface is minimum. Critical Case II is in the application stage. In

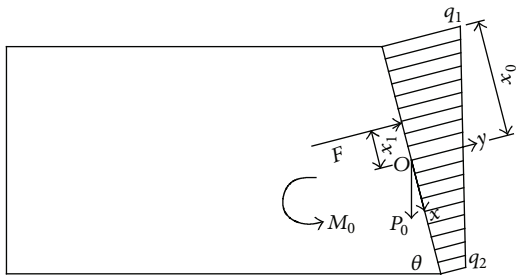

Figure 7: Mechanical model one of steel-concrete interface.

this stage, the orthotropic bridge deck slab is installed and bridge deck pavement is ready. When wheel load is located at the most unfavorable loading position (see Figure 5), the stress on top edge of steel-concrete interface is minimum and the stress on bottom edge of interface is maximum. Under the above two critical cases, if tensile stress is ensured not to happen to top edge and bottom edge of interface and compressive stress is ensured not to exceed compressive strength of the concrete at interface, the stress distribution under other general load cases can be determined to satisfy the structural requirements.

4.2. Theoretical Inference for the Optimal Position of the Transverse External Tendon

4.2.1. Stress Analysis on Critical Case I. Under this case, only the self-weight of steel cantilever and the action of external prestressed tendon are considered. Suppose that any point "O" on the steel cantilever interface is reference point for the force analysis and the equivalent stress analysis is performed based on which. Meanwhile, simplify self-weight of steel cantilever beam as "P_0" concentrated force and "M_0" bending moment that go through the reference center "O." Transverse external prestress is "F" and the distance between its load position and bending center is "x_1." Length of interface is "l," the distance between top edge of interface and bending center is "x_0," and the distance between bottom edge of interface and bending center is "$l - x_0$." Counterforce on the top edge of interface is "q_1" and counterforce on the bottom edge of interface is "q_2." As elasticity modulus of steel is much larger than that of concrete, the stress on the interface is supposed to be in linear distribution. Mechanical model for Critical Case I should be referred to in Figure 7.

In Figure 7, it could be concluded that

$$F - P_0 \cos\theta = \int_{-x_0}^{l-x_0} q(x)\, dx \tag{6}$$

$$Fx_1 + \int_{-x_0}^{l-x_0} q(x) \cdot x\, dx - M_0 = 0. \tag{7}$$

From (6), q_1 and q_2 can be expressed as

$$\begin{aligned} q_1 &= \frac{2(F - P_0\cos\theta)}{l} - q_2 \\ q_2 &= \frac{2(F - P_0\cos\theta)}{l} - q_1. \end{aligned} \tag{8}$$

In order to ensure good collaboration of the steel cantilever and original box girder, it should meet the requirements that the tensile stress will not happen to bottom edge of interface and compressive stress at top edge will not exceed compressive strength $[\sigma]$ of the concrete at interface. Thus, it needs to meet $q_1 \le [\sigma]t$, where "t" represents the width of the concrete postpouring diaphragm, and it also needs to meet $q_2 \ge 0$.

With the above safety requirements, (8) can be changed as

$$\begin{aligned} q_1 &\le \frac{2(F - P_0\cos\theta)}{l} \\ q_2 &\ge \frac{2(F - P_0\cos\theta)}{l} - [\sigma]\cdot t. \end{aligned} \tag{9}$$

From $q_1 \le [\sigma]\cdot t$ and $q_1 \le 2(F - P_0\cos\theta)/l$, the following equation is gotten:

$$q_1 \le a_0, \tag{10}$$

wherein $a_0 = \min\{[\sigma]\cdot t, 2(F - P_0\cos\theta)/l\}$.

From $q_2 \ge 0$ and $q_2 \ge 2(F - P_0\cos\theta)/l - [\sigma]\cdot t$, the following equation is gotten:

$$q_2 \ge b_0, \tag{11}$$

wherein $b_0 = \max\{0, 2(F - P_0\cos\theta)/l - [\sigma]\cdot t\}$.

Then, from (7), taking $x_0 = l/2$, it could be concluded that

$$Fx_1 - \frac{1}{2}(q_1 - q_2)\cdot l\cdot\left(\frac{2l}{3} - \frac{l}{2}\right) - M_0 = 0. \tag{12}$$

Joining (8) into (12), we can get

$$Fx_1 - \frac{l^2}{6}\left[\frac{(F - P_0\cos\theta)}{l} - q_2\right] = M_0 \tag{13}$$

$$Fx_1 - \frac{l^2}{6}\left[q_1 - \frac{(F - P_0\cos\theta)}{l}\right] = M_0. \tag{14}$$

From (10) and (13), the following equation can be gotten:

$$x_1 \le \left[\frac{a_0 l^2 - (F - P_0\cos\theta)\, l}{6} + M_0\right]\cdot\frac{1}{F}. \tag{15}$$

From (11) and (14), the following equation can be gotten:

$$x_1 \le \left[\frac{(F - P_0\cos\theta)\, l - b_0 l^2}{6} + M_0\right]\cdot\frac{1}{F}. \tag{16}$$

Joining (15) and (16) together, the upper limit of x_1 is given by

$$\begin{aligned} x_1 \le \min\Bigg\{&\left[\frac{a_0 l^2 - (F - P_0\cos\theta)\, l}{6} + M_0\right] \\ &\cdot\frac{1}{F}, \left[\frac{(F - P_0\cos\theta)\, l - b_0 l^2}{6} + M_0\right]\cdot\frac{1}{F}\Bigg\}, \end{aligned} \tag{17}$$

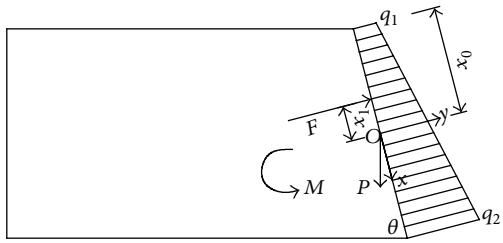

Figure 8: Mechanical model two of steel-concrete interface.

4.2.2. Stress Analysis on Critical Case II. Simplify the dead load on steel cantilever and wheel load as "P" concentrated force and "M" bending moment that go through the reference point "O." The transverse external prestress is "F" and the distance between its load position and bending center is "x_1." Length of the interface is "l," the distance between top edge of cross section and bending center is "x_0," and the distance between bottom edge of interface and bending center is "$l - x_0$." Counterforce on top edge of interface is "q_1" and counterforce on bottom edge of interface is "q_2." The stress on the interface is also supposed to be in linear distribution. Mechanical model for Critical Case II is shown in Figure 8.

From Figure 8, it could be concluded that

$$F - P\cos\theta = \int_{-x_0}^{l-x_0} q(x)\,dx \tag{18}$$

$$Fx_1 + \int_{-x_0}^{l-x_0} q(x)\cdot x\,dx - M = 0. \tag{19}$$

From equilibrium of friction along x-axis, it can be gotten that

$$P\cdot\sin\theta < \mu\cdot\int_{-x_0}^{l-x_0} q(x)\cdot dx. \tag{20}$$

From (18) and (20), the lower limit of external prestress "F" could be valued as

$$F > P\cdot\left(\frac{\sin\theta}{\mu} + \cos\theta\right). \tag{21}$$

In order to ensure good collaboration of steel cantilever and original box girder in Critical Case II, it should meet the requirements that tensile stress will not happen to top edge of interface and compressive stress on the bottom edge of interface will not exceed compressive strength of the concrete at interface. Thus, it needs to meet $q_1 \geq 0$ and $q_2 \leq [\sigma]t$ at the same time.

Referring to the derivation process of Critical Case I, lower limit of "x_1" could be expressed as

$$x_1 \geq \max\left\{\left[M - \frac{(F - P\cos\theta)\,l - al^2}{6}\right]\cdot\frac{1}{F}, \left[M - \frac{bl^2 - (F - P\cos\theta)\,l}{6}\right]\cdot\frac{1}{F}\right\}. \tag{22}$$

4.2.3. Load Position of Transverse Prestress and Value of External Prestress. Combining (17) and (22), theoretical value range of "x_1" and the load position of transverse prestressed tendon could be expressed as

$$\begin{aligned} x_1 &\geq \max\left\{\left[M - \frac{(F - P\cos\theta)\,l - al^2}{6}\right]\cdot\frac{1}{F}, \left[M - \frac{bl^2 - (F - P\cos\theta)\,l}{6}\right]\cdot\frac{1}{F}\right\} \\ x_1 &\leq \min\left\{\left[\frac{a_0 l^2 - (F - P_0\cos\theta)\,l}{6} + M_0\right]\cdot\frac{1}{F}, \left[\frac{(F - P_0\cos\theta)\,l - b_0 l^2}{6} + M_0\right]\cdot\frac{1}{F}\right\}. \end{aligned} \tag{23}$$

Reasonable values of "F" and "x_1" are the important premise to ensure the stress on the interface satisfy the requirements. To sum up, in the steel cantilever widening method, when making design for transverse external prestressed tendon, (21) should be referred to, according to which, limit for transverse external prestress "F" is provided. Within this range, type and number of prestressed tendons could be set to confirm the value of "F." Then, from (23), value range of "x_1" could be calculated, namely, theoretical range for load position of transverse external prestress tendon. The value of "F" can be adjusted until the load position of transverse prestressed tendon is reasonable and practical.

5. Structural Optimization Scheme of Steel Cantilever

Integrating the topological optimization design for the boundary and layout of steel cantilever and the theoretical derivation result for optimal position of transverse prestressed tendon, the structural optimization scheme of steel cantilever used in concrete box girder widening is proposed. First, make topological optimization analysis on the setting area and design the boundary and layout of steel cantilever beam. Second, based on the optimized shape and combining two critical cases, value range of transverse external prestress and reasonable action range of transverse prestressed tendon could be deduced. Third, select proper value of "F" to ensure that position of transverse external prestressed tendons is reasonable and practical and then make detail design on stiffening rib near interface of steel cantilever beam. Finally, make accurate finite element analysis on contact stress at steel-concrete interface under critical case to verify if the values of design parameters are reasonable. Steel cantilever could be designed according to this optimization analysis scheme, which could effectively reduce trials and save computing resources.

6. Application

6.1. Actual Bridge Example. In Figure 9, it shows the section of a two-lane bridge. This bridge is a reinforced concrete continuous box girder bridge having a width of 9.5 m. The

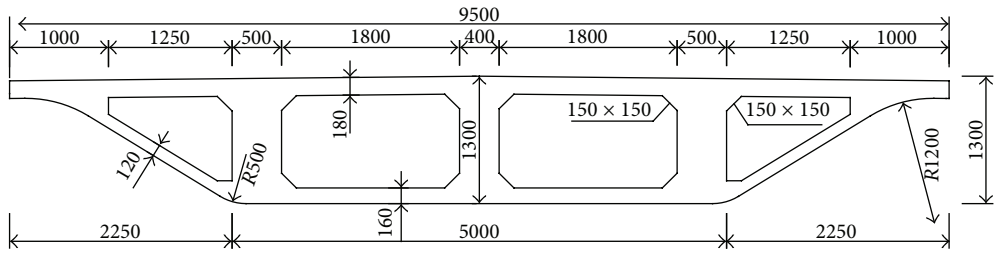

Figure 9: Standard cross section of Dalian northeast road overpass (unit: mm).

beam depth is 1.3 m; the thicknesses of roof and bottom plate are 18 cm and 16 cm, respectively. And the thicknesses of webs are shown in Figure 9. The results of health survey indicate that the bridge is in good condition. In order to ease traffic pressure of this bridge, it needs to be widened from two lanes to four lanes. This bridge is of an important geographical location with intensive underground pipelines and surrounding buildings and the traffic is not allowed to be stopped. In order to reduce building demolition and prevent traffic confliction on the ground, the steel cantilever widening concrete box girder method without piers is adopted to widen the bridge.

6.2. Optimization Design for the Shape of Steel Cantilever. As it is illustrated in Section 3.1, fully distributed dead load and uniform wheel load are the major load case to control the shape design of steel cantilever. For this bridge, pavement layer of pitch is 8 cm and pavement layer of concrete is 10 cm. Thickness of the roof of orthotropic bridge deck slab is 14 mm and thickness of U-shaped rib is 6 mm. A pair of steel cantilever beams are set every 3 m, thickness of the web is 14 mm, and thickness of bottom plate is 20 mm. Combined with the above actual loading conditions, dead uniform load "q_0" and wheel uniform load "q_1" are calculated as $q_0 = 21.9$ kN/m and $q_1 = 140.8$ kN/m (axle weight of vehicle is 130 kN which considers dynamic load magnification factor as 1.3), respectively. Load arrangement form is the same as in the above Figures 5 and 6.

The inclination angle of interface "θ" should be determined by comprehensively considering the following factors: transverse external prestressed tendons should be vertical to the interface; the external prestressed tendons which cross the original box girder should try to minimize the damage of the original structure; bending radius "R" of transverse external prestressed tendons should meet the minimum specified value which is 1.5 m for epoxy coated strands. With integration of the above factors, the inclination angle of interface here is valued as $\theta = 75.5^\circ$ and the bending radius of transverse prestressed tendons is $R = 2$ m.

As referred to in Section 3.2, the objective function of the topological optimization problem is to make the stiffness of the steel cantilever the largest. Design variable is the relative density of the element for the materials within design area. In order to ensure that the steel cantilever transmits the loads to the interface effectively, Load Case 1 and Load Case 2 are considered together to confirm the boundary and layout

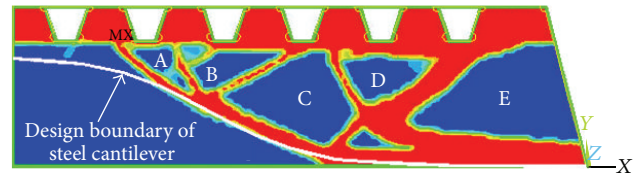

Figure 10: Topological optimization result for load weight coefficient (1, 0).

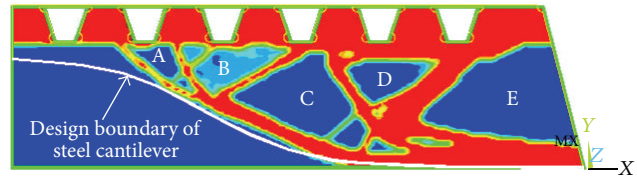

Figure 11: Topological optimization result for load weight coefficient (0.5, 0.5).

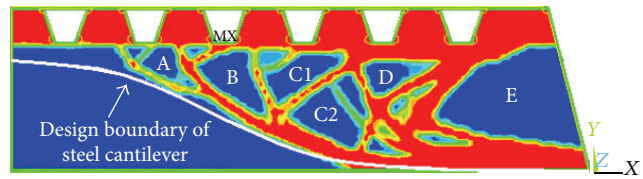

Figure 12: Topological optimization result for load weight coefficient (0, 1).

of steel cantilever. As to this minimum compliance design problem, the material distribution results for three kinds of weight coefficients (the weight coefficients of Load Case 1 and Load Case 2 are selected as (1, 0), (0.5, 0.5), and (0, 1)) are compared. Besides, the optimization results for different volume coefficients (20% to 60%) are compared too. Based on the layout of them, the material distribution of 40% is selected for the more reasonable shape and hole parameters from the point of actual engineering. The optimization results for different kinds of weight coefficients when the volume coefficient is 40% are given in Figures 10 to 12. As can be seen from them, on the premise of the same volume coefficient, the optimization results for different weight coefficients are similar, wherein blue area represents the area that does not need to arrange materials during structure design and red areas represent the areas that need to arrange materials. The

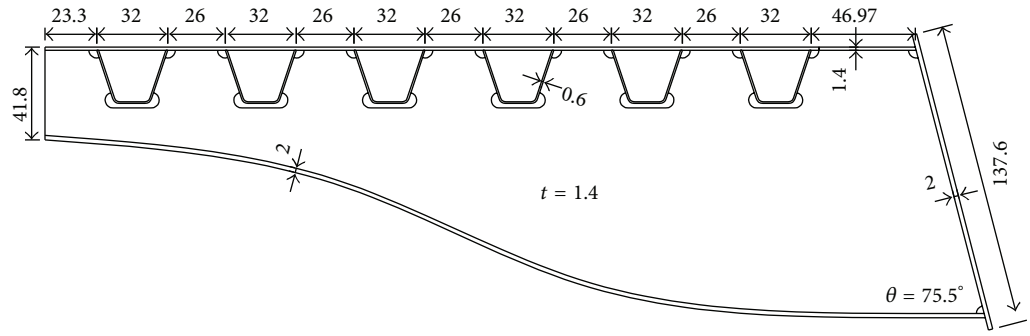

Figure 13: Steel cantilever optimization appearance design (unit: cm).

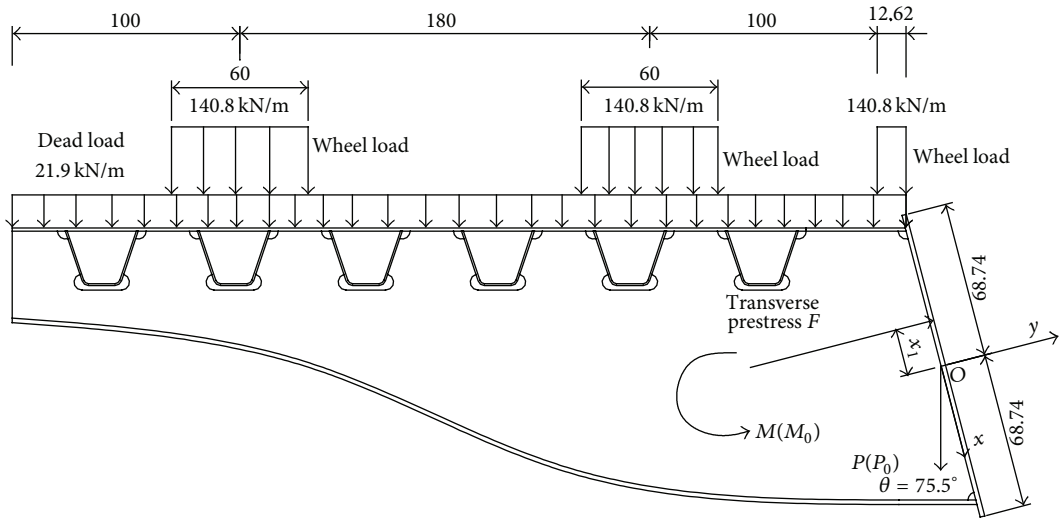

Figure 14: Steel cantilever mechanical model (unit: cm).

results of topological optimization are used to confirm the boundary of steel cantilever and the positions of function holes. As it is shown in Figures 10 to 11, in the domain of the boundary of the steel cantilever, function holes which are used to settle pipelines should be placed in the blue area marked as A, B, C, and D. The area marked as E should not be punched because, under the transverse prestressed load, domain E is the key area of the prestress transmitting. But for this bridge, lighting at bridge deck is provided by street lamps on the ground and there are no other requirements for pipelines to pass by in early stage. Thus, functional holes are not needed to be set in steel cantilever beam. The streamlined boundary of steel cantilever is extracted as it is shown in Figure 13. In the future, the function holes can be set in the blue area marked as A, B, C, and D when they are needed.

6.3. Design for Load Position of Transverse Prestressed Tendons. Based on the shape and size of steel cantilevers that have been confirmed, under combined action of dead load, the most unfavorable live load and prestress, the mechanical model for steel cantilever beam is established as in Figure 14. The uniform load caused by bridge deck pavement is 21.9 kN/m and uniform force made by single wheel is 140.8 kN/m, which is Critical Case II as illustrated in Section 4.1. The dead load on steel cantilever beam and wheel load are simplified as a concentrated force "P" and bending moment "M" that go through the bending center "O." The other critical case refers to the fact that only self-weight of steel cantilever beam and action of external prestressed tendons are considered during construction. Self-weight of steel cantilever beam is simplified as a concentrated force "P_0" and bending moment "M_0" that go through the bending center. The concrete strength grade of original girder is C30. In order to supply sufficient resistance to the steel cantilever beam, the concrete postpouring diaphragm needs enough compressive strength. So, C50 is selected for the postpouring diaphragm. During the derivation process, ultimate compressive strength of concrete $[\sigma]$ is valued as 22.4 MPa according to the regulations for bridges ⟨JTG D62-2004⟩. Specific values of other parameters under the two critical cases should be referred to in Table 1.

According to (23), the range of theoretical load position of transverse prestressed tendons in this example is calculated to be 0.19 m $< x_1 <$ 0.32 m. Within this range, the specific position of transverse prestressed tendons should be determined by considering these factors: when the transverse prestressed tendons go through the original girder, the damage to original girder should be minimized and the bending radius "R"

Table 1: Steel cantilever mechanics parameter.

Load case	M (M_0) (kNm)	F (kN)	P (P_0) (kN)	Cos θ	[σ] (MPa)	l (m)	x_1 (m)
Dead load + live load	555.43	1430	252.92	0.25	22.4	1.226	Lower limit 0.19
Self-weight	181.95	1430	85.98	0.25	22.4	1.226	Upper limit 0.32

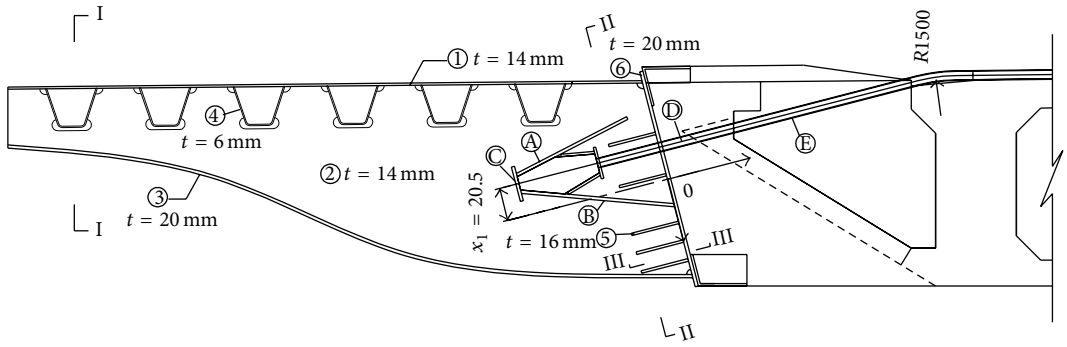

①: roof, 14 mm
②: web, 14 mm
③: bottom flange plate, 20 mm
④: U-shaped rib, 6 mm
⑤: small stiffening rib, 16 mm
⑥: base plate, 20 mm
Ⓐ: upper diagonal rib, 20 mm
Ⓑ: lower diagonal rib, 20 mm
Ⓒ: anchor plate, 20 mm
Ⓓ: prestressed tendon
Ⓔ: preembedded steel tube

Figure 15: Steel cantilever elevational drawing (unit: mm).

of transverse external prestressed tendons should meet the minimum specified value of epoxy coating steel strands.

Based on above factors and actual conditions of this girder, the position of transverse external prestressed tendons is determined as shown in Figure 15, wherein x_1 takes 20.5 cm and bending radius of transverse prestressed tendons is R = 2 m. The transverse prestress is 1430 kN, which could be offered by 10φ15.2 mm prestressed tendons, which are set symmetrically on both sides of steel cantilever slab as shown in Figure 17. The steel cantilevers at both sides of box girder are transversely combined with original box girder by 2 bundles (each bundles is composed by 5φ15.2 mm prestressed tendons) of external prestressed epoxy steel strands.

6.4. Detailed Design of Stiffening Rib. Stiffening rib of steel cantilever should be designed in detail on the basis of confirmed shape of steel cantilever and load position of transverse prestressed tendons. During the designing process, the reasonable stress on interface is an important reference index. In order to ensure that the steel cantilever and original girder are reliably combined, principles of the stress on the interface between steel cantilever beam and concrete postpouring diaphragm should be confirmed as follows: the key regions of concrete postpouring diaphragm interface which are under the base plate at web, roof, and bottom flange plate as shown in Figure 15 should keep in compression to avoid from being separated from steel cantilever and the maximum compressive stress of concrete interface should be ensured not to exceed local compressive admissible value of postpouring diaphragm concrete.

Under direction of the above principles, stiffening ribs of steel cantilever are designed in detail. In order to make the force at steel cantilever able to transmit to original girder uniformly, a steel base plate with thickness of 20 mm is placed at the interface between steel cantilever and concrete diaphragm and several stiffening ribs are set on the base plate. Setting stiffening ribs could also guarantee that the external force is transmitted to the interface effectively and evenly. Transverse prestressed tendons especially at both sides of web need to be anchored to Anchor Plate C that is vertical to the webs and the prestress is transferred to interface through Diagonal Rib A, Diagonal Rib B, and Web ② as shown in Figure 15. Specific size of various components should be referred to in Figures 15 and 16. Structure of the actual bridge should be referred to in Figure 18.

6.5. Stress Analysis on Steel-Concrete Interface. After detailed design, the reasonability and feasibility of the whole optimal design should be verified by analyzing the stress on the steel-concrete interface.

According to above design parameters, finite element model is established and the girder with 3 m long is taken from the widened girder to analyze. In this paper, ANSYS FEA software is used to analyze the stress on the interface. SOLID95 with 20 nodes is used to simulate original concrete box girder and postpouring concrete diaphragm. SHELL63 is used to simulate steel plate structures including steel cantilever beam, orthotropic bridge deck slab, stiffening rib, and steel base plate. Link 10 tension-only element is used to simulate prestressed tendons. Concrete element at the interface is divided into hexahedral mesh grids and the steel

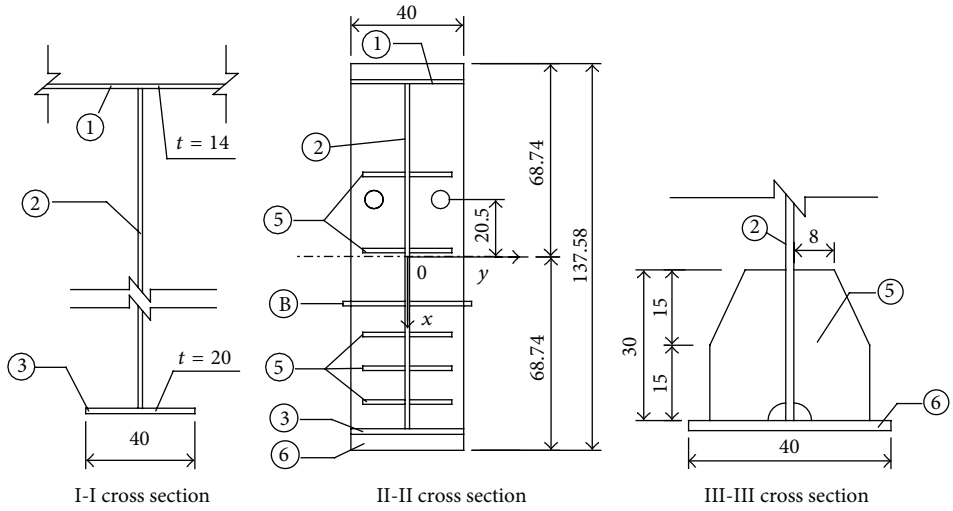

Figure 16: Section schematic diagram (unit: mm).

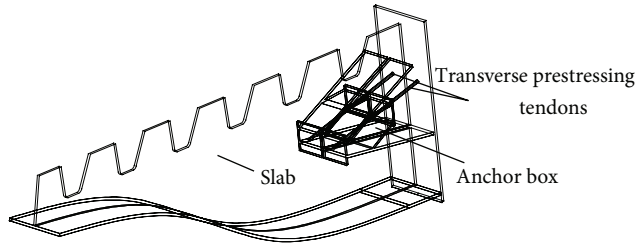

Figure 17: Details of the steel cantilever beam.

Figure 18: A case for optimization design of bridge.

base plate of steel cantilever is divided into the same mesh to ensure that the interface is connected truly and reliably. Link 10 compression-only element is used to connect the steel base plate and the concrete, which can simulate axial force in the direction of y, while the contact conditions in other directions are simulated by the coupled equations. Finite element model is shown in Figures 19 and 20.

Local stress analysis on widened bridge structure is loaded by 20t vehicle with 70 kN front shaft and 130 kN back shaft. The most unfavorable condition is the case when the back shaft is loaded on the cantilever. According to the regulations of bridges ⟨JTG D62-2004⟩, impact effect should be included here and impact coefficient should take 1.3. Thus, the load of back shaft should be exerted as $1.3 \times 130\,\text{kN} = 169\,\text{kN}$.

Two critical cases are adopted as follows.

Critical Case I is in the construction state. In this stage the self-weight and prestress are considered. The objective of Case I is checking if compressive stress on top of the interface exceeds allowable value of C50 and if the bottom of the interface open when prestressed tendon is stretched.

Critical Case II is in the service status. Self-weight, dead load, prestress, and live load of four lanes are considered in this stage. The objective is checking if top of the interface

Figure 19: Finite element model.

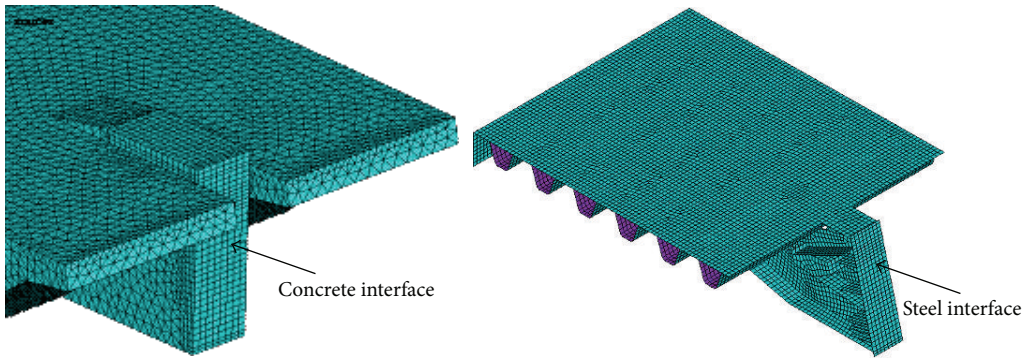

Figure 20: Finite element model of interface.

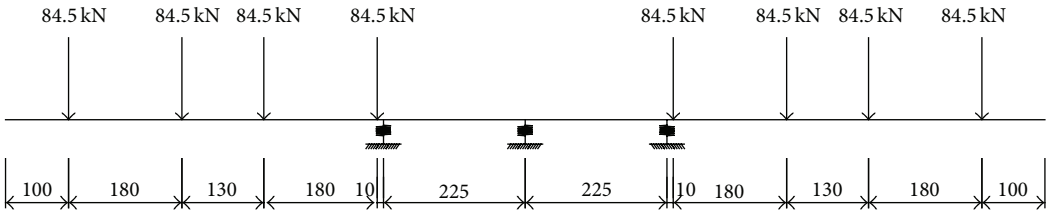

Figure 21: Load spread schematic diagram of model two.

between concrete and steel beam opens and if the compressive stress on the bottom exceeds admissible value of C50. Load arrangement should be referred to in Figure 21.

Stress on the interface for Case I is shown in Figure 22. It could be concluded from this figure that the key regions of interface at web, roof, and bottom flange is under compression. Local maximum compressive stress of concrete interface is 14.4 MPa and this value is smaller than compressive strength of C50 concrete used for postpouring diaphragm as 22.4 MPa. And from enlarged stress nephogram for normal stress at bottom edge of the interface, it could be concluded that tensile stress does not happen to bottom edge of interface under this case.

Stress on interface for Case II should be referred to in Figure 23. It could be concluded that the key regions of the interface is also under compression. Local maximum compressive stress for concrete is 16.9 MPa, which is smaller than compressive stress of concrete postpouring diaphragm, so as to ensure that the concrete at interface is safely compressed. In this case, the top of the interface is easy to open, while the enlarged cloud diagram for the stress at top edge shows that this position is under compression too.

Thus, it could be concluded that, under both of the two critical cases, the interface between steel cantilever beam and concrete postpouring diaphragm is ensured to be closed and the concrete at interface is ensured not to be crushed. The stress results show the interface is reasonably compressed, which meets the design requirements.

7. Conclusions

The structural optimization method of steel cantilever used in concrete box girder bridge widening is illustrated in this paper, which is a new box girder widening method with

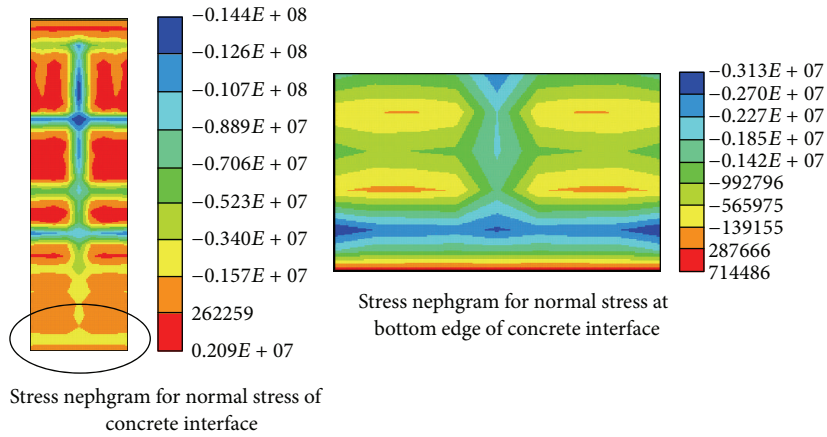

Figure 22: Concrete interface normal stress diagram of Case I.

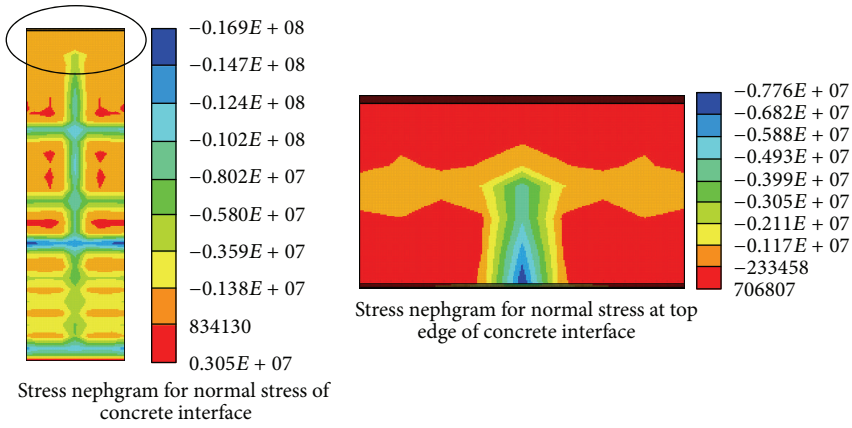

Figure 23: Concrete interface normal stress diagram of Case II.

various advantages. In order to promote actual application of this method, relevant researches on the structural optimization of steel cantilever are made and the following could be concluded.

(1) The authors have introduced the topological optimization theory to get reasonable material distribution results within design area for steel cantilever. And this topological result provides theoretical basis for the determination of shape and arrangement of function holes of steel cantilever beam.

(2) Authors have made stress analysis on the interface between steel cantilever and concrete postpouring diaphragm. In order to prevent tensile stress from happening to the interface under any load cases and make compressive stress not to exceed admissible value for compressive strength of the postpouring diaphragm, basic mechanical model for steel cantilever beam under two critical load cases has been established and the analytical expression of the optimal action range of transverse prestressed tendons has been deduced according to plane cross-section assumption.

(3) In this paper, an optimization design scheme based on the stress at steel-concrete interface has been given, which is applied to a real bridge. The analysis results indicate that using this optimization design scheme to make optimization design on steel cantilever could get the scheme that meets design requirements with reasonable stress. This method could reduce unnecessary trials and save computing resource to the greatest extent, so as to realize rapid and accurate design.

This structural optimization method provides the theoretical support to the promotion of steel cantilever widening concrete box girder method and also promotes the application of structural optimization theory in bridge design.

Conflict of Interests

The authors declare that there is no conflict of interests regarding the publication of this paper.

Acknowledgments

The research described in this paper was financially supported by the science and technology funds of Liaoning Education Department (20131021) and the National Natural Science Foundation of China (51308090).

References

[1] S. Allahdadian and B. Boroomand, "Design and retrofitting of structures under transient dynamic loads by a topology optimization scheme," in *Proceedings of the 3rd International Conference on Seismic Retrofitting*, pp. 1–9, Iranian NorthWest Retrofitting Center, Iranian Retrofitting Researchers Institute, Tabriz, Iran, October 2010.

[2] L. Stromberg, A. Beghini, W. F. Baker, and G. H. Paulino, "Design of structural braced frames using group optimization," in *Proceedings of the 20th Analysis and Computation Specialty Conference*, vol. 10, pp. 267–277, 2012.

[3] L. L. Beghini, A. Beghini, N. Katz, W. F. Baker, and G. H. Paulino, "Connecting architecture and engineering through structural topology optimization," *Engineering Structures*, vol. 59, pp. 716–726, 2014.

[4] J. K. Guest, R. Lotfi, A. T. Gaynor, and M. Jalalpour, "Structural topology optimization: moving beyond linear elastic design objectives," in *Proceedings of the 20th Analysis and Computation Specialty Conference*, pp. 245–256, Chicago, Ill, USA, March 2012.

[5] L. L. Stromberg, A. Beghini, W. F. Baker, and G. H. Paulino, "Application of layout and topology optimization using pattern gradation for the conceptual design of buildings," *Structural and Multidisciplinary Optimization*, vol. 43, no. 2, pp. 165–180, 2011.

[6] B. Briseghella, L. Fenu, C. Lan, E. Mazzarolo, and T. Zordan, "Application of topological optimization to bridge design," *Journal of Bridge Engineering*, vol. 18, no. 8, pp. 790–800, 2013.

[7] H. Guan, Y.-J. Chen, Y.-C. Loo, Y.-M. Xie, and G. P. Steven, "Bridge topology optimisation with stress, displacement and frequency constraints," *Computers & Structures*, vol. 81, no. 3, pp. 131–145, 2003.

[8] E. Fauche, S. Adriaenssens, and J. H. Prevost, "Structural optimization of a thin-shell bridge structure," *Journal of the International Association for Shell and Spatial Structures*, vol. 51, no. 2, p. 153, 2010.

[9] V. Goremikins, K. Rocens, and D. Serdjuks, "Topology optimization of cable Truss web for prestressed suspension bridge," *World Academy of Science, Engineering and Technology*, vol. 73, pp. 41–47, 2013.

[10] M. Daifuku, T. Nishizu, A. Takezawa, M. Kitamura, H. Terashita, and Y. Ohtsuki, "Design methodology using topology optimization for anti-vibration reinforcement of generators in a ship's engine room," *Proceedings of the Institution of Mechanical Engineers Part M: Journal of Engineering for the Maritime Environment*, 2014.

[11] M. Bruggi, "Generating strut-and-tie patterns for reinforced concrete structures using topology optimization," *Computers & Structures*, vol. 87, no. 23-24, pp. 1483–1495, 2009.

[12] M. Victoria, O. M. Querin, and P. Marti, "Generation of strut-and-tie models by topology design using different material properties in tension and compression," *Structural and Multidisciplinary Optimization*, vol. 44, no. 2, pp. 247–258, 2011.

[13] Y. Yang, C. D. Moen, and J. K. Guest, "Three-dimensional force flow paths and reinforcement design in concrete via stress-dependent truss-continuum topology optimization," *Journal of Engineering Mechanics*, vol. 141, no. 1, Article ID 04014106, 2014.

[14] M. Bruggi and A. Taliercio, "Topology optimization of the fiber-reinforcement retrofitting existing structures," *International Journal of Solids and Structures*, vol. 50, no. 1, pp. 121–136, 2013.

[15] M. Bruggi, G. Milani, and A. Taliercio, "Design of the optimal fiber-reinforcement for masonry structures via topology optimization," *International Journal of Solids and Structures*, vol. 50, no. 13, pp. 2087–2106, 2013.

[16] M. Bruggi, G. Milani, and A. Taliercio, "Simple topology optimization strategy for the FRP reinforcement of masonry walls in two-way bending," *Computers and Structures*, vol. 138, no. 1, pp. 86–101, 2014.

[17] Q. Wang and Z. Zhang, "Orthotropic steel cantilever widening method of concrete box girder," *Structural Engineering International*, vol. 21, no. 2, pp. 228–232, 2011.

[18] Q. Wang, L. Shi, and Z. Zhang, "Application of a new kind of widening method in Dalian Northeast Road overpass improvement project," in *Proceedings of the 9th International Conference on Civil and Environmental Engineering*, Dalian, China, November 2010.

[19] M. Majowiecki, "The free form design (FFD) in steel structural architecture—aesthetic values and reliability," *Steel Construction*, vol. 1, no. 1, pp. 3–15, 2008.

[20] M. Majowiecki, "Ethics and structural reliability in free-form design (FFD)," *Journal of the International Association for Shell and Spatial Structures*, vol. 48, no. 4, pp. 29–50, 2007.

[21] M. P. Bendsøe and N. Kikuchi, "Generating optimal topologies in structural design using a homogenization method," *Computer Methods in Applied Mechanics and Engineering*, vol. 71, no. 2, pp. 197–224, 1988.

[22] M. P. Bendsøe, *Optimization of Structural Topology, Shape, and Material*, Springer, Berlin, Germany, 1995.

[23] M. P. Bendsøe and O. Sigmund, *Topology Optimization: Theory, Methods, and Applications*, Springer, Berlin, Germany, 2003.

[24] H. P. Mlejnek and R. Schirrmacher, "An engineer's approach to optimal material distribution and shape finding," *Computer Methods in Applied Mechanics and Engineering*, vol. 106, no. 1-2, pp. 1–26, 1993.

[25] Y. M. Xie and G. P. Steven, "A simple evolutionary procedure for structural optimization," *Computers and Structures*, vol. 49, no. 5, pp. 885–896, 1993.

[26] Y. M. Xie and G. P. Steven, *Evolutionary Structural Optimization*, Springer, Berlin, Germany, 1997.

[27] X. Y. Yang, Y. M. Xie, G. P. Steven, and O. M. Querin, "Bidirectional evolutionary method for stiffness optimization," *AIAA Journal*, vol. 37, no. 11, pp. 1483–1488, 1999.

[28] O. M. Querin, V. Young, G. P. Steven, and Y. M. Xie, "Computational efficiency and validation of bi-directional evolutionary structural optimization," *Computer Methods in Applied Mechanics and Engineering*, vol. 189, no. 2, pp. 559–573, 2000.

[29] X. Huang and Y. M. Xie, "Topology optimization of nonlinear structures under displacement loading," *Engineering Structures*, vol. 30, no. 7, pp. 2057–2068, 2008.

[30] M. P. Bendsøe, "Optimal shape design as a material distribution problem," *Structural Optimization*, vol. 1, no. 4, pp. 193–202, 1989.

[31] M. P. Bendsøe and O. Sigmund, "Material interpolation schemes in topology optimization," *Archive of Applied Mechanics*, vol. 69, no. 9-10, pp. 635–654, 1999.

[32] G. I. N. Rozvany, "Aims, scope, methods, history and unified terminology of computer-aided topology optimization in structural mechanics," *Structural and Multidisciplinary Optimization*, vol. 21, no. 2, pp. 90–108, 2001.

[33] X. Zhou, L. Chen, and Z. Huang, "The SIMP-SRV method for stiffness topology optimization of continuum structures," *International Journal of CAD/CAM*, vol. 7, no. 1, 2009.

[34] Ministry of Transport of the People's Republic of China (MOT), *Code for Design of Highway Reinforced Concrete and Prestressed Concrete Bridges and Culverts*, JTG D62-2004, Ministry of Transport of the People's Republic of China (MOT), Beijing, China, 2004.

[35] O. Sigmund, "A 99 line topology optimization code written in Matlab," *Structural and Multidisciplinary Optimization*, vol. 21, no. 2, pp. 120–127, 2001.

[36] M. P. Bendsøe and O. Sigmund, *Topology Optimization, Theory, Methods, and Applications*, Springer, Berlin, Germany, 2004.

[37] M. Bruggi, "On the automatic generation of strut and tie patterns under multiple load cases with application to the aseismic design of concrete structures," *Advances in Structural Engineering*, vol. 13, no. 6, pp. 1167–1181, 2010.